DEVELOPMENT OF A USER-GUIDED PROGRAM FOR PREDICTING TIME-DEPENDENT DEFORMATIONS IN PRESTRESSED BRIDGE GIRDERS

by

Claire Elizabeth Schrantz

A thesis submitted to the Graduate Faculty of
Auburn University
in partial fulfillment of the
requirements for the Degree of
Master of Science

Auburn, Alabama
May 7, 2012

Keywords: camber, concrete, prestress losses, creep, relaxation, shrinkage, time-step analysis

Approved by

Robert W. Barnes, Chair, Associate Professor of Civil Engineering
Anton K. Schindler, Associate Professor of Civil Engineering
Hassan H. Abbas, Assistant Professor of Civil Engineering

ABSTRACT

A Visual Basic (VB) computer program was developed to predict time-dependent deformations and associated material stresses in prestressed concrete bridge girders. The VB program allows the user to select a model for the development of the concrete modulus of elasticity (MOE) over time as well as the creep and shrinkage models used in the calculations. The program includes two test-based and three code-prediction models for MOE growth. The test-based models include the "Constant E_c" and "Two-Point E_c" models. The code-prediction models include AASHTO LRFD '05(+)—2005 and later, ACI 209R-92, and CEB 90. The creep and shrinkage models include AASHTO LRFD '05(+), AASHTO LRFD '04(-)—2004 and earlier, ACI 209R-92, CEB 90, and Modified CEB 90. The Modified CEB 90 model is based on previous research by Kavanaugh (2008).

Experimental data from three previous research studies at Auburn University were used to evaluate the strain- and camber-prediction capabilities of the program. Strain and camber measurements were collected from six full-scale AASHTO Type I girders and five AASHTO BT-54 girders. Camber measurements for sixteen 15-in. deep prestressed T-beams were also used. The AASHTO Type I girders and T-beams were constructed using conventional and self-consolidating concrete (SCC) mixtures. Four moderate- strength SCC mixtures and three high-strength SCC mixtures were used. The moderate-strength SCC mixtures had 28-day concrete strengths between 8500 and 9800 psi, while the high-strength SCC mixtures had 28-day concrete

strengths between 13100 and 13600 psi. The 28-day concrete strengths of the conventional mixtures ranged from 6300 to 7200 psi.

Various combinations of models for the concrete MOE development and creep and shrinkage calculations were used to predict the strain and camber of prestressed flexural members. The program results were compared to experimental measurements to evaluate the accuracy of the camber predictions. A sensitivity analysis was also performed to determine the effects of design parameters on strain and camber results.

ACKNOWLEDGEMENTS

I would like to thank Dr. Robert Barnes for his immense knowledge, guidance, and patience over the years. I would also like to thank Dr. Anton Schindler for his assistance throughout this project.

This project would not have been possible without the hard work and support of Graduate Research Assistants Kurtis Boehm, Darren Dachelet, Nicole Donnee, Bryan Kavanaugh, and Triple Sawyer, as well as concrete lab technician Billy Wilson. I would also like to thank The Alabama Department of Transportation and Auburn University Highway Research Center for the financial support of various portions of the research described in this thesis.

Most importantly, I would like to thank God and my family for the unconditional love and support. I dedicate all of my work to them.

TABLE OF CONTENTS

ABSTRACT ii

ACKNOWLEDGEMENTS iv

LIST OF TABLES xiii

LIST OF FIGURES xvii

CHAPTER 1: INTRODUCTION 1

1.1 BACKGROUND 1

1.2 RESEARCH OBJECTIVES AND WORK PLAN 2

1.3 RESEARCH SCOPE 3

1.4 ORGANIZATION OF THESIS 4

1.5 NOTATION 5

CHAPTER 2: CAMBER IN PRETENSIONED MEMBERS 6

2.1 INTRODUCTION 6

2.2 CAMBER 6

2.3 FACTORS INFLUENCING CAMBER 7

2.3.1 Steel Relaxation 8

2.3.2 Elastic Shortening of Concrete 10

2.3.3 Concrete Compressive Strength 11

2.3.4 Concrete Modulus of Elasticity 11

2.3.4.1 AASHTO LRFD Pre-2005 and Post-2005 12

2.3.4.2 ACI 209 14

2.3.4.3 CEB 90 16

2.3.5 Creep 18

2.3.5.1 AASHTO LRFD (2005 and Later) 19

2.3.5.2 AASHTO LRFD (2004 and Earlier) 20

2.3.5.3 ACI 209 22

2.3.5.4 CEB 90 24

2.3.5.5 Modified CEB 90 26

2.3.6 Shrinkage 26

2.3.6.1 AASHTO LRFD (2005 and Later) 27

2.3.6.2 AASHTO LRFD (2004 And Earlier) 27

2.3.6.3 ACI 209 29

2.3.6.4 CEB 90 30

2.4 PREVIOUS STUDIES 31

2.4.1 HINKLE (2006) 32

2.4.2 AL-OMAISHI, TADROS, AND SEGUIRANT (2009) 33

CHAPTER 3: COMPUTER PROGRAM DEVELOPMENT 35

3.1 ANALYTICAL APPROACH 35

3.1.1 METHODOLOGY 35

3.1.2 CROSS-SECTIONAL DEFORMATIONS 38

3.1.2.1 INCREMENTAL STRAIN 39

3.1.2.2 INCREMENTAL CURVATURE 43

3.1.3 TIME ARRAY FUNCTION 45

3.2 ANALYTICAL METHODS 48

3.2.1 MATURITY OF CONCRETE 48

3.2.2 CONCRETE MODULUS OF ELASTICITY 50

3.2.2.1 CONSTANT E_C 50

3.2.2.2 TWO-POINT E_C 50

3.2.3 CREEP AND SHRINKAGE 52

3.2.3.1 AASHTO LRFD 52
3.2.3.2 ACI 209 53
3.2.3.3 CEB 90 53
3.2.3.4 MODIFIED CEB 90 54
3.3 PROGRAM EXECUTION 54
3.3.1 USER-DEFINED INPUT 55
3.3.1.1 CROSS-SECTIONAL GEOMETRY 55
3.3.1.2 GLOBAL VARIABLES 58
3.3.1.3 GLOBAL ARRAYS 58
3.3.2 INTERNAL CALCULATIONS 60
3.3.2.1 INITIAL TRANSFORMED SECTION PROPERTIES 60
3.3.2.2 INITIAL PRESTRESS LOSSES 60
3.3.2.3 TRANSFORMED SECTION PROPERTIES 61
3.3.2.4 CREEP AND SHRINKAGE CORRECTION FACTORS 61
3.3.2.5 TIME LOOP—INCREMENTAL STRAINS, STRESSES, AND CURVATURES 62
3.3.2.6 CAMBER CALCULATIONS 65
3.3.3 PROGRAM FLOW CHART 67

3.3.4 PROGRAM OUTPUT 67

3.4 INTERVAL SELECTION 68

3.4.1 DISCRETIZATION ANALYSIS 68

3.4.1.1 TIME INTERVALS 70

3.4.1.2 CROSS SECTIONS 75

3.4.2 SELECTION SUMMARY 79

CHAPTER 4: EXPERIMENTAL METHODS 80

4.1 INTRODUCTION 80

4.2 EXPERIMENTAL PROGRAM 80

4.3 DATA ACQUISITION 85

4.3.1 STRAIN MEASUREMENTS 85

4.3.2 CAMBER MEASUREMENTS 88

4.4 PREVIOUS RESEARCH 90

4.4.1 LEVY (2007) 90

4.4.2 STALLINGS, BARNES, AND ESKILDSEN (2003) 93

4.5 PROGRAM INPUT 95

4.5.1 PROPERTY AND EVENT SUMMARY 95

4.5.2 Prestressing Stand and Reinforcing Steel Summary 96

CHAPTER 5: RESULTS 97

5.1 STRAIN PREDICTIONS 97

5.1.1 Temperature-Induced Strains 97

5.1.2 AASHTO Type I Girders 103

5.1.2.1 Strain Predictions Using Test-Based E_C Models 104

5.1.2.2 Strain Predictions Using Code-Prediction E_C Models 125

5.1.3 BT-54 Girders 146

5.2 STRAND STRESS PREDICTIONS 154

5.2.1 AASHTO Type I Girders 154

5.3 CAMBER PREDICTIONS 157

5.3.1 Temperature-Induced Curvatures 158

5.3.2 AASHTO Type I Girders 160

5.3.2.1 Camber Predictions Using Test-Based E_C Models 160

5.3.2.2 Camber Predictions Using Code-Prediction E_C Models 165

5.3.3 T-Beams 174

5.3.3.1 Camber Predictions Using Test-Based E_C Models 175

5.3.3.2 Camber Predictions Using Code-Prediction E_C Models 181

5.3.4 BT-54 Girders 190

CHAPTER 6: SENSITIVITY ANALYSIS 195

6.1 APPROACH 195

6.2 EFFECT OF CONCRETE PROPERTIES 195

6.2.1 Cement Type 195

6.2.2 Slump 198

6.3 EFFECT OF CONSTRUCTION VARIABLES 202

6.3.1 Jacking Stress 202

6.3.2 Curing Methods 203

6.4 EFFECTS OF MATURITY 208

CHAPTER 7: SUMMARY, CONCLUSIONS, AND RECOMMENDATIONS 212

7.1 SUMMARY 212

7.2 CONCLUSIONS 213

7.2.1 Strain Predictions 213

7.2.2 Strand Stress Predictions 215

7.2.3 Camber Predictions 216

7.2.3 GENERAL CONCLUSIONS 219

7.3 RECOMMENDATIONS FOR FUTURE WORK 220

REFERENCES 222

APPENDIX A: NOTATION 226

APPENDIX B: AASHTO TYPE I RESEARCH.....229

APPENDIX C: T-BEAM RESEARCH.....236

APPENDIX D: AASHTO BT-54 RESEARCH 239

APPENDIX E: STRAIN MEASUREMENTS 240

APPENDIX F: MEASURED CAMBER 257

APPENDIX G: PREDICTED CAMBER.....266

APPENDIX H: VISUAL BASIC PROGRAM.....296

APPENDIX I: SENSITIVITY ANALYSIS – INTERVAL SELECTION 309

APPENDIX J: SENSITIVITY ANALYSIS – VISUAL BASIC PROGRAM.....314

APPENDIX K: VISUAL BASIC PROGRAM USER INTERFACE 318

APPENDIX L: VISUAL BASIC PROGRAM CODE 344

LIST OF TABLES

Table 2-1: Coarse Aggregate Coefficients (Iravani 1996) 13

Table 2-2: Values of Constants for Strength Development 15

Table 2-3: Characteristic Strength f_{ck} Values (MPa) 17

Table 2-4: Effect of Aggregate Type on Modulus of Elasticity (CEB-FIP 1990) 18

Table 2-5: Parameters used in the Modified CEB 90 Method (Kavanaugh 2008) 26

Table 3-1: Parameter Summary for Time Functions 46

Table 3-2: Modifications for Concrete Age at Time of Loading 53

Table 3-3: Components for Camber Equation 66

Table 3-4: Profile Details for Interval Selection Test Case 69

Table 3-5: Design Parameters for Interval Selection Test Case 70

Table 4-1: Summary of Fresh Concrete Properties (Boehm 2008) 82

Table 4-2: Summary of Hardened Concrete Properties Reported by Boehm (2008) 83

Table 4-3: Curing Details used by Boehm (2008) 84

Table 4-4: Vibrating Wire Strain Gage (VWSG) Locations 86

Table 4-5: VWSG Reading Times Relative to Transfer 88

Table 4-6: Level Reading Locations Relative to East End of Girder 89

Table 4-7: Summary of Specimen Material Properties (Levy 2007) 92

Table 4-8: Calculated f_{pj} based on given f_{pbt} Values 93

Table 5-1: AASHTO Type I Girder Zone Geometry 98

Table 5-2: Slump and Slump Flow – AASHTO Type I Girders 104

Table 5-3: BT-54 Design Parameters 147

Table 5-4: ACI 209 Correction Factors for BT-54 Girders (Stallings et al. 2003).....147

Table 5-5: Strand Stress Comparisons.....155

Table 5-6: T-Beam Lengths (Levy 2007) 174

Table 5-7: Slump and Slump Flow – T-Beams (Levy 2007).....175

Table 5-8: BT-54 Camber - Experimental Results from Stallings et. al (2003) 191

Table 5-9: BT-54 Camber Comparison – AASHTO / ACI 193

Table 5-10: BT-54 Camber Comparison – CEB 90 / Modified CEB.....194

Table 6-1: CEB-FIP Cement Classifications 196

Table 6-2: STD-M-1 Camber – Varying Jacking Stress.....203

Table 6-3: STD-M-1 Adjusted Concrete Age – Varying Curing Temperature 209

Table B-1: AASHTO Type 1 Mix Designs (Boehm 2008) 229

Table B-2: Summary of Hardened Concrete Property Test Results (Boehm 2008).....229

Table B-3: Effective Prestress at Measured Transfer Length Ages (Boehm 2008) 232

Table C-1: Concrete Mixture Proportions (Levy 2007) 236

Table C-2: Summary of Fresh Property Test Results (Levy 2007) 237

Table C-3: Hardened Concrete Property Summary (Levy 2007) 237

Table C-4: Time of Events Summary (Levy 2007) 238

Table D-1: HPC Mix Proportions (Stallings et al. 2003).....239

Table E-1: STD-M-1 Strain Measurements.....240

Table E-2: STD-M-2 Strain Measurements.....241

Table E-3: SCC-MS-1 Strain Measurements.....242

Table E-4: SCC-MS-2 Strain Measurements....243
Table E-5: SCC-HS-1 Strain Measurements....244
Table E-6: SCC-HS-2 Strain Measurements....245
Table E-7: STD-M Strain without Temperature Effects....246
Table E-8: SCC-MS Strains without Temperature Effects....247
Table E-9: SCC-HS Strains without Temperature Effects....247
Table E-10: STD-M Top VWSG – Percent Error in Strain....248
Table E-11: STD-M Middle VWSG – Percent Error in Strain....249
Table E-12: STD-M Bottom VWSG – Percent Error in Strain....250
Table E-13: SCC-MS Top VWSG – Percent Error in Strain....251
Table E-14: SCC-MS Middle VWSG – Percent Error in Strain....252
Table E-15: SCC-MS Bottom VWSG – Percent Error in Strain....253
Table E-16: SCC-HS Top VWSG – Percent Error in Strain....254
Table E-17: SCC-HS Middle VWSG – Percent Error in Strain....255
Table E-18: SCC-HS Bottom VWSG – Percent Error in Strain....256
Table G-1: STD-M (AASHTO Type I) Percent Error in Camber....274
Table G-2: STD-M (AASHTO Type I) Percent Error in Camber Growth....275
Table G-3: SCC-MS (AASHTO Type I) Percent Error in Camber....276
Table G-4: SCC-MS (AASHTO Type I) Percent Error in Camber Growth....277
Table G-5: SCC-HS (AASHTO Type I) Percent Error in Camber....278
Table G-6: SCC-HS (AASHTO Type I) Percent Error in Camber Growth....279
Table G-7: STD-M-A & -B Percent Error in Camber....280
Table G-8: STD-M-A & -B Percent Error in Camber Growth....281

Table G-9: STD-M-C & -D Percent Error in Camber 282
Table G-10: STD-M-C & -D Percent Error in Camber Growth 283
Table G-11: SCC-MA-A & -B Percent Error in Camber 284
Table G-12: SCC-MA-A & -B Percent Error in Camber Growth 285
Table G-13: SCC-MA-C & -D Percent Error in Camber 286
Table G-14: SCC-MA-C & -D Percent Error in Camber Growth 287
Table G-15: SCC-MS-A & -B Percent Error in Camber 288
Table G-16: SCC-MS-A & -B Percent Error in Camber Growth 289
Table G-17: SCC-MS-C & -D Percent Error in Camber 290
Table G-18: SCC-MS-C & -D Percent Error in Camber Growth 291
Table G-19: SCC-HS-A & -B Percent Error in Camber 292
Table G-20: SCC-HS-A & -B Percent Error in Camber Growth 293
Table G-21: SCC-HS-C & -D Percent Error in Camber 294
Table G-22: SCC-HS-C & -D Percent Error in Camber Growth 295
Table H-1: Property and Event Summary 302
Table H-2: Prestressing Strand and Reinforcing Steel Summary 304
Table H-3: Reinforcing Steel Properties 306
Table H-4: Prestressing Steel Properties 306
Table H-5: AASHTO Girder Section Properties 307
Table H-6: AASHTO Girder Dimensions 307
Table H-7: Maximum Number of Strands in AASHTO Girders 308

LIST OF FIGURES

Figure 2-1: Prestressing Strand Stress vs. Time (Tadros et. al 2003) 9

Figure 2-2: Creep Factor k_c for Volume-to-Surface Ratio (AASHTO 2004) 21

Figure 2-3: Shrinkage Factor k_s for Volume-to-Surface Ratio (AASHTO 2004) 28

Figure 2-4: Experimental Shrinkage Results (Al-Omaishi et al. 2009) 34

Figure 2-5: Experimental Creep Results (Al-Omaishi et al. 2009) 34

Figure 3-1: Strain Variation across a Concrete Section (Collins and Mitchell 1997) 36

Figure 3-2: Relationship between Stresses and Strains (Collins and Mitchell 1997) 37

Figure 3-3: Time Function Plots for 2^{nd} Power 47

Figure 3-4: Time Function Plots for s = 0.2 48

Figure 3-5: STD-M-1 E_c Development with Time 52

Figure 3-6: Moment Area Method using Curvature Diagram 65

Figure 3-7: Test Case Strand Pattern - AASHTO Type I Girder 69

Figure 3-8: LG1 Stress vs. Number of Time Intervals 71

Figure 3-9: Bottom Fiber Stress vs. Number of Time Intervals 71

Figure 3-10: Midspan Curvature vs. Number of Time Intervals 72

Figure 3-11: Midspan Camber vs. Number of Time Intervals 72

Figure 3-12: Percent Difference in LG1 Stress at Midspan 73

Figure 3-13: Percent Difference in Bottom Fiber Stress at Midspan 74

Figure 3-14: Percent Difference in Midspan Curvature and Camber 74

Figure 3-15: Initial Midspan Camber vs. Number of Cross Sections 75
Figure 3-16: Midspan Camber at 28 Days vs. Number of Cross Sections 76
Figure 3-17: Midspan Camber at 365 Days vs. Number of Cross Sections 76
Figure 3-18: Percent Difference in Initial Midspan Camber 77
Figure 3-19: Percent Difference in 28-Day Midspan Camber 78
Figure 3-20: Percent Difference in 365-Day Midspan Camber 78
Figure 4-1: AASHTO Type I Girder Cross Section (Boehm 2008) 81
Figure 4-2: AASHTO Type I Girder Identification (Boehm 2008) 82
Figure 4-3: Placement of Curing Blankets (Boehm 2008) 83
Figure 4-4: Typical Cast-in-Place Deck Details (Boehm 2008) 84
Figure 4-5: Model 4200 Vibrating Wire Strain Gage (Geokon 2007) 85
Figure 4-6: Typical Vibrating Wire Strain Gage at Deck 87
Figure 4-7: CR10X Data Logger and Keyboard 87
Figure 4-8: T-Beam Cross Section (Levy 2007) 91
Figure 4-9: T-Beam Identification System (Levy 2007) 91
Figure 4-10: BT-54 Cross Section Details (Stallings et. al 2003) 94
Figure 4-11: Typical BT-54 Girder Elevation (Stallings et. al 2003) 95
Figure 5-1: Concrete Stresses associated with Temperature Effects 99
Figure 5-2: STD-M-1 VWSG Readings 100
Figure 5-3: STD-M-2 VWSG Readings 101
Figure 5-4: SCC-MS-1 VWSG Readings 101
Figure 5-5: SCC-MS-2 VWSG Readings 102
Figure 5-6: SCC-HS-1 VWSG Readings 102

Figure 5-7: SCC-HS-2 VWSG Readings.....103

Figure 5-8: STD-M-1 Predicted Strains at Top VWSG with Constant E_c.....105

Figure 5-9: STD-M-1 Predicted Strains at Top VWSG with Two-Point E_c.....106

Figure 5-10: STD-M-2 Predicted Strains at Top VWSG with Constant E_c.....106

Figure 5-11: STD-M-2 Predicted Strains at Top VWSG with Two-Point E_c.....107

Figure 5-12: STD-M-1 Predicted Strains at Middle VWSG with Constant E_c 107

Figure 5-13: STD-M-1 Predicted Strains at Middle VWSG with Two-Point E_c.....108

Figure 5-14: STD-M-2 Predicted Strains at Middle VWSG with Constant E_c 108

Figure 5-15: STD-M-2 Predicted Strains at Middle VWSG with Two-Point E_c.....109

Figure 5-16: STD-M-1 Predicted Strains at Bottom VWSG with Constant E_c 109

Figure 5-17: STD-M-1 Predicted Strains at Bottom VWSG with Two-Point E_c 110

Figure 5-18: STD-M-2 Predicted Strains at Bottom VWSG with Constant E_c 110

Figure 5-19: STD-M-2 Predicted Strains at Bottom VWSG with Two-Point E_c 111

Figure 5-20: SCC-MS-1 Predicted Strains at Top VWSG with Constant E_c 112

Figure 5-21: SCC-MS-1 Predicted Strains at Top VWSG with Two-Point E_c 113

Figure 5-22: SCC-MS-2 Predicted Strains at Top VWSG with Constant E_c 113

Figure 5-23: SCC-MS-2 Predicted Strains at Top VWSG with Two-Point E_c 114

Figure 5-24: SCC-MS-1 Predicted Strains at Middle VWSG with Constant E_c 114

Figure 5-25: SCC-MS-1 Predicted Strains at Middle VWSG with Two-Point E_c 115

Figure 5-26: SCC-MS-2 Predicted Strains at Middle VWSG with Constant E_c 115

Figure 5-27: SCC-MS-2 Predicted Strains at Middle VWSG with Two-Point E_c 116

Figure 5-28: SCC-MS-1 Predicted Strains at Bottom VWSG with Constant E_c.....116

Figure 5-29: SCC-MS-1 Predicted Strains at Bottom VWSG with Two-Point E_c.....117

Figure 5-30: SCC-MS-2 Predicted Strains at Bottom VWSG with Constant E_c 117

Figure 5-31: SCC-MS-2 Predicted Strains at Bottom VWSG with Two-Point E_c 118

Figure 5-32: SCC-HS-1 Predicted Strains at Top VWSG with Constant E_c 119

Figure 5-33: SCC-HS-1 Predicted Strains at Top VWSG with Two-Point E_c 120

Figure 5-34: SCC-HS-2 Predicted Strains at Top VWSG with Constant E_c 120

Figure 5-35: SCC-HS-2 Predicted Strains at Top VWSG with Two-Point E_c 121

Figure 5-36: SCC-HS-1 Predicted Strains at Middle VWSG with Constant E_c 121

Figure 5-37: SCC-HS-1 Predicted Strains at Middle VWSG with Two-Point E_c 122

Figure 5-38: SCC-HS-2 Predicted Strains at Middle VWSG with Constant E_c 122

Figure 5-39: SCC-HS-2 Predicted Strains at Middle VWSG with Two-Point E_c 123

Figure 5-40: SCC-HS-1 Predicted Strains at Bottom VWSG with Constant E_c 123

Figure 5-41: SCC-HS-1 Predicted Strains at Bottom VWSG with Two-Point E_c.....124

Figure 5-42: SCC-HS-2 Predicted Strains at Bottom VWSG with Constant E_c 124

Figure 5-43: SCC-HS-2 Predicted Strains at Bottom VWSG with Two-Point E_c.....125

Figure 5-44: STD-M-1 Predicted Strains at Top VWSG with AASHTO/ACI E_c.....126

Figure 5-45: STD-M-1 Predicted Strains at Top VWSG with CEB 90 E_c 127

Figure 5-46: STD-M-2 Predicted Strains at Top VWSG with AASHTO/ACI E_c.....127

Figure 5-47: STD-M-2 Predicted Strains at Top VWSG with CEB 90 E_c 128

Figure 5-48: STD-M-1 Predicted Strains at Middle VWSG with AASHTO/ACI E_c 128

Figure 5-49: STD-M-1 Predicted Strains at Middle VWSG with CEB 90 E_c 129

Figure 5-50: STD-M-2 Predicted Strains at Middle VWSG with AASHTO/ACI E_c 129

Figure 5-51: STD-M-2 Predicted Strains at Middle VWSG with CEB 90 E_c 130

Figure 5-52: STD-M-1 Predicted Strains at Bottom VWSG with AASHTO/ACI E_c 130

Figure 5-53: STD-M-1 Predicted Strains at Bottom VWSG with CEB 90 E_c 131

Figure 5-54: STD-M-2 Predicted Strains at Bottom VWSG with AASHTO/ACI E_c 131

Figure 5-55: STD-M-2 Predicted Strains at Bottom VWSG with CEB 90 E_c 132

Figure 5-56: SCC-MS-1 Predicted Strains at Top VWSG with AASHTO/ACI E_c 133

Figure 5-57: SCC-MS-1 Predicted Strains at Top VWSG with CEB 90 E_c.....134

Figure 5-58: SCC-MS-2 Predicted Strains at Top VWSG with AASHTO/ACI E_c 134

Figure 5-59: SCC-MS-2 Predicted Strains at Top VWSG with CEB 90 E_c.....135

Figure 5-60: SCC-MS-1 Predicted Strains at Middle VWSG with AASHTO/ACI E_c 135

Figure 5-61: SCC-MS-1 Predicted Strains at Middle VWSG with CEB 90 E_c.....136

Figure 5-62: SCC-MS-2 Predicted Strains at Middle VWSG with AASHTO/ACI E_c 136

Figure 5-63: SCC-MS-2 Predicted Strains at Middle VWSG with CEB 90 E_c.....137

Figure 5-64: SCC-MS-1 Predicted Strains at Bottom VWSG with AASHTO/ACI E_c.....137

Figure 5-65: SCC-MS-1 Predicted Strains at Bottom VWSG with CEB 90 E_c 138

Figure 5-66: SCC-MS-2 Predicted Strains at Bottom VWSG with AASHTO/ACI E_c.....138

Figure 5-67: SCC-MS-2 Predicted Strains at Bottom VWSG with CEB 90 E_c 139

Figure 5-68: SCC-HS-1 Predicted Strains at Top VWSG with AASHTO/ACI E_c.....140

Figure 5-69: SCC-HS-1 Predicted Strains at Top VWSG with CEB 90 E_c 141

Figure 5-70: SCC-HS-2 Predicted Strains at Top VWSG with AASHTO/ACI E_c.....141

Figure 5-71: SCC-HS-2 Predicted Strains at Top VWSG with CEB 90 E_c 142

Figure 5-72: SCC-HS-1 Predicted Strains at Middle VWSG with AASHTO/ACI E_c.....142

Figure 5-73: SCC-HS-1 Predicted Strains at Middle VWSG with CEB 90 E_c 143

Figure 5-74: SCC-HS-2 Predicted Strains at Middle VWSG with AASHTO/ACI E_c.....143

Figure 5-75: SCC-HS-2 Predicted Strains at Middle VWSG with CEB 90 E_c 144

Figure 5-76: SCC-HS-1 Predicted Strains at Bottom VWSG with AASHTO/ACI E_c 144

Figure 5-77: SCC-HS-1 Predicted Strains at Bottom VWSG with CEB 90 E_c.....145

Figure 5-78: SCC-HS-2 Predicted Strains at Bottom VWSG with AASHTO/ACI E_c 145

Figure 5-79: SCC-HS-2 Predicted Strains at Bottom VWSG with CEB 90 E_c.....146

Figure 5-80: Creep and Shrinkage Correction Factors – VB Program Output.....148

Figure 5-81: BT-54 Creep Coefficients (Stallings et al. 2003).....149

Figure 5-82: BT-54 Predicted Creep Coefficients.....150

Figure 5-83: BT-54 Predicted Strains at Top VWSG.....151

Figure 5-84: BT-54 Predicted Strains at Top VWSG – Early Age.....152

Figure 5-85: BT-54 Predicted Strains at Bottom VWSG 153

Figure 5-86: BT-54 Predicted Strains at Bottom VWSG – Early Age.....153

Figure 5-87: Predicted Strand Stresses in LG1 for STD-M Girders.....156

Figure 5-88: Predicted Strand Stresses in LG1 for SCC-MS Girders 156

Figure 5-89: Predicted Strand Stresses in LG1 for SCC-HS Girders 157

Figure 5-90: Temperature-Induced Curvature for STD-M Girders.....158

Figure 5-91: Temperature-Induced Curvature for SCC-MS Girders.....159

Figure 5-92: Temperature-Induced Curvature for SCC-HS Girders 159

Figure 5-93: STD-M-1 Predicted Camber with Constant E_c 161

Figure 5-94: STD-M-2 Predicted Camber with Constant E_c 162

Figure 5-95: SCC-MS-1 Predicted Camber with Constant E_c.....163

Figure 5-96: SCC-MS-2 Predicted Camber with Constant E_c.....163

Figure 5-97: SCC-HS-1 Predicted Camber with Constant E_c.....164

Figure 5-98: SCC-HS-2 Predicted Camber with Constant E_c.....164

Figure 5-99: STD-M-1 Predicted Camber with AASHTO/ACI E_c 166
Figure 5-100: STD-M-1 Predicted Camber with CEB 90 E_c.....166
Figure 5-101: STD-M-2 Predicted Camber with AASHTO/ACI E_c 167
Figure 5-102: STD-M-2 Predicted Camber with CEB 90 E_c.....167
Figure 5-103: SCC-MS-1 Predicted Camber with AASHTO/ACI E_c.....169
Figure 5-104: SCC-MS-1 Predicted Camber with CEB 90 E_c 169
Figure 5-105: SCC-MS-2 Predicted Camber with AASHTO/ACI E_c.....170
Figure 5-106: SCC-MS-2 Predicted Camber with CEB 90 E_c 170
Figure 5-107: SCC-HS-1 Predicted Camber with AASHTO/ACI E_c.....172
Figure 5-108: SCC-HS-1 Predicted Camber with CEB 90 E_c 172
Figure 5-109: SCC-HS-2 Predicted Camber with AASHTO/ACI E_c.....173
Figure 5-110: SCC-HS-2 Predicted Camber with CEB 90 E_c 173
Figure 5-111: STD-M-A, B Predicted Camber with Constant E_c.....176
Figure 5-112: STD-M-C, D Predicted Camber with Constant E_c.....176
Figure 5-113: SCC-MA-A, B Predicted Camber with Constant E_c.....177
Figure 5-114: SCC-MA-C, D Predicted Camber with Constant E_c.....178
Figure 5-115: SCC-MS-A, B Predicted Camber with Constant E_c 178
Figure 5-116: SCC-MS-C, D Predicted Camber with Constant E_c 179
Figure 5-117: SCC-HS-A, B Predicted Camber with Constant E_c 180
Figure 5-118: SCC-HS-C, D Predicted Camber with Constant E_c 180
Figure 5-119: STD-M-A, B Predicted Camber with AASHTO/ACI E_c.....181
Figure 5-120: STD-M-A, B Predicted Camber with CEB 90 E_c 182
Figure 5-121: STD-M-C, D Predicted Camber with AASHTO/ACI E_c.....182

Figure 5-122: STD-M-C, D Predicted Camber with CEB 90 E_c 183

Figure 5-123: SCC-MA-A, B Predicted Camber with AASHTO/ACI E_c.....184

Figure 5-124: SCC-MA-A, B Predicted Camber with CEB 90 E_c 184

Figure 5-125: SCC-MA-C, D Predicted Camber with AASHTO/ACI E_c.....185

Figure 5-126: SCC-MA-C, D Predicted Camber with CEB 90 E_c 185

Figure 5-127: SCC-MS-A, B Predicted Camber with AASHTO/ACI E_c 186

Figure 5-128: SCC-MS-A, B Predicted Camber with CEB 90 E_c.....186

Figure 5-129: SCC-MS-C, D Predicted Camber with AASHTO/ACI E_c 187

Figure 5-130: SCC-MS-C, D Predicted Camber with CEB 90 E_c.....187

Figure 5-131: SCC-HS-A, B Predicted Camber with AASHTO/ACI E_c 188

Figure 5-132: SCC-HS-A, B Predicted Camber with CEB 90 E_c 189

Figure 5-133: SCC-HS-C, D Predicted Camber with AASHTO/ACI E_c 189

Figure 5-134: SCC-HS-C, D Predicted Camber with CEB 90 E_c 190

Figure 5-135: BT-54 Predicted Camber 192

Figure 5-136: BT-54 Predicted Early-Age Camber.....192

Figure 6-1: BT-54 Predicted Strains at Top VWSG - Varying Cement Type.....197

Figure 6-2: BT-54 Predicted Strains at Bottom VWSG - Varying Cement Type 197

Figure 6-3: BT-54 Predicted Camber - Varying Cement Type 198

Figure 6-4: BT-54 Predicted Strains at Top VWSG - Varying Concrete Slump.....200

Figure 6-5: BT-54 Predicted Strains at Bottom VWSG - Varying Concrete Slump.....200

Figure 6-6: BT-54 Predicted Camber - Varying Concrete Slump 201

Figure 6-7: BT-54 Predicted Early Age Camber - Varying Concrete Slump.....202

Figure 6-8: SCC-MS-1 Predicted Strains at Top VWSG – Varying Cure Type 204

Figure 6-9: SCC-MS-1 Predicted Strains at Middle VWSG – Varying Cure Type 204
Figure 6-10: SCC-MS-1 Predicted Strains at Bottom VWSG – Varying Cure Type.....205
Figure 6-11: SCC-HS-1 Predicted Strains at Top VWSG – Varying Cure Type.....206
Figure 6-12: SCC-HS-1 Predicted Strains at Middle VWSG – Varying Cure Type.....206
Figure 6-13: SCC-HS-1 Predicted Strains at Bottom VWSG – Varying Cure Type 207
Figure 6-14: AASHTO Type I SCC Predicted Camber – Varying Cure Type 208
Figure 6-15: AASHTO Type I STD-M Predicted Camber – Maturity.....210
Figure 6-16: AASHTO Type I SCC-MS Predicted Camber – Maturity 210
Figure 6-17: AASHTO Type I SCC-HS Predicted Camber – Maturity 211
Figure B-1: Temperature Development Curves for STD-M-1 (Boehm 2008).....230
Figure B-2: Temperature Development Curves for SCC-MS-1 (Boehm 2008).....230
Figure B-3: Temperature Development Curves for SCC-MS-2 (Boehm 2008).....231
Figure B-4: Temperature Development Curves for SCC-HS-1 (Boehm 2008) 231
Figure B-5: Temperature Development Curves for SCC-HS-2 (Boehm 2008) 232
Figure B-6: VWSG Temperature Readings for STD-M Girders.....233
Figure B-7: VWSG Temperature Readings for SCC-MS Girders.....234
Figure B-8: VWSG Temperature Readings for SCC-HS Girders 235
Figure F-1: Measured Midspan Camber versus Time 257
Figure F-2: STD-M-1 Measured Camber 258
Figure F-3: STD-M-2 Measured Camber 258
Figure F-4: SCC-MS-1 Measured Camber.....259
Figure F-5: SCC-MS-2 Measured Camber.....259
Figure F-6: SCC-HS-1 Measured Camber.....260

Figure F-7: SCC-HS-2 Measured Camber....260
Figure F-8: STD-M Smoothed Camber....261
Figure F-9: SCC-MS Smoothed Camber....261
Figure F-10: SCC-HS Smoothed Camber....262
Figure F-11: STD-M-A & -B Smoothed Camber....262
Figure F-12: STD-M-C & -D Smoothed Camber....263
Figure F-13: SCC-MA-A & -B Smoothed Camber....263
Figure F-14: SCC-MA-C & -D Smoothed Camber....264
Figure F-15: SCC-MS-A & -B Smoothed Camber....264
Figure F-16: SCC-MS-A & -B Smoothed Camber....265
Figure F-17: SCC-HS-A, -B, -C & -D Smoothed Camber....265
Figure G-1: STD-M-1 Predicted Camber with Two-Point E_c....266
Figure G-2: STD-M-2 Predicted Camber with Two-Point E_c....267
Figure G-3: SCC-MS-1 Predicted Camber with Two-Point E_c....267
Figure G-4: SCC-MS-2 Predicted Camber with Two-Point E_c....268
Figure G-5: SCC-HS-1 Predicted Camber with Two-Point E_c....268
Figure G-6: SCC-HS-2 Predicted Camber with Two-Point E_c....269
Figure G-7: STD-M-A, B Predicted Camber with Two-Point E_c....269
Figure G-8: STD-M-C, D Predicted Camber with Two-Point E_c....270
Figure G-9: SCC-MA-A, B Predicted Camber with Two-Point E_c....271
Figure G-10: SCC-MA-C, D Predicted Camber with Two-Point E_c....271
Figure G-11: SCC-MS-A, B Predicted Camber with Two-Point E_c....272
Figure G-12: SCC-MS-C, D Predicted Camber with Two-Point E_c....272

Figure G-13: SCC-HS-A, B Predicted Camber with Two-Point E_c 273

Figure G-14: SCC-HS-C, D Predicted Camber with Two-Point E_c 273

Figure H-1: Visual Basic Program Flow Chart.....301

Figure I-1: Comparison of Percent Differences in Initial Midspan Camber 309

Figure I-2: Comparison of Percent Differences in 28-Day Midspan Camber 310

Figure I-3: Comparison of Percent Differences in 365-Day Midspan Camber 311

Figure I-4: Initial Midspan Camber vs. Number of Cross Sections (Straight) 312

Figure I-5: Midspan Camber at 28 Days vs. Number of Cross Sections (Straight).....312

Figure I-6: Midspan Camber at 365 Days vs. Number of Cross Sections (Straight).....313

Figure J-1: SCC-MS-2 Predicted Strains at Top VWSG – Varying Cure Type.....314

Figure J-2: SCC-MS-2 Predicted Strains at Middle VWSG – Varying Cure Type.....315

Figure J-3: SCC-MS-2 Predicted Strains at Bottom VWSG – Varying Cure Type 315

Figure J-4: SCC-HS-2 Predicted Strains at Top VWSG – Varying Cure Type 316

Figure J-5: SCC-HS-2 Predicted Strains at Middle VWSG – Varying Cure Type 316

Figure J-6: SCC-HS-2 Predicted Strains at Bottom VWSG – Varying Cure Type.....317

Figure K-1: Selection of Standard or User-Defined Cross Section 318

Figure K-2: Input of Cross-Sectional Properties 319

Figure K-3: Confirmation of Standard Cross-Sectional Properties 319

Figure K-4: Input of Concrete Properties 320

Figure K-5: Concrete Modulus of Elasticity Development 321

Figure K-6: Input of Prestressing Steel Properties 322

Figure K-7: Instructions for Prestressing Strand Input 323

Figure K-8: Input of Prestressing Steel Layout 324

Figure K-9: Input of Prestressing Steel Layout – Draped Strands.....325
Figure K-10: Input of Reinforcing Steel Properties and Layout.....325
Figure K-11: Input of Event Times, Curing, and Maturity Information.....326
Figure K-12: Selection and Input of Creep and Shrinkage Model Information.....327
Figure K-13: Display of ACI 209 Creep and Shrinkage Correction Factors.....328
Figure K-14: Display of AASHTO (+'05) Creep and Shrinkage Correction Factors.....328
Figure K-15: Input of Analysis Intervals.....329
Figure K-16: Output Summary Form – Initial Calculations.....330
Figure K-17: Initial Transformed Section Properties.....331
Figure K-18: Initial Prestress Losses and Stress Immediately after Transfer.....332
Figure K-19: Strains and Stresses Immediately after Release.....333
Figure K-20: Initial Curvatures and Midspan Camber.....334
Figure K-21: Output Summary Form – Time-Dependent Calculations.....335
Figure K-22: Transformed Section Properties.....336
Figure K-23: Incremental Relaxation Losses.....337
Figure K-24: Incremental Unrestrained Strains and Curvature.....338
Figure K-25: Incremental Curvature, Strains, and Stresses.....339
Figure K-26: Output Summary Form – Final Results.....340
Figure K-27: Total Strains and Stresses.....341
Figure K-28: Total Curvatures.....342
Figure K-29: Total Camber at Midspan.....343

CHAPTER ONE

INTRODUCTION

1.1 BACKGROUND

As the use of high-strength concrete and self-consolidating concrete (SCC) becomes more practical for prestressed bridge design, the accuracy of current prediction models used for camber calculations is questioned. Many of these models are based on outdated research and formulated using assumptions no longer valid in current prestressed bridge girder construction practice. Camber growth can affect several aspects of the design and construction phases and is therefore important to various parties involved in a typical prestressed bridge construction project.

Overestimating camber during the design phase may result in a bridge that ultimately sags under superimposed dead loads. Underestimating camber may adversely influence the design efficiency by causing extra tendons to be incorporated. Inaccuracy in camber prediction can also result in misalignment issues in the field, which further increase the cost of construction.

Camber can be defined as the net upward deflection along the length of the girder due to the eccentricity of the prestressing forces. Camber and camber growth depend on various factors such as concrete strength, modulus of elasticity, creep and shrinkage properties, curing conditions, maturity of concrete at prestress force release, initial strand stress, environmental conditions during storage, and the length of time in storage. Camber calculations can be based

on time-step procedures and material prediction models to account for these time-dependent factors. The time-step procedures and prediction models must be evaluated to determine if adjustments to the prediction models are necessary to increase the accuracy of camber calculations. An automated method incorporating these adjustments could greatly simplify the overall design process and provide accurate predictions of camber development over time. Ultimately, more efficient prestressed designs could be implemented or construction problems due to inaccurate camber prediction can be minimized.

1.2 RESEARCH OBJECTIVES AND WORK PLAN

The primary objective of this work is the development of an automated process for predicting camber and evaluating the practical accuracy of different material-behavior modeling assumptions during the design phase of prestressed bridge girders. Specific objectives are stated below:

1. Create a user-friendly interface that allows for a variety of design scenarios while providing typical design parameters when possible to minimize user-defined input.
2. Validate the prediction accuracy of the automated process by comparing results to experimental research.
3. Perform a sensitivity analysis to quantify the effects of certain design parameters on the overall process.
4. Identify any program limitations and recommend future modifications that can be implemented to better predict camber.

The following work plan was used to accomplish the objectives:

1. Develop incremental time-step relationships for cross-sectional behavior that satisfy strain compatibility and equilibrium for the various factors affecting prestress loss and camber.
2. Incorporate user-defined variables into prestress loss and camber calculations.
3. Compile a library of various creep, shrinkage, and concrete stiffness models allowing the user to choose how time-dependent variables are calculated.
4. Create a user-friendly program that automates time-dependent prestress loss and camber calculations for bridge girders up to deck placement.
5. Run the program using design parameters from experimental research and compare the calculated camber values to actual field measurements.
6. Perform a sensitivity analysis by running multiple design scenarios with slight variations in design parameters.

1.3 RESEARCH SCOPE

The work presented in this thesis incorporates data from previous research studies on the use of high-performance and self-consolidating concrete in AASHTO Type I bridge girders, AASHTO BT-54 bridge girders, and other prestressed flexural members. Previously unpublished strain and camber measurements from research studies described by Boehm (2008) and Levy (2007), as well as previously published results (Stallings et al. 2003), were used to evaluate the performance of the program. In addition, design material behavior models were incorporated into the computer program for evaluation—including those of the *AASHTO LRFD Bridge Design Specifications* the 2004 and earlier edition and the 2005 and later edition, ACI Committee Report

209, and CEB-FIP Model Code 1990. These codes provide models for predicting time-dependent material properties including the concrete modulus of elasticity (MOE), creep, and shrinkage.

1.4 ORGANIZATION OF THESIS

Chapter 2 of this thesis provides a detailed background on the camber associated with prestressed bridge girders as well as an overview of past and current prediction models. The chapter also includes a literature review of prestress losses, the effects of concrete creep and shrinkage, and other factors influencing camber. A summary of previous camber prediction studies is also provided.

Chapter 3 gives an overview of the computer program theory and presents derivations for the incremental time-step calculations and other equations used within the program. AASHTO LRFD, ACI 209R-92, CEB-FIP 90, and "Modified CEB" models are all addressed. A program flow chart outlines the user-defined input, internal calculations, and output. Results are described from a sensitivity analysis that was performed to determine the number of time intervals and cross sections to be used during the calculations.

Chapter 4 details the experimental research programs and data acquisition methods used for strain and camber measurements. Information from previous research used to analyze the time-step procedure is also given.

Chapter 5 describes an evaluation of the accuracy of the various material prediction models by comparing the program results to the measurements obtained from the experimental research described in Chapter 4. Comparing the experimental and theoretical values also provides a better understanding of the material models included in the program. A sensitivity

analysis in Chapter 6 provides a more in-depth evaluation of the program and the effect of design parameters on strain and camber results.

Chapter 7 summarizes the findings and conclusions of the work in this thesis. General observations on the accuracy of prediction models are listed. Recommendations for future work are also given.

1.5 NOTATION

The computer program developed for this thesis utilizes several symbols and variables for the user-defined input, internal calculations, and results. A list of the symbols and definitions can be found in Appendix A.

CHAPTER TWO

CAMBER IN PRETENSIONED MEMBERS

2.1 INTRODUCTION

The objective of this chapter is to discuss how prestress losses, concrete modulus of elasticity, compressive strength, creep, shrinkage, and other factors influence camber. A review of prediction models and previous studies highlights the need for an accurate means of predicting camber growth over time.

2.2 CAMBER

Initial camber is created when a prestress force is transferred at the time of release. Camber is the upward deflection in flexural members due to an eccentrically applied prestressing force. Simultaneously, the member's self-weight causes a downward deflection. The summation of the upward and downward deflection components yields the initial camber immediately after release.

Estimating long-term camber is not as straightforward as initial camber because of several factors affecting camber growth over time. The ACI Committee 435 report on deflection control in concrete structures states: "The word 'estimate' should be taken literally in that the properties of concrete which affect deflections (particularly long term deflections) are variable and not determinable with precision" (ACI 435 1995). Some of the time-dependent factors include prestress losses, concrete modulus of elasticity, concrete compressive strength, creep,

and shrinkage. A closer look at how each of these factors influences camber is provided in this chapter.

Stallings et.al (2003) implemented an incremental time-step analysis to predict strains, prestress losses, and camber in high-performance bridge girders. Results using standard creep and shrinkage parameters based on ACI 209R (1992) were compared to those based on measured high-performance concrete (HPC) parameters. When using the standard material parameters, the predicted camber values exceeded the measured values. Analysis using the HPC parameters provided better correlation between the predicted and measured cambers. Stallings et al. (2003) concluded that accurate material parameters are crucial for accurate camber and prestress loss predictions.

2.3 FACTORS INFLUENCING CAMBER

Camber in prestressed bridge girders can be divided into two parts: initial elastic camber and long-term camber that changes over time. The eccentricity of the prestress force and initial prestress losses affect the initial camber. However, long-term camber is affected by several interrelated time-dependent factors. Creep deformations tend to increase the camber over time. On the other hand, creep, shrinkage, and steel relaxation all reduce the effective prestress force in the strands over time. These prestress losses decrease the rate of camber growth and are therefore a vital component to understanding long-term camber.

Prestress losses can be divided into two categories as well: initial losses prior to release and long-term time-dependent losses. The initial prestress losses in pretensioned members are caused by relaxation of the prestressing steel between jacking and transfer and the initial elastic shortening of the concrete. Steel relaxation also affects the long-term prestress losses. Concrete

creep, shrinkage, and modulus of elasticity are other time-dependent factors affecting long-term prestress losses and ultimately camber. These factors are discussed in the following sections.

2.3.1 STEEL RELAXATION

Steel relaxation is the loss of prestress that occurs when prestressing strands are subjected to essentially constant strain over a period of time. Because of creep, the stress in the tendon decreases (or relaxes) with time to maintain the state of constant strain (Youakim et al. 2007). This decrease in stress is known as intrinsic relaxation and must be included with the decrease in stress due to creep and shrinkage of the concrete to evaluate the prestress losses and camber over time.

Steel relaxation is a function of the initial prestress, yield strength of the reinforcement, and duration of prestress loading. The type of prestressing reinforcement, either stress-relieved or low-relaxation strands, also affects the magnitude of steel relaxation. Equation 2-1 expresses steel relaxation as an incremental prestress loss for a given time interval using the equations provided by Nilson (1987).

$$\Delta f_{p,R} = f_{pi}\left[\frac{(\log t_2 - \log t_1)}{K_L}\right] \times \left[\left(\frac{fpi}{f_{py}}\right) - 0.55\right] \qquad \textit{Equation 2-1}$$

where, K_L = 10 (stress-relieved); 45 (low-relaxation),

f_{pi} = initial stress in prestressing reinforcement (beginning of interval),

f_{py} = yield strength of the prestressing reinforcement,

t_1 = time at the beginning of interval (relative to jacking), and

t_2 = time at the end of interval (relative to jacking).

To compute the initial prestress loss due to steel relaxation prior to release, f_{pi} is replaced with the jacking stress (f_{pj}). The time interval then becomes the time between prestress transfer and jacking (t_i).

$$\Delta f_{p,R} = f_{pj}\left[\frac{(\log t_i)}{K_L}\right] \times \left[\left(\frac{f_{pi}}{f_{py}}\right) - 0.55\right] \qquad \textit{Equation 2-2}$$

Figure 2-1 breaks down the components of prestress losses over time. This includes the initial steel relaxation that occurs between tensioning and transfer as well as relaxation over time.

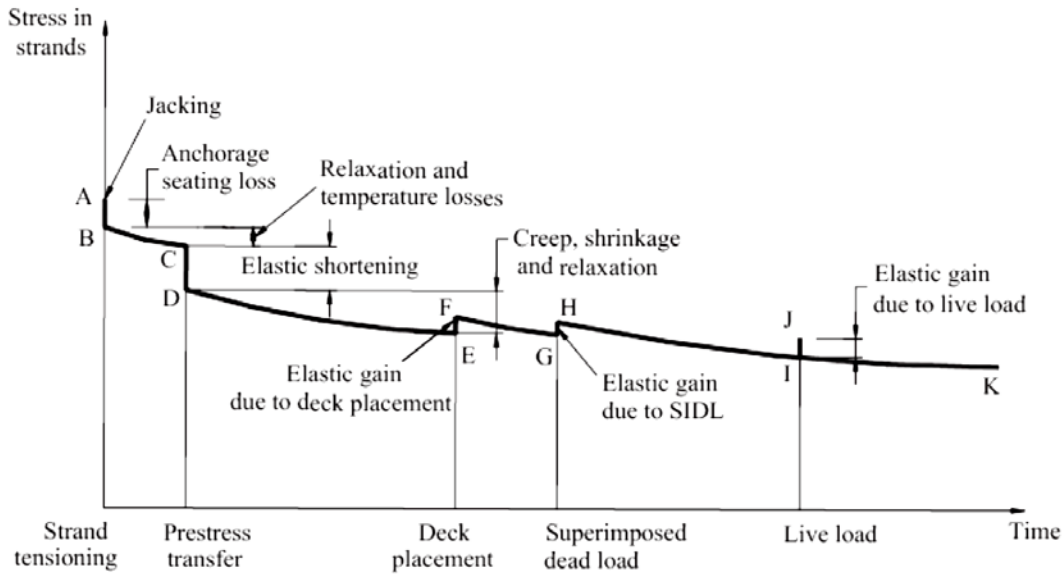

Figure 2-1: Prestressing Strand Stress vs. Time (Tadros et. al 2003)

2.3.2 ELASTIC SHORTENING OF CONCRETE

When a prestressing force is applied to a concrete member, the resulting axial compression causes the concrete element to shorten. The strands simultaneously shorten due to their bond with the surrounding concrete (ACI 435R-95). The changes in length create a strain in the concrete and prestressing strand. Assuming a perfect bond relationship, the change in concrete strain must equal the strain change in the prestressing strand. Therefore, the prestress loss due to elastic shortening of the concrete ($\Delta f_{p,ES}$) can be calculated using the incremental concrete strain and modulus of elasticity of the prestressing strand, as shown in Equation 2-3.

$$\Delta f_{p,ES} = E_p \left[\Delta \varepsilon_{cen} + \Delta \phi y\right] \qquad \textit{Equation 2-3}$$

where, $\Delta \varepsilon_{cen} = \frac{-N_o}{E_{ci} A_{tr,initial}}$

= change in strain at the centroid of the cross section

$N_o = \sum E_p \varepsilon_{p,initial} A_{ps}$ = axial load on cross section due to prestress transfer

$\varepsilon_{p,initial} = \frac{f_{pbt}}{E_p} = \frac{f_{pj} + \Delta f_{p,R}}{E_p}$

= strain in prestressing steel immediately before transfer

$\Delta \phi = \frac{M_G - M_o}{E_{ci} I_{tr,initial}}$ = change in cross-sectional curvature

$M_o = \sum N_o y_{p,cen}$ = moment on cross section due to prestress transfer

E_p = modulus of elasticity of prestressing steel

M_G = moment due to self-weight

y = distance from centroid to the point being considered (positive downward)

As stated in the ACI Committee 423 (2011) report on estimating prestress losses, accurately estimating the elastic shortening is important for two reasons:

- Design codes limit the concrete and prestressing steel stresses immediately after transfer effectively constraining the member size, prestress amount, and concrete strength at transfer.
- Both instantaneous and (time-dependent) creep responses are strongly dependent on the stresses at transfer. Inaccurate elastic shortening estimations can magnify errors in predicted camber and long-term prestress losses.

2.3.3 Concrete Compressive Strength

Kelly, Breen, and Bradberry (1987) found that beams made of lower strength concrete exhibited the greatest camber during erection, the greatest time-dependent creep and shrinkage effects, and the least final camber at the end of service life. Beams made of high-strength concrete exhibited opposite trends for the same prestress force.

2.3.4 Concrete Modulus of Elasticity

In general, the concrete modulus of elasticity (MOE) is proportional to the square root of the compressive strength. This is evident based on the equations used by AASHTO LRFD, ACI 209R (1992), and CEB (1990) prediction methods covered in the following sections. These

strength-based relationships are also dependent on the other factors such as cement and aggregate type, curing methods, and unit weight of concrete.

2.3.4.1 AASHTO LRFD PRE-2005 AND POST-2005

With pre-2005 AASHTO LRFD formulas not providing reliable estimates for long-term HPC material properties, NCHRP Research Project 18-07 implemented an experimental program to extend the pre-2005 AASHTO LRFD prediction formulas to concrete strengths up to 15 ksi. The paper by Al-Omaishi et al. (2009) summarizes the experimental results for concrete MOE, creep, and shrinkage. The concrete MOE values were compared to those calculated by pre-2005 AASHTO LRFD and the ACI Committee 363 Report (1992). According to pre-2005 AASHTO LRFD Specifications:

$$E_c = 33{,}000 w_c^{1.5} \left(f'_c\right)^{1/2} \qquad \textbf{\textit{Equation 2-4}}$$

where, E_c = modulus of elasticity of concrete (ksi)

w_c = unit weight of concrete (kcf)

f'_c = compressive strength of concrete (ksi)

As stated in the ACI Committee 363 Report, Equation 2-4 may overestimate the MOE for compressive strengths over 6 ksi. The following equation is recommended by ACI 363 (1992) to estimate the concrete MOE.

$$E_c = \left(\frac{w_c}{0.145}\right)^{1.5} \left[1000 + 1265\left(f'_c\right)^{1/2}\right] \qquad \textbf{\textit{Equation 2-5}}$$

As shown in Equations 2-4 and 2-5, the pre-2005 AASHTO LRFD and ACI 363 prediction models are not dependent on the aggregate type. Research by Iravani (1996) and

Myers and Carrasquillo (1999) found a direct correlation between the type of aggregate and measured concrete MOE. For the same compressive strength and unit weight, a relatively stiff course aggregate produced a significantly higher MOE. Shams and Kahn (2000) also concluded that the measured concrete MOE was greatly affected by the aggregate type. Table 2-1 provides the coarse aggregate coefficient, C_{ca}, for various aggregate types as recommended by Iravani (1996). The coarse aggregate coefficient is applied directly to the relationship between the concrete compressive strength and MOE, similar to the correction factor (K_1) in Equation 2-6.

Table 2-1: Coarse Aggregate Coefficients (Iravani 1996)

Cca	Coarse Aggregate Type
0.71	Sandstone Gravel
0.76	Siliceous Gravel
0.92	Limestone
0.92	Dolomite
0.97	Quartzite
0.82	Granite
0.97	Trap Rock
0.90	Diabase
0.61	Sandstone

The research for NCHRP Project 18-07 included the aggregate types and sources in its experimental program. The results led to a proposed elastic modulus prediction method that includes an aggregate stiffness factor K_1. The proposed formula, shown in Equation 2-6, provided improved results for high strength concrete with unusually stiff or soft aggregates.

$$E_c = 33{,}000 K_1 w_c^{1.5} \left(f'_c\right)^{1/2} \qquad \textit{Equation 2-6}$$

where, K_1 = correction factor for source of aggregate to be taken as 1.0

unless determined by physical test, and as approved by the authority of jurisdiction

w_c = unit weight of concrete (kcf)

The proposed formula shown in Equation 2-6 was adopted by the AASHTO Bridge Design Specifications, Interims 2005 and 2006, as well as the Fourth Edition in 2007. Unlike pre-2005 AASHTO LRFD concrete MOE prediction methods, the AASHTO LRFD 2005+ method accounts for the effect of aggregate type.

The AASHTO LRFD prediction methods for concrete MOE are dependent on the compressive strength. AASHTO LRFD uses ACI 209R-92 provisions for the concrete strength development. The ACI 209 provisions for estimating compressive strength and modulus of elasticity growth over time are reviewed in the following section.

2.3.4.2 ACI 209

ACI 209R-92 considers the following equation satisfactory for computing the modulus of elasticity values versus time. The equation was developed by Pauw (1960) and adopted by ACI 318.

$$E_c = g_{ct}\left[w^3\left(f'_c\right)_t\right]^{1/2} \qquad \textit{Equation 2-7}$$

where, w = unit weight of concrete (pcf)

$\left(f'_c\right)_t$ = compressive strength of concrete at a certain time, t (psi)

g_{ct} = 33

The ACI 209R-92 equation for calculating compressive strength versus time is shown in Equation 2-8. The constants α and β are functions of cement type and curing method. Table 2-2 summarizes of the recommended values determined by Branson and Christiason (1971).

$$\left(f'_c\right)_t = \left[\frac{t}{(\alpha+\beta t)}\right] \times \left(f'_c\right)_{28} \qquad \textit{Equation 2-8}$$

where, $\left(f'_c\right)_{28}$ = 28-day specified concrete compressive strength

t = age of concrete (days)

Table 2-2: Values of Constants for Strength Development

Curing Type	Cement Type	α	β
Moist	I	4.0	0.85
Moist	III	2.3	0.92
Steam	I	1.0	0.95
Steam	III	0.7	0.98

The constants for predicting strength growth over time are not applicable for concrete containing Type II or Type V cements or containing blends of portland cement and pozzolanic materials. The strength development for these concretes are slower and may continue well beyond one year (ACI 209 1992).

ACI 209R-92 recommendations use the terms “moist” and “steam” to describe the types of curing methods. Moist curing refers to non-accelerated curing, meaning there is no additional temperature increase beyond the normal ambient effects. Steam curing refers to accelerated curing, meaning the curing temperature is elevated beyond normal ambient effects.

Because AASHTO LRFD uses the ACI 209R-92 provisions for strength development, the MOE calculations for the two methods can yield the same result for a given concrete unit

weight. However, this is only valid if the aggregate stiffness constant K_1 specified in the AASHTO LRFD provisions is taken as 1.0.

The ASHTO LRFD and ACI 209R-92 concrete MOE models use the specified compressive strength (f'_c) of concrete which is less than the mean strength (f'_{cr}) at 28 days. While the understrength is preferred for safety-related design calculations, the discrepancy between design strength and mean strength can create an inherent underestimation in the concrete MOE prediction models, which can result in significant inaccuracy in serviceability-related predictions. As expected, Huo, Al-Omaishi, and Tadros (2001) found ACI 209 underestimated measured MOE values.

2.3.4.3 CEB 90

The European code CEB-FIP Model Code 1990 (CEB 90) provides prediction methods for the development of concrete compressive strength and MOE over time. Unlike the AASHTO LRFD and ACI 209R-92 provisions, the CEB 90 calculates the MOE based on the mean compressive strength at 28 days. As shown in Equation 2-9, the mean compressive strength f_{cm} can be estimated using the characteristic compressive strength.

$$f_{cm} = f_{ck} + \Delta f \qquad \textit{Equation 2-9}$$

where, f_{ck} = characteristic compressive strength (MPa)

Δf = 8 MPa

CEB 90 defines the characteristic compressive strength as the "strength below which 5 percent of all possible strength measurements for the specified concrete may be expected to fall." Table 2-3 shows the characteristic strength (f_{ck}) values for various concrete grades.

Table 2-3: Characteristic Strength f_{ck} Values (MPa)

Concrete Grade	C12	C20	C30	C40	C50	C60	C70	C80
f_{ck} - cylinder	12	20	30	40	50	60	70	80
f_{ck} - cube	15	25	37	50	60	70	80	90

The concrete MOE at 28 days can be estimated using the mean compressive strength at 28 days. CEB 90 specifies the following equation be used when estimating the MOE for normal weight concrete made of quartzitic aggregates.

$$E_{ci} = E_{co}\left[\frac{f_{cm}}{f_{cmo}}\right]^{1/3} \qquad \textit{Equation 2-10}$$

where, E_{ci} = modulus of elasticity at a concrete age of 28 days (MPa)

E_{co} = 2.15 x 10^4 MPa

f_{cmo} = 10 MPa

To account for the effect of aggregate types on the modulus of elasticity, CEB 90 provides the coefficients listed in Table 2-4 for various aggregates. The modulus of elasticity calculated in Equation 2-10 is multiplied by the corresponding coefficient to determine the MOE for concrete made of basalt, dense limestone, limestone or sandstone. Based on the coefficient variance for limestone aggregate, an average of 1.0 can be used when specific aggregate properties are not known.

Table 2-4: Effect of Aggregate Type on Modulus of Elasticity (CEB-FIP 1990)

Aggregate Type	Coefficient
Basalt, dense limestone	1.2
Quartzitic aggregates	1.0
Limestone aggregates	0.9
Sandstone aggregates	0.7

2.3.5 CREEP

Creep is defined as "the time-dependent increase of strain in hardened concrete subjected to sustained stress" (ACI 209 1992). As stated by Collins and Mitchell (1991), it is "hard to estimate the amount of creep concrete will exhibit without tests determining the creep characteristics of the concrete." As shown in the following AASHTO LRFD, ACI 209, and CEB 90 creep models, the creep characteristics of concrete are affected by concrete composition, volume/surface ratio, curing conditions, age at loading, and duration of loading.

The creep associated with accelerated-cured concrete can be thirty to fifty percent lower than that associated with non-accelerated-cured concrete (Neville 1983). Using concrete mixtures with hard coarse aggregates can also reduce the amount of creep when compared to mixtures using soft coarse aggregates (Mokhtarzadeh and French 2000). Several studies also noted that concrete with higher compressive strength exhibits less creep than lower compressive strength concrete (Hinkle 2006).

2.3.5.1 AASHTO LRFD (2005 AND LATER)

The creep strain is determined by multiplying the creep coefficient to the compressive strain caused by permanent loads. The creep coefficient can be calculated as follows:

$$\psi(t, t_i) = 1.9 k_s k_{hc} k_f k_{td} t_i^{-0.118} \qquad \textit{Equation 2-11}$$

where, k_s = volume-to-surface ratio factor = $1.45 - 0.13\left(\frac{V}{S}\right) > 1.0$

k_{hc} = humidity factor for creep = $1.56 - 0.008H$

k_f = concrete strength factor = $\frac{5}{(1+f'_{ci})}$

k_{td} = time development factor = $\frac{t}{(61-4f'_{ci}+t)}$

H = relative humidity (%)

t = maturity of concrete (days); relative to time of loading for creep calculations

t_i = age of concrete at time of load application (day)

V/S = volume-to-surface ratio (in.)

f'_{ci} = specified compressive strength of concrete at time of prestressing (ksi)

The creep model is based on the method described in the NCHRP 496 report which uses accelerated-curing days for t_i. Therefore, when using non-accelerated-cured specimens, the

loading age must be divided by 7 days to determine the t_i specified in AASHTO LFRD (2005 and later).

The concrete maturity, t, associated with the time development factor is relative to the age at loading for creep calculations. Therefore, no correction for curing-type is required and t should be the actual days between time of loading and the time being considered for analysis.

2.3.5.2 AASHTO LRFD (2004 AND EARLIER)

The methods for determining creep used in AASHTO LRFD (2004 and earlier) are taken from Collins and Mitchell (1991). The computation for the creep coefficient is shown in Equation 2-12.

$$\psi(t,t_i) = 3.5k_c k_f \left(1.58 - \frac{H}{120}\right) t_i^{-0.118} \times \frac{(t-t_i)^{0.6}}{10.0+(t-t_i)^{0.6}} \qquad \textit{Equation 2-12}$$

where, k_f = concrete strength factor = $\frac{1}{0.67+\left(\frac{f'_c}{9}\right)}$

k_c = volume-to-surface ratio factor

H = relative humidity (%)

t = maturity of concrete (days); relative to time of loading for creep calculations

t_i = age of concrete when load is initially applied (days)

f'_c = specified compressive strength at 28 days (ksi)

The volume-to-surface ratio factor k_c can be estimated using Figure 2-2 or Equation 2-13. Both were developed based on a maximum volume-to-surface ratio of 6.0 inches (PCI 1977).

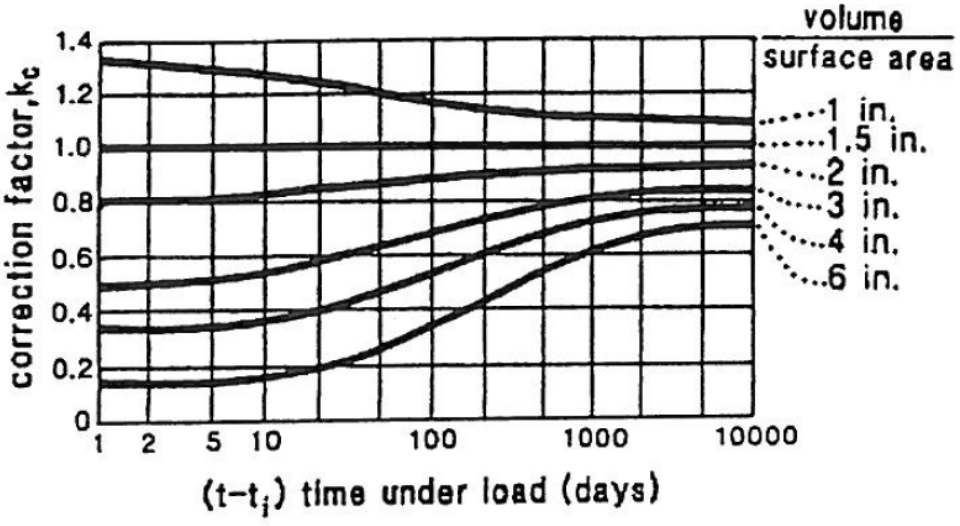

Figure 2-2: Creep Factor k_c for Volume-to-Surface Ratio (AASHTO 2004)

$$k_c = \left[\frac{t}{\{26\exp(0.36V/S)\}+t}\right] \times \left[\frac{1.80+\{1.77\exp(-0.54V/S)\}}{2.587}\right]$$

Equation 2-13

For creep calculations, the code does not explicitly state which type of curing is the basis for t_i. However, the statement "one day of accelerated curing by steam or radiant heat may be taken as equal to seven days of normal curing" implies that accelerated (steam) curing requires modification. Therefore, t_i is assumed to be based on the length of "normal" or non-accelerated curing. To compensate for accelerated curing, the accelerated-curing loading age is multiplied by 7 to get an equivalent number of non-accelerated curing days. Alternatively, Collins and

Mitchell (1991) refer to adding days to compensate for accelerated curing. For one day of accelerated curing, there is no difference to the loading age when adding 6 days or multiplying by 7. However, the difference significantly increases as the accelerated-curing period exceeds 24 hours. For accelerated-curing periods of 18 to 24 hours, the difference in the loading age factor is less than 3 percent.

Research by Townsend (2003) and Shams and Kahn (2000) found that the AASHTO LRFD prediction model generated creep strains closest to the experimentally measured creep values.

2.3.5.3 ACI 209

According to the ACI 209R-92 creep model, creep is a function of concrete composition, slump, V/S ratio, relative humidity, and age at loading, . The procedure is applicable to normal and lightweight concretes using Type I or III cement and moist or steam curing. As shown in Equation 2-14, correction factors must be applied to the ultimate creep coefficient for any condition other than "standard" conditions.

$$v_{ult} = 2.35 \times \left(\gamma_{la}\gamma_{\lambda}\gamma_{vs}\gamma_{\psi}\gamma_{s}\gamma_{a}\right) \qquad \textit{Equation 2-14}$$

where, γ_{la} = loading age correction factor

= $1.25(t_{la})^{-0.118}$ (for moist curing)

= $1.13(t_{la})^{-0.094}$ (for steam curing)

γ_{λ} = relative humidity correction factor = 1.27 – 0.0067RH

γ_{vs} = volume-to-surface ratio correction factor

$$= \frac{2}{3}[1 + 1.13exp(-0.54V/S)]$$

γ_{ψ} = fine aggregate correction factor = 0.88 + 0.0024ψ

γ_s = slump correction factor = 0.82 + 0.067 s

γ_a = air content correction factor = 0.46 + 0.09 α

t_{la} = loading age (days)

ψ = ratio of fine aggregate to total aggregate by weight (%)

s = slump (in.)

α = air content (%)

ACI 209R-92 does not address creep correction factors for moist-curing less than seven days and steam-curing less than one day. The creep model also assumes the relative humidity will never drop below 40 percent. If relative humidity is lower than 40 percent, the correction factor for creep will be higher than one. Similar to AASHTO LRFD, the ACI 209 model uses the volume-to-surface ratio to account for member size.

The creep coefficient v_t, shown in Equation 2-15, is determined by applying the creep age correction factor to the ultimate creep coefficient calculated in Equation 2-14. The creep age correction factor is the same for 7-day moist curing and 1-3 day steam curing.

$$v_t = \left[\frac{t^{0.60}}{10+t^{0.60}}\right] v_{ult} \qquad \textbf{\textit{Equation 2-15}}$$

where, t = time after loading (days)

v_{ult} = ultimate creep coefficient

Research by Mokhtarzadeh and French (2000) found that the ACI 209R-92 creep model was a good predictor of creep strain, while Stallings and Glover (2000) found the creep model to be very conservative. Hinkle (2006) also found a majority of studies that concluded that ACI 209 over-predicts the measured values of creep.

2.3.5.4 CEB 90

The creep coefficient at any given time is calculated by applying the notational creep coefficient to the development of creep with time. The notational creep coefficient is estimated by the following:

$$\phi_0 = \phi_{RH}[\beta(f_{cm})][\beta(t_0)] \qquad \textit{Equation 2-16}$$

where, $\phi_{RH} = 1 + \left[\frac{1-\left(\frac{RH}{100}\right)}{0.46\left(\frac{h}{100}\right)^{1/3}}\right]$

$$\beta(f_{cm}) = \frac{5.3}{\left(\frac{f_{cm}}{10\ MPa}\right)^{0.5}}$$

$$\beta(t_0) = \frac{1}{\left(0.1 + \frac{t_0}{1\ day}\right)^{0.2}}$$

RH = relative humidity (%)

h = notational size of member (mm) = $\frac{2A_c}{u}$

f_{cm} = mean compressive strength at 28 days (MPa) = f'_c + 6.5

t_0 = age of concrete at loading (days)

The development of creep with time is shown in Equation 2-17. The creep coefficient at any time after loading is calculated by multiplying the creep development factor by the notional creep coefficient (ϕ_0) as shown in Equation 2-18.

$$\beta_c(t-t_0) = \left[\frac{(t-t_0)/t_1}{\beta_H+(t-t_0)/t_1}\right]^{0.5} \qquad \textit{Equation 2-17}$$

$$\phi(t,t_0) = \phi_0\beta_c(t-t_0) \qquad \textit{Equation 2-18}$$

where, t = age of concrete (days)

t_1 = 1 day

$\beta_H = 150\left[1+\left(1.2\frac{RH}{RH_0}\right)^{18}\right]\frac{h}{h_0}+250 \leq 1500$

RH_0 = 100%

h_0 = 100 mm

CEB 90 takes into account the effect of temperature on the maturity of concrete. The age of concrete, *t*, can be replaced with the temperature-adjusted concrete age, t_T, calculated as follows:

$$t_T = \sum \Delta t_i exp\left\{13.65 - \frac{4000}{273+\{T(\Delta t_i)/T_0\}}\right\} \qquad \textit{Equation 2-19}$$

Chapter 3 shows how the above equation is used to adjust the age of concrete at loading based on the curing conditions specified by the program user. The effect of cement type on the creep coefficient by modifying the age at loading is also reviewed.

2.3.5.5 MODIFIED CEB 90

The modified CEB creep model is based on previous research by Kavanaugh (2008). The research, conducted at Auburn University, investigated the creep performance of conventional and SCC mixtures designed for use in prestressed concrete bridge girders. Non-accelerated curing formulas and accelerated-curing formulas were derived to modify specific creep parameters based on curing type. The modified CEB functions for the creep parameters are summarized in Table 2-5.

Table 2-5: Parameters used in the Modified CEB 90 Method (Kavanaugh 2008)

Parameter	Original Formulation	Non-Accelerated-Cured Formulation	Accelerated-Cured Formulation
$\beta(f_{cm})$	$\frac{5.3}{(f_{cm}/f_{cmo})^{0.5}}$	$\frac{5.3}{(f_{cm}/f_{cmo})^{0.5}}$	$\frac{4.65}{(f_{cm}/f_{cmo})^{0.5}}$
$\beta(t_0)$	$\frac{1}{0.1+(t_0/t_1)^{0.2}}$	$\frac{1}{0.26+(t_0/t_1)^{0.18}}$	$\frac{1}{0.26+(t_0/t_1)^{0.18}}$
$\beta(t-t_0)$	$\left[\frac{(t_0/t_1)/t_1}{\beta_H+(t_0/t_1)/t_1}\right]^{0.3}$	$\left[\frac{(t_0/t_1)/t_1}{\beta_H+(t_0/t_1)/t_1}\right]^{0.27}$	$\left[\frac{(t_0/t_1)/t_1}{\beta_H+(t_0/t_1)/t_1}\right]^{0.35}$

2.3.6 SHRINKAGE

Shrinkage is a property of concrete that occurs during the drying process as concrete cures. The four types of shrinkage include plastic shrinkage, autogenous shrinkage, drying shrinkage, and carbonation shrinkage. Shrinkage is affected by aggregate, w/c ratio, size of the concrete element, ambient conditions, amount of reinforcing, admixtures, and type of cement (Nawy 1989).

Paulson, Nilson, and Hover (1991) indicated that high-strength concrete tends to have 1/3 less drying shrinkage than normal strength concrete. In regards to relative humidity, research by

Shams and Kahn (2000) as well as Mangoba, Mayberry, and Saiidi (1999) found shrinkage decreased as relative humidity increased.

2.3.6.1 AASHTO LRFD (2005 AND LATER)

As shown in Equation 2-20, many of the factors used to calculate the creep coefficient (see Equation 2-11) are also used to calculate the strain due to shrinkage. The relative humidity factor, however, is different for creep and shrinkage.

$$\varepsilon_{sh} = k_s k_{hs} k_f k_{td} 0.48 \times 10^{-3} \qquad \textit{Equation 2-20}$$

where, k_{hs} = humidity factor for shrinkage = 2.00 – 0.014 H

H = relative humidity (%)

In addition to the shrinkage factors above, a 20 percent increase in shrinkage is specified for concrete "exposed to drying before 5 days of curing have elapsed." The AASHTO LRFD 2005 code does not clarify if these are non-accelerated-cured days or accelerated-cured days. However, this percent increase is stated in the 2004 code, and earlier versions, so the curing period can be assumed to mean five days of non-accelerated curing. For accelerated curing, the critical curing period is adjusted by dividing the "normal" five-day period by a factor of seven. Therefore, for accelerated-curing periods less than 5/7 day (17 hours), the shrinkage is increased by 20 percent.

2.3.6.2 AASHTO LRFD (2004 AND EARLIER)

$$\varepsilon_{sh} = -k_s k_h \left[\frac{t}{35+t}\right] 0.51 \times 10^{-3} \qquad \textit{Equation 2-21}$$

where, k_s = size factor

k_h = humidity factor = $140 - H/70$ (for H< 80%)

= $3(100 - H)/70$ (for H >= 80%)

t = drying time; relative to the end of curing (days)

H = relative humidity (%)

The size factor k_s can be estimated using Figure 2-3 or Equation 2-22. Similar to the volume-to-surface ratio factor for creep, the shrinkage factor was developed based on a maximum V/S of 6.0 inches (PCI 1977).

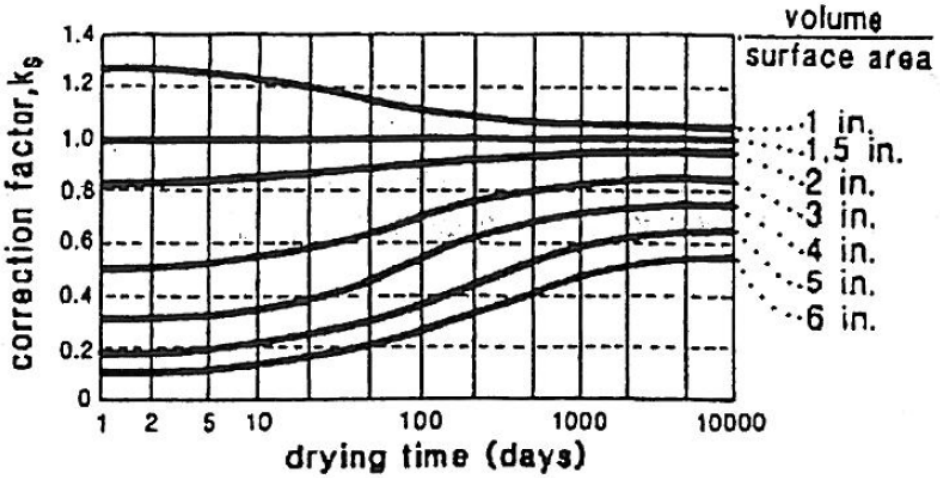

Figure 2-3: Shrinkage Factor k_s for Volume-to-Surface Ratio (AASHTO 2004)

$$k_s = \left[\frac{t}{\frac{\{26\exp(0.36V/S)\} + t}{45 + t}}\right] \times \left[\frac{1064 - 94\,(V/S)}{923}\right]$$

Equation 2-22

AASHTO LRFD (2004 and earlier) also includes a shrinkage correction factor based on the duration of curing. For "concrete exposed to drying before five days of curing," shrinkage should be increased by 20 percent. It is assumed the five days are for non-accelerated curing.

2.3.6.3 ACI 209

According to ACI 209R-92, the total shrinkage strain is dependent on the ultimate shrinkage strain and the shrinkage rate. Similar to the ultimate creep coefficient calculation, correction factors must be applied to the ultimate shrinkage strain to account for non-standard conditions.

$$\varepsilon_{sh,ult} = \left(\gamma_\lambda \gamma_{vs} \gamma_\psi \gamma_s \gamma_c \gamma_a \gamma_{cp}\right) 780 \times 10^{-6} \qquad \textit{Equation 2-23}$$

where, γ_λ = humidity correction factor

$$= min \begin{cases} 1.4 - 0.01RH \\ 3.0 - 0.03RH \end{cases}$$

γ_{vs} = V/S ratio correction factor = $1.2\exp(-0.12\frac{V}{S})$

γ_ψ = fine aggregate percentage correction factor

$$= min \begin{cases} 0.3 + 0.014FA \\ 0.9 + 0.002FA \end{cases}$$

γ_s = slump correction factor = $0.89 + 0.041s$

γ_c = cement content correction factor = $0.75 + 0.00036c$

γ_a = air content correction factor = $0.95 + 0.008a$

c = cement content (lbs/yd^3)

ACI 209R-92 also provides a shrinkage correction factor for "concrete moist cured during a period other than seven days." Based on the tabulated values given in ACI's Table 2.5.3 for ages 1 to 90 days, Equation 2-24 expresses the shrinkage correction factor for curing period in terms of the duration of moist (non-accelerated) curing (t). For a moist-cured period of seven days, γ_{cp} = 1.0. The code does not mention correction factors for steam (accelerated) curing periods other than 1-3 days.

$$\gamma_{cp} = -0.1015 \ln(t) + 1.202 \qquad \textbf{\textit{Equation 2-24}}$$

To determine the shrinkage at any time, the ultimate shrinkage strain is applied to a specific shrinkage rate dependent on the curing method. After 7 days of moist (non-accelerated) curing, the development of shrinkage over time can be determined by:

$$\varepsilon_{sh}(t) = \left[\frac{t}{35+t}\right] \varepsilon_{sh,ult} \qquad \textbf{\textit{Equation 2-25}}$$

After 1-3 days of steam (accelerated) curing, the development of shrinkage over time becomes:

$$\varepsilon_{sh}(t) = \left[\frac{t}{55+t}\right] \varepsilon_{sh,ult} \qquad \textbf{\textit{Equation 2-26}}$$

where, t = time after the end of the initial wet curing (days)

2.3.6.4 CEB 90

Similar to ACI 209R-92, the total shrinkage strain at any given time is dependent on the notional shrinkage coefficient and the development of shrinkage with time, or shrinkage rate. The notional shrinkage coefficient is calculated as follows:

$$\varepsilon_{cso}(t) = \varepsilon_s(f_{cm})\beta_{RH} \qquad \textbf{\textit{Equation 2-27}}$$

where, $\varepsilon_s(f_{cm}) = \left[160 + 10\beta_{sc}\left(9 - \frac{f_{cm}}{10\ MPa}\right)\right] \times 10^{-6}$

β_{RH} = -1.55β_{SRH} (for 40% ≤ RH < 99%)

= 0.25 (for RH ≥ 99%)

$\beta_{SRH} = 1 - \left(\frac{RH}{100}\right)^3$

β_{SC} = 4 (for slowly hardening cements SL)

= 5 (for normal or rapid hardening cements N and R)

= 8 (for rapid hardening high strength cements RS)

When applying the shrinkage rate shown in Equation 2-28 to the notional shrinkage coefficient, the shrinkage strain for any time after initial curing is determined by Equation 2-29.

$$\beta_S(t - t_s) = \left[\frac{(t-t_s)}{350\left(\frac{h}{100\,mm}\right)^2 + (t-t_s)}\right]^{0.5} \qquad \textit{Equation 2-28}$$

$$\varepsilon_{cs}(t, t_s) = \varepsilon_{cso}\beta_s(t - t_s) \qquad \textit{Equation 2-29}$$

where, t = age of concrete (days)

t_s = age of concrete at the beginning of shrinkage (days)

h = notational size of member = $2A_c/u$

2.4 PREVIOUS STUDIES

This section reviews relevant findings from previous research on the time-dependent behavior of high-strength concrete. Hinkle (2006) investigated camber in high strength prestressed bridge

girders. Research by Al-Omaishi, Tadros, and Seguirant (2009) focused on the elastic modulus, shrinkage, and creep of high strength concrete bridge girders.

2.4.1 HINKLE (2006)

Hinkle implemented an experimental program consisting of 27 AASHTO bulb tees. The girders were 79 inches deep with lengths ranging from 127'-4" to 137'-3". The normal weight, high-strength mixtures had a specified 28-day design strength of 9000 psi and release strength of 6100 psi. The prestressing steel consisted of 0.6" diameter, Grade 270, low relaxation, seven-wire strands. The strands were prestressed to 75 percent of the ultimate tensile strength; approximately 44 kips per strand. The beams were moist cured for 18 hours to one day. Camber measurements were taken at weekly intervals for three to four weeks and then decreased to monthly intervals. The measurements were taken early in the morning to avoid temperature effects on the short-term camber growth.

Hinkle used a multiplier method and an incremental time step method to predict camber. The incremental time step calculations were based on the time step method presented in Nilson (1987). The deflection at each time step was then calculated according to the Moment Area Method. The camber predictions for both methods were compared to the experimental measurements. Camber predictions from the beam design software, CONSPAN, were also included in the analysis.

Findings from Hinkle's research concluded that the predictions using the CONSPAN design software and multiplier methods drastically overestimated camber. The software program over-predicted the measured camber by an average of 58 percent. The multiplier methods only over-predicted camber by an average of 21 percent and could therefore be used as a "rough

estimate" during the design phase. Hinkle recommended the Modified PCI Multiplier developed by Tadros (1985) be used over the original PCI Multiplier Method developed by Martin (1977).

Hinkle found the best camber predictions were calculated using the incremental time step method. The Shams and Kahn (2000) compressive strength equation best predicted the compressive strength measured during cylinder testing. In general, the Shams and Kahn model for creep, shrinkage, and modulus of elasticity resulted in the most accurate camber predictions when using the incremental time step method.

2.4.2 AL-OMAISHI, TADROS, AND SEGUIRANT (2009)

The study by Al-Omaishi et al. (2009) included research from the National Cooperative Highway Research Program (NCHRP) research project no. 18-07. Al-Omaishi et al. used the experimental results to validate the prediction formulas in pre-2005 AASHTO LRFD specifications and the ACI 209 committee report. Based on research findings, proposed methods were introduced to better predict modulus of elasticity, creep, and shrinkage of high strength concrete.

The concrete mixtures included in the experimental program ranged from 8 ksi to 12 ksi. DEMEC gauges were used to measure the shrinkage and creep strains. The initial strain readings were taken immediately before and after prestress transfer. Shrinkage readings and creep measurements were taken daily for the first week, weekly for the first month, and monthly for about a year. Figures 2-4 and 2-5 show the experimental creep and shrinkage results presented by Al-Omaishi et al. (2009).

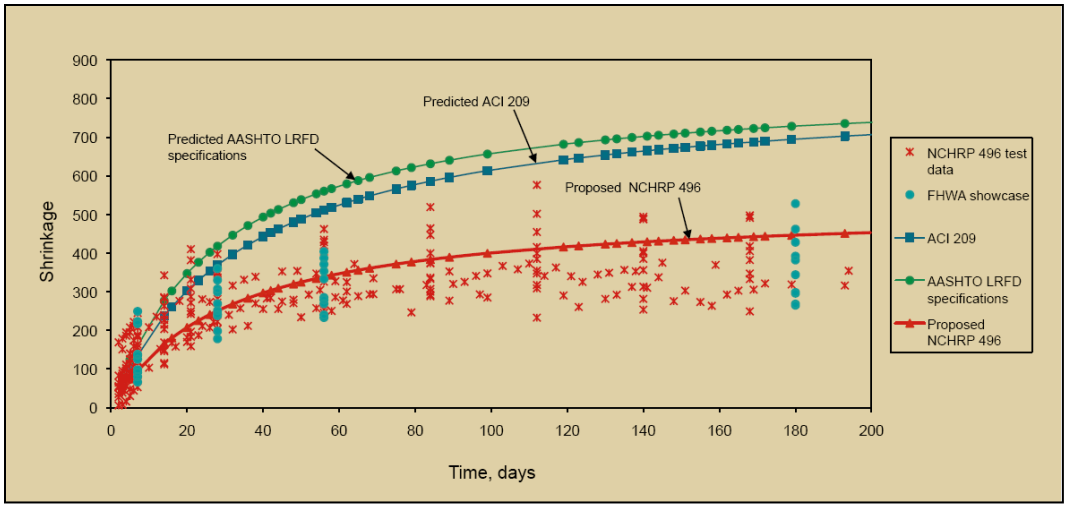

Figure 2-4: Experimental Shrinkage Results (Al-Omaishi et al. 2009)

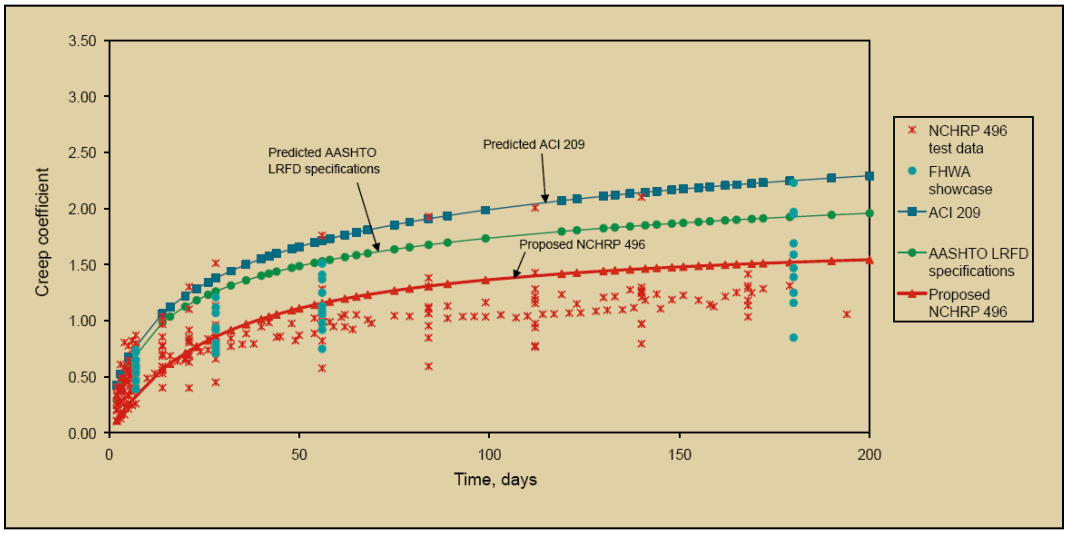

Figure 2-5: Experimental Creep Results (Al-Omaishi et al. 2009)

Al-Omaishi et al. (2009) concluded that the pre-2005 AASHTO and ACI 209 prediction formulas do not provide reliable estimates of the long-term behavior of high strength concrete. Research by Stallings et al. (2003) verified the need for more accurate prediction methods when using high strength concrete. The proposed methods presented by Al-Omaishi et al. were adopted into the 2005 and 2006 interim provisions of the AASHTO LRFD specifications.

CHAPTER THREE

COMPUTER PROGRAM DEVELOPMENT

3.1 ANALYTICAL APPROACH

This section reviews the analytical approach used for the Visual Basic (VB) program numerical time-step analysis procedure. It includes a methodology based on basic mechanics principles and summarizes the derivation process for the equations used.

3.1.1 METHODOLOGY

The numerical methods used throughout the derivation process implement a time-step procedure based on compatibility, linear elastic stress-strain behavior, and equilibrium. Instantaneous deformations are computed similarly to the linear-elastic, uncracked response procedure from Collins and Mitchell (1997)—using transformed section properties to accurately incorporate the restraining effects of reinforcement without repeated iterations. Instantaneous computations are performed for each time step, and the cross-section deformations and stresses are updated based on the results. Analysis then proceeds for the next step using the updated time-dependent material properties and deformations. This section describes the fundamental relationships that were derived from mechanics principles and then used in the computations.

Assuming that plane sections remain plane, the strain at any location is equal to the centroidal strain at that cross section plus the cross-sectional curvature times the distance from that location to the centroid of the section when the section is transformed to reflect the relative stiffness of the constituent materials (concrete and steel). Thus, the strain calculations used in the program are based on the centroid of the transformed section. Based on the strain variation shown in Figure 3-1, the basic equations for strain in the concrete, reinforcing steel, and prestressing steel are given in Equations 3-1, 3-2, and 3-3, respectively.

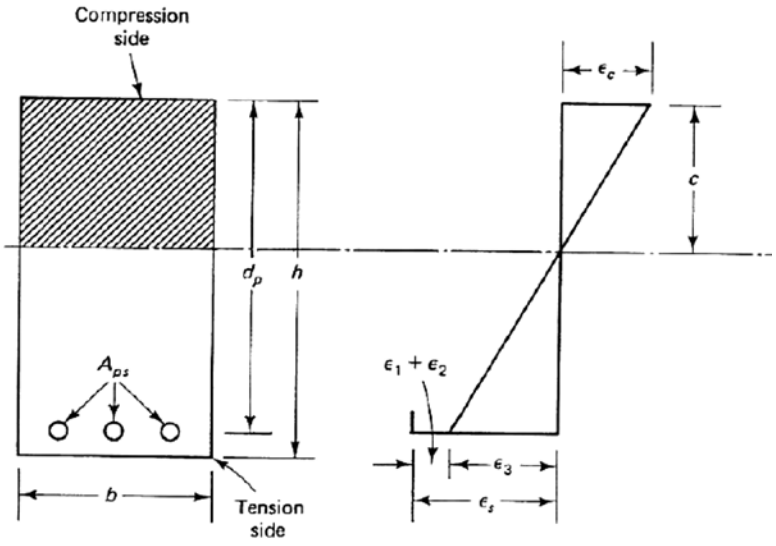

Figure 3-1: Strain Variation across a Concrete Section (Collins and Mitchell 1997)

$$\varepsilon_c = \varepsilon_{cen} + \phi y \qquad \textit{Equation 3-1}$$

$$\varepsilon_s = \varepsilon_{cen} + \phi y_s \qquad \textit{Equation 3-2}$$

$$\varepsilon_p = \varepsilon_{cen} + \phi y_p + \Delta\varepsilon_p \qquad \textit{Equation 3-3}$$

where, ε_c = stain in concrete (in./in.)

ε_s = strain in reinforcing steel (in./in.)

ε_p = strain in prestressing steel (in./in.)

$\Delta\varepsilon_p$ = initial difference in prestressing steel strain and strain in adjacent concrete (in./in.)

ε_{cen} = strain at centroid of the transformed section (in./in.)

ϕ = curvature; slope of strain profile

y = distance from centroid of the transformed section, where positive y is downward (in.)

In addition to the strains caused by stress, thermal and shrinkage strains must also be taken into account. Figure 3-2 shows how the thermal and shrinkage strains, which have no stress associated with them when unrestrained, are included with the linear relationship of the stress-induced strains.

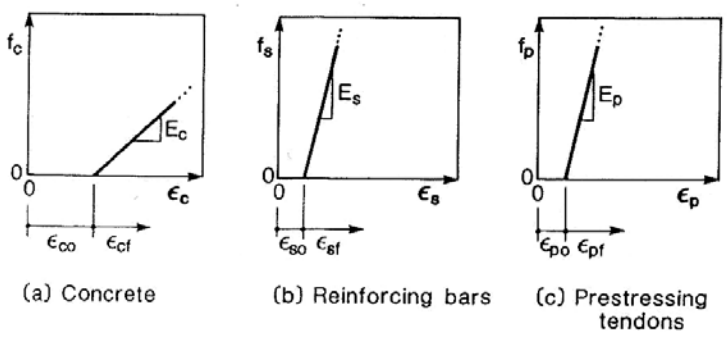

Figure 3-2: Relationship between Stresses and Strains (Collins and Mitchell 1997)

As shown above, the total strain for each cross-sectional component is the sum of the stress-independent strain and stress-dependent strain.

where, ε_{co} = shrinkage strain plus thermal strain in the concrete

ε_{cso} = thermal strain in the reinforcing steel

ε_{po} = thermal strain in the prestressing steel

The final principle used during the derivation process is equilibrium. As shown in Equation 3-4, integrating the stress over the cross-sectional area must equal the applied axial load, N.

$$N = \int_A \sigma \, dA = \int_{A_c} f_c \, dA_c + \int_{A_s} f_s \, dA_s + \int_{A_p} f_p \, dA_p \qquad \textbf{\textit{Equation 3-4}}$$

Similarly, integrating the stresses multiplied by the distance from the centroidal axis must equal the applied moment, M.

$$M = \int_{A_c} f_c y \, dA_c + \int_{A_s} f_s y \, dA_s + \int_{A_p} f_p y \, dA_p \qquad \textbf{\textit{Equation 3-5}}$$

3.1.2 Cross-Sectional Deformations

Using the three basic principles of compatibility, linear elastic behavior, and equilibrium, a derivation process was implemented to determine the incremental strain and curvature for each cross section. For each time-step in which the externally applied load does not change, the change in axial force and bending moment on a cross section is equal to zero. Therefore, the derivation process begins with the equilibrium equations 3-6 and 3-7.

$$\Delta N = \int_{A_c} \Delta f_c \, dA_c + \int_{A_p} \Delta f_p \, dA_p + \int_{A_s} \Delta f_s \, dA_s = 0$$

$$= \int_{A_c} \Delta f_c \, dA_c + \sum(\Delta f_p \, A_p) + \sum(\Delta f_s A_s) = 0 \qquad \textbf{\textit{Equation 3-6}}$$

$$\Delta M = \int_{A_c} \Delta f_c \mathrm{y}\, dA_c + \int_{A_p} \Delta f_p\, \mathrm{y} dA_p + \int_{A_s} \Delta f_s\, \mathrm{y} dA_s = 0$$

$$= \int_{A_c} \Delta f_c\, \mathrm{y} dA_c + \sum(\Delta f_p y_p A_p) + \sum(\Delta f_s y_s A_s) = 0 \qquad \textbf{\textit{Equation 3-7}}$$

3.1.2.1 INCREMENTAL STRAIN

The various changes in stress can be related back to changes in strain based on the linear elastic stress-strain relationship previously discussed. As shown in Equation 3-8, the total change in concrete strain includes the "free, unrestrained" creep, shrinkage, and temperature strains in addition to the stress-induced strains. The shrinkage and temperature strains are assumed constant for a given cross section; however, the creep strain is a function of y because the stress varies over the depth of the cross section.

$$\Delta\varepsilon_c = \frac{\Delta f_c}{E_c} + \Delta\varepsilon_{c,cr} + \Delta\varepsilon_{c,sh} + \Delta\varepsilon_{c,T} \qquad \textbf{\textit{Equation 3-8}}$$

Rearranging Equation 3-8, the total change in concrete stress at a particular cross section over a given time interval becomes:

$$\Delta f_c = E_c \left[\Delta\varepsilon_c - \left(\Delta\varepsilon_{c,cr} + \Delta\varepsilon_{c,sh} + \Delta\varepsilon_{c,T}\right)\right] \qquad \textbf{\textit{Equation 3-9}}$$

Similarly, the change in stress for prestressed reinforcing and non-prestressed reinforcing becomes:

$$\Delta f_p = E_p \left(\Delta\varepsilon_p\right) + \Delta f_{p,R} \qquad \textbf{\textit{Equation 3-10}}$$

$$\Delta f_s = E_s \left(\Delta\varepsilon_s\right) \qquad \textbf{\textit{Equation 3-11}}$$

where, $\Delta f_{p,R}$ = change in stress due to relaxation

E_p = modulus of elasticity of prestressing steel

E_s = modulus of elasticity of non-prestressed reinforcing steel

Substituting Equations 3-9 though 3-11 into Equation 3-6 yields the following:

$$0 = \int_{A_c} E_c \left[\Delta\varepsilon_c - \left(\Delta\varepsilon_{c,cr} + \Delta\varepsilon_{c,sh} + \Delta\varepsilon_{c,T}\right)\right] dA_c + \sum \left[(E_p \Delta\varepsilon_p + \Delta f_{p,R}) A_p\right] + \sum \left[(E_s \Delta\varepsilon_s) A_s\right] \qquad \textbf{Equation 3-12}$$

The relationship among the concrete and steel strains can be further simplified due to the "perfect bond" behavior in which the change in concrete and steel strains at a particular location must be equal, as shown below.

$$\Delta\varepsilon_c(y) = \Delta\varepsilon_s(y) = \Delta\varepsilon_p(y) \qquad \textbf{Equation 3-13}$$

Incorporating the perfect bond relationship, Equations 3-1 through 3-3 can be written in terms on incremental strains and curvature.

$$\Delta\varepsilon_c = \Delta\varepsilon_{cen} + \Delta\phi y \qquad \textbf{Equation 3-14}$$

$$\Delta\varepsilon_s = \Delta\varepsilon_c = \Delta\varepsilon_{cen} + \Delta\phi y_s \qquad \textbf{Equation 3-15}$$

$$\Delta\varepsilon_p = \Delta\varepsilon_c = \Delta\varepsilon_{cen} + \Delta\phi y_p \qquad \textbf{Equation 3-16}$$

Similar to Equation 3-14, the incremental creep strain can be written in terms of the creep strain at the centroid of the transformed section and the creep curvature.

$$\Delta\varepsilon_{c,cr} = \Delta\varepsilon_{cen,cr} + \Delta\phi_{cr} y \qquad \textbf{Equation 3-17}$$

By substituting Equations 3-14 through 3-17 into Equation 3-12, the cross-sectional force equilibrium is in terms of the incremental change in strain at the centroid of the transformed section, $\Delta\varepsilon_{cen}$.

$$0 = \int_{A_c} E_c \left[(\Delta\varepsilon_{cen} + \Delta\phi y) - \left(\Delta\varepsilon_{cen,cr} + \Delta\phi_{cr} y + \Delta\varepsilon_{c,sh} + \Delta\varepsilon_{c,T}\right)\right] dA_c +$$

$$\sum \left[\left\{E_p\left(\Delta\varepsilon_{cen} + \Delta\phi y_p\right) + \Delta \mathrm{f}_{\mathrm{p,R}}\right\} A_p\right] + \sum \left[E_s(\Delta\varepsilon_{cen} + \Delta\phi y_s)\, A_s\right]$$

Equation 3-18

In order to solve for $\Delta\varepsilon_{cen}$, the terms in Equation 3-18 are grouped into curvature-dependent terms and those independent of location, *y*. The incremental thermal strain is assumed to be zero.

$$0 = E_c A_c\left[\Delta\varepsilon_{cen} - \left(\Delta\varepsilon_{cen,cr} + \Delta\varepsilon_{c,sh}\right)\right] + \sum\left(E_p A_p \Delta\varepsilon_{cen}\right) + \sum(E_s A_s \Delta\varepsilon_{cen}) +$$

$$\sum\left(A_p \Delta f_{p,R}\right) + E_c\Delta\phi \left[\int_{A_c} y dA_c + \left(\frac{E_p}{E_c}\right)\sum y_p A_p + \left(\frac{E_s}{E_c}\right)\sum y_s\, A_s\right] -$$

$$E_c\Delta\phi_{cr} \int_{A_c} y dA_c \qquad \textbf{\textit{Equation 3-19}}$$

As shown below, the curvature-dependent terms in Equation 3-19 are the result when integrating *y* over the transformed section.

$$\int_{A_c} y dA_{tr} = \int_{A_c} y\, dA_c + \left(\frac{E_p}{E_c}\right)\sum y_p A_p + \left(\frac{E_s}{E_c}\right)\sum y_s\, A_s$$

$$= \int_{A_c} y\, dA_c + \sum n_p y_p A_p + \sum n_s y_s\, A_s = 0 \qquad \textbf{\textit{Equation 3-20}}$$

Since the y-values are defined with respect to the centroid of the transformed section, this integral is equal to zero. The equilibrium equation can be further simplified as follows:

$$0 = \Delta\varepsilon_{cen}\left[E_c A_c + \sum E_p A_p + \sum E_s A_s\right] - E_c A_c\left(\Delta\varepsilon_{cen,cr} + \Delta\varepsilon_{c,sh}\right) + \sum\left(A_p \Delta f_{p,R}\right) - E_c \Delta\phi_{cr} \int_{A_c} y \, dA_c$$

Equation 3-21

Solving for $\Delta\varepsilon_{cen}$ yields,

$$\Delta\varepsilon_{cen} = \frac{E_c A_c\left(\Delta\varepsilon_{cen,cr} + \Delta\varepsilon_{c,sh}\right) + E_c \Delta\phi_{cr} \int_{A_c} y \, dA_c - \sum\left(A_p \Delta f_{p,R}\right)}{E_c A_c + E_p \sum A_p + E_s \sum A_s}$$

Equation 3-22

When dividing all terms by E_c, the denominator becomes the definition for the area of the transformed section as shown in Equation 3-23. The integration of *y* over the concrete area is shown in Equation 3-24. Unlike the integration in Equation 3-20, this integral is *not* equal to zero because y is defined relative to the centroid of the transformed section rather than the centroid of the concrete area.

$$A_{tr} = A_c + \left(\frac{E_p}{E_c}\right) A_p + \left(\frac{E_s}{E_c}\right) A_s$$

Equation 3-23

$$\int_{A_c} y \, dA_c = -\left[\sum n_p y_p A_p + \sum n_s y_s A_s\right]$$

Equation 3-24

Applying the definitions in Equations 3-23 and 3-24, the incremental strain at the centroid of the transformed cross section becomes:

$$\Delta\varepsilon_{cen} = \frac{A_c}{A_{tr}}\left(\Delta\varepsilon_{cen,cr} + \Delta\varepsilon_{c,sh}\right) - \left[\frac{\Delta\phi_{c,cr}\left\{\sum\left(n_p y_p A_p\right) + \sum\left(n_s y_s A_s\right)\right\} + \frac{1}{E_c}\sum\left(A_p \Delta f_{p,R}\right)}{A_{tr}}\right]$$

Equation 3-25

3.1.2.2 INCREMENTAL CURVATURE

As shown in the previous section, the derivation for incremental strain at the centroid of the transformed section is based on the equilibrium equation for the change in axial load, ΔN. Similarly, the incremental curvature can be derived from the equilibrium equation for the change in bending moment, ΔM. Substituting Equations 3-9 through 3-11 into the equilibrium Equation 3-7 converts the incremental stress variables to incremental strain variables.

$$0 = \int_{A_c} y\, E_c \left[\Delta\varepsilon_c - \left(\Delta\varepsilon_{c,cr} + \Delta\varepsilon_{c,sh} + \Delta\varepsilon_{c.T}\right)\right] dA_c + \sum \left[y_p\left(E_p\Delta\varepsilon_p + \Delta f_{p,R}\right)A_p\right] + \sum \left[y_s(E_s\Delta\varepsilon_s)A_s\right] \qquad \textbf{Equation 3-26}$$

The incremental strain at the centroid of the transformed section is used to relate these various strains in terms of the incremental curvature. This can be seen by incorporating Equations 3-14 through 3-17 into the Equation 3-26.

$$0 = E_c \int_{A_c}\left[y(\Delta\varepsilon_{cen} + \Delta\phi y) - \left(\Delta\varepsilon_{cen,cr} + \Delta\phi_{cr}y + \Delta\varepsilon_{c,sh}\right)\right]dA_c + \sum \left[\left\{y_pE_p\left(\Delta\varepsilon_{cen} + \Delta\phi y_p\right) + y_p\Delta f_{p,R}\right\}A_p\right] + \sum \left[y_sE_s(\Delta\varepsilon_{cen} + \Delta\phi y_s)A_s\right]$$

Equation 3-27

Similar to the derivation of $\Delta\varepsilon_{cen}$, the terms in Equation 3-27 are grouped into curvature-dependent terms and those dependent on $\Delta\varepsilon_{cen}$.

$$0 = \Delta\varepsilon_{cen}E_c\left[\int_{A_c} y\, dA_c + \left(\frac{E_p}{E_c}\right)\sum y_pA_p + \left(\frac{E_s}{E_c}\right)\sum y_sA_s\right] + E_c\Delta\phi\left[\int_{A_c} y^2dA_c + \left(\frac{E_p}{E_c}\right)\sum {y_p}^2A_p + \left(\frac{E_s}{E_c}\right)\sum {y_s}^2A_s\right] - E_c\left(\Delta\varepsilon_{cen,cr} + \Delta\varepsilon_{c,sh}\right)\int_{A_c} ydA_c - E_c\Delta\phi_{cr}\int_{A_c} y^2dA_c + \sum\left(y_pA_p\Delta f_{p,R}\right) \qquad \textbf{Equation 3-28}$$

The first group of terms is dependent on $\Delta\varepsilon_{cen}$ and includes the integral of *y* over the transformed area as shown in Equation 3-29. The *y*-values are defined with respect to the centroid of the transformed area; therefore, this entire integral is equal to zero.

$$\int y\, dA_{tr} = \int_{A_c} y\, dA_c + \left(\frac{E_p}{E_c}\right)\sum y_p A_p + \left(\frac{E_s}{E_c}\right)\sum y_s A_s = 0 \qquad \textbf{\textit{Equation 3-29}}$$

The second group of terms in Equation 3-28 is dependent on $\Delta\phi$ and the bracketed factor represents the moment of inertia (second moment of the area) for the transformed section (see Equation 3-30). In addition, the integral of *y* over the net concrete section was used during the incremental strain variation and can be seen in Equation 3-24. Finally, Equation 3-30 can be rearranged to obtain $\int_{A_c} y^2 dA_c$.

$$I_{tr} = \int_{A_c} y^2\, dA_c + \sum n_p {y_p}^2 A_p + \sum n_s {y_s}^2 A_s \qquad \textbf{\textit{Equation 3-30}}$$

$$\int_{A_c} y^2\, dA_c = I_{tr} - \left(\sum n_p {y_p}^2 A_p + \sum n_s {y_s}^2 A_s\right) \qquad \textbf{\textit{Equation 3-31}}$$

Applying the fundamental definitions shown in Equations 3-29 through 3-31, the incremental curvature becomes:

$$\Delta\phi = \Delta\phi_{cr}\left[1 - \frac{\left\{\sum n_p {y_p}^2 A_p + \sum n_s {y_s}^2 A_s\right\}}{I_{tr}}\right] - \left[\frac{\left\{\left(\Delta\varepsilon_{cen,cr} + \Delta\varepsilon_{c,sh}\right)\left(\sum n_p y_p A_p + \sum n_s y_s A_s\right) + \sum n_p \left(\frac{\Delta f_{p,R}}{E_p}\right) y_p A_p\right\}}{I_{tr}}\right]$$

Equation 3-32

Although the shrinkage strain is taken as uniform over the concrete cross section, it can be seen from this derivation that shrinkage can have an effect—however slight—on curvature change because of the eccentric restraint provided by the (conventional and prestressed) reinforcement. The incremental strains at various locations within a cross section can now be calculated using the incremental strain at the centroid of the transformed section ($\Delta\varepsilon_{cen}$) and the incremental curvature ($\Delta\phi$). With the basic parameters defined, the remaining calculations are reviewed in the Program Execution section.

3.1.3 TIME ARRAY FUNCTION

The computer program uses a time-step procedure to calculate incremental and total strains, stresses, and camber over time. A time array function was developed and utilized to determine the ages at which the incremental calculations were performed. The time array function used for the time-step procedure was derived using an approach similar to the CEB 90 growth development for the concrete compressive strength over time shown in Equation 3-33.

$$\beta_{cc}(t) = exp\left\{s\left[1 - \left(\frac{28}{t}\right)^{1/2}\right]\right\} \qquad \textbf{\textit{Equation 3-33}}$$

The nonlinear function creates smaller time intervals at the beginning of the analysis period when time-dependent changes are more rapid. Equation 3-34 shows a modified version of the mathematical expression from Equation 3-33 rewritten in terms of the maximum time for analysis (t_{max}) and the total number of time intervals (N) specified by the user.

$$\frac{i}{N} = exp\left\{s\left[1 - \left(\frac{t_{max}}{t_i}\right)^{1/\alpha}\right]\right\} \qquad \textbf{\textit{Equation 3-34}}$$

where, i = specific time interval (1 to N)

t_i = time at interval *i*

s = unknown variable

α = unknown exponent

As shown in Equation 3-35, solving for t_i creates a time function in terms of an unknown variable (*s*) and exponent (α).

$$t_i = t_{max}\left[1 - \left(\frac{1}{s}\right)\ln\left(\frac{i}{N}\right)\right]^{-\alpha} \qquad \textit{Equation 3-35}$$

Several time functions were investigated by changing the unknown variable (*s)* and exponent (α) until the desired rate was produced. Table 3-1 summarizes the parameters for each time function. All cases were based on one hundred time intervals.

Table 3-1: Parameter Summary for Time Functions

Case	s	α	Case	s	α
1	0.15	1.5	10	0.30	2.0
2	0.20	1.5	11	0.35	2.0
3	0.25	1.5	12	0.40	2.0
4	0.30	1.5	13	0.15	2.5
5	0.35	1.5	14	0.20	2.5
6	0.40	1.5	15	0.25	2.5
7	0.15	2.0	16	0.30	2.5
8	0.20	2.0	17	0.35	2.5
9	0.25	2.0	18	0.40	2.5

Figure 3-3 shows the plots for the time functions when α = 2. Inspection of Case 8 reveals that slightly over 90% of the 100 time intervals are accounted for halfway through the total analysis time period.

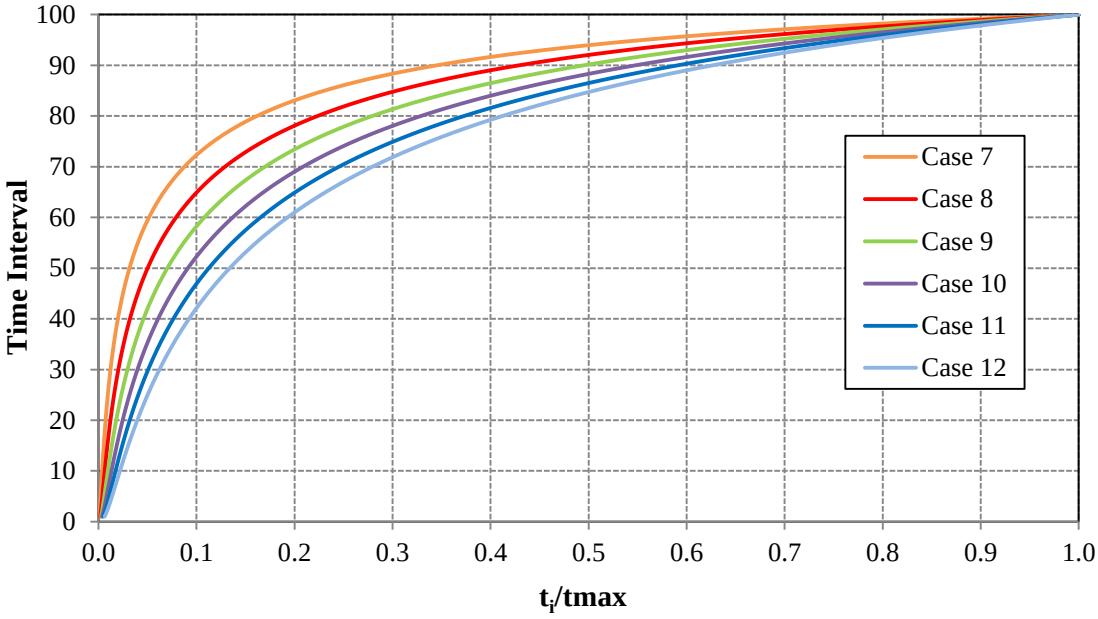

Figure 3-3: Time Function Plots for α = 2

Figure 3-4 shows the plots for the time functions with s = 0.2. Case 14 is similar to Case 8 in terms of percent expended at the halfway point. However, the growth rate for Case 14 is steep for earlier time intervals. Therefore, the time array function used in the program is based on the Case 8 parameters and shown in Equation 3-36.

$$t_i = t_{max}\left[1 - \left(\frac{1}{0.2}\right)\ln\left(\frac{i}{N}\right)\right]^{-2} \qquad \textit{Equation 3-36}$$

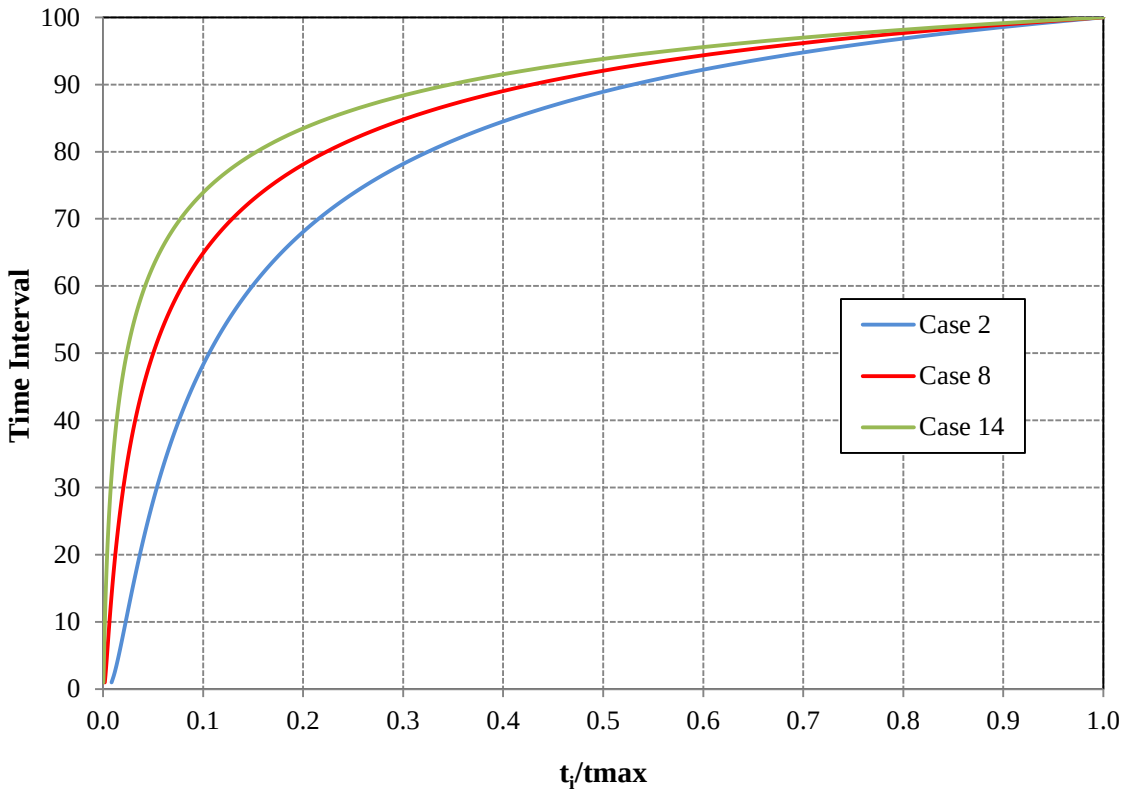

Figure 3-4: Time Function Plots for s = 0.2

3.2 ANALYTICAL METHODS

To calculate time-dependent camber, the concrete modulus of elasticity, creep, and shrinkage over time must be known. As discussed in Chapter 2, there are several prediction methods for calculating the time-dependent variables including those of AASHTO LRFD, ACI 209R-92, and CEB 90. The program includes these prediction models as well as those reviewed in this section.

3.2.1 MATURITY OF CONCRETE

The program accounts for concrete maturity based on user-defined information. AASHTO and ACI models do not account for temperature effects on concrete maturity. Therefore, the user

can input an equivalent concrete age at transfer to account for maturity when using these prediction models. The CEB 90 model is used to adjust the maturity of concrete based on the average curing temperature $T(\Delta t_i)$ and duration of curing Δt_i defined by the user.

$$t_{0,T} = \Delta t_i exp\left\{13.65 - \left[\frac{4000}{273+\frac{T(\Delta t_i)}{T_0}}\right]\right\} \qquad \textbf{\textit{Equation 3-37}}$$

The program also includes a modified CEB maturity function based on previous research by Kavanaugh (2008). The original CEB equation was updated with an activation energy of 45,000 J/mol which provided the following equation for both non-accelerated and accelerated-curing conditions.

$$t_{0,T} = \Delta t_i exp\left\{18.47 - \left[\frac{5410}{273+\frac{T(\Delta t_i)}{T_0}}\right]\right\} \qquad \textbf{\textit{Equation 3-38}}$$

The time intervals generated by the time array function are relative to transfer not casting. To calculate the concrete age, the time between casting and transfer must be accounted for. When maturity is neglected, the time between casting and transfer is simply added to the time array values. When maturity is calculated based on the CEB 90 and Modified CEB equations above, the duration of curing is replaced with the equivalent age between casting and transfer.

The user interface for collecting the maturity information is shown in Figure K-11 in Appendix K. The Visual Basic code for the maturity calculations and development of an adjusted concrete age array can be found in Module 10 of Appendix L.

3.2.2 CONCRETE MODULUS OF ELASTICITY

The concrete modulus of elasticity (MOE) is a function of various concrete properties and curing types depending on the prediction model selected for analysis. The AASHTO '05(+), ACI 209, and CEB 90 specify models that calculate the concrete MOE using the concrete compressive strength. Thus, these models are designated as "strength-based" in the program, and they are called "code-prediction" MOE models in this thesis. To further investigate the concrete MOE effect on predicting camber, two models were added to the program that allow the incorporation of actual MOE test results: "Constant E_c" and "Two-Point E_c." These models are referred to as "stiffness-based" in the program and "test-based" in this thesis. Figure K-5 in Appendix K shows the models the user may select from to calculate the concrete MOE development over time.

3.2.2.1 CONSTANT E_C

The first test-based model neglects the change of concrete MOE over time. The concrete MOE at transfer is assumed to remain constant for subsequent time intervals after transfer. Based on the user-defined input for the concrete MOE at the time of transfer, a one-dimensional global array for the concrete's modulus of elasticity is calculated.

3.2.2.2 TWO-POINT E_C

The second test-based model uses user-supplied MOE values at transfer and 28 days to establish a MOE growth curve over time. The growth curve is generated using the time-dependent coefficient $\beta_{cc}(t)$ found in the CEB 90 equation for development of strength with time (see Equation 3-33).

In Equation 3-33, the coefficient *s* is dependent on the type of cement. Using the relationship shown in Equation 3-39, the original CEB equation can be modified such that the coefficient *s* is dependent on the concrete MOE at transfer and 28 days. As shown in Equation 3-41, solving for *s* yields the growth rate factor based on the two measured concrete MOE values.

$$\beta_{cc} = \frac{E_{c,initial}}{E_{c,28}} \qquad when\ t = t_{initial} \qquad \textbf{Equation 3-39}$$

$$\frac{E_{c,initial}}{E_{c,28}} = exp\left\{s\left[1 - \left(\frac{28}{t_{initial}}\right)^{1/2}\right]\right\} \qquad \textbf{Equation 3-40}$$

$$s = \frac{\ln\left(\frac{E_{c,inital}}{E_{c,28}}\right)}{\left[1-\left(\frac{28}{t_{inital}}\right)^{1/2}\right]} \qquad \textbf{Equation 3-41}$$

The two-point E_c model uses the concrete MOE at 28 days and the growth rate to calculate the concrete MOE over time. As shown in Equation 3-42, the concrete MOE for any time interval ($E_{c,i}$) is a function of the concrete age at the beginning of the interval (age_{i-1}), the concrete MOE at 28 days ($E_{c,28}$), and the growth rate (*s*).

$$E_{c,i} = E_{c,28} exp\left\{s\left[1 - \left(\frac{28}{age_{i-1}}\right)^{1/2}\right]\right\} \qquad \textbf{Equation 3-42}$$

The computer program allows the user to specify either a test-based or code-prediction model to predict the concrete MOE development over time. A closer look at the effect each concrete MOE model has on strain and camber predictions can be found in Chapters 5 and 6. Figure 3-5 shows the change in concrete MOE over time for one of the AASHTO Type I girders (STD-M-1) described in the experimental program in Chapter 4. For this particular girder, the code-prediction models significantly underestimated the concrete MOE at transfer (5700 ksi) which, as shown in Figure 3-5, is the basis for the test-based models.

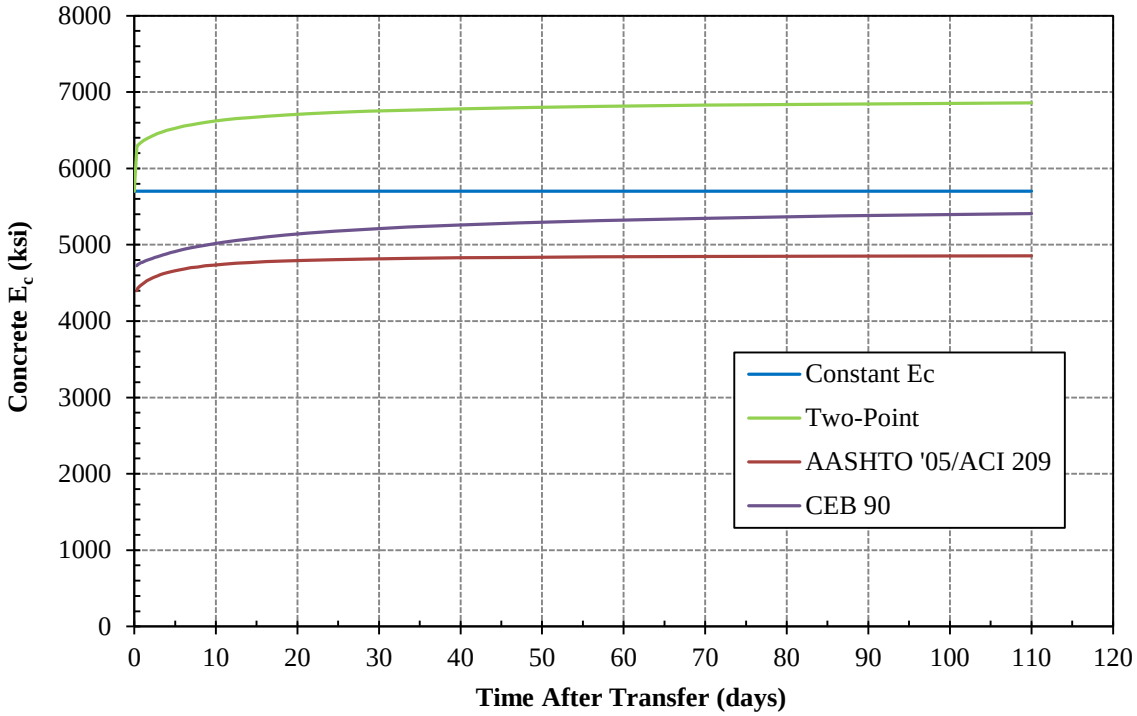

Figure 3-5: STD-M-1 E_c Development with Time

3.2.3 CREEP AND SHRINKAGE

Curvature, and ultimately camber, is a function of the creep strain, creep curvature, and shrinkage strain (to a lesser extent). The creep strain and curvature are dependent on the creep coefficient. Therefore, to calculate time-dependent camber, the prediction models discussed in Chapter 2 can be utilized to determine the creep and shrinkage strains over time.

The program allows the user to choose among AASHTO ’05(+), AASHTO ’04(-), ACI 209, CEB 90, and Modified CEB models to calculate creep and shrinkage strains over time (see Figure K-12).

3.2.3.1 AASHTO LRFD

AASHTO LRFD uses the “age of the concrete when load is initially applied” or t_i for the creep calculations. As covered in Chapter 2, the basis for calculating t_i is not consistent between the

2004 and 2005 versions. Therefore, two AASHTO models are included in the camber program: 2004 or earlier versions, '04(-), and 2005 or later versions, '05(+). Table 3-2 summarizes the modifications for the concrete age t_i depending on the AASHTO model and curing type.

Table 3-2: Modifications for Concrete Age at Time of Loading

Code	**AASHTO '04(–)**		**AASHTO '05(+)**	
Curing Type	**Moist Cured**	**Steam Cured**	**Moist Cured**	**Steam Cured**
t_i	Moist Cured Loading Age	Steam Cured Loading Age x 7	Moist Cured Loading Age / 7	Steam Cured Loading Age

3.2.3.2 ACI 209

The camber program uses the AASHTO and ACI creep and shrinkage factors discussed in Chapter 2 to calculate the creep coefficient and shrinkage strain over time. See Module 8 in Appendix L for the Visual Basic code used to calculate the correction factors based on the method selected by the user.

3.2.3.3 CEB 90

In addition to the temperature-adjusted concrete age ($t_{0,T}$) shown in Equation 3-37, the CEB 90 model also modifies the concrete age at loading based on the cement type. The final adjusted concrete age equation and variables are given below.

$$t_0 = t_{0,T}\left\{\left[\frac{9}{2+\left(\frac{t_{0,T}}{t_{1,T}}\right)^{1.2}}\right]+1\right\}^{\alpha} \qquad \textit{Equation 3-43}$$

where, $t_{0,T}$ = age of concrete at loading adjusted according to temperature (days)

$t_{1,T}$ = 1 day

α = -1 for slowly hardening cements SL; 0 for normal or rapid hardening cements N and R; and 1 for rapid hardening, high-strength cements RS

The CEB 90 model uses the final adjusted concrete age t_0 to calculate the notional creep coefficient and the development of creep with time. However, the shrinkage calculations are relative to the concrete age at the end of curing. To account for the duration of curing, the program uses a shrinkage time array for the incremental shrinkage calculations. The development of the shrinkage time array is covered in the "Program Execution" section.

3.2.3.4 MODIFIED CEB 90

As discussed in Chapter 2, the Modified CEB 90 method is based on previous research by Kavanaugh (2008) which incorporates the effect of curing type on creep. The calculations for the notional creep coefficient and development of creep over time vary depending on either non-accelerated or accelerated curing. The modified functions used in the program are summarized in Table 2-4.

3.3 PROGRAM EXECUTION

The program incorporates the analytical approach and numerical methods previously presented in this thesis. The following sections discuss the user-defined input, internal calculations, and generated output of the program. In conclusion, a program flow chart is presented to summarize the sequencing of the time-step procedure and overall execution process.

3.3.1 USER-DEFINED INPUT

The user must define several design parameters including material properties, cross-sectional geometry, time of events, and curing details. The user interface created to obtain these variables can be seen in Figures K-1 through K-15 in Appendix K. The required concrete and prestressing steel properties are shown in Figures K-4 and K-6, respectively. If conventional reinforcing steel is present, the user must also specify its modulus of elasticity as shown in Figure K-10.

When inputting the time of events, casting of the girder is used as the event of reference. The time of jacking must be specified in hours before casting, while the time of transfer must be specified in hours after casting. The user also needs to identify the type (moist or steam) and length of curing. If the user elects to include the effects of maturity, an average curing temperature or equivalent age at transfer must be provided. See Figure K-11 for the input screen used to collect the time of events, curing, and maturity information.

3.3.1.1 CROSS-SECTIONAL GEOMETRY

The user may select from a list of standard AASHTO girders (Type I through VI) or directly input gross cross-sectional properties. The cross-sectional properties and dimensions for the standard AASHTO girders are shown in Tables H-5 through H-7 in Appendix H. Figure K-2 shows the input required if the user does not select from the list of standard AASHTO sections.

When inputting the prestressing strand layout, the program allows the user to include straight, draped, and debonded strands. To locate the prestressing strands (in particular, draped and debonded strands) at any cross section along the length of the prestressed member, the following terminology was developed.

- *Layer* – a set of strands located at the same cross-sectional depth
- *Layer Group* – a subset of strands within a *Layer* that have the same draping or debonding characteristics; each *Layer Group* must be classified as one of the following:
    - Fully bonded, straight strands
    - Debonded, straight strands
    - Draped strands (fully bonded)
- *Layer Group Detail Length* – dependent on the *Layer Group* classification
    - Fully bonded, straight strands = 0
    - Debonded strands = debonded (jacketed) length measured from the end of the girder
    - Draped Strands = distance between draping point and midspan (may be equal to zero)

Based on the above terminology, one *Layer* can consist of multiple *Layer Groups*; however, a *Layer Group* cannot extend into multiple *Layers*. Each *Layer Group* can have only one value for the *Layer Group Detail Length*. Therefore, the strands in each debonded *Layer Group* must have the same debonded (jacketed) length. The strands in each draped *Layer Group* must have the same draping location relative to midspan. The distance for each *Layer Group* to the bottom of the girder is measured from the centroid of the *Layer Group* at the midspan cross section.

If draped *Layer Groups* are specified, the user must also input the distance from the bottom of the girder to the centroid of the draped *Layer Group* for a cross section at the end of the girder (see Figure K-9). The program then calculates the draped *Layer Group*'s cross-

sectional depth along the length of the girder assuming a constant slope between the hold-down point and end of the girder.

These guidelines are presented to the user in Figure K-7. The interface for collecting the prestressing strand layout at midspan is shown in Figure K-8. The program allows the user to input up to thirty prestressing steel *Layer Groups* and assumes the strand pattern is symmetric about midspan. The user must also specify the strand type, nominal strand diameter, and jacking stress for each *Layer Group*. The prestressing steel properties built into the program database are shown in Figure H-4. The user is limited to the following seven-wire strand diameters:

- 0.5 in.
- 0.5 in. oversized (area = 0.164 $in.^2$)
- 0.5 in. oversized (area = 0.167 $in.^2$)
- 0.6 in.

The user is allowed to input up to five conventional reinforcing steel layers. As shown in Figure K-10, the user must specify the number of bars and bar size in each layer as well as the distance from the bottom of the girder to the centroid of the steel layer. All bars in a reinforcing steel layer must be the same size. The reinforcing steel properties built into the program database are shown in Figure H-3.

As shown in Figure K-15, the program allows the user to specify the number of cross sections to be used for analysis. Because the program assumes the cross-sectional geometry is symmetric about midspan, the user must provide the number of cross sections to be taken along *half* of the girder length. A minimum of one cross section is required and corresponds to the

cross section at midspan. The program output is limited to forty cross sections, which was judged to be sufficient for most draped and debonded layouts.

3.3.1.2 GLOBAL VARIABLES

Based the user-defined input, the program generates global variables to be used throughout the program calculations. *Module 1* in Appendix L shows the program code that translates the user-defined input into global variables. A brief description of these variables, including the notation used in the program, is shown in Appendix A. The subscript "*k*" stands for a specific prestressing steel *Layer Group* (LG) or reinforcing steel layer. The subscript "*j*" represents a particular cross section along the length of the girder whose location is measured relative to midspan. The subscript "*i*" represents a specific time interval and is discussed more in-depth later in this chapter.

3.3.1.3 GLOBAL ARRAYS

Before time-step calculations can be executed, the user input must also be organized into global arrays using the subscripts *i, j,* and *k.* The program generates global arrays for prestressing steel, reinforcing steel, time intervals, concrete age, shrinkage age, jacking time, and the concrete modulus of elasticity. *Module 2* in Appendix L shows the program code that translates the user-defined input and global variables (see *Module 1*) into global arrays.

Two-dimensional arrays (*k, j*) are generated for the prestressing steel and reinforcing steel using the information provided in Figures K-8 through K-10. The arrays are dimensioned based on the number of prestressing steel *Layer Groups*, reinforcing steel layers, and cross sections specified by the user.

The time array is a one-dimensional array (*i*) calculated using the time function previously discussed in this chapter. The array is dimensioned based on the number of time intervals specified by the user. As shown in Figure K-15, the program allows the user to denote the maximum time (measured in days) and number of time intervals to be used for analysis. The program output is limited to forty time intervals. Because the ultimate goal of the time-step procedure is to calculate camber, the time array is defined relative to time of prestress transfer.

Creep calculations are dependent on the concrete age at the time of transfer. The concrete age array is generated by adding the time between casting and transfer to the original time array. The concrete age can then be adjusted (using the *AdjustedAge* variable) to include the effects of maturity. If the user chooses to neglect maturity, the *AdjustedAge* is simply the time between casting and transfer. However, if the user chooses to include maturity, the *AdjustedAge* is calculated based on the equations provided by the analytical methods.

Alternatively, shrinkage calculations are dependent on the concrete age after initial curing. Therefore, the shrinkage age array is generated by subtracting the length of the curing period from the concrete age array.

Steel relaxation calculations are dependent on the time relative to jacking. The jacking time array is created by adding the time elapsed between jacking and transfer to the original time array which begins at transfer. The jacking time array is calculated using the global variables *JackingTime* and *TransferTime* which are based on the user input provided in Figure K-11.

The program generates a one-dimensional array (*i*) for the concrete MOE development over time. The calculations are based on the selected development model and information provided by the user (see Figure K-5). The concrete age array is included in the calculations for

all models except for the "Constant E_c" model, which is based solely on the initial concrete MOE.

3.3.2 INTERNAL CALCULATIONS

The following initial and time-step calculations are presented for a single cross section (*k*). The same procedure is valid for multiple cross sections.

3.3.2.1 INITIAL TRANSFORMED SECTION PROPERTIES

The initial transformed section properties correspond to the time immediately after release (t = 0). The transformed section calculations use the cross-sectional geometry defined by the user and the global arrays generated by the program. The distance to the centroid of the transformed section ($y_{tr,initial}$) is calculated using the area of steel in each prestressing strand *Layer Group* (LG) and reinforcing steel layer as well as the layer locations within the cross section. The contribution of prestressing strands and reinforcing steel to the moment of inertia immediately after release ($I_{tr,initial}$) is dependent on the distance from each LG/layer to the centroid of the transformed section. See *Module 3* in Appendix L for the program code that calculates the initial transformed section properties.

3.3.2.2 INITIAL PRESTRESS LOSSES

As stated in Chapter 2, the initial prestress losses are due to steel relaxation and elastic shortening of concrete. The loss due to steel relaxation is added to the jacking stress (f_{pj}) to determine the prestress immediately before transfer (f_{pbt}). The loss due to the elastic shortening of concrete is added to f_{pbt} to determine the prestress after transfer (f_{pt}). Because the initial prestress losses are independent of the time function, the steel relaxation and elastic shortening

results are saved in two-dimensional arrays (*k, j*) based on the number of *Layer Groups* and number of cross sections. See *Module 4* in Appendix L for the complete program code used to calculate the initial prestress losses.

The stresses and strains immediately after transfer are calculated at each prestressing steel LG, reinforcing steel layer, top and bottom of the concrete section, and the centroid of the transformed area. The two-dimensional (*k, j*) initial stress and strain arrays are created by calculating these values at each cross section. *Module 5* in Appendix L shows the development of the initial stress and strain arrays. The initial arrays are transferred into the time loop (time-step calculations) and represent the stresses and strains at $i = 0$.

3.3.2.3 TRANSFORMED SECTION PROPERTIES

The same approach used for calculating the initial transformed section properties is used to calculate the changing section properties over time. The transformed section properties change as the concrete MOE changes. The relative restraint offered by the steel reinforcement decreases as the concrete stiffness increases. *Module 6* and *Module 7* in Appendix L show the program code for calculating the transformed section properties and net concrete properties, respectively. Both sets of section properties are presented in three-dimensional arrays. The transformed section properties are used to calculate incremental strains and stresses at each prestressing steel LG and reinforcing steel layer location. The net concrete properties are used to calculate the incremental strains and stresses at the top, bottom, and centroid of the concrete section.

3.3.2.4 CREEP AND SHRINKAGE CORRECTION FACTORS

Before beginning the time-step calculations, any applicable creep and shrinkage correction factors are calculated. The program calculates the standard AASHTO and ACI correction factors

discussed in Chapter 2 as well as the cure-dependent factors previously covered in this chapter. The program code for calculating the creep and shrinkage correction factors is located in *Module 8* of Appendix L. The user is able to review the calculated correction factors (see Figures K-13 and K-14) based on the creep and shrinkage model selected (see Figure K-12).

3.3.2.5 TIME LOOP—INCREMENTAL STRAINS, STRESSES, AND CURVATURES

The time-step calculations are executed within a time loop (starting at $i = 1$) based on the number of time intervals used for the analysis. As previously stated, the initial strains, stresses, and curvature correspond to $i = 0$.

The incremental relaxation loss is the first calculation within the time loop. For the first time-step ($i = 1$), the stress at transfer is used to calculate the incremental relaxation loss. For each time-step thereafter, the prestress force at the end of the previous time-step is used for the relaxation loss calculation.

Next, the creep coefficient is calculated using the creep and shrinkage model selected by the user. The incremental unrestrained creep strain at the centroid of the transformed section and incremental unrestrained creep curvature are then calculated using the creep coefficient. The incremental unrestrained shrinkage strain is also calculated for the cross section. While the creep strain varies across the cross section, the incremental unrestrained shrinkage strain remains constant.

Now, the incremental strain at the centroid of the transformed section and the incremental curvature can be computed using Equation 3-25 and Equation 3-32, respectively.

As shown in the derivation process, the incremental strain is calculated at the centroid of the transformed section. However, the program calculates the incremental concrete strain and stress at various locations within a cross section using the incremental strain at the centroid of the net concrete section. Equation 3-44 shows the relationship between the incremental strain at the centroid of the transformed section and net concrete section.

$$\Delta\varepsilon_{net} = \Delta\varepsilon_{cen} + \Delta\phi(y_{tr} - y_c) \qquad \textbf{\textit{Equation 3-44}}$$

where, $\Delta\varepsilon_{net}$ = incremental strain at centroid of the net concrete section

$\Delta\varepsilon_{cen}$ = incremental strain at centroid of the transformed section

y_{tr} = distance from centroid of the transformed section to the extreme bottom fiber

y_c = distance from centroid of the net concrete section to the extreme bottom fiber

The incremental strain at any location becomes a function of its distance from the centroid of the net section (y) where positive y is downward. The basic relationship is shown in Equation 3-45.

$$\Delta\varepsilon = \Delta\varepsilon_{net} + \Delta\phi(y) \qquad \textbf{\textit{Equation 3-45}}$$

The unrestrained, incremental creep and shrinkage strains are used to calculate the incremental stresses. The unrestrained, incremental shrinkage strain is constant across the entire cross section. However, the creep strain varies. As shown in Equation 3-46, the unrestrained,

incremental creep curvature is used to translate the creep strain from the centroid of the transformed section to the centroid of the net concrete section.

$$\Delta\varepsilon_{cr(u),net} = \Delta\varepsilon_{cr(u),cen} + \Delta\phi_{cr(u)}(y_{tr} - y_{net}) \qquad \textbf{\textit{Equation 3-46}}$$

where, $\Delta\varepsilon_{cr(u),net}$ = unrestrained, incremental creep strain at the centroid of the net concrete section

$\Delta\varepsilon_{cr(u),cen}$ = unrestrained, incremental creep strain at the centroid of the transformed section

$\Delta\phi_{cr(u)}$ = unrestrained, incremental creep curvature

The incremental concrete stress is calculated by removing the unrestrained, incremental creep and shrinkage strains from the total incremental strain.

$$\Delta f_c = E_c\left[\Delta\varepsilon_c - \left(\Delta\varepsilon_{cr(u)} + \Delta\varepsilon_{sh(u)}\right)\right] \qquad \textbf{\textit{Equation 3-47}}$$

As shown in Equations 3-48 and 3-49, the incremental stress in each reinforcing steel layer and prestressing strand *Layer Group* is a function of the incremental strain at that location and the steel modulus of elasticity. The incremental steel relaxation loss must be accounted for when calculating the incremental stress in the prestressing steel.

$$\Delta f_s = E_s\,(\Delta\varepsilon_s) \qquad \textbf{\textit{Equation 3-48}}$$

$$\Delta f_p = E_p\left(\Delta\varepsilon_p\right) + \Delta f_{p,R} \qquad \textbf{\textit{Equation 3-49}}$$

where, Δf_s = incremental stress in reinforcing steel layer

Δf_p = incremental stress in prestressing layer group

The incremental strains and stresses are calculated for each time step. The total strains and stresses at the end of each time step are then calculated by adding the incremental values with the total strains and stresses from the end of the previous time step. This incremental, time-step procedure is the basis for the program's outer time loop (*i*). The complete program code for the time loop calculations is provided in *Module 9* in Appendix L.

3.3.2.6 CAMBER CALCULATIONS

The camber calculations are based on the moment-area method and assume a simply-supported, symmetrical beam that has a uniformly distributed self-weight. The camber is only computed at midspan and is based on approximate straight-line changes in curvature between analyzed cross sections. As shown in Figure 3-6, the resulting symmetric curvature distribution can be visualized as a series of trapezoids approximating the theoretical curvature function. This allows the area under the curvature curve to be divided into rectangular and triangular area components.

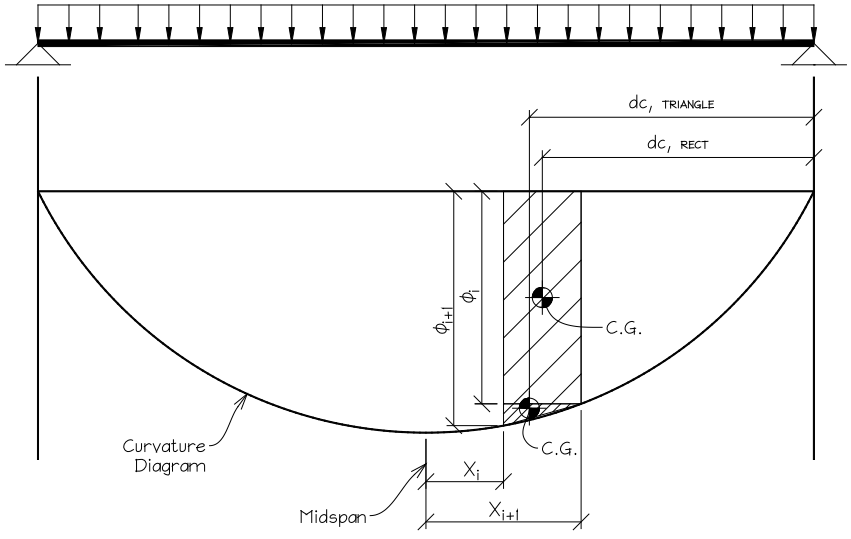

Figure 3-6: Moment-Area Method using Curvature Diagram

Table 3-3 summarizes the variables to be used for each area component. The d_c variable represents the distance from the centroid of the triangular or trapezoidal area to the end of the beam. As shown in Figure 3-6, x_i and x_{i+1} are measured from midspan and Δx is the difference between the two.

Table 3-3: Components for Camber Equation

Component	Height	Area	d_c
Rectangle	ϕ_i	$\phi_i(\Delta x)$	$L/2 - [x_i + 1/2(\Delta x)]$
Triangle	$\phi_{i+1} - \phi_i$	$½(\phi_{i+1} - \phi_i)(\Delta x)$	$L/2 - [x_i + 2/3(\Delta x)]$

Using this moment-area approach, the standard deflection equation (Equation 3-50) can be rewritten in terms of the triangular and rectangular area components.

$$\Delta = \int_0^{0.5L} \phi x \, dx \qquad \textbf{\textit{Equation 3-50}}$$

$$\Delta = \sum\left[(Ad_c)_{rect} + (Ad_c)_{triangle}\right] \qquad \textbf{\textit{Equation 3-51}}$$

Substituting the components shown in Table 3-3 into Equation 3-51 relates the midspan camber to the curvature values along the length of the beam. The camber calculation is shown in Equation 3-52.

$$\Delta = \sum\left(\frac{\Delta x}{2}\right)\left[\phi_i\left\{\frac{L}{2} - \frac{2}{3}(x_i) - \frac{1}{3}(x_j)\right\} + \phi_j\left\{\frac{L}{2} - \frac{1}{3}(x_i) - \frac{2}{3}(x_j)\right\}\right] \qquad \textbf{\textit{Equation 3-52}}$$

The accuracy of this approximation increases with the number of cross sections selected for analysis. The midspan camber at the end of each time interval is calculated using a three-dimensional total curvature array (*1, j, i*) which contains curvatures at every cross section for each time interval. If the user specifies only one cross section to be used for the camber

calculation, the total curvature array is dimensioned based on the number of time intervals only *(1, 1, i)* and contains only curvatures at the midspan cross section. Therefore, if only one cross section is used for analysis, the camber is dependent on the curvature at midspan and the length of the beam as shown in Equation 3-53.

$$\Delta = \frac{\phi L^2}{8} \qquad \textbf{\textit{Equation 3-53}}$$

The initial and time-dependent midspan camber calculations are shown in *Module 10* of Appendix L.

3.3.3 PROGRAM FLOW CHART

The program flow chart helps to visualize the intricate relationship among the incremental strains, stresses, and curvatures for each cross section. The inner loop shows how the program collects the incremental values along the length of the girder The outer time loop shows how the incremental results are used to calculate total strains, stresses, curvature, and camber at the end of each time interval. The program flow chart is shown in Figure H-1 in Appendix H.

3.3.4 PROGRAM OUTPUT

Results from the time-step calculations are saved in three-dimensional arrays (*k, j, i*) for each LG/layer (*k*) at each cross section (*j*) at the end of each time interval (*i*). This allows the user to view the stress, strain, and curvature results at specific locations for each time interval. Figures K-16 through K-29 located in Appendix K show the program's output forms. The user is able to control which output is displayed and can therefore limit viewing unwanted results.

The output format is dependent on the number of cross sections and time intervals the user selects for analysis. The distance from midspan is displayed with the results for each cross

section based on the length of the girder and number of cross sections selected. The time at the beginning and end of each time interval is also displayed based on the time function defined at the beginning of Chapter 3.

3.4 INTERVAL SELECTION

Before executing and analyzing the program, a standardized number of time intervals and cross sections used in the calculations must be determined. An interval selection test case was developed to investigate the effects the number of cross sections and time intervals have on camber results.

3.4.1 DISCRETIZATION ANALYSIS

The interval selection test case is based on the ALDOT Standard S4040CD AASHTO Type I girder strand pattern which consists of fully bonded, straight strands and bedonded strands. A cross section of the strand pattern is shown in Figure 3-7. The strand details for each layer group (LG) are summarized in Table 3-4 using the input format of the program. Other design parameters used for the interval selection are summarized in Table 3-5. For the time-dependent variables (modulus of elasticity, creep, and shrinkage), the AASHTO '05(+) prediction methods discussed in Chapter 3 were used. Maintaining these constant variables, a discretization analysis was performed to indentify the appropriate number of cross sections and time intervals to be maintained when further analyzing the program.

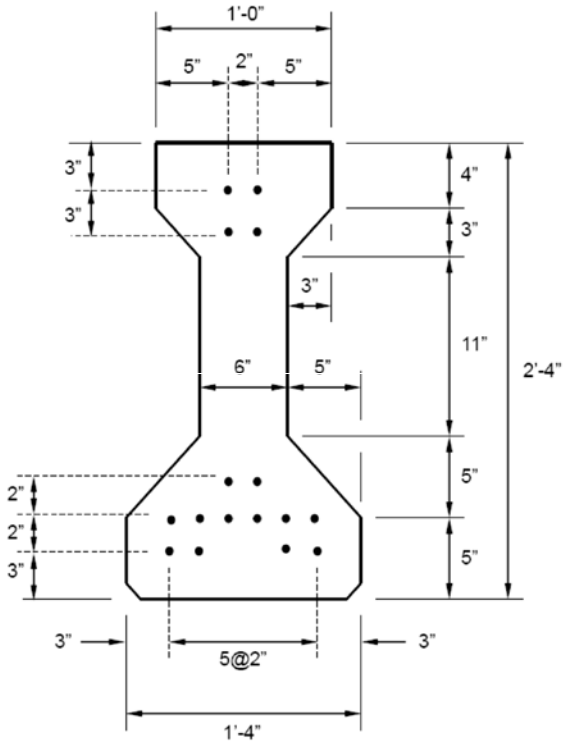

Figure 3-7: Test Case Strand Pattern - AASHTO Type I Girder

Table 3-4: Profile Details for Interval Selection Test Case

LG	Group Type	Number of Strands	Strand Type	Nominal Dia. (in.)	Jacking Stress (ksi)	Distance from Bottom	Detail Length (in.)
1	Fully Bonded, Straight	2	Low-relax	0.5	202.5	3	0
2	Debonded	2	Low-relax	0.5	202.5	3	72
3	Fully Bonded, Straight	6	Low-relax	0.5	202.5	5	0
4	Fully Bonded, Straight	2	Low-relax	0.5	202.5	7	0
5	Fully Bonded, Straight	2	Low-relax	0.5	202.5	19	0
6	Fully Bonded, Straight	2	Low-relax	0.5	32.7	25	0

Table 3-5: Design Parameters for Interval Selection Test Case

Material Properties		
f'_{ci}	psi	4500
f'_{c}	psi	5000
E_{ci}	ksi	5700
E_{c28}	ksi	6200
w_c	pcf	145
E_p	ksi	28500
f_{pu}	ksi	270
f_{py}	ksi	243
V/S	in.	3.07
Cement Type	-	Type III
Length of Girder	in.	465
Time of Events		
Curing	18-hour steam cure	
Stressing	Strands stressed 6 hours before casting	
Transfer	Transfer at 18 hours after casting	

3.4.1.1 TIME INTERVALS

In addition to the constant variables described above, a sensitivity analysis on the number of time intervals was based on one cross section (at midspan) and a total time of 365 days. Results for the following were collected when increasing the number of time intervals from 1 to 100 over the 365 day period: strand stress in layer group one (LG1), bottom fiber stress, midspan curvature, and midspan camber. Figures 3-8 through 3-11 indicate a plateau effect when using 40 or more time intervals.

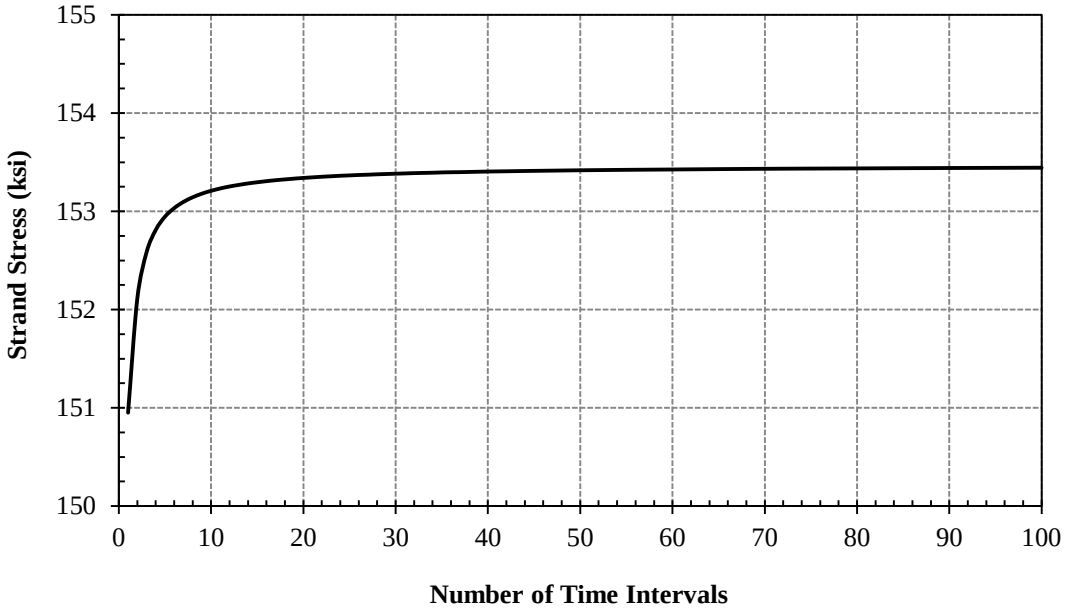

Figure 3-8: LG1 Stress vs. Number of Time Intervals

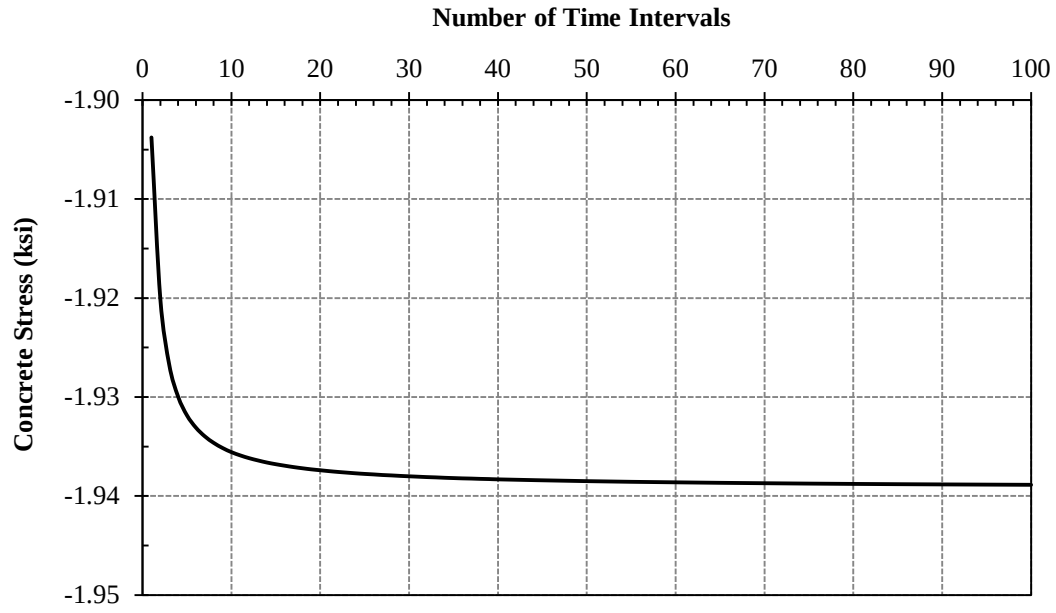

Figure 3-9: Bottom Fiber Stress vs. Number of Time Intervals

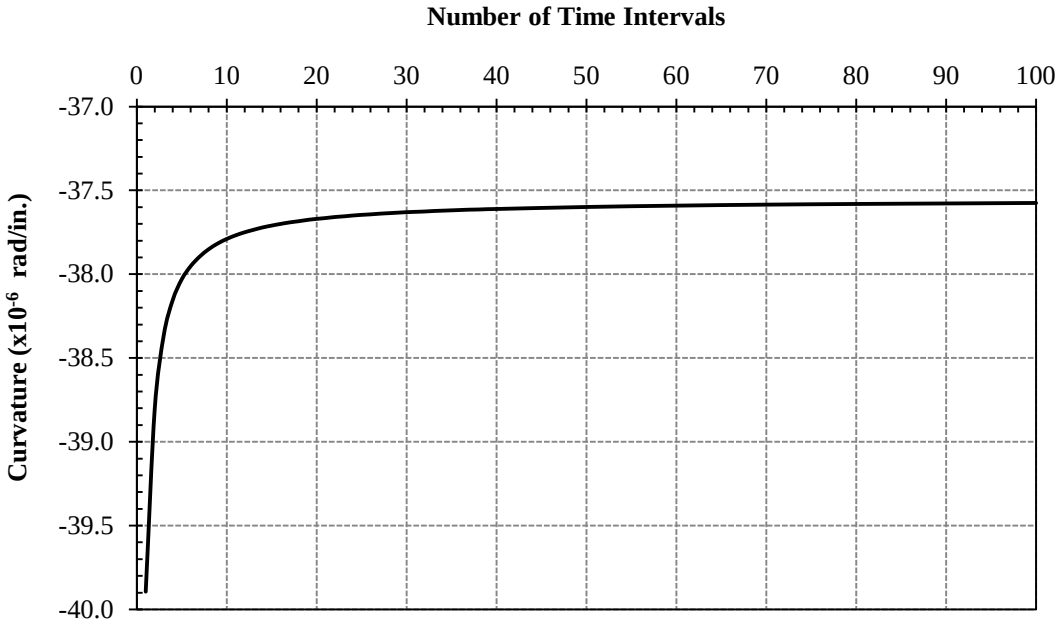

Figure 3-10: Midspan Curvature vs. Number of Time Intervals

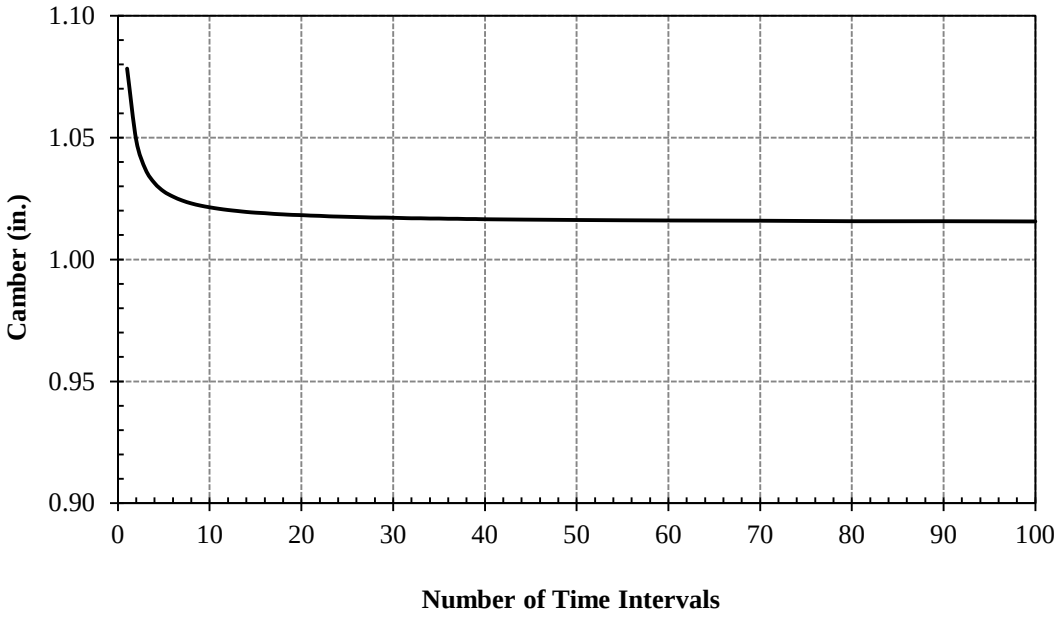

Figure 3-11: Midspan Camber vs. Number of Time Intervals

The values for LG1 stress, bottom fiber stress, curvature, and camber at midspan were calculated using 1 through 40, 50, 60, 70, 80, 90 and 100 time intervals over the 365-day period. The results using 100 time intervals were established as the ultimate values. The percent difference was then calculated between the results using the various time intervals (up to 90) and the ultimate values associated with 100 time intervals. As shown in Figures 3-12 through 3-14, the percent difference when using 40 time intervals is less than ±0.10 percent for all ultimate values. More specifically, the program under-estimated both the stress in LG1 and the bottom fiber by 0.03 percent. The curvature and camber were over-predicted by 0.10 percent when compared to the ultimate value. Based on these results and to set a realistic limit on program output, forty was chosen as an adequate number of time intervals to subdivide a given time period of analysis.

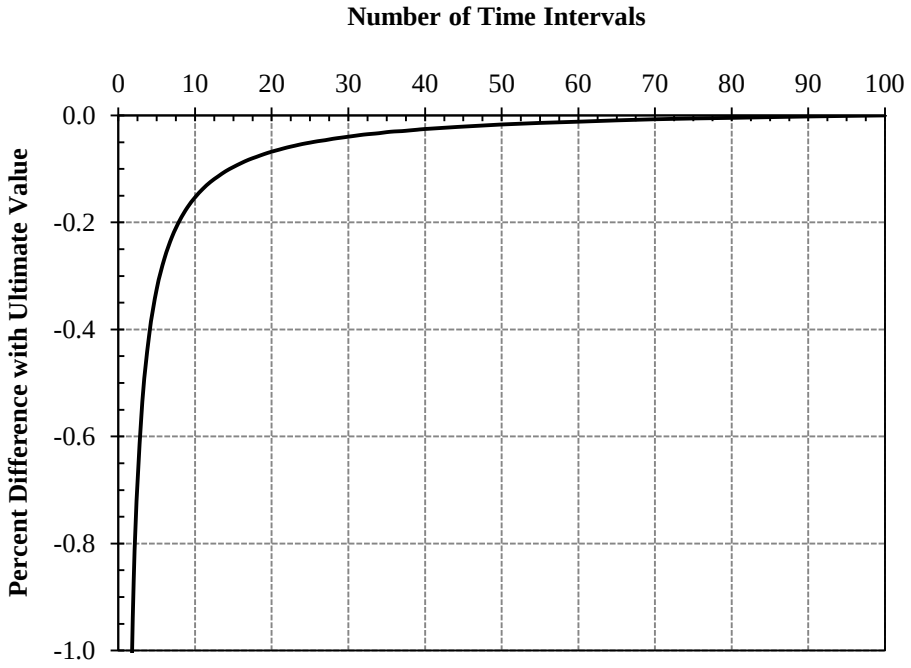

Figure 3-12: Percent Difference in LG1 Stress at Midspan

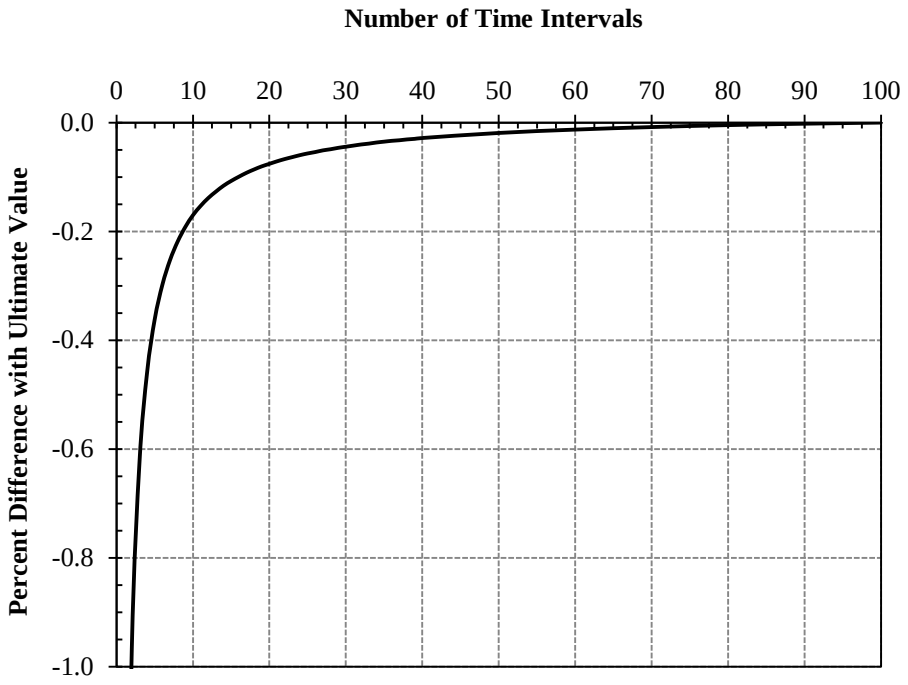

Figure 3-13: Percent Difference in Bottom Fiber Stress at Midspan

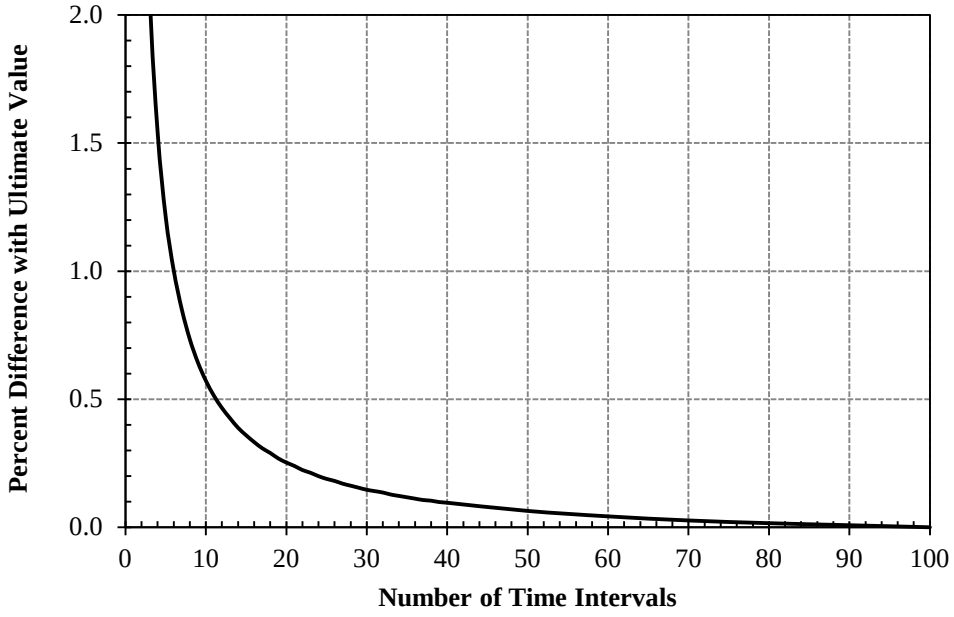

Figure 3-14: Percent Difference in Midspan Curvature and Camber

3.4.1.2 CROSS SECTIONS

A similar approach was taken to determine the number of cross sections used along the length of a girder when further analyzing the camber prediction program. Based on the time interval selection results summarized in the previous section, forty time intervals over a period of 365 days were used for the sensitivity analysis on the number of cross sections. Midspan camber results immediately following transfer, 28 days after transfer, and 365 days after transfer were recorded when increasing the number of cross sections from 1 to 100. Figures 3-15 through 3-17 show the camber results oscillating about a central value. This oscillation is primarily due to the debonded strands at the end of the member. As the number of cross sections increases, the amplitude of the oscillation decreases. However, the amplitude shows little decay beyond thirty-five cross sections as the peak magnitudes remain fairly constant for all three sets of camber results.

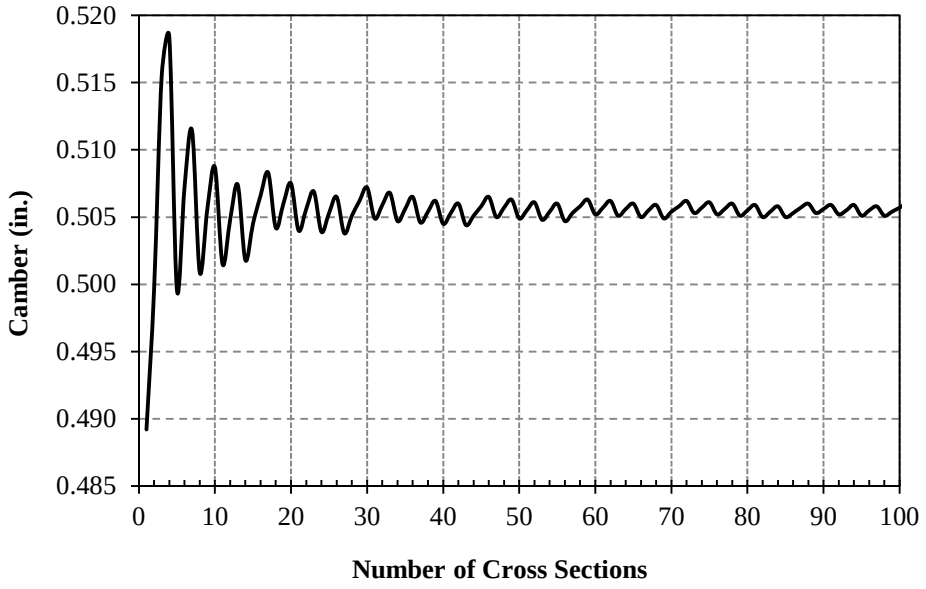

Figure 3-15: Initial Midspan Camber vs. Number of Cross Sections

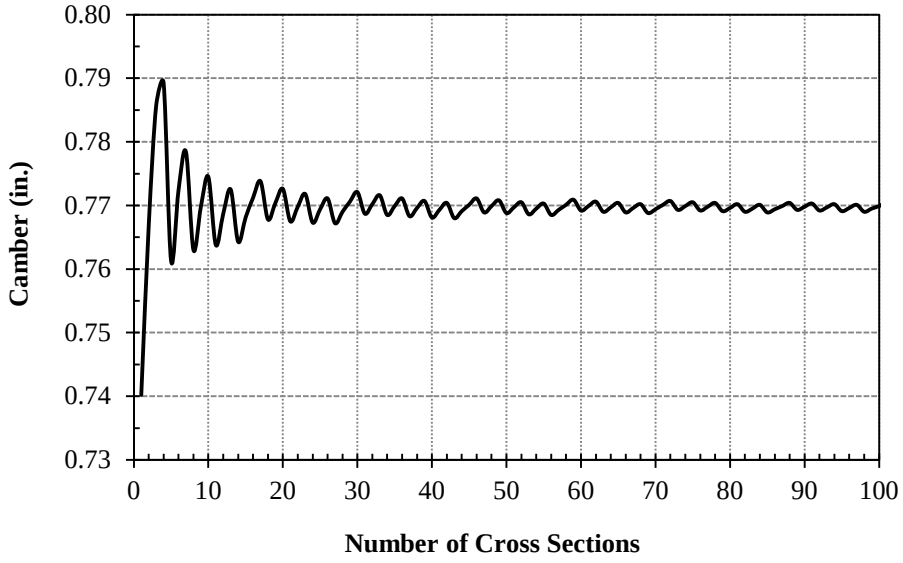

Figure 3-16: Midspan Camber at 28 Days vs. Number of Cross Sections

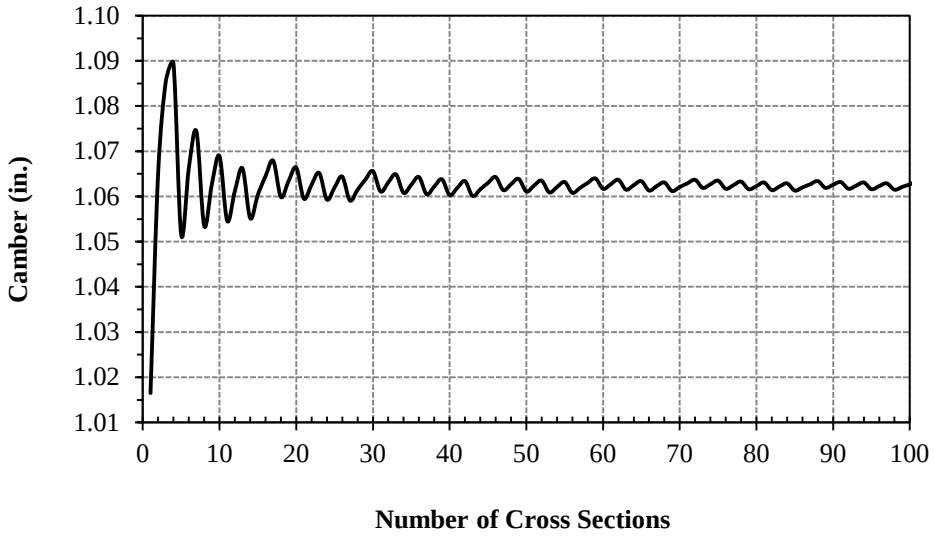

Figure 3-17: Midspan Camber at 365 Days vs. Number of Cross Sections

The midspan camber results associated with 100 cross sections were established as the ultimate values. The percent difference between the predicted camber using up to 99 cross sections and the ultimate value was then calculated for the three different instances in time: immediately after transfer, 28 days after transfer and 365 days after transfer. Similar to the camber results, the percent difference plots followed the same oscillating pattern as the number of cross sections increased. Figures 3-18 through 3-20 show the percent difference with the ultimate camber is approximately zero percent when thirty-five cross sections were used along half the girder length.

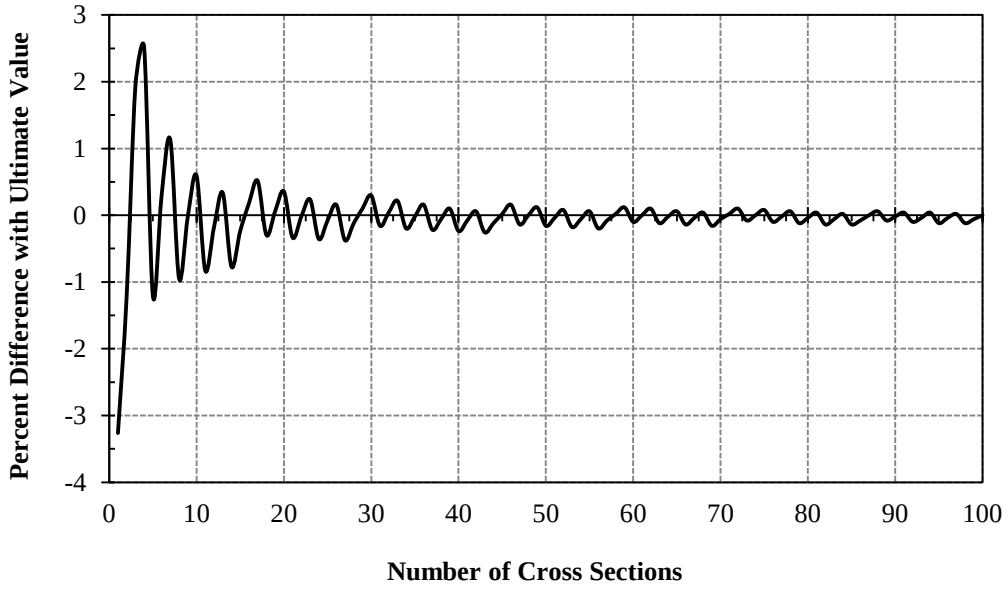

Figure 3-18: Percent Difference in Initial Midspan Camber

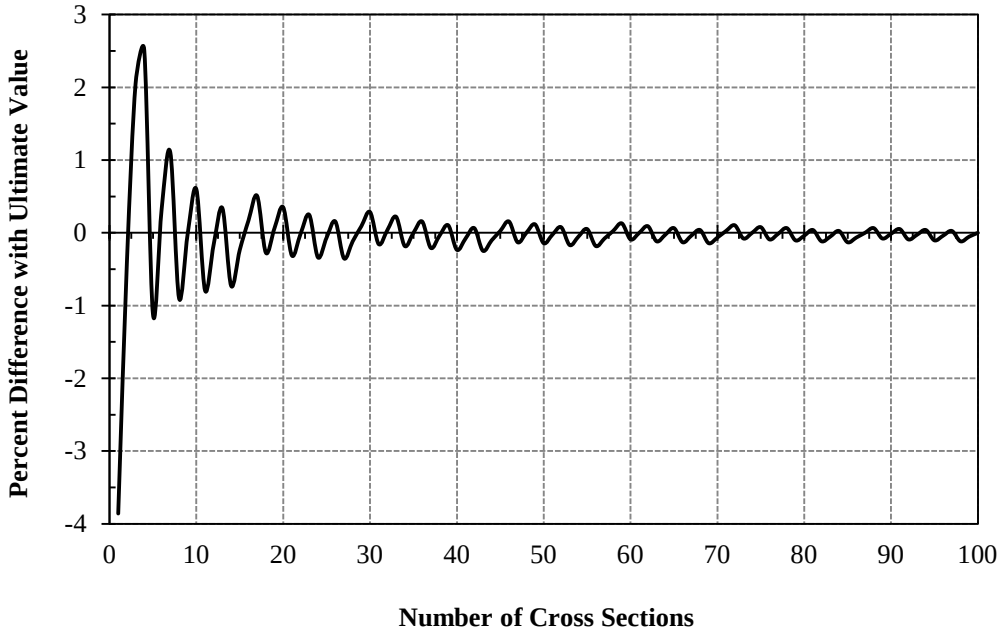

Figure 3-19: Percent Difference in 28-Day Midspan Camber

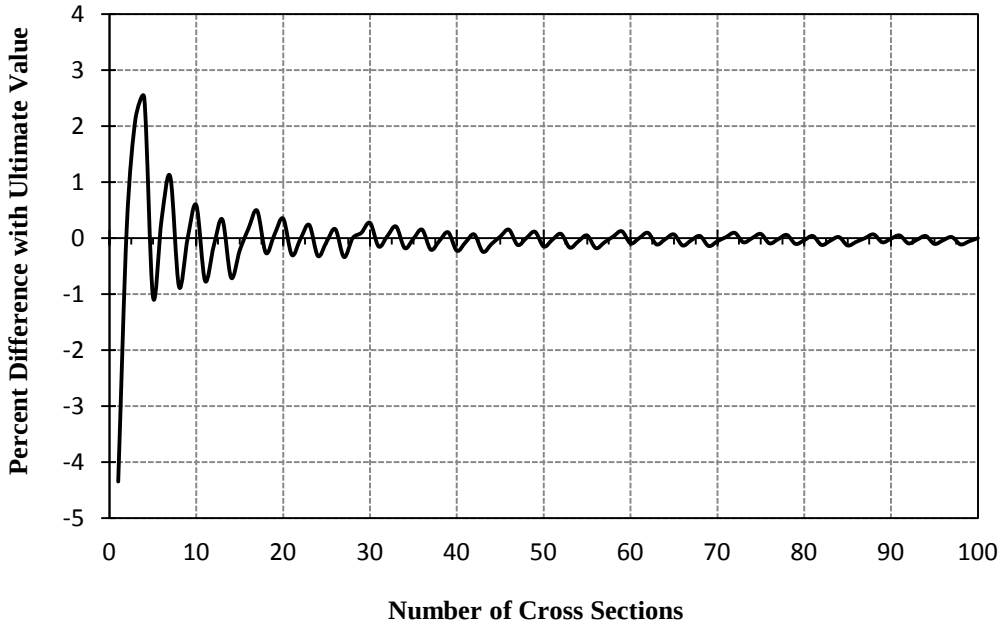

Figure 3-20: Percent Difference in 365-Day Midspan Camber

Percent difference plots were also generated based on ultimate values corresponding to 20, 30, 40, and 50 cross sections. Figures I-1 through I-3 in Appendix I compare these various plots to the percent difference plot based on 100 cross sections. The percent difference remains fairly consistent for a given number of cross sections regardless of the time at which camber is calculated.

3.4.2 SELECTION SUMMARY

Based on the discretization analyses performed on the number of time intervals and cross sections, standardized intervals were selected to further execute the computer program and analyze the prediction models. Considering the plateau effect shown on various graphical results when increasing the number of time intervals, forty was chosen as the standard number of time intervals (TI) to be taken over any given period of time. Taking a closer look at the oscillating patterns, which decrease as the number of cross sections increase, thirty-five was chosen as the standard number of cross sections (CS) to be taken along half of the girder length. The standard intervals (TI = 40 and CS = 35) were used for all camber program runs as shown in the program input summary in Chapter 4. Note the program output screens display results for the first 40 cross sections (from midspan to the end of the girder) and the first 40 time intervals only (from transfer to the total analysis time).

CHAPTER FOUR

EXPERIMENTAL METHODS

4.1 INTRODUCTION

Experimental measurements from multiple research studies were used to analyze the camber prediction models included in the Visual Basic (VB) program. The experimental program developed for this thesis was part of a larger ALDOT-sponsored program which included research by Boehm (2008). Previous research by Levy (2007) and Stallings, Barnes, and Eskildsen (2003) also generated relevant data that were used to further analyze the VB program. The following sections summarize these three experimental programs.

4.2 EXPERIMENTAL PROGRAM

The Alabama Department of Transportation (ALDOT) sponsored an investigation by the Auburn University Highway Research Center to study the effects of self-consolidating concrete (SCC) in precast, prestressed concrete bridge girders. As part of the overall study, Boehm (2008) examined the structural behavior of SCC in full-scale bridge girders. The experimental program used in this thesis utilized the girders from the Boehm (2008) research. This section presents the portion of the research data relevant to this study.

The full-scale AASHTO Type I bridge girders were 40-ft long and pretensioned with eight prestressing strands. The bottom layer of prestress consisted of six strands located three inches from the bottom of the girder. An additional two strands were located three inches from

the top of the girder. All prestressing steel was ½-in. "special", low-relaxation, Grade 270, seven wire prestressing strand. According to the reported values from the manufacturer, the "oversized" strand had a cross-sectional area of 0.164 in.^{2}, an elastic modulus of 28,900 ksi and diameter of 0.515 inches. Figure 4-1 shows a typical cross section.

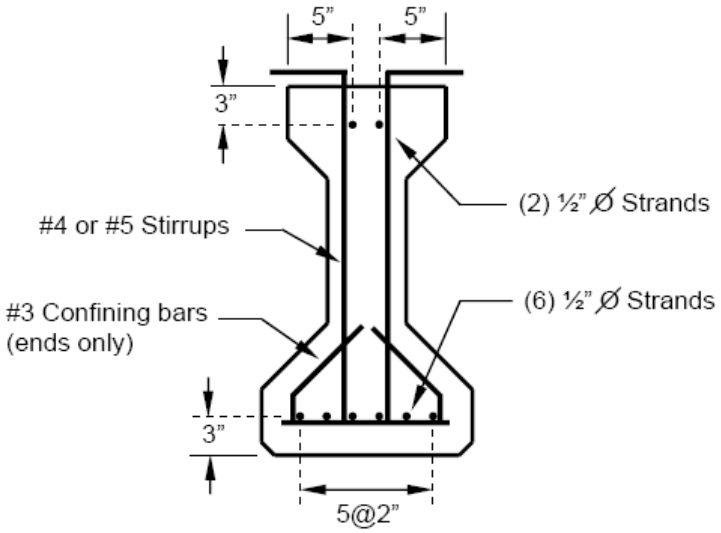

Figure 4-1: AASHTO Type I Girder Cross Section (Boehm 2008)

A total of six girders were constructed at the Hanson Prestress Plant in Pelham, Alabama. To study the effects of SCC, two girders were cast with conventional concrete and four girders were cast with SCC. Boehm (2008) introduced a specimen identification system to distinguish among the six test specimens. The identification system is summarized in Figure 4-2 and will be used throughout this study.

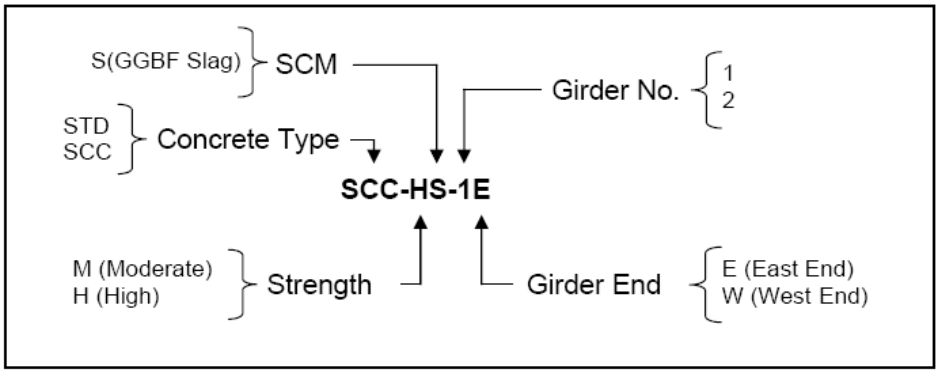

Figure 4-2: AASHTO Type I Girder Identification (Boehm 2008)

In addition to the cross section properties, material properties for each girder are also pertinent for camber analysis. Table 4-1 summarizes the fresh concrete properties for the conventional, moderate-strength SCC, and high-strength SCC mixtures.

Table 4-1: Summary of Fresh Concrete Properties (Boehm 2008)

PROPERTIES	MIXTURE					
	STD-M		SCC-MS		SCC-HS	
	-1	-2	-1	-2	-1	-2
Water / Cement	0.42		0.36		0.28	
Sand / Aggregate	0.37		0.47		0.46	
Slump Flow (in.)	6.75	6.5	26.25	27.75	28	28.25
Unit Weight (lb/ft^3)	Unknown	Unknown	148.5	150.3	153.6	153.2
Air (%)	3.4	3	3.8	1.8	1.5	1.5
VSI	—	—	1.5	1	1	1
T-50 (sec.)	—	—	4.5	3.1	Unknown	5
J-ring (in.)	—	—	26.25	28.6	28	26.25
L-Box (H_1/H_2)	—	—	0.67	0.86	0.8	Unknown

Boehm (2008) performed several hardened concrete property tests. The results are summarized in Table B-2 in Appendix B. The results using the match cured samples were selected for the initial concrete strength and modulus of elasticity values. The 28-day strength

and modulus of elasticity values were based on the ASTM 6x12 cylinder tests. The hardened concrete properties used for camber analysis are summarized in Table 4-2.

Table 4-2: Summary of Hardened Concrete Properties Reported by Boehm (2008)

Girder ID	f'_{ci} (psi)	E_{ci} (ksi)	f'_{c28} (psi)	E_{c28} (ksi)
STD-M-1	4780	5700	6600	6750
STD-M-2	4780	5700	7200	7300
SCC-MS-1	5540	5250	9780	7400
SCC-MS-2	5540	5250	9790	7500
SCC-HS-1	10430	7000	13160	8600
SCC-HS-2	10430	7000	13580	8300

Figure 4-3 shows the placement of curing blankets over a girder. Accelerated (steam) curing was applied to the two standard concrete girders for a period of 18 hours. Curing of the SCC girders was not accelerated and lasted 18 hours. The curing details are summarized in Table 4-3.

Figure 4-3: Placement of Curing Blankets (Boehm 2008)

Table 4-3: Curing Details used by Boehm (2008)

Girder ID	Curing Type	Length (hours)
STD-M-1	Accelerated	18
STD-M-2	Accelerated	18
SCC-MS-1	Non-accelerated	18
SCC-MS-2	Non-accelerated	18
SCC-HS-1	Non-accelerated	18
SCC-HS-2	Non-accelerated	18

The girders were transported to the Auburn University Structural Research Laboratory where a 48 in. by 3.5 in. deck was added to each girder. Bridge overhang brackets and plywood formwork were used to cast the deck. The deck and girder cross section is shown in Figure 4-4.

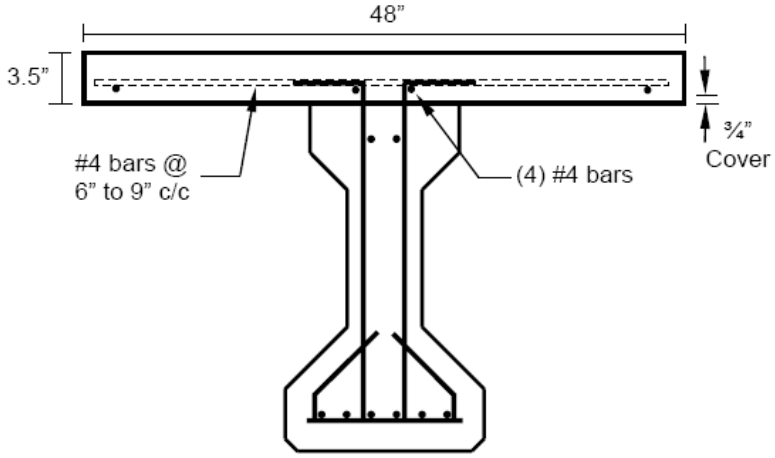

Figure 4-4: Typical Cast-in-Place Deck Details (Boehm 2008)

4.3 DATA ACQUISITION

Strain, temperature, and camber data were collected on the prestressed bridge girders previously described in this chapter. Strain and temperature readings were taken for each girder at various times after casting. Camber measurements for each girder were taken immediately before transfer and with each strain reading thereafter. Ambient temperature and relative humidity were also recorded once the girders were moved to the Auburn University Structural Research Laboratory. The following sections provide more details on how the strain, temperature, and camber data were collected.

4.3.1 STRAIN MEASUREMENTS

The Geokon Model VCE-4200 vibrating wire strain gage (VWSG) was used to measure strains in the prestressed bridge girders. A nominal batch factor of 0.96 was provided by the manufacturer based on calibration results for the 4200 model. Figure 4-5 shows the VWSG and thermistor used to measure strain and temperature.

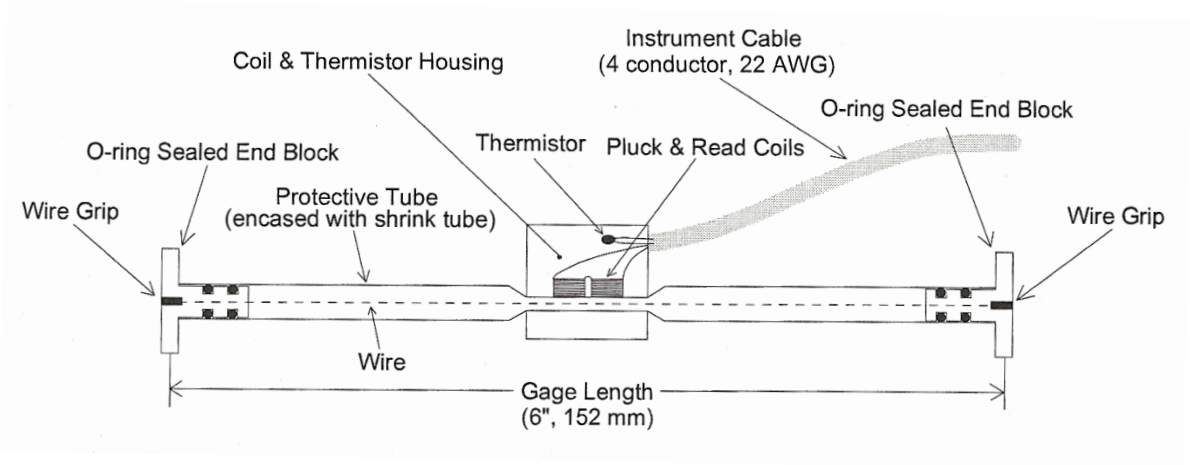

Figure 4-5: Model 4200 Vibrating Wire Strain Gage (Geokon 2007)

Before the girder forms were set in-place, three vibrating wire strain gages were installed at midspan of each girder: one at the top, middle, and bottom of the girder cross section. The strain gages were mounted along the centerline of the cross section using standard rebar ties. All VWSG locations were measured from the bottom of the girder. Table 4-4 summarizes the VWSG locations in each girder.

Table 4-4: Vibrating Wire Strain Gage (VWSG) Locations

Girder ID	Top VWSG	Middle VWSG	Bottom VWSG
STD-M-1	24.38”	11.88”	3.25”
STD-M-2	23.50”	12.38”	3.25”
SCC-MS-1	24.25”	12.75”	3.25”
SCC-MS-2	24.13”	12.88”	3.25”
SCC-HS-1	24.25”	12.88”	3.00”
SCC-HS-2	24.06”	13.00”	3.38”

A fourth strain gage was installed in each girder after the reinforcement for the cast-in-place deck was secured. The VWSG was placed at approximately mid-depth of the deck at midspan. Figure 4-6 shows a typical VWSG secured to the deck reinforcement.

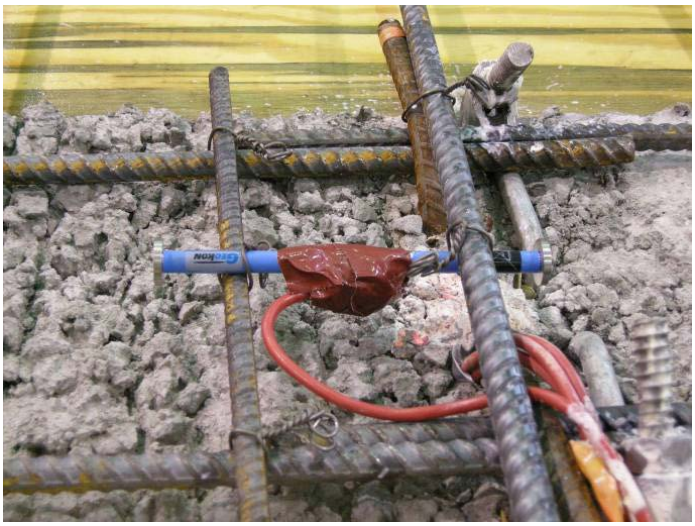

Figure 4-6: Typical Vibrating Wire Strain Gage at Deck

The strain and temperature readings were recorded using Campbell Scientific's CR10X automatic data acquisition system. The CR10X is a fully programmable data logger containing several "instructions" with built-in computations. Instruction 28 was used to measure the vibrating wire strain. The built-in function excites the vibrating wire sensor with a swept frequency and measures the response period (T) in milliseconds. Instruction 4 was used to read the vibrating wire temperature sensor.

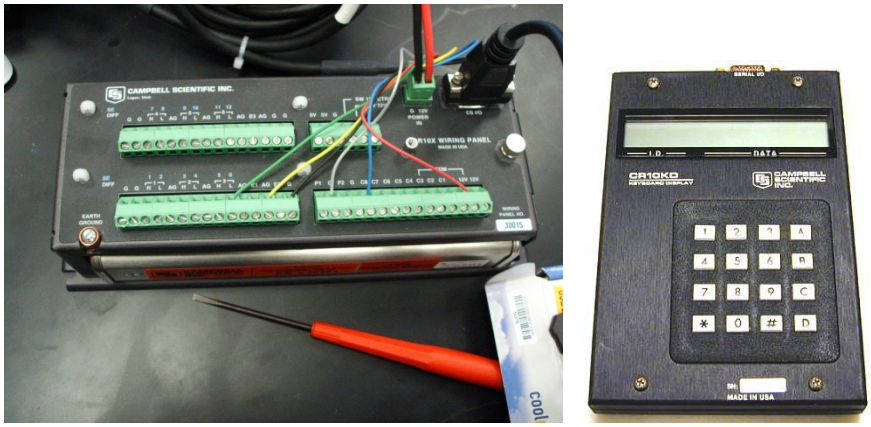

Figure 4-7: CR10X Data Logger and Keyboard

Initial strain and temperature readings were taken shortly after casting of each girder. VWSG readings continued to be recorded at various times until superimposed loads were applied for testing. Table 4-5 shows the time period strain and temperature readings were taken for each girder. All VWSG reading times are in days and are relative to transfer, hence the negative values for the initial readings taken shortly after casting.

Table 4-5: VWSG Reading Times Relative to Transfer

Girder ID	Initial Reading (days)	Final Reading (days)	Total Time (days)
STD-M-1	-0.86	109.98	110.84
STD-M-2	-0.86	109.98	110.84
SCC-MS-1	-0.95	159.92	160.87
SCC-MS-2	-0.95	166.92	167.86
SCC-HS-1	-0.93	214.02	214.95
SCC-HS-2	-0.93	214.02	214.95

When calculating the strain at each gage location, two reference points were established: post-casting and pre-transfer. As shown in the Appendix E tables, the strain readings immediately after casting were 20με to 150με higher than the readings taken prior to release. However, this was not the case with STD-M-2 which had relatively constant readings between casting and transfer. A closer look at the strain results based on the post-casting and pre-transfer reference points is covered in Chapter 5.

4.3.2 Camber Measurements

A surveyor's level and 0.01-inch-precision steel rule were used to measure camber in the prestressed bridge girders. The rule was mounted on stadia rod, which was placed at each

measurement point. Measurements were taken at five points along the length of each girder. These points were centered on top of the girder and located at the east end, east-end quarter span, midspan, west-end quarter span, and west end. Table 4-6 shows the distance, in inches, from these five points to the east end of the girder. The east end was established for reference purposes only and was based on the girder position in the prestress bed. Two to four level readings were taken at each location for a single camber measurement. The reading averages were used to calculate the camber at that given time.

Table 4-6: Level Reading Locations Relative to East End of Girder

Reading Location from East End (in.)	East End	East ¼	Midspan	West ¼	West End
	2	120	240	360	248

The method for measuring camber previously described was not feasible for times between the deck being poured and the end of its curing period. The deck was cured with wet burlap and polyethylene plastic for approximately three days. During this time, camber was measured using a calibrated gauge located directly under the girder at midspan. Once curing of the concrete deck was completed, level reading points were marked on top of the deck at the same locations shown in Table 4-6.

Camber was measured each time strain and temperature readings were taken. The date and time were recorded for every set of strain, temperature, and camber measurements. This information was used to calculate the "age" of the girder which was expressed in days after transfer. The current weather conditions were recorded while the girders were at the prestress plant. Ambient temperature and relative humidity were recorded for every measurement once

the girders were located in the Auburn University Structural Research Laboratory. The camber results for each girder are presented in Chapter 5.

4.4 PREVIOUS RESEARCH

Previous research was used to further analyze the strain and camber prediction accuracy of the Visual Basic (VB) program covered in Chapter 3. The following sections summarize the research by Levy (2007) and Stallings, Barnes, and Eskildsen (2003) relevant to this study. Research by Levy generated camber measurements while the research by Stallings et al. included camber and strain measurements.

4.4.1 LEVY (2007)

To research bond behavior of prestressed reinforcement, Levy tested sixteen eccentrically prestressed T-beams. One conventional concrete mixture and three self-consolidating concrete (SCC) mixtures were used. The mix designs are shown in Table C-1 located in Appendix C. Four T-beams with varying lengths (9'-8", 13'-0", 16'-4" and 23'-0") were constructed for each of the four concrete mixtures. As shown in Figure 4-8, the prestressed reinforcement consists of two seven-wire, low-relaxation, Grade 270 ½" special diameter strands (0.164 $in.^2$). The compression reinforcement consists of four Grade 60 No. 3 reinforcing bars. Figure 4-9 shows the specimen identification used for Levy's research.

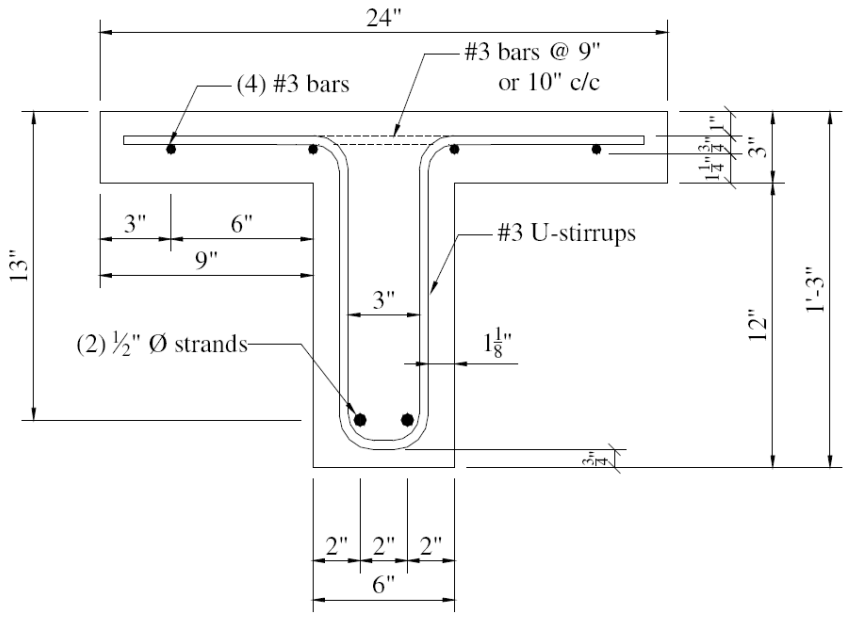

Figure 4-8: T-Beam Cross Section (Levy 2007)

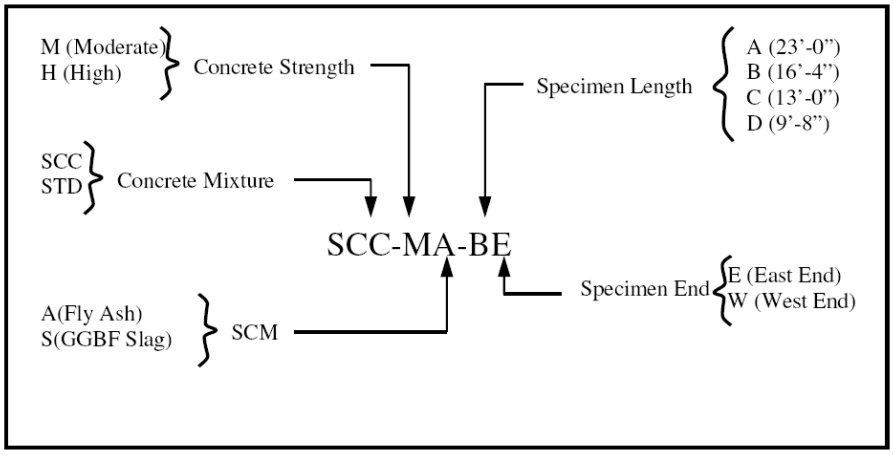

Figure 4-9: T-Beam Identification System (Levy 2007)

Levy (2007) conducted fresh and hardened concrete property testing on all mixtures. The fresh and hardened concrete properties are summarized in Table C-2 and C-3, respectively.

The strand stresses immediately before transfer (f_{pbt}) and immediately after transfer (f_{pt}) are summarized for each T-beam in Table 4-7. However, as stated in Chapter 3, the program calculates f_{pbt} and f_{pt} based on the jacking stress (f_{pj}) defined by the user.

Table 4-7: Summary of Specimen Material Properties (Levy 2007)

Specimen	f'_{ci} (psi)	f_{pbt} (ksi)	f_{pt} (ksi)	$f_{pe,4}$ (ksi)	Transfer Length (in.)			
					Live End		Dead End	
					Initial	4-day	Initial	4-day
STD-M-A	5000	209	197	193	34.0	32.0	22.0	22.0
STD-M-B		202	190	186	24.0	26.5	27.0	27.5
STD-M-C		202	191	188	21.0	24.0	24.0	24.5
STD-M-D		209	197	192	32.0	32.5	19.0	23.5
SCC-MA-A	5500	200	189	184	21.0	25.5	19.0	22.0
SCC-MA-B		196	184	178	27.5	28.5	21.5	22.0
SCC-MA-C		196	186	180	23.5	26.0	21.0	26.0
SCC-MA-D		200	189	183	23.5	26.0	20.0	26.0
SCC-MS-A	5300	211	200	196	31.0	31.0	20.0	20.5
SCC-MS-B		207	196	192	40[a]	44[a]	20.5	22.0
SCC-MS-C		207	195	191	43.5	44.5	25.0	24.0
SCC-MS-D		211	199	194	37.5	40.0	16.5	17.0
SCC-HS-A	9990	210	201	197	18.0	20.5	14.0	18.0
SCC-HS-B		210	200	197	20.0	19.0	12.0	14.0
SCC-HS-C		210	201	197	20.5	22.0	11.0	14.0
SCC-HS-D		210	200	196	25.0	25.5	16.0	19.5

NOTE: [a] Value estimated using maximum strain on opposite end of specimen.

An iterative process was used to calculate the jacking stress associated with the specified f_{pbt} values given in Table 4-7. The jacking stress used in the first iteration was determined by adding an assumed initial steel relaxation loss of 2 ksi to the stress immediately before transfer. The actual steel relaxation loss and f_{pbt} were then calculated based on the jacking stress. This

process continued until the calculated f_{pbt} matched the specified value. Table 4-8 summarizes of the required jacking stress based on the given f_{pbt} for each T-beam.

Table 4-8: Calculated f_{pj} based on given f_{pbt} Values

Beam ID	$f_{pj,req'd}$ (ksi)	$f_{pbt,calc}$ (ksi)	$f_{pbt,actual}$ (ksi)	Δf_{pbt} (ksi)
STD-M-A	212.4	209.0	209	0
STD-M-B	205.0	202.0	202	0
STD-M-C	205.0	202.0	202	0
STD-M-D	212.4	209.0	209	0
SCC-MA-A	202.2	200.0	200	0
SCC-MA-B	198.0	196.0	196	0
SCC-MA-C	198.0	196.0	196	0
SCC-MA-D	202.2	200.0	200	0
SCC-MS-A	214.5	211.0	211	0
SCC-MS-B	210.3	207.0	207	0
SCC-MS-C	210.3	207.0	207	0
SCC-MS-D	214.5	211.0	211	0
SCC-HS-A	213.7	210.0	210	0
SCC-HS-B	213.7	210.0	210	0
SCC-HS-C	213.7	210.0	210	0
SCC-HS-D	213.7	210.0	210	0

4.4.2 STALLINGS, BARNES, AND ESKILDSEN (2003)

Stallings et al. (2003) studied camber and prestress losses in high performance concrete (HPC) bridge girders. The experimental program included field and laboratory measurements on five AASHTO BT-54 girders. The girders were instrumented with vibrating wire strain gages, thermocouples, and electrical resistance strain gages. Similar to this study, the data was recorded using the Campbell Scientific CR10X data logger.

The concrete mix design used for all BT-54 girders is shown in Table D-1 located in Appendix D. An average modulus of elasticity of 5740 ksi was calculated using the test results for 32 cylinders at various ages from release to 56-days.

The cross section details in Figure 4-10 show the prestressed strand pattern at midspan and at the end of the girder. The hold down point and slope of the draped strands can be seen in the typical BT-54 girder elevation in Figure 4-11. The span length for all girders was equal to 112.25 ft with 7½ in. bearing at each end.

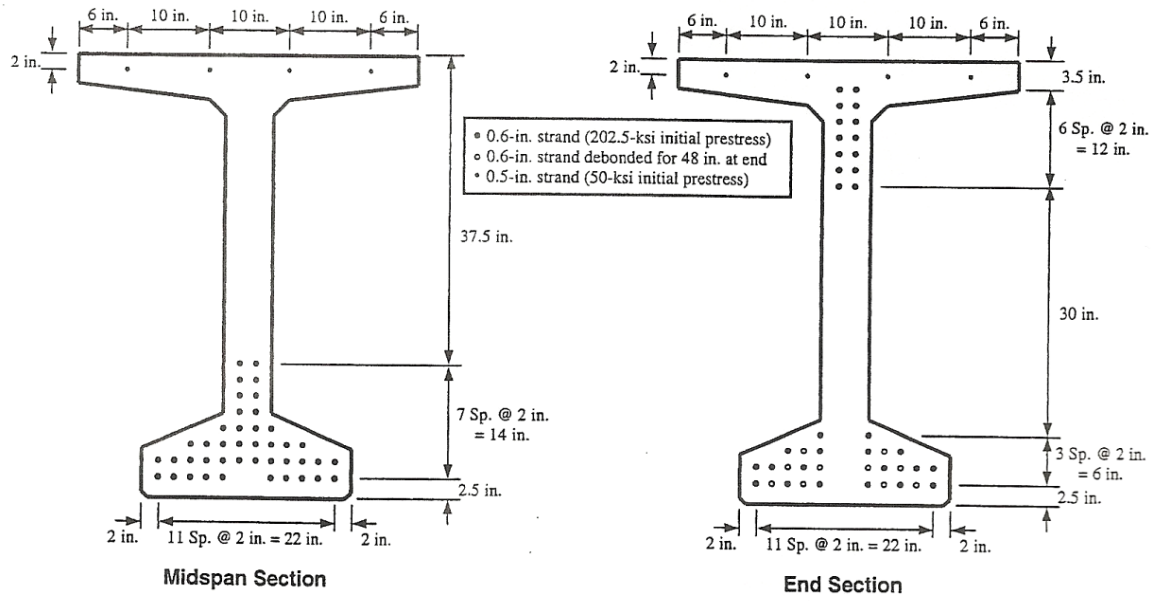

Figure 4-10: BT-54 Cross Section Details (Stallings et. al 2003)

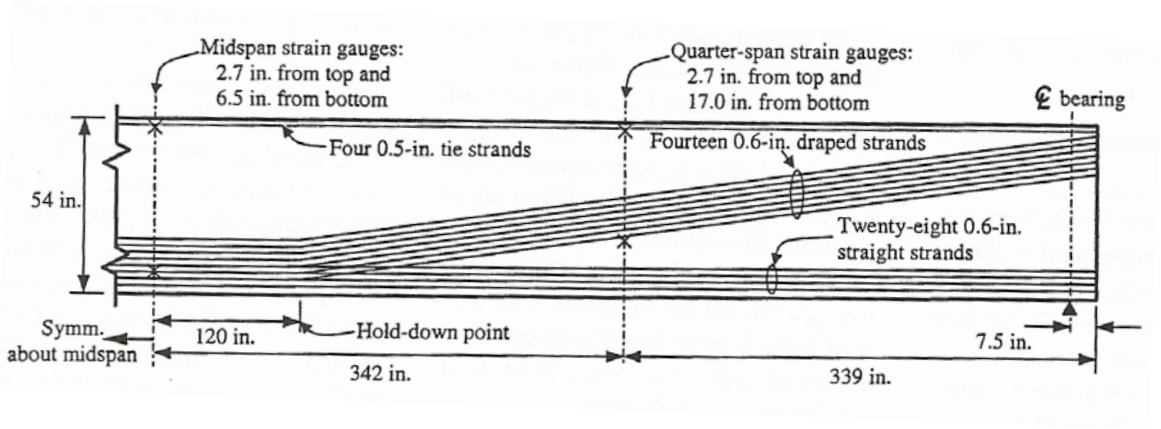

Figure 4-11: Typical BT-54 Girder Elevation (Stallings et. al 2003)

4.5 PROGRAM INPUT

The research by Boehm (2008), Levy (2007), and Stallings et al. (2003) provides 23 unique cases to evaluate the program output. The detailed identification systems shown in Figures 4-2 and 4-9 were used to distinguish among the six AASHTO Type I girders and sixteen T-beams.

4.5.1 PROPERTY AND EVENT SUMMARY

Table H-1 located in Appendix H summarizes information collected from the Boehm (2008), Levy (2007), and Stallings et al. (2003) research. The table is formatted based on the specimen identification systems introduced in Section 4.4 and the VB program's input forms. The table includes information on the cross section properties, concrete mix design, fresh and hardened concrete properties, prestressing and reinforcing steel properties, jacking and transfer times, and curing details. The data presented in Table H-1 were used to complete the program's input screens shown in Figures K-2 through K-4, K-6, K-11, and K15.

Two slump values are provided for each AASHTO Type I girder, T-beam, and BT-54 girder. The first value is an "adjusted" slump based on mixture proportions. The adjusted value accounts for low water content and is equivalent to a "water slump" estimated assuming there are

no water-reducing admixtures in the mixture. The second value is the actual slump (for conventional mixtures) or slump flow (for SCC mixtures) measured during testing. A comparison between using the measured and "adjusted" values is covered in the sensitivity analysis in Chapter 6.

The concrete mixture designs for the AASHTO Type I and BT-54 girders specified limestone aggregate. The CEB 90 concrete MOE model specifies varying correction factors for either dense or regular limestone (see Table 2-4). Therefore, an approximate average of 1.0 was used as the correction factor for the source of aggregate.

4.5.2 Prestressing Stand and Reinforcing Steel Summary

Table H-2 located in Appendix H summaries the prestressing strand and reinforcing steel details for each specimen. The strand and reinforcing layouts are based the cross sections shown in Section 4.4. The data in Table H-2 are used to complete the program's input screens shown in Figures K-8 through K-10.

As previously discussed in this chapter, the jacking stresses for the T-beams were calculated based on the stresses immediately before transfer. Therefore, the f_{pj} values provided in Table H-2 match those shown in Table 4-8.

CHAPTER FIVE

RESULTS

5.1 STRAIN PREDICTIONS

As covered in Chapter 3, the Visual Basic (VB) program utilizes a variety of models for estimating concrete modulus of elasticity, creep, and shrinkage over time. This section takes a closer look at how accurately these models, and combinations thereof, predict concrete strain in a prestressed concrete section. The concrete MOE models used in the analysis include the Constant E_c, Two-Point E_c, AASHTO '05+, ACI 209, and CEB 90 models. The creep and shrinkage models include AASHTO '04-, AASHTO '05+, ACI 209, CEB 90, and modified CEB 90.

The program calculates concrete strains and stresses at the top, bottom, and centroid of the transformed section (see output screen in Figure K-27). Assuming linear elastic behavior, these strains are used to determine the strain at the top, middle, and bottom VWSG located at midspan of each girder. The predicted strains are compared to the experimental VWSG measurements for the AASHTO Type I and BT-54 girders.

5.1.1 TEMPERATURE-INDUCED STRAINS

The total strain in concrete includes the strain caused by stress, unrestrained creep and shrinkage, and temperature change. However, the program does not address thermal strains when

calculating the incremental concrete strains over time. To better evaluate the program's strain predictions, the thermal strain component of the experimental strain measurements must be removed.

The temperature effects were estimated using the thermocouple readings from the three VWSG's located at midspan of each AASHTO Type I girder. The thermocouple readings taken immediately prior to transfer were established as the point of reference when calculating the temperature change. Based on the AASHTO Type I girder cross section geometry, the zones shown in Table 5-1 were used to estimate the stresses over the cross section. The y-parameters are measured from the top of the girder where y_1 is the distance to the top of the zone and $\dot{y}$ is the distance to the centroid of the zone.

Table 5-1: AASHTO Type I Girder Zone Geometry

Parameter	A	B1	B2	B3	C	D1	D2	D3	D4	D5	E
width (in.)	12	11	9	7	6	7	9	11	13	15	16
y_1 (in.)	0	4	5	6	7	18	19	20	21	22	23
height (in.)	4	1	1	1	11	1	1	1	1	1	5
A ($in.^2$)	48	11	9	7	66	7	9	11	13	15	80
$\dot{y}$ (in.)	2.0	4.5	5.5	6.5	12.5	18.5	19.5	20.5	21.5	22.5	25.5
I ($in.^4$)	8695	1310.1	884.5	556.2	1224.2	67.4	151.3	286	483.3	755.4	8312.3

The average free temperature stress was calculated at the centroid of each zone assuming a linear temperature gradient established by the three thermocouple readings. The stress at release of restraint was calculated using the estimated force and moment required to restrain the temperature strain. As shown in Figure 5-1, the summation of the two stress components yields the net stress on the concrete section.

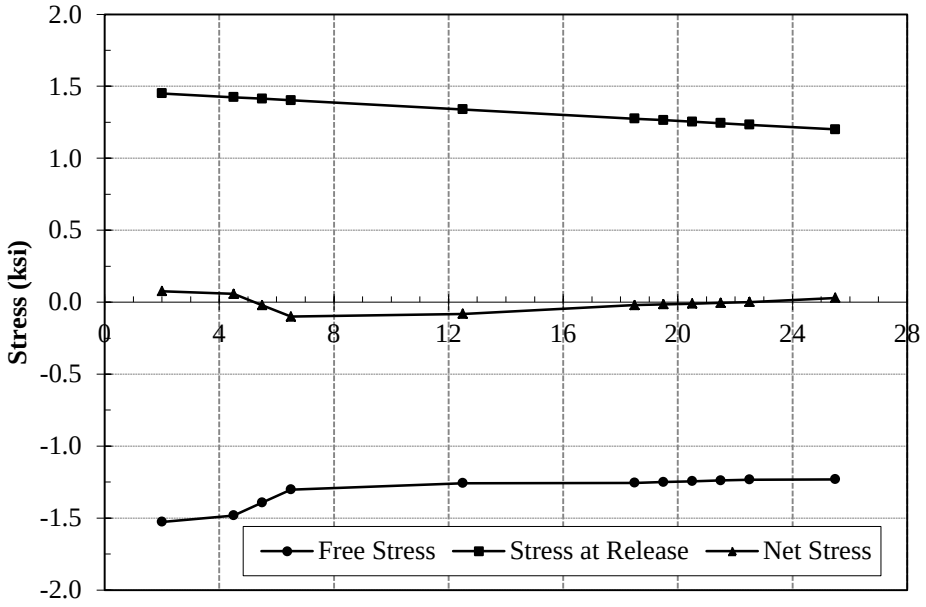

Figure 5-1: Concrete Stresses associated with Temperature Effects

Theoretically, the "stress at release" values are used to calculate the thermal strain. However, the "net stress" was used to calculate the non-linear temperature gradient on the cross section. This is due to a level of self-correction built into the VWSG's which compensates for the difference between the "net stress" and "stress at release" values. As the temperature increases, the vibrating wire becomes more flexible. The difference between the coefficient of thermal expansion for concrete (1.16×10^{-5} με/°F) and the VWSG steel (1.22×10^{-5} με/°F) must also be taken into account. Therefore, the thermal strain component can be estimated as follows:

$$\epsilon_{\Delta T} = \frac{f_{c,net}}{E_c} + \left(\alpha_c - \alpha_{vwsg}\right)\Delta T \qquad \textit{Equation 5-1}$$

where, $f_{c,net} =$ net stress on the concrete section

$\alpha_c =$ coefficient of thermal expansion for concrete

$\alpha_{vwsg} =$ coefficient of thermal expansion for the VWSG steel

$\Delta T =$ temperature change

Removing the thermal component from the total strain measurement yields a "corrected" strain that can be directly compared to the program's strain predictions. See Tables E-7 through E-9 in Appendix E for a summary of the corrected strains at each VWSG location. Figures 5-2 through 5-7 show the measured and corrected strains at the three VWSG locations for each AASHTO Type I girder.

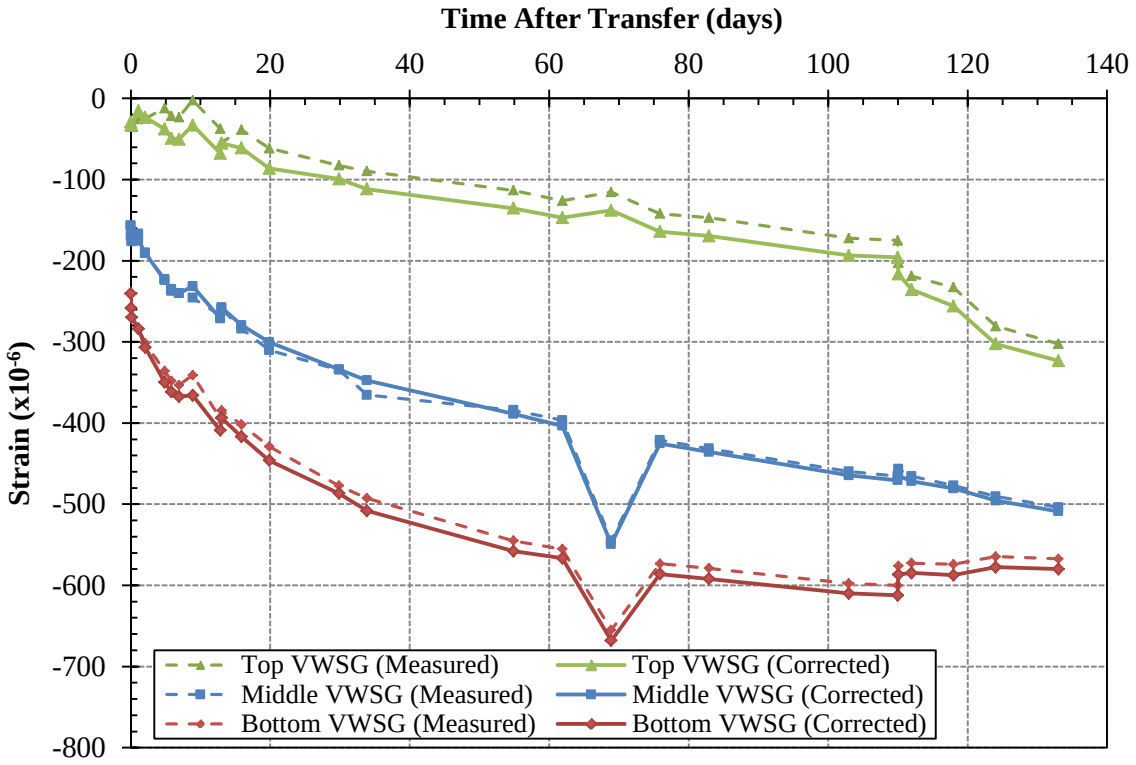

Figure 5-2: STD-M-1 VWSG Readings

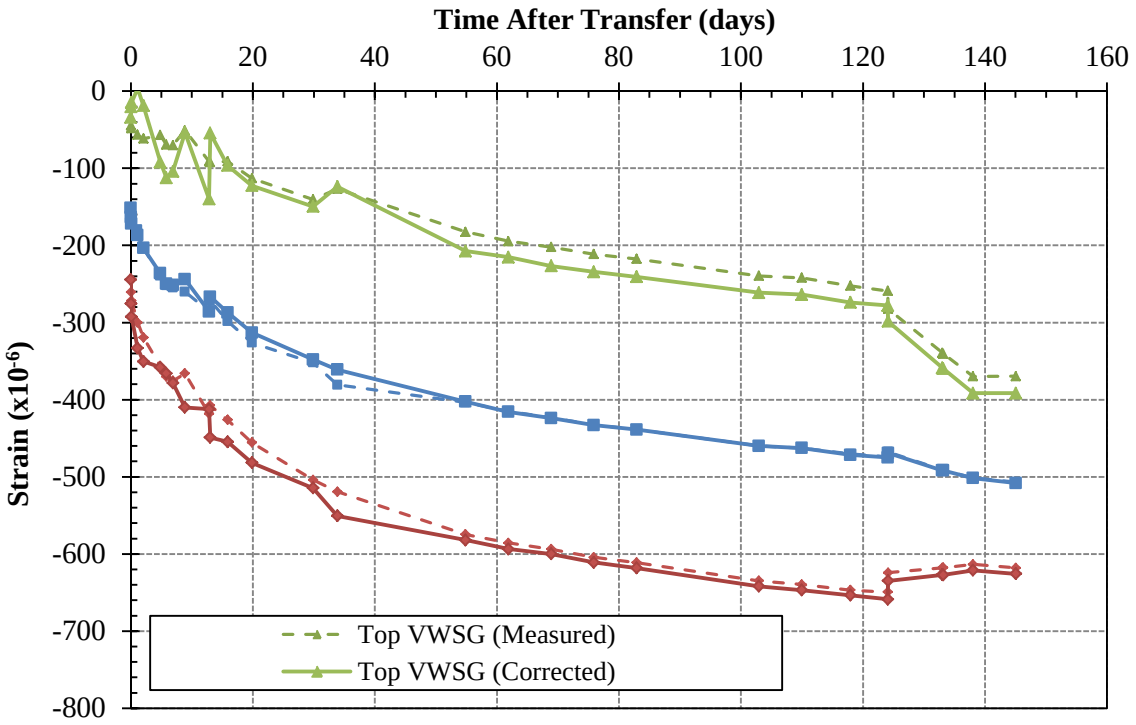

Figure 5-3: STD-M-2 VWSG Readings

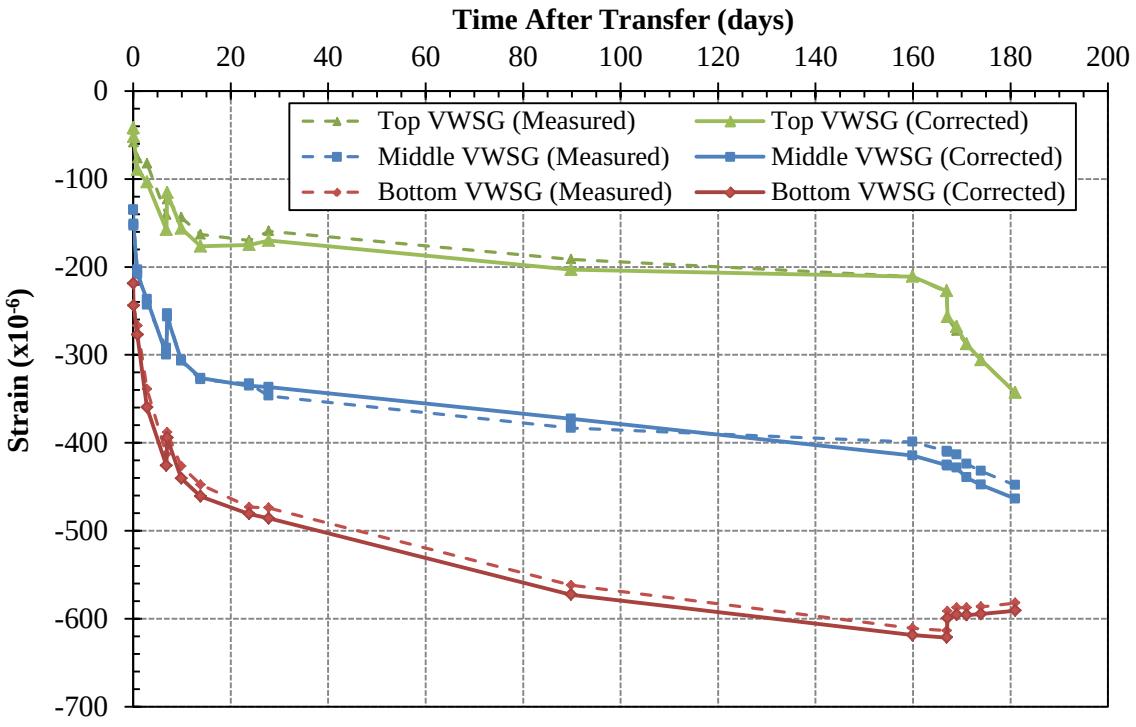

Figure 5-4: SCC-MS-1 VWSG Readings

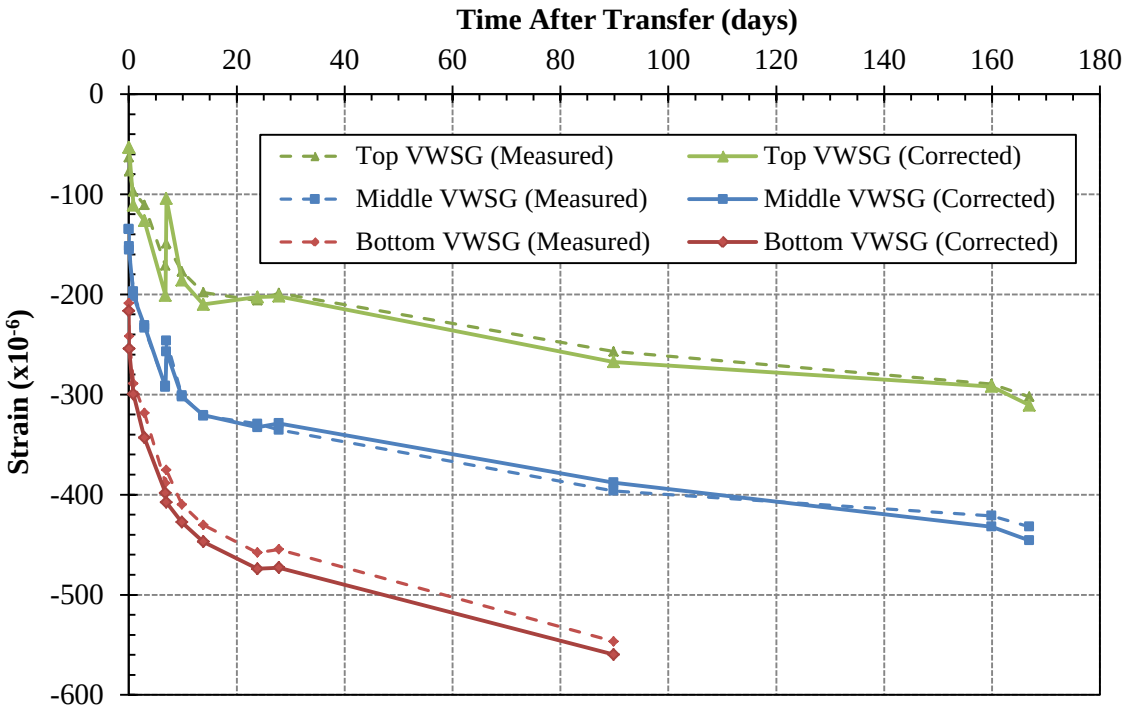

Figure 5-5: SCC-MS-2 VWSG Readings

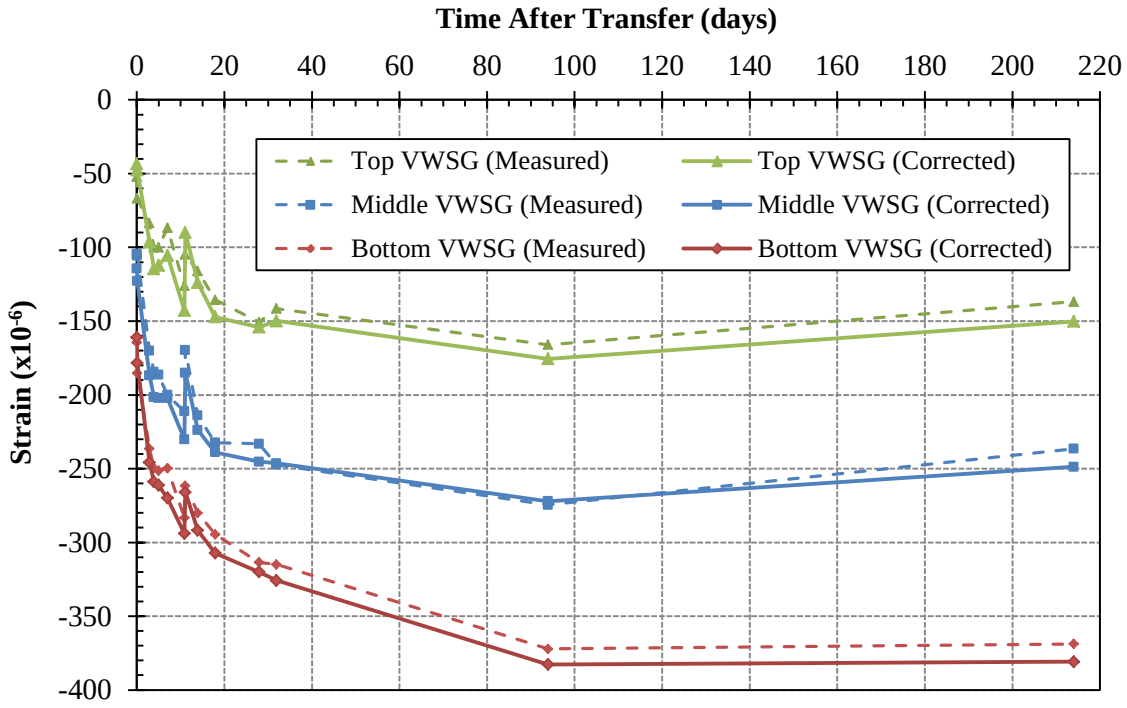

Figure 5-6: SCC-HS-1 VWSG Readings

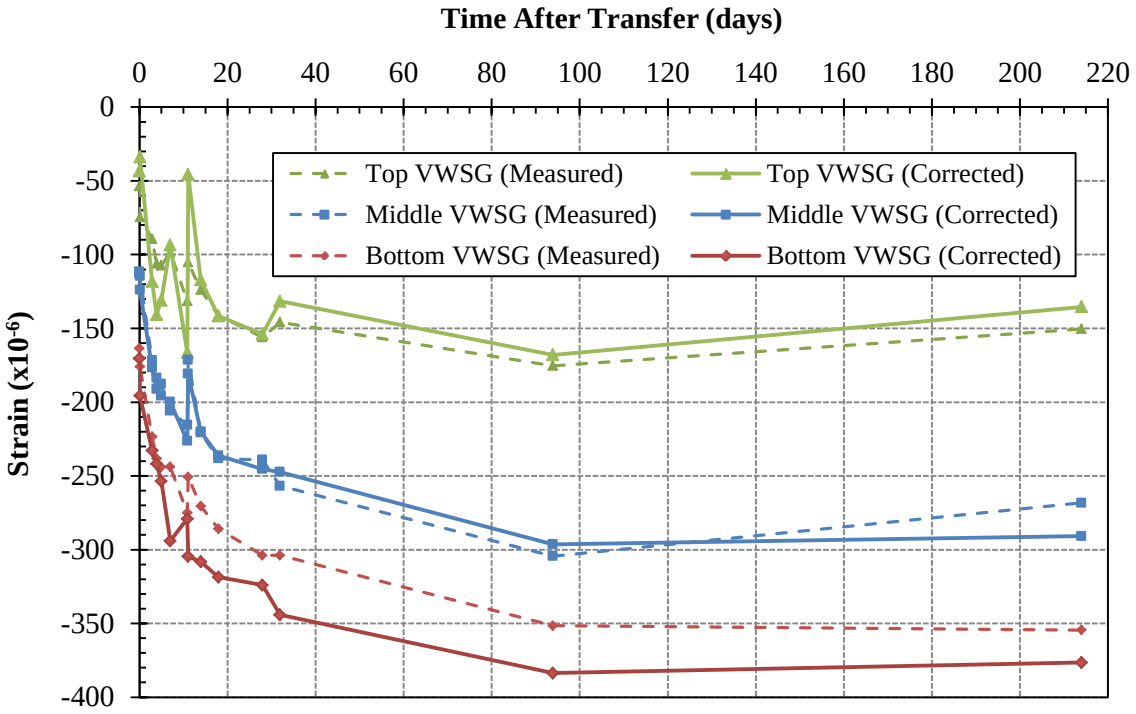

Figure 5-7: SCC-HS-2 VWSG Readings

5.1.2 AASHTO TYPE I GIRDERS

Two AASHTO Type I girders were constructed using "standard" (STD) concrete mixtures and exposed to accelerated-curing for 18 hours. For the STD girders, two sets of results are presented for the ACI 209 creep and shrinkage model: one using the slump value determined from concrete testing and the other using an "adjusted" slump value based on the mixture proportions. The results based on the "adjusted" slump are designated by ACI 209*.

Four AASHTO Type I girders were constructed using self-consolidating concrete (SCC) and exposed to non-accelerated-curing for 18 hours. High slump flow values typical to SCC mixtures cannot be input as a conventional slump value as this will cause unrealistic creep and shrinkage correction factors and strain predictions. For the results presented in this chapter, the "adjusted" slump was used in lieu of the actual slump flow for all SCC girders. The sensitivity

analysis in Chapter 6 addresses the effect of both the actual and "adjusted" slump on strain predictions. The actual and adjusted slump values for the AASHTO Type I girders are summarized in Table 5-2.

Table 5-2: Slump and Slump Flow – AASHTO Type I Girders

Girder	Actual Slump (in.)	Actual Slump Flow (in.)	Adjusted Slump (in.)
STD-M-1	6.75	NA	1
STD-M-2	6.5	NA	1
SCC-MS-1	NA	26.25	0
SCC-MS-2	NA	27.75	0
SCC-HS-1	NA	28	0
SCC-HS-2	NA	28.25	0

The AASHTO Type I results presented in this chapter are based on accelerated-curing for STD girders and non-accelerated-curing for SCC girders. The sensitivity analysis in Chapter 6 compares strain results for the SCC girders using both non-accelerated and accelerated-curing.

5.1.2.1 Strain Predictions Using Test-Based E_C Models

The program includes two test-based models for estimating the concrete modulus of elasticity over time: the "Constant E_c" model and the "Two-Point E_c" model. The "Constant E_c" model uses the measured concrete modulus of elasticity at transfer for all time intervals. The "Two-Point E_c" model estimates the concrete MOE development over time using the MOE values measured at transfer and 28 days after casting.

Figures 5-8 through 5-19 show the predicted concrete strains for the STD-M AASHTO Type I girders. Results using six different creep and shrinkage models are presented for each

test-based E_c model. The measured strain data points shown in the figures refer to the "corrected" strain measurements which neglect the effects of temperature.

Tables E-10 through E-12 in Appendix E summarize the percent errors between the measured and predicted STD-M strains shown in the figures. Strains at the top VWSG locations were generally over-estimated. However, the CEB and Modified CEB creep and shrinkage models under-estimated long-term strains at the top VWSG approximately 25 percent. The AASHTO '04 (-) and ACI 209* creep and shrinkage models best predicted long-term strains at the top and middle VWSG locations. The ACI 209 model based on the actual slump better predicted strain at the bottom VWSG's.

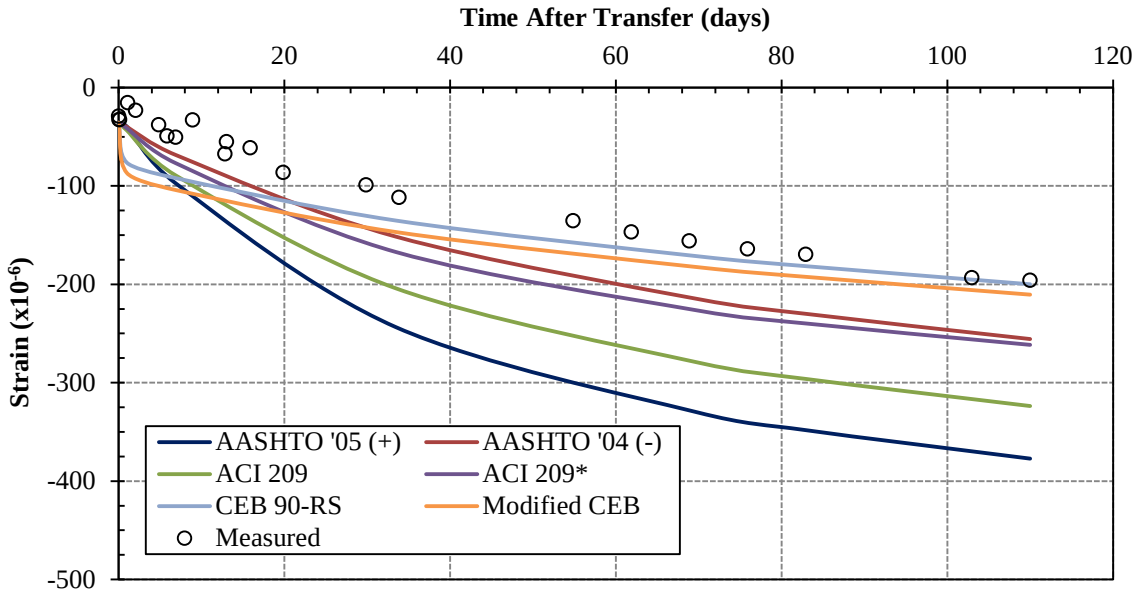

Figure 5-8: STD-M-1 Predicted Strains at Top VWSG with Constant E_c

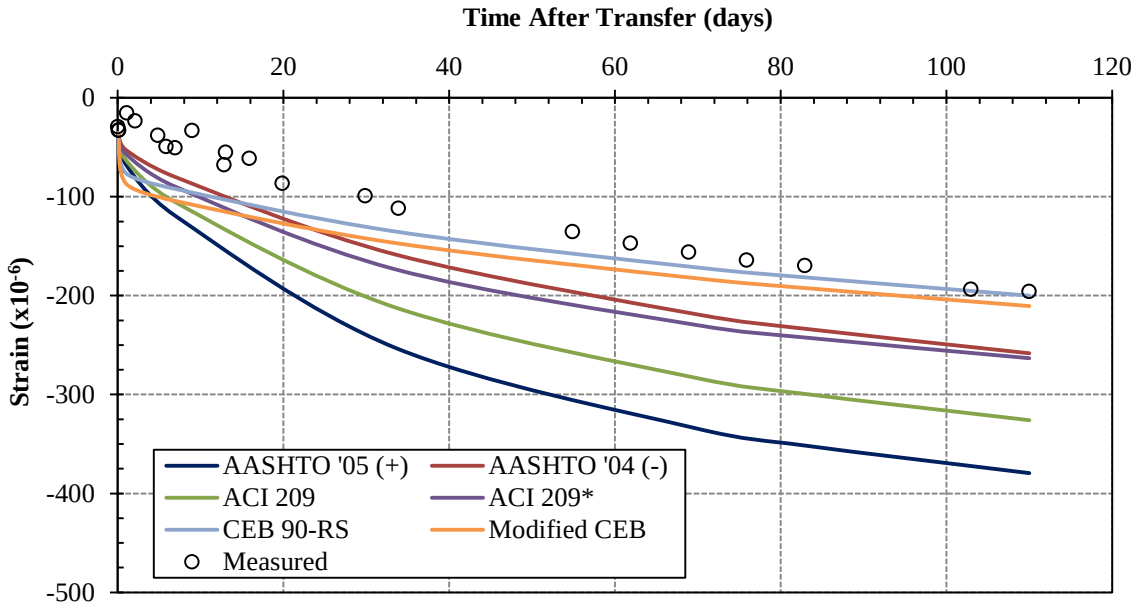

Figure 5-9: STD-M-1 Predicted Strains at Top VWSG with Two-Point E_c

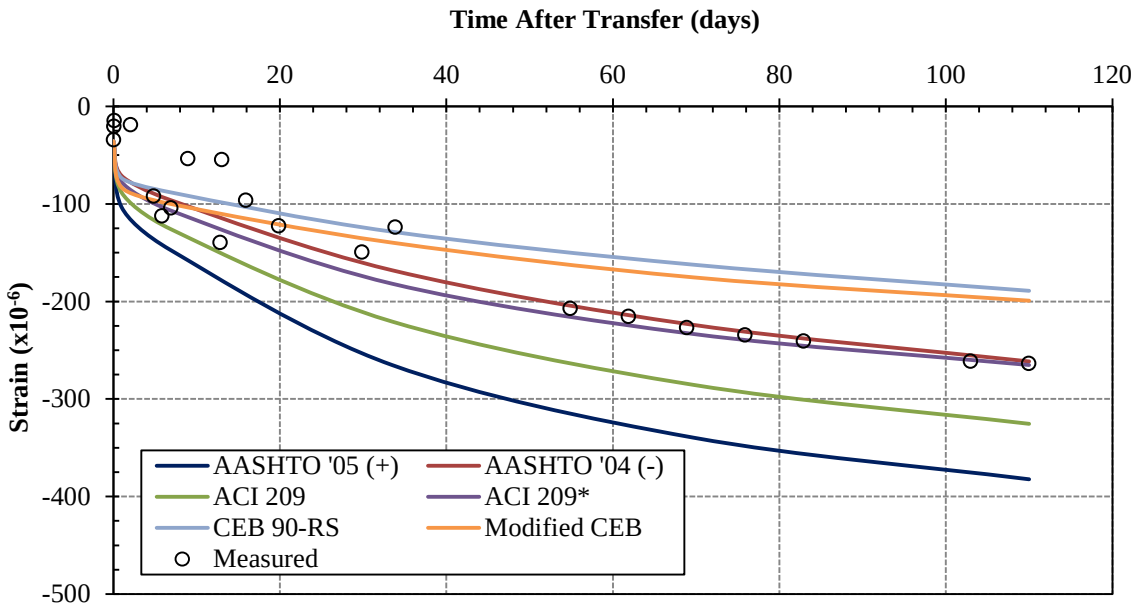

Figure 5-10: STD-M-2 Predicted Strains at Top VWSG with Constant E_c

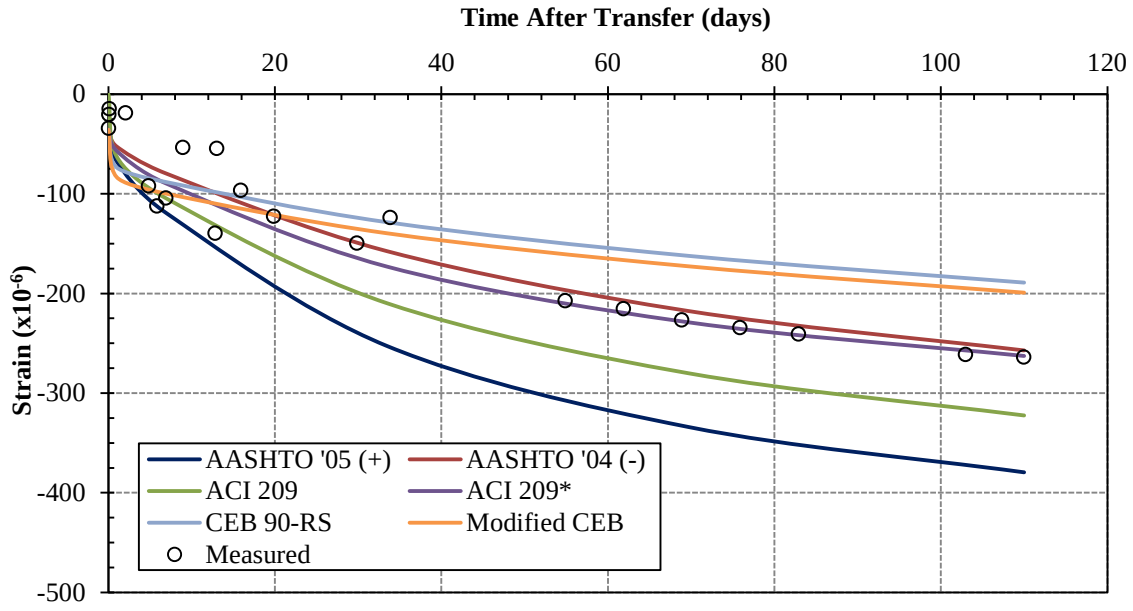

Figure 5-11: STD-M-2 Predicted Strains at Top VWSG with Two-Point E_c

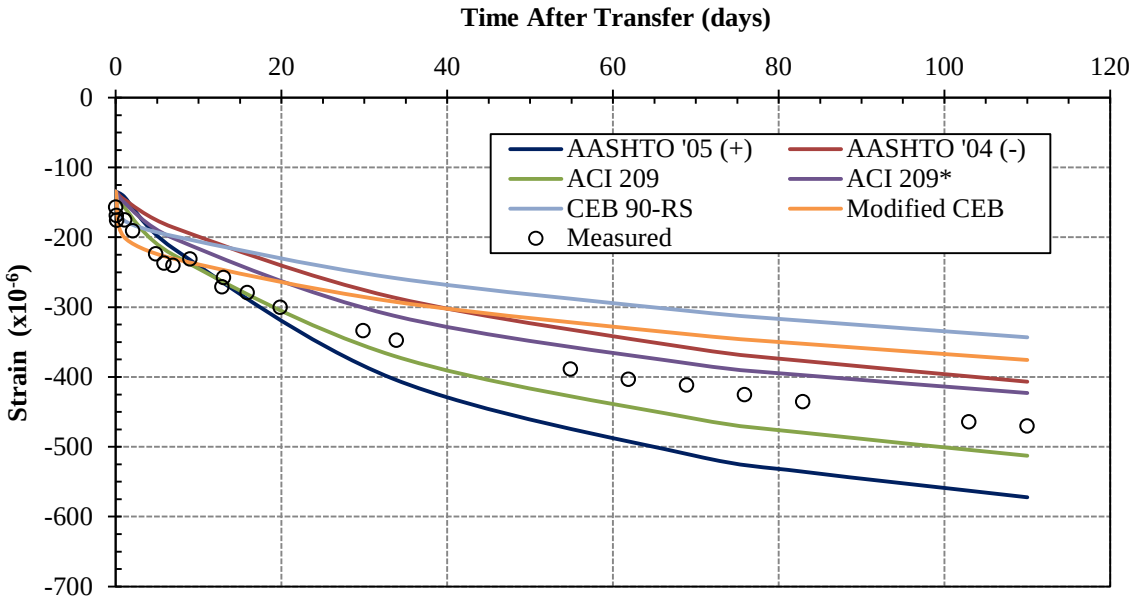

Figure 5-12: STD-M-1 Predicted Strains at Middle VWSG with Constant E_c

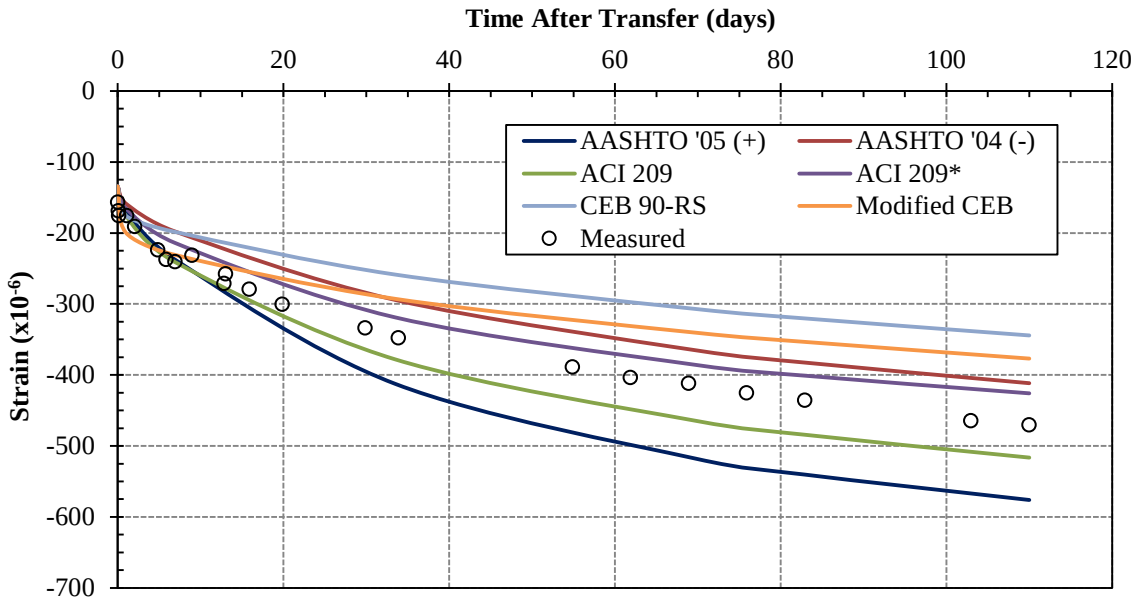

Figure 5-13: STD-M-1 Predicted Strains at Middle VWSG with Two-Point E_c

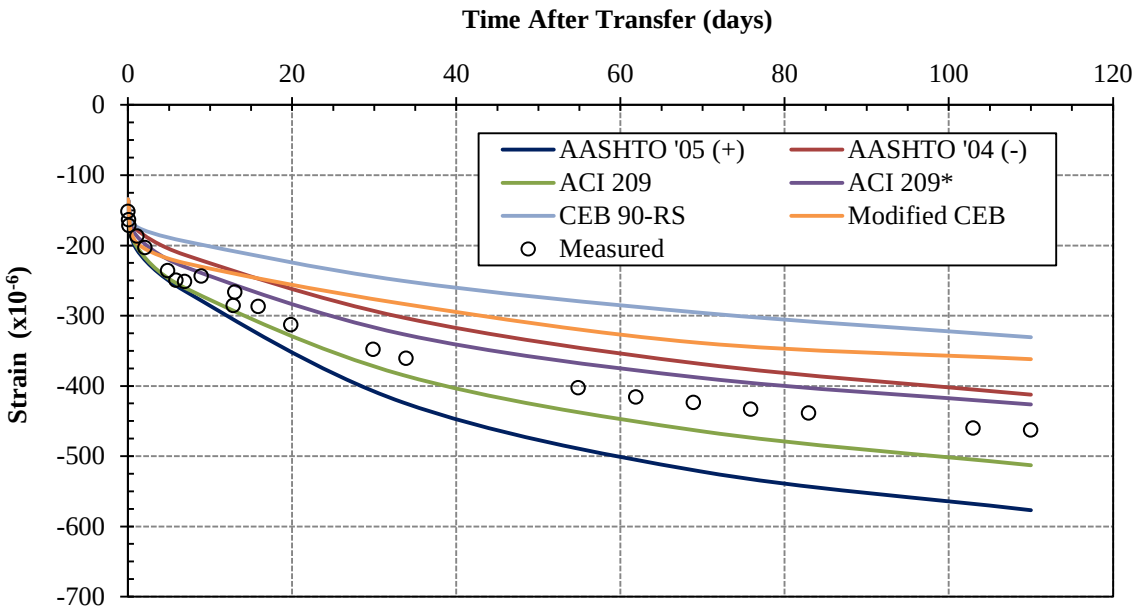

Figure 5-14: STD-M-2 Predicted Strains at Middle VWSG with Constant E_c

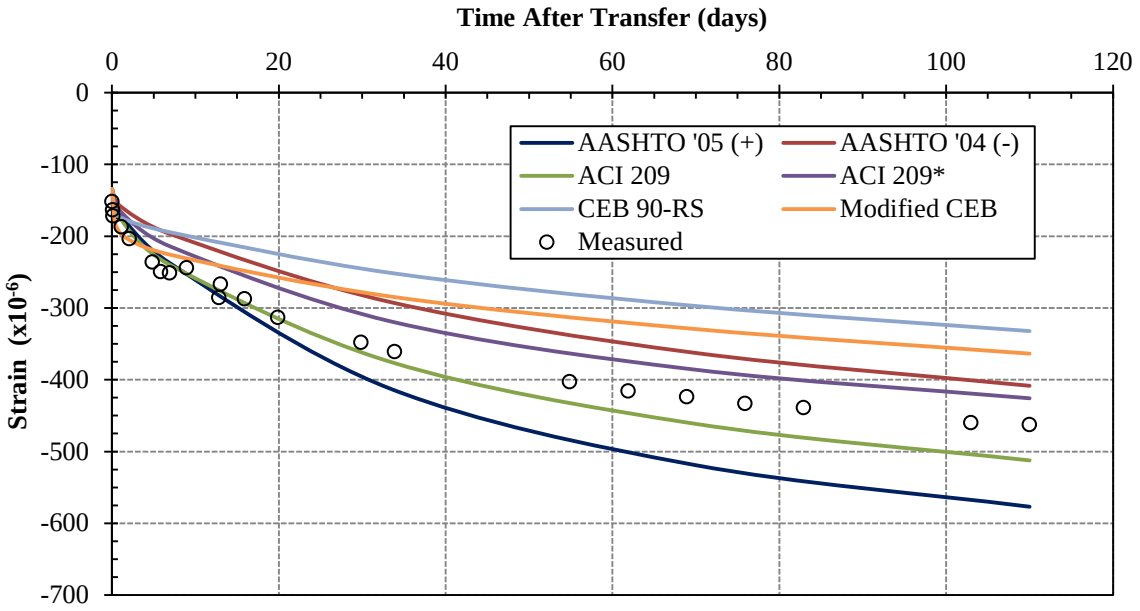

Figure 5-15: STD-M-2 Predicted Strains at Middle VWSG with Two-Point E_c

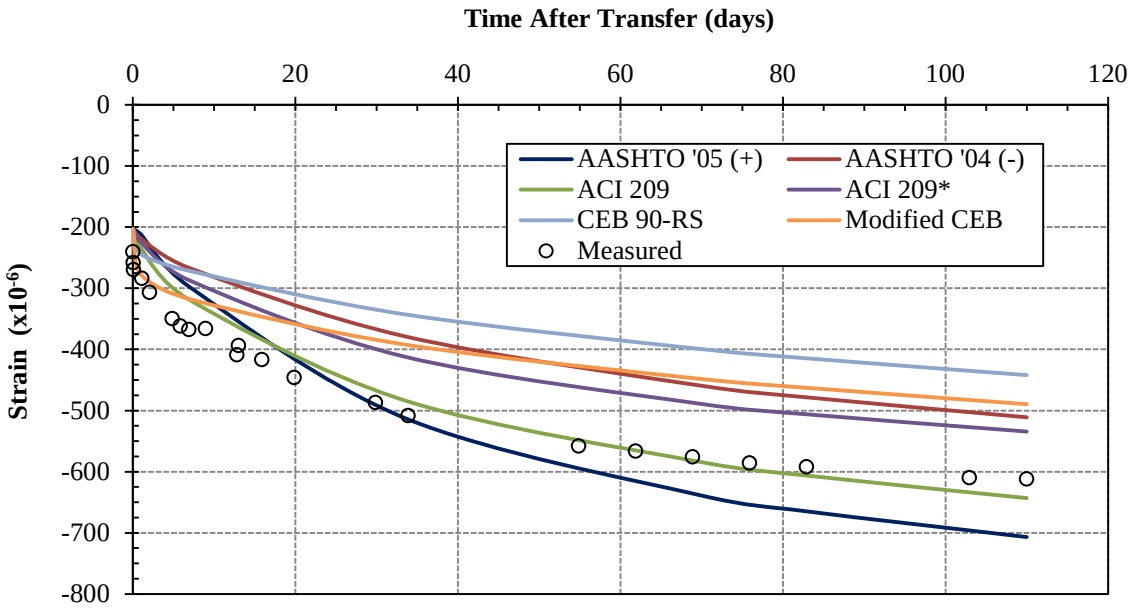

Figure 5-16: STD-M-1 Predicted Strains at Bottom VWSG with Constant E_c

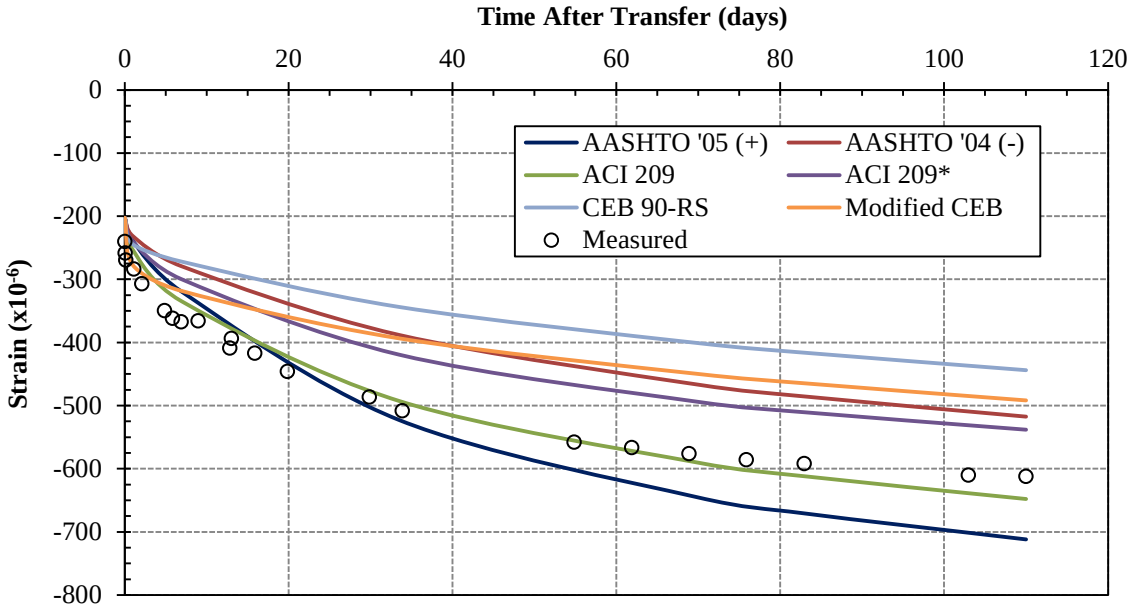

Figure 5-17: STD-M-1 Predicted Strains at Bottom VWSG with Two-Point E_c

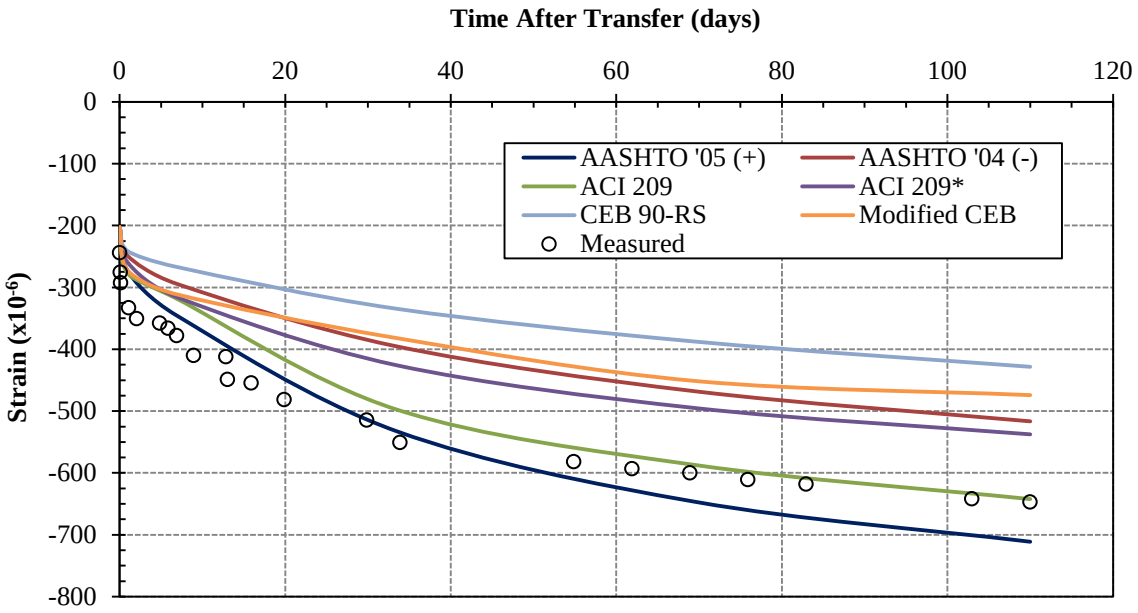

Figure 5-18: STD-M-2 Predicted Strains at Bottom VWSG with Constant E_c

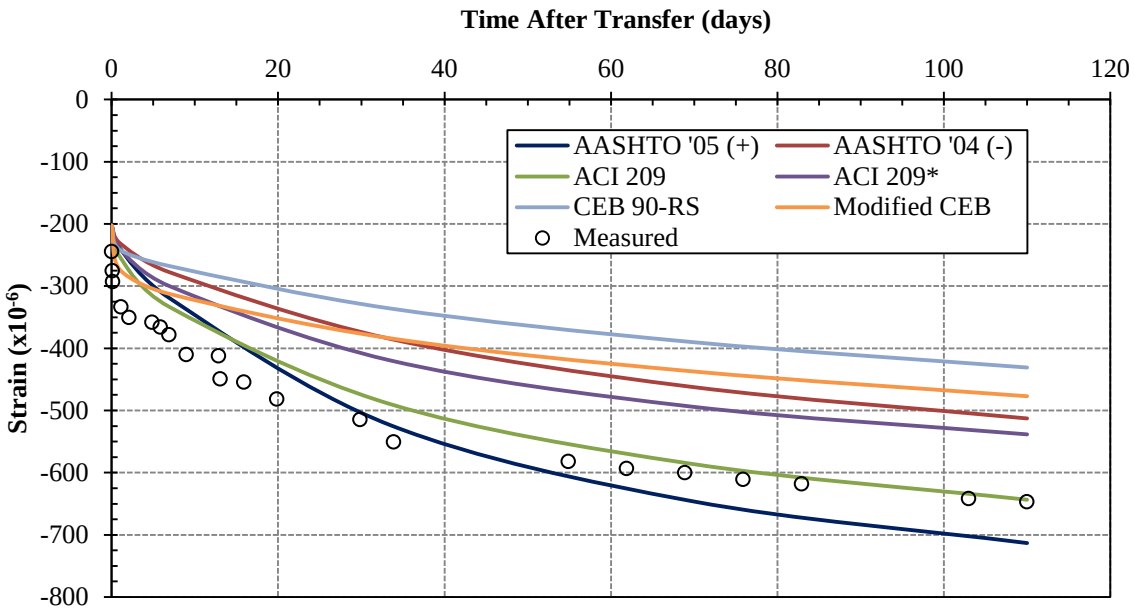

Figure 5-19: STD-M-2 Predicted Strains at Bottom VWSG with Two-Point E_c

Figures 5-20 through 5-31 show the predicted concrete strains for the SCC-MS AASHTO Type I girders. Results using five different creep and shrinkage models are presented for each test-based E_c model. The measured strain data points shown in the figures refer to the "corrected" strain measurements which neglect the effects of temperature.

Tables E-13 through E-15 in Appendix E summarize the percent errors between the measured and predicted SCC-MS strains shown in the figures. The CEB and Modified CEB creep and shrinkage models under-estimated the concrete strains at all locations approximately 25 to 35 percent. The AASHTO '05 (+) and ACI 209* models best predicted short-term strains while the AASHTO '04 (-) was the best predictor of long-term concrete strains at all VWSG locations.

The "Constant E_c" and "Two-point E_c" best predicted the concrete strain immediately after transfer at the bottom VWSG locations. The difference between these predicted and

measured strains was -0.02 percent for SCC-MS-1 and 0.81 percent for SCC-MS-2. Strains immediately after transfer at the middle VWSG locations were over-estimated 1.7 and 2.4 percent. Strains immediately after transfer at the top VWSG locations were under-estimated 4.6 and 21.3 percent for SCC-MS-1 and SCC-MS-2, respectively.

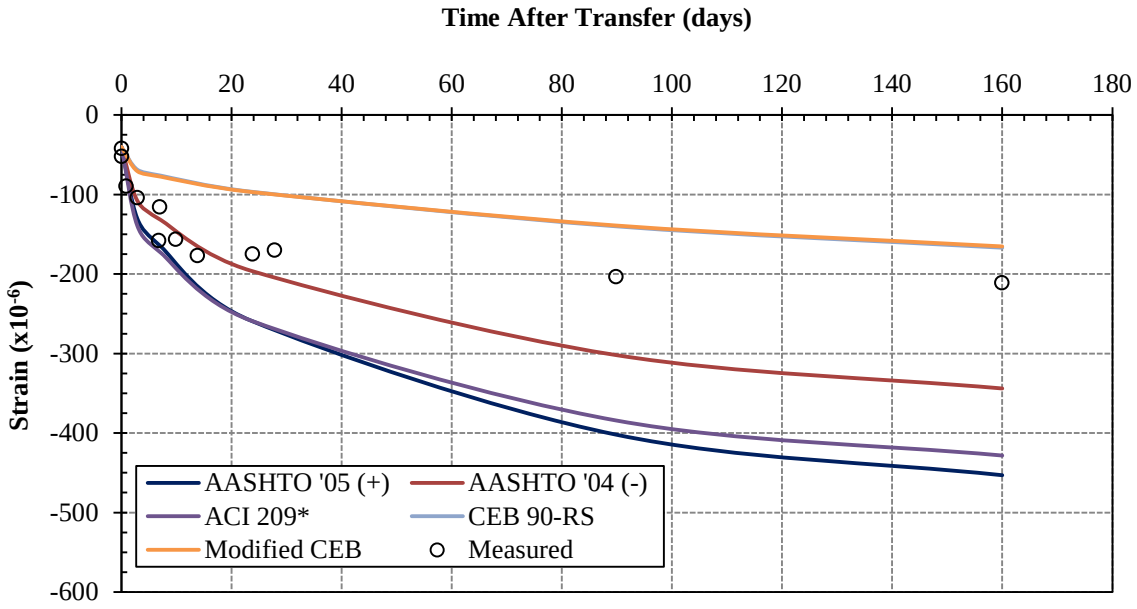

Figure 5-20: SCC-MS-1 Predicted Strains at Top VWSG with Constant E_c

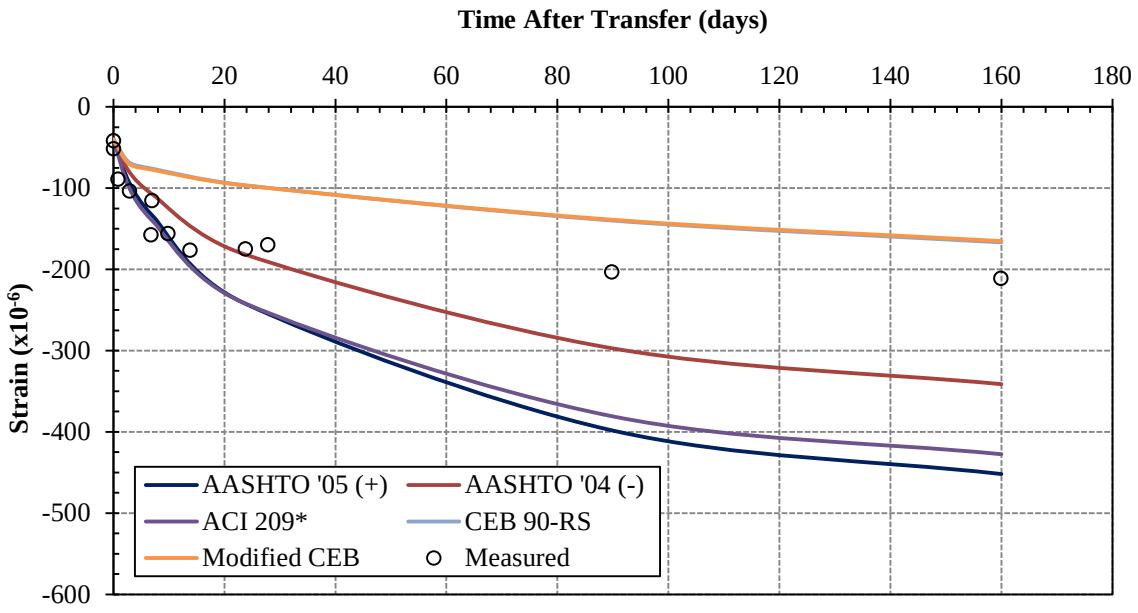

Figure 5-21: SCC-MS-1 Predicted Strains at Top VWSG with Two-Point E_c

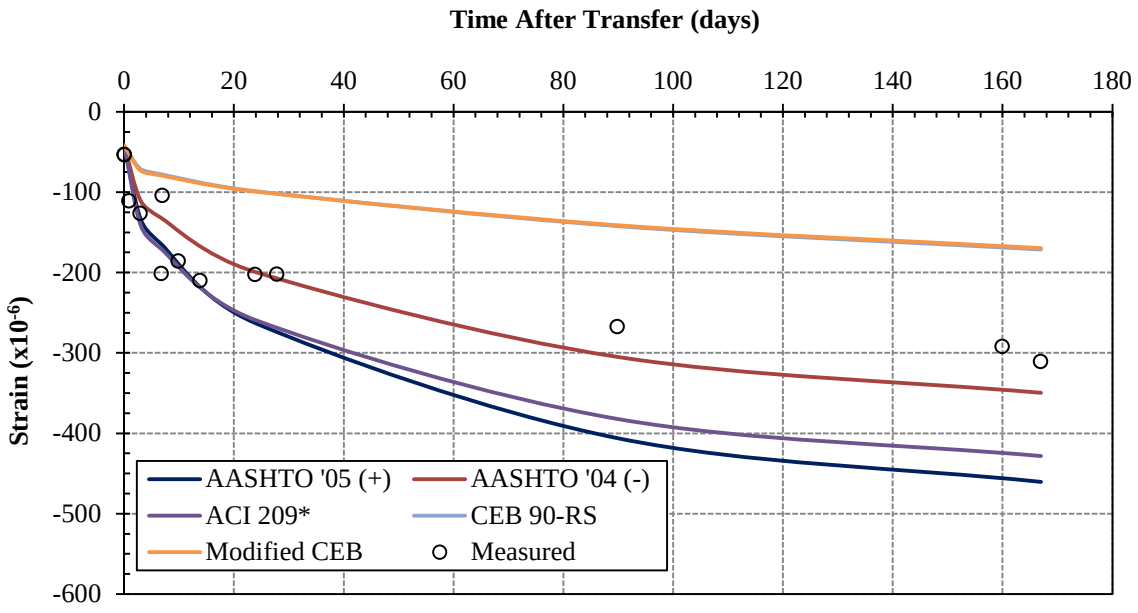

Figure 5-22: SCC-MS-2 Predicted Strains at Top VWSG with Constant E_c

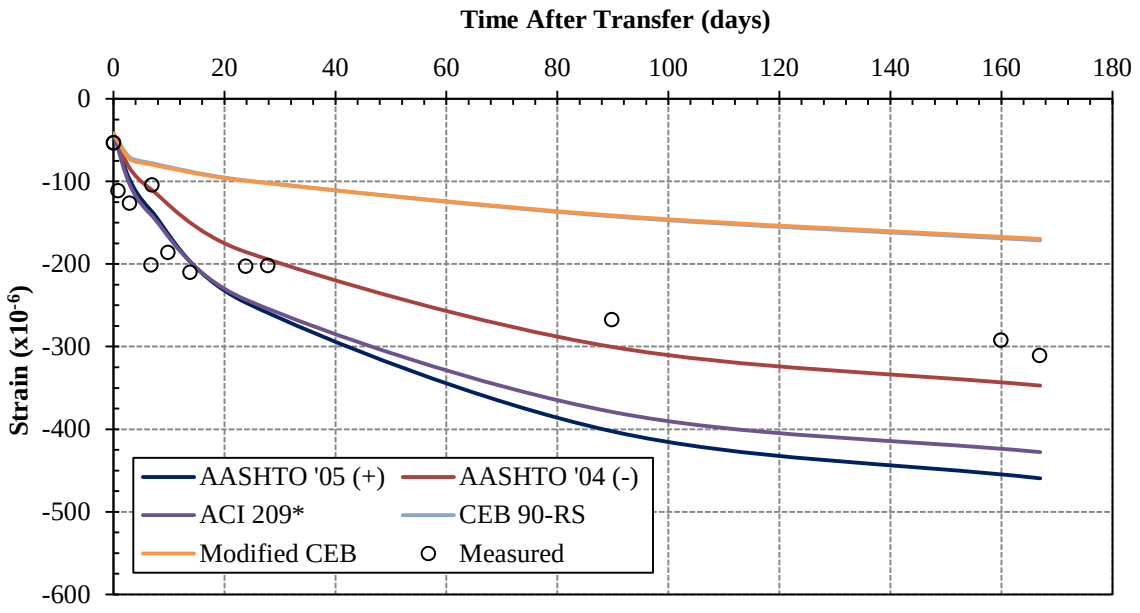

Figure 5-23: SCC-MS-2 Predicted Strains at Top VWSG with Two-Point E_c

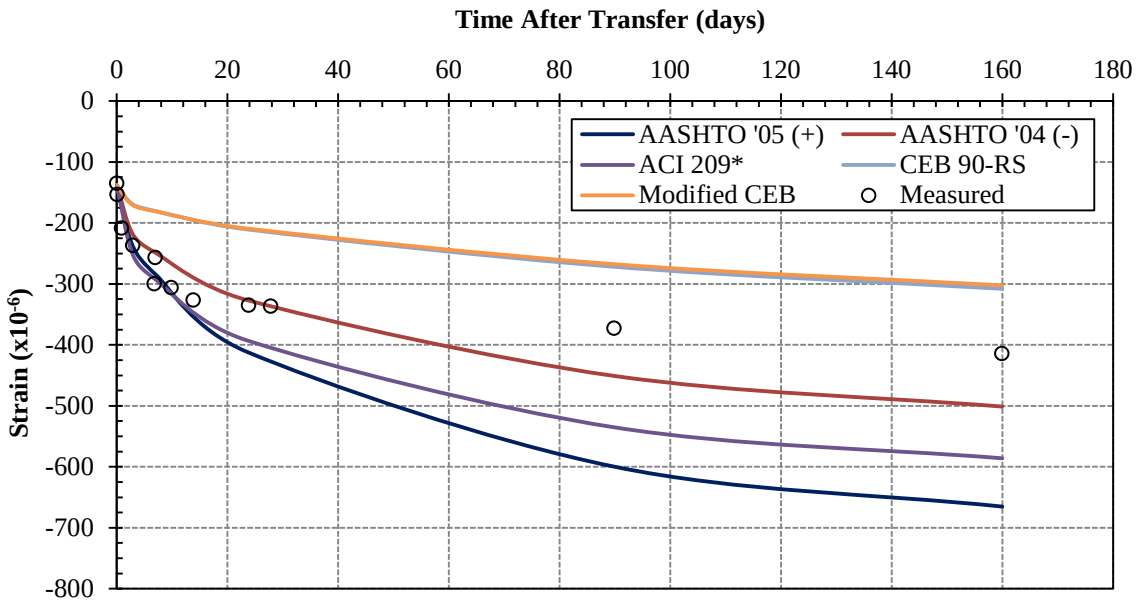

Figure 5-24: SCC-MS-1 Predicted Strains at Middle VWSG with Constant E_c

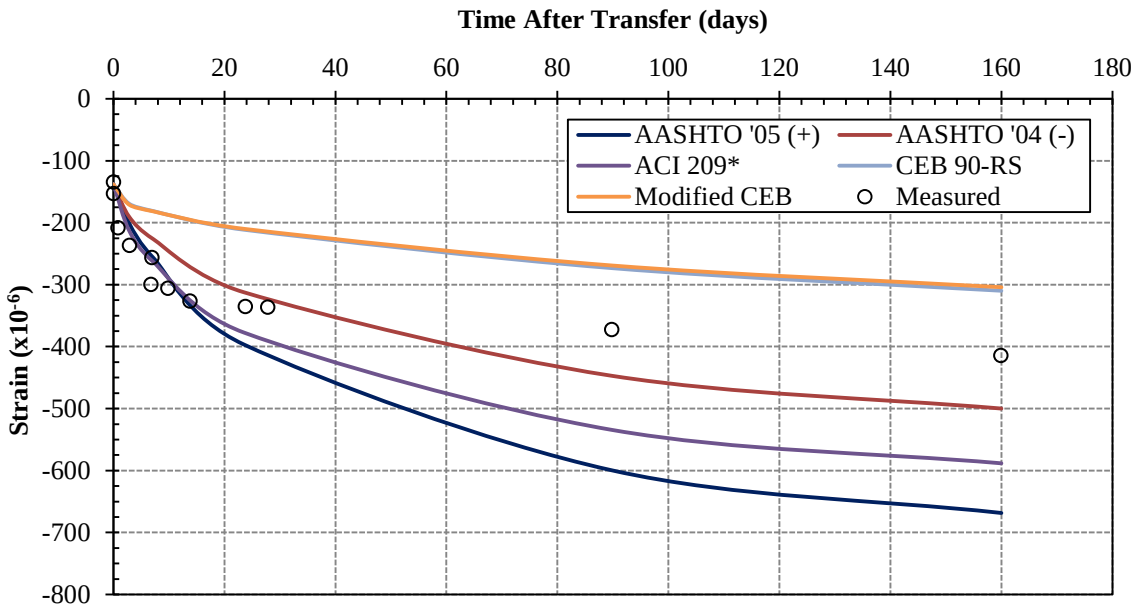

Figure 5-25: SCC-MS-1 Predicted Strains at Middle VWSG with Two-Point E_c

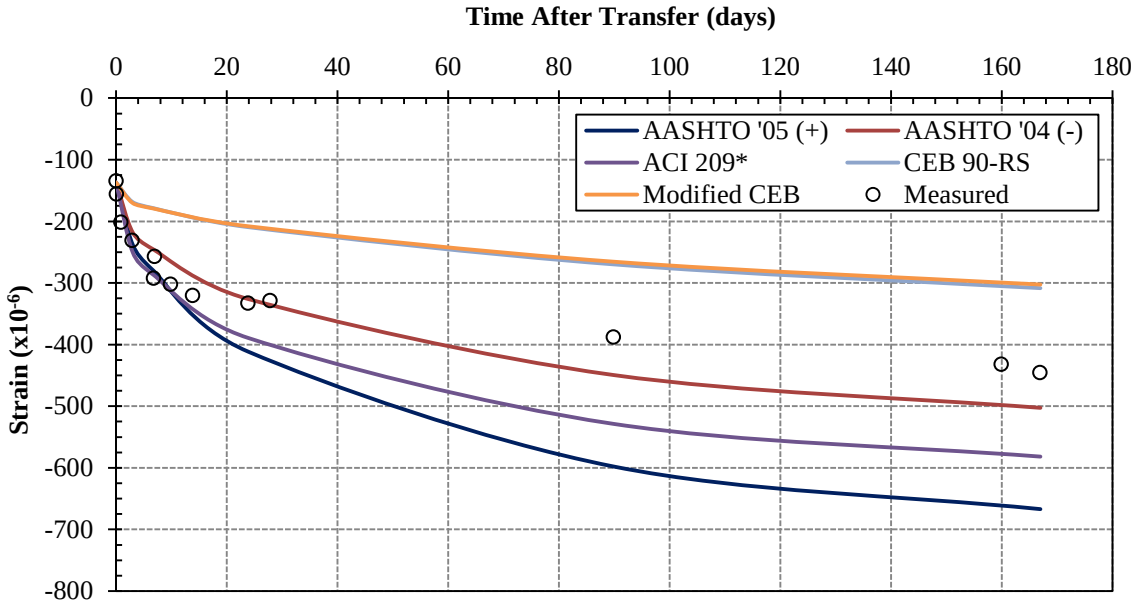

Figure 5-26: SCC-MS-2 Predicted Strains at Middle VWSG with Constant E_c

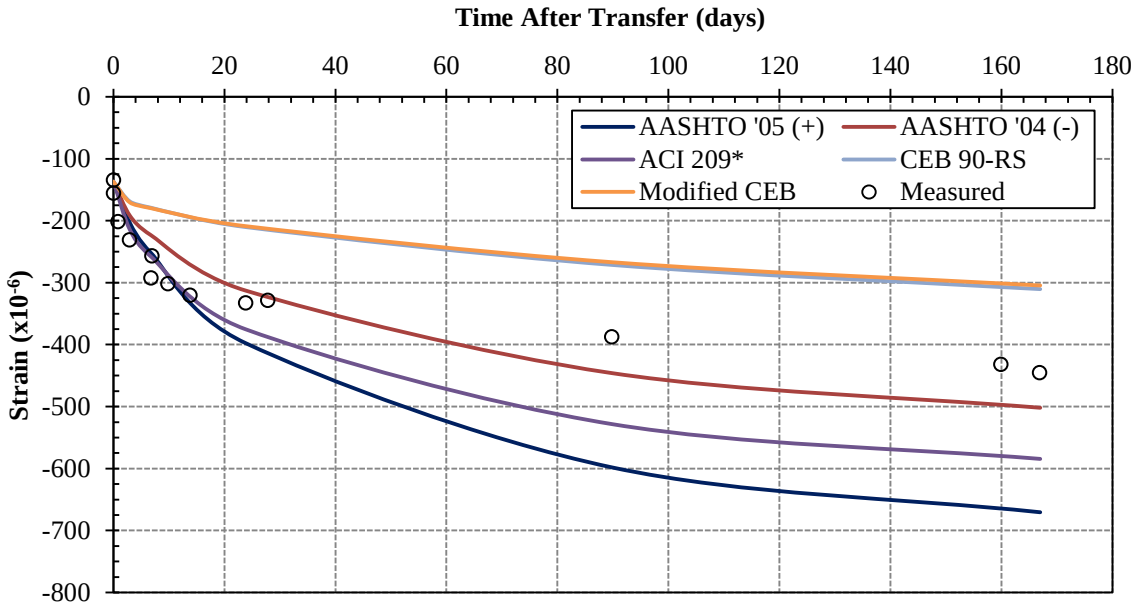

Figure 5-27: SCC-MS-2 Predicted Strains at Middle VWSG with Two-Point E_c

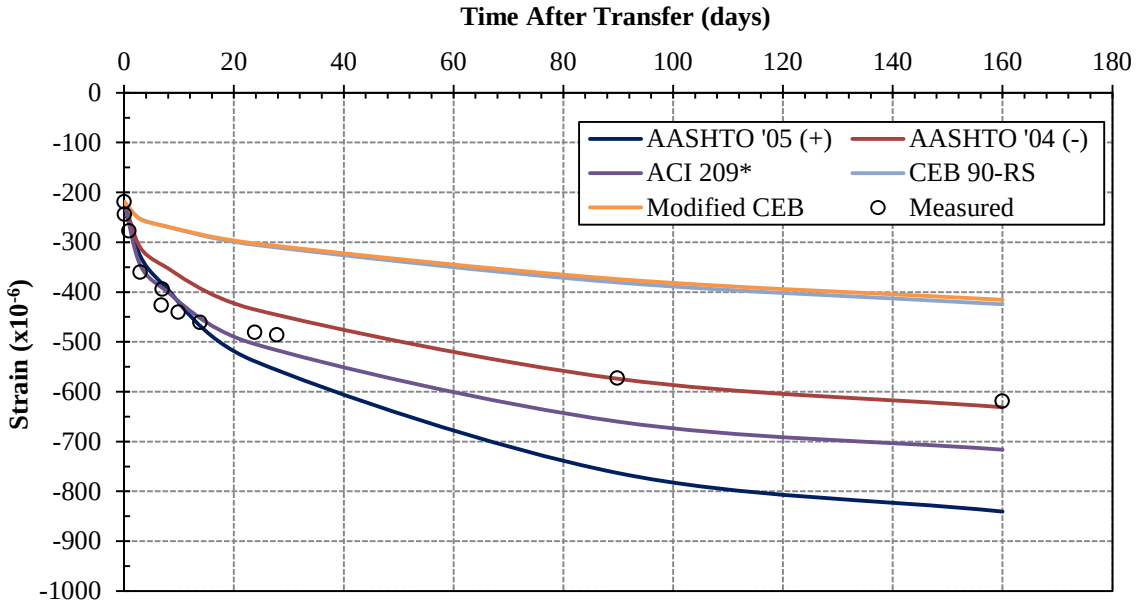

Figure 5-28: SCC-MS-1 Predicted Strains at Bottom VWSG with Constant E_c

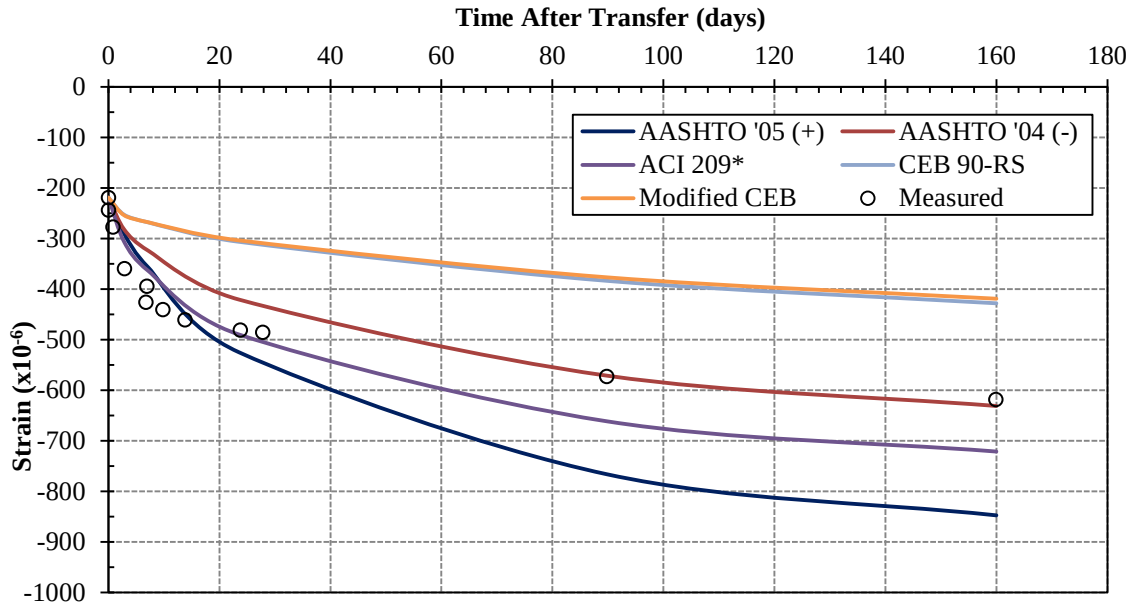

Figure 5-29: SCC-MS-1 Predicted Strains at Bottom VWSG with Two-Point E_c

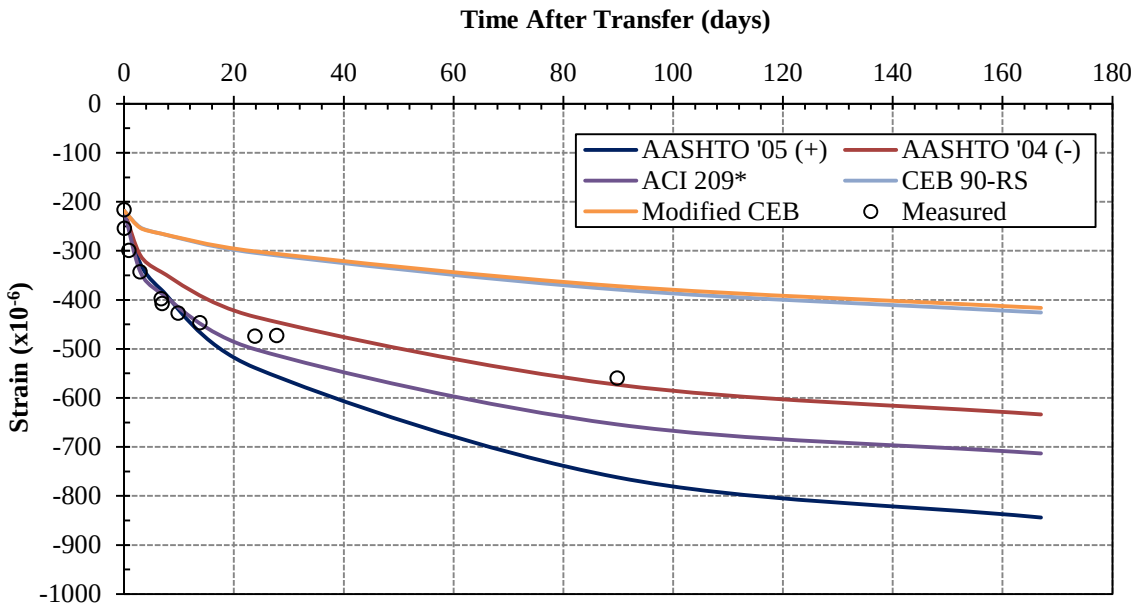

Figure 5-30: SCC-MS-2 Predicted Strains at Bottom VWSG with Constant E_c

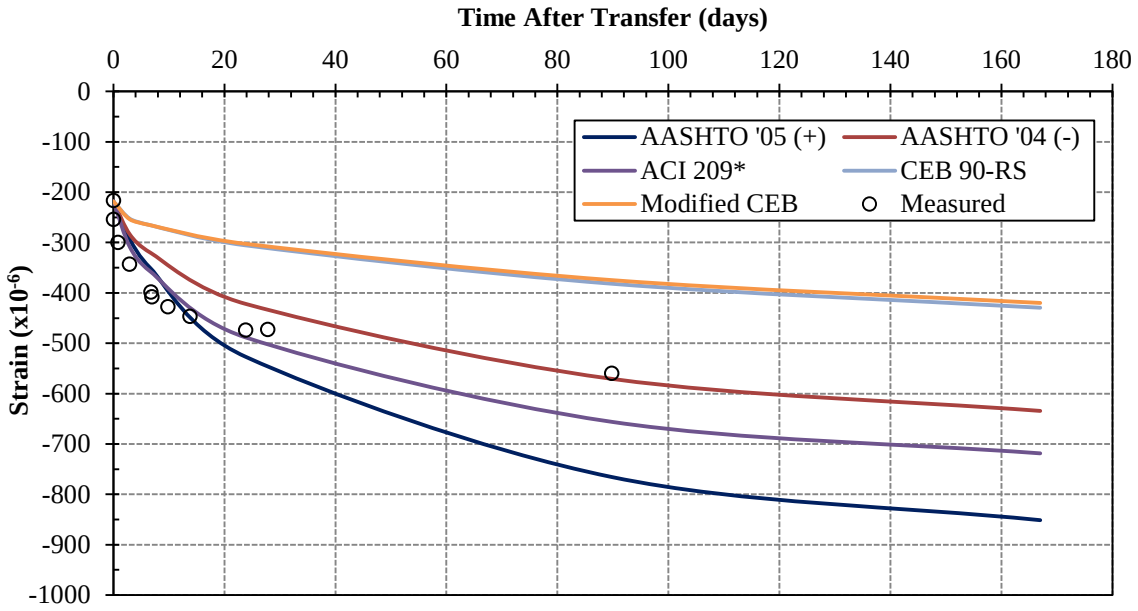

Figure 5-31: SCC-MS-2 Predicted Strains at Bottom VWSG with Two-Point E_c

Figures 5-32 through 5-43 show the predicted concrete strains for the SCC-HS AASHTO Type I girders. Results using five different creep and shrinkage models are presented for each test-based E_c model. The measured strain data points shown in the figures refer to the "corrected" strain measurements which neglect the effects of temperature.

Tables E-16 through E-18 in Appendix E summarize the percent errors between the measured and predicted SCC-HS strains shown in the figures. The CEB and Modified CEB creep and shrinkage models under-estimated the concrete strains at all locations, similar to the SCC-MS girders. The AASHTO '04 (-) was the best predictor of early concrete strains at all VWSG locations. None of the creep and shrinkage models were good predictors of long-term concrete strains in the SCC-HS girders.

Consistent with the SCC-MS results, the "Constant E_c" and "Two-point E_c" models best predicted the concrete strain immediately after transfer at the bottom VWSG locations. The

average predicted strain at the bottom VWSG for the two SCC-HS girders is 165.0 με. The average measured strain at the same location for the two SCC-HS girders is 165.7 με which is a difference of only -0.5 percent. On average, the strains immediately after transfer at the middle VWSG locations were under-estimated 9.2 percent while strains immediately after transfer at the top VWSG locations were under-estimated 25.9 percent.

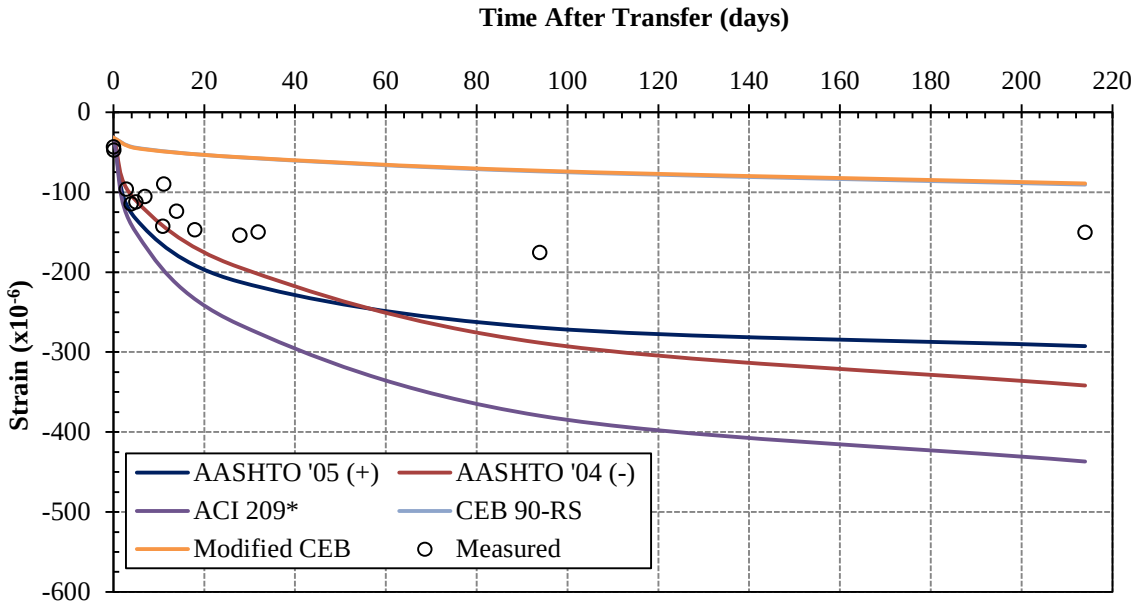

Figure 5-32: SCC-HS-1 Predicted Strains at Top VWSG with Constant E_c

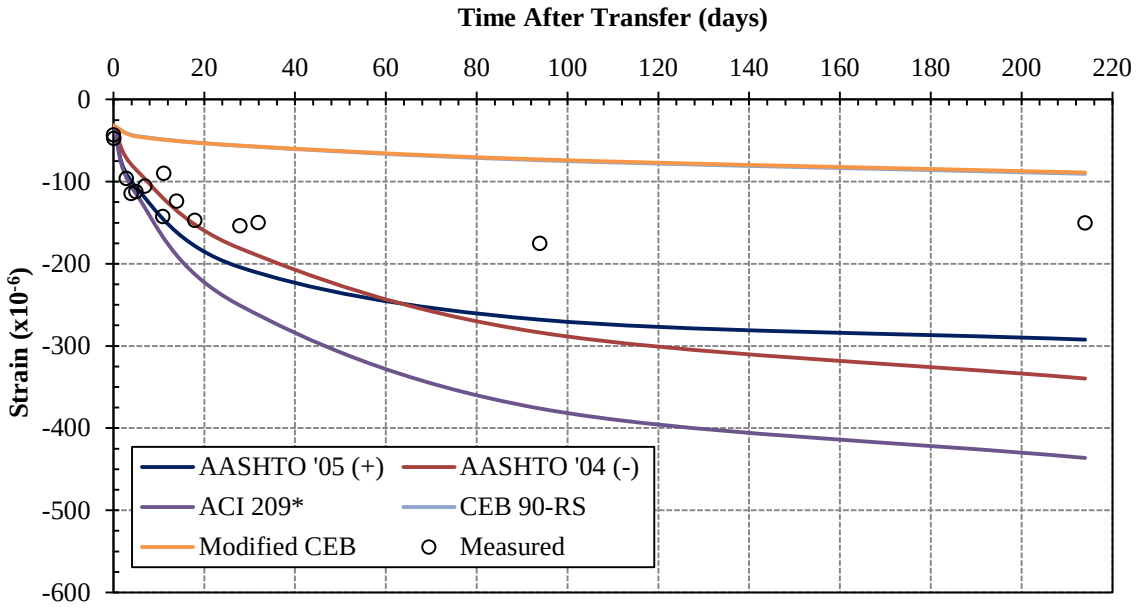

Figure 5-33: SCC-HS-1 Predicted Strains at Top VWSG with Two-Point E_c

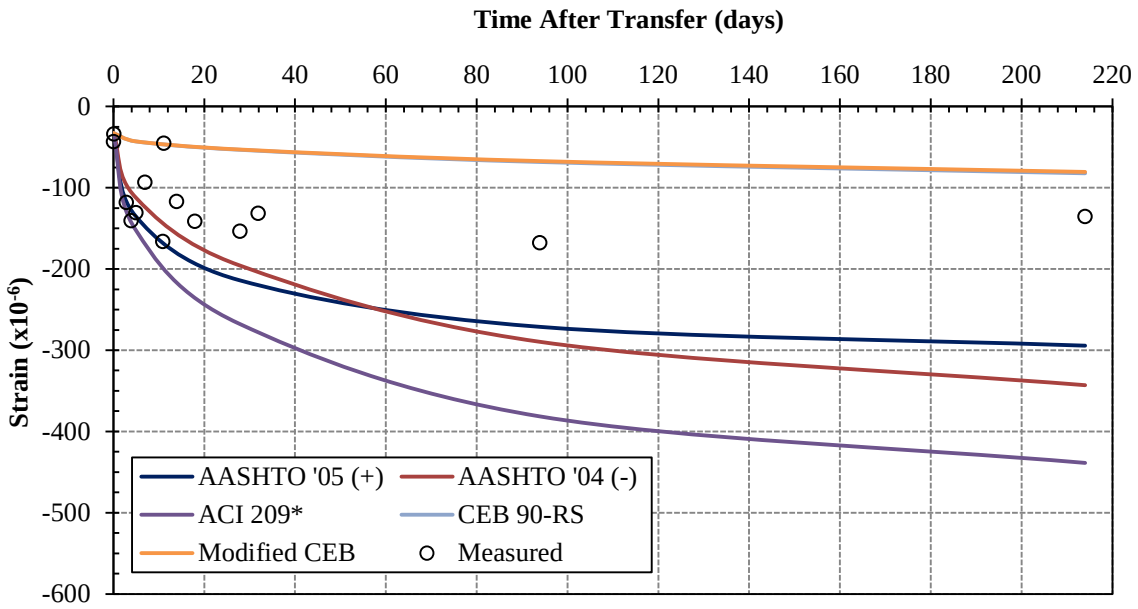

Figure 5-34: SCC-HS-2 Predicted Strains at Top VWSG with Constant E_c

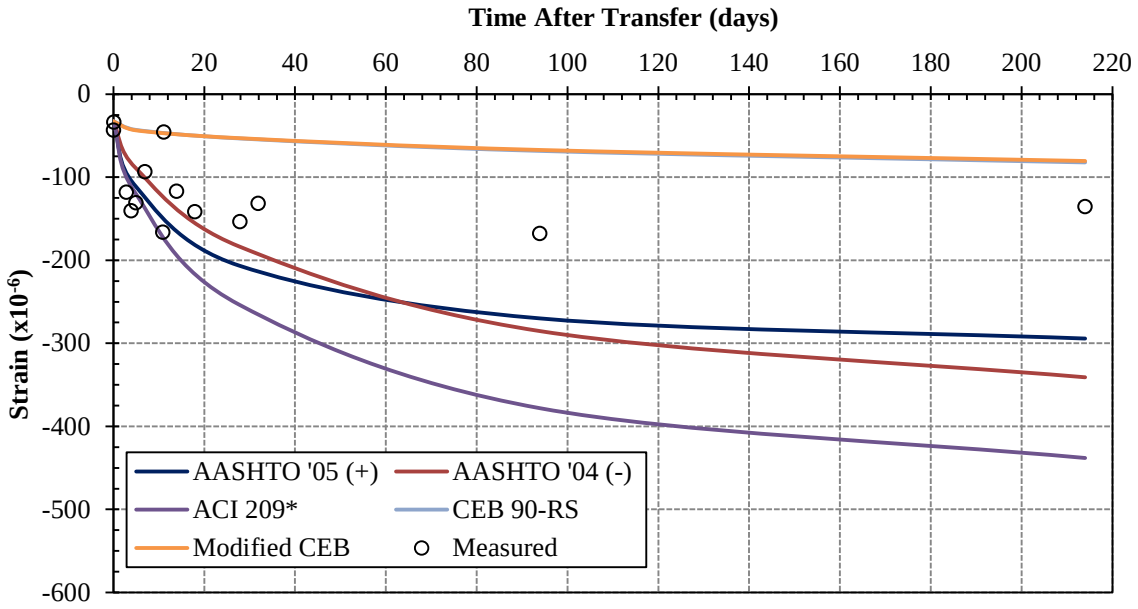

Figure 5-35: SCC-HS-2 Predicted Strains at Top VWSG with Two-Point E_c

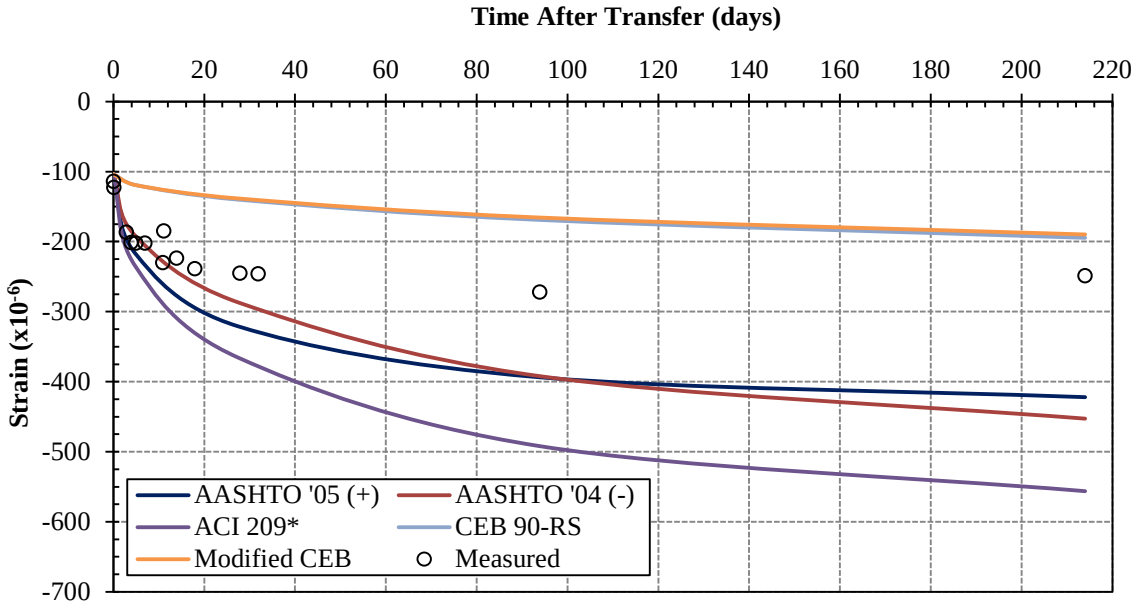

Figure 5-36: SCC-HS-1 Predicted Strains at Middle VWSG with Constant E_c

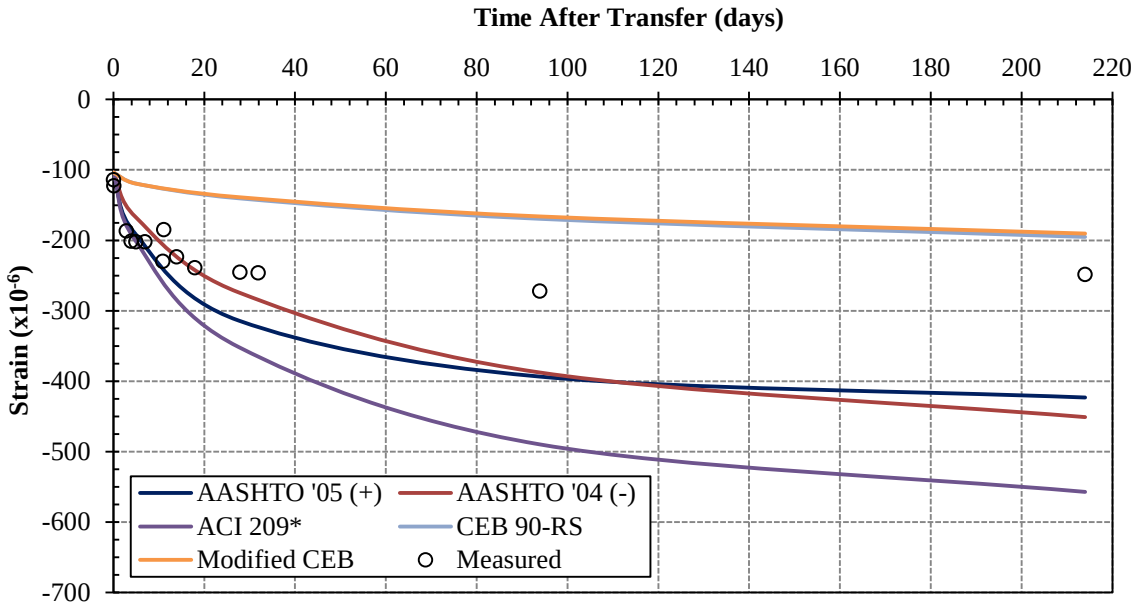

Figure 5-37: SCC-HS-1 Predicted Strains at Middle VWSG with Two-Point E_c

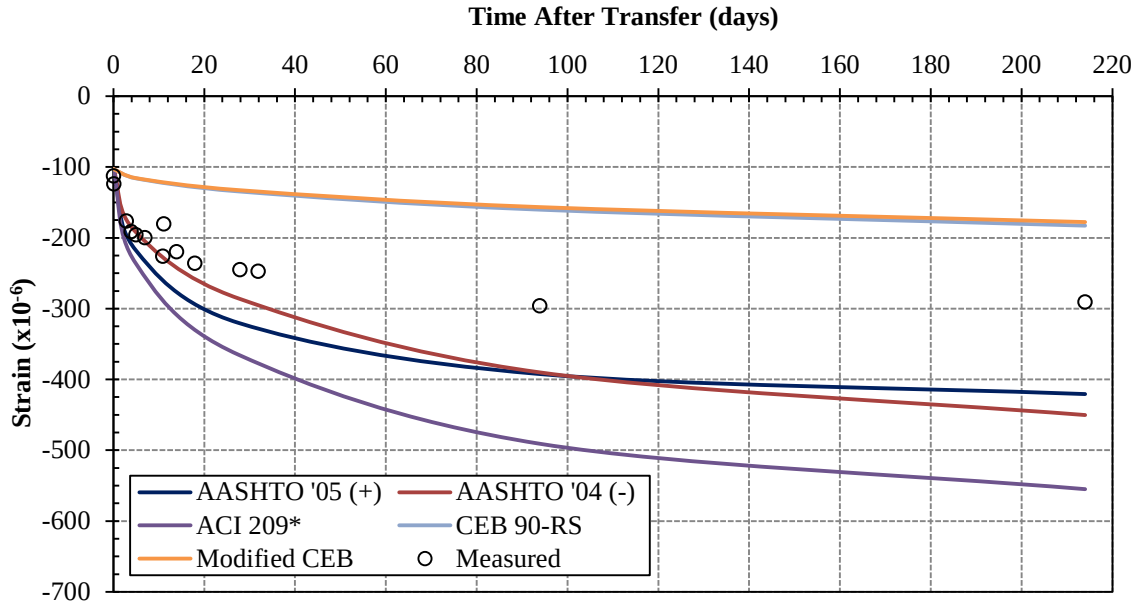

Figure 5-38: SCC-HS-2 Predicted Strains at Middle VWSG with Constant E_c

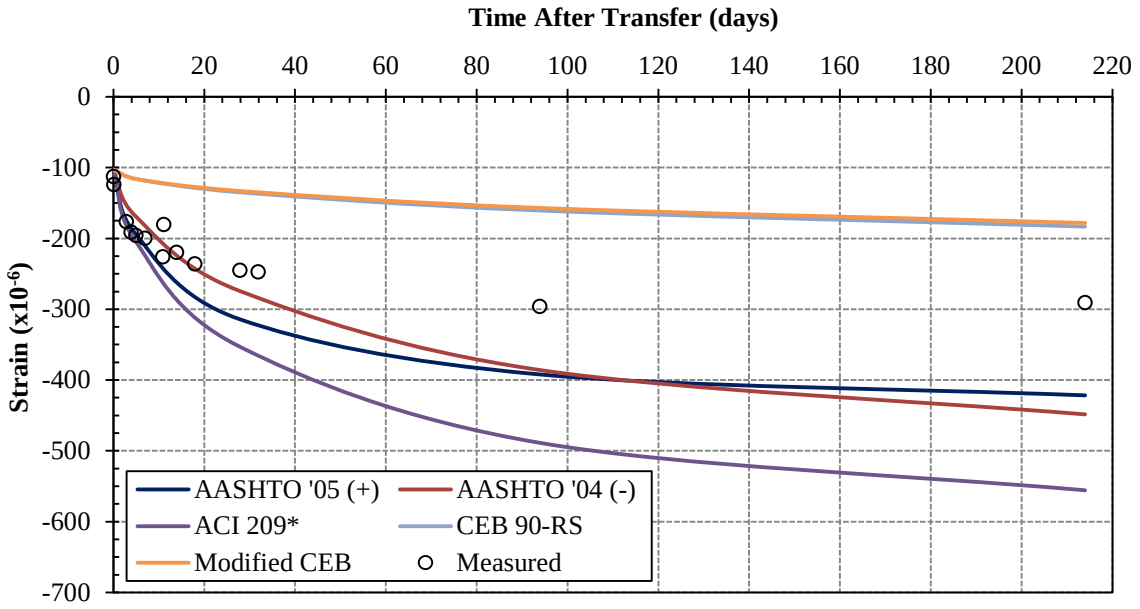

Figure 5-39: SCC-HS-2 Predicted Strains at Middle VWSG with Two-Point E_c

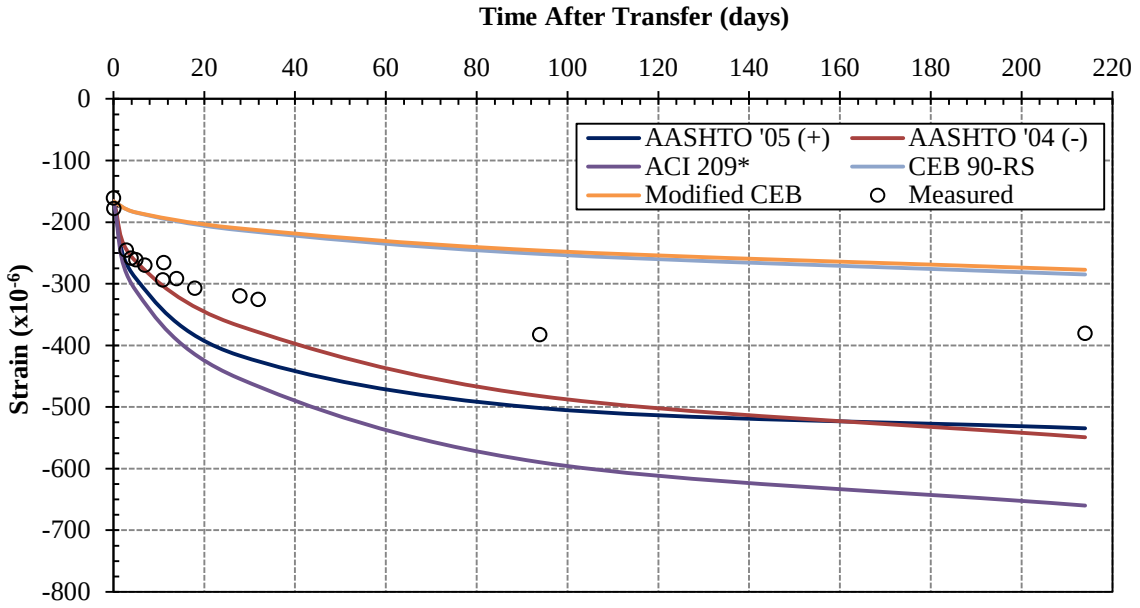

Figure 5-40: SCC-HS-1 Predicted Strains at Bottom VWSG with Constant E_c

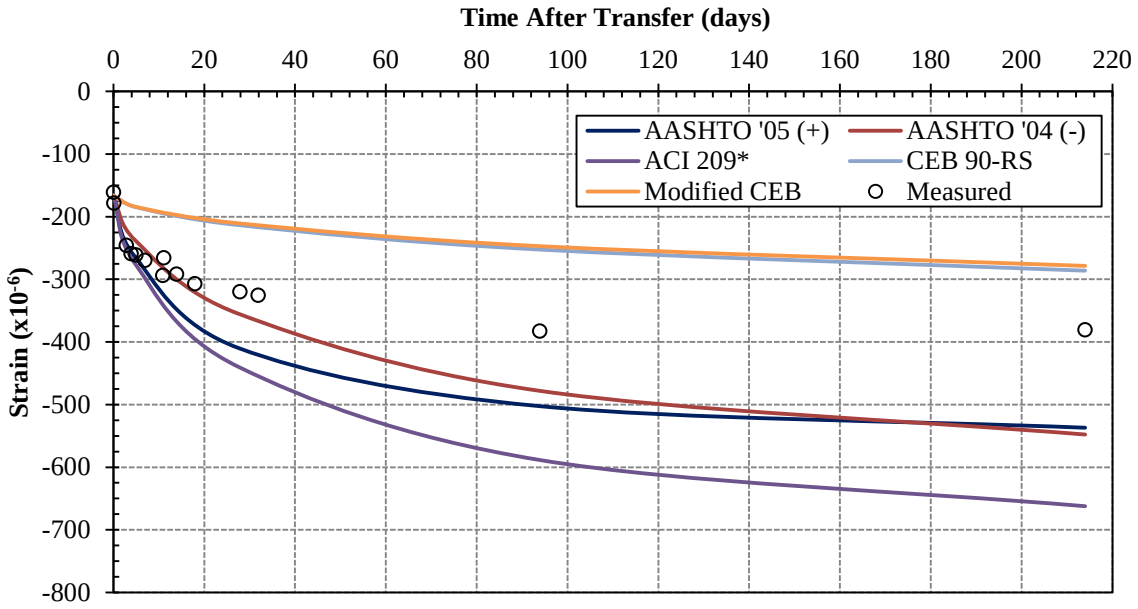

Figure 5-41: SCC-HS-1 Predicted Strains at Bottom VWSG with Two-Point E_c

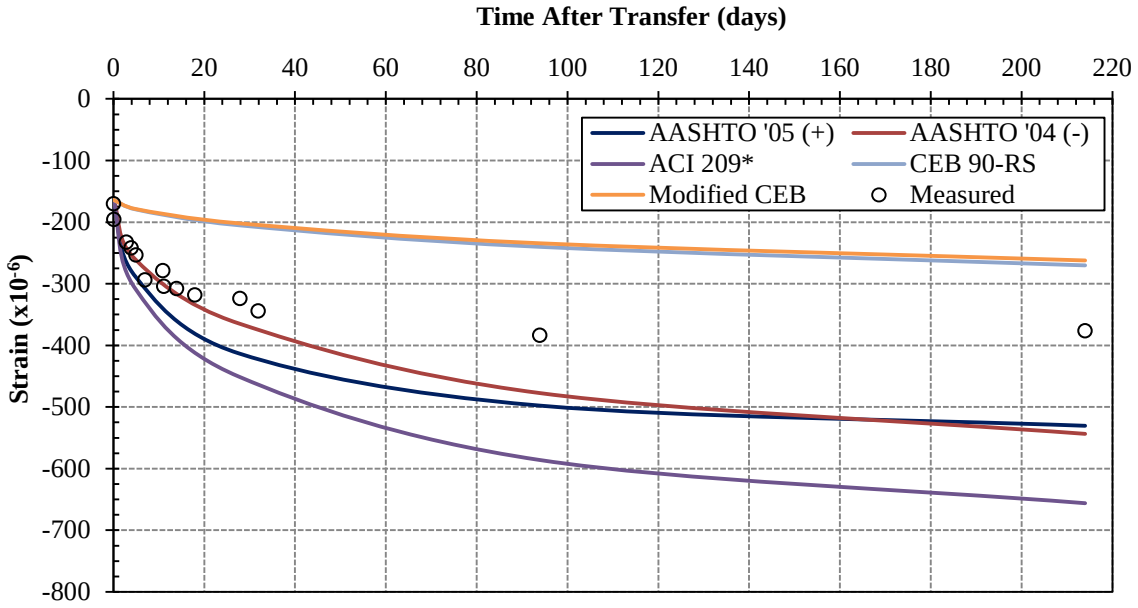

Figure 5-42: SCC-HS-2 Predicted Strains at Bottom VWSG with Constant E_c

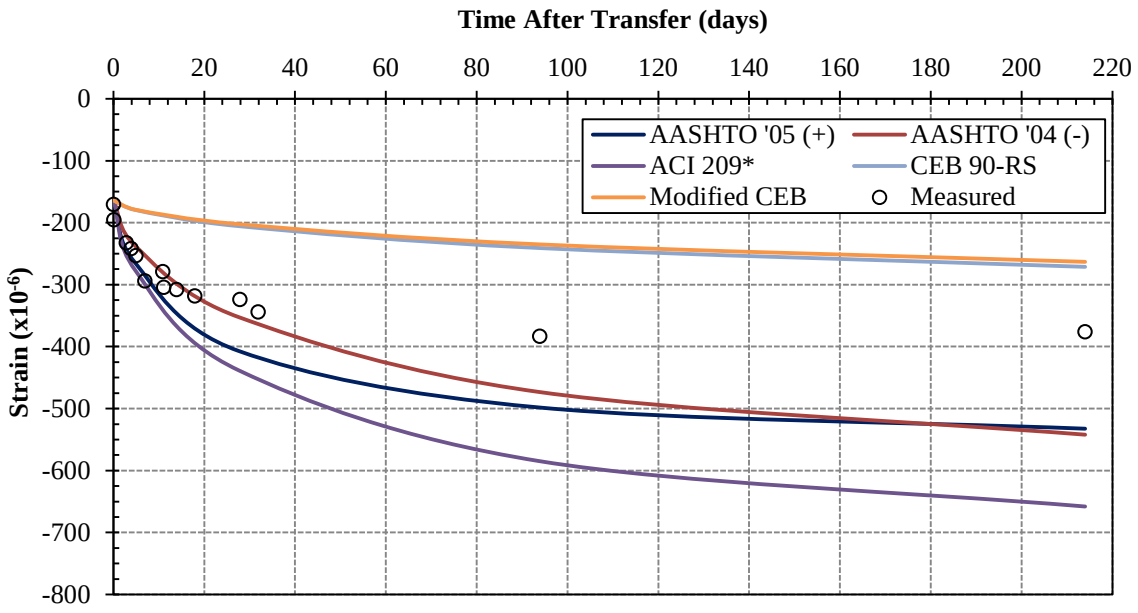

Figure 5-43: SCC-HS-2 Predicted Strains at Bottom VWSG with Two-Point E_c

5.1.2.2 Strain Predictions Using Code-Prediction E_C Models

The program allows the user to select among three code-prediction models for the concrete MOE development over time: AASHTO ’05(+), ACI 209, and CEB 90. The AASHTO ’05(+) model uses the strength development rate from the ACI 209 model and therefore predicts the same concrete strains as ACI 209.

Figures 5-44 through 5-55 show the predicted concrete strains for the STD-M AASHTO Type I girders. Results using six different creep and shrinkage models are presented for the CEB 90 E_c model and the combined AASHTO ’05(+)/ACI 209 E_c model. The measured strain data points shown in the figures refer to the “corrected” strain measurements which neglect the effects of temperature.

Tables E-10 through E-12 in Appendix E summarize the percent errors between the measured and predicted STD-M strains shown in the figures. The AASHTO ’05(+) and ACI 209

creep and shrinkage models generally over-estimated the concrete strains at all locations. The AASHTO ’04(-) and ACI 209* creep and shrinkage models best predicted long-term strains at the top VWSG locations when the CEB 90 E_c model was used. The AASHTO ’04(-) creep and shrinkage model was also a good predictor of concrete strain at the middle VWSG in the STD-M-1 girder when using the CEB 90 E_c model.

The CEB 90 E_c model best predicted strains at the middle VWSG 110 days after transfer when using the ACI 209* creep and shrinkage model. The percent difference between these predicted and measured long-term strains is 0.05 percent and 0.04 percent for STD-M-1 and STD-M-2, respectively.

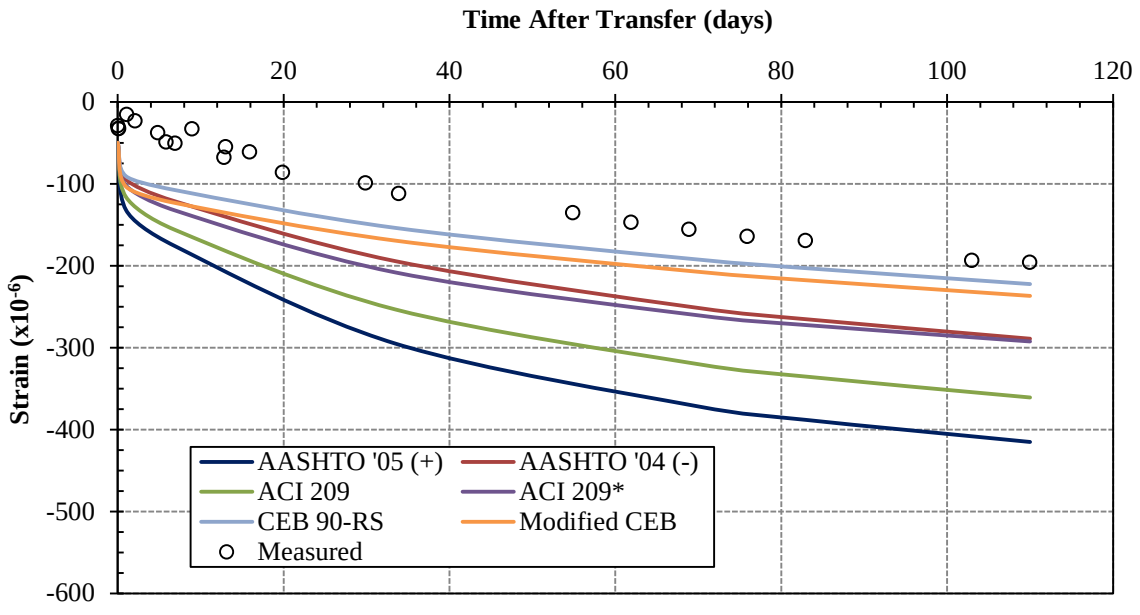

Figure 5-44: STD-M-1 Predicted Strains at Top VWSG with AASHTO/ACI E_c

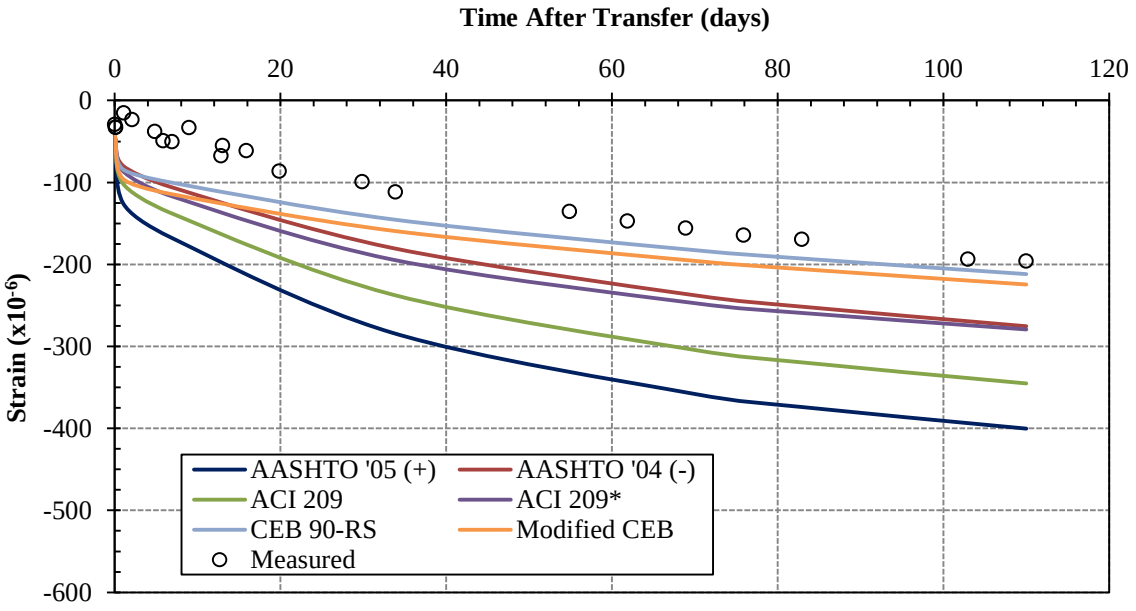

Figure 5-45: STD-M-1 Predicted Strains at Top VWSG with CEB 90 E_c

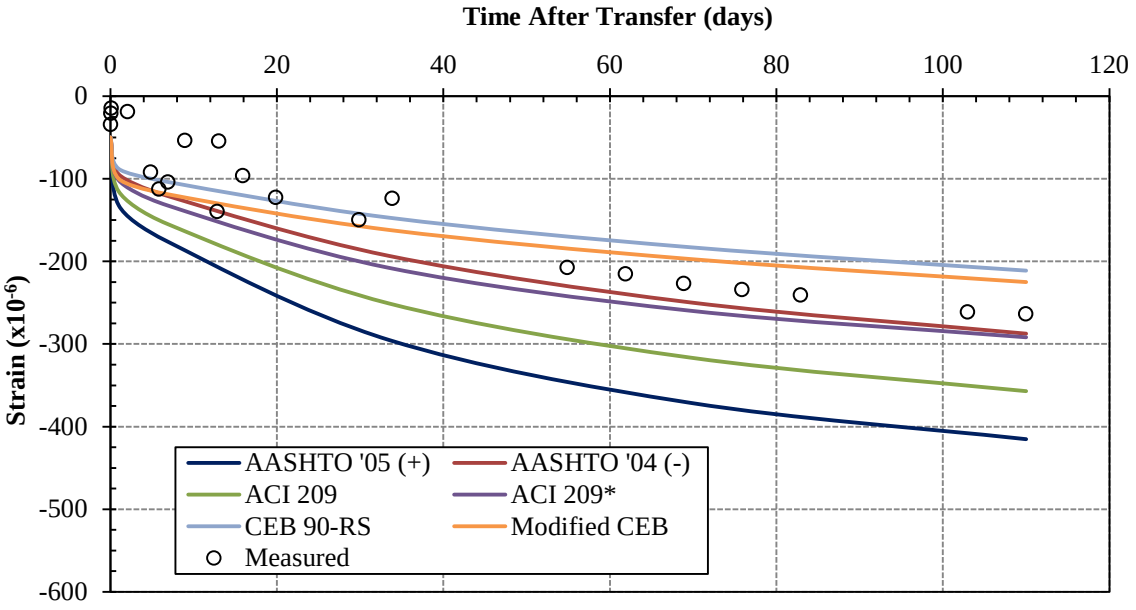

Figure 5-46: STD-M-2 Predicted Strains at Top VWSG with AASHTO/ACI E_c

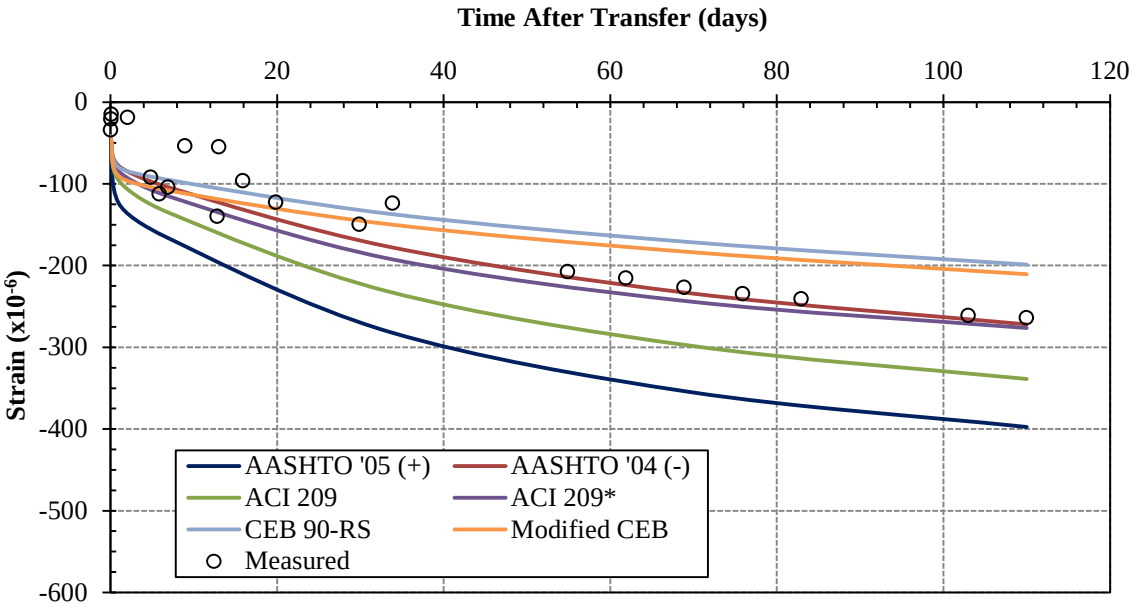

Figure 5-47: STD-M-2 Predicted Strains at Top VWSG with CEB 90 E_c

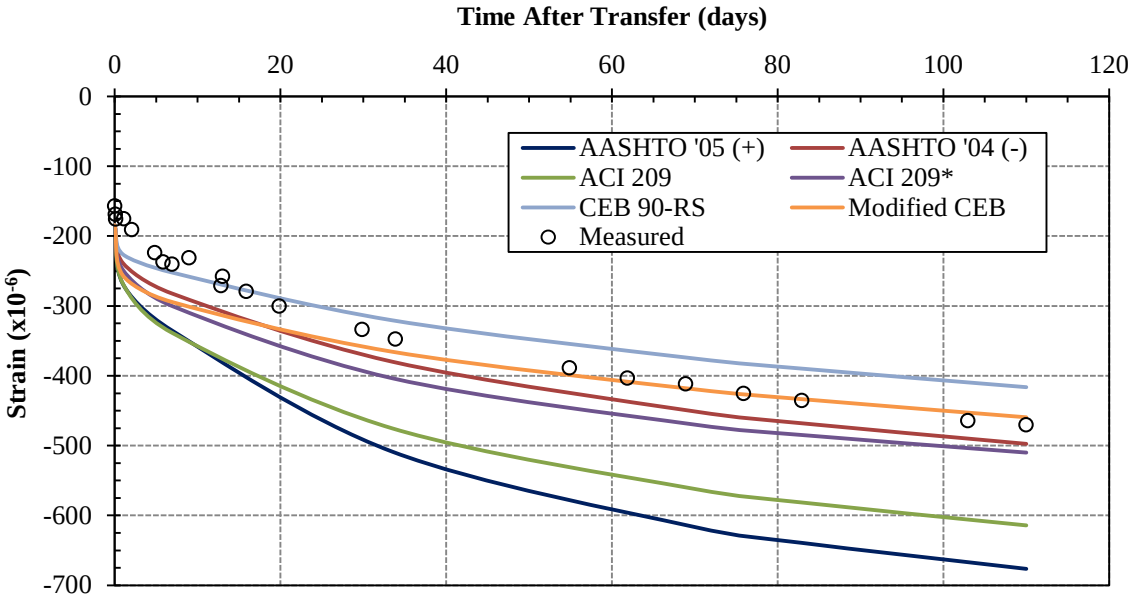

Figure 5-48: STD-M-1 Predicted Strains at Middle VWSG with AASHTO/ACI E_c

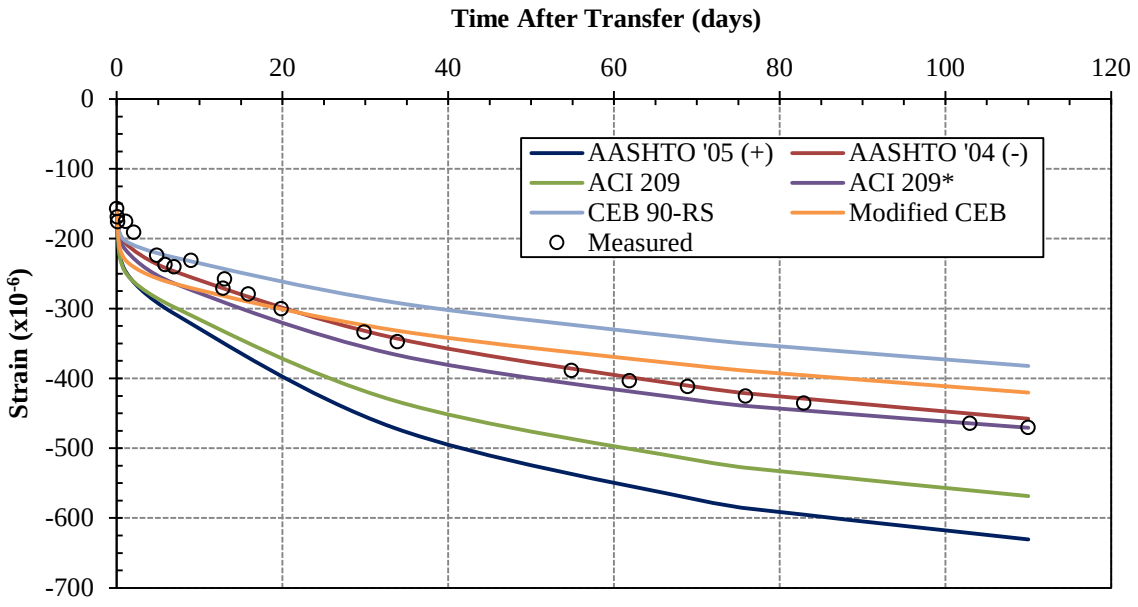

Figure 5-49: STD-M-1 Predicted Strains at Middle VWSG with CEB 90 E_c

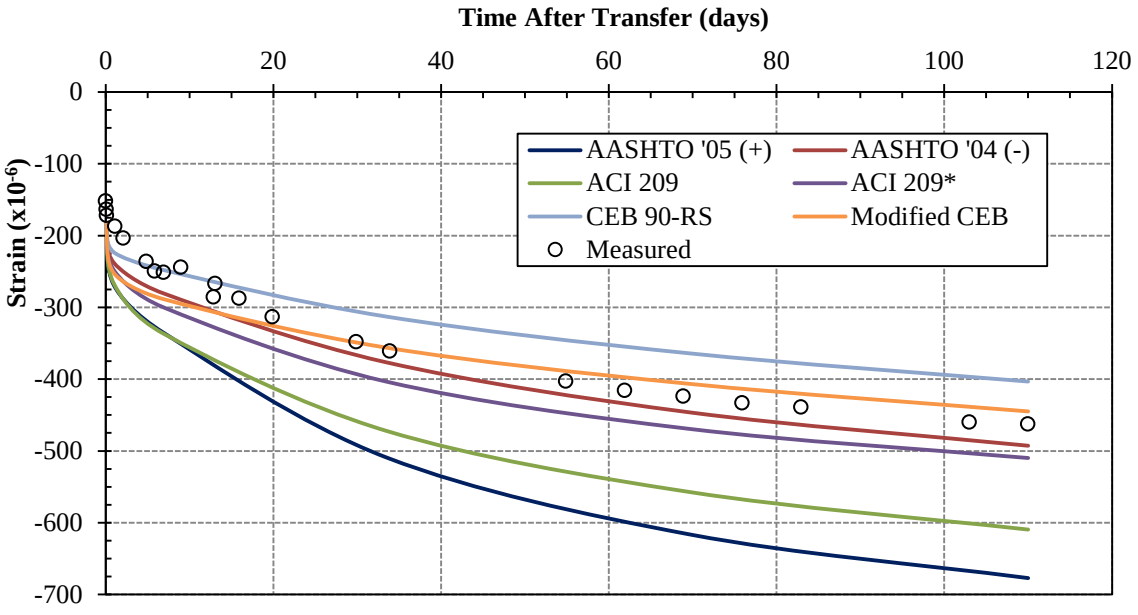

Figure 5-50: STD-M-2 Predicted Strains at Middle VWSG with AASHTO/ACI E_c

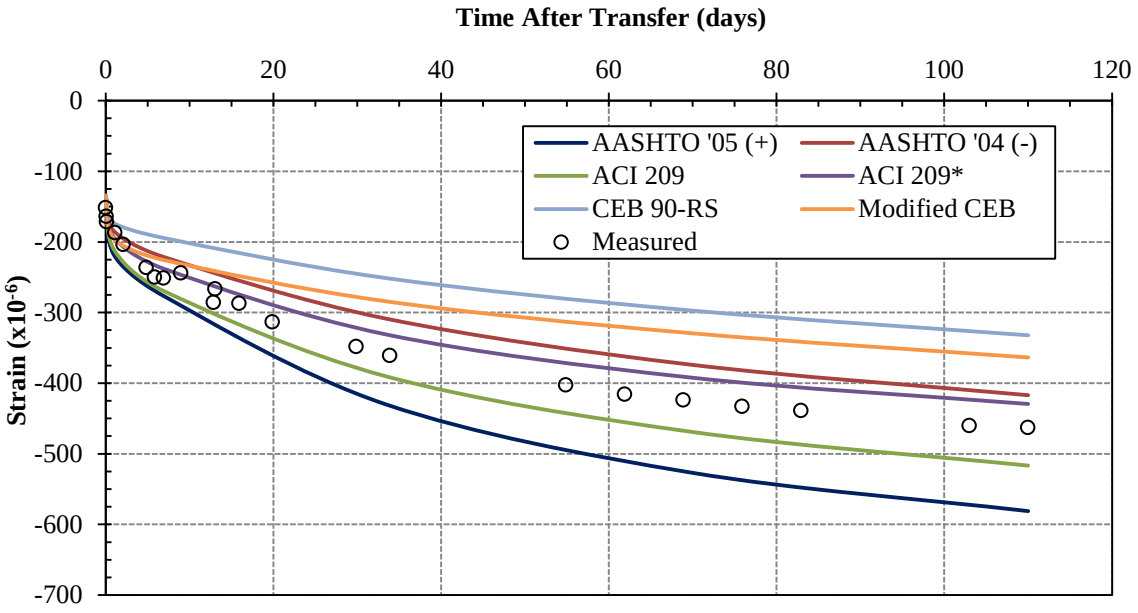

Figure 5-51: STD-M-2 Predicted Strains at Middle VWSG with CEB 90 E_c

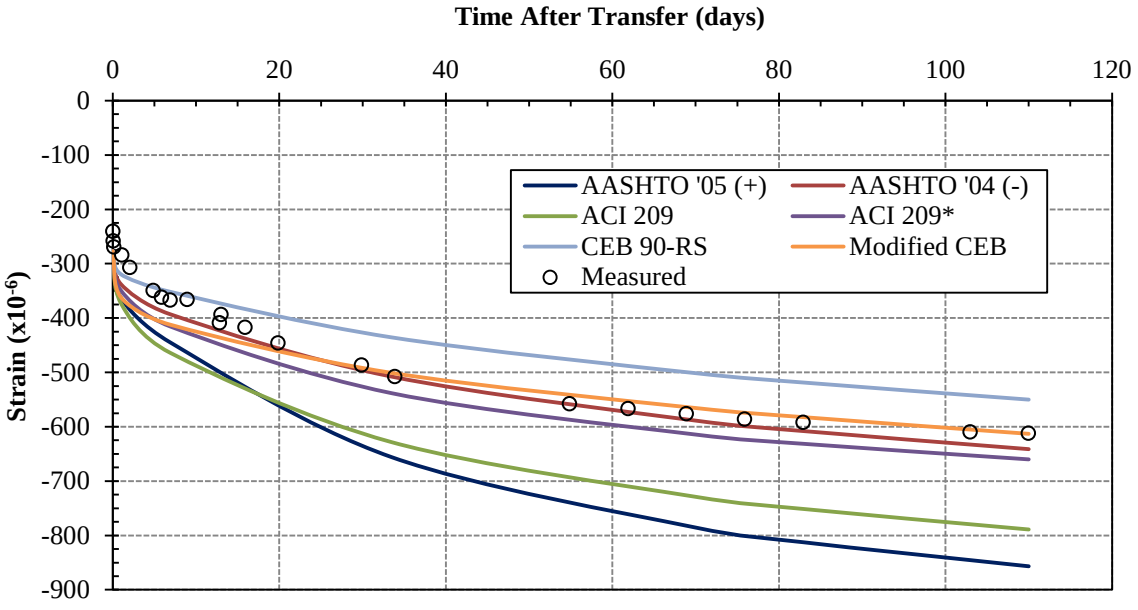

Figure 5-52: STD-M-1 Predicted Strains at Bottom VWSG with AASHTO/ACI E_c

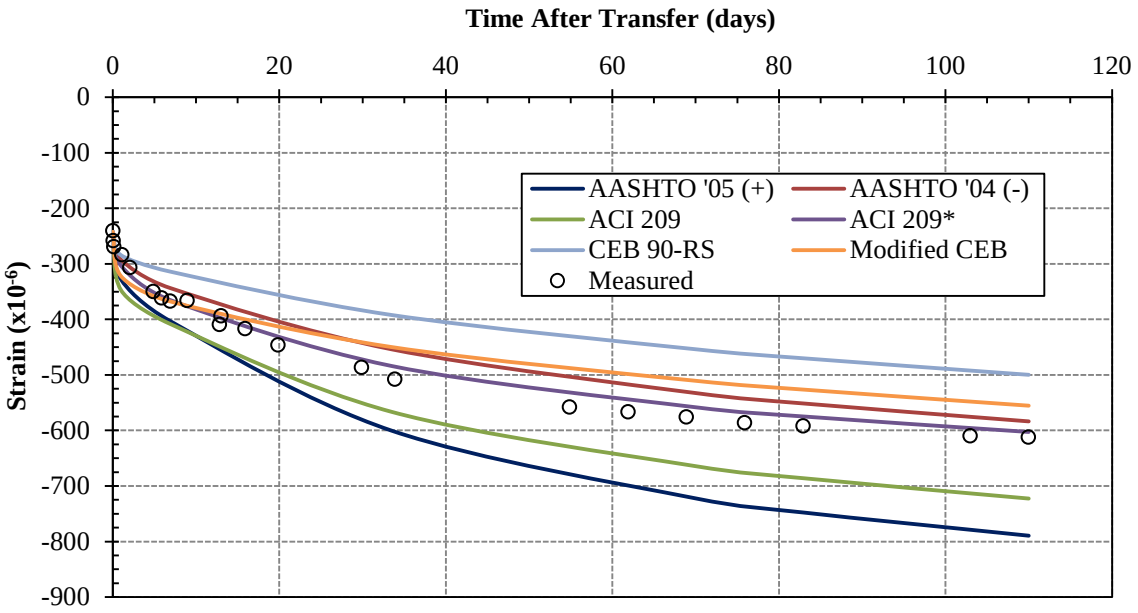

Figure 5-53: STD-M-1 Predicted Strains at Bottom VWSG with CEB 90 E_c

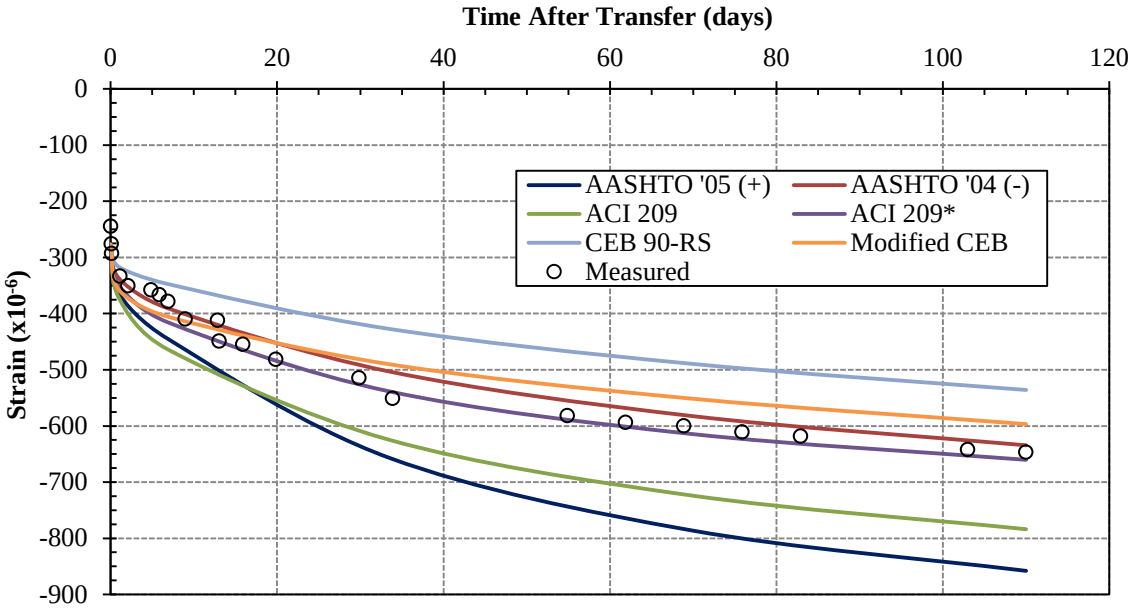

Figure 5-54: STD-M-2 Predicted Strains at Bottom VWSG with AASHTO/ACI E_c

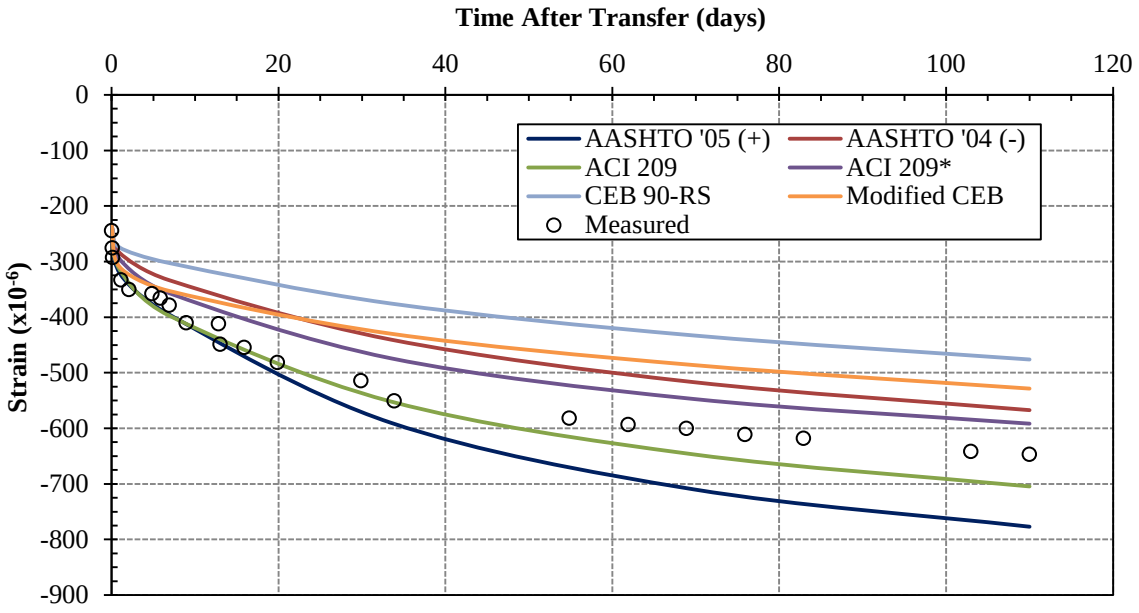

Figure 5-55: STD-M-2 Predicted Strains at Bottom VWSG with CEB 90 E_c

Figures 5-56 through 5-67 show the predicted concrete strains for the SCC-MS AASHTO Type I girders when using code-prediction E_c models. Results for five different creep and shrinkage models are presented: AASHTO '05(+), AASHTO '04(-), ACI 209*, CEB 90, and Modified CEB 90. The measured strain data points shown in the figures refer to the "corrected" strain measurements which neglect the effects of temperature.

Tables E-13 through E-15 in Appendix E summarize the percent errors between the measured and predicted SCC-MS strains shown in the figures. The CEB 90 and Modified CEB 90 creep and shrinkage models consistently under-estimate the concrete strain at all VWSG locations.

Generally, the AASHTO '04(-) creep and shrinkage model over-estimates concrete strain at the middle and bottom VWSG locations less than 20 percent. Using either the AASHTO '05(+) or ACI 209 E_c model, the AASHTO '04(-) creep and shrinkage model over-estimates

strain at the bottom VWSG in the SCC-MS-1 girder 0.4 percent three days after transfer and 1.7 percent seven days after transfer (see Figure 5-64). When using the CEB 90 E_c model, the AASHTO '04(-) creep and shrinkage model under-predicts the same strain -0.6 percent 90 days after transfer and 1.2 percent 160 days after transfer (see Figure 5-65).

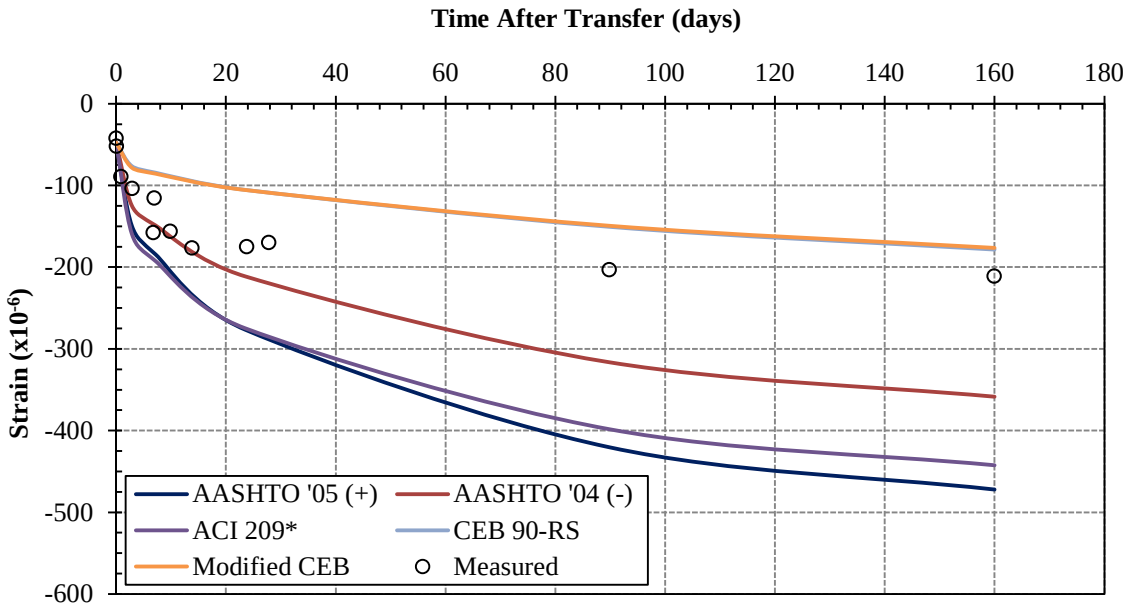

Figure 5-56: SCC-MS-1 Predicted Strains at Top VWSG with AASHTO/ACI E_c

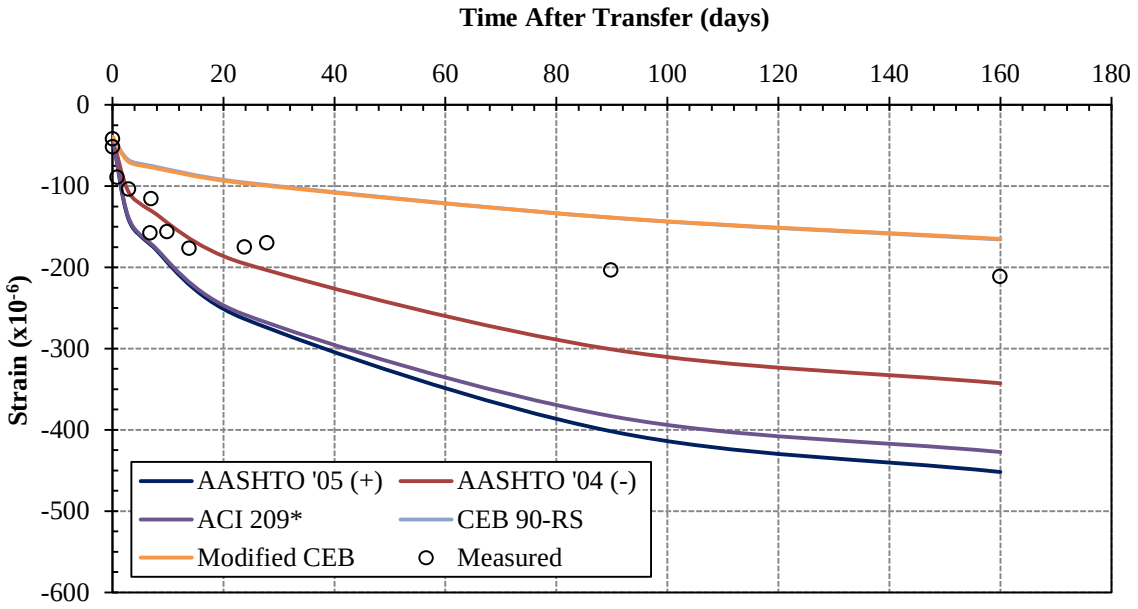

Figure 5-57: SCC-MS-1 Predicted Strains at Top VWSG with CEB 90 E_c

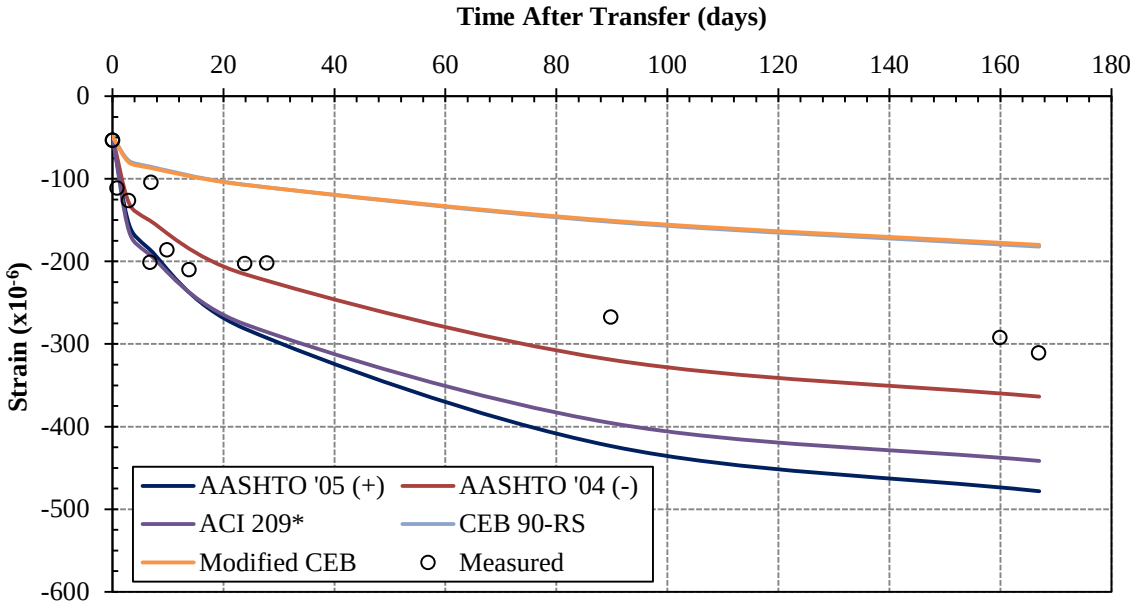

Figure 5-58: SCC-MS-2 Predicted Strains at Top VWSG with AASHTO/ACI E_c

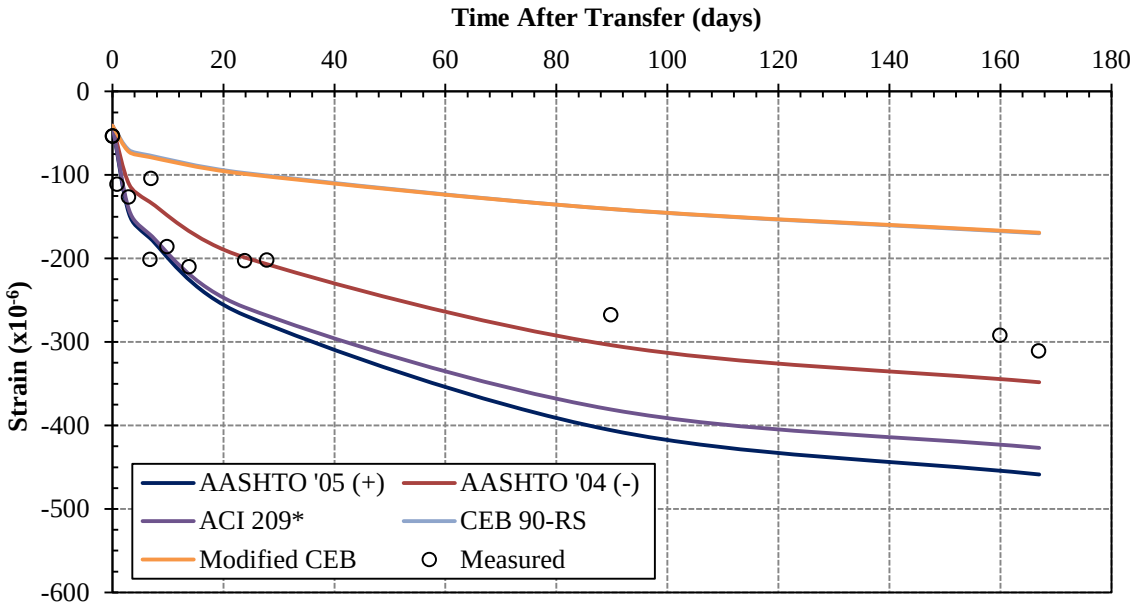

Figure 5-59: SCC-MS-2 Predicted Strains at Top VWSG with CEB 90 E_c

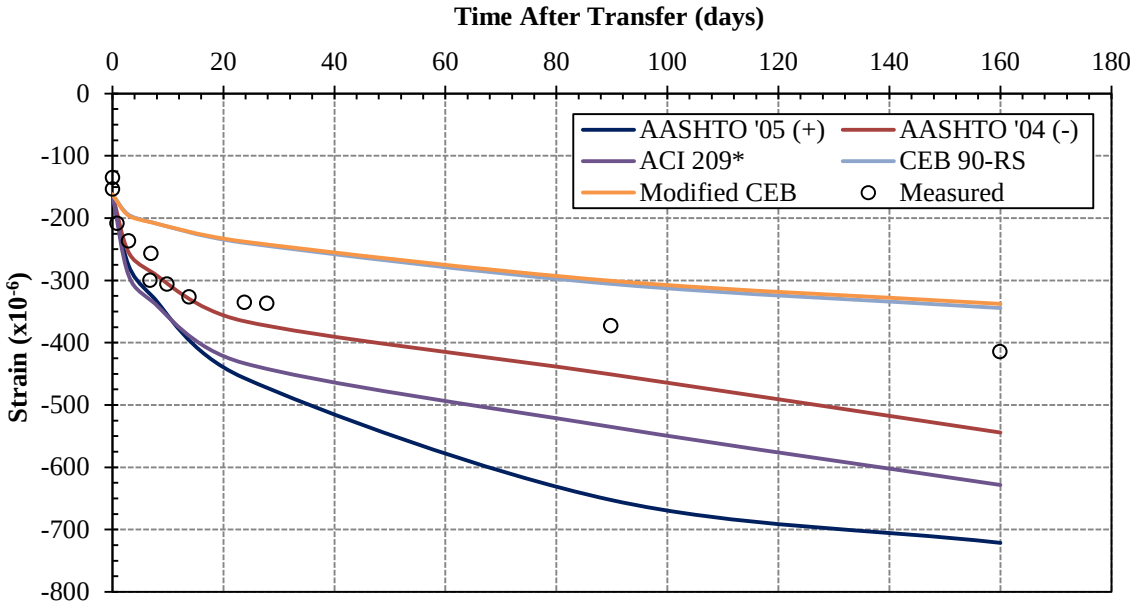

Figure 5-60: SCC-MS-1 Predicted Strains at Middle VWSG with AASHTO/ACI E_c

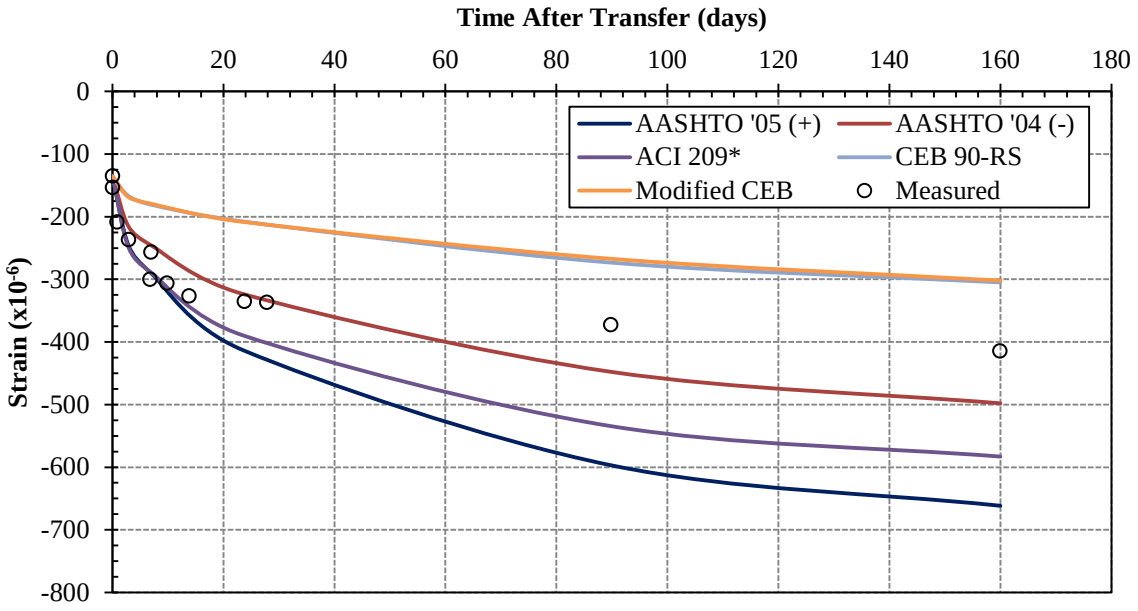

Figure 5-61: SCC-MS-1 Predicted Strains at Middle VWSG with CEB 90 E_c

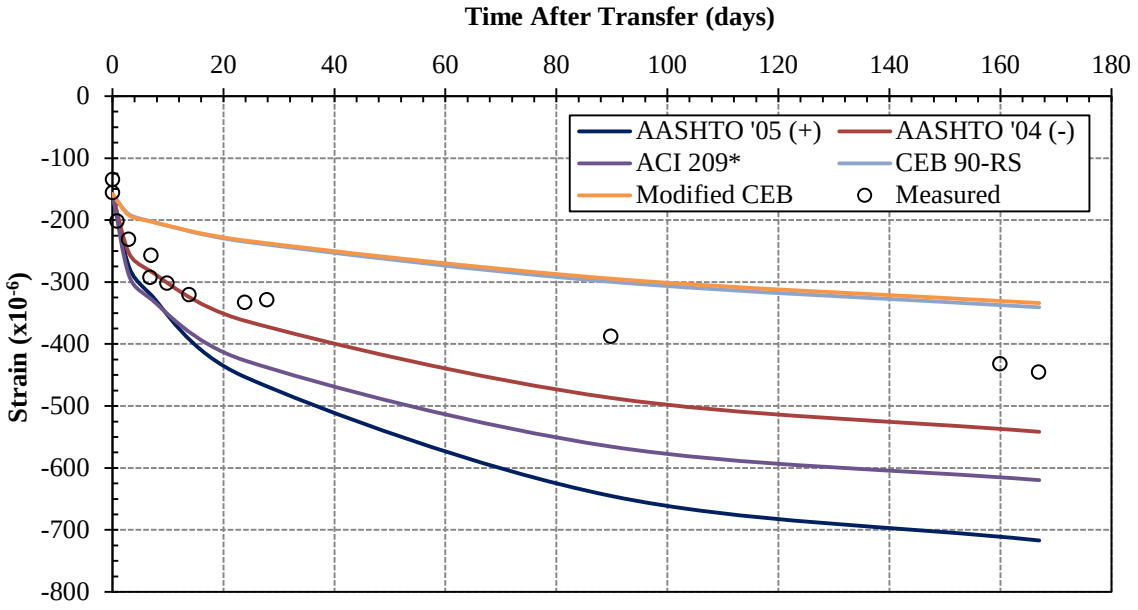

Figure 5-62: SCC-MS-2 Predicted Strains at Middle VWSG with AASHTO/ACI E_c

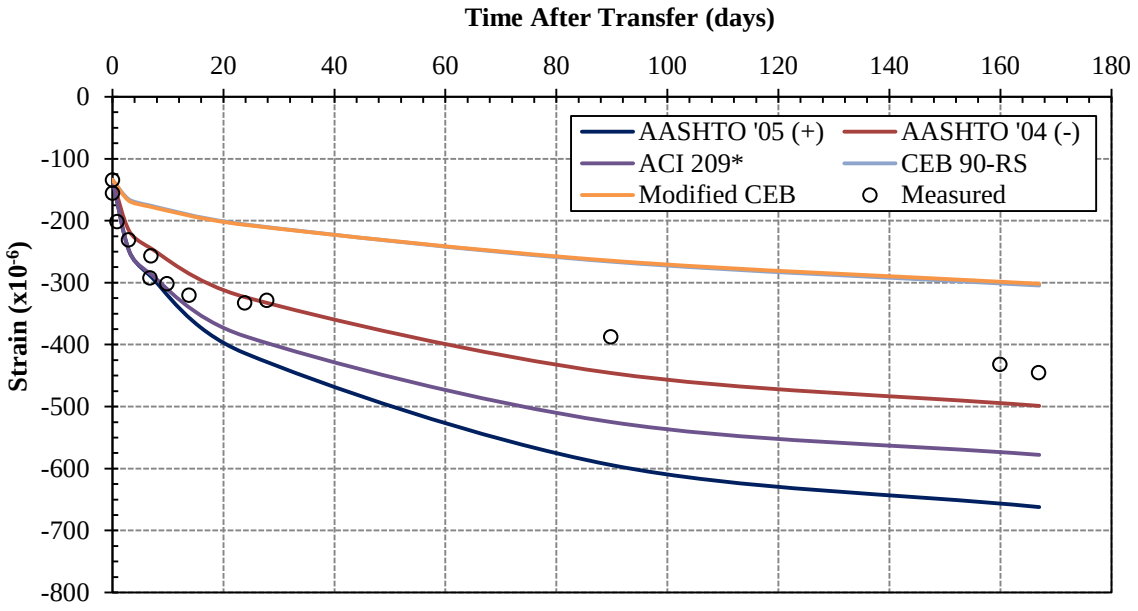

Figure 5-63: SCC-MS-2 Predicted Strains at Middle VWSG with CEB 90 E_c

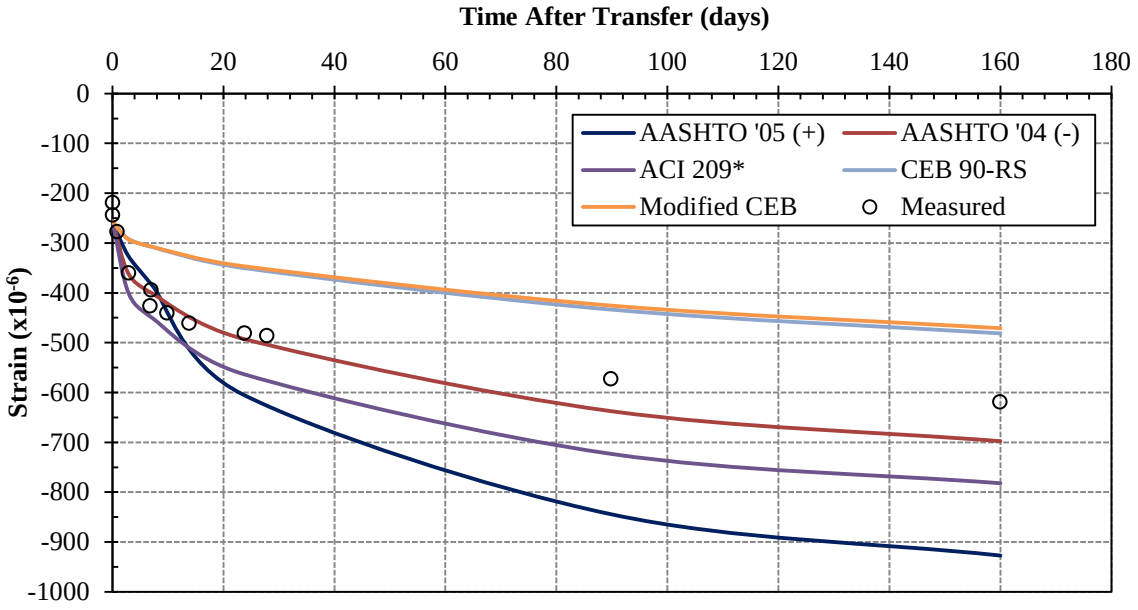

Figure 5-64: SCC-MS-1 Predicted Strains at Bottom VWSG with AASHTO/ACI E_c

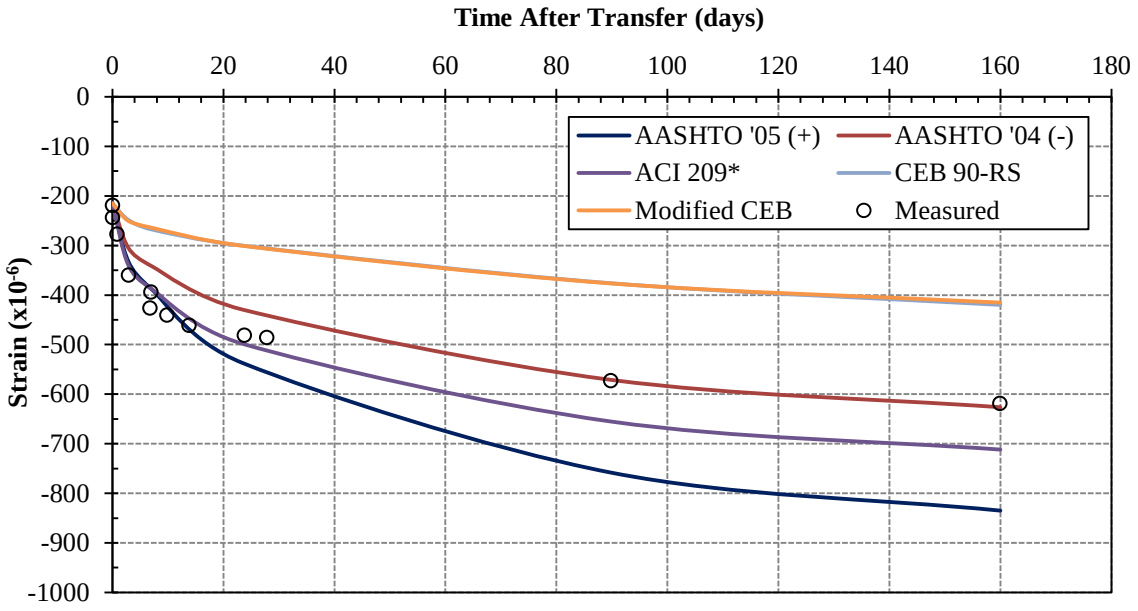

Figure 5-65: SCC-MS-1 Predicted Strains at Bottom VWSG with CEB 90 E_c

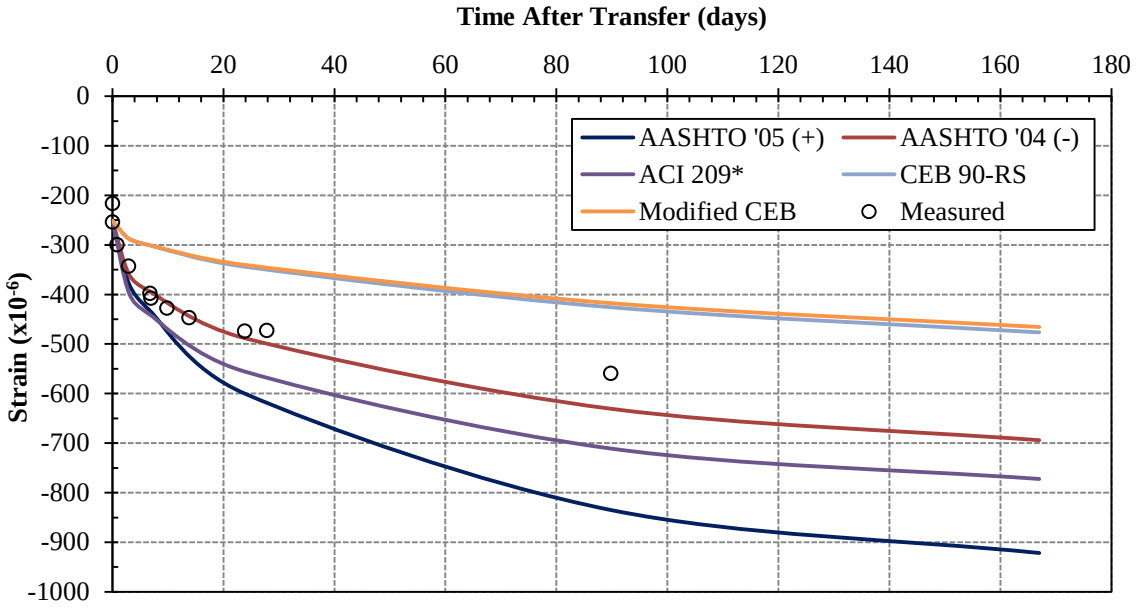

Figure 5-66: SCC-MS-2 Predicted Strains at Bottom VWSG with AASHTO/ACI E_c

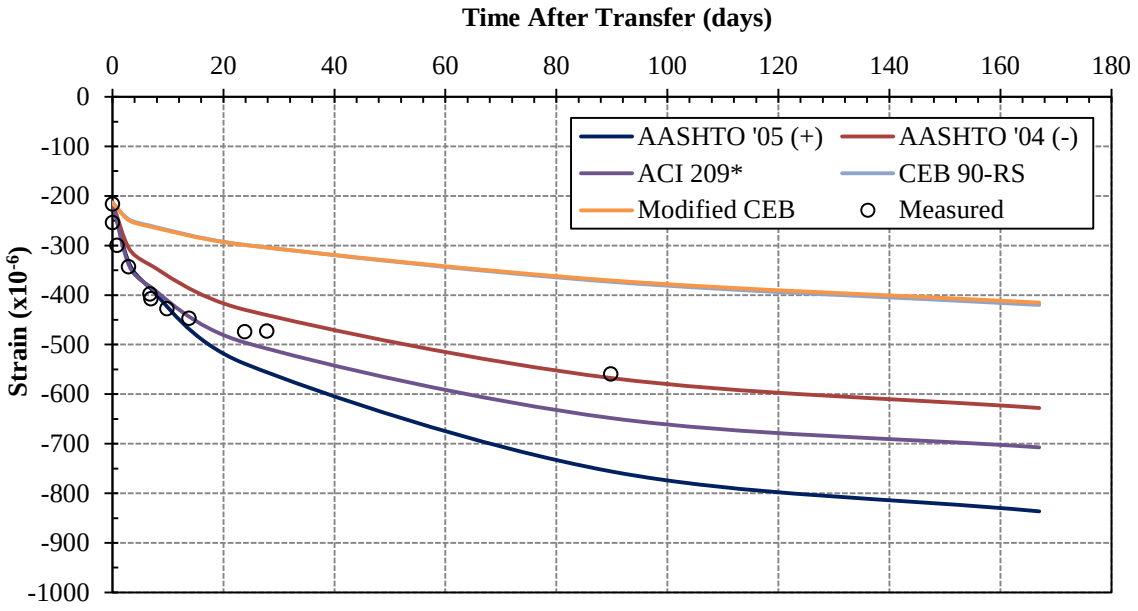

Figure 5-67: SCC-MS-2 Predicted Strains at Bottom VWSG with CEB 90 E_c

Figures 5-68 through 5-79 show the predicted concrete strains for the SCC-HS AASHTO Type I girders when using code-prediction E_c models. Results for five different creep and shrinkage models are presented: AASHTO '05(+), AASHTO '04(-), ACI 209*, CEB 90, and Modified CEB 90. The measured strain data points shown in the figures refer to the "corrected" strain measurements which neglect the effects of temperature.

Tables E-16 through E-18 in Appendix E summarize the percent errors between the measured and predicted SCC-HS strains shown in the figures. The AASHTO '04(-) creep and shrinkage model best predicts early-age concrete strains. At 28 days after transfer, AASHTO '04(-) over-predicts the strain at all VWSG locations an average of 27 percent. Similar to the SCC-MS results, the CEB 90 and Modified CEB 90 creep and shrinkage models consistently under-predict the concrete strains at all VWSG locations. However, the CEB 90 model is the best predictor of long-term strains. At 214 days after transfer and depending on the code-

prediction E_c model selected, the CEB 90 creep and shrinkage model under-predicts strain at the bottom VWSG 14 to 23 percent, strain at the middle VWSG 11 to 33 percent, and strain at the top VWSG 33 to 37 percent.

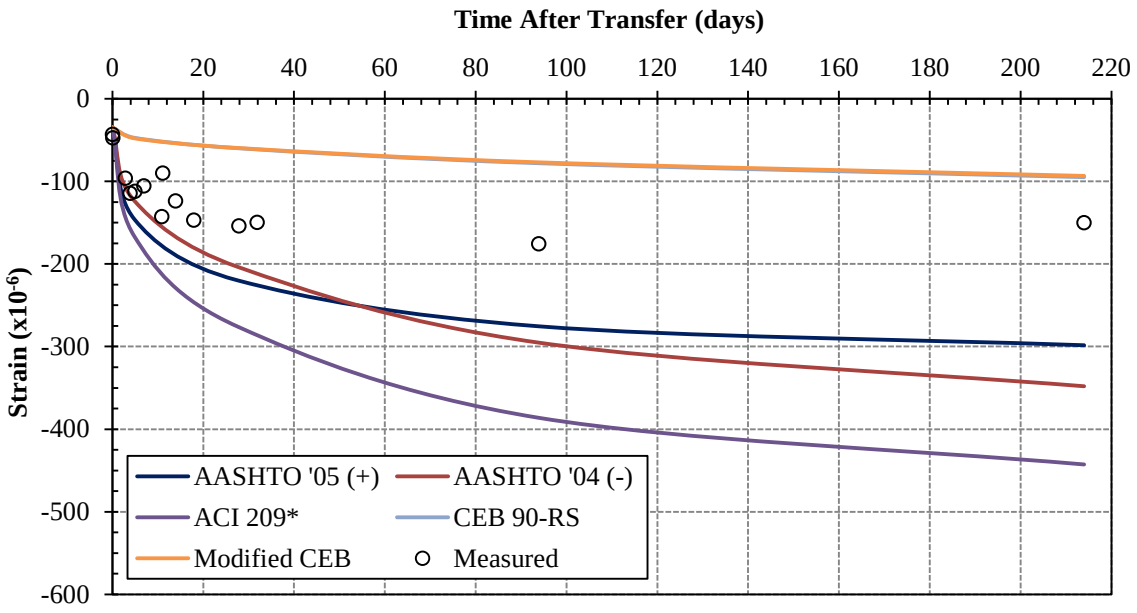

Figure 5-68: SCC-HS-1 Predicted Strains at Top VWSG with AASHTO/ACI E_c

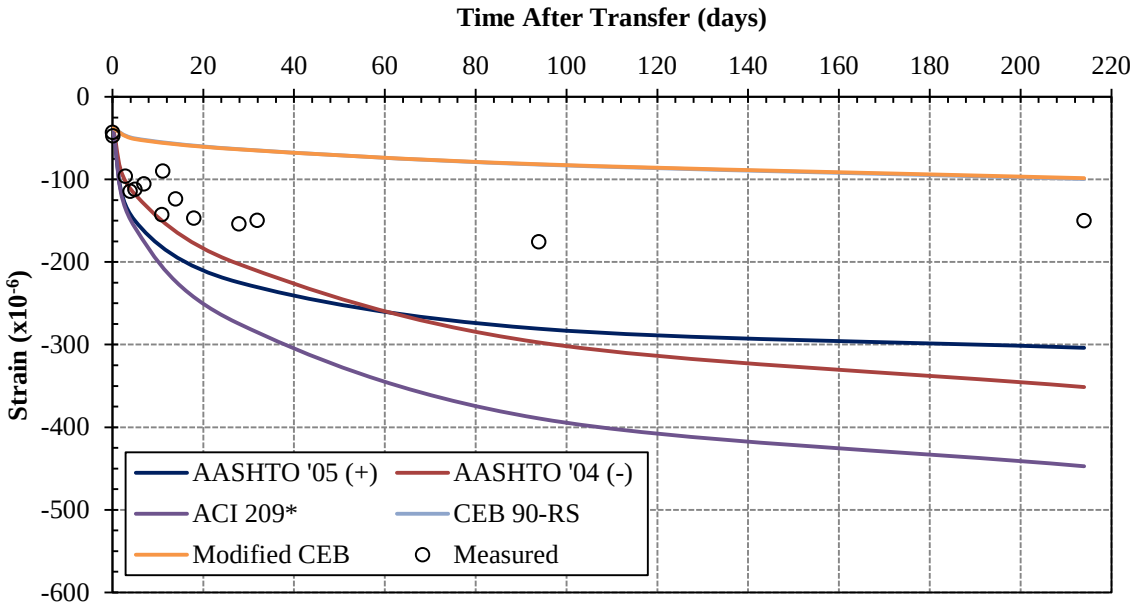

Figure 5-69: SCC-HS-1 Predicted Strains at Top VWSG with CEB 90 E_c

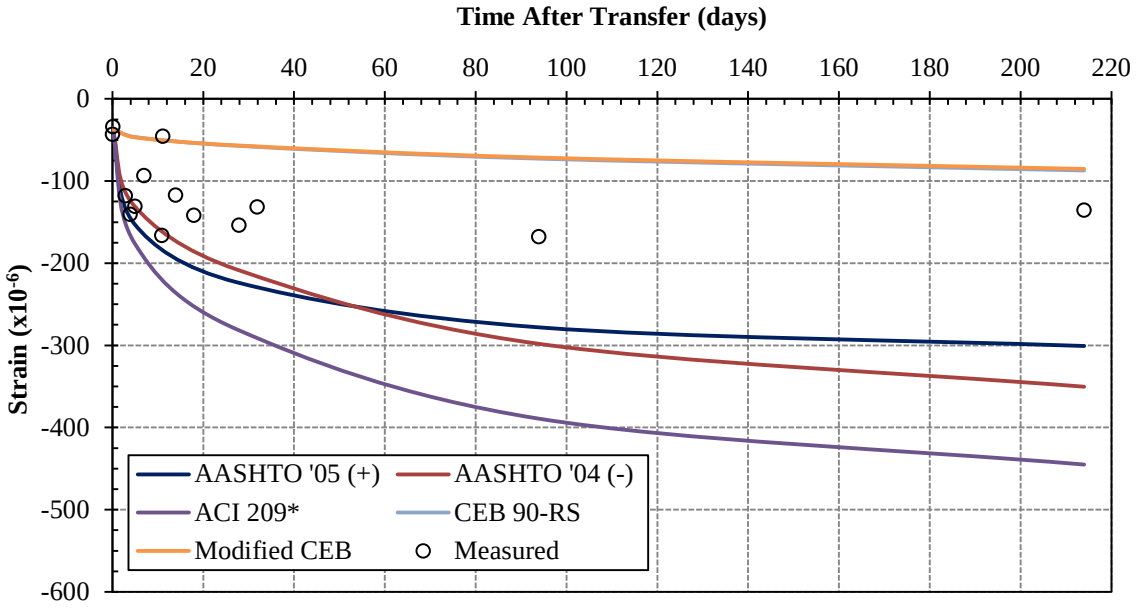

Figure 5-70: SCC-HS-2 Predicted Strains at Top VWSG with AASHTO/ACI E_c

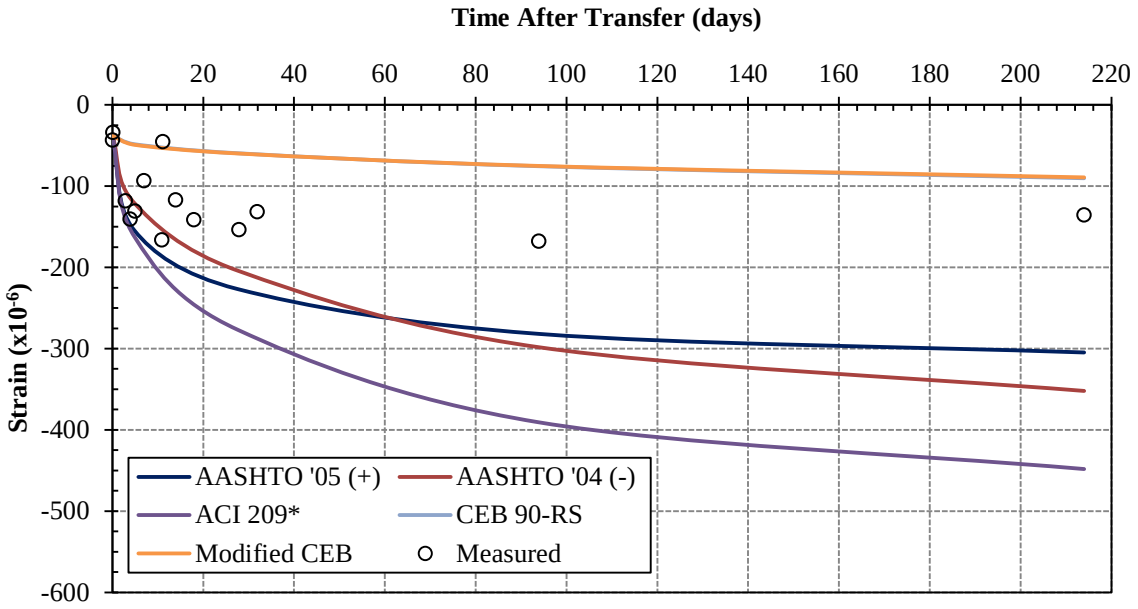

Figure 5-71: SCC-HS-2 Predicted Strains at Top VWSG with CEB 90 E_c

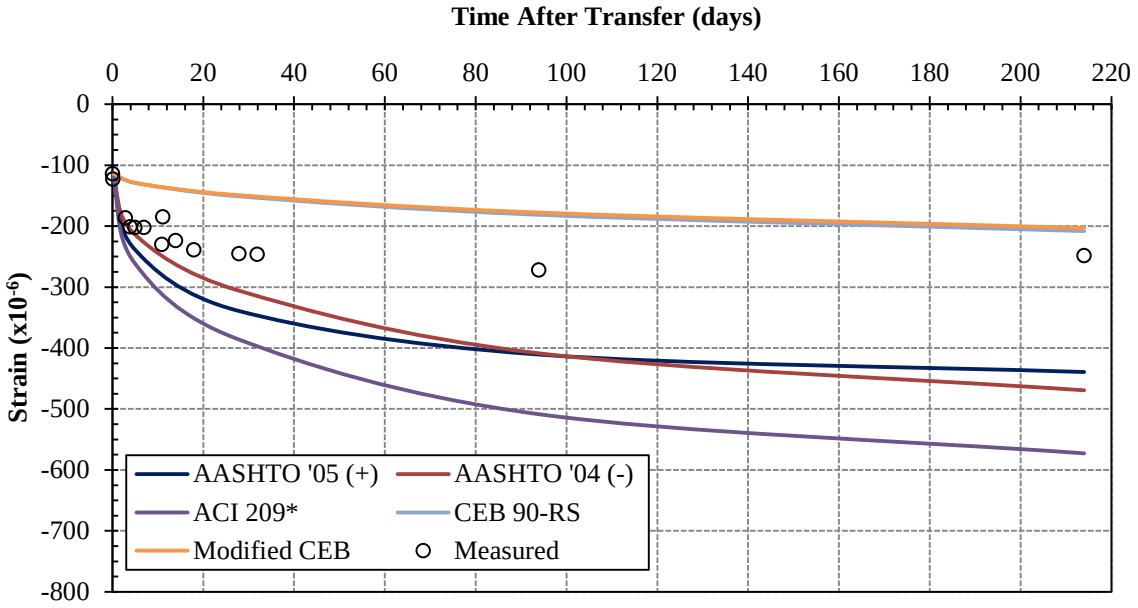

Figure 5-72: SCC-HS-1 Predicted Strains at Middle VWSG with AASHTO/ACI E_c

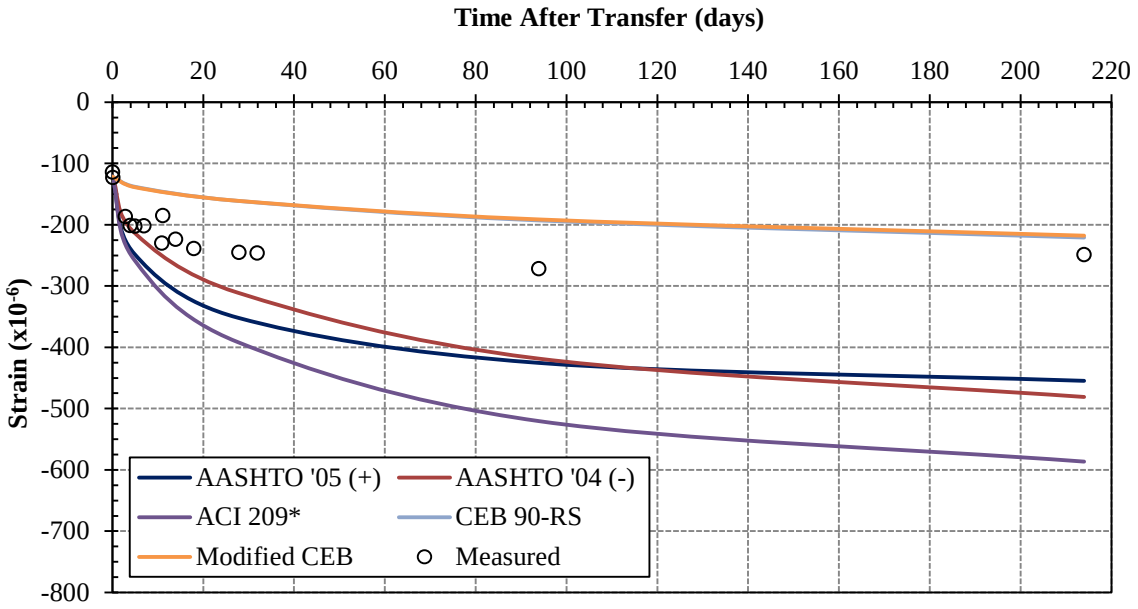

Figure 5-73: SCC-HS-1 Predicted Strains at Middle VWSG with CEB 90 E_c

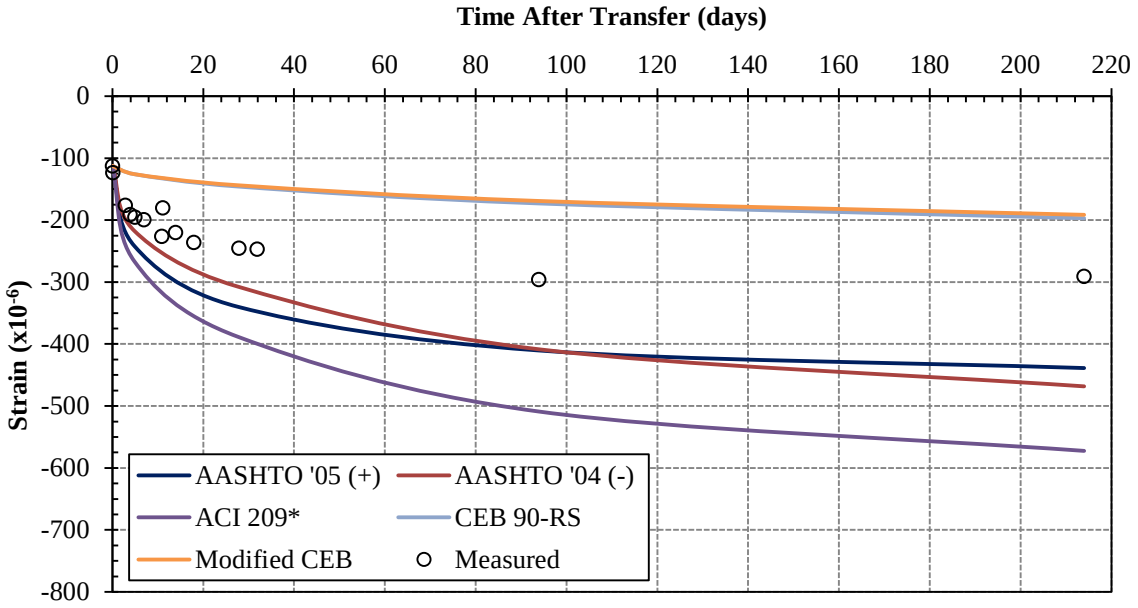

Figure 5-74: SCC-HS-2 Predicted Strains at Middle VWSG with AASHTO/ACI E_c

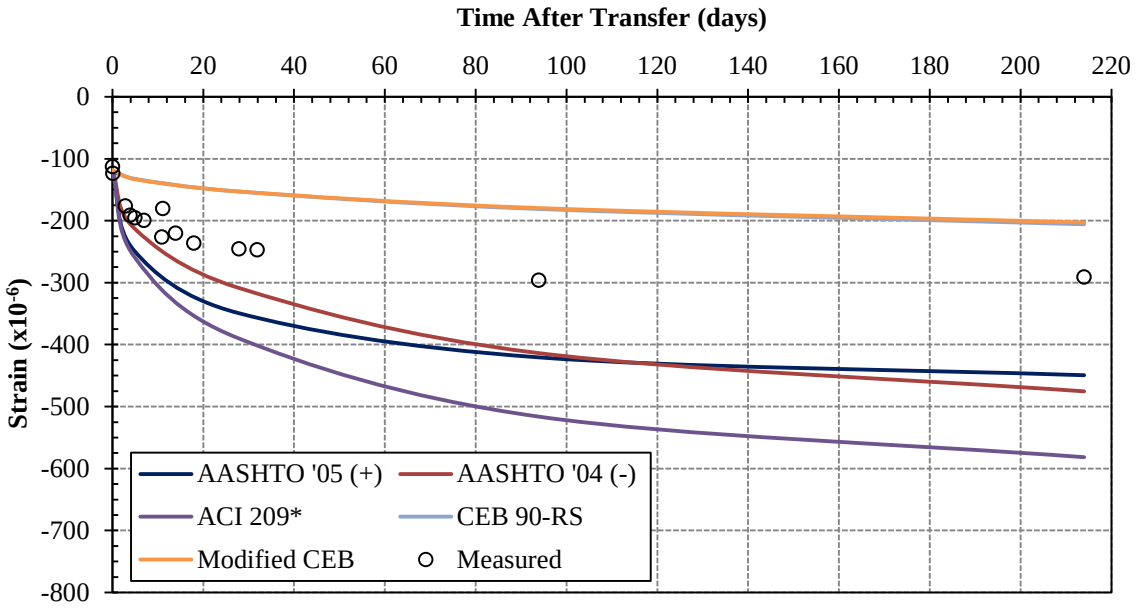

Figure 5-75: SCC-HS-2 Predicted Strains at Middle VWSG with CEB 90 E_c

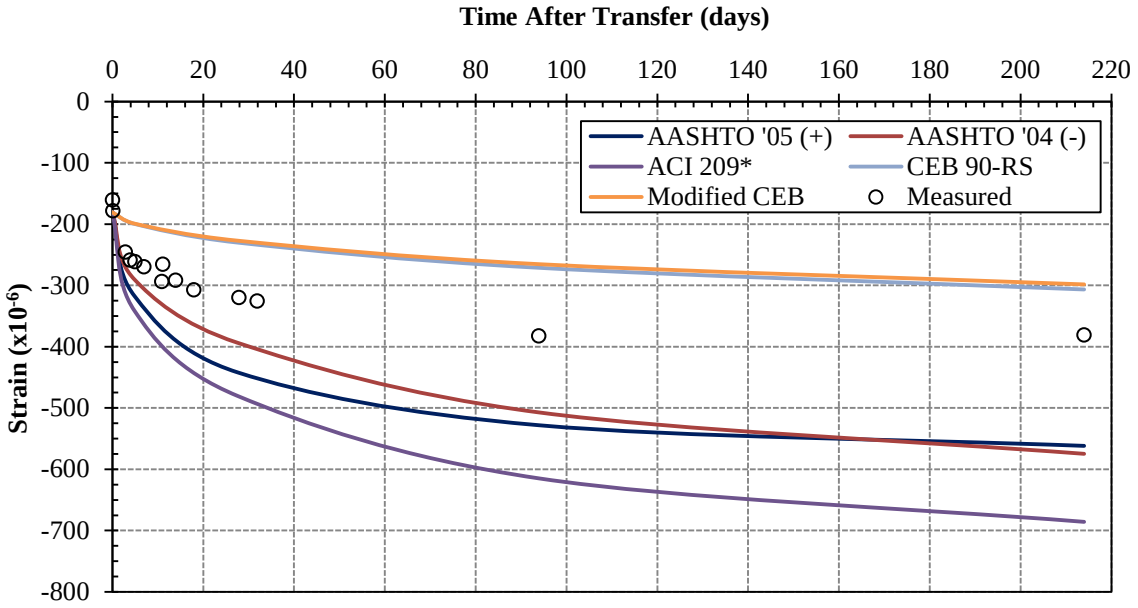

Figure 5-76: SCC-HS-1 Predicted Strains at Bottom VWSG with AASHTO/ACI E_c

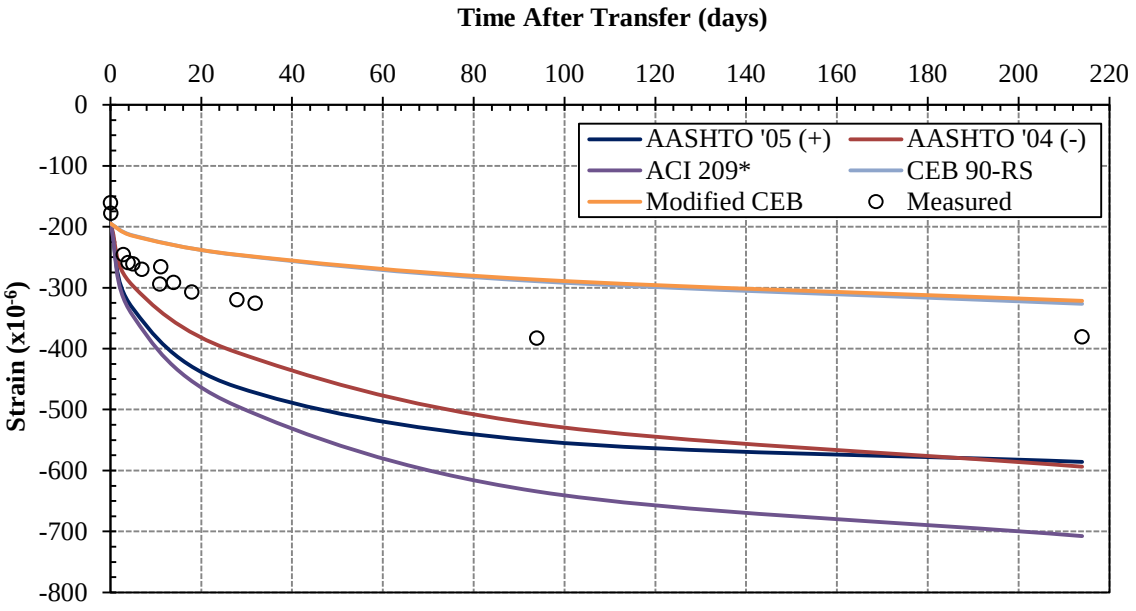

Figure 5-77: SCC-HS-1 Predicted Strains at Bottom VWSG with CEB 90 E_c

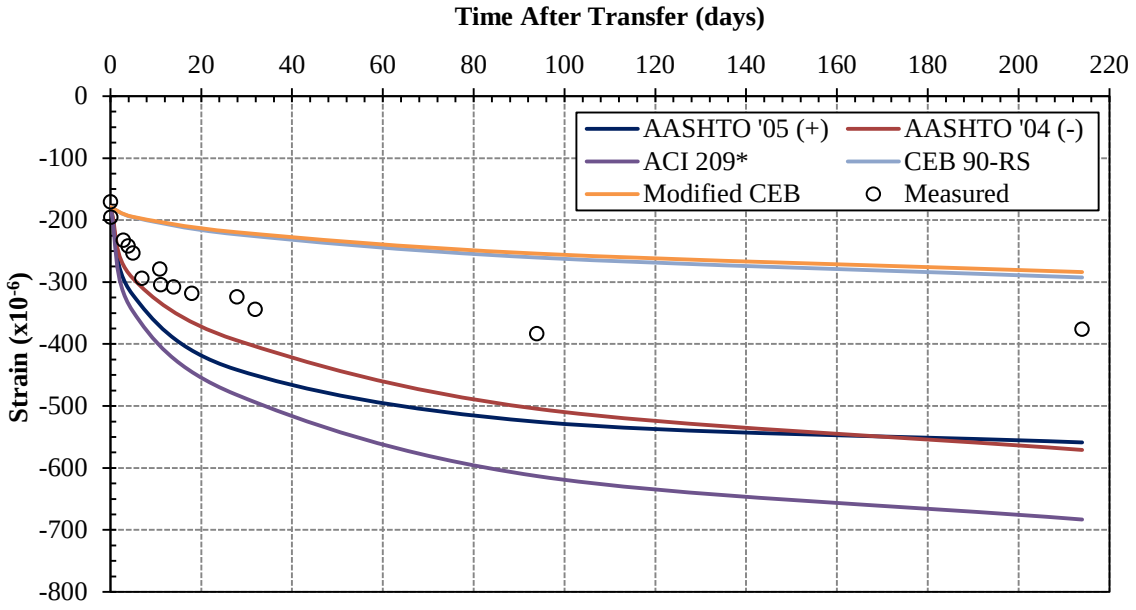

Figure 5-78: SCC-HS-2 Predicted Strains at Bottom VWSG with AASHTO/ACI E_c

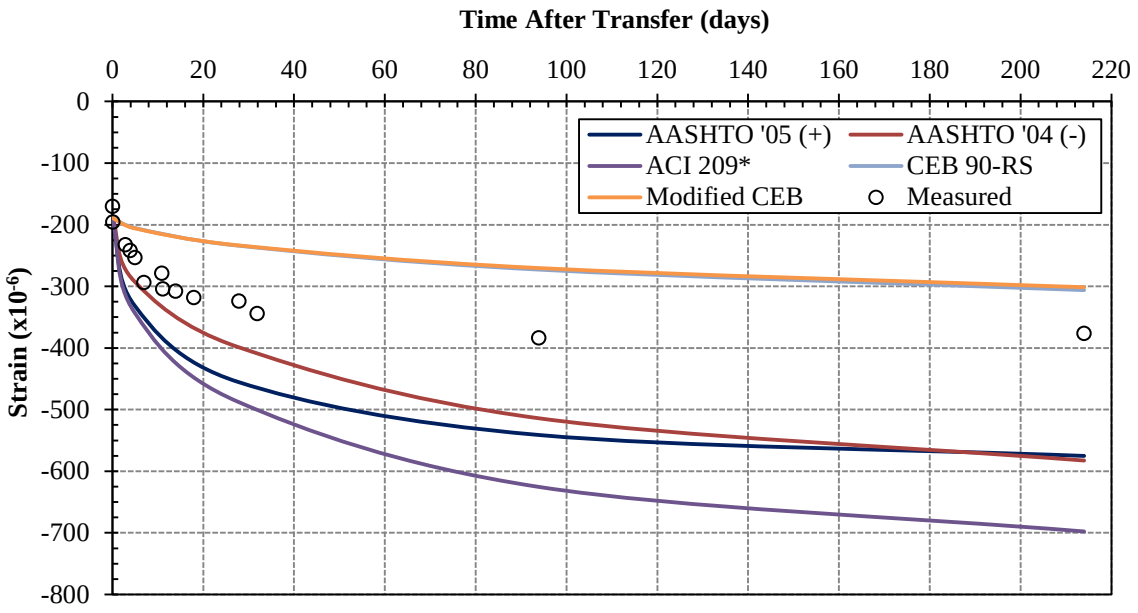

Figure 5-79: SCC-HS-2 Predicted Strains at Bottom VWSG with CEB 90 E_c

5.1.3 BT-54 GIRDERS

The results for five AASHTO BT-54 girders presented by Stallings et al. (2003) were based on a concrete modulus of elasticity of 5740 ksi at all ages. Therefore, all of the program results for the BT-54 girders were calculated using the "Constant E_c" model for the concrete MOE development over time. The creep and shrinkage models used for analysis include: AASHTO '05(+), AASHTO '04(-), ACI 209*, CEB 90 and Modified CEB 90.

The ACI 209* model uses an "adjusted" slump of 0.5 inches based on mixture proportions. The BT-54 design parameters used to calculate the ACI 209 correction factors are given in Table 5-3. The correction factors, excluding the slump correction factor, as calculated by Stallings et al. (2003) are shown in Table 5-4. The slump correction factors provided in Table 5-4 are based on the "adjusted" slump of 0.5 inches instead of the actual slump of 8 inches.

Table 5-3: BT-54 Design Parameters

Parameter	Value
Relative Humidity	70 %
Volume/Surface	3.07 in.
Adjusted Slump	0.5 in.
Fine Aggregate	37 %
Water	265 pcy
Total Cement Content	904 pcy
Air Content	4.2%

Table 5-4: ACI 209 Correction Factors for BT-54 Girders (Stallings et al. 2003)

Factor	Shrinkage	Creep
Relative Humidity	0.700	0.801
Volume/Surface	0.836	0.815
Slump (Adjusted)	0.911	0.854
Fine Aggregate %	0.818	0.969
Cement Content	1.075	NA
Air Content	0.984	1.000
Product of Factors	0.461	0.540

The computer program calculates the ACI 209 correction factors based on user input of the parameters shown in Table 5-3. Figure 5-80 shows the output screen listing the creep and shrinkage correction factors when the ACI 209 creep and shrinkage model is selected. The slump correction factors shown in Figure 5-80 are calculated using the actual slump of 8 inches

and are much greater than the slump correction factors shown in Table 5-4 which are based on the “adjusted” slump.

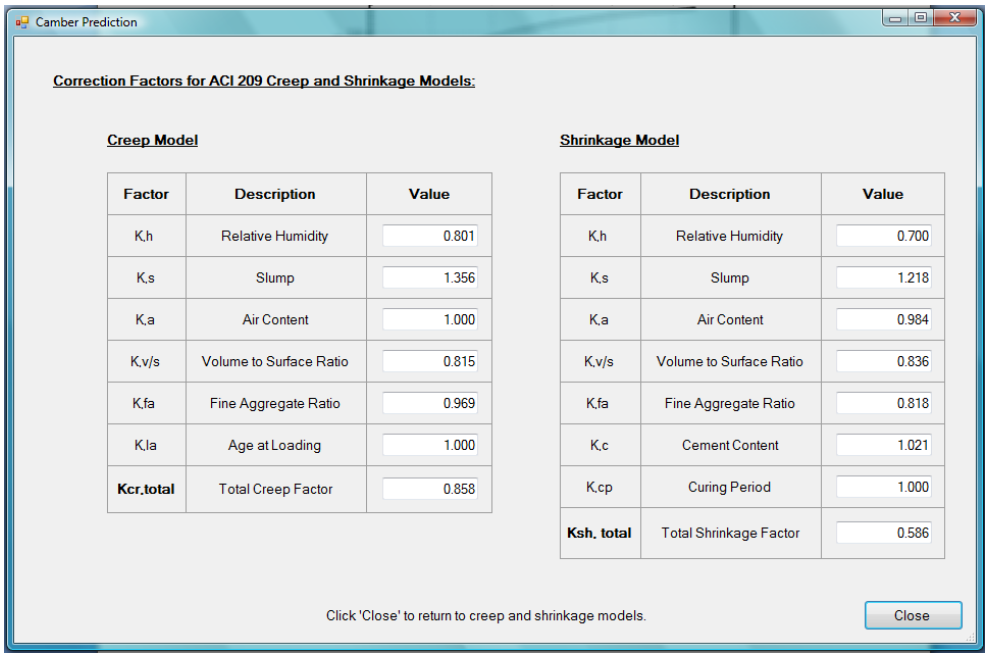

Figure 5-80: Creep and Shrinkage Correction Factors – VB Program Output

Research by Stallings et al. (2003) measured the creep coefficients at various ages. The creep test results are shown in Figure 5-81. The relationship between creep coefficient and time when using the standard ACI 209 conditions is also shown.

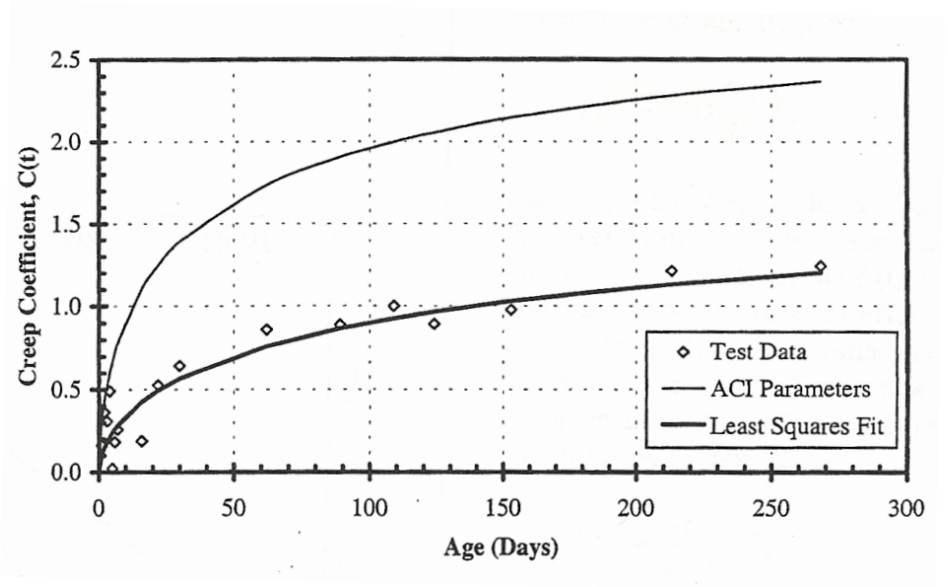

Figure 5-81: BT-54 Creep Coefficients (Stallings et al. 2003)

The computer program calculates an incremental creep coefficient for each time interval. See Figure K-24 in Appendix K for the output screen showing the incremental creep coefficients. The total creep coefficient any time after transfer is the summation of the preceding incremental creep coefficients. The total creep coefficient over time as predicted by the computer program is shown in Figure 5-82. When using the "adjusted" slump for the ACI 209 creep and shrinkage model, the program generates a creep coefficient curve similar to the "Least Squares Fit" presented in Figure 5-81.

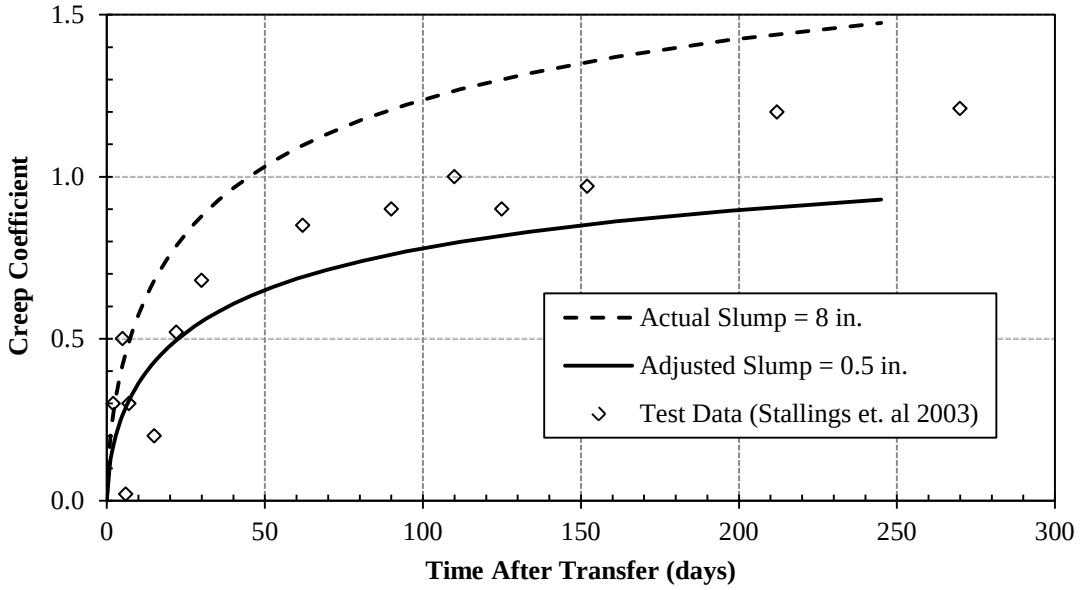

Figure 5-82: BT-54 Predicted Creep Coefficients

The ACI 209R-92 creep and shrinkage model used the correction factors and creep coefficients to predict incremental concrete strains at the top, bottom, and centroid of the transformed section. Based on the resulting strain gradient, the concrete strain at the top and bottom VWSG locations are determined. The ACI 209* predicted strains are compared to the experimental strain measurements of five BT-54 girders in Figures 5-83 through 5-86. Predicted strains based on the AASHTO '05(+), AASHTO '04(-), CEB 90, and Modified CEB 90 creep and shrinkage models are also shown.

The predicted concrete strains at the top VWSG are shown in Figure 5-83. The AASHTO creep and shrinkage models best predict long-term strains (beyond 150 days after transfer) without over-estimating. However, the ACI 209* model provides a good average for the long-term strains at the top VWSG location.

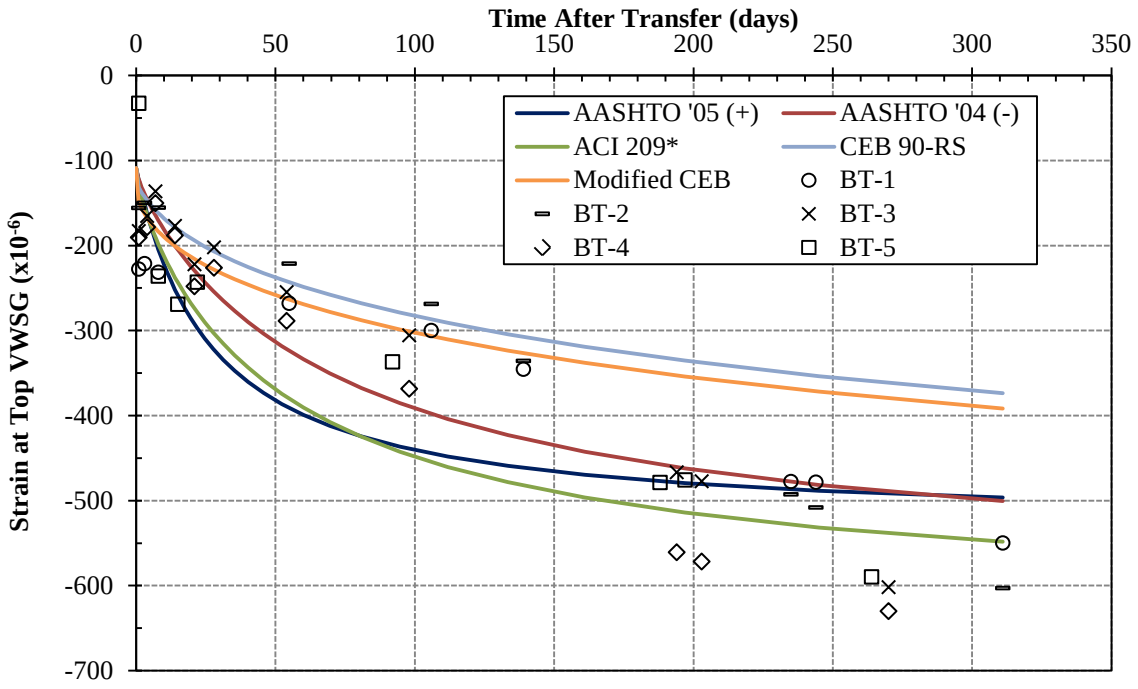

Figure 5-83: BT-54 Predicted Strains at Top VWSG

Figure 5-84 takes a closer look at the early-age strains at the top VWSG. The strain predictions using the CEB 90 creep and shrinkage model correlate well with the BT-3 strain measurements before 28 days while the Modified CEB model better correlates after 28 days. The AASHTO '05(+) and ACI 209* creep and shrinkage models provide similar strain predictions up to 80 days after transfer. The CEB 90 model best predicts the BT-2 strain measurements up to 120 days after transfer.

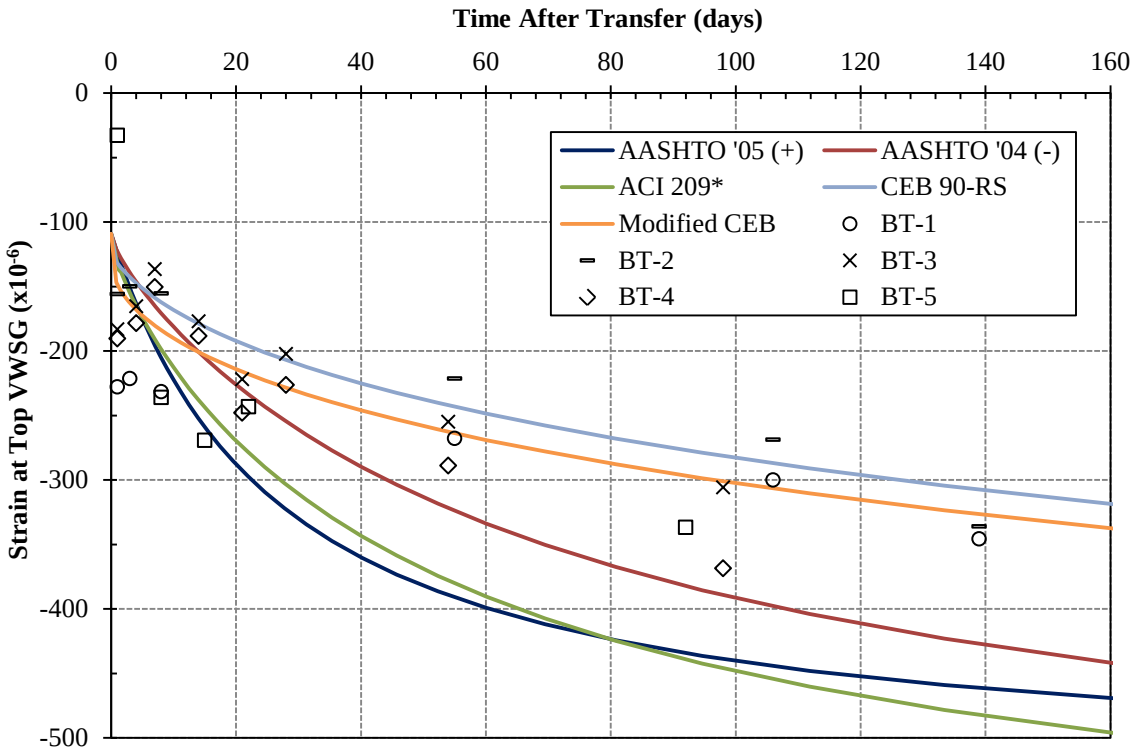

Figure 5-84: BT-54 Predicted Strains at Top VWSG – Early Age

The predicted concrete strains at the bottom VWSG are shown in Figures 5-85 and 5-86. In general, the AASHTO '05(+) and ACI 209* creep and shrinkage models best predict the long-term strains. However, the strain measurements for BT-5 just prior to 200 days after transfer are better predicted by AASHTO '04(-) and the Modified CEB model. At 197 days after transfer, the measured strain at BT-5's bottom VWSG was under-predicted 0.05 percent using the AASHTO '04(-) model. The Modified CEB model over-predicted the strain in the bottom VWSG by 0.42 percent.

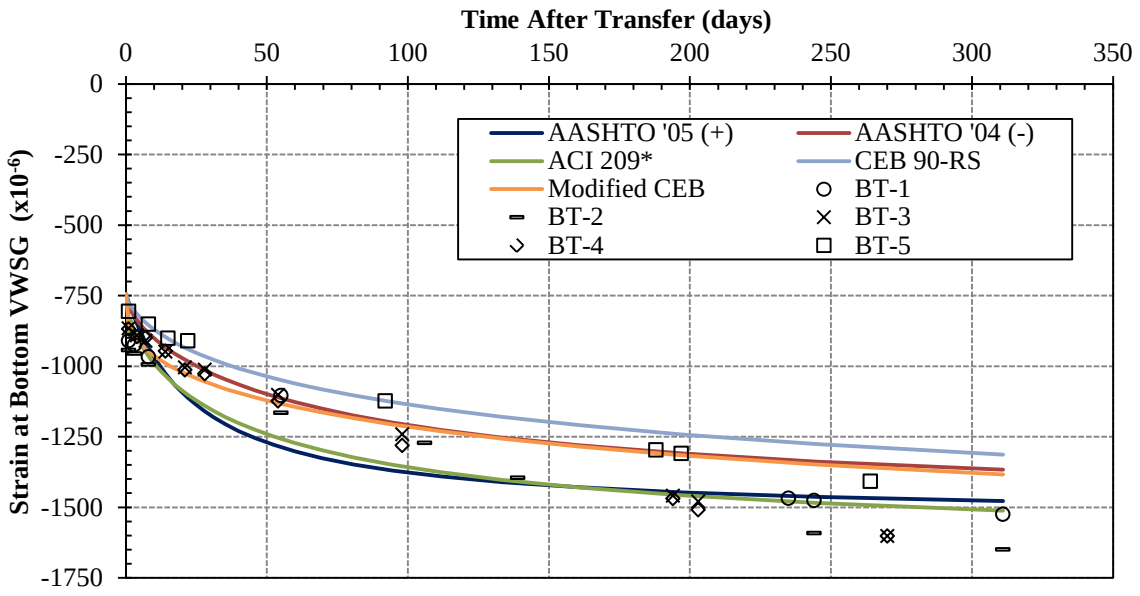

Figure 5-85: BT-54 Predicted Strains at Bottom VWSG

Figure 5-86 takes a closer look at the early-age strains at the bottom VWSG. In general, the Modified CEB model better predict the early-age strains. However, CEB 90 best predicts the strains measured for girder BT-5.

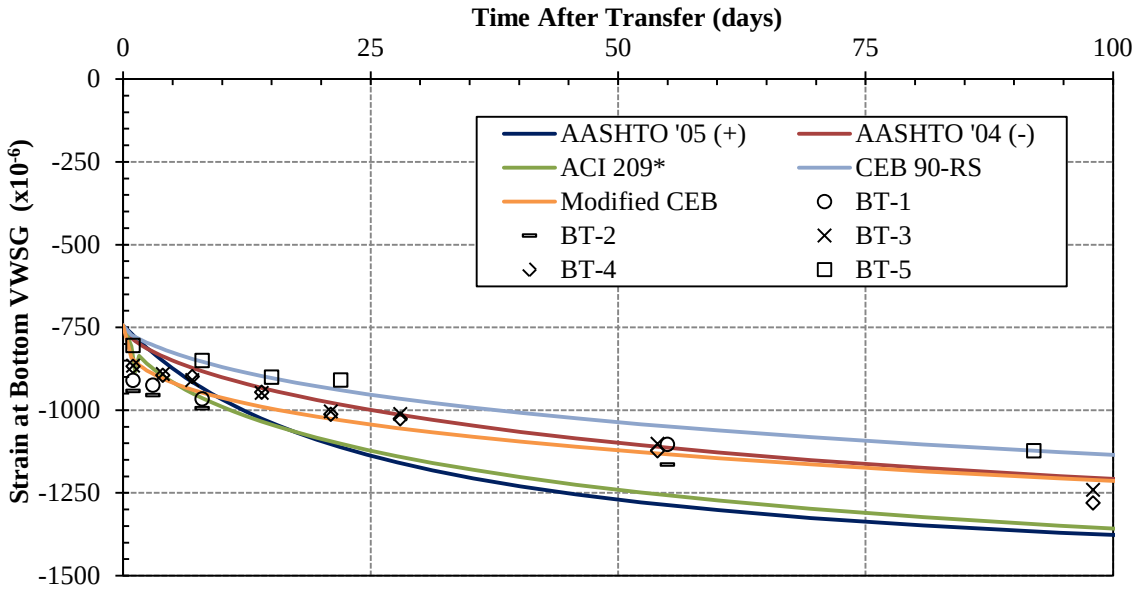

Figure 5-86: BT-54 Predicted Strains at Bottom VWSG – Early Age

5.2 STRAND STRESS PREDICTIONS

The program calculates initial prestress losses to predict the strand stresses immediately before and after transfer. These initial prestress losses include relaxation of steel and elastic shortening of concrete. After transfer, incremental strains and curvatures at the centroid of the transformed section are used to calculate the total strains and stresses at various cross sections along the girder and locations within each cross section. Previous research findings for the AASHTO Type I girders are presented in this section to evaluate the program's strand stress predictions.

5.2.1 AASHTO TYPE I GIRDERS

A portion of the research performed by Boehm (2008) included the effect of SCC on the transfer length of AASTHO Type I girders. Strand force transducer readings were used to calculate the strand stresses immediately before transfer. DEMEC strain gauge readings were used to calculate the strand stresses immediately after transfer and the effective prestress in the strands up to 28 days after transfer. The results from Boehm's research are presented in Table B-3 located in Appendix B of this thesis.

DEMEC strain gauge readings were taken at both ends of each girder. Table 5-5 compares the average of the measured strand stresses at each end to the program's predicted stresses. The predicted stresses presented in this section correspond to the six prestressing strands located in *Layer Group* 1 (LG1) of the AASHTO Type I girders.

Table 5-5: Strand Stress Comparisons

Girder	Measured f_{pbt} (ksi)	Predicted f_{pbt} (ksi)	% Diff	Measured f_{pt} (ksi)	Predicted f_{pt} (ksi)	% Diff
STD-M-1	200	200.7	0.4	192	193.3	0.7
STD-M-2	200	200.7	0.4	192	193.3	0.7
SCC-MS-1	196	200.6	2.4	187	192.7	3.0
SCC-MS-2	196	200.7	2.4	187.7	192.7	2.7
SCC-HS-1	202	200.7	-0.7	195	194.6	-0.2
SCC-HS-2	202	200.7	-0.7	195	194.6	-0.2

To compare the strand stresses up to 28 days after transfer, the "Constant E_c" model was used for the concrete MOE development with time. The creep and shrinkage models used for analysis included the following: AASHTO '05 (+), AASHTO '04 (-), ACI 209*, and CEB 90. The "adjusted" slump values were used in the ACI 209* model for all girders. Figures 5-87 through 5-89 compare the predicted strand stresses in LG1 (layer group at bottom of girder) to the measured stresses from Boehm's research. None of the models provide a fast enough rate of time-dependent deformation for the 28-day period, particularly within the first seven days after transfer.

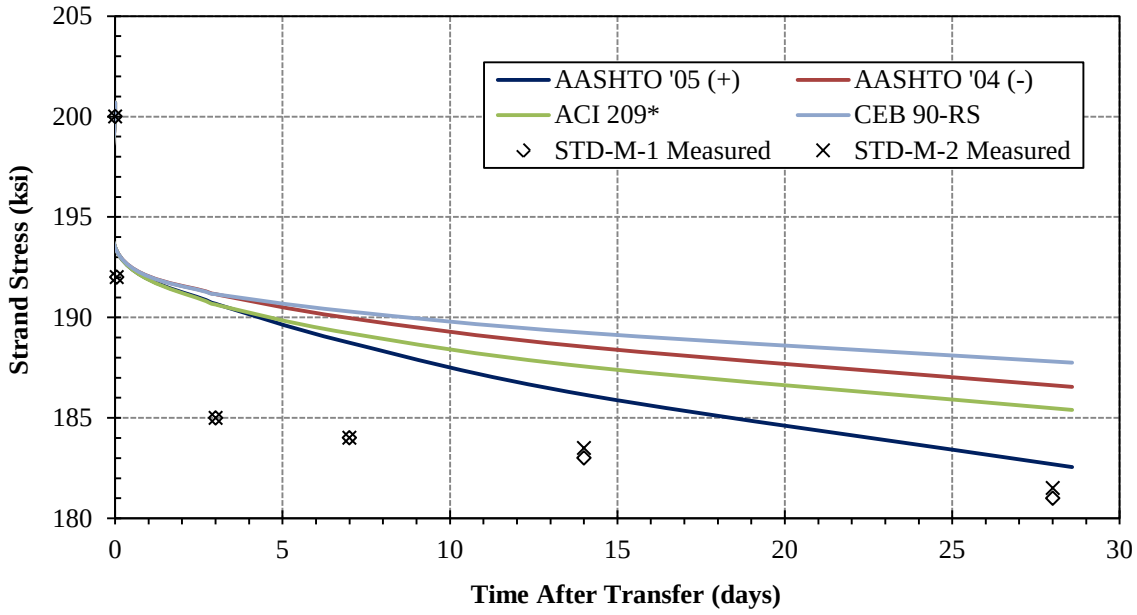

Figure 5-87: Predicted Strand Stresses in LG1 for STD-M Girders

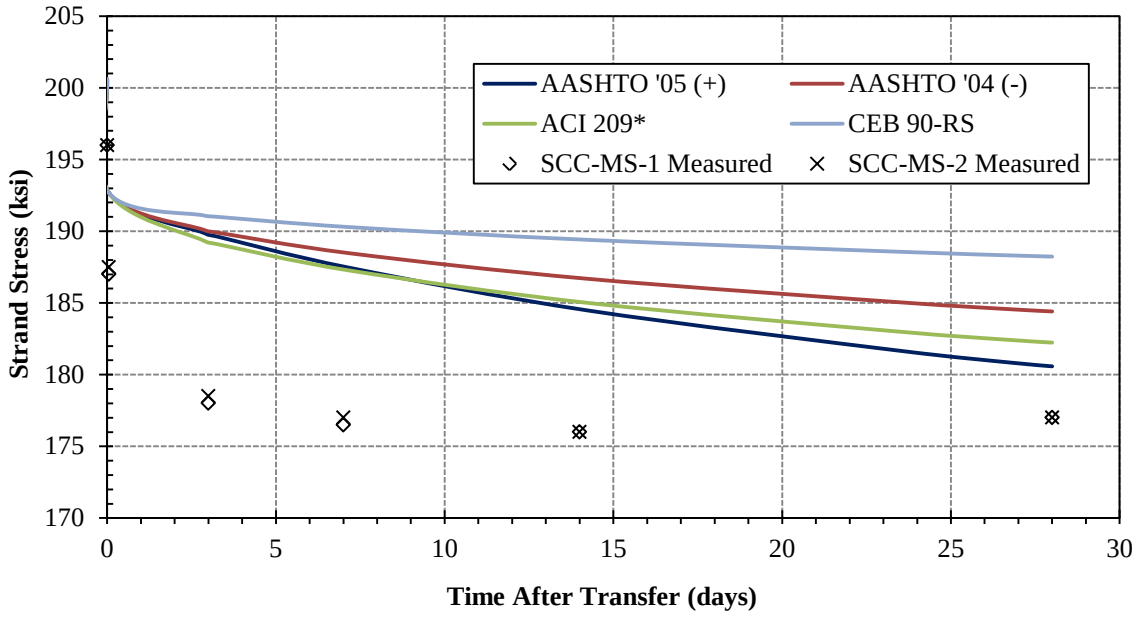

Figure 5-88: Predicted Strand Stresses in LG1 for SCC-MS Girders

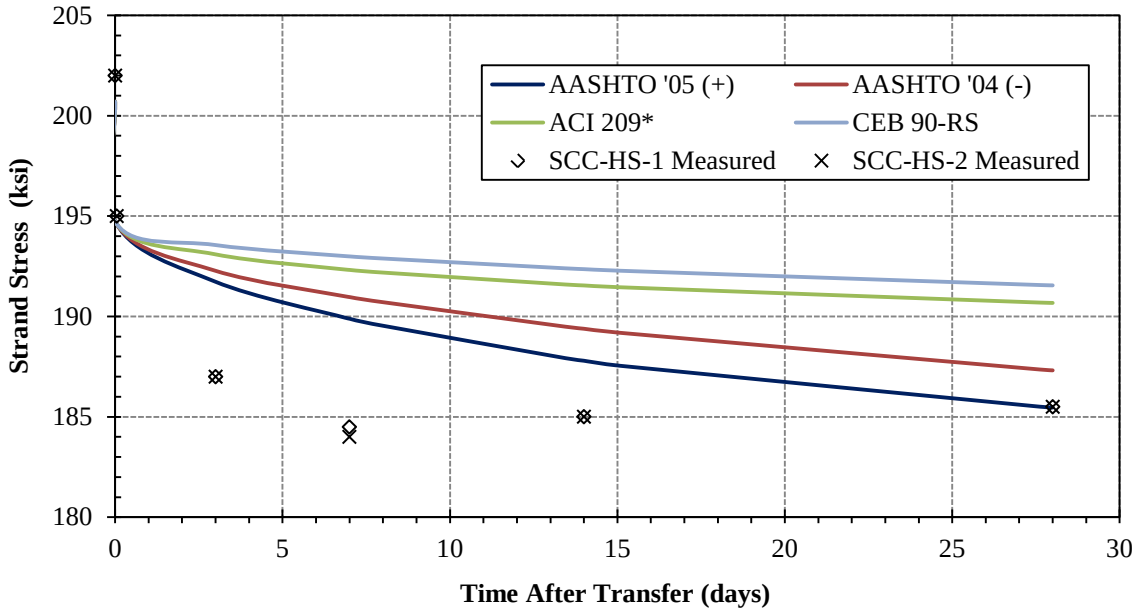

Figure 5-89: Predicted Strand Stresses in LG1 for SCC-HS Girders

5.3 CAMBER PREDICTIONS

The program calculates the camber at midspan of prestressed flexural members. Experimental camber measurements for six AASHTO Type I girders, sixteen T-beams, and five BT-54 girders reviewed in Chapter 4 are presented in this section. The measured camber is compared to camber predictions using various combinations of concrete modulus of elasticity, creep, and shrinkage models in the VB program. The concrete MOE models include Constant E_c, Two-Point E_c, AASHTO '05 (+), ACI 209, and CEB 90. The creep and shrinkage models include AASHTO '05 (+), AASHTO '04 (-), ACI 209, CEB 90, and modified CEB 90.

The measured camber for the T-beams and BT-54 girders was taken directly from previous research by Levy (2007) and Stallings et al. (2003). However, the camber measurements for the AASHTO Type I girders were adjusted based on the VWSG temperature

readings. The temperature effects on camber for the AASHTO Type I girders are presented in the next section.

5.3.1 TEMPERATURE-INDUCED CURVATURES

Similar to temperature-induced strains, VWSG temperature readings were used to calculate temperature-induced curvatures for the AASHTO Type I girders. The top and bottom VWSG temperature readings for the STD-M, SCC-MS, and SCC-HS girders are shown in Figures B-6, B-7, and B-8, respectively. Figures 5-90 through 5-92 show the temperature-induced curvatures for the AASHTO Type I girders at various times after transfer.

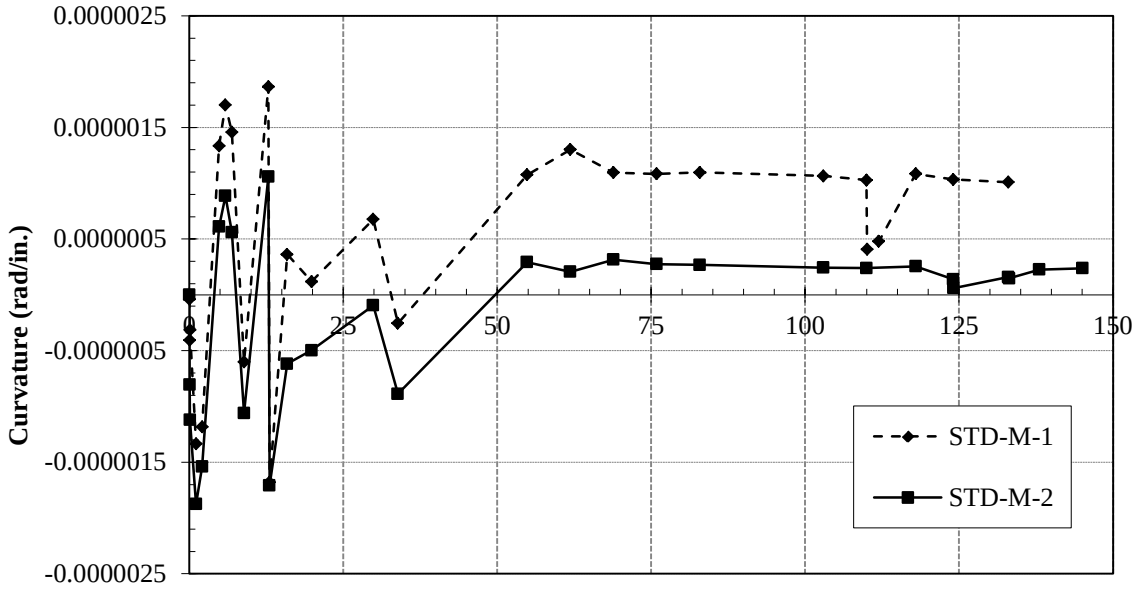

Figure 5-90: Temperature-Induced Curvature for STD-M Girders

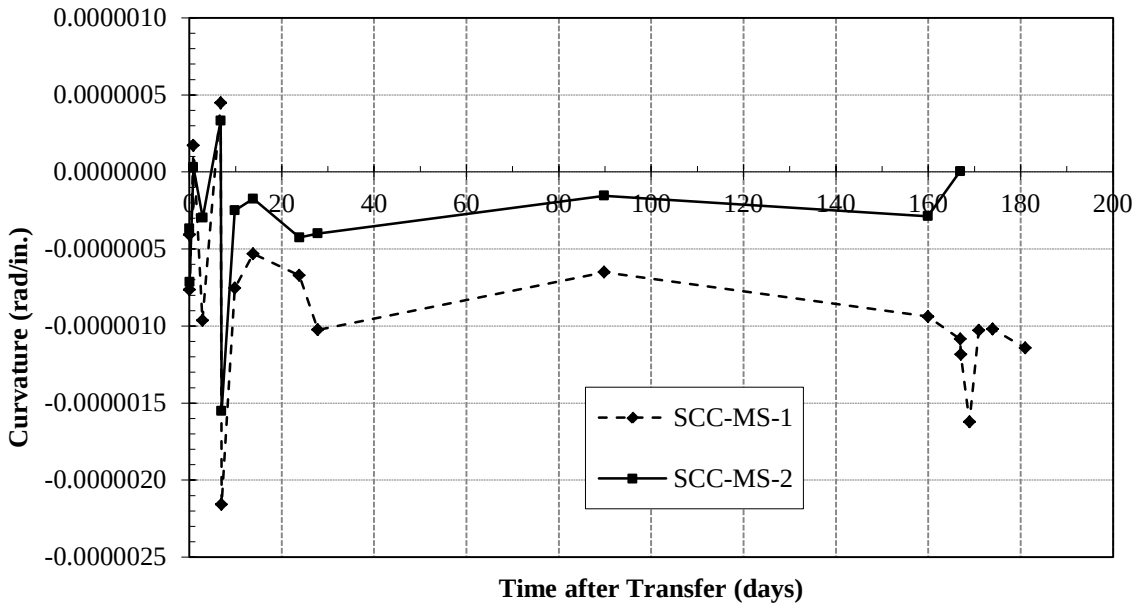

Figure 5-91: Temperature-Induced Curvature for SCC-MS Girders

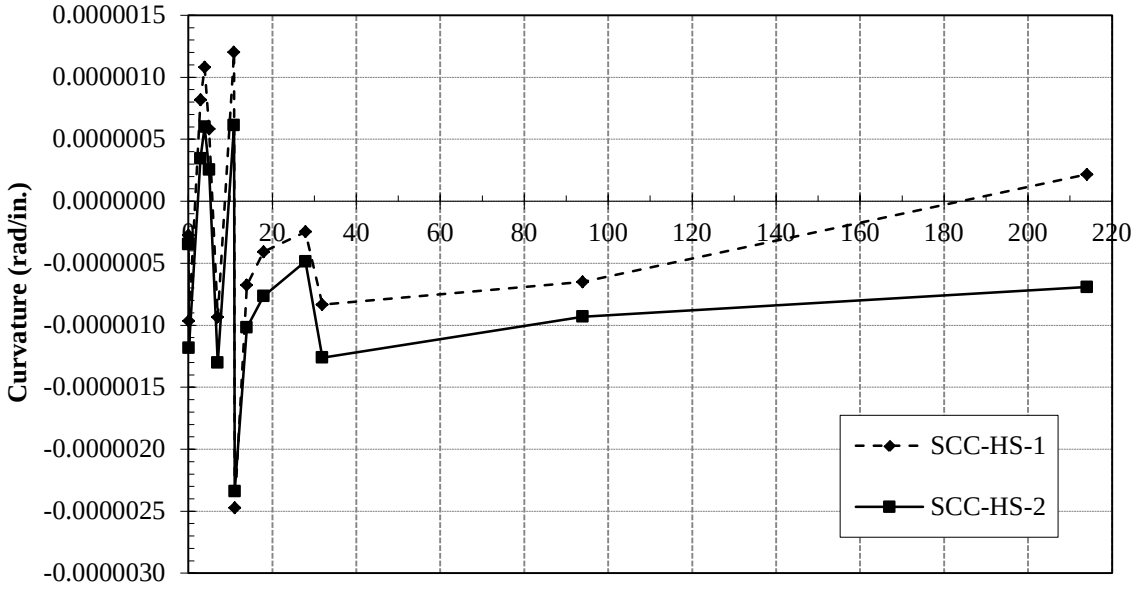

Figure 5-92: Temperature-Induced Curvature for SCC-HS Girders

5.3.2 AASHTO TYPE I GIRDERS

Camber was measured at midspan and quarter-span of each AASHTO Type I girder. See Figures F-2 through F-7 in Appendix F for the measured camber of each girder at various times after prestress transfer. Removing the temperature-induced curvature component from the measured camber produces "corrected" camber values. The measured and "corrected" camber values for all AASHTO Type I girders are shown in Figure F-1. Throughout this section, the "corrected" camber values are compared to the program's camber predictions.

The same approach for predicting strains in the AASHTO Type I girders was used to evaluate the program's camber predictions. For the STD girders, two sets of results are presented for the ACI 209 creep and shrinkage model: one using the slump value determined from concrete testing and the other using an "adjusted" slump value based on mixture proportions. The results based on the "adjusted" slump are designated by ACI 209*.

The SCC camber results presented in this chapter are based on non-accelerated-curing conditions and the use of an "adjusted" slump flow in lieu of the actual slump flow. To review the slump values for the AASHTO Type I girders, see Table 5-2. The effect on camber predictions when using actual slump versus "adjusted" slump as well as curing conditions (accelerated versus non-accelerated) is covered in the sensitivity analysis presented in Chapter 6.

5.3.2.1 CAMBER PREDICTIONS USING TEST-BASED E_C MODELS

The Constant E_c and Two-Point E_c models yielded very similar camber results with a maximum range of ±0.005 inches for corresponding values. The camber plots when using a constant concrete MOE over time are presented in this section. For the camber results using the Two-Point E_c model, see Figures G-1 through G-6 in Appendix G.

Figures 5-93 and 5-94 show the predicted camber plots for the STD AASHTO Type I girders. All creep and shrinkage models under-predict the camber for all ages. The CEB 90 model under-predicts camber up to 41 percent which is the most of all the models. The ACI 209 better predicts early-age camber (less than 10 days after transfer) while the AASHTO '05(+) creep and shrinkage model better predicts long-term camber. Table G-1 located in Appendix G summarizes the percent error in camber predictions at various ages for the STD-M-1 and STD-M-2 girders. Table G-2 shows the error in proportional camber growth at various ages relative to the initial camber.

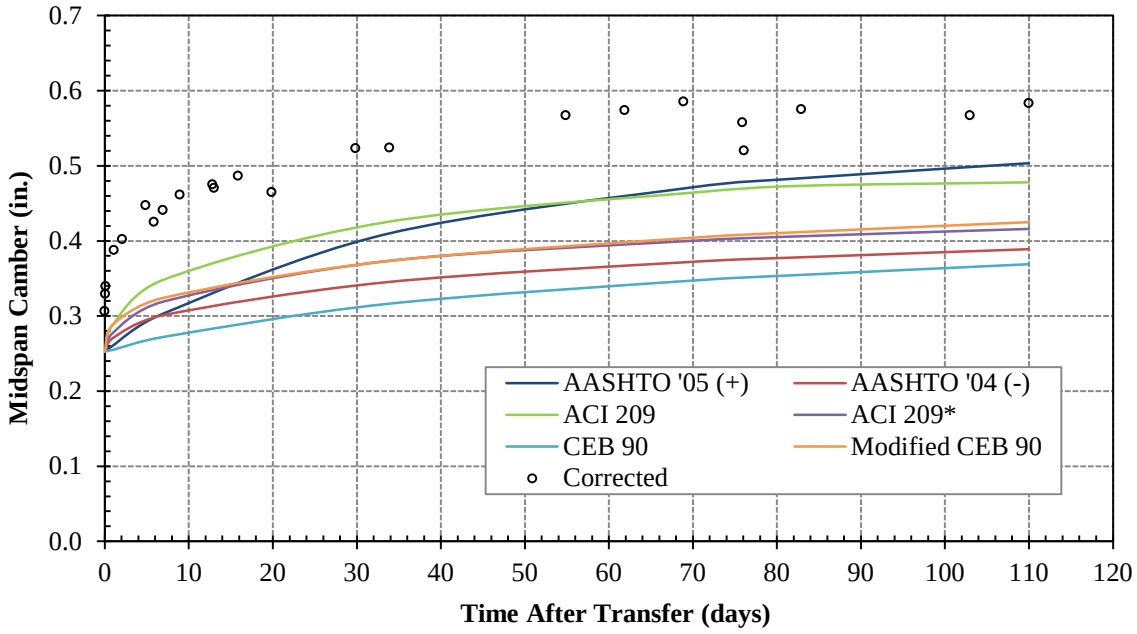

Figure 5-93: STD-M-1 Predicted Camber with Constant E_c

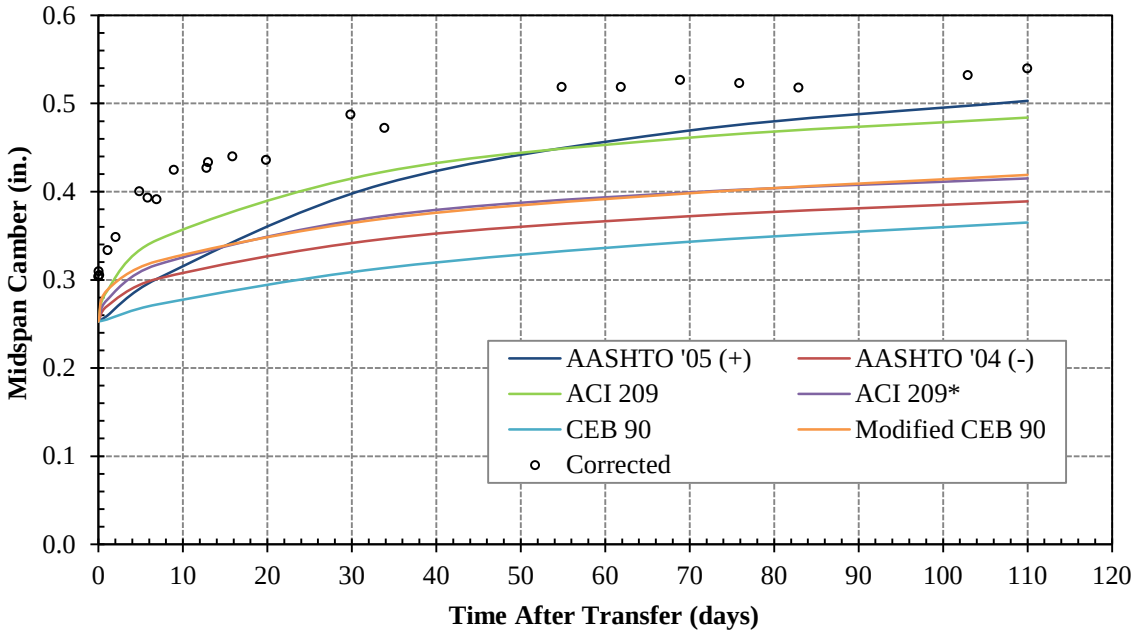

Figure 5-94: STD-M-2 Predicted Camber with Constant E_c

Figures 5-95 through 5-98 show the predicted camber plots for the SCC AASHTO Type I girders. The Constant E_c model over-estimated the SCC-MS-1 initial camber 2.6 percent and the SCC-MS-2 initial camber 28 percent. Initial camber for the two SCC-HS girders was measured at 0.173 inches and 0.125 inches. The program predicted an initial camber of 0.204 inches for the two SCC-HS girders, a difference of 18 and 64 percent, respectively.

The SCC-MS-1 camber at 160 days after transfer was under-predicted an average of 9.2 percent using the AASHTO '04(-) and ACI 209* creep and shrinkage models. The CEB 90 and Modified CEB models are the best predictors of long-term camber for the other three SCC girders. In general, the camber growth rates using the AASHTO '04(-) creep and shrinkage model correlate the best with the measured camber growth rates. See Tables G-3 through G-6 in Appendix G for a summary of the percent error in camber and camber growth at various ages for each SCC girder.

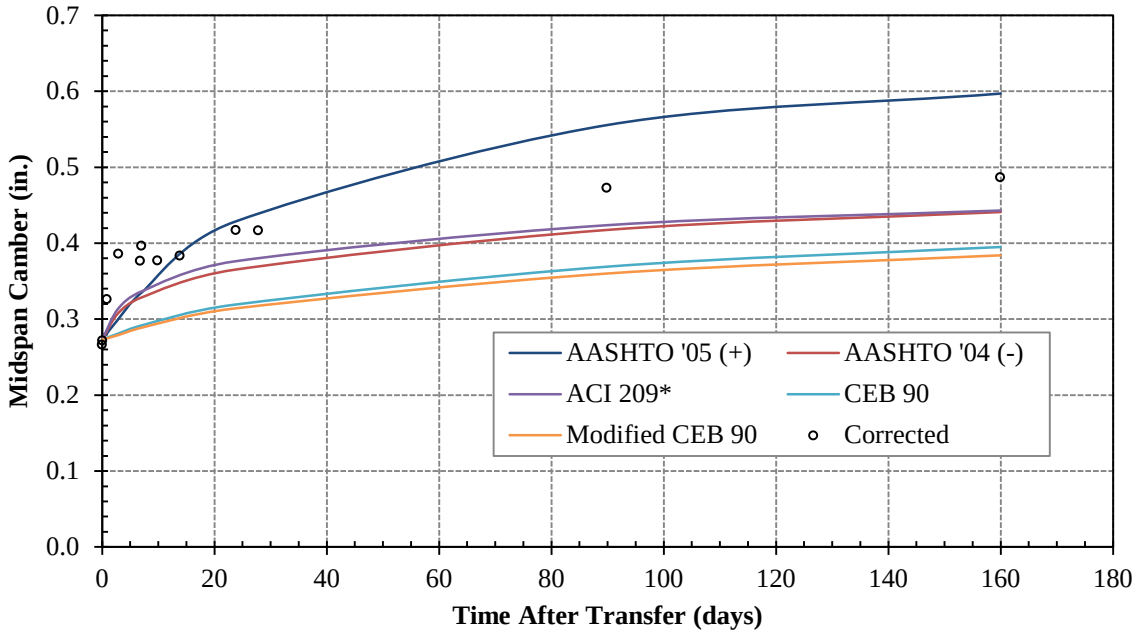

Figure 5-95: SCC-MS-1 Predicted Camber with Constant E_c

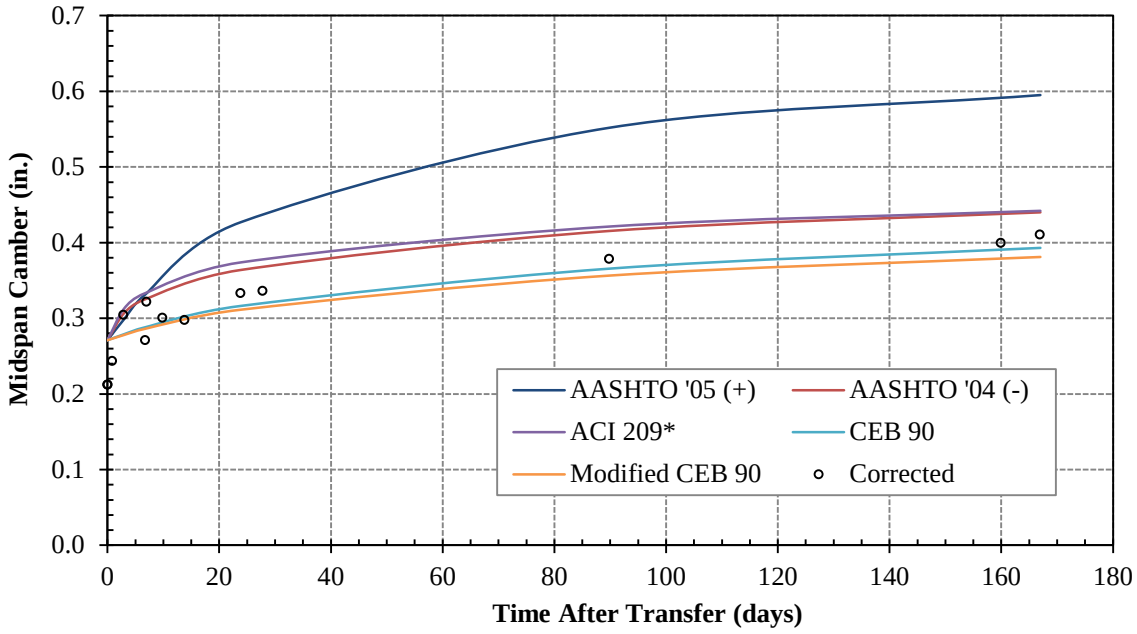

Figure 5-96: SCC-MS-2 Predicted Camber with Constant E_c

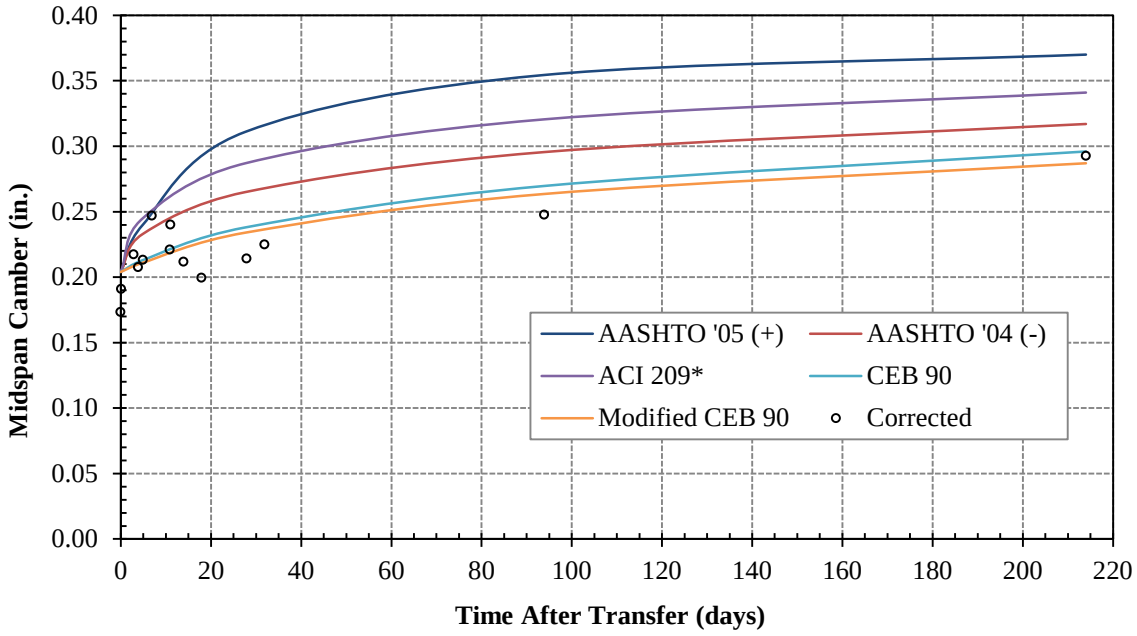

Figure 5-97: SCC-HS-1 Predicted Camber with Constant E_c

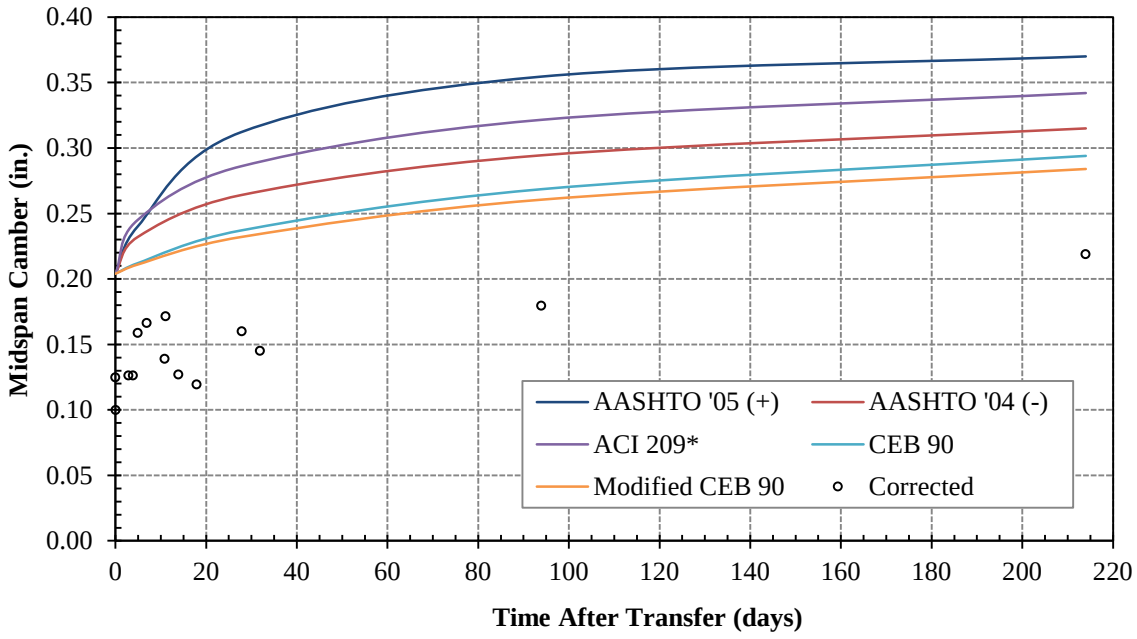

Figure 5-98: SCC-HS-2 Predicted Camber with Constant E_c

5.3.2.2 CAMBER PREDICTIONS USING CODE-PREDICTION E_C MODELS

The code-prediction E_c models include AASHTO ’05 (+), ACI 209, and CEB 90. The AASHTO ’05 (+) model uses the ACI 209 concrete compressive strength development rate and therefore yields the same results as the ACI 209 model. The following camber results were generated by varying the creep and shrinkage model for a given E_c model.

Figures 5-99 through 5-102 show the camber results for the STD-M AASHTO Type I girders when using code-prediction E_c models. The CEB 90 E_c model is the best predictor of initial camber. The camber immediately after transfer was measured to be 0.306 inches for STD-M-1 and 0.304 inches for STD-M-2. Using the CEB 90 E_c model, the program calculates an initial camber of 0.302 inches for STD-M-1 and 0.294 inches for STD-M-2. The average difference for the measured and predicted initial camber is 2.3 percent.

The AASHTO ‘05(-) and ACI 209 creep and shrinkage models better predict the long-term camber when the CEB 90 E_c model is used for the concrete modulus development over time. Using the AASHTO ‘05(+) or ACI 209 E_c model, the Modified CEB 90 creep and shrinkage model best predicts long-term camber of STD-M-1 while the AASHTO ’04(-) model best predicts STD-M-2 long-term camber. The CEB 90 creep and shrinkage model under-predicts camber at all ages regardless of the E_c model.

Table G-1 located in Appendix G provides a summary the percent error in camber predictions at various ages for the STD-M-1 and STD-M-2 girders. Table G-2 shows the percent error in proportional camber growth at various ages relative to the initial camber.

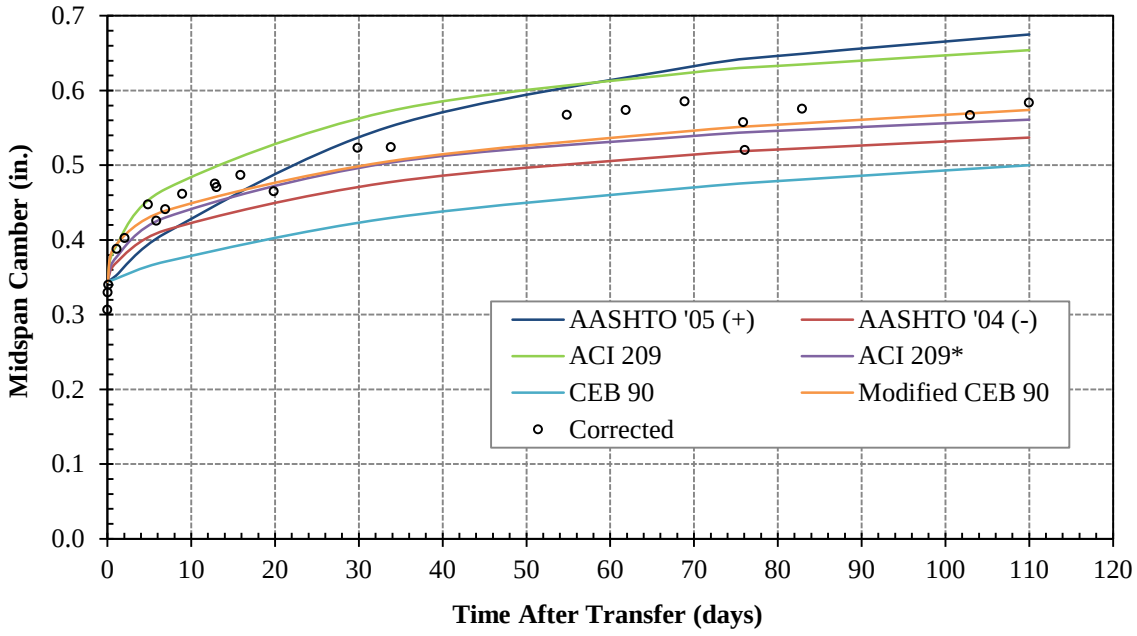

Figure 5-99: STD-M-1 Predicted Camber with AASHTO/ACI E_c

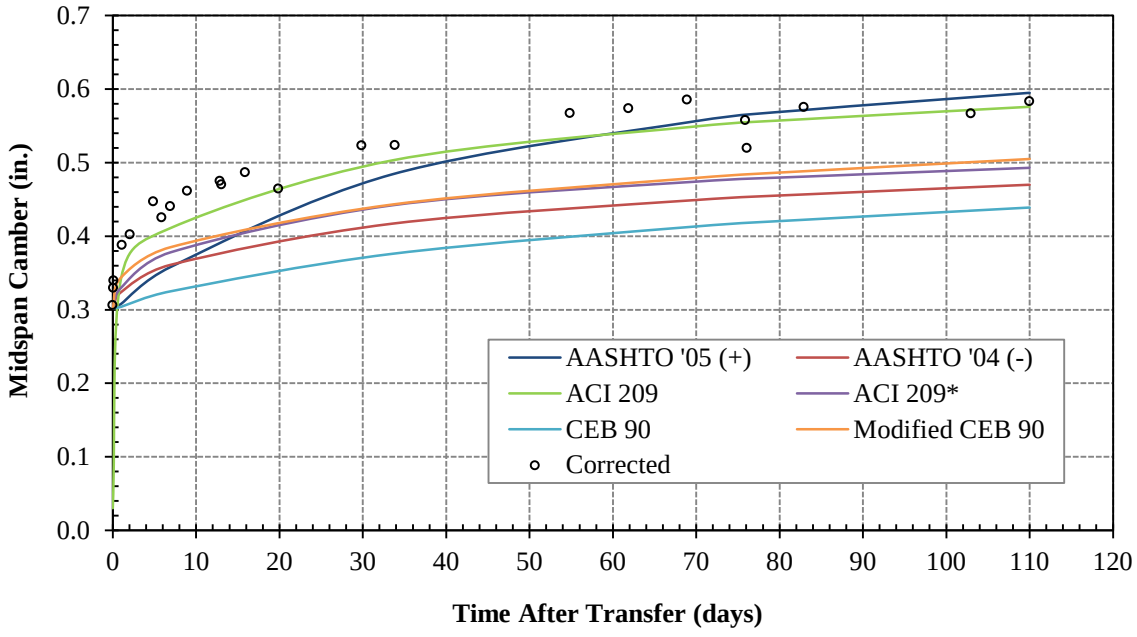

Figure 5-100: STD-M-1 Predicted Camber with CEB 90 E_c

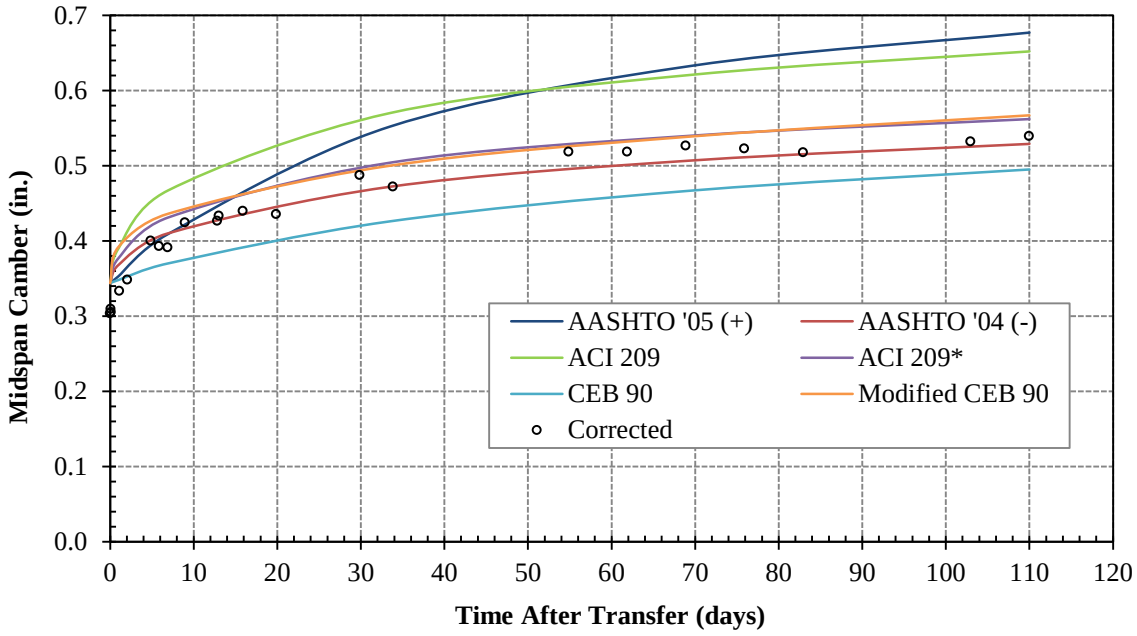

Figure 5-101: STD-M-2 Predicted Camber with AASHTO/ACI E_c

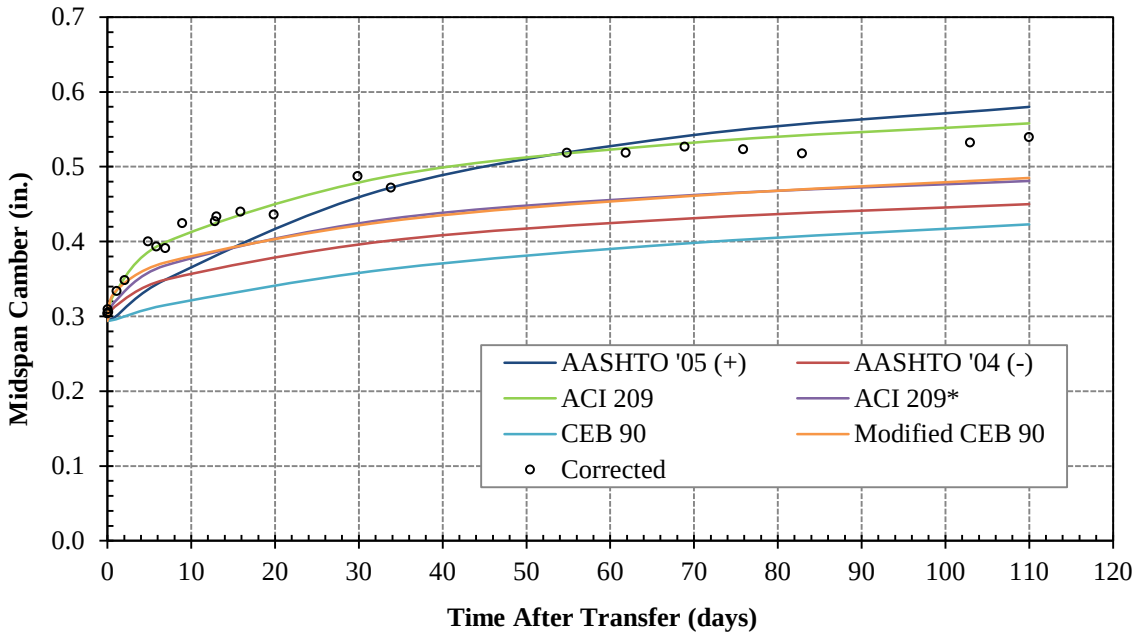

Figure 5-102: STD-M-2 Predicted Camber with CEB 90 E_c

Camber plots for the AASHTO Type I SCC-MS girders are shown in Figures 5-103 through 5-106. Similar to the STD-M results, the CEB 90 E_c model is the best predictor of initial camber. The camber immediately after transfer was measured to be 0.266 inches for SCC-MS-1 and 0.212 inches for SCC-MS-2. Using the CEB 90 E_c model, the program calculates an initial camber of 0.268 inches for STD-M-1 and 0.265 inches for STD-M-2 which is a difference of 0.7 percent and 25 percent, respectively.

At 90 days after transfer, the AASHTO '04(-) creep and shrinkage model over-predicts the SCC-MS-1 camber 4.1 percent while the ACI 209* model over-predicts the SCC-MS-1 camber 5.6 percent. The same two models over-predict the SCC-MS-2 camber at 90 days by an average of 29 percent. When using the AASHTO '05(+) or ACI 209 E_c model, the Modified CEB 90 creep and shrinkage model best predicts the SCC-MS-2 camber at 90 days and 167 days after transfer.

Table G-3 in Appendix G shows the percent difference between the measured and predicted SCC-MS cambers at various ages. Table G-4 shows the percent difference in proportional camber growth at various ages relative to initial camber.

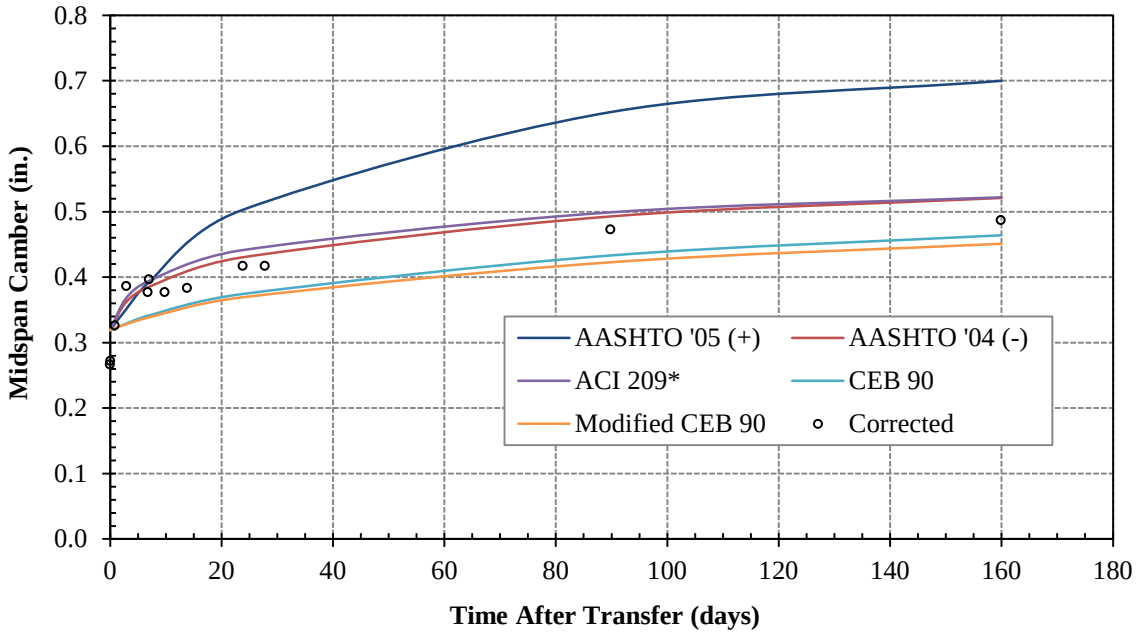

Figure 5-103: SCC-MS-1 Predicted Camber with AASHTO/ACI E_c

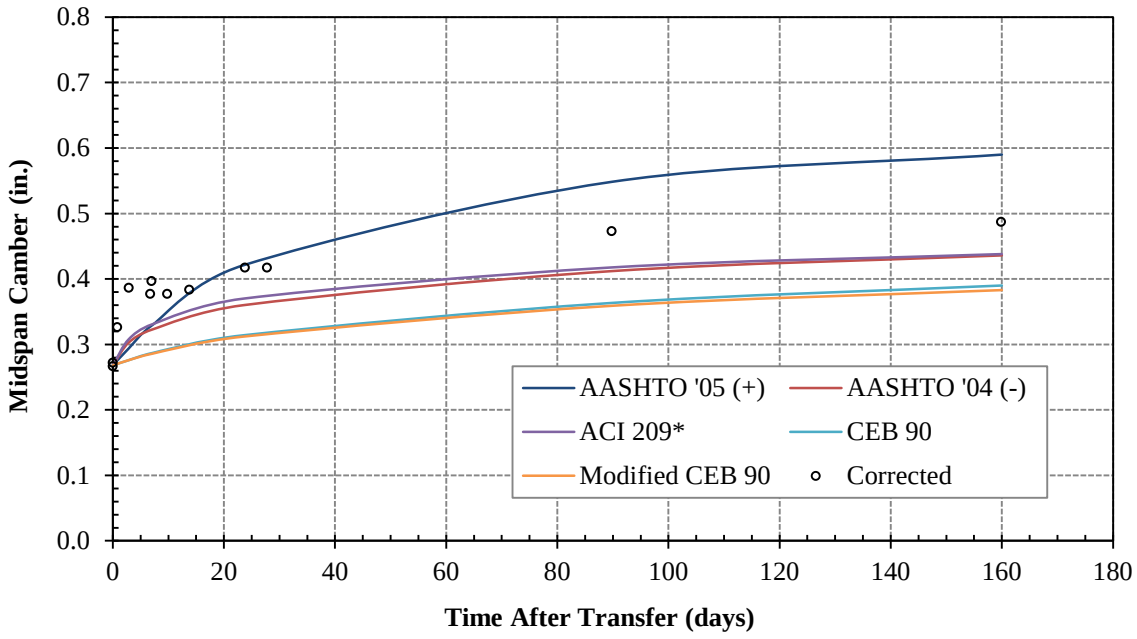

Figure 5-104: SCC-MS-1 Predicted Camber with CEB 90 E_c

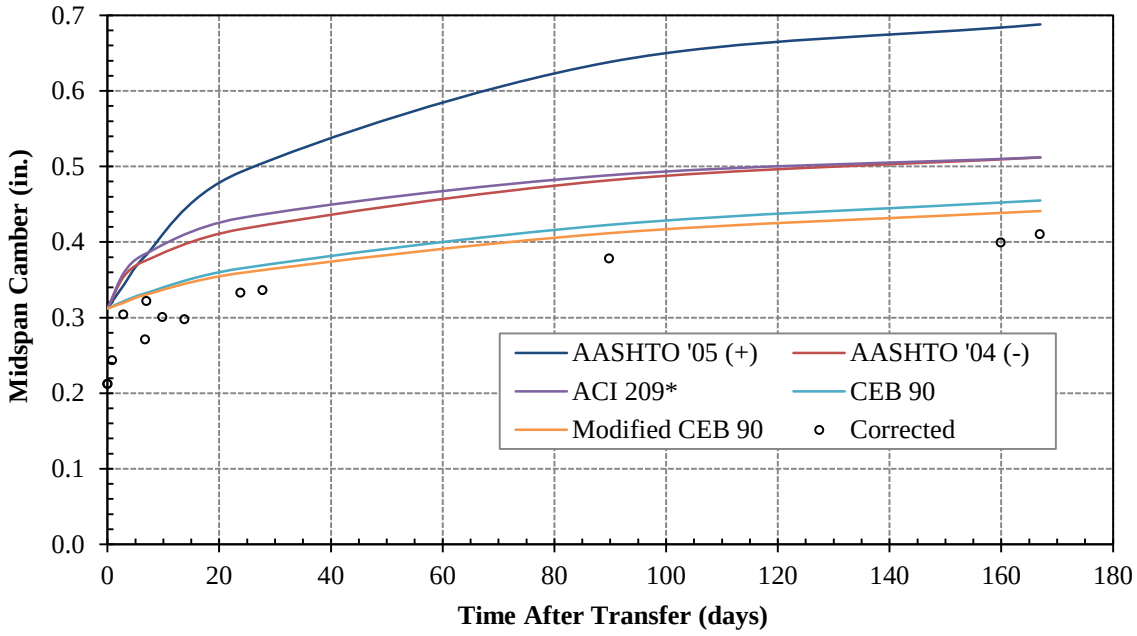

Figure 5-105: SCC-MS-2 Predicted Camber with AASHTO/ACI E_c

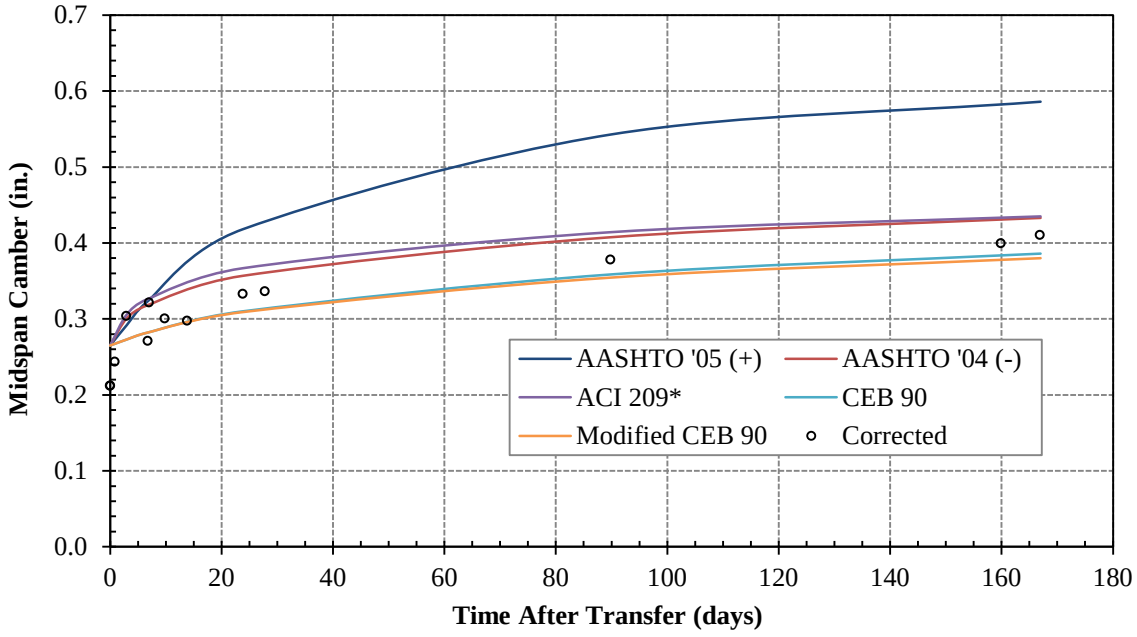

Figure 5-106: SCC-MS-2 Predicted Camber with CEB 90 E_c

Camber plots for the AASHTO Type I SCC-HS girders are shown in Figures 5-107 through 5-110. The code-prediction E_c models over-predict initial camber of the SCC-HS girders 28 to 89 percent. As shown in the figures, the AASHTO and ACI creep and shrinkage models drastically over-predict long-term camber. The best predictions of long-term camber use the CEB 90 and Modified CEB 90 creep and shrinkage models.

The SCC-HS-1 measured camber at 214 days after transfer was 0.293 inches. Using the AASHTO '05(+) or ACI 209 E_c model along with the Modified CEB 90 creep and shrinkage model, the program predicted a camber of 0.312 inches which is a difference is 6.5 percent. When using the CEB 90 creep and shrinkage model, the percent difference in SCC-HS-1 camber at 214 days is increased to 10 percent. The same models over-estimate the SCC-HS-2 camber at 214 days an average of 44 percent.

Table G-5 in Appendix G shows the percent difference between the measured and predicted SCC-HS cambers at various ages. The percent difference in proportional camber growth at various ages is summarized in Table G-6.

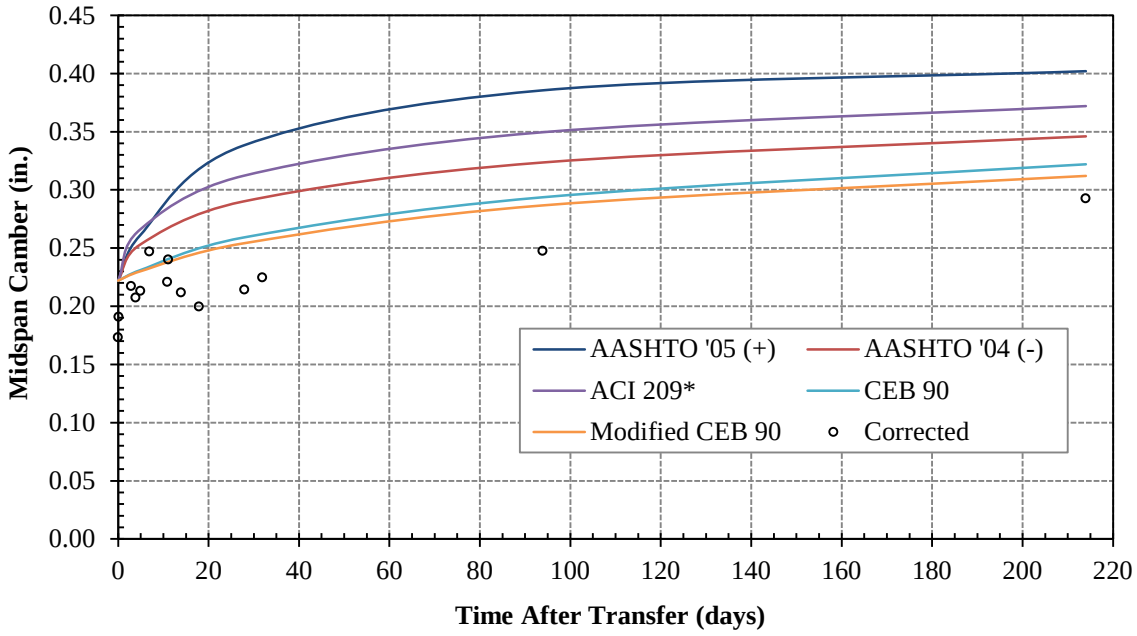

Figure 5-107: SCC-HS-1 Predicted Camber with AASHTO/ACI E_c

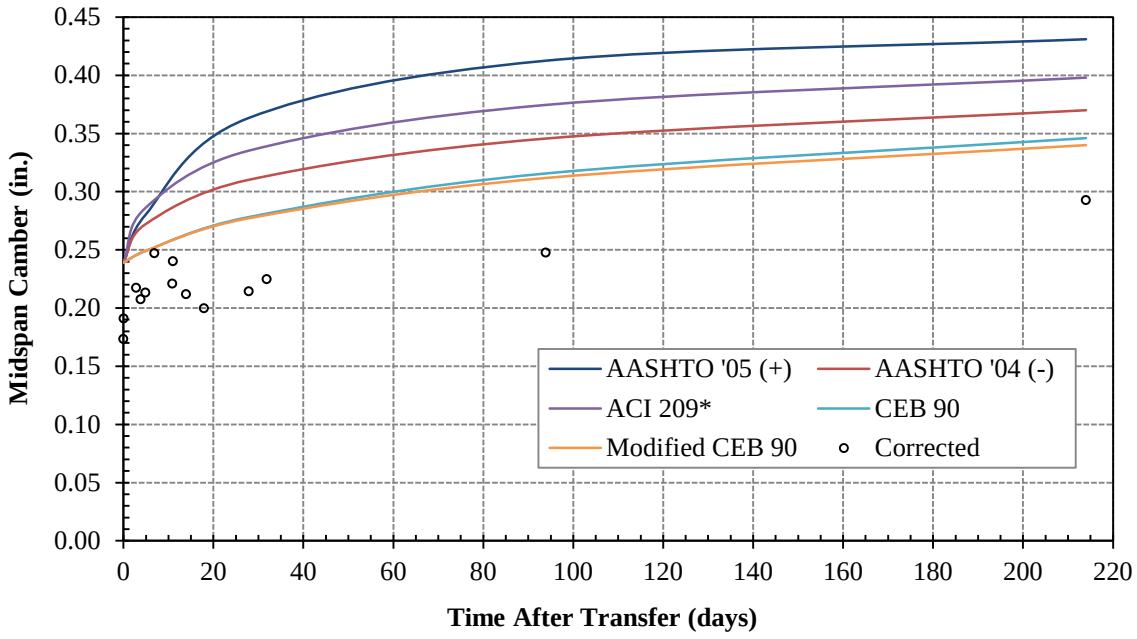

Figure 5-108: SCC-HS-1 Predicted Camber with CEB 90 E_c

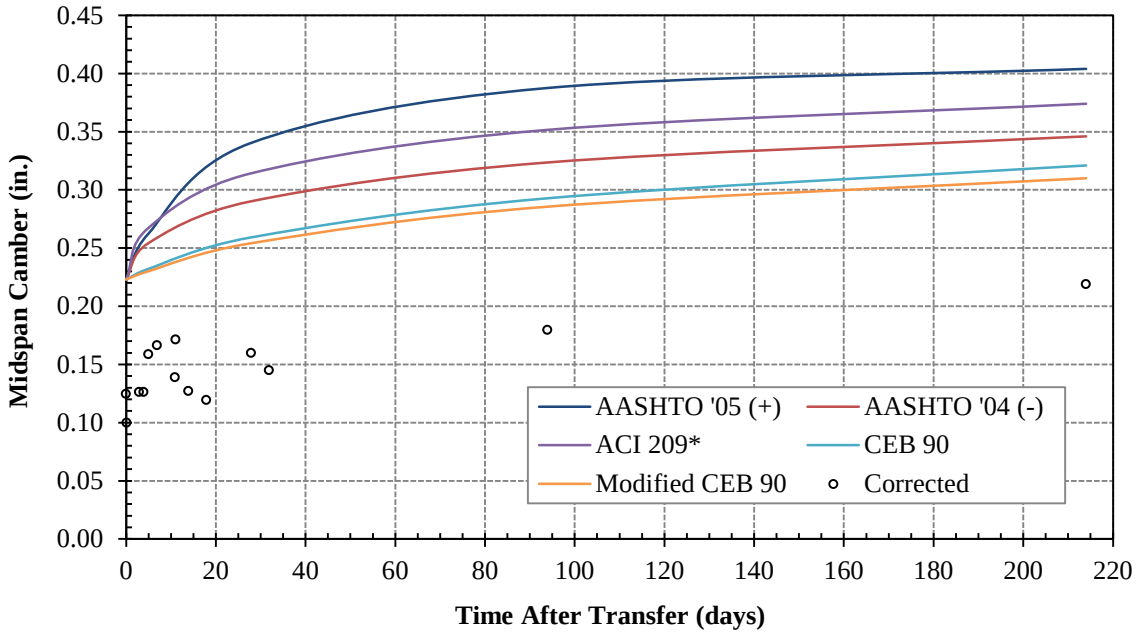

Figure 5-109: SCC-HS-2 Predicted Camber with AASHTO/ACI E_c

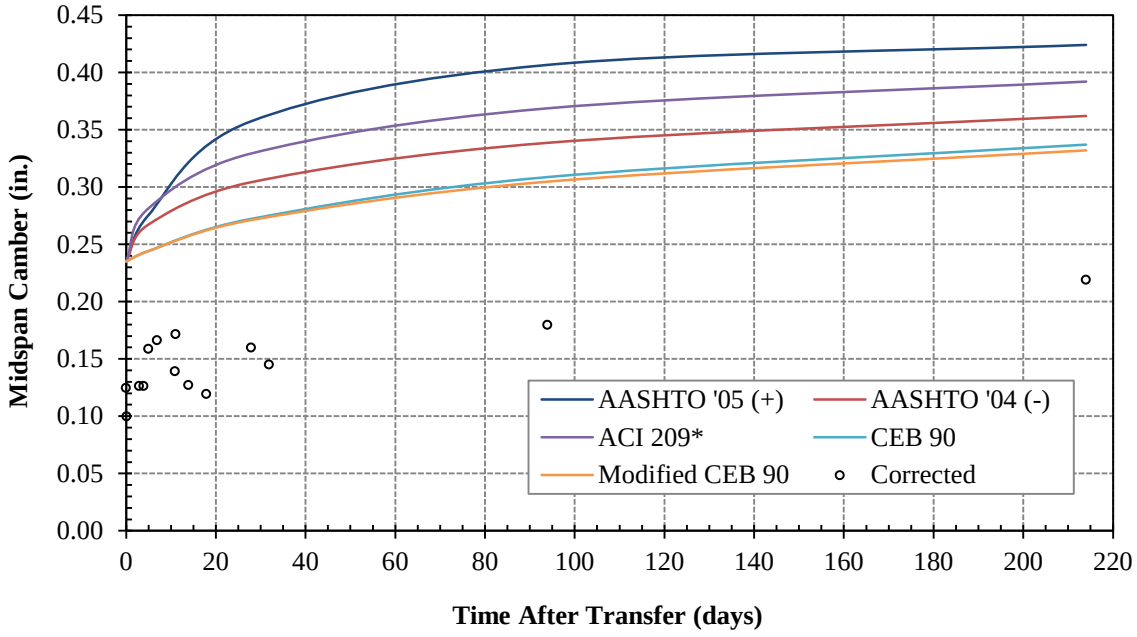

Figure 5-110: SCC-HS-2 Predicted Camber with CEB 90 E_c

5.3.3 T-BEAMS

Previous research by Levy (2007) measured the camber of sixteen prestressed flexural members. The sixteen T-beams were constructed using four concrete mixtures and four overall member lengths. See Figure 4-9 in Chapter 4 for the specimen identification developed by Levy and used throughout this thesis. The T-beam lengths are summarized in Table 5-6.

Table 5-6: T-Beam Lengths (Levy 2007)

Girder	Length (in.)
A	276
B	196
C	156
D	116

Three of the four mixtures consisted of self-consolidating concrete (SCC) and had slump flow values greater than 25 inches. Similar to the AASHTO Type I girders, the concrete mix slump and slump flow values were adjusted based on mix proportioning. The actual and "adjusted" values for the T-beams are shown in Table 5-7. The camber predictions calculated using the ACI 209 creep and shrinkage model with the "adjusted" slump values in lieu of the actual slump and slump flow values are designated by ACI 209* in the figures. The sensitivity analysis in Chapter 6 evaluates the effect on camber predictions when using actual versus "adjusted" slump and slump flow.

Table 5-7: Slump and Slump Flow – T-Beams (Levy 2007)

Girder	Actual Slump (in.)	Actual Slump Flow (in.)	Adjusted Slump (in.)
STD-M	9.5	NA	1
SCC-MA	NA	29	0
SCC-MS	NA	28.5	0
SCC-HS	NA	26	0

Levy concluded that short T-beams have long transfer lengths. The results presented in this section neglect any prestress force build-up associated with long transfer lengths. For the short T-beams C and D, the transfer length takes up a majority of the beam. Therefore, the results presented in this section include a large discrepancy in prestress force for cross sections near the ends of the beams. Further analysis can be performed using multiple debonded *Layer Groups* to "build-up" the prestress force and generate a more accurate prestress force at the ends of the beams.

5.3.3.1 CAMBER PREDICTIONS USING TEST-BASED E_C MODELS

Similar to the AASHTO Type I girders, the T-beam camber predictions using the Constant E_c and Two-Point E_c models are within ±0.005 inches of each other for each camber value. The camber results using the Constant E_c model are presented in this section. See Figures G-8 through G-14 in Appendix G for the results based on the Two-Point E_c model.

Figures 5-111 and 5-112 show the STD-M camber results when using the Constant E_c model for the concrete MOE development over time. Tables G-7 and G-9 in Appendix G summarize the percent difference in measured and predicted camber and camber growth at various ages after transfer. See Tables G-8 and G-10 for the percent difference in the measured and predicted proportional camber growth at various ages.

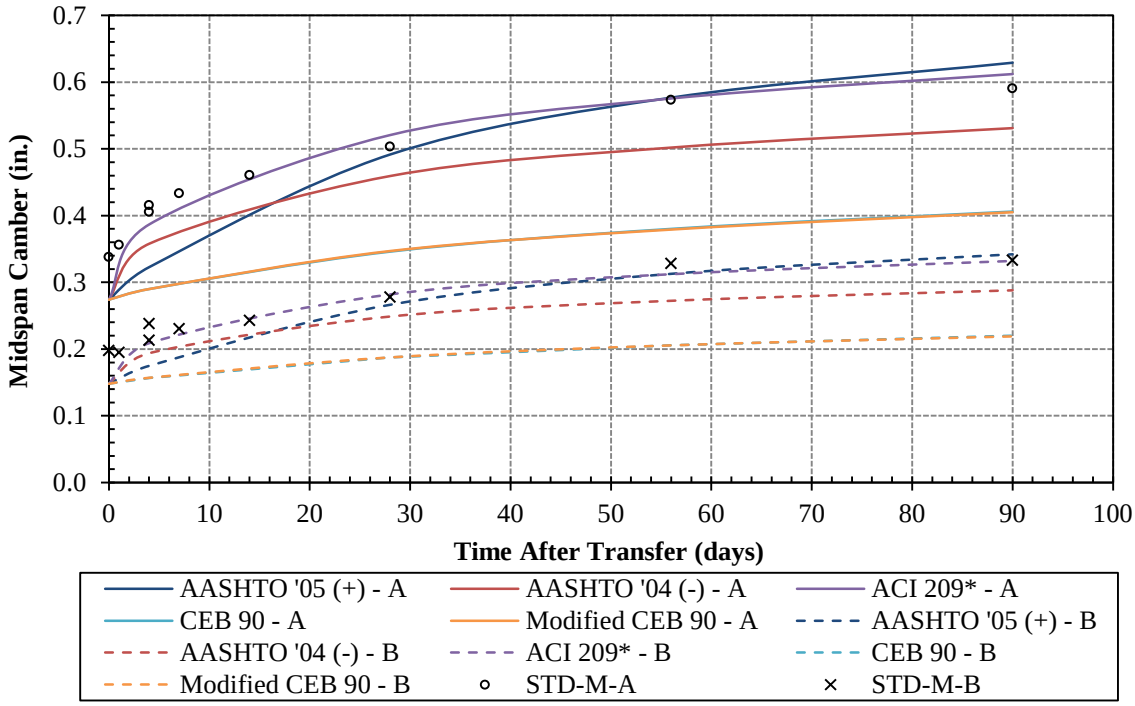

Figure 5-111: STD-M-A, B Predicted Camber with Constant E_c

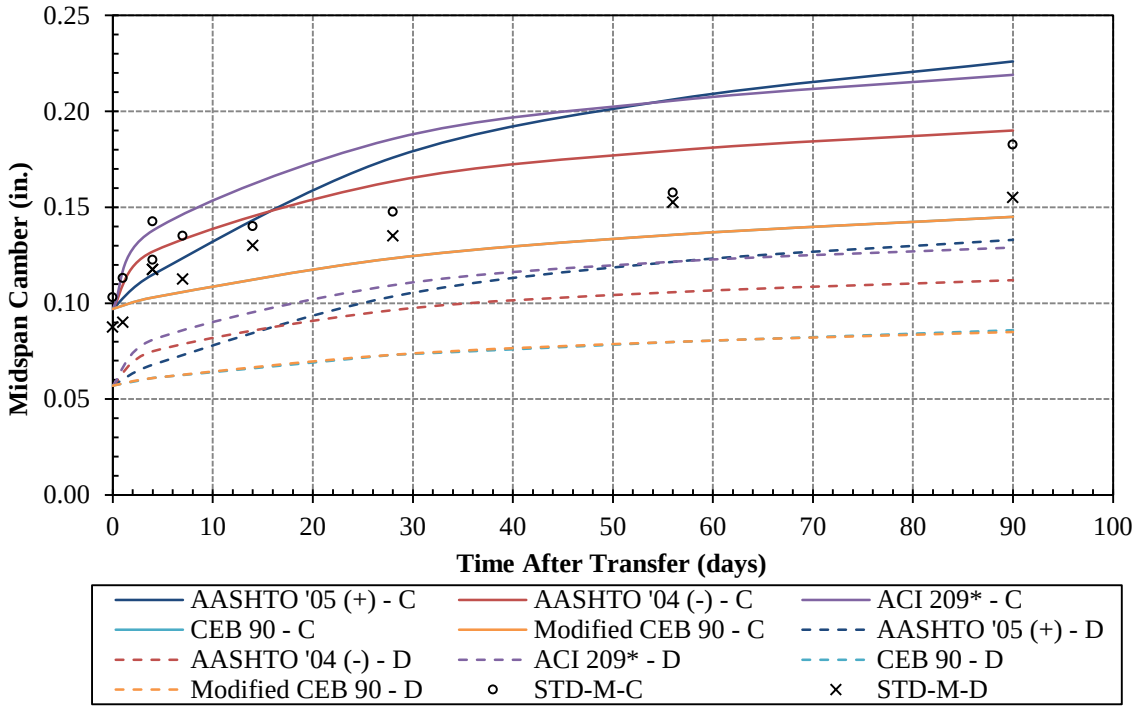

Figure 5-112: STD-M-C, D Predicted Camber with Constant E_c

Figures 5-113 and 5-114 show the SCC-MA camber results when using the Constant E_c model for the concrete modulus of elasticity development over time. Tables G-11 and G-13 located in Appendix G summarize the percent difference in measured and predicted camber at various ages for the SCC-MA beams. The percent differences in the measured and predicted proportional camber growth are shown in Tables G-12 and G-14.

The camber results for the SCC-MS beams are shown in Figures 5-115 and 5-116. Tables G-15 and G-17 in Appendix G show the percent difference in measured and predicted camber at various ages for the SCC-MS beams. Tables G-16 and G-17 show the percent difference in the measured and predicted proportional camber growth relative to the initial camber.

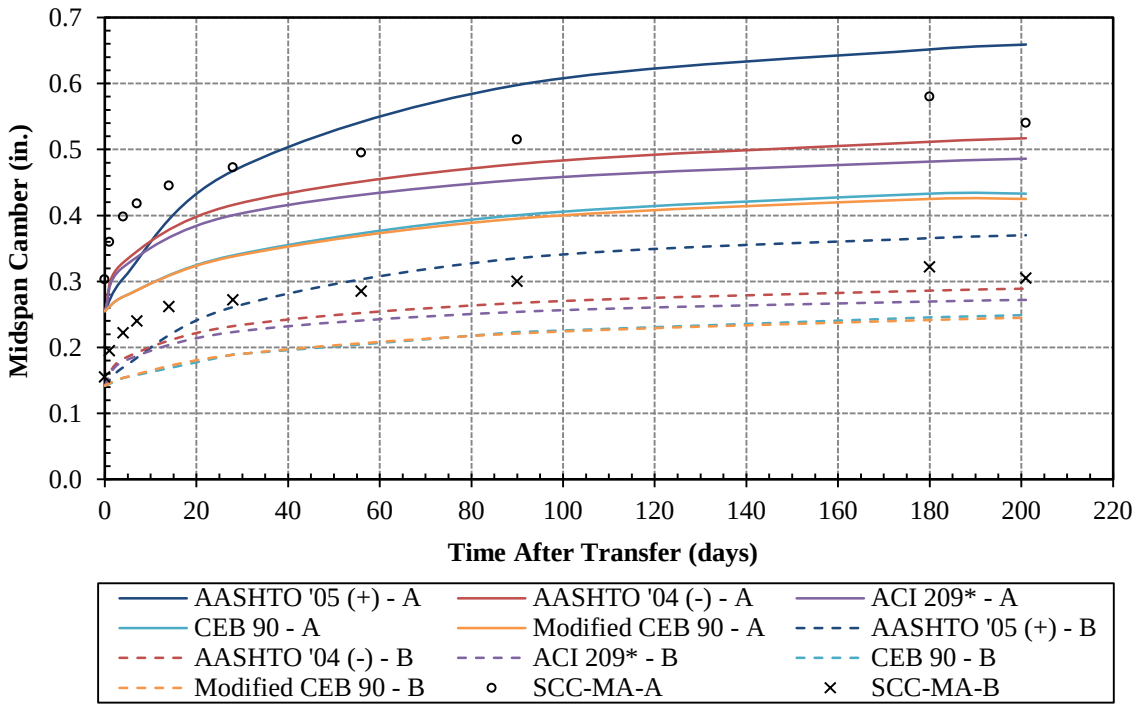

Figure 5-113: SCC-MA-A, B Predicted Camber with Constant E_c

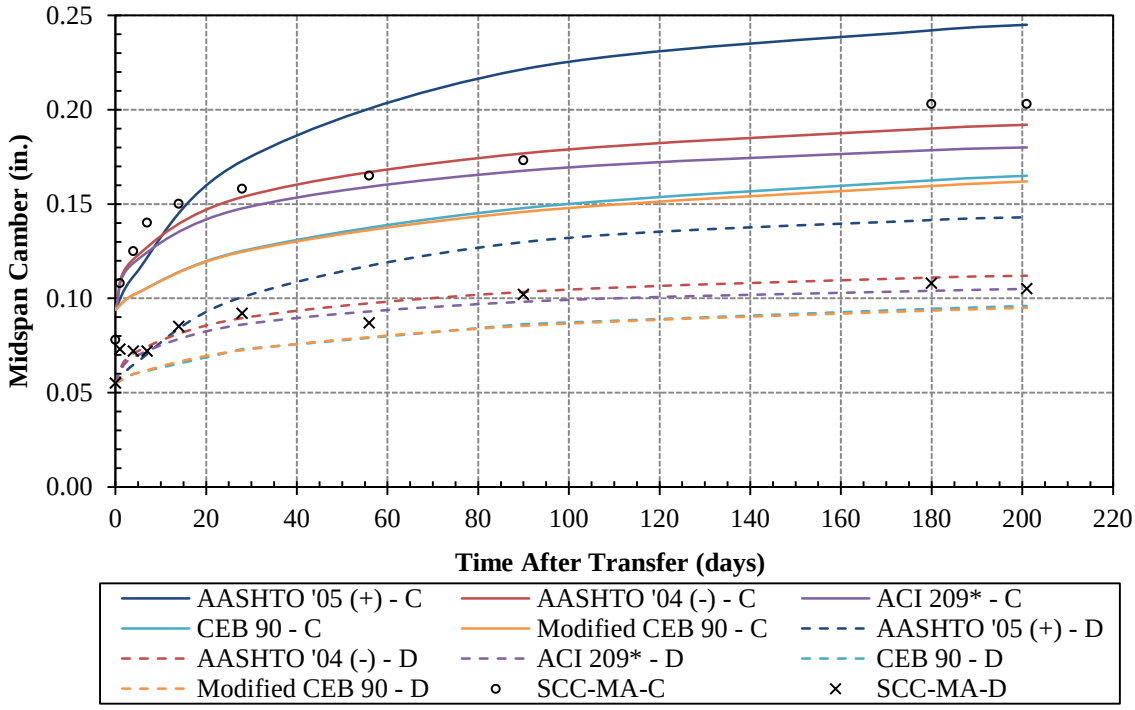

Figure 5-114: SCC-MA-C, D Predicted Camber with Constant E_c

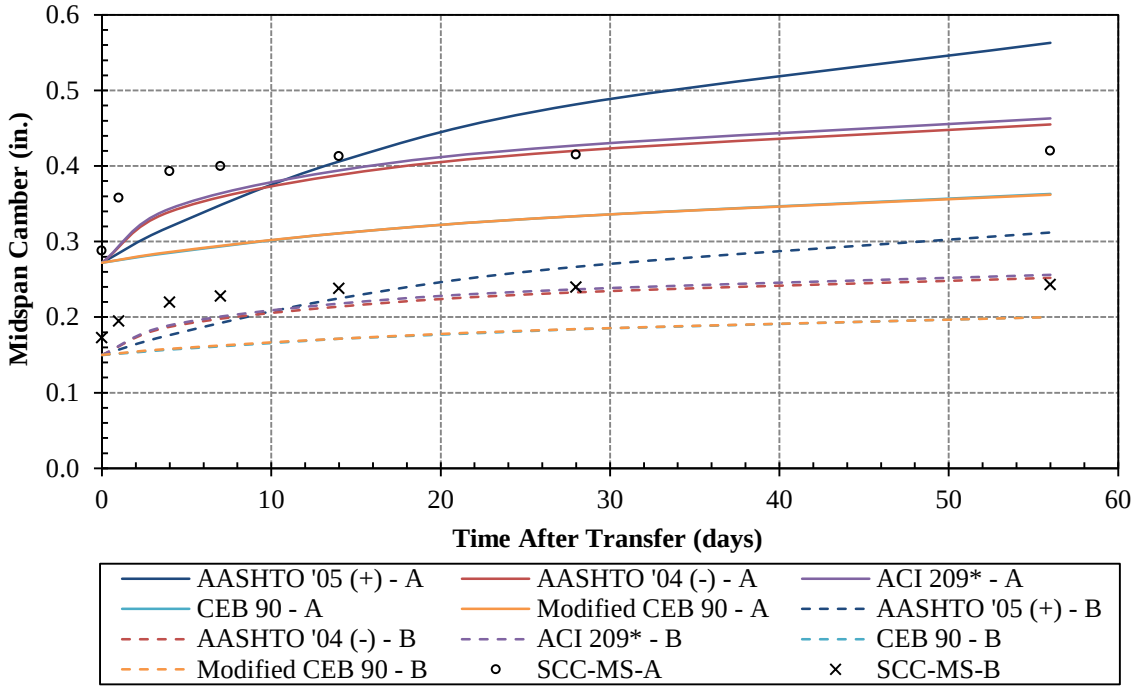

Figure 5-115: SCC-MS-A, B Predicted Camber with Constant E_c

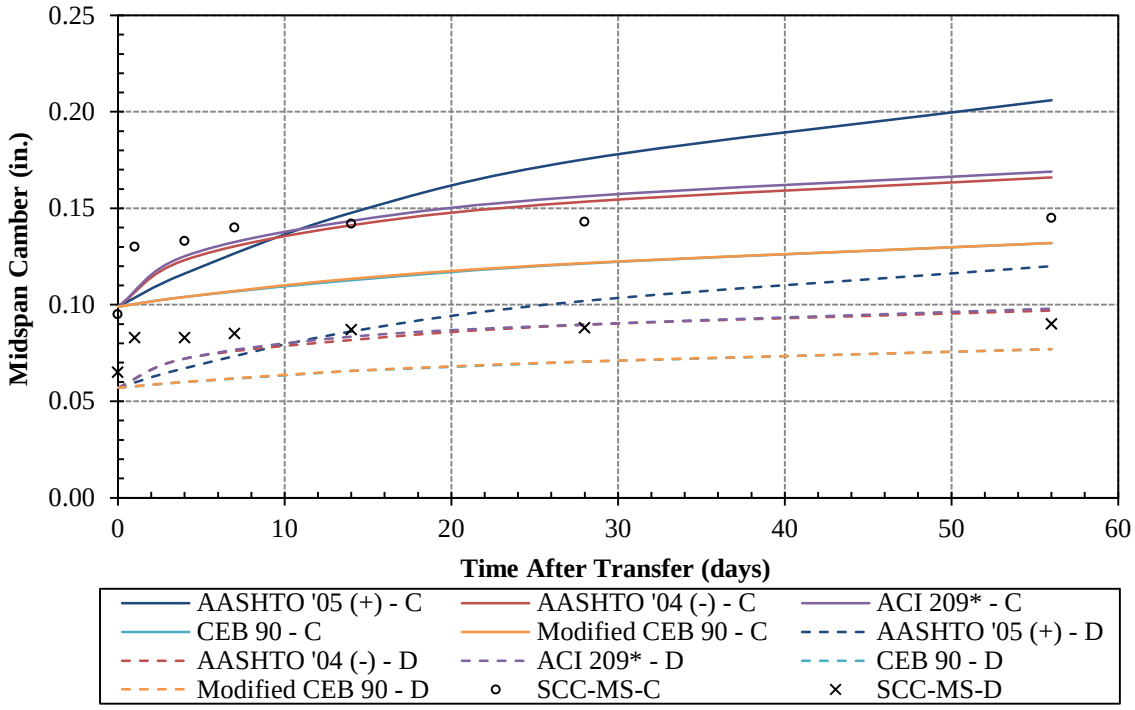

Figure 5-116: SCC-MS-C, D Predicted Camber with Constant E_c

The camber results for the SCC-HS beams are shown in Figures 5-117 and 5-118. Tables G-19 and G-21 in Appendix G show the percent difference in measured and predicted camber at various ages for the SCC-MS beams. The percent differences in the measured and predicted proportional camber growth are shown in Tables G-20 and G-22.

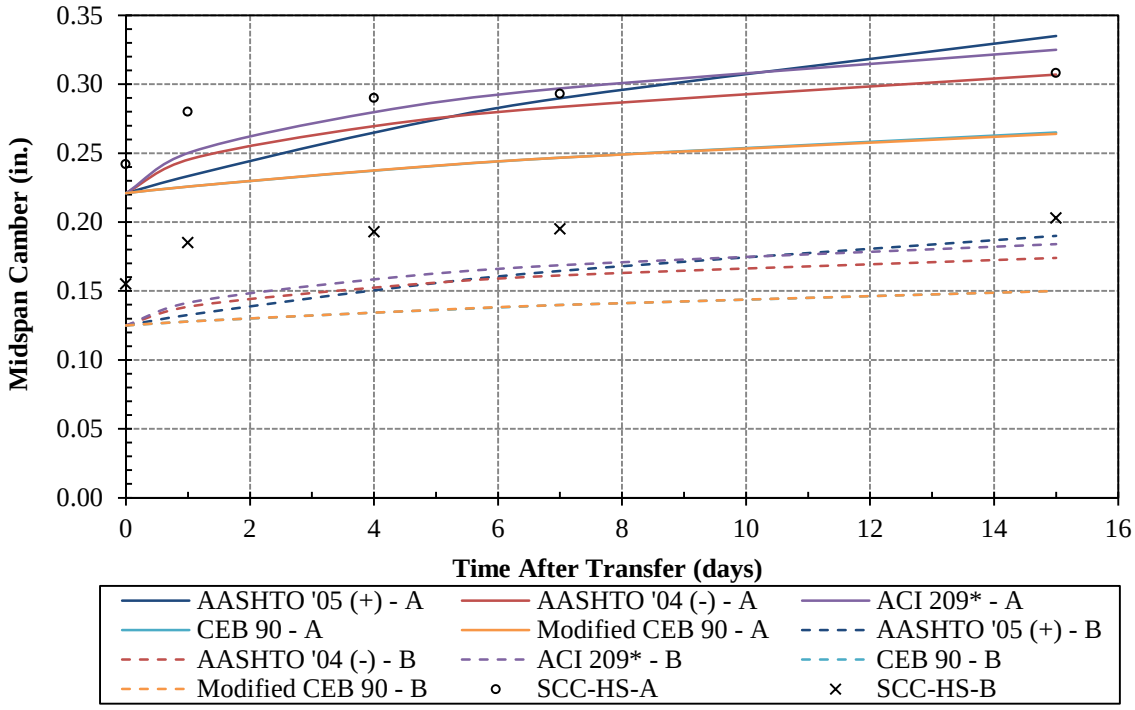

Figure 5-117: SCC-HS-A, B Predicted Camber with Constant E_c

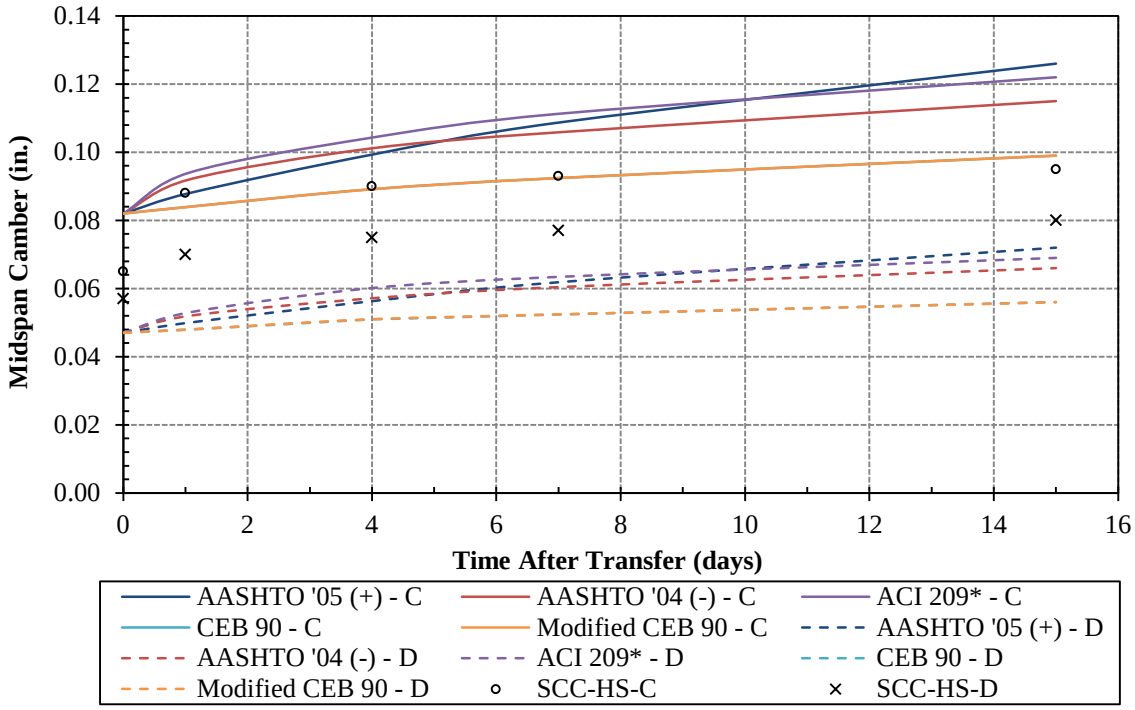

Figure 5-118: SCC-HS-C, D Predicted Camber with Constant E_c

5.3.3.2 CAMBER PREDICTIONS USING CODE-PREDICTION E_C MODELS

The camber predictions using the AASHTO ’05 (+), ACI 209, and CEB 90 models for concrete modulus of elasticity development over time are presented in this section. The AASHTO ’05 (+) model uses the ACI 209 rate for strength development over time. The two models, therefore, yield the same camber results.

Figures 5-119 through 5-122 show the camber results for the four STD-M beams when using various creep and shrinkage models with a code-prediction E_c model. The percent difference in measured and predicted camber and camber growth at various ages after transfer is summarized in Tables G-7 through G-10 in Appendix G.

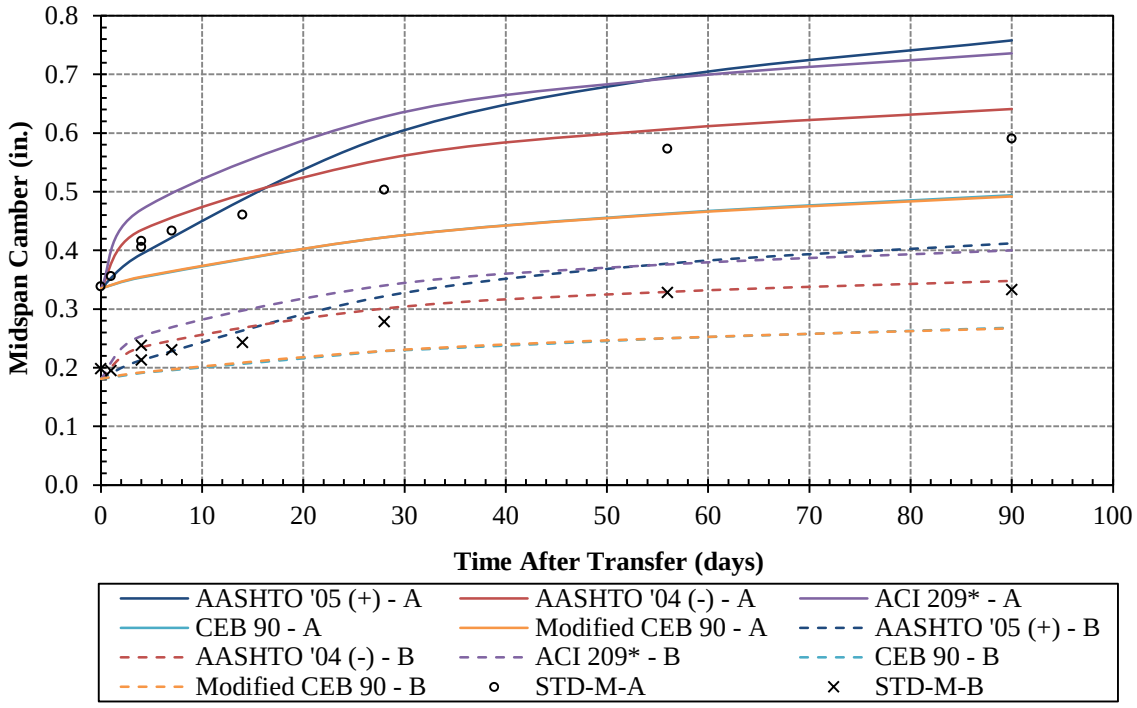

Figure 5-119: STD-M-A, B Predicted Camber with AASHTO/ACI E_c

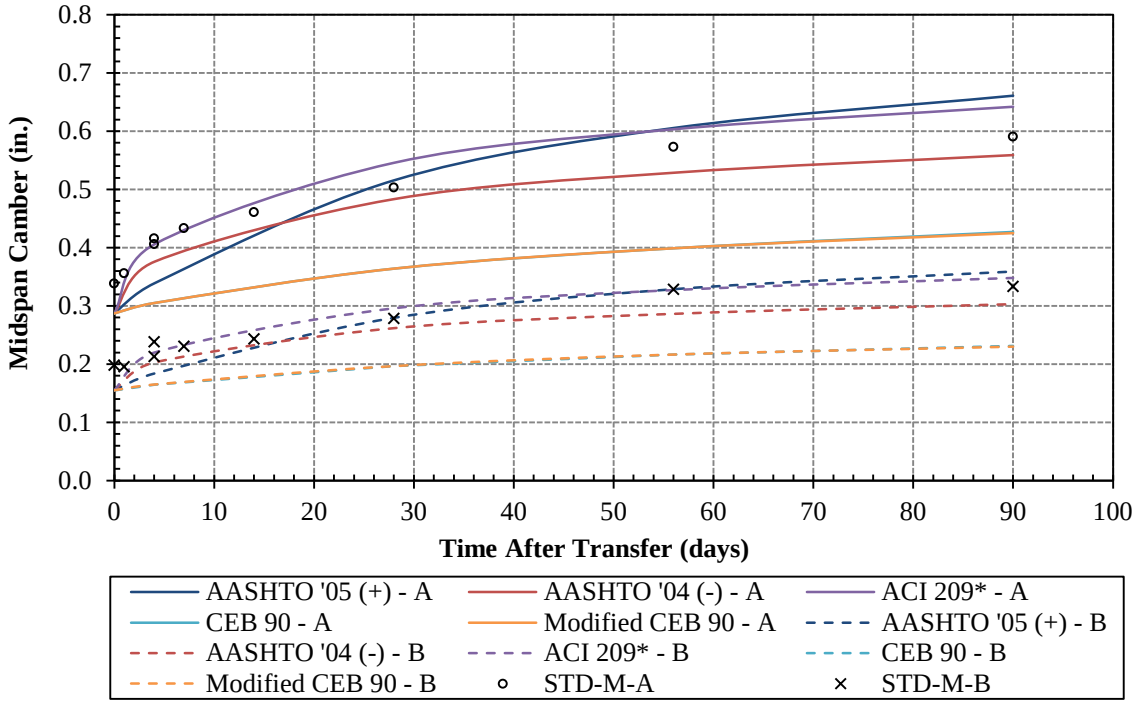

Figure 5-120: STD-M-A, B Predicted Camber with CEB 90 E_c

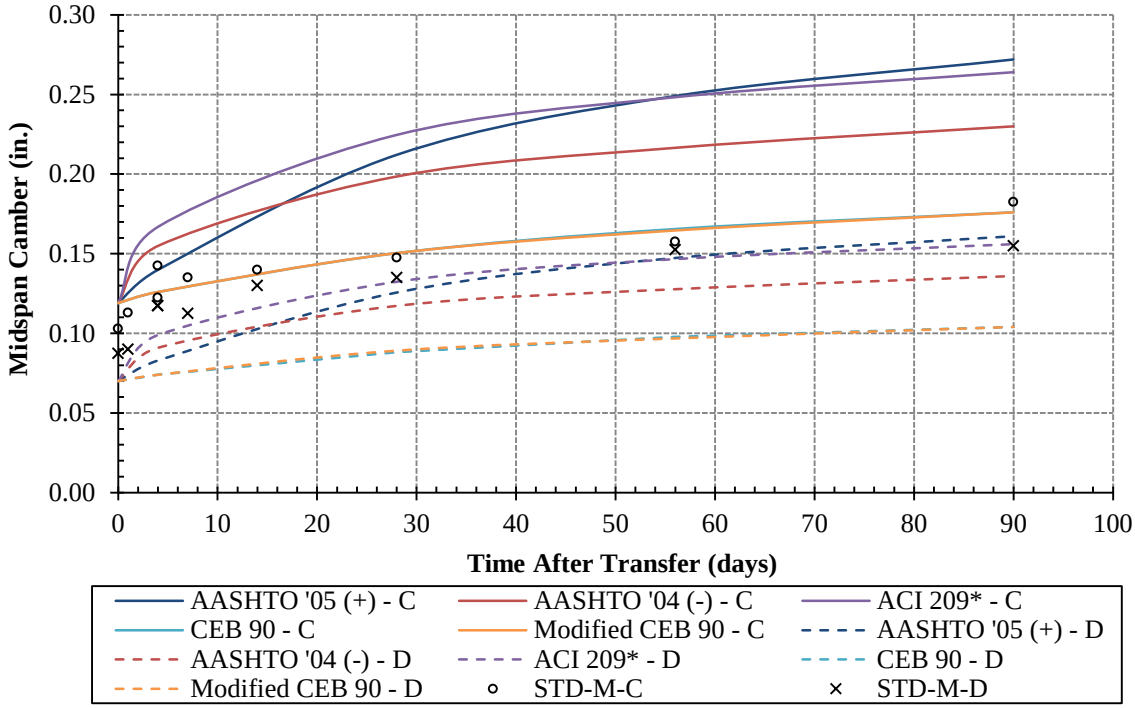

Figure 5-121: STD-M-C, D Predicted Camber with AASHTO/ACI E_c

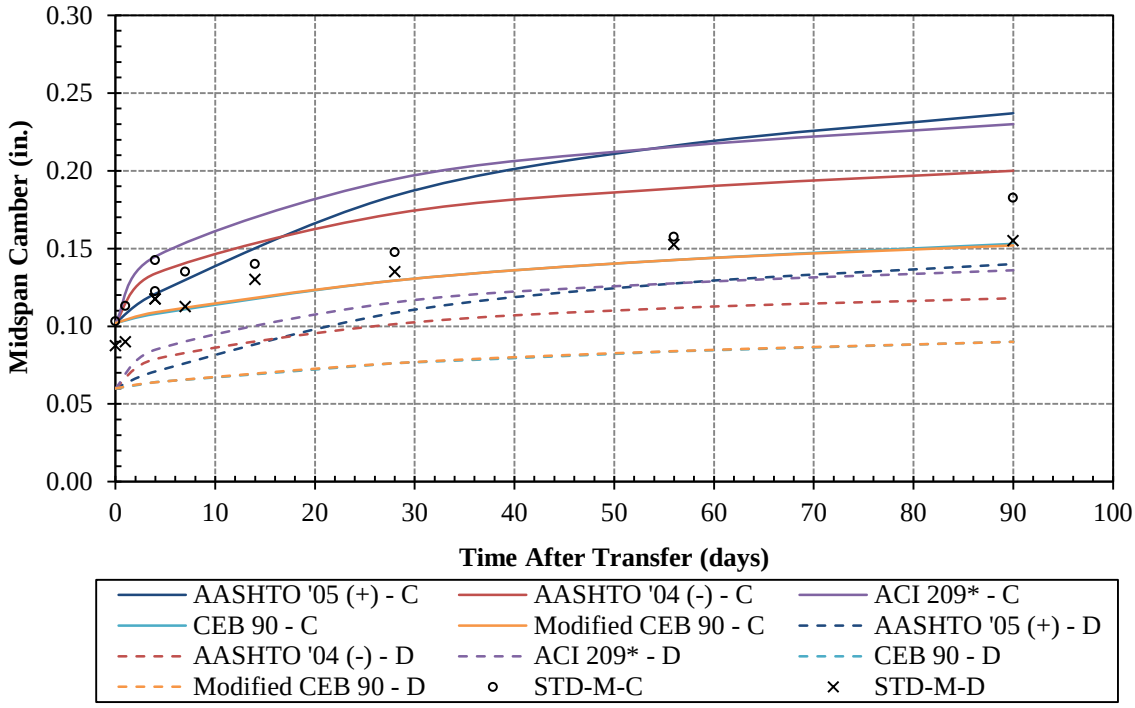

Figure 5-122: STD-M-C, D Predicted Camber with CEB 90 E_c

Figures 5-123 through 5-126 show the SCC-MA camber results when using various creep and shrinkage models with code-prediction E_c models. Tables G-11 and G-13 in Appendix G show the percent difference in measured and predicted camber at various ages. The percent differences in the measured and predicted proportional camber growth are shown in Tables G-12 and G-14.

The camber results for the SCC-MS beams are shown in Figures 5-127 through 5-130. The percent differences in measured and predicted camber and proportional camber growth in the SCC-MS beams at various ages after transfer are presented in Tables G-15 through G-18 in Appendix G.

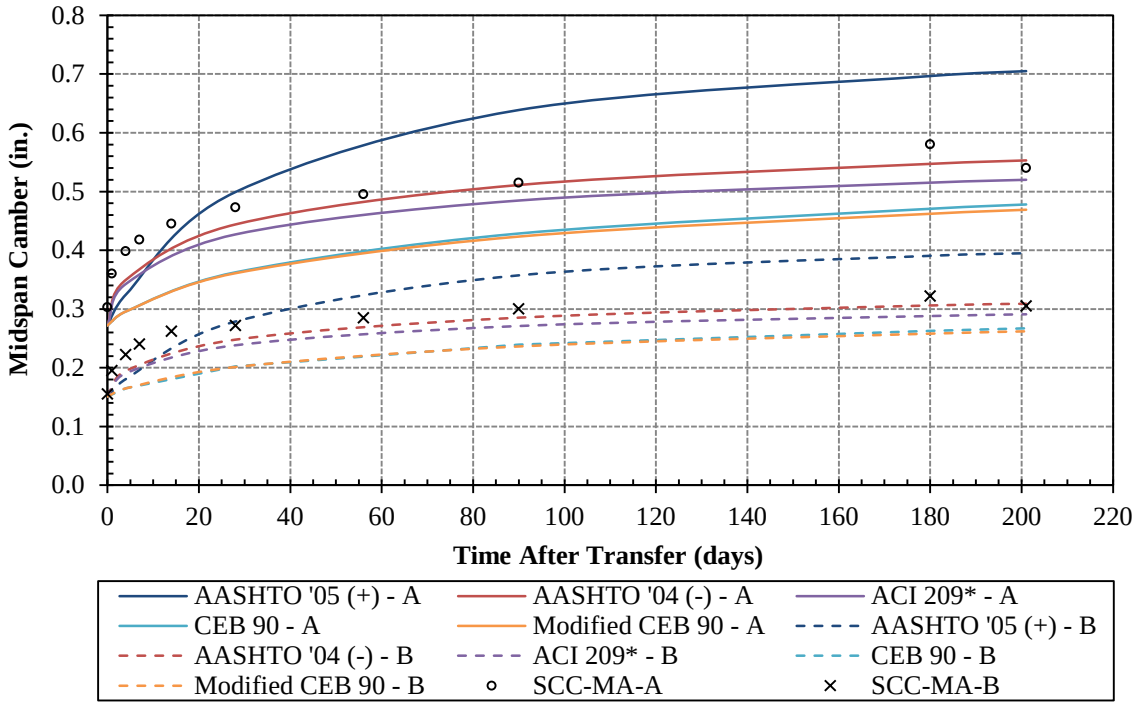

Figure 5-123: SCC-MA-A, B Predicted Camber with AASHTO/ACI E_c

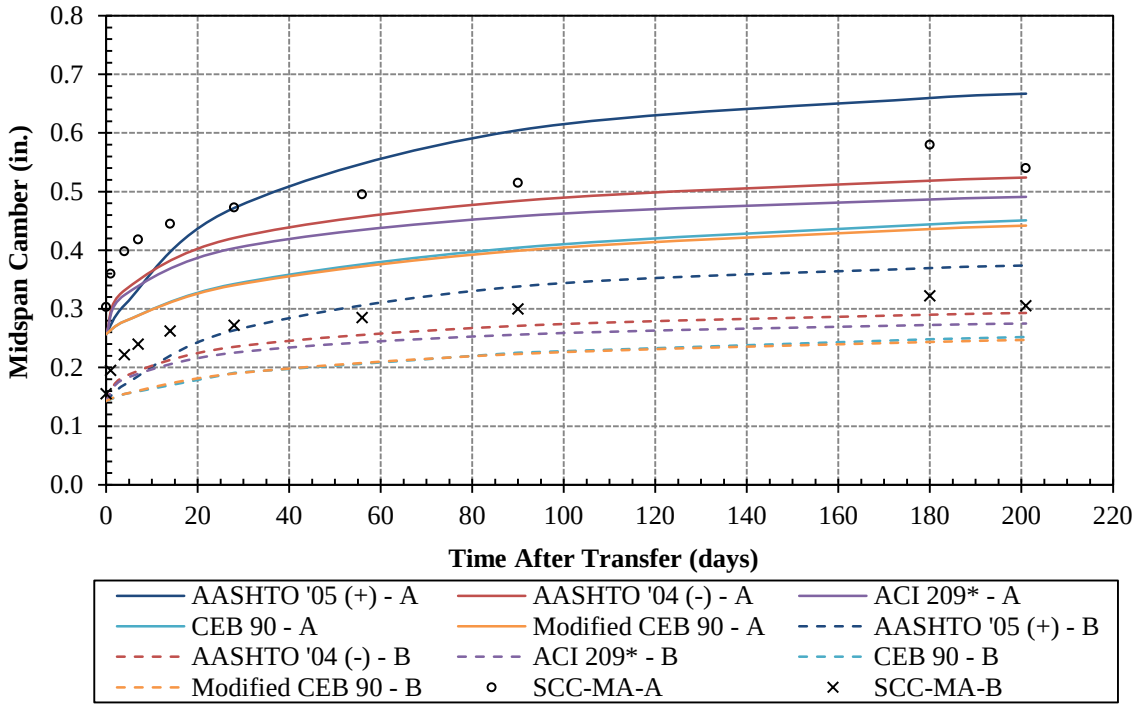

Figure 5-124: SCC-MA-A, B Predicted Camber with CEB 90 E_c

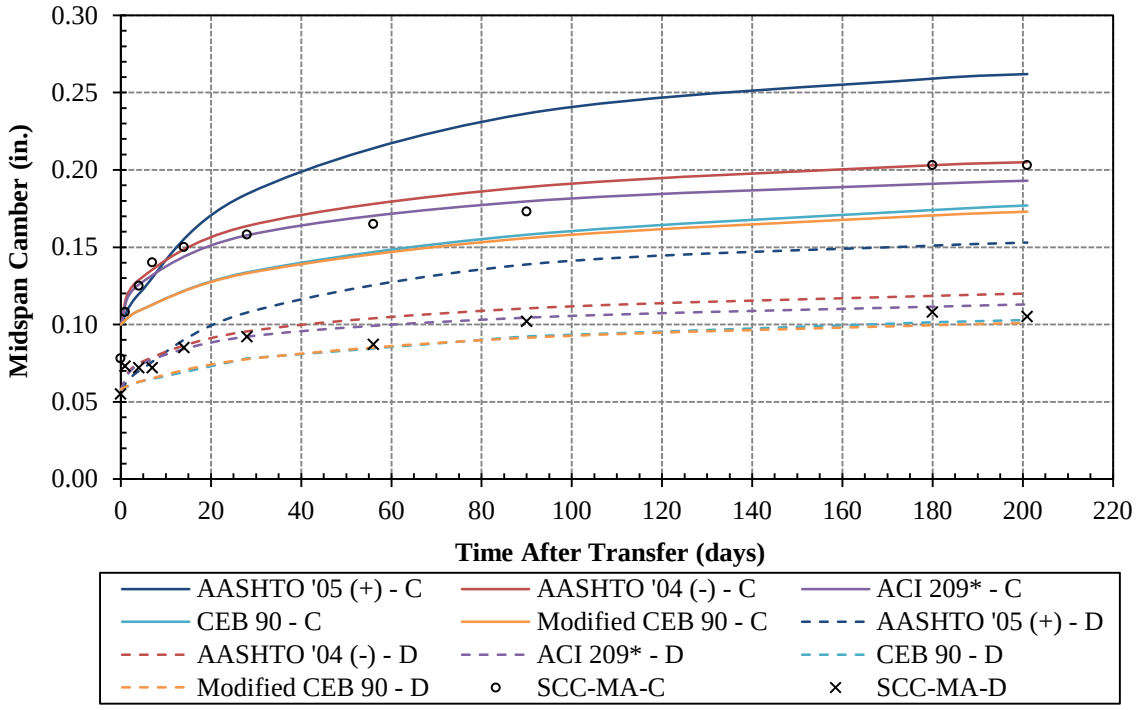

Figure 5-125: SCC-MA-C, D Predicted Camber with AASHTO/ACI E_c

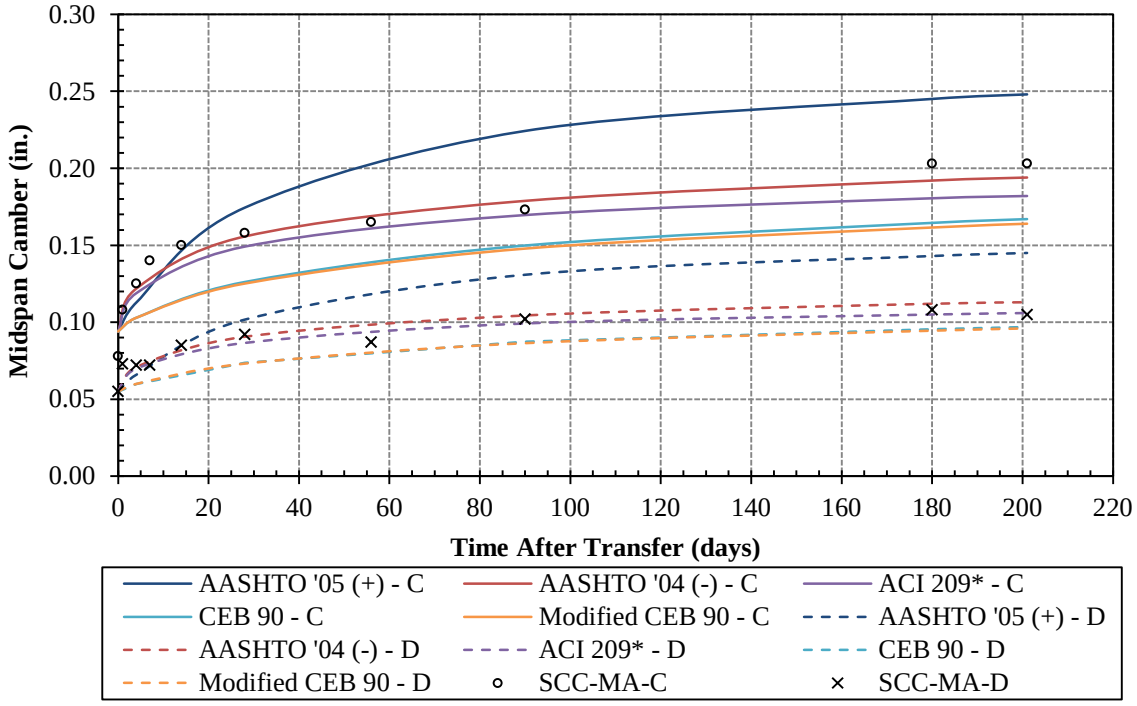

Figure 5-126: SCC-MA-C, D Predicted Camber with CEB 90 E_c

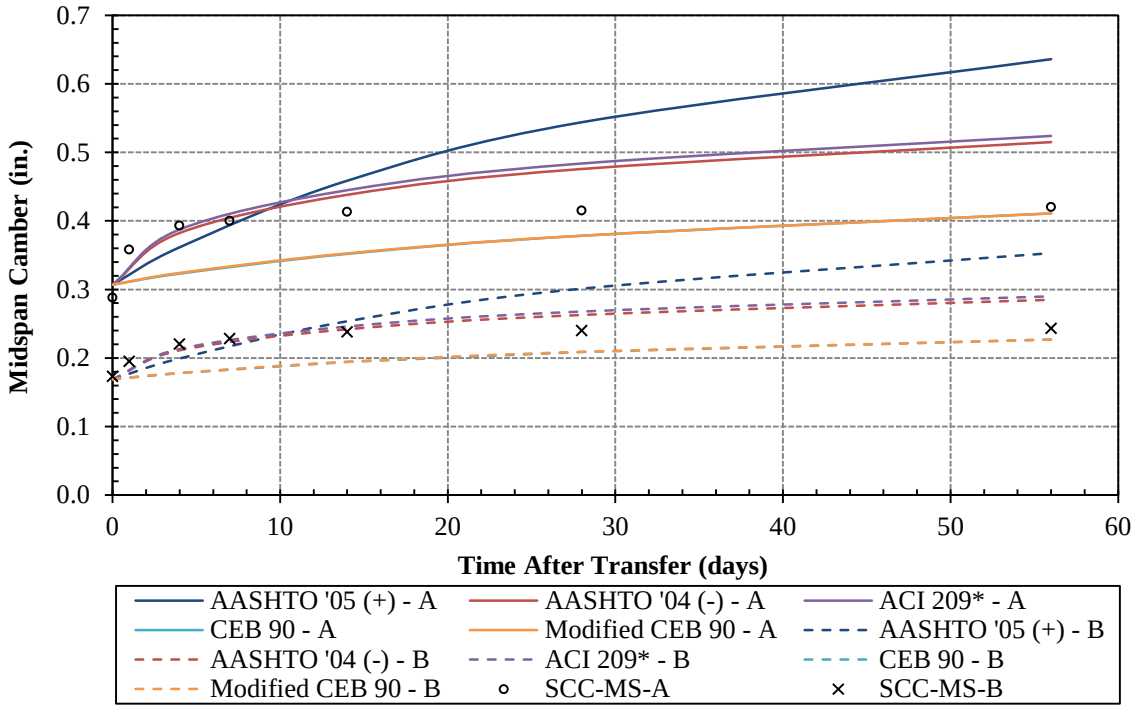

Figure 5-127: SCC-MS-A, B Predicted Camber with AASHTO/ACI E_c

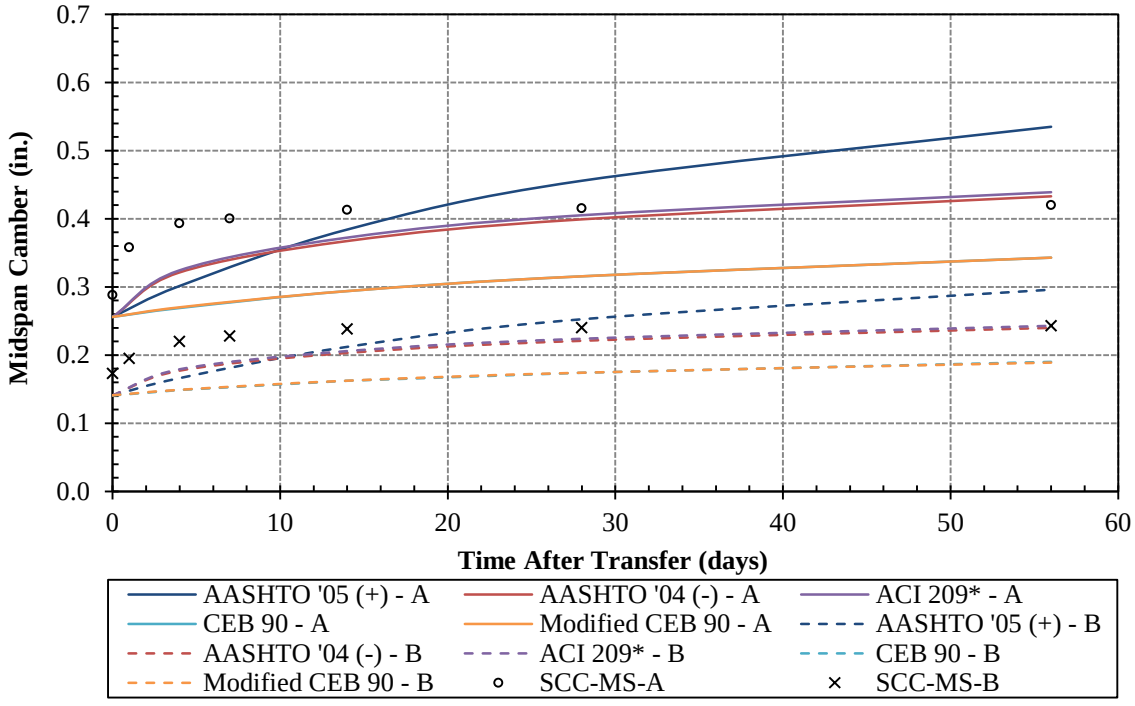

Figure 5-128: SCC-MS-A, B Predicted Camber with CEB 90 E_c

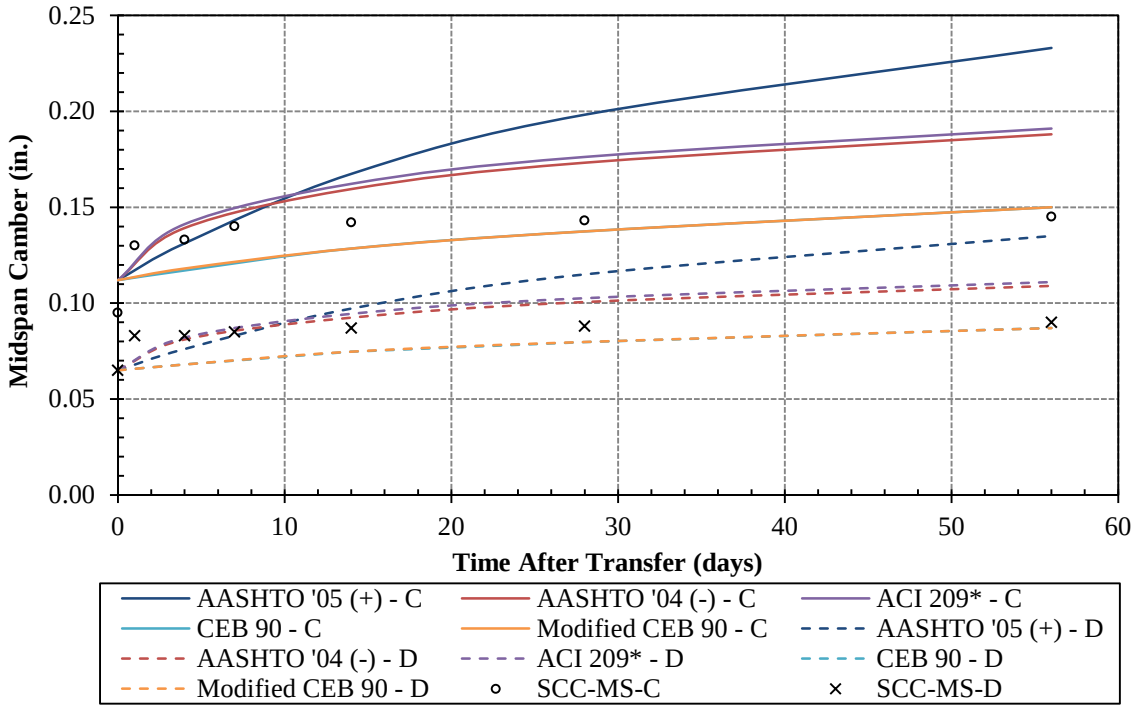

Figure 5-129: SCC-MS-C, D Predicted Camber with AASHTO/ACI E_c

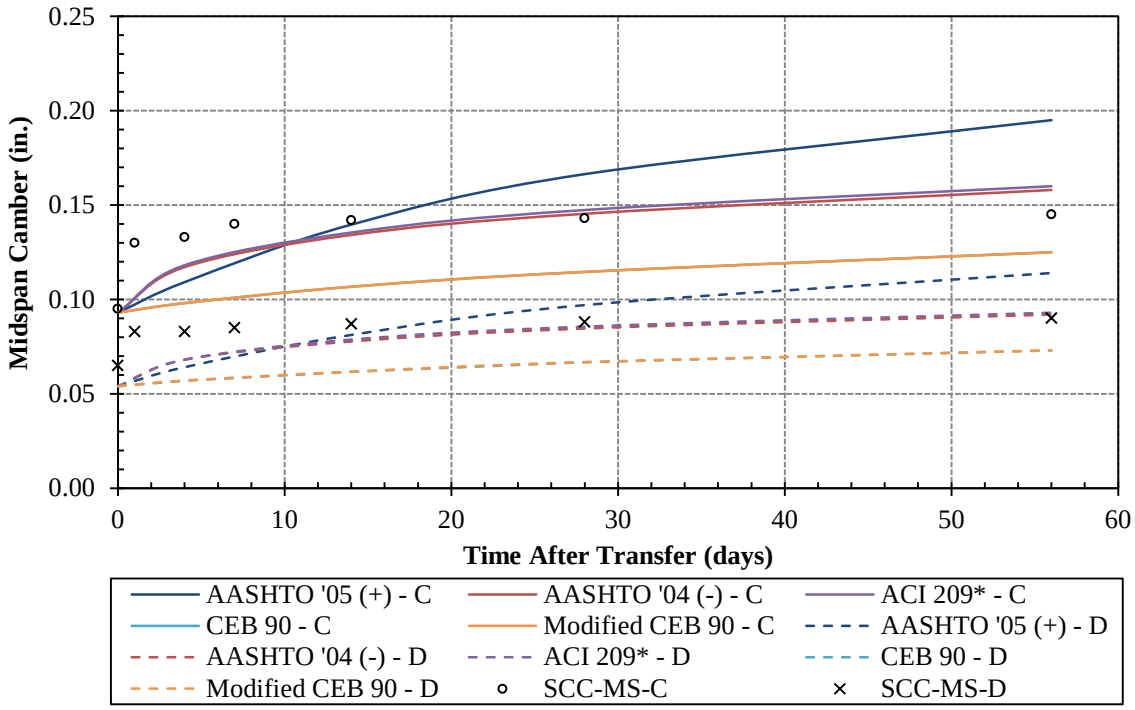

Figure 5-130: SCC-MS-C, D Predicted Camber with CEB 90 E_c

Figures 5-131 through 5-134 show the SCC-HS camber results when using various creep and shrinkage models with code-prediction E_c models. Tables G-19 and G-21 in Appendix G show the percent difference in measured and predicted camber at various ages. The percent differences in the measured and predicted proportional camber growth at various ages of the SCC-HS beams are shown in Tables G-20 and G-22.

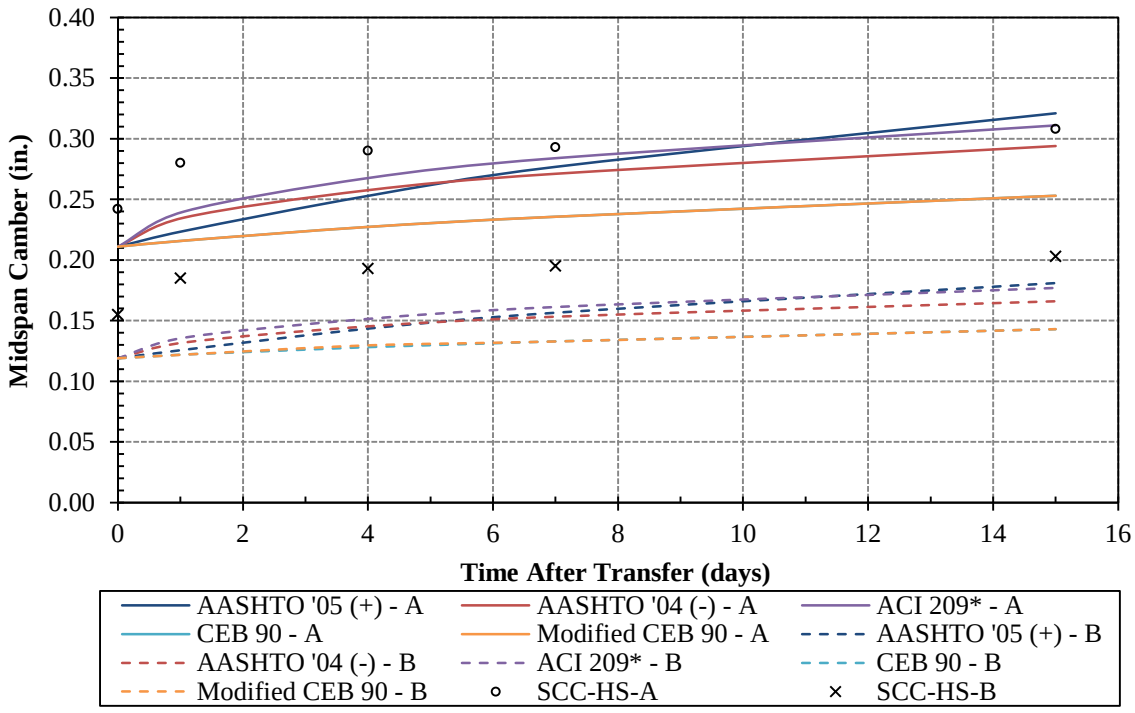

Figure 5-131: SCC-HS-A, B Predicted Camber with AASHTO/ACI E_c

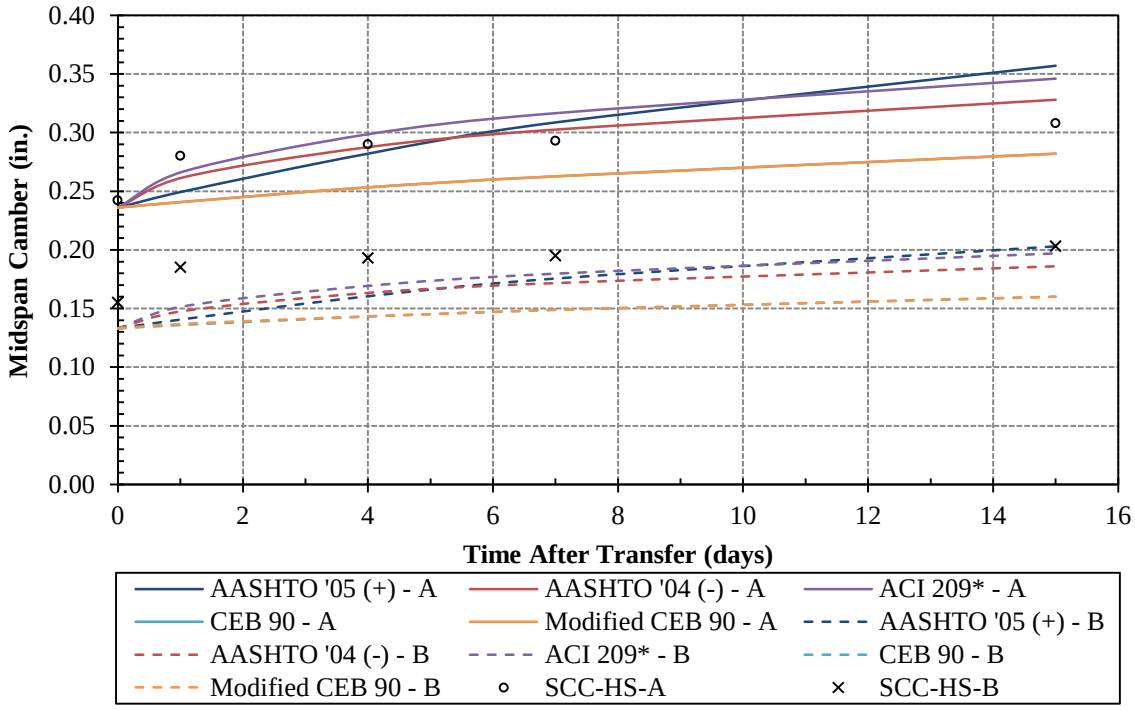

Figure 5-132: SCC-HS-A, B Predicted Camber with CEB 90 E_c

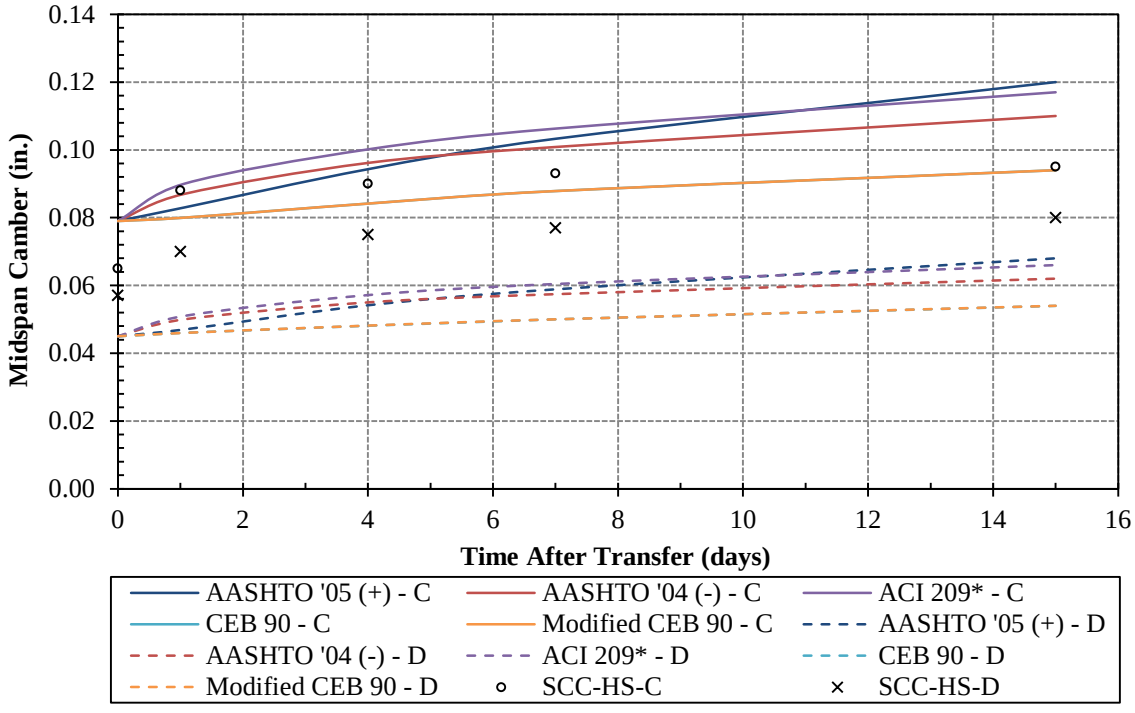

Figure 5-133: SCC-HS-C, D Predicted Camber with AASHTO/ACI E_c

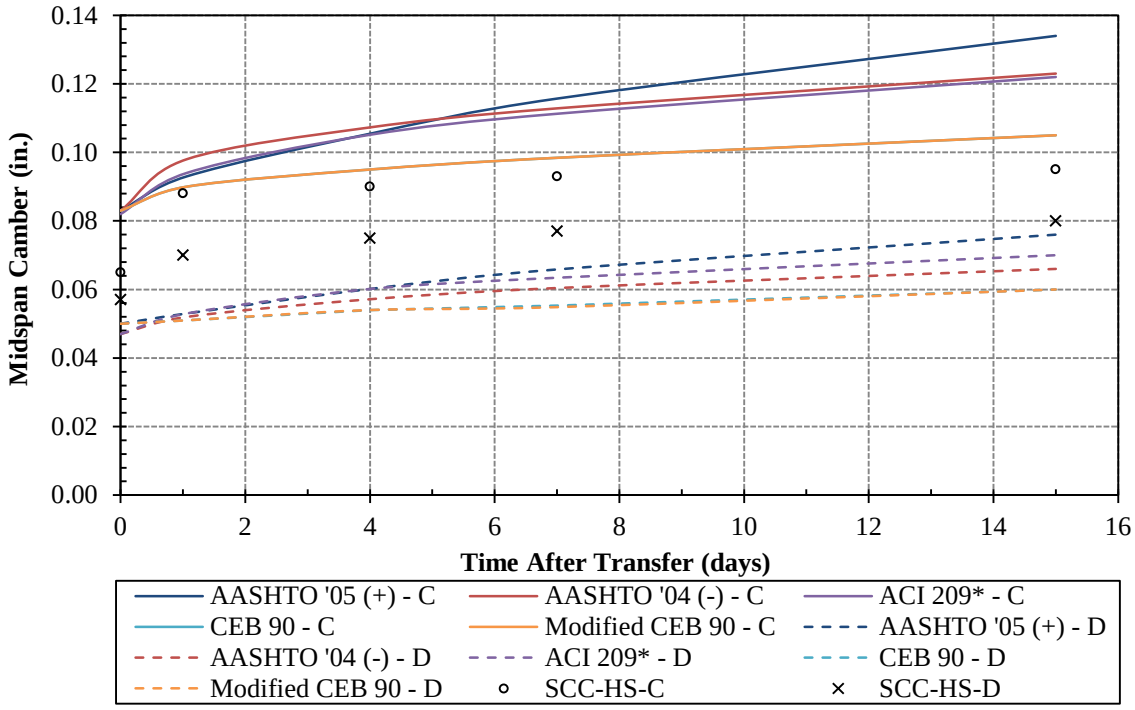

Figure 5-134: SCC-HS-C, D Predicted Camber with CEB 90 E_c

5.3.4 BT-54 GIRDERS

Findings by Stallings et al. (2003) stated "no identifiable increase in E_c was noted after transfer of prestress." Therefore, the average concrete modulus of 5740 ksi was used for the Constant E_c model. Since the program input data were the same for all five BT-54 girders, the five sets of experimental camber measurements are compared to one set of camber predictions. Table 5-8 summarizes the camber results from the Stallings et al. research. The calculated camber values were determined by an incremental time-step method using high-performance concrete (HPC) parameters.

Table 5-8: BT-54 Camber - Experimental Results from Stallings et. al (2003)

Girder	Age (Days)	Camber (in.)		
		Measured	Calculated	% Difference
BT-1	1	3.34	3.02	-10
	295	4.55	4.31	-5
BT-2	1	3.63	3.02	-17
	295	4.90	4.31	-12
BT-3	1	3.19	3.02	-5
	242	4.09	4.24	+4
BT-4	1	3.28	3.02	-8
	242	4.20	4.24	+1
BT-5	1	3.34	3.02	-10
	234	4.17	4.23	+1

The following creep and shrinkage models were included in the program analysis: AASHTO ’05 (+), AASHTO ’04 (-), ACI 209, CEB, and modified CEB. The slump determined from concrete testing was used in the ACI 209 model. The “adjusted” slump based on mixture proportions was used in the ACI 209* model. The CEB creep and shrinkage model was evaluated assuming cement type RS. See the sensitivity analysis in Chapter 6 for further discussion of cement type and its effect on strain and camber predictions. The camber predictions using the various creep and shrinkage models while maintaining a constant E_c are shown in Figures 5-135 and 5-136.

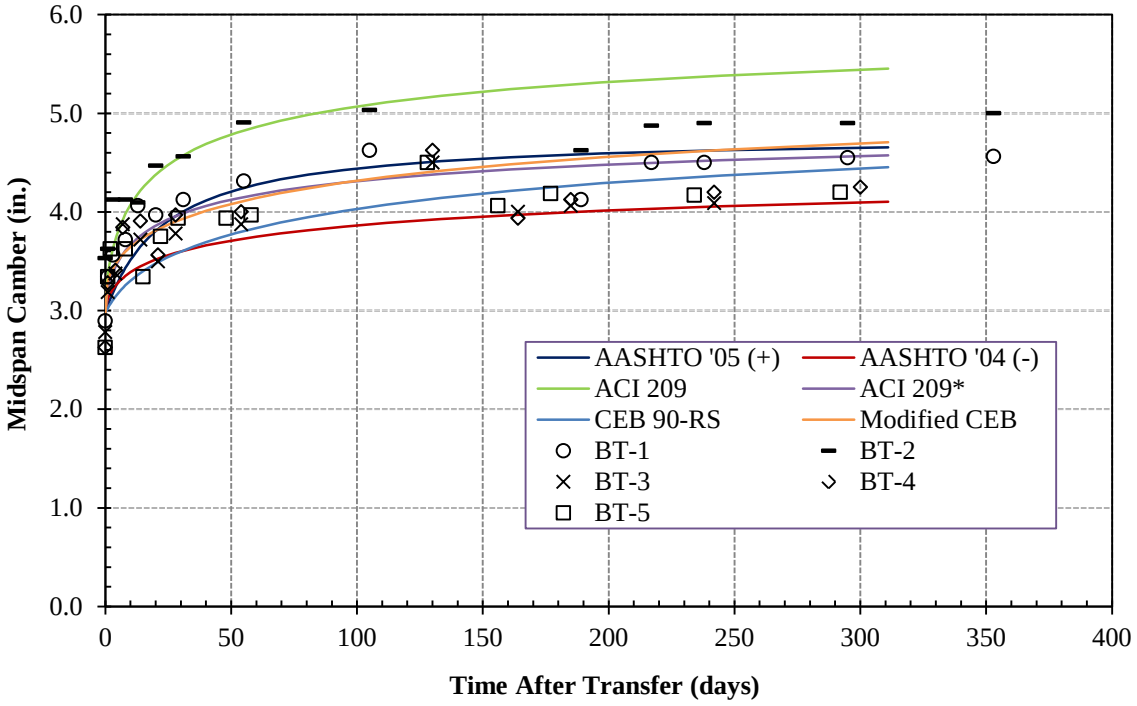

Figure 5-135: BT-54 Predicted Camber

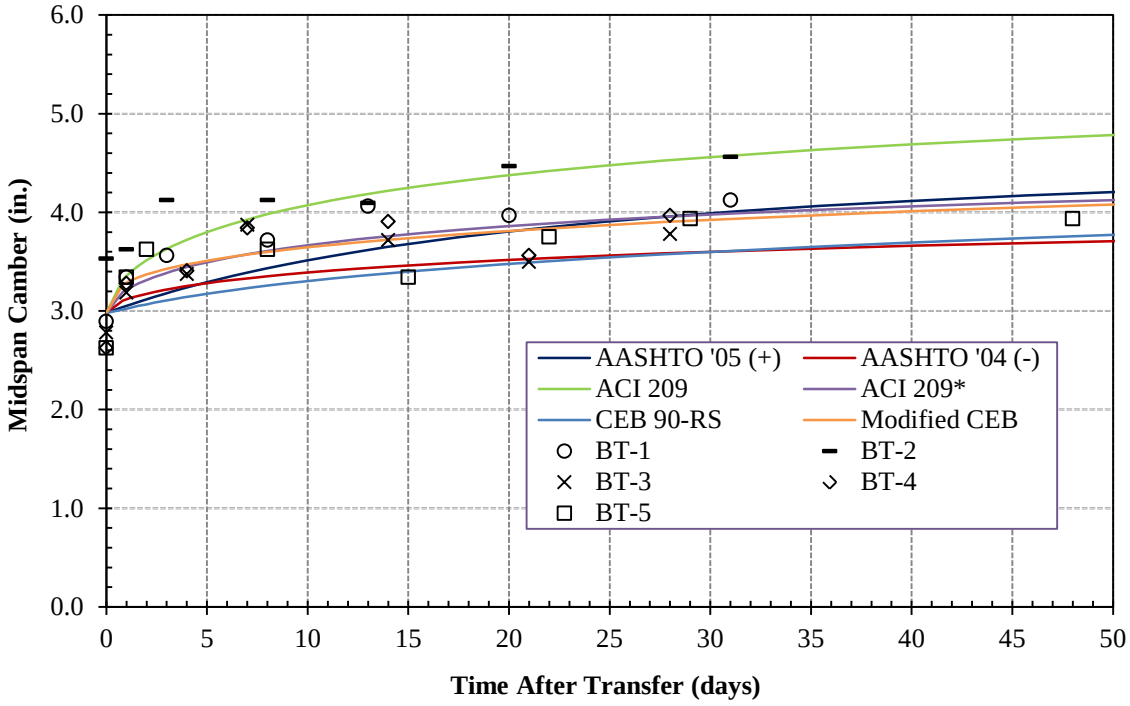

Figure 5-136: BT-54 Predicted Early-Age Camber

As shown in Figure 5-136, the ACI 209 model best predicts early-age camber for BT-2. The percent difference between the ACI 209 predicted values and measured camber at 1 day ranges from -7.6 to 0.4 percent. However, the ACI 209 model over-predicts long-term camber up to 31 percent. In general, the ACI 209* and Modified CEB creep and shrinkage models better predict early-age camber. These two models also provide the best estimate for camber growth over time.

The CEB 90 creep and shrinkage model slightly under-estimates long-term camber while the Modified CEB 90 model slightly over-estimates long-term camber. The percent difference between the CEB 90 predicted values and measured camber prior to casting of deck ranges from -9.5 to 6.7 percent. See Tables 5-9 and 5-10 for the percent differences of all creep and shrinkage models.

Table 5-9: BT-54 Camber Comparison – AASHTO / ACI

Girder	Age (Days)	Measured Camber (in.)	Predicted Camber (in.)					
			AASHTO '05 (+)		AASHTO '04 (-)		ACI 209	
			Predicted	% Diff	Predicted	% Diff	Predicted	% Diff
BT-1	1	3.34	3.05	-8.6	3.12	-6.7	3.35	0.4
	295	4.55	4.65	2.2	4.09	-10.0	5.43	19.4
BT-2	1	3.63	3.05	-15.9	3.12	-14.1	3.35	-7.6
	295	4.90	4.65	-5.1	4.09	-16.5	5.43	10.9
BT-3	1	3.19	3.05	-4.3	3.12	-2.3	3.35	5.1
	242	4.09	4.62	13.1	4.05	-0.9	5.38	31.5
BT-4	1	3.28	3.05	-6.9	3.12	-5.0	3.35	2.2
	242	4.20	4.62	10.1	4.05	-3.5	5.38	28.0
BT-5	1	3.34	3.05	-8.6	3.12	-6.7	3.35	0.4
	234	4.17	4.62	10.7	4.05	-3.0	5.37	28.7

Table 5-10: BT-54 Camber Comparison – CEB 90 / Modified CEB

Girder	Age (Days)	Measured Camber (in.)	Predicted Camber (in.)					
			CEB 90 - R		CEB 90 - RS		Modified CEB	
			Predicted	% Diff	Predicted	% Diff	Predicted	%
BT-1	1	3.34	3.10	-7.1	3.02	-9.5	3.29	-1.6
	295	4.55	4.68	2.9	4.43	-2.5	4.69	3.0
BT-2	1	3.63	3.10	-14.6	3.02	-16.7	3.29	-9.5
	295	4.90	4.68	-4.5	4.43	-9.5	4.69	-4.3
BT-3	1	3.19	3.10	-2.8	3.02	-5.2	3.29	3.0
	242	4.09	4.61	12.7	4.37	6.7	4.62	13.1
BT-4	1	3.28	3.10	-5.5	3.02	-7.8	3.29	0.2
	242	4.20	4.61	9.8	4.37	4.0	4.62	10.1
BT-5	1	3.34	3.10	-7.1	3.02	-9.5	3.29	-1.6
	234	4.17	4.60	10.2	4.35	4.4	4.61	10.6

CHAPTER SIX

SENSITIVITY ANALYSIS

6.1 APPROACH

To better understand the behavior of time-dependent camber, the basic variables in the camber calculations can be included in a sensitivity analysis. The analysis presented in this chapter covers the effect variances in concrete properties and construction parameters have on strain and camber predictions.

6.2 EFFECT OF CONCRETE PROPERTIES

Estimating creep over time and its effect on camber is a function of the concrete properties. To further analyze the program's strain and camber predictions, the following concrete properties were included in a sensitivity analysis: cement type and slump.

6.2.1 CEMENT TYPE

The CEB 90 classifies cement types based on their strength class and rate of strength development. A general description for each cement type is provided in Table 6-1.

Table 6-1: CEB-FIP Cement Classifications

Cement Classification	Description
SL	Slowly hardening cement
N	Normal hardening cement
R	Rapid hardening cement
RS	Rapid hardening, high strength cement

The BT-54 girders were used to evaluate the effect of cement type on concrete strain and camber predictions. The CEB 90 MOE model and the CEB 90 creep and shrinkage models were used during the analysis. The sensitivity analysis was limited to cement types R and RS. As shown in Equation 3-43, no adjustments are made to the concrete age at loading when Type R cement is used. Figures 6-1 and 6-2 show the effect of cement type on top and bottom concrete strain predictions. Specifying Type R cement overestimates the bottom fiber strain at all ages. This is primarily because the initial concrete MOE was underestimated by assuming Type R cement. Beyond 50 days after transfer, the degree of separation in strain results when using Type R versus Type RS remains fairly constant. The results when specifying Type RS cement correlate very well with the measured bottom fiber strain at all ages.

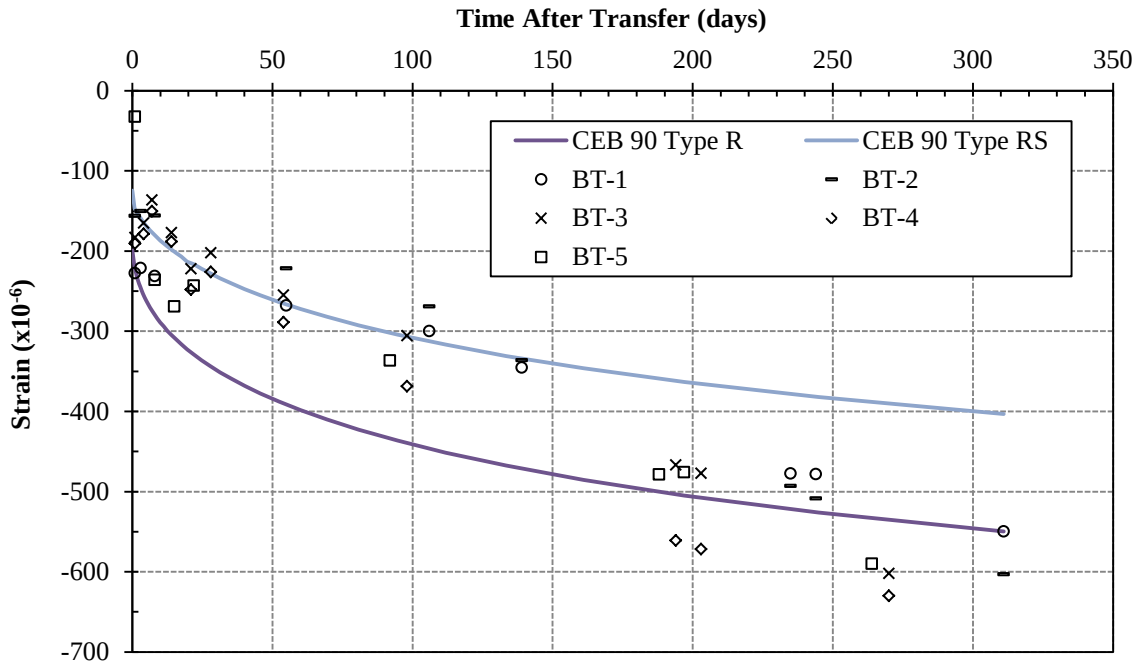

Figure 6-1: BT-54 Predicted Strains at Top VWSG - Varying Cement Type

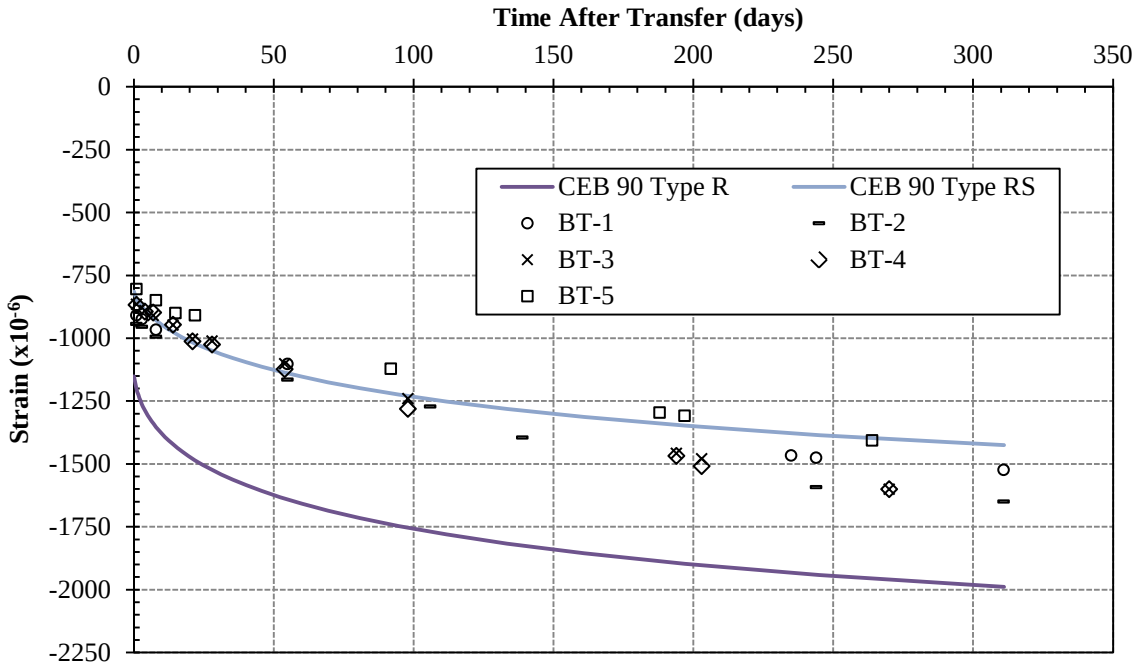

Figure 6-2: BT-54 Predicted Strains at Bottom VWSG - Varying Cement Type

Figure 6-3 shows the effect of cement type on camber predictions. The initial camber and the early-age camber growth when using cement Type R are larger than when using cement Type RS. Beyond 50 days after transfer, the degree of separation in camber results when using Type R versus Type RS remains constant. The results when specifying Type RS cement correlate very well with the measured camber at all ages.

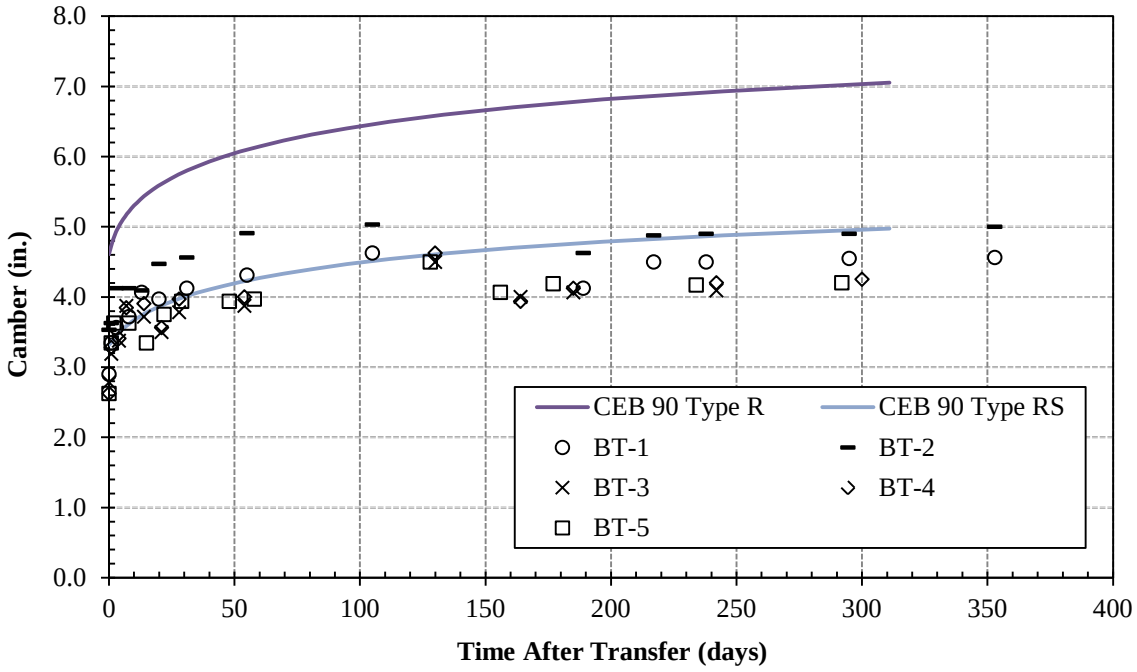

Figure 6-3: BT-54 Predicted Camber - Varying Cement Type

6.2.2 SLUMP

The AASHTO BT-54 girders were used to evaluate the effect of slump on the program's strain and camber predictions. Using the "Constant E_c" model for the concrete MOE development, four slump values were inserted into the ACI 209 creep and shrinkage model. The actual slump for the BT-54 girders was 8 inches. To produce a correction factor exactly equal to one, a slump equal to 2.68 inches was included in the sensitivity analysis. Based on the mixture proportions,

the appropriate adjusted “water” slump for these girders is less than 1 inch. As stated in Chapter 4, the adjusted “water” slump estimation assumes no water-reducing admixture in the mixture. The analysis was performed using both 0 and 1 inch values of adjusted slump to bound the actual expected behavior. The following figures show the predicted strains and camber of the BT-54 girder when varying the slump from 0 to 8 inches.

Figures 6-4 and 6-5 show the effect of slump on the strain at the top and bottom VWSG. In general, the strains prior to 150 days after transfer are overestimated. The predicted strains using a one-inch slump are a good average of the strain measurements taken after 200 days. At 311 days after transfer, the top and bottom strain in BT-1 measured -550 με and -1525 με, respectively. When using a one-inch slump in the ACI 209 creep and shrinkage model, the VB program calculates a top and bottom strain of -486 με and -1665 με. The difference between the top strain values is -11.7 percent and the difference between the bottom strain values is 9.2 percent.

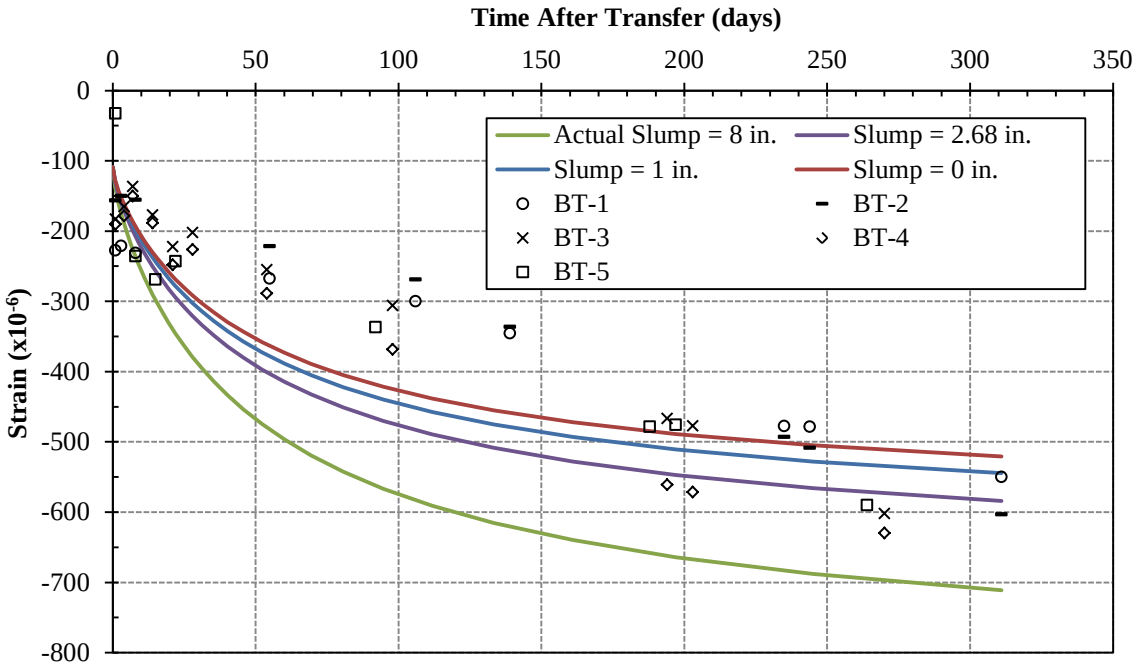

Figure 6-4: BT-54 Predicted Strains at Top VWSG - Varying Concrete Slump

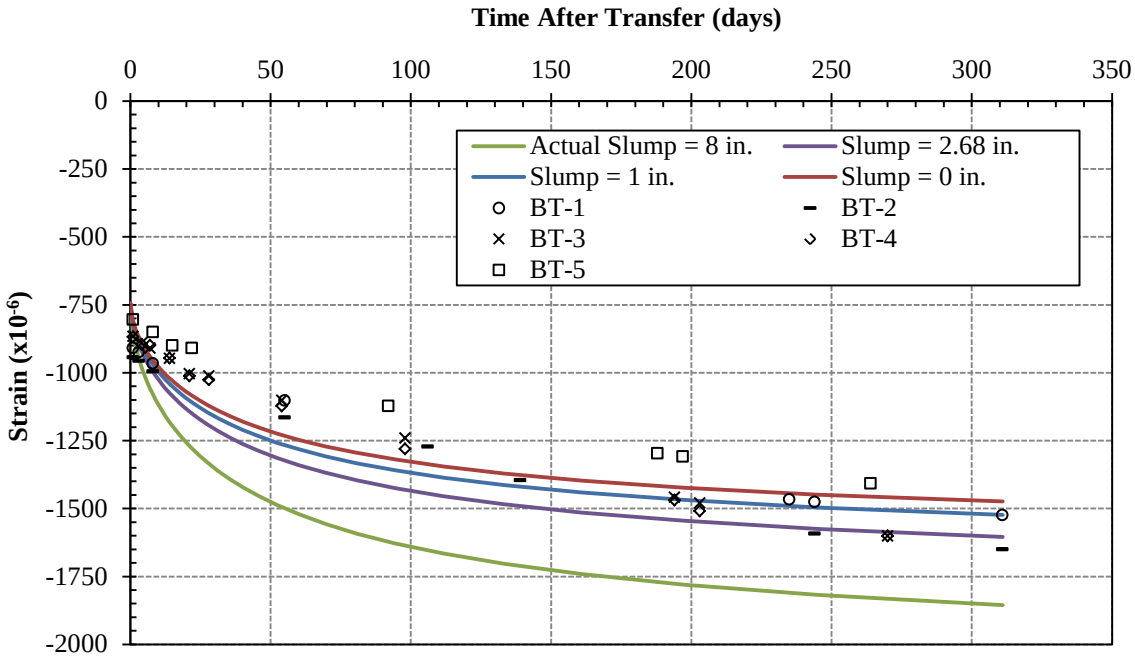

Figure 6-5: BT-54 Predicted Strains at Bottom VWSG - Varying Concrete Slump

Figure 6-6 shows the effect of slump on the AASHTO BT-54 camber predictions. Using a concrete slump of zero inches in the ACI 209 creep and shrinkage model best predicts the long-term camber of girders BT-1, BT-3, BT-4, and BT-5. The camber predictions based on the actual slump of 8 inches best predicts BT-2 camber up to 100 days after transfer. After 100 days, the BT-2 camber correlates best with the camber predictions using a slump of 2.68 inches which corresponds to a slump correction factor equal to one.

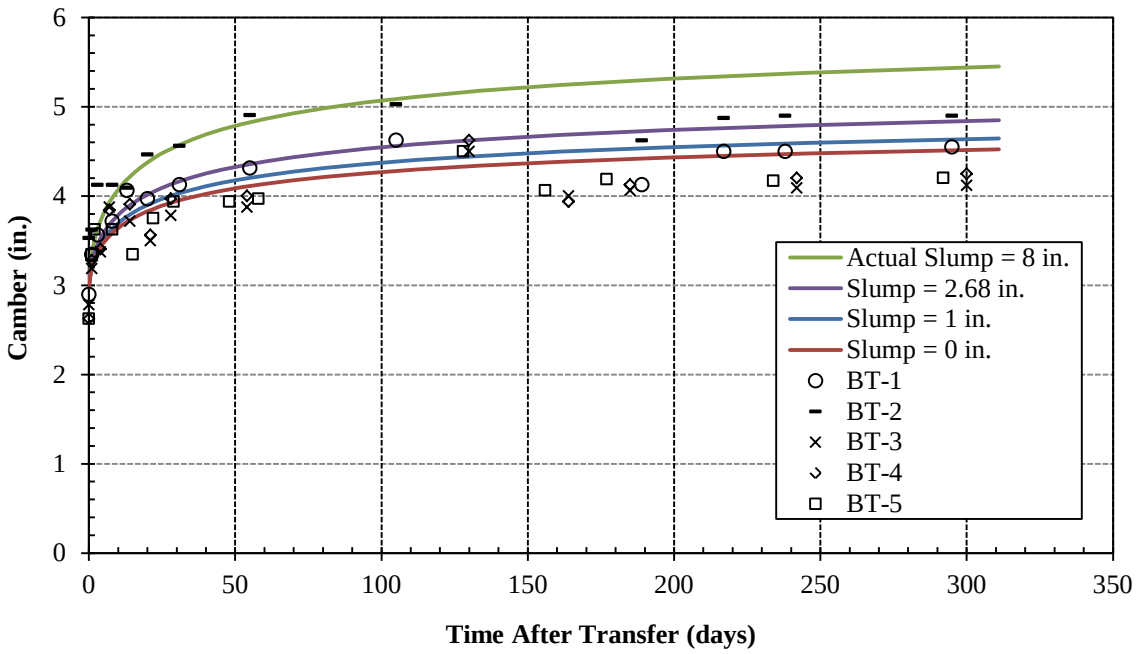

Figure 6-6: BT-54 Predicted Camber - Varying Concrete Slump

A closer look at the effect on early-age camber when varying slump in the ACI 209 creep and shrinkage model can be seen in Figure 6-7. Up to 60 days after transfer, the best predictor of BT-1 camber is based on a concrete slump of 2.68 inches. For BT-3 and BT-4 camber less than 10 days after transfer, the predictions based on a slump value of zero inches provide the best-fit.

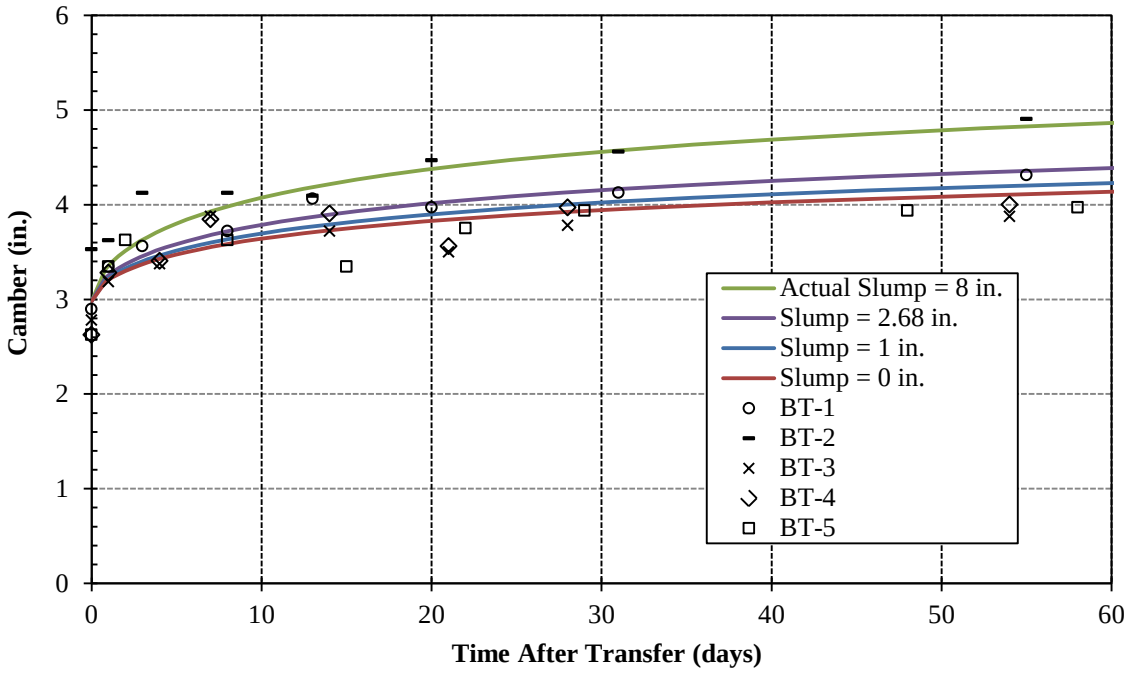

Figure 6-7: BT-54 Predicted Early Age Camber - Varying Concrete Slump

6.3 EFFECT OF CONSTRUCTION VARIABLES

The construction variables addressed in the sensitivity analysis include jacking stress and curing method. Varying the jacking stress can indirectly account for varying steel relaxation and prestress force immediately prior to release.

6.3.1 JACKING STRESS

The AASHTO Type I STD-M-1 girder was used to investigate the effect on the program's camber results when varying jacking stress up to 2 percent. Based on the results presented in Chapter 5, the best model combination for predicting STD-M camber is the CEB 90 E_c model and the ACI 209 creep and shrinkage model. Therefore, these models were used for the analysis. Table 6-2 shows the camber results when varying the jacking stress +/- 2 percent in each layer group. The original jacking stresses and camber predictions are given for reference.

Table 6-2: STD-M-1 Camber – Varying Jacking Stress

Jacking Stress	Percent Change	Camber (in.)					
		Initial		28 Days		110 Days	
		Measured	% Diff	Measured	% Diff	Measured	% Diff
202.5	-	0.30	-	0.50	-	0.58	-
30.5	-						
206.6	+2	0.31	+3.0	0.51	+3.2	0.60	+3.3
30.5	-						
206.6	+2	0.31	+3.0	0.51	+2.8	0.60	+3.0
31.1	+2						
198.5	-2	0.30	-3.0	0.48	-3.2	0.56	-3.1
30.5	-						
198.5	-2	0.30	-3.0	0.48	-3.0	0.56	-3.0
29.9	-2						

6.3.2 CURING METHODS

The strain and camber results for all AASHTO Type I SCC girders were evaluated assuming accelerated (steam) and non-accelerated (moist) curing conditions for the ACI 209 creep and shrinkage model. The adjusted slump was also used for analysis. The AASHTO '05(+)/ACI 209 model was used for the concrete MOE development over time.

Figures 6-8 through 6-10 show the strain predictions for SCC-MS-1. The strains at the top, middle, and bottom VWSG were best predicted using accelerated curing. Similar results were found for SCC-MS-2. See Figures J-1 through J-3 in Appendix J for the SCC-MS-2 strain predictions.

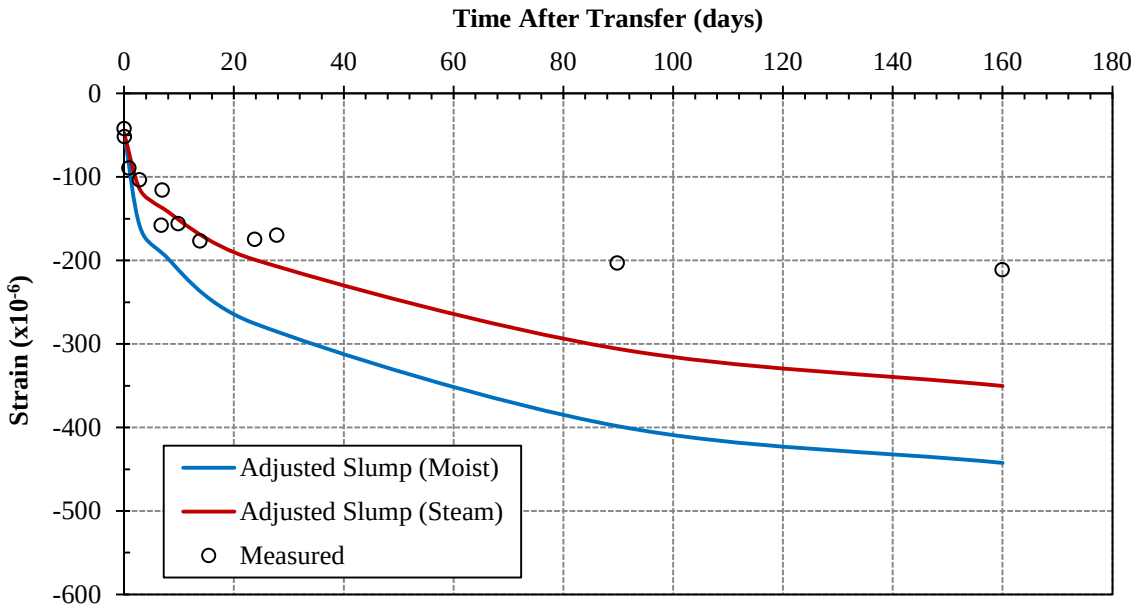

Figure 6-8: SCC-MS-1 Predicted Strains at Top VWSG – Varying Cure Type

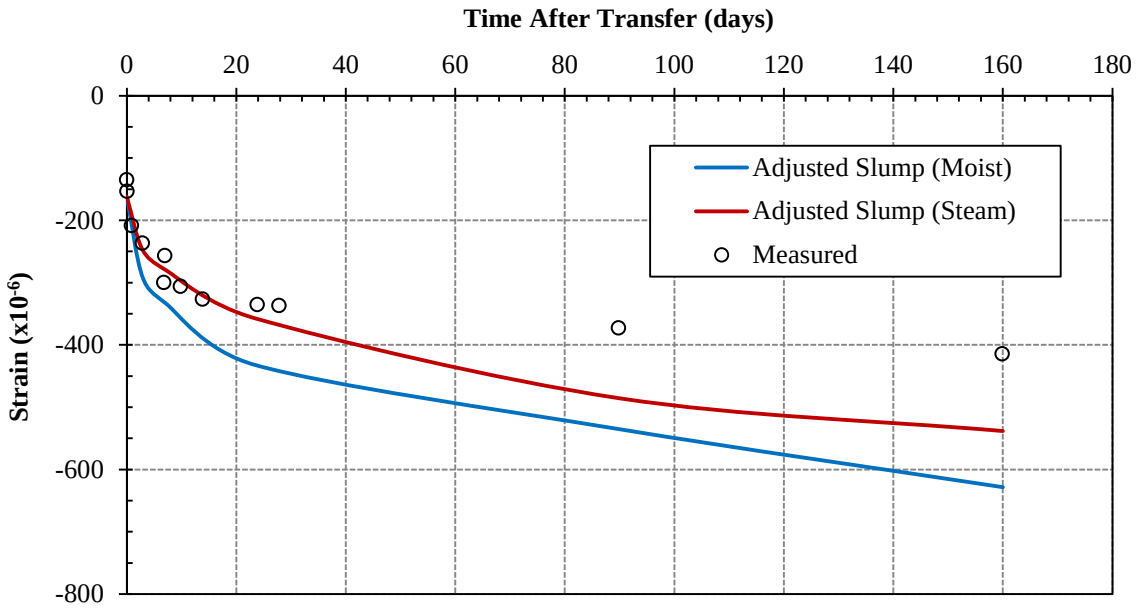

Figure 6-9: SCC-MS-1 Predicted Strains at Middle VWSG – Varying Cure Type

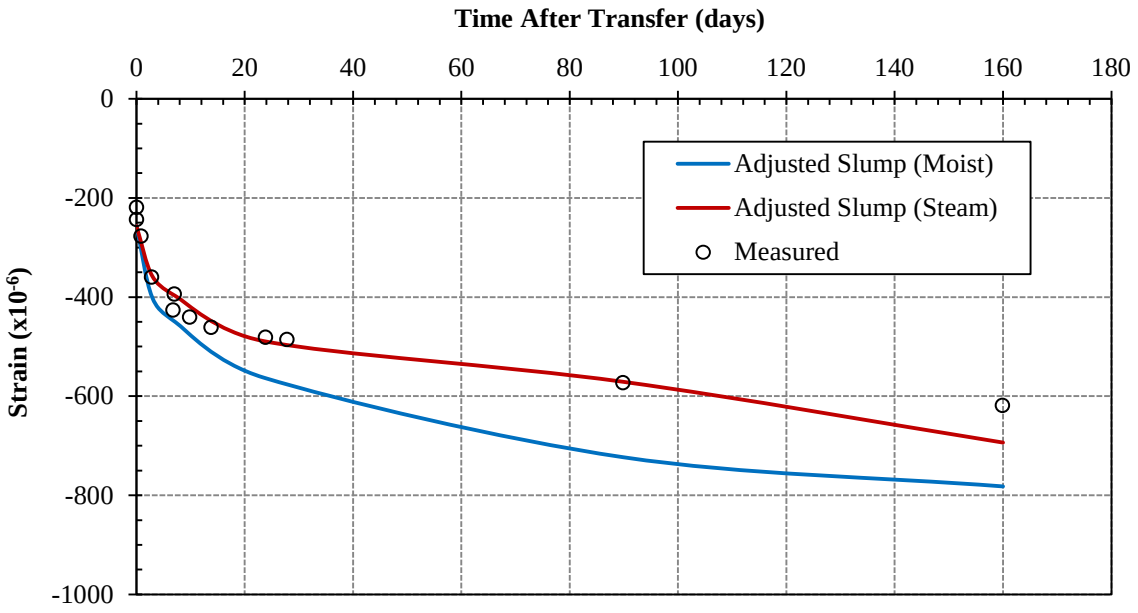

Figure 6-10: SCC-MS-1 Predicted Strains at Bottom VWSG – Varying Cure Type

Figures 6-11 through 6-13 show the strain predictions for SCC-HS-1. Again, using accelerated curing yielded the best predictions for strain at the top, middle, and bottom VWSG locations. See Figures J-4 through J-6 in Appendix J for the effect of slump and curing conditions on the SCC-HS-2 strain predictions.

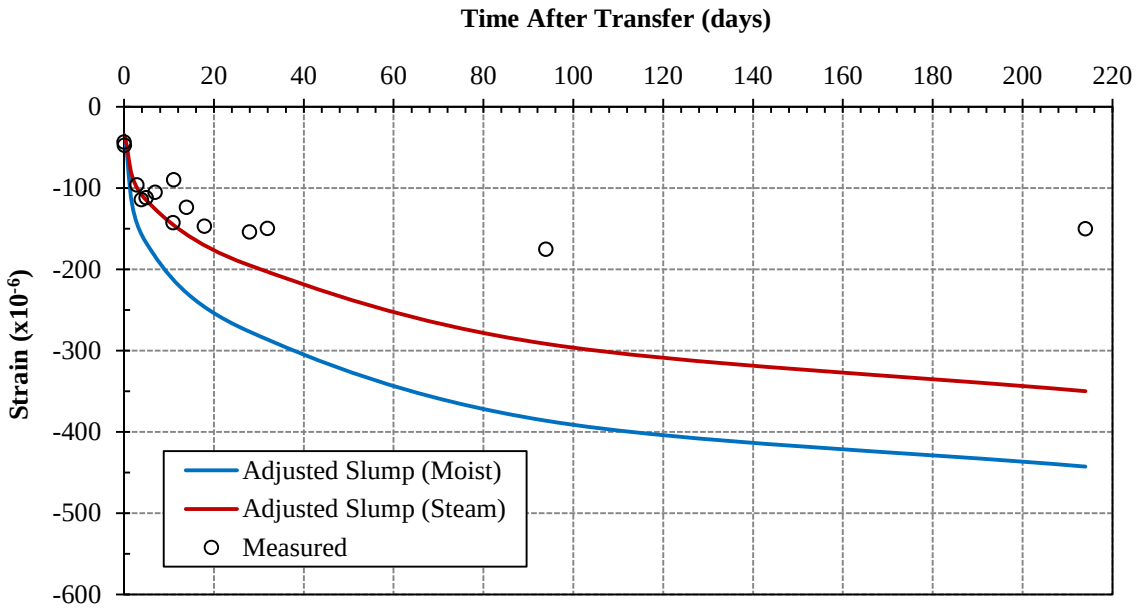

Figure 6-11: SCC-HS-1 Predicted Strains at Top VWSG – Varying Cure Type

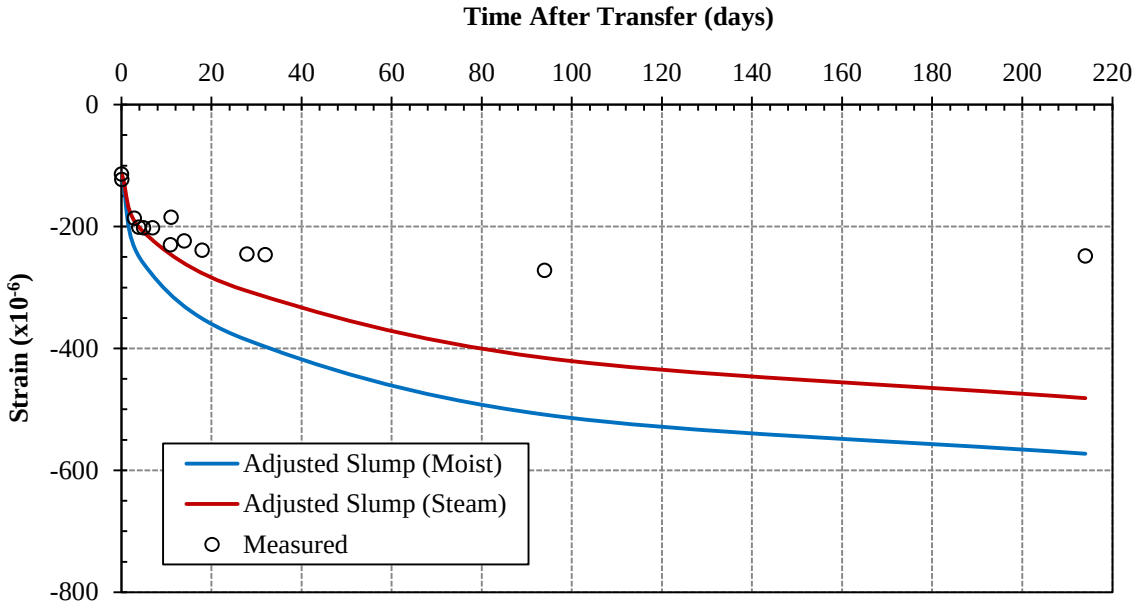

Figure 6-12: SCC-HS-1 Predicted Strains at Middle VWSG – Varying Cure Type

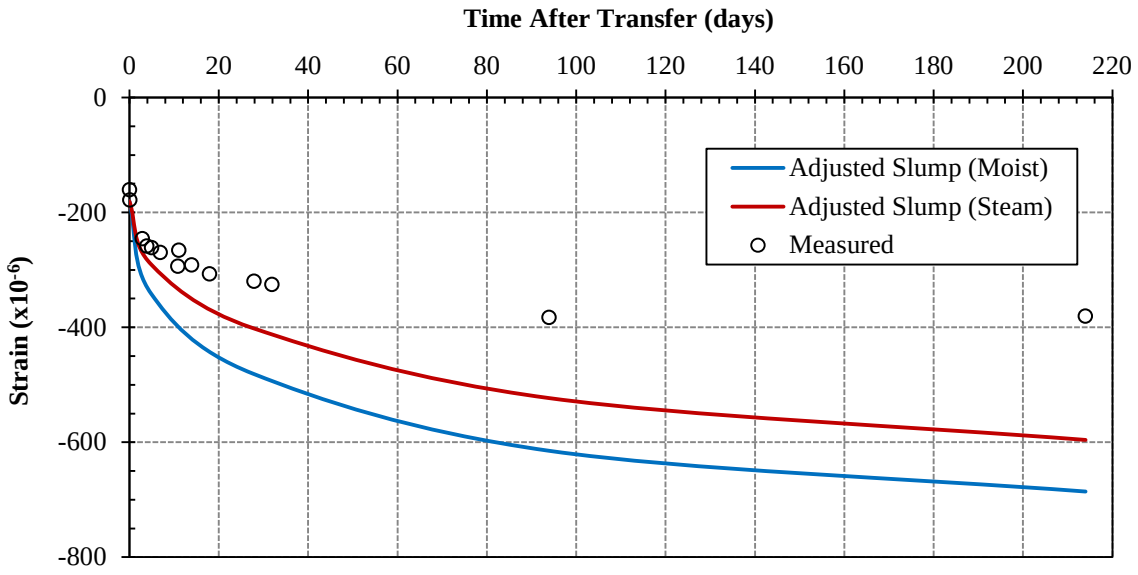

Figure 6-13: SCC-HS-1 Predicted Strains at Bottom VWSG – Varying Cure Type

Figure 6-14 shows the SCC-MS-1 and SCC-HS-1 camber results assuming accelerated (steam) and non-accelerated (moist) curing conditions. The effect of curing type on camber predictions is minimal. This can be expected since the ACI 209 creep model does not have a correction factor directly allocated for the curing type. Instead, the loading age correction factor is modified based on the curing type as shown in Equation 2-14. Conversely, as shown in Equation 2-24, the ACI 209 shrinkage model has a curing period correction factor directly accounting for accelerated versus non-accelerated curing conditions. This explains the larger difference in strain predictions shown in Figures 6-8 through 6-13.

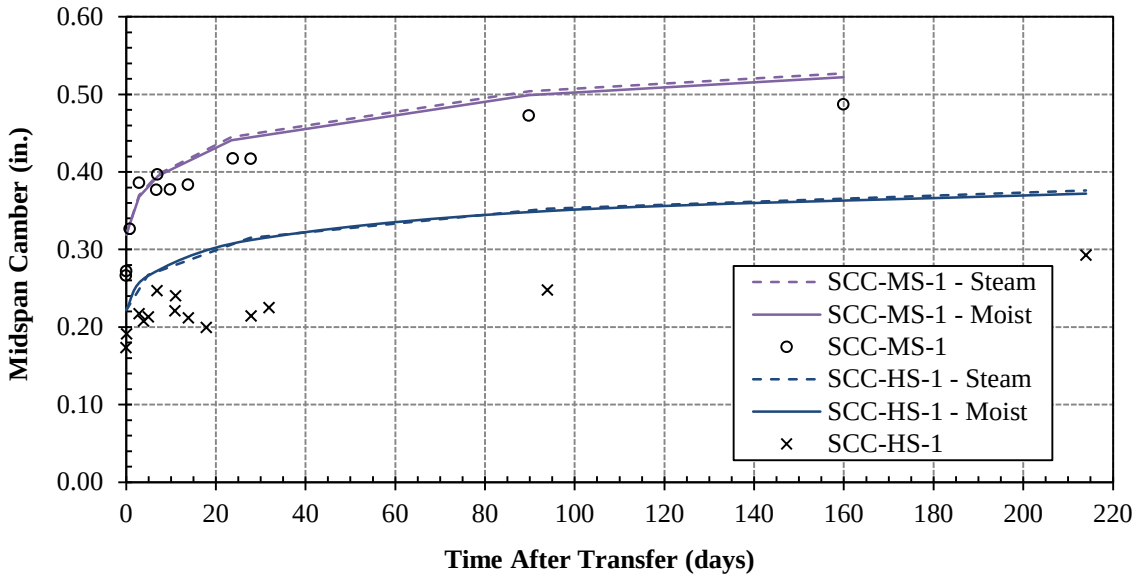

Figure 6-14: AASHTO Type I SCC Predicted Camber – Varying Cure Type

6.4 EFFECTS OF MATURITY

The program allows the user to either include or neglect the effects of maturity associated with curing. For maturity to be included in the analysis, the user must provide an average curing temperature or equivalent concrete age at transfer (see Figure K-11 in Appendix K). The six AASHTO Type I girders from Boehm's research were selected as the test specimens to compare camber results when neglecting and including maturity. An average curing temperature of 140 degrees Fahrenheit was used when including maturity in the analysis. All camber results were based on the CEB 90 concrete MOE model and CEB 90 creep and shrinkage model.

Using the CEB 90 Equations 3-37 and 3-43 provided in Chapter 3, the maturity of concrete was adjusted for an average curing temperature ranging from 100˚ to 160˚F. Table 6-3 below shows the adjusted concrete age for the STD-M-1 girder based on curing temperature only ($t_{0,T}$) and the adjusted concrete age based on curing temperature and cement type (t_0). Cement

Type RS was used in the analysis. Neglecting maturity, the concrete chronological age at transfer is 0.875 days.

Table 6-3: STD-M-1 Adjusted Concrete Age – Varying Curing Temperature

Average Curing Temperature (˚F)	$t_{0,T}$ (days)	t_0 (days)
100	1.91	6.02
120	2.97	7.67
140	4.50	9.52
160	6.64	11.74

Figures 6-15 through 6-17 show the camber results for the AASHTO Type I girders when maturity is included and neglected in the CEB 90 analysis. As shown in Figure 6-15, neglecting maturity provides better camber predictions for the STD-M girders. The results for the SCC-MS girders, shown in Figure 6-16, are not as straightforward. Neglecting maturity better predicts camber for the SCC-MS-1 girder, whereas the SCC-MS-2 camber is better predicted when the effects of maturity are included in the analysis. However, the actual curing temperature for the SCC-MS-2 girder is approximately 115 degrees Fahrenheit instead of 140 degrees. The SCC-HS camber results are shown in Figure 6-17. Including the effects of maturity provides better camber predictions for both SCC-HS girders. Note the average curing temperature for the SCC-HS girders is 122 degrees Fahrenheit.

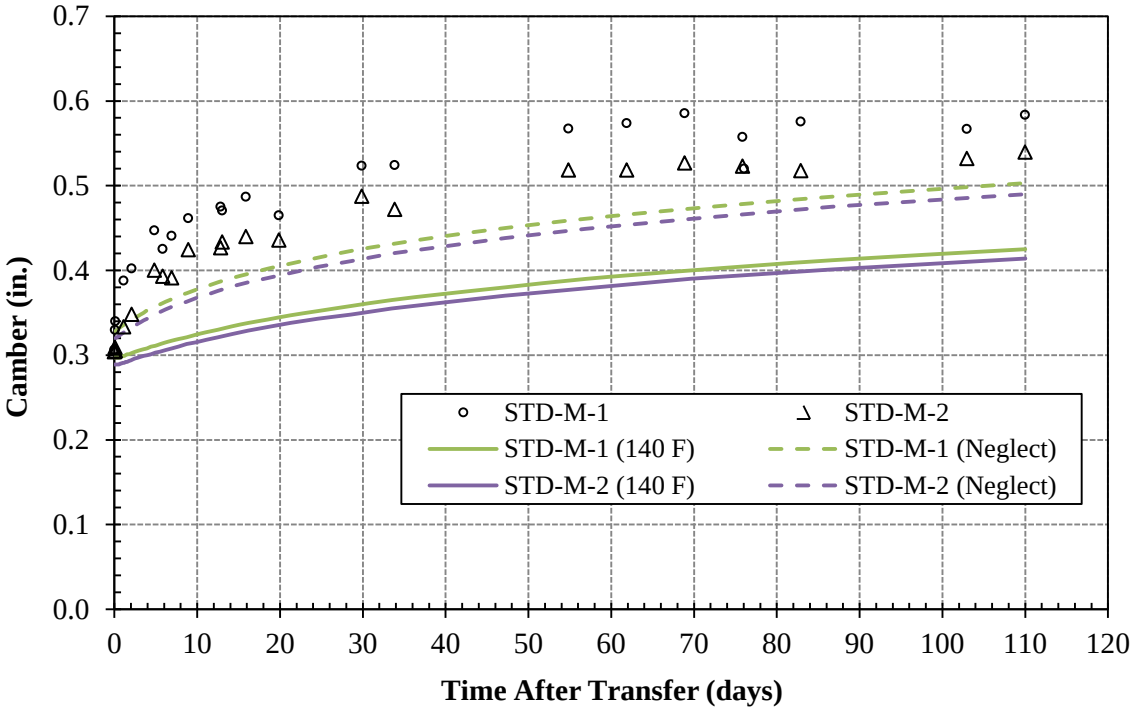

Figure 6-15: AASHTO Type I STD-M Predicted Camber – Maturity

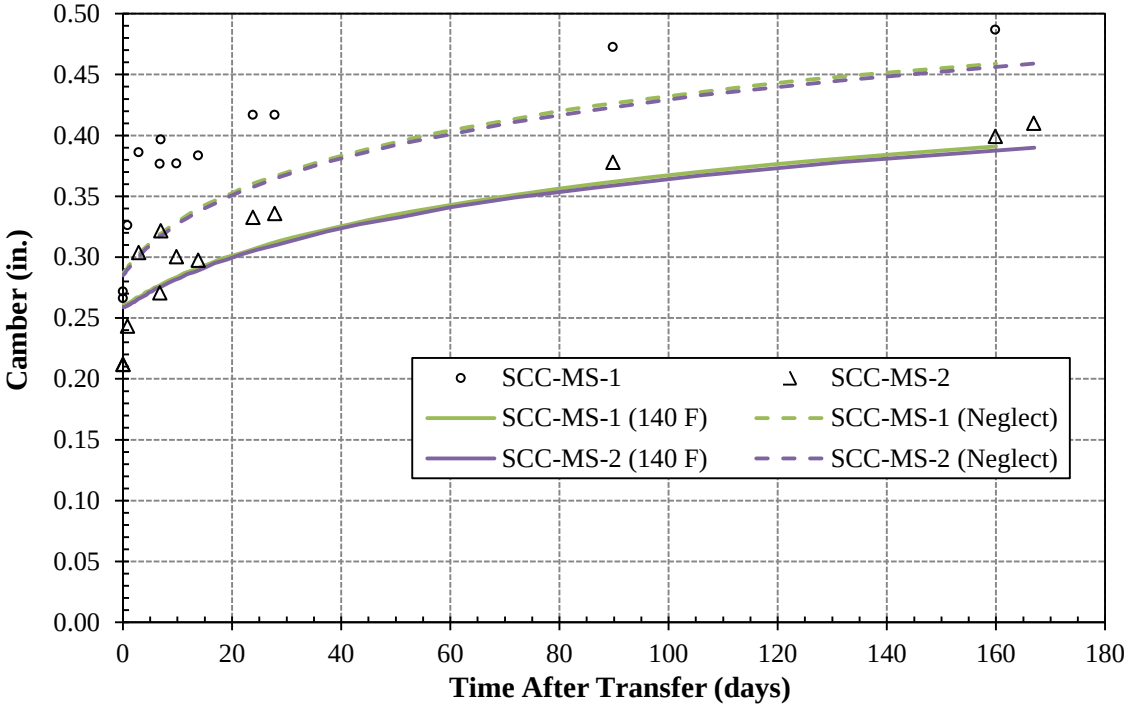

Figure 6-16: AASHTO Type I SCC-MS Predicted Camber – Maturity

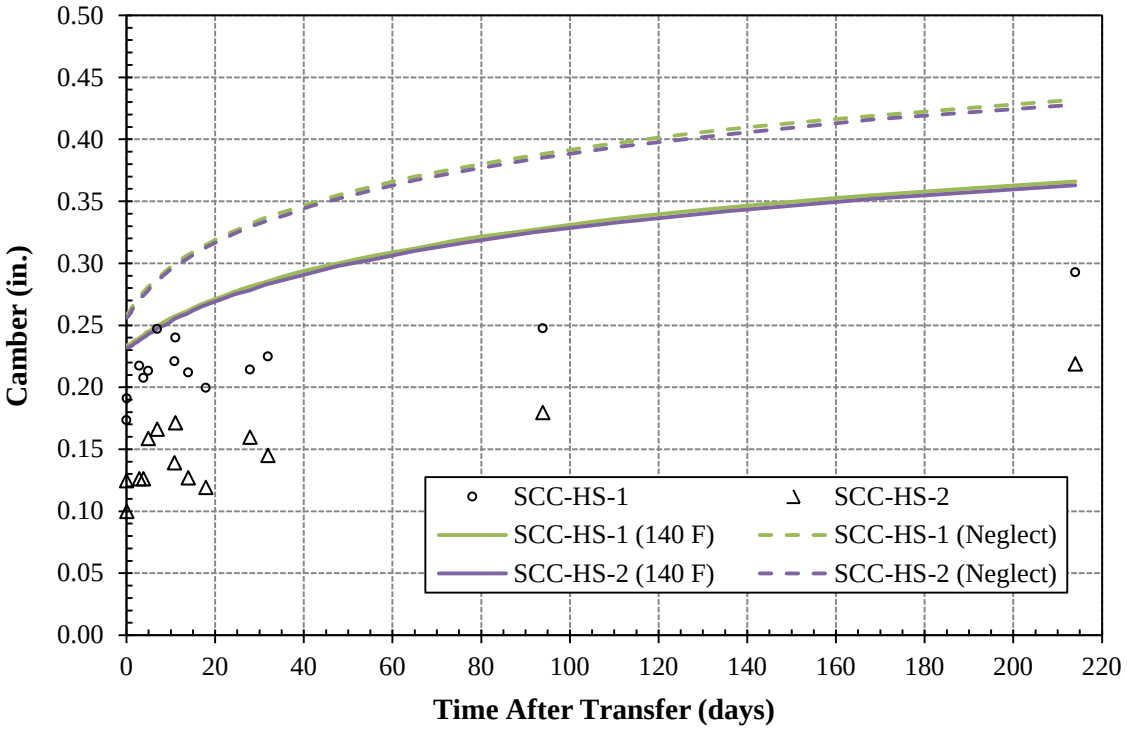

Figure 6-17: AASHTO Type I SCC-HS Predicted Camber – Maturity

CHAPTER SEVEN

SUMMARY, CONCLUSIONS, AND RECOMMENDATIONS

7.1 SUMMARY

A Visual Basic (VB) program was developed to predict time-dependent camber of prestressed flexural members. The computer program allows the user to select a model for the development of the concrete modulus of elasticity over time as well as creep and shrinkage calculations. The program includes two test-based and three code-prediction concrete modulus models. The test-based models include the "Constant E_c" and "Two-Point E_c" model. The code-prediction models include AASHTO '05(+), ACI 209, and CEB 90. The creep and shrinkage models include AASHTO '05(+), AASHTO '04(-), ACI 209, CEB 90, and Modified CEB 90. The Modified CEB 90 model is based on previous research by Kavanaugh (2008).

Experimental data from previous research by Boehm (2008), Levy (2007), and Stallings et al. (2003), was used to evaluate the program's strain and camber prediction capabilities. New strain and camber measurements were collected from six AASTHO Type I girders included in Boehm's experimental program. The camber measurements for sixteen prestressed T-beams were used from Levy's research. Lastly, strain and camber measurements for five AASTHO BT-54 girders were used from Stallings et al. research. The program input was based on the design parameters presented in the experimental programs. Various combinations of models for

the concrete modulus development and creep and shrinkage calculations were used to predict the strain and camber for each prestressed member.

7.2 CONCLUSIONS

To evaluate the program, experimental measurements were compared to the concrete strain, strand stress, and camber predictions. The following sections state general conclusions from the program evaluation and sensitivity analysis.

7.2.1 STRAIN PREDICTIONS

For the AASTHO Type I STD-M girders:

- Strains at the top VWSG locations were generally over-estimated. However, the CEB 90 and Modified CEB 90 creep and shrinkage models under-estimated long-term strains at the top VWSG approximately 25 percent when test-based E_c models were used.
- Using test-based E_c models, the ACI 209 creep and shrinkage model best predicted strains at the bottom VWSG.
- Using code-prediction E_c models, the AASHTO ’05(+) and ACI 209 creep and shrinkage models generally over-estimated the concrete strains at all locations.
- Test-based E_c models under-estimate strains at the bottom VWSG up to 28 days after transfer. Therefore, code-prediction E_c models better predict bottom strains indicative of prestress losses.

For the AASHTO Type I SCC-MS girders:

- Based on bottom VWSG measurements immediately after transfer, the "Constant E_c" model is the best test-based model for predicting initial prestress losses. The AASHTO '05(+)/ACI 209 E_c model is the best code-prediction model.
- The AASHTO '04(-) creep and shrinkage model is the best predictor of bottom strains when using either test-based or code-prediction E_c models.
- In general, the CEB 90 and Modified CEB 90 creep and shrinkage models consistently under-estimate the concrete strain at all VWSG locations.
- For the ACI 209 creep and shrinkage model, the strains at all locations were best predicted when using the adjusted slump and assuming accelerated curing.

For AASHTO Type I SCC-HS girders:

- Test-based E_c models are the best predictors of bottom strains. The "Constant E_c" model is the best test-based model.
- In general, the AASHTO '04(-) creep and shrinkage model best predicts bottom strains up to 28 days after transfer.
- In general, the CEB 90 creep and shrinkage model is the best predictor of long-term strains without over-estimating.
- Similar to the SCC-MS results, the CEB 90 and Modified CEB 90 creep and shrinkage models consistently under-predict the concrete strains at all VWSG locations.
- For the ACI 209 creep and shrinkage model, the strains at all locations were best predicted when using the adjusted slump and assuming accelerated curing.

Strain predictions for the AASHTO BT-54 girders were based on the test-based "Constant E_c" model only. The following are general conclusions based on the analysis results presented in Chapter 5.

- The AASHTO creep and shrinkage models best predict long-term strains at the top VWSG without over-estimating while the ACI 209 model over-estimates long-term strain at the top VWSG location approximately 15 to 20 percent.
- In general, the AASHTO '04(-) and the Modified CEB models better predict the early-age strains at the bottom VWSG.
- In general, the AASHTO '05(+) creep and shrinkage model best predicts the long-term strains at the bottom VWSG.

7.2.2 Strand Stress Predictions

The program calculates initial prestress losses to predict the strand stresses immediately before and after transfer. The predicted strand stresses in LG 1 were compared to previous research findings for the AASHTO Type I girders. The following provides a summary of the results.

- For the STD-M girders, the program over-predicted the strand stresses immediately before transfer and immediately after transfer less than 1 percent.
- For the SCC-MS girders, the program over-predicted the strand stresses immediately before transfer and immediately after transfer less than 3 percent.
- For the SCC-HS girders, the program under-predicted the strand stresses immediately before transfer and immediately after transfer less than 1 percent.

7.2.3 CAMBER PREDICTIONS

For the AASHTO Type I STD-M girders:

- Considering camber is highly sensitive to E_{ci} and much less sensitive to *later* E_c values, the "Constant E_c" and "Two-Point E_c" models yielded very similar camber results with a maximum range of ±0.005 inches for corresponding camber values.
- When using a test-based E_c model, all creep and shrinkage models under-predict the camber for all ages. The CEB 90 model under-predicts camber up to 41 percent which is the most of all the models.
- When using a test-based E_c model, the ACI 209 creep and shrinkage model better predicts early-age camber (up to 10 days after transfer) while the AASHTO '05(+) creep and shrinkage model better predicts long-term camber.
- Compared to other code-predicted E_c models, the CEB 90 E_c model is the best predictor of initial camber and therefore provides the best relationship between concrete strength and the initial stiffness. This may be partially attributable to the fact that the CEB 90 E_c model is based on the mean compressive strength (f_{cm}) while the AASHTO and ACI provisions are based on a lower specified compressive strength (f'_c).
- The CEB 90 creep and shrinkage model under-predicts camber at all ages regardless of the E_c model.
- The best model combination for predicting STD-M camber includes the CEB 90 E_c model and ACI 209 creep and shrinkage model.

For the AASHTO Type I SCC girders:

- The "Constant E_c" model over-estimated the SCC-MS-1 initial camber 3 percent and the SCC-MS-2 initial camber 28 percent. The "Constant E_c" model over-estimated the SCC-HS-1 initial camber 18 percent and the SCC-MS-2 initial camber 64 percent.
- Using test-based E_c models, the AASHTO '04(-) and ACI 209* creep and shrinkage models are the best predictors for SCC-MS-1 long-term camber. The CEB 90 and Modified CEB 90 models are the best predictors of long-term camber for the other three SCC girders.
- The camber growth rates using the AASHTO '04(-) creep and shrinkage model correlate the best with the measured camber growth rates when using a test-based E_c model.
- The CEB 90 E_c model is the best predictor of initial camber for the SCC-MS girders. Again, using a mean concrete compressive strength provides better stiffness predictions compared to using f'_c.
- The code-prediction E_c models over-predict initial camber of the SCC-HS girders 28 to 89 percent.
- The best predictions of SCC-HS long-term camber use the CEB 90 and Modified CEB 90 creep and shrinkage models. The AASHTO and ACI creep and shrinkage models drastically over-predict the long-term camber.

For the STD-M T-beams:

- Using test-based E_c models, the ACI 209* best predicts initial camber for the STD-M-A and STD-M-B beams and the AASHTO ‘04(-) best predicts camber for the STD-M-C beam.
- Using the AASHTO ‘05(+) or ACI 209 E_c model, the AASHTO ‘04(-) model best predicts the camber for STD-M-A and STD-M-B at all ages.
- All models under-estimate the camber for the STD-M-D beam. The best camber prediction resulted when using the AASHTO ’05(+) or ACI 209 E_c model with the ACI 209* creep and shrinkage model.

For the SCC-MA and SCC-MS beams:

- In general, all creep and shrinkage models under-estimate the initial camber. The best initial camber predictions for all SCC-MS beams use the AASHTO ‘05(+) or ACI 209 E_c model.
- The CEB 90 and Modified CEB 90 creep and shrinkage models predict the least amount of camber.
- The AASHTO ‘05(+) creep and shrinkage model over-estimates long-term camber for all E_c models.
- The camber growth rate for the SCC-MS beams correlates best with the AASHTO ‘04(-) and ACI 209* creep and shrinkage models.

For the SCC-HS T-beams:

- When using test-based E_c models, all creep and shrinkage models under-estimate the initial camber except for SCC-HS-C.
- The SCC-HS camber growth rate correlates best with the CEB 90 and Modified CEB 90 creep and shrinkage model.

For the AASHTO BT-54 girders:

- Assuming a constant E_c over time, the AASHTO '04(-) creep and shrinkage model best predicts long-term camber without over-estimating.
- The CEB 90 creep and shrinkage model best predicts bottom strains and camber when using cement Type RS.

7.2.3 General Conclusions

Taking a closer look at the bottom VWSG strain and camber predictions, the following general conclusions were made for predicting time-dependent deformations in prestressed bridge girders.

- In general, code-prediction E_c models are better predictors of bottom strains in girders constructed with non-SCC and SCC (normal to moderate-strength).
- For high-strength SCC girders, test-based E_c models better predict bottom strains.
- For non-SCC girders, test-based E_c models under-predict bottom strains up to 28 days. As a result, all creep and shrinkage models under-estimate camber for non-SCC girders even though the measured rate of camber growth correlates well with the ACI 209, CEB 90, and Modified CEB creep and shrinkage models.

- The AASHTO ‘04(-) creep and shrinkage model is the best predictor of bottom strains when using code-prediction E_c models.
- The “Constant E_c” model is the best test-based model for predicting prestress losses. The AASHTO ‘05(+)/ACI 209 E_c model is the best code-prediction model for predicting prestress losses.
- Using the AASHTO ‘05(+)/ACI 209 E_c model, the AASHTO ‘04(-) and ACI 209* creep and shrinkage models better predict the camber growth rate for normal-strength non-SCC and moderate-strength SCC girders.
- Using the actual slump in the ACI 209 creep and shrinkage model can result in significant errors in time-dependent deformations and prestress losses. An adjusted slump (water slump) should be used in the ACI 209 model.
- Using the “Constant E_c” model, the CEB 90 and Modified CEB creep and shrinkage models better predict the camber growth rate for high-strength SCC girders.
- In general, the CEB 90 and Modified CEB creep and shrinkage models are the best predictors of long-term camber in SCC girders.

7.3 RECOMMENDATIONS FOR FUTURE WORK

Further development and analysis of the Visual Basic program is recommended to improve the time-dependent deformation predictions for prestressed bridge girders. Improvements to the program can be made to simplify the user-interface and presentation of results. Items to be addressed in further research include the following:

- A variety of case studies testing the program’s full capabilities should be implemented to continue debugging the program.

- A more in-depth sensitivity analysis can be performed to include design considerations such as concrete compressive strength and transfer length.
- To account for long transfer lengths, the prestress force can be introduced in multiple debonded layer groups.
- Further development of the code-provision models should be investigated. In particular, recommendations for the appropriate implementation of mean concrete compressive strength estimates in the AASHTO/ACI E_c models should be developed.
- Cross-sectional information on additional standard AASHTO girders can be added to the program to reduce the amount of user input required.
- A user guide, including sample problems and screen shots, should be developed to help the user execute the program.
- The possibility of linking to other database programs in order to graphically present program results needs to be investigated.

REFERENCES

AASHTO. 2004. *AASHTO LRFD Bridge Design Specifications*. 3rd ed. Washington D.C.: American Association of State Highway and Transportation Officials (AASHTO).

AASHTO. 2005. *AASHTO LRFD Bridge Design Specifications*. 2005 Interim Revisions, Washington D.C.: American Association of State Highway and Transportation Officials (AASHTO).

AASHTO. 2006. *AASHTO LRFD Bridge Design Specifications*. 2006 Interim Revisions, Washington D.C.: American Association of State Highway and Transportation Officials (AASHTO).

AASHTO. 2007. *AASHTO LRFD Bridge Design Specifications*. 4rd ed. Washington D.C.: American Association of State Highway and Transportation Officials (AASHTO).

ACI 209. 1992. "Prediction of Creep, Shrinkage, and Temperature Effects in Concrete Structures." Farmington Hills, Michigan: American Concrete Institute, 209R-92 (Reapproved 1997).

ACI 363. 1992. "Report on High-Strength Concrete." Farmington Hills, Michigan: American Concrete Institute, 363R-92 (Reapproved 1997).

ACI 435. 1995. "Control of Deflection in Concrete Structures (ACI 435R)". In *ACI Manual of Concrete Practice 2001: Part 1*. Farmington Hills, Michigan: American Concrete Institute, 435R-21 – R435-25.

Ahlborn, T.M. and Gilbertson, C.G. 2004. A Probabilistic Comparison of Prestress Loss Methods in Prestressed Concrete Beams. *PCI Journal 49*, no. 5: 52 – 61.

Al-Omaishi, N., M.K Tadros, and S.J. Seguirant. 2009. Elastic modulus, shrinkage, and creep of high strength concrete as adopted by AASHTO. *PCI Journal*, Summer 2009: 44-63.

Boehm, Kurtis. 2008. Structural Performance of Self-Consolidating Concrete in AASHTO Type I Prestressed Girders. M.S. Thesis, Auburn University.

Branson, D.E. and Christiason, M.I. 1971. Time-Dependent Concrete Properties Related to Design – Strength and Elastic Properties, Creep and Shrinkage. Symposium on Creep, Shrinkage, and Temperature Effects: SP-27-13. American Concrete Institute, Detroit: 257 – 277.

Collins, M. P. and Mitchell, D. 1997. Prestressed Concrete Structures. Response Publications, Montreal, Canada.

Geokon Instruction Manual. Model 4200/4202/4210 Vibrating Wire Strain Gages. Rev J 04/07.

Hinkle, Stephen D. 2006. Investigation of Time-Dependent Deflection in Long Span, High Strength, Prestressed Concrete Bridge Beams. M.S. Thesis, Virginia Polytechnic Institute and State University.

Huo, X.S., N. Al-Omaishi, and M.K. Tadros. 2001. Creep, Shrinkage, Modulus of Elasticity of High-Performance Concrete. *ACI Materials Journal 98*, no. 6: 440 – 449.

Iravani, S. 1996. Mechanical Properties of High-Performance Concrete. *ACI Materials Journal 43*, no. 5.

Kahn, L.F. and Lopez, M. 2005. Prestress Losses in High Performance Lightweight Concrete Pretensioned Bridge Girders. *PCI Journal* September-October 2005: 84 – 93.

Kavanaugh, Bryan. 2008. Creep Behavior of Self-Consolidating Concrete. M.S. Thesis, Auburn University.

Martin, Leslie D. 1977. A Rational Method for Estimating Camber and Deflection of Precast Prestressed Members. *PCI Journal 22*, no. 1: 100-108.

Levy, Kelly. 2007. Bond Behavior of Prestressed Reinforcement in Beams Constructed with Self-Consolidating Concrete. M.S. Thesis, Auburn University.

Magura, D.D, Sozen, M. A., and C.P. Siess. 1964. A Study of Stress Relaxation in Prestressing Reinforcement. *PCI Journal 41*, no. 5: 78-89.

Neville, Adam M. 1997. "Aggregate Bond and Modulus of Elasticity of Concrete". *PCI Journal 95*, no. 1: 71 – 74.

Nilson, Arthur H. *Design of Prestressed Concrete (2nd ed.).* John Wiley and Sons Inc. New York, New York. 1987.

Sethi, Vivek. 2006. Unbonded Monostrands for Camber Adjustment. M.S. Thesis, Who Knows.

Shams, M. and Kahn, L.F. 2000. "Time-Dependent Behavior of High-Performance Concrete". Georgia Tech Structural Engineering, Mechanics and Materials Research Report No. 00-5, Georgia Department of Transportation Research Project No. 9510, April 2000: 395 pp.

Stallings, J.M., R.W. Barnes, and S. Eskildsen. 2003. Camber and Prestress Losses in Alabama HPC Bridge Girders. *PCI Journal 48*, no. 5: 90-104.

Tadros, M.K., A. Ghali, and A.W. Meyer. 1985. Prestressed Loss and Deflection of Precast Concrete Members. *PCI Journal 30*, no. 1: 114-141.

Tadros, M.K., N. Al-Omaishi, S.J. Seguirant, and J.T. Gallt. 2003. Prestress Losses in Pretensioned High-Strength Concrete Bridge Girders. NCHRP Report 496, National Cooperative Highway Research Program (NCHRP).

Youakim, Samer A., Amin Ghali, Susan E. Hida, and Vistasp M. Karbhari. 2007. Prediction of Long-Term Prestress Losses. *PCI Journal 52*, no. 2:116 – 130.

APPENDIX A

NOTATION

Symbol	Definition/Description
A_c	area of concrete
A_g	area of gross cross section
$A_{p,k}$	area of each strand in a prestressing steel layer
$A_{ps,k}$	total area of prestressing steel in each layer
$A_{r,k}$	area of each bar in reinforcing steel layer
$A_{rs,k}$	total area of reinforcing steel in each layer
A_{tr}	area of transformed cross section
$(Ay)_{p,k}$	$(A_{ps,i})*(y_{cen,pi})$ for each prestressing steel layer
$(Ay)_{s,k}$	$(A_{rs,i})*(y_{cen,si})$ for each reinforcing steel layer
$(Ay^2)_{p,k}$	$(A_{ps,i})*(y_{cen,pi})^2$ for each prestressing steel layer
$(Ay^2)_{s,k}$	$(A_{rs,i})*(y_{cen,si})^2$ for each reinforcing steel layer
CS	a specific cross section along the length of a girder
E_c	modulus of elasticity of concrete
E_{ci}	modulus of elasticity of concrete at time of initial prestress
E_p	modulus of elasticity of prestressing steel
E_s	modulus of elasticity of reinforcing steel
$e_{p,k}$	distance from c.g.c. to c.g.p. of each prestressing layer
$e_{s,k}$	distance from c.g.c. to c.g.s. of each reinforcing layer
$F_{pt,k}$	force in each prestressing steel layer immediately after transfer
f'_c	specified 28-day compressive strength of concrete
$f_{cgp,k}$	concrete stress at the center of gravity of each prestressing steel layer
f'_{ci}	compressive strength of concrete at time of initial prestress

$f_{p,kji}$	total prestress in each prestressing steel layer for each cross section (j) at the end of each time interval (i)
$f_{pbt,k}$	stress in each prestressing steel layer immediately before transfer
$f_{pj,k}$	jacking stress in each prestressing steel layer
$f_{pt,k}$	stress in each prestressing steel layer immediately after transfer
f_{pu}	prestressing steel ultimate strength
f_{py}	prestressing steel yield strength
$f_{p,R,k}$	initial prestress loss in each layer due to relaxation before transfer
$f_{p,ES,k}$	initial prestress loss in each layer due to elastic shortening loss
h	depth of girder cross section
I_g	gross moment of inertia
I_{tr}	transformed moment of inertia
i	time interval
j	cross section
k	layer of prestressing/reinforcing steel
K'_L	factor accounting for type of steel (45 for low relaxation, 10 for other)
L	length of girder
M_g	moment due to self-weight only
n_p	modular ratio w.r.t. prestressing steel
$n_{p,k}$	number of prestressing stands in each prestressing steel layer
n_s	modular ratio w.r.t. reinforcing steel
$n_{s,k}$	number of steel bars in each reinforcing steel layer
p	prestressing steel/prestressing steel layer
r	reinforcing steel
s	reinforcing steel layer
t_i	time of prestress transfer relative to original jacking (days)
TI	a specific time interval within a given time period
w_g	self-weight of girder (plf)
y_c	distance from centroid of the net concrete section to the extreme bottom fiber
$y_{cen,pk}$	distance from centroid of transformed area to each prestressing steel layer

$y_{cen,sk}$	distance from centroid of transformed area to each reinforcing steel layer
$y_{p,k}$	distance from prestressing steel layer to the extreme bottom fiber
$y_{s,k}$	distance from the reinforcing steel layer to the extreme bottom fiber
y_{tr}	distance from centroid of transformed section to the extreme bottom fiber
$\Delta_{c,initial}$	initial camber due to prestress (positive = upward deflection)
$\Delta_{d,initial}$	initial deflection due to self-weight (positive = downward deflection)
$\Delta f_{p,k}$	incremental change in prestress in each layer
$(\Delta\varepsilon_{c,cr(u)})_{cen}$	incremental unrestrained creep strain in concrete at centroid of transformed section
$(\Delta\varepsilon_{c,sh(u)})_{cen}$	incremental unrestrained shrinkage strain in concrete at centroid of transformed section
$\Delta\varepsilon_{cen}$	incremental strain at the centroid of the transformed section
$\Delta\phi_{cr(u)}$	incremental curvature due to unrestrained creep
$\Delta\phi$	incremental curvature
$\varepsilon_{cen,ji}$	total strain for each cross section (j) in each time interval (i)
ϕ_{ji}	total curvature for each cross section (j) in each time interval (i)

APPENDIX B

AASHTO TYPE I RESEARCH

Table B-1: AASHTO Type 1 Mix Designs (Boehm 2008)

Mixture Constituents	Units (per yd^3)	Mixtures		
		STD-M	SCC-MS	SCC-HS
Water	gal	32.4	34.2	31.2
Cement (Type III)	lb	640	553	650
GGBF Slag (Grade 100)	lb	0	237	279
# 78 Crushed Limestone	lb	2034	1608	1601
Red Bluff Sand	lb	1110	1317	1267
Air-Entraining Admixture	fl oz	0.6	0.6	0.6
HRWR Admixture	fl oz	19.2	51.0	93.0
Viscosity-Modifying Admixture	fl oz	0	16.0	0
Retarding Admixture (Delvo)	fl oz	19.2	24.0	28.0

Table B-2: Summary of Hardened Concrete Property Test Results (Boehm 2008)

HARDENED PROPERTIES		MIXTURES											
		STD-M-1		STD-M-2		SCC-MS-1		SCC-MS-2		SCC-HS-1		SCC-HS-2	
Compressive Strength		f'_c (psi)	E_c (ksi)	f'_c (psi)	E_c (ksi)	f'_c (psi)	E_c (ksi)	f'_c (psi)	E_c (ksi)	f'_c (psi)	E_c (ksi)	f'_c (psi)	E_c (ksi)
Air Cured	Transfer	4990	6050	4860	5550	5110	5200	4500	4950	10190	6750	10720	7150
	7	5790	5900	5740	6050	7110	6100	7210	5850	11710	7350	—	—
	28	6330	6350	6120	5800	8390	6450	8530	6350	12200	7500	12030	7550
	91	6610	6050	6370	6050	8840	5900	9110	6200	12340	7900	—	—
	Post-Test	6720	6150	6540	5800	8850	5850	9160	5900	13080	7100	12810	7200
Match Cured	Transfer	4780	5700	—	—	5540	5250	—	—	10430	7000	—	—
ASTM 6x12	28	6600	6750	7200	7300	9780	7400	9790	7500	13160	8600	13580	8300
CIP Deck (Post-Test)	West End	5720	4950	5370	5350	5480	5350	5080	5300	3720	4100	4820	4550
	East End	5630	5000	5410	5150	5270	5400	5210	5150	3800	3900	4680	4450
Modulus of Rupture		f_r (psi)		f_r (psi)		f_r (psi)		f_r (psi)		f_r (psi)		f_r (psi)	
Air-Cured	Post-Test	900		—	—	840		—	—	940		—	—
ASTM	Post-Test	1110		—	—	1420		—	—	1980		—	—

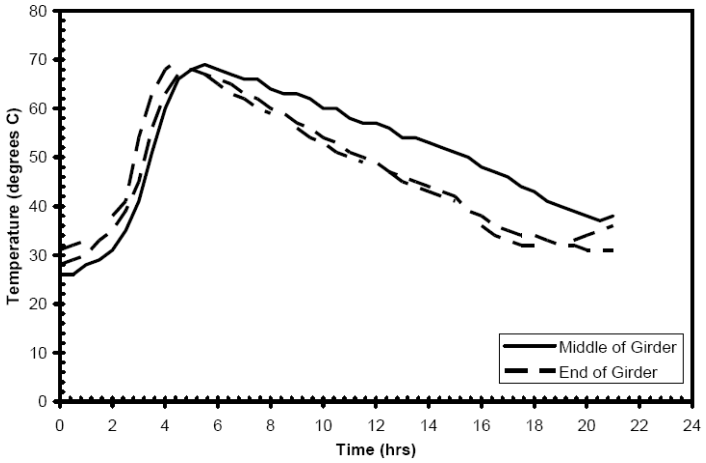

Figure B-1: Temperature Development Curves for STD-M-1 (Boehm 2008)

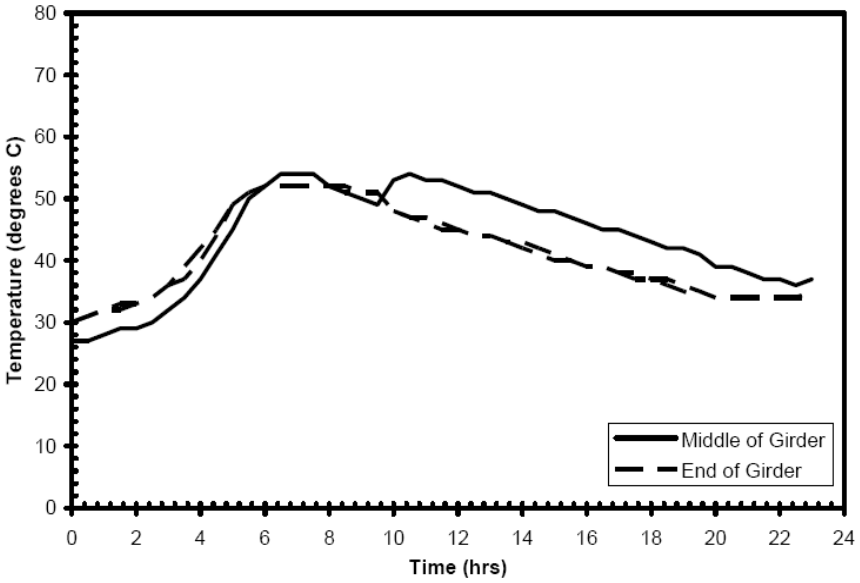

Figure B-2: Temperature Development Curves for SCC-MS-1 (Boehm 2008)

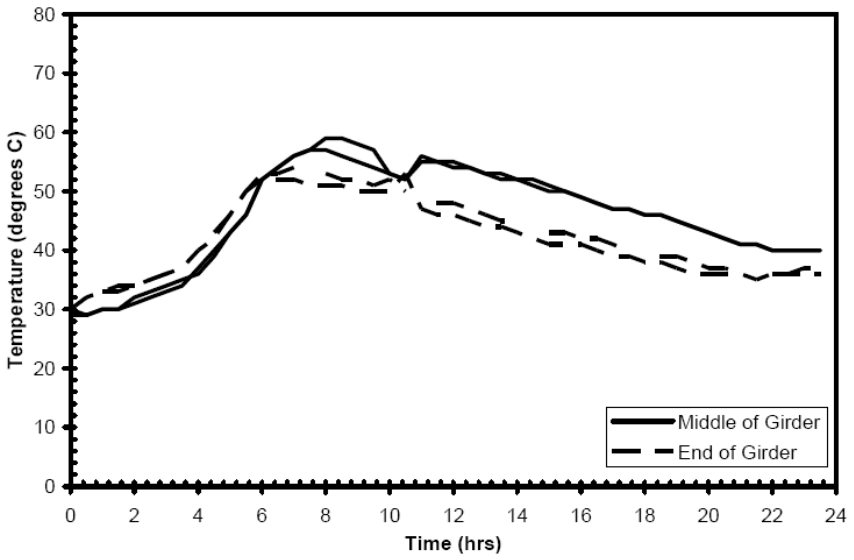

Figure B-3: Temperature Development Curves for SCC-MS-2 (Boehm 2008)

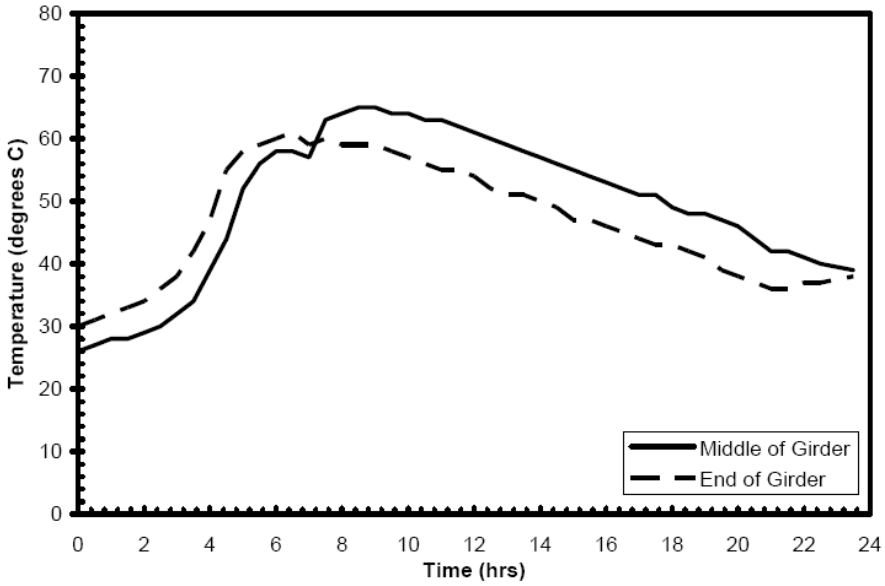

Figure B-4: Temperature Development Curves for SCC-HS-1 (Boehm 2008)

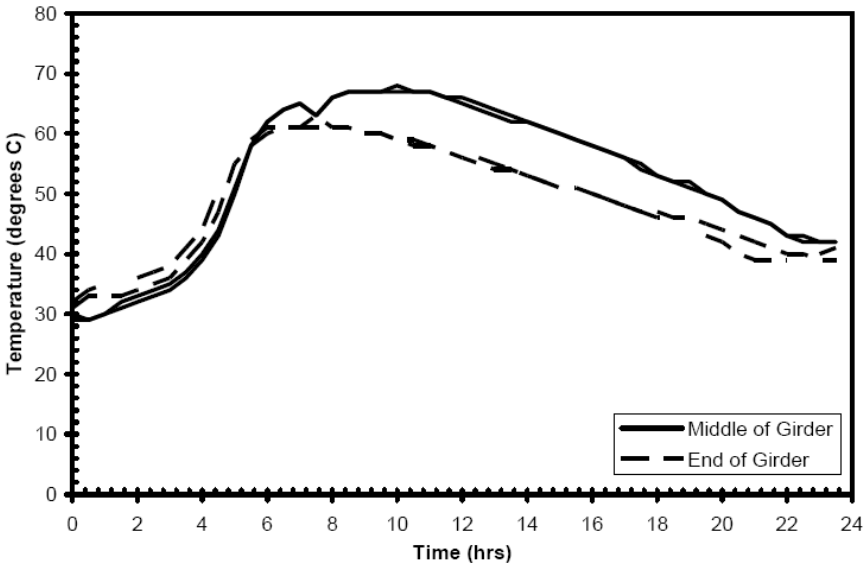

Figure B-5: Temperature Development Curves for SCC-HS-2 (Boehm 2008)

Table B-3: Effective Prestress at Measured Transfer Length Ages (Boehm 2008)

Specimen ID	f_{pbt} ksi	f_{pt} ksi	$f_{pe,3}$ ksi	$f_{pe,7}$ ksi	$f_{pe,14}$ ksi	$f_{pe,28}$ ksi	$f_{pe,2\ mon}$ ksi	$f_{pe,3\ mon}$ ksi
STD-M-1W	200	193	186	185	184	182	178	177
STD-M-1E	200	191	184	183	182	180	176	174
STD-M-2E	200	192	185	184	183	181	176	175
STD-M-2W	200	192	185	184	184	182	177	177
SCC-MS-1W	196	187	178	177	176	177	176	175
SCC-MS-1E	196	187	178	176	176	177	175	175
SCC-MS-2E	196	187	178	177	176	177	175	175
SCC-MS-2W	196	188	179	177	176	177	175	175
SCC-HS-1W	202	195	187	185	185	186	185	184
SCC-HS-1E	202	195	187	184	185	185	185	184
SCC-HS-2E	202	195	187	184	185	186	185	184
SCC-HS-2W	202	195	187	184	185	185	185	184

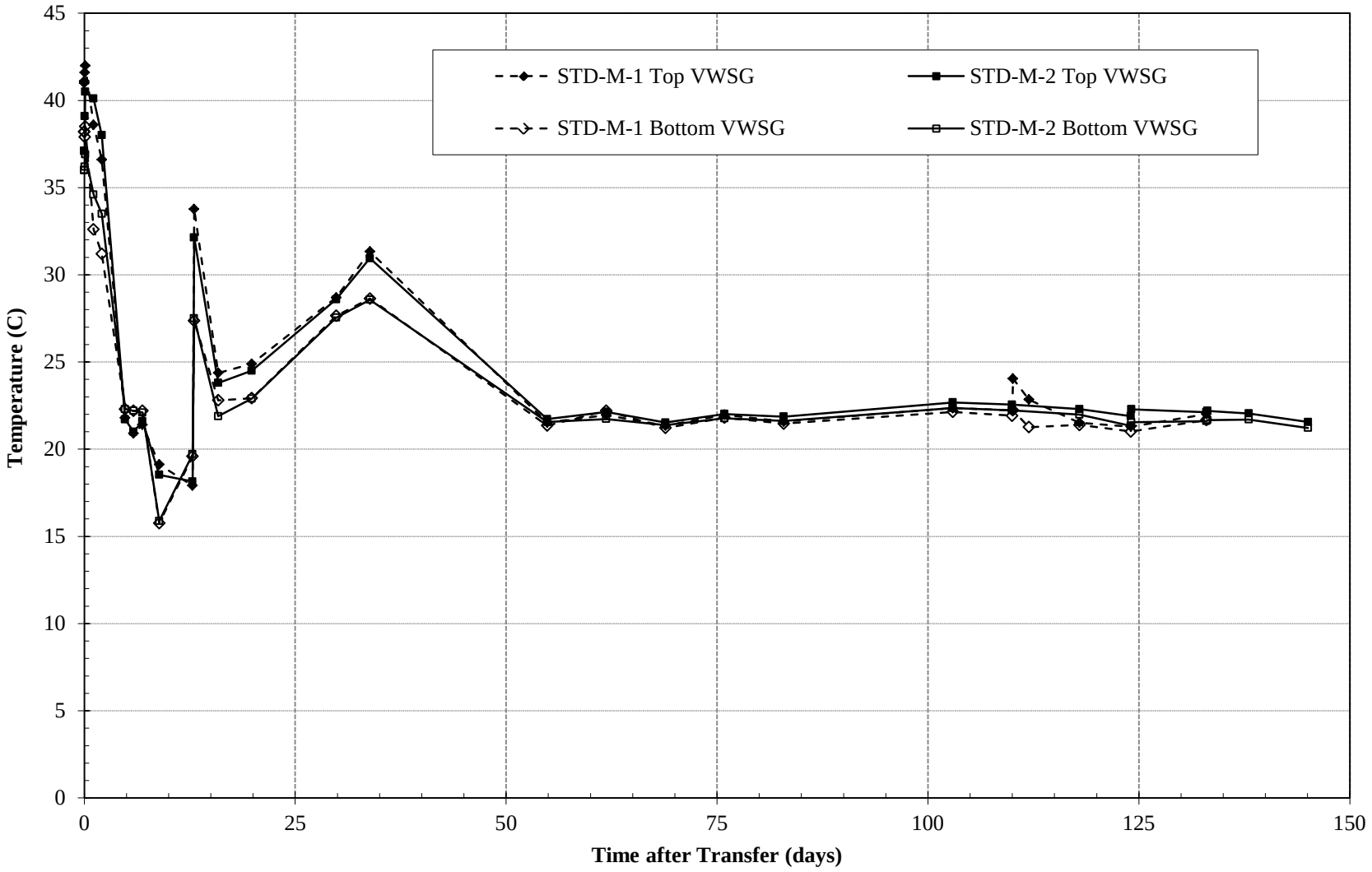

Figure B-6: VWSG Temperature Readings for STD-M Girders

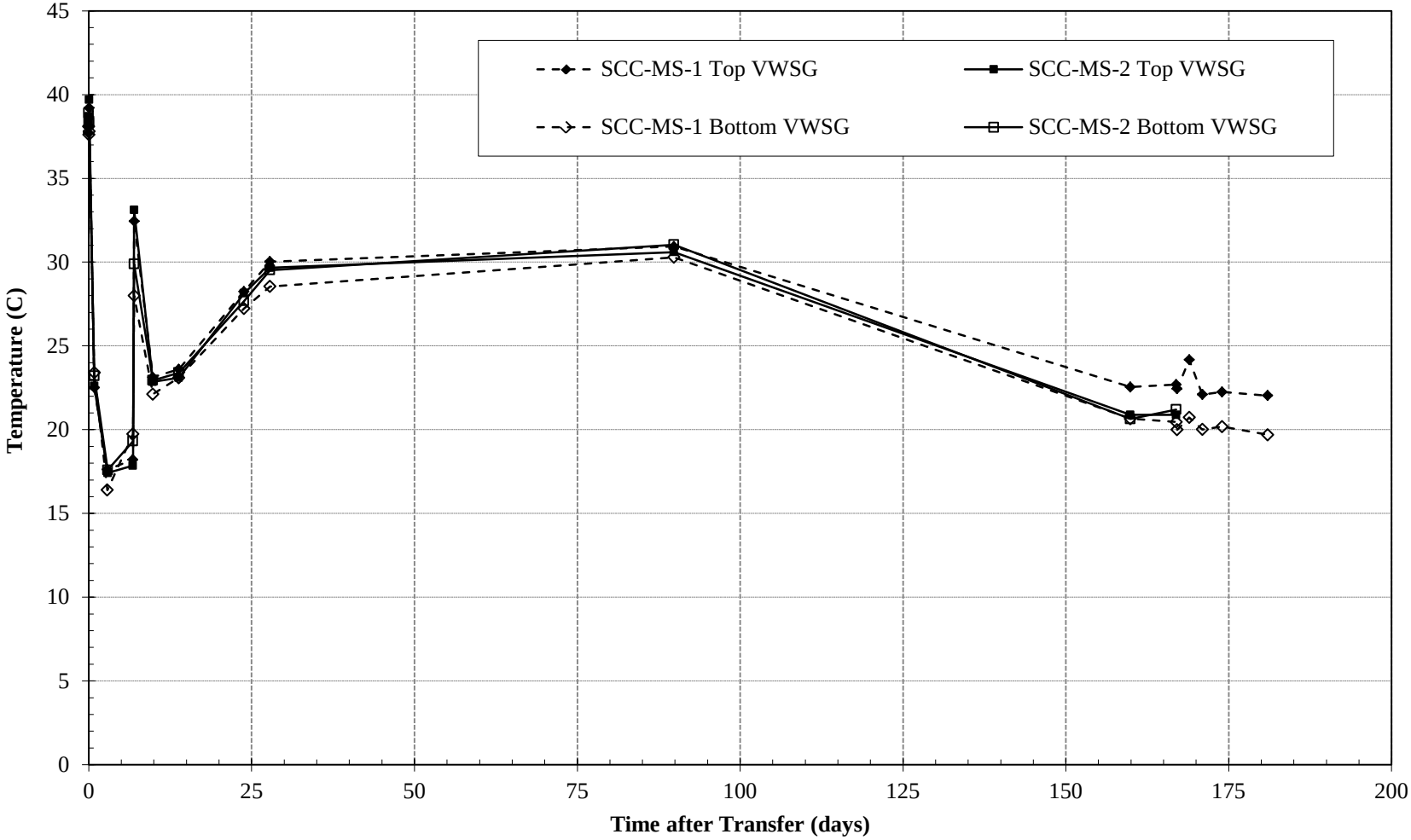

Figure B-7: VWSG Temperature Readings for SCC-MS Girders

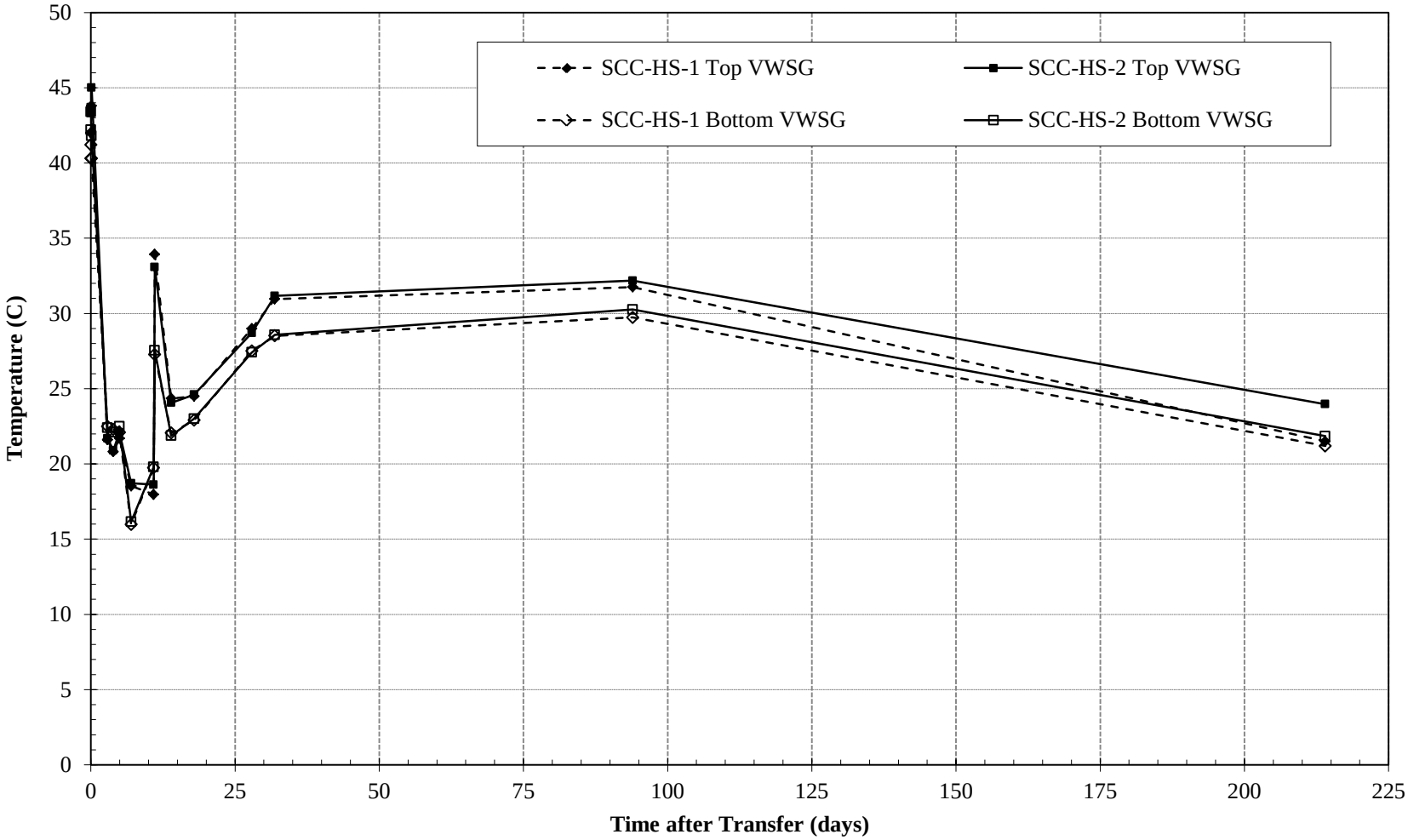

Figure B-8: VWSG Temperature Readings for SCC-HS Girders

APPENDIX C

T-BEAM RESEARCH

Table C-1: Concrete Mixture Proportions (Levy 2007)

Mixture Constituents	Mixtures			
	STD-M	SCC-MA	SCC-MS	SCC-HS
Water (pcy)	270	270	270	260
Cement (pcy)	640	525	375	650
Fly Ash (pcy)	0	225	0	0
GGBF Slag (pcy)	0	0	375	279
Coarse Agg. (pcy)	1964	1607	1613	1544
Fine Agg. (pcy)	1114	1316	1323	1265
AEA (oz/cwt)	0.33	0.00	0.00	0.00
WRA (oz/cwt)	4.0	4.0	6.0	6.0
HRWRA (oz/cwt)	3.5	4.0	4.5	5.0
VMA (oz/cwt)	0.0	2.0	2.0	2.0
w/cm	0.40	0.36	0.36	0.28
s/agg	0.46	0.46	0.46	0.46

Table C-2: Summary of Fresh Property Test Results (Levy 2007)

FRESH PROPERTIES	MIXTURES			
	STD-M	SCC-MA	SCC-MS	SCC-HS
Slump Flow (in.)	9.5	29	28.5	26
Unit Weight (lb/ft^3)	142.2	151.8	148.4	155.2
Air (%)	11.0	2.0	5.0	3.0
VSI	-	1.0	1.0	1.0
T-50 (sec.)	-	2.47	1.54	3.75
J-Ring Difference (in.)	-	1.5	2	2.5
L-Box (H_2/H_1)	-	0.84	0.92	0.63
Placement Temperature (°F)	82	62	89	95

Table C-3: Hardened Concrete Property Summary (Levy 2007)

PROPERTY	MIXTURES			
	STD-M	SCC-MA	SCC-MS	SCC-HS
f'_{ci} (psi)	5000	5500	5300	9990
E_{ci}(ksi)	4900	4900	4950	6050
$f'_{c,28(ASTM)}$ (psi)	5990	8840	9640	13150
$f'_{c,28(AC)}$ (psi)	6320	8540	9170	13380
$E_{c,28(AC)}$ (ksi)	5150	5400	6950	7050
$f_{ct,28(AC)}$ (psi)	560	760	840	830

Table C-4: Time of Events Summary (Levy 2007)

Specimen	Casting Date	Prestress Transfer Date	Flexural Test Date	Concrete Age at Test (days)
STD-M-A	11/14/2005	11/17/2005	5/19/2006	186
STD-M-B	11/14/2005	11/17/2005	6/5/2006	203
STD-M-C	11/14/2005	11/17/2005	6/8/2006	206
STD-M-D	11/14/2005	11/17/2005	6/21/2006	219
SCC-MA-A	12/13/2005	12/14/2005	7/27/2006	226
SCC-MA-B	12/13/2005	12/14/2005	7/20/2006	219
SCC-MA-C	12/13/2005	12/14/2005	7/18/2006	217
SCC-MA-D	12/13/2005	12/14/2005	7/6/2006	205
SCC-MS-A	6/26/2006	6/29/2006	8/31/2006	66
SCC-MS-B	6/26/2006	6/29/2006	9/7/2006	73
SCC-MS-C	6/26/2006	6/29/2006	9/12/2006	78
SCC-MS-D	6/26/2006	6/29/2006	9/21/2006	87
SCC-HS-A	8/21/2006	8/22/2006	10/5/2006	45
SCC-HS-B	8/21/2006	8/22/2006	10/3/2006	43
SCC-HS-C	8/21/2006	8/22/2006	9/28/2006	38
SCC-HS-D	8/21/2006	8/22/2006	9/26/2006	36

APPENDIX D

AASHTO BT-54 RESEARCH

Table D-1: HPC Mix Proportions (Stallings et al. 2003)

Material	Quantity
Type III Cement	752 lbs/yd^3
Type C Fly Ash	152 lbs/yd^3
#67 Limestone	1822 lbs/yd^3
#89 Sand	374 lbs/yd^3
#100 Sand	695 lbs/yd^3
Water	265 lbs/yd^3
Superplasticizers	14 oz per 100lb of cementitious material
Retarder	1.4 oz per 100lb of cementitious material
Air Entrainment	0.44 oz per 100lb of cementitious material
Air Content	4.2% (Average)
Slump	8 in. (Average)

APPENDIX E: STRAIN MEASUREMENTS

Table E-1: STD-M-1 Strain Measurements

					Using Post-Casting as Reference			*Using Pre-Release as Reference*		
	Time After Transfer (days)	VWSG Reading			Top VWSG (με)	Middle VWSG (με)	Bottom VWSG (με)	Top VWSG (με)	Middle VWSG (με)	Bottom VWSG (με)
		Top (με)	Middle (με)	Bottom (με)						
Post-Casting	-0.86	2750	2808	2953	-	-	-	-	-	-
Pre-Transfer	0	2680.1	2780.6	2936.5	-69.9	-27.4	-16.5	-	-	-
	0.00	2649.1	2617.5	2685.9	-100.9	-190.5	-267.1	-31.0	-163.1	-250.6
	0.07	2644.1	2603.6	2667.8	-105.9	-204.4	-285.2	-36.0	-177.0	-268.7
	0.12	2644.1	2596.8	2655.7	-105.9	-211.2	-297.3	-36.0	-183.8	-280.8
	1.10	2653.5	2606.7	2641.4	-96.5	-201.3	-311.6	-26.6	-173.9	-295.1
	2.07	2654.2	2582.6	2622.1	-95.8	-225.4	-330.9	-25.9	-198.0	-314.4
	4.84	2667.5	2548.4	2586.5	-82.5	-259.6	-366.5	-12.6	-232.2	-350.0
	5.84	2657.4	2535.9	2573.7	-92.6	-272.1	-379.3	-22.7	-244.7	-362.8
	6.91	2655.9	2530.6	2568.5	-94.1	-277.4	-384.5	-24.2	-250.0	-368.0
	8.95	2677.7	2524.6	2581.3	-72.3	-283.4	-371.7	-2.4	-256.0	-355.2
	12.83	2641.1	2502.1	2526.1	-108.9	-305.9	-426.9	-39.0	-278.5	-410.4
	13.02	2623.6	2510.3	2536.0	-126.4	-297.7	-417.0	-56.5	-270.3	-400.5
	15.89	2639.6	2484.9	2517.9	-110.4	-323.1	-435.1	-40.5	-295.7	-418.6
	19.86	2616.0	2457.3	2489.7	-134.0	-350.7	-463.3	-64.1	-323.3	-446.8
	29.86	2594.0	2432.1	2439.4	-156.0	-375.9	-513.6	-86.1	-348.5	-497.1
	33.86	2586.8	2399.9	2423.4	-163.2	-408.1	-529.6	-93.3	-380.7	-513.1
	54.86	2562.1	2380.3	2368.8	-187.9	-427.7	-584.2	-118.0	-400.3	-567.7
	61.89	2548.8	2367.5	2358.0	-201.2	-440.5	-595.0	-131.3	-413.1	-578.5
	68.89	2541.1	2356.5	2350.0	-208.9	-451.5	-603.0	-139.0	-424.1	-586.5
	75.89	2532.0	2342.0	2339.3	-218.0	-466.0	-613.7	-148.1	-438.6	-597.2
	76.07	-	-	-	-	-	-	-	-	-
	82.92	2527.0	2331.0	2333.4	-223.0	-477.0	-619.6	-153.1	-449.6	-603.1
	102.97	2500.6	2301.7	2313.8	-249.4	-506.3	-639.2	-179.5	-478.9	-622.7
	109.98	2497.7	2295.7	2311.5	-252.3	-512.3	-641.5	-182.4	-484.9	-625.0

Table E-2: STD-M-2 Strain Measurements

	Time After Transfer (days)	VWSG Reading			*Using Post-Casting as Reference*			*Using Pre-Release as Reference*		
		Top (με)	Middle (με)	Bottom (με)	Top VWSG (με)	Middle VWSG (με)	Bottom VWSG (με)	Top VWSG (με)	Middle VWSG (με)	Bottom VWSG (με)
Post-Casting	-0.86	2776	2631	2862	-	-	-	-	-	-
Pre-Transfer	0	2762.6	2645.4	2864.2	-13.4	14.4	2.2	-	-	-
	0.00	2727.0	2487.5	2609.8	-49.0	-143.5	-252.2	-35.6	-157.9	-254.4
	0.07	2716.4	2474.7	2592.9	-59.6	-156.3	-269.1	-46.2	-170.7	-271.3
	0.12	2712.6	2465.5	2581.0	-63.4	-165.5	-281.0	-50.0	-179.9	-283.2
	1.10	2703.6	2458.5	2551.8	-72.4	-172.5	-310.2	-59.0	-186.9	-312.4
	2.07	2698.4	2433.2	2531.6	-77.6	-197.8	-330.4	-64.2	-212.2	-332.6
	4.84	2703.2	2396.2	2492.8	-72.8	-234.8	-369.2	-59.4	-249.2	-371.4
	5.84	2690.2	2382.9	2478.7	-85.8	-248.1	-383.3	-72.4	-262.5	-385.5
	6.91	2689.6	2380.1	2473.0	-86.4	-250.9	-389.0	-73.0	-265.3	-391.2
	8.95	2709.5	2374.4	2482.9	-66.5	-256.6	-379.1	-53.1	-271.0	-381.3
	12.83	2667.8	2347.8	2428.5	-108.2	-283.2	-433.5	-94.8	-297.6	-435.7
	13.02	2666.5	2362.4	2439.7	-109.5	-268.6	-422.3	-96.1	-283.0	-424.5
	15.89	2667.8	2334.7	2420.2	-108.2	-296.3	-441.8	-94.8	-310.7	-444.0
	19.86	2644.8	2305.6	2389.5	-131.2	-325.4	-472.5	-117.8	-339.8	-474.7
	29.86	2616.4	2278.8	2339.2	-159.6	-352.2	-522.8	-146.2	-366.6	-525.0
	33.86	2630.6	2248.7	2323.2	-145.4	-382.3	-538.8	-132.0	-396.7	-541.0
	54.86	2572.6	2224.9	2265.6	-203.4	-406.1	-596.4	-190.0	-420.5	-598.6
	61.89	2559.9	2213.1	2254.2	-216.1	-417.9	-607.8	-202.7	-432.3	-610.0
	68.89	2552.0	2204.4	2245.7	-224.0	-426.6	-616.3	-210.6	-441.0	-618.5
	75.89	2542.4	2194.9	2234.7	-233.6	-436.1	-627.3	-220.2	-450.5	-629.5
	76.07	-	-	-	-	-	-	-	-	-
	82.92	2536.0	2188.5	2227.6	-240.0	-442.5	-634.4	-226.6	-456.9	-636.6
	102.97	2513.0	2166.5	2202.8	-263.0	-464.5	-659.2	-249.6	-478.9	-661.4
	109.98	2510.6	2163.4	2197.9	-265.4	-467.6	-664.1	-252.0	-482.0	-666.3

Table E-3: SCC-MS-1 Strain Measurements

	Time After Transfer (days)	VWSG Reading			*Using Post-Casting as Reference*			*Using Pre-Release as Reference*		
		Top (με)	Middle (με)	Bottom (με)	Top VWSG (με)	Middle VWSG (με)	Bottom VWSG (με)	Top VWSG (με)	Middle VWSG (με)	Bottom VWSG (με)
Post-Casting	-0.95	2921.3	2800.6	3010.9	-	-	-	-	-	-
Pre-Transfer	0	2808.8	2753.0	2931.7	-112.5	-47.6	-79.2	-	-	-
	0.01	2763.1	2611.8	2704.2	-158.2	-188.8	-306.7	-45.7	-141.2	-227.5
	0.06	2747.8	2595.4	2676.7	-173.5	-205.2	-334.2	-61.0	-157.6	-255.0
	0.86	2729.1	2541.4	2653.8	-192.2	-259.2	-357.1	-79.7	-211.6	-277.9
	2.90	2723.0	2499.4	2578.6	-198.3	-301.2	-432.3	-85.8	-253.6	-353.1
	6.79	2662.2	2448.3	2501.1	-259.1	-352.3	-509.8	-146.6	-304.7	-430.6
	6.98	2680.6	2489.3	2527.3	-240.7	-311.3	-483.6	-128.2	-263.7	-404.4
	9.84	2659.1	2433.1	2487.3	-262.2	-367.5	-523.6	-149.7	-319.9	-444.4
	13.82	2638.9	2411.1	2465.3	-282.4	-389.5	-545.6	-169.9	-341.9	-466.4
	23.82	2631.8	2406.2	2438.9	-289.5	-394.4	-572.0	-177.0	-346.8	-492.8
	27.82	2642.8	2391.9	2437.9	-278.5	-408.7	-573.0	-166.0	-361.1	-493.8
	89.84	2609.5	2353.8	2346.4	-311.8	-446.8	-664.5	-199.3	-399.2	-585.3
	159.92	2588.8	2337.3	2295.4	-332.5	-463.3	-715.5	-220.0	-415.7	-636.3

Table E-4: SCC-MS-2 Strain Measurements

	Time After Transfer (days)	VWSG Reading			*Using Post-Casting as Reference*			*Using Pre-Release as Reference*		
		Top (με)	Middle (με)	Bottom (με)	Top VWSG (με)	Middle VWSG (με)	Bottom VWSG (με)	Top VWSG (με)	Middle VWSG (με)	Bottom VWSG (με)
Post-Casting	-0.95	2823.6	2819.7	2868.3	-	-	-	-	-	-
Pre-Transfer	0	2764.9	2752.6	2768.1	-58.7	-67.1	-100.2	-	-	-
	0.01	2699.0	2611.8	2550.4	-124.6	-207.9	-317.9	-65.9	-140.8	-217.7
	0.06	2684.5	2594.4	2516.1	-139.1	-225.3	-352.2	-80.4	-158.2	-252.0
	0.86	2663.5	2547.5	2467.1	-160.1	-272.2	-401.2	-101.4	-205.1	-301.0
	2.90	2649.6	2509.4	2436.5	-174.0	-310.3	-431.8	-115.3	-243.2	-331.6
	6.79	2586.5	2449.0	2363.6	-237.1	-370.7	-504.7	-178.4	-303.6	-404.5
	6.98	2609.6	2496.1	2377.1	-214.0	-323.6	-491.2	-155.3	-256.5	-391.0
	9.84	2580.4	2439.0	2341.3	-243.2	-380.7	-527.0	-184.5	-313.6	-426.8
	13.82	2558.5	2417.9	2319.9	-265.1	-401.8	-548.4	-206.4	-334.7	-448.2
	23.84	2550.3	2409.7	2291.1	-273.3	-410.0	-577.2	-214.6	-342.9	-477.0
	27.82	2557.9	2403.3	2294.5	-265.7	-416.4	-573.8	-207.0	-349.3	-473.6
	89.84	2497.1	2339.8	2198.8	-326.5	-479.9	-669.5	-267.8	-412.8	-569.3
	159.92	2463.3	2313.9	-	-360.3	-505.8	-	-301.6	-438.7	-
	166.92	2450.0	2302.6	-	-373.6	-517.1	-	-314.9	-450.0	-

Table E-5: SCC-HS-1 Strain Measurements

	Time After Transfer (days)	VWSG Reading			*Using Post-Casting as Reference*			*Using Pre-Release as Reference*		
		Top (με)	Middle (με)	Bottom (με)	Top VWSG (με)	Middle VWSG (με)	Bottom VWSG (με)	Top VWSG (με)	Middle VWSG (με)	Bottom VWSG (με)
Post-Casting	-0.93	2982.5	2773.4	2949.5	-	-	-	-	-	-
Pre-Transfer	0	2795.2	2615.2	2776.1	-187.3	-158.2	-173.4	-	-	-
	0.01	2741.0	2506.4	2604.9	-241.5	-267.0	-344.6	-54.2	-108.8	-171.2
	0.12	2725.5	2505.2	2583.1	-257.0	-268.2	-366.4	-69.7	-110.0	-193.0
	2.89	2708.1	2438.1	2529.8	-274.4	-335.3	-419.7	-87.1	-177.1	-246.3
	3.89	2691.1	2423.2	2516.2	-291.4	-350.2	-433.3	-104.1	-192.0	-259.9
	4.95	2691.1	2421.0	2514.3	-291.4	-352.4	-435.2	-104.1	-194.2	-261.8
	6.93	2704.7	2406.8	2516.0	-277.8	-366.6	-433.5	-90.5	-208.4	-260.1
	10.88	2663.9	2395.3	2481.1	-318.6	-378.1	-468.4	-131.3	-219.9	-295.0
	11.07	2686.0	2438.6	2503.6	-296.5	-334.8	-445.9	-109.2	-176.6	-272.5
	13.93	2674.4	2392.3	2484.5	-308.1	-381.1	-465.0	-120.8	-222.9	-291.6
	17.91	2654.0	2373.1	2469.3	-328.5	-400.3	-480.2	-141.2	-242.1	-306.8
	27.91	2638.2	2372.4	2449.5	-344.3	-401.0	-500.0	-157.0	-242.8	-326.6
	31.91	2647.8	2357.5	2448.1	-334.7	-415.9	-501.4	-147.4	-257.7	-328.0
	93.93	2622.3	2329.2	2388.4	-360.2	-444.2	-561.1	-172.9	-286.0	-387.7
	214.02	2652.7	2368.8	2391.9	-329.8	-404.6	-557.6	-142.5	-246.4	-384.2

Table E-6: SCC-HS-2 Strain Measurements

	Time After Transfer (days)	VWSG Reading			*Using Post-Casting as Reference*			*Using Pre-Release as Reference*		
		Top (μЄ)	Middle (μЄ)	Bottom (μЄ)	Top VWSG (μЄ)	Middle VWSG (μЄ)	Bottom VWSG (μЄ)	Top VWSG (μЄ)	Middle VWSG (μЄ)	Bottom VWSG (μЄ)
Post-Casting	-0.93	2705.6	2953.0	2847.2	-	-	-	-	-	-
Pre-Transfer	0	2559.7	2807.0	2686.0	-145.9	-146.0	-161.2	-	-	-
	0.01	2503.9	2690.9	2515.6	-201.7	-262.1	-331.6	-55.8	-116.1	-170.4
	0.12	2482.0	2687.8	2502.7	-223.6	-265.2	-344.5	-77.7	-119.2	-183.3
	2.89	2466.6	2628.2	2453.3	-239.0	-324.8	-393.9	-93.1	-178.8	-232.7
	3.89	2449.2	2615.8	2437.8	-256.4	-337.2	-409.4	-110.5	-191.2	-248.2
	4.95	2447.8	2611.6	2431.9	-257.8	-341.4	-415.3	-111.9	-195.4	-254.1
	6.93	2457.2	2592.5	2432.0	-248.4	-360.5	-415.2	-102.5	-214.5	-254.0
	10.88	2422.7	2582.6	2399.4	-282.9	-370.4	-447.8	-137.0	-224.4	-286.6
	11.07	2450.1	2628.4	2424.7	-255.5	-324.6	-422.5	-109.6	-178.6	-261.3
	13.93	2430.6	2577.2	2404.3	-275.0	-375.8	-442.9	-129.1	-229.8	-281.7
	17.91	2412.8	2558.9	2388.2	-292.8	-394.1	-459.0	-146.9	-248.1	-297.8
	27.91	2397.2	2557.9	2369.5	-308.4	-395.1	-477.7	-162.5	-249.1	-316.5
	31.91	2407.8	2539.5	2369.5	-297.8	-413.5	-477.7	-151.9	-267.5	-316.5
	93.93	2377.1	2489.9	2319.8	-328.5	-463.1	-527.4	-182.6	-317.1	-366.2
	214.02	2403.0	2527.5	2316.7	-302.6	-425.5	-530.5	-156.7	-279.5	-369.3

Table E-7: STD-M Strain without Temperature Effects

Time after Transfer (days)	STD-M-1			STD-M-2		
	Top VWSG (μЄ)	Middle VWSG (μЄ)	Bottom VWSG (μЄ)	Top VWSG (μЄ)	Middle VWSG (μЄ)	Bottom VWSG (μЄ)
0.00	-29	-157	-240	-34	-152	-244
0.07	-33	-169	-258	-21	-164	-276
0.12	-33	-176	-270	-15	-172	-293
1.10	-15	-175	-284	3	-187	-333
2.07	-23	-191	-307	-19	-203	-351
4.84	-38	-224	-350	-92	-236	-358
5.84	-49	-237	-362	-112	-250	-366
6.91	-50	-240	-367	-104	-251	-378
8.89	-33	-231	-366	-54	-244	-410
12.83	-68	-271	-409	-140	-286	-412
13.02	-55	-258	-394	-55	-267	-449
15.89	-61	-279	-417	-96	-287	-455
19.86	-86	-300	-446	-123	-313	-482
29.86	-99	-334	-487	-150	-348	-515
33.86	-112	-348	-508	-124	-361	-551
54.86	-135	-389	-558	-207	-403	-582
61.89	-147	-404	-567	-215	-416	-594
68.89	-138	-549	-668	-227	-424	-600
75.89	-164	-425	-586	-234	-433	-611
82.92	-170	-436	-592	-241	-439	-618
102.97	-194	-464	-610	-261	-460	-642
109.98	-196	-470	-612	-264	-463	-647

Table E-8: SCC-MS Strains without Temperature Effects

Time after Transfer (days)	SCC-MS-1			SCC-MS-2		
	Top VWSG (με)	Middle VWSG (με)	Bottom VWSG (με)	Top VWSG (με)	Middle VWSG (με)	Bottom VWSG (με)
0.01	-42	-135	-219	-53	-135	-217
0.06	-52	-153	-244	-54	-156	-254
0.86	-89	-208	-277	-111	-202	-300
2.84	-104	-237	-360	-126	-231	-343
6.79	-158	-300	-426	-201	-293	-398
6.98	-116	-257	-394	-104	-257	-408
9.84	-156	-306	-440	-186	-302	-428
13.82	-177	-327	-461	-210	-321	-447
23.82	-175	-335	-481	-203	-333	-474
27.82	-170	-337	-486	-202	-329	-473
89.84	-203	-373	-573	-267	-388	-560
159.92	-211	-415	-619	-292	-432	-
166.92	-227	-425	-622	-311	-446	-

Table E-9: SCC-HS Strains without Temperature Effects

Time after Transfer (days)	SCC-HS-1			SCC-HS-2		
	Top VWSG (με)	Middle VWSG (με)	Bottom VWSG (με)	Top VWSG (με)	Middle VWSG (με)	Bottom VWSG (με)
0.01	-43	-114	-161	-43	-113	-171
0.12	-47	-123	-178	-34	-124	-196
2.89	-96	-187	-246	-118	-177	-233
3.89	-115	-201	-259	-141	-191	-242
4.95	-112	-202	-261	-131	-196	-254
7.00	-105	-202	-270	-94	-200	-294
10.88	-143	-230	-294	-166	-226	-279
11.07	-90	-185	-266	-46	-181	-305
13.93	-124	-224	-292	-117	-220	-308
17.91	-147	-239	-307	-142	-236	-319
27.91	-154	-245	-320	-154	-245	-324
31.91	-150	-246	-326	-132	-247	-344
93.93	-175	-272	-383	-168	-296	-384
214.02	-150	-249	-381	-135	-291	-376

Table E-10: STD-M Top VWSG – Percent Error in Strain

	STD-M-1						STD-M-2					
	Creep and Shrinkage Model						Creep and Shrinkage Model					
	AASHTO '05 (+)	AASHTO '04 (-)	ACI 209	ACI 209*	CEB 90	Modified CEB 90	AASHTO '05 (+)	AASHTO '04 (-)	ACI 209	ACI 209*	CEB 90	Modified CEB 90
Ec Model	Percent Error in Strain - Top VWSG After Transfer						Percent Error in Strain - Top VWSG After Transfer					
AASHTO '05 (+)	70.6	70.6	70.6	70.6	70.6	70.6	46.2	46.2	46.2	46.2	46.2	46.2
ACI 209	70.6	70.6	70.6	70.6	70.6	70.6	46.2	46.2	46.2	46.2	46.2	46.2
CEB 90-RS	47.7	47.7	47.7	47.7	47.7	47.7	22.7	22.7	22.7	22.7	22.7	22.7
Constant Ec	22.0	22.0	22.0	22.0	22.0	22.0	4.5	4.5	4.5	4.5	4.5	4.5
2-Point	22.0	22.0	22.0	22.0	22.0	22.0	4.5	4.5	4.5	4.5	4.5	4.5
Ec Model	Percent Error in Strain -Top VWSG at 6.91 Days						Percent Error in Strain -Top VWSG at 6.91 Days					
AASHTO '05 (+)	248.8	140.4	209.5	162.5	113.2	144.3	69.1	16.1	48.7	27.1	-0.3	14.0
ACI 209	248.8	140.4	209.5	162.5	113.2	144.3	69.1	16.1	48.7	27.1	-0.3	14.0
CEB 90-RS	232.3	109.9	173.1	131.5	98.6	126.5	59.6	-0.2	29.5	10.4	-8.8	3.8
Constant Ec	93.0	35.8	77.0	52.3	82.3	106.3	41.6	-7.6	20.9	2.6	-15.3	-3.9
2-Point	135.9	58.4	108.6	77.7	82.3	106.4	14.3	-23.6	0.3	-14.0	-15.3	-4.2
Ec Model	Percent Error in Strain -Top VWSG at 33.48 Days						Percent Error in Strain -Top VWSG at 33.48 Days					
AASHTO '05 (+)	163.9	73.9	126.6	86.2	37.6	51.5	138.5	56.3	102.8	68.0	18.9	30.9
ACI 209	163.9	73.9	126.6	86.2	37.6	51.5	138.5	56.3	102.8	68.0	18.9	30.9
CEB 90-RS	153.3	60.9	111.6	73.5	29.7	42.0	127.2	43.1	87.6	54.9	10.5	20.8
Constant Ec	117.8	35.5	82.5	49.5	20.9	31.3	114.3	35.8	78.3	46.9	3.8	12.9
2-Point	126.0	41.6	89.5	55.0	20.9	31.3	104.3	27.4	69.6	39.9	3.9	12.8
Ec Model	Percent Error in Strain -Top VWSG at 69.68 Days						Percent Error in Strain -Top VWSG at 69.68 Days					
AASHTO '05 (+)	138.1	61.0	105.0	66.8	23.2	32.8	63.7	10.1	39.6	14.5	-19.4	-13.1
ACI 209	138.1	61.0	105.0	66.8	23.2	32.8	63.7	10.1	39.6	14.5	-19.4	-13.1
CEB 90-RS	129.2	52.1	94.8	58.3	16.9	25.3	56.5	3.2	31.5	7.7	-24.4	-19.1
Constant Ec	111.5	37.6	79.0	45.1	9.8	16.9	49.8	-1.2	25.9	2.9	-28.4	-22.7
2-Point	114.2	40.2	81.5	47.2	9.9	16.9	47.3	-4.0	23.5	1.0	-28.4	-23.8
Ec Model	Percent Error in Strain -Top VWSG at 110 Days						Percent Error in Strain -Top VWSG at 110 Days					
AASHTO '05 (+)	111.8	47.5	84.1	49.2	13.5	20.8	57.4	9.0	35.4	10.7	-19.9	-14.7
ACI 209	111.8	47.5	84.1	49.2	13.5	20.8	57.4	9.0	35.4	10.7	-19.9	-14.7
CEB 90-RS	104.2	40.5	76.1	42.5	8.1	14.5	50.7	3.1	28.5	4.8	-24.6	-20.2
Constant Ec	92.4	30.4	65.2	33.4	2.0	7.4	45.0	-0.9	23.4	0.5	-28.3	-24.5
2-Point	93.6	31.8	66.3	34.3	2.1	7.4	43.9	-2.5	22.3	-0.4	-28.3	-24.5

Table E-11: STD-M Middle VWSG – Percent Error in Strain

	STD-M-1						STD-M-2					
	Creep and Shrinkage Model						Creep and Shrinkage Model					
	AASHTO '05 (+)	AASHTO '04 (-)	ACI 209	ACI 209*	CEB 90	Modified CEB 90	AASHTO '05 (+)	AASHTO '04 (-)	ACI 209	ACI 209*	CEB 90	Modified CEB 90
Ec Model	Percent Error in Strain - Middle VWSG After Transfer						Percent Error in Strain - Middle VWSG After Transfer					
AASHTO '05 (+)	17.6	17.6	17.6	17.6	17.6	17.6	21.6	21.6	21.6	21.6	21.6	21.6
ACI 209	17.6	17.6	17.6	17.6	17.6	17.6	21.6	21.6	21.6	21.6	21.6	21.6
CEB 90-RS	2.7	2.7	2.7	2.7	2.7	2.7	3.3	3.3	3.3	3.3	3.3	3.3
Constant Ec	-14.3	-14.3	-14.3	-14.3	-14.3	-14.3	-11.3	-11.3	-11.3	-11.3	-11.3	-11.3
2-Point	-14.3	-14.3	-14.3	-14.3	-14.3	-14.3	-11.3	-11.3	-11.3	-11.3	-11.3	-11.3
Ec Model	Percent Error in Strain -Middle VWSG at 6.91 Days						Percent Error in Strain -Middle VWSG at 6.91 Days					
AASHTO '05 (+)	39.5	17.4	40.8	24.8	4.9	22.5	33.5	11.6	34.0	19.4	-1.3	14.8
ACI 209	39.5	17.4	40.8	24.8	4.9	22.5	33.5	11.6	34.0	19.4	-1.3	14.8
CEB 90-RS	27.8	2.6	23.9	9.8	-5.7	10.0	20.1	-4.6	15.5	2.7	-13.3	0.7
Constant Ec	-10.3	-22.7	-6.4	-16.3	-17.6	-4.2	5.4	-15.1	3.6	-8.3	-22.8	-10.4
2-Point	-1.2	-17.7	0.3	-11.0	-17.4	-3.9	-5.5	-21.7	-4.6	-14.9	-22.7	-10.2
Ec Model	Percent Error in Strain -Middle VWSG at 33.48 Days						Percent Error in Strain -Middle VWSG at 33.48 Days					
AASHTO '05 (+)	46.3	9.3	36.7	16.1	-7.8	5.2	41.0	4.3	30.8	11.8	-13.3	-1.4
ACI 209	46.3	9.3	36.7	16.1	-7.8	5.2	41.0	4.3	30.8	11.8	-13.3	-1.4
CEB 90-RS	35.5	-1.6	24.2	5.2	-16.2	-4.8	28.5	-7.8	16.7	-0.6	-23.0	-12.6
Constant Ec	15.8	-17.7	6.3	-10.2	-25.8	-16.0	17.3	-16.2	6.5	-9.6	-30.6	-21.6
2-Point	18.7	-15.3	8.8	-8.3	-25.6	-15.8	14.4	-19.1	4.0	-11.7	-30.4	-21.3
Ec Model	Percent Error in Strain -Middle VWSG at 69.68 Days						Percent Error in Strain -Middle VWSG at 69.68 Days					
AASHTO '05 (+)	49.6	9.4	36.4	14.0	-8.9	1.8	45.4	5.3	31.5	10.7	-14.1	-4.1
ACI 209	49.6	9.4	36.4	14.0	-8.9	1.8	45.4	5.3	31.5	10.7	-14.1	-4.1
CEB 90-RS	39.2	0.0	25.5	4.7	-16.8	-7.3	33.3	-5.3	19.0	-0.1	-23.1	-14.5
Constant Ec	24.4	-12.8	11.6	-7.3	-25.6	-17.5	23.0	-13.1	9.5	-8.4	-30.2	-20.1
2-Point	25.8	-11.3	12.8	-6.3	-25.4	-17.3	22.3	-14.5	8.8	-9.0	-29.9	-22.4
Ec Model	Percent Error in Strain -Middle VWSG at 110 Days						Percent Error in Strain -Middle VWSG at 110 Days					
AASHTO '05 (+)	43.8	5.7	30.6	8.4	-11.5	-2.3	46.3	6.5	31.7	10.2	-12.8	-3.8
ACI 209	43.8	5.7	30.6	8.4	-11.5	-2.3	46.3	6.5	31.7	10.2	-12.8	-3.8
CEB 90-RS	34.0	-2.7	20.8	0.0	-18.8	-10.7	34.4	-3.5	20.0	0.0	-21.6	-13.8
Constant Ec	21.6	-13.5	9.0	-10.1	-27.0	-20.2	24.7	-10.9	10.8	-7.9	-28.5	-21.8
2-Point	22.5	-12.5	9.8	-9.5	-26.8	-19.9	24.7	-11.7	10.7	-8.0	-28.2	-21.4

Table E-12: STD-M Bottom VWSG – Percent Error in Strain

	STD-M-1						STD-M-2					
	Creep and Shrinkage Model						Creep and Shrinkage Model					
	AASHTO '05 (+)	AASHTO '04 (-)	ACI 209	ACI 209*	CEB 90	Modified CEB 90	AASHTO '05 (+)	AASHTO '04 (-)	ACI 209	ACI 209*	CEB 90	Modified CEB 90
Ec Model	Percent Error in Strain - Bottom VWSG After Transfer						Percent Error in Strain - Bottom VWSG After Transfer					
AASHTO '05 (+)	15.2	15.2	15.2	15.2	15.2	15.2	13.4	13.4	13.4	13.4	13.4	13.4
ACI 209	15.2	15.2	15.2	15.2	15.2	15.2	13.4	13.4	13.4	13.4	13.4	13.4
CEB 90-RS	0.8	0.8	0.8	0.8	0.8	0.8	-3.5	-3.5	-3.5	-3.5	-3.5	-3.5
Constant Ec	-15.8	-15.8	-15.8	-15.8	-15.8	-15.8	-17.1	-17.1	-17.1	-17.1	-17.1	-17.1
2-Point	-15.8	-15.8	-15.8	-15.8	-15.8	-15.8	-17.1	-17.1	-17.1	-17.1	-17.1	-17.1
Ec Model	Percent Error in Strain -Bottom VWSG at 6.91 Days						Percent Error in Strain -Bottom VWSG at 6.91 Days					
AASHTO '05 (+)	21.1	7.0	26.3	13.1	-4.3	12.2	17.7	3.3	22.2	9.9	-8.2	7.2
ACI 209	21.1	7.0	26.3	13.1	-4.3	12.2	17.7	3.3	22.2	9.9	-8.2	7.2
CEB 90-RS	9.7	-6.5	11.1	-0.6	-14.5	0.1	4.5	-11.8	5.0	-5.7	-20.0	-6.7
Constant Ec	-19.1	-27.5	-13.3	-22.0	-26.2	-13.6	-8.6	-22.2	-6.7	-16.5	-29.4	-17.7
2-Point	-13.1	-24.0	-8.9	-18.4	-26.0	-13.4	-15.7	-26.7	-11.9	-20.8	-29.3	-17.4
Ec Model	Percent Error in Strain -Bottom VWSG at 33.48 Days						Percent Error in Strain -Bottom VWSG at 33.48 Days					
AASHTO '05 (+)	29.1	-0.1	23.7	5.9	-14.3	-1.4	19.3	-8.7	13.4	-2.2	-22.4	-11.0
ACI 209	29.1	-0.1	23.7	5.9	-14.3	-1.4	19.3	-8.7	13.4	-2.2	-22.4	-11.0
CEB 90-RS	18.1	-10.7	11.5	-4.8	-22.8	-11.5	7.1	-20.0	0.2	-13.9	-31.8	-22.0
Constant Ec	0.8	-25.5	-4.8	-18.9	-32.6	-22.8	-3.3	-28.2	-9.7	-22.7	-39.2	-30.6
2-Point	2.9	-23.6	-3.1	-17.5	-32.4	-22.6	-4.9	-30.1	-11.1	-23.8	-39.0	-30.3
Ec Model	Percent Error in Strain -Bottom VWSG at 69.68 Days						Percent Error in Strain -Bottom VWSG at 69.68 Days					
AASHTO '05 (+)	36.2	2.1	26.4	6.5	-13.1	-1.9	30.9	-3.0	20.6	2.3	-18.5	-8.2
ACI 209	36.2	2.1	26.4	6.5	-13.1	-1.9	30.9	-3.0	20.6	2.3	-18.5	-8.2
CEB 90-RS	25.2	-7.6	15.2	-3.2	-21.3	-11.5	18.3	-13.9	7.8	-8.8	-27.9	-19.0
Constant Ec	10.8	-20.4	1.3	-15.2	-30.7	-22.2	7.8	-22.0	-2.1	-17.5	-35.4	-24.8
2-Point	11.9	-19.1	2.3	-14.3	-30.5	-22.0	7.6	-23.0	-2.4	-17.7	-35.0	-27.2
Ec Model	Percent Error in Strain -Bottom VWSG at 110 Days						Percent Error in Strain -Bottom VWSG at 110 Days					
AASHTO '05 (+)	39.9	4.7	28.9	7.8	-10.2	0.1	32.6	-1.9	21.2	2.1	-17.1	-7.8
ACI 209	39.9	4.7	28.9	7.8	-10.2	0.1	32.6	-1.9	21.2	2.1	-17.1	-7.8
CEB 90-RS	29.0	-4.7	18.0	-1.6	-18.4	-9.3	20.1	-12.3	8.9	-8.5	-26.4	-18.3
Constant Ec	15.5	-16.5	5.0	-12.7	-27.8	-20.0	9.9	-20.1	-0.7	-16.9	-33.8	-26.7
2-Point	16.3	-15.5	5.8	-12.1	-27.5	-19.7	10.3	-20.7	-0.5	-16.8	-33.4	-26.3

Table E-13: SCC-MS Top VWSG – Percent Error in Strain

	SCC-MS-1						SCC-MS-2					
	Creep and Shrinkage Model						Creep and Shrinkage Model					
	AASHTO '05 (+)	AASHTO '04 (-)	ACI 209	ACI 209*	CEB 90	Modified CEB 90	AASHTO '05 (+)	AASHTO '04 (-)	ACI 209	ACI 209*	CEB 90	Modified CEB 90
Ec Model	Percent Error in Strain - Top VWSG After Transfer						Percent Error in Strain - Top VWSG After Transfer					
AASHTO '05 (+)	13.0	13.0	13.0	13.0	13.0	13.0	-8.6	-8.6	-8.6	-8.6	-8.6	-8.6
ACI 209	13.0	13.0	13.0	13.0	13.0	13.0	-8.6	-8.6	-8.6	-8.6	-8.6	-8.6
CEB 90-RS	-6.5	-6.5	-6.5	-6.5	-6.5	-6.5	-23.2	-23.2	-23.2	-23.2	-23.2	-23.2
Constant Ec	-4.6	-4.6	-4.6	-4.6	-4.6	-4.6	-21.3	-21.3	-21.3	-21.3	-21.3	-21.3
2-Point	-4.6	-4.6	-4.6	-4.6	-4.6	-4.6	-21.3	-21.3	-21.3	-21.3	-21.3	-21.3
Ec Model	Percent Error in Strain -Top VWSG at 2.88 Days						Percent Error in Strain -Top VWSG at 3.00 Days					
AASHTO '05 (+)	44.3	20.5	191.9	53.8	-26.3	-24.4	23.0	2.6	152.6	29.5	-38.1	-36.5
ACI 209	44.3	20.5	191.9	53.8	-26.3	-24.4	23.0	2.6	152.6	29.5	-38.1	-36.5
CEB 90-RS	35.3	3.0	154.9	33.3	-34.5	-32.5	15.9	-12.1	120.3	12.3	-44.5	-42.7
Constant Ec	25.6	3.9	156.1	34.2	-33.7	-31.9	5.5	-12.6	117.4	11.4	-43.7	-42.1
2-Point	-9.7	-22.6	73.3	-3.4	-33.7	-31.9	-21.8	-33.0	52.7	-17.1	-43.7	-42.1
Ec Model	Percent Error in Strain -Top VWSG at 7.18 Days						Percent Error in Strain -Top VWSG at 6.70 Days					
AASHTO '05 (+)	59.5	28.8	228.5	66.5	-27.0	-25.9	77.6	44.0	270.6	83.6	-18.5	-17.1
ACI 209	59.5	28.8	228.5	66.5	-27.0	-25.9	77.6	44.0	270.6	83.6	-18.5	-17.1
CEB 90-RS	50.3	13.5	196.9	49.1	-34.8	-33.3	67.9	26.6	233.2	63.8	-26.6	-24.8
Constant Ec	43.2	14.3	198.1	50.0	-34.0	-32.9	57.3	26.3	230.8	63.2	-25.6	-24.1
2-Point	16.7	-6.1	137.4	22.3	-34.0	-32.9	29.0	4.6	164.8	34.0	-25.6	-24.1
Ec Model	Percent Error in Strain -Top VWSG at 89.84 Days						Percent Error in Strain -Top VWSG at 89.84 Days					
AASHTO '05 (+)	106.9	55.7	317.9	96.1	-25.9	-26.5	58.3	19.3	224.4	47.9	-43.2	-43.7
ACI 209	106.9	55.7	317.9	96.1	-25.9	-26.5	58.3	19.3	224.4	47.9	-43.2	-43.7
CEB 90-RS	97.7	48.0	303.9	88.5	-31.7	-31.7	51.7	13.6	213.9	42.4	-47.4	-47.4
Constant Ec	97.9	48.6	304.9	89.1	-31.1	-31.6	51.8	14.0	214.7	42.9	-46.8	-47.2
2-Point	95.9	46.2	301.5	87.4	-31.1	-31.6	50.5	12.3	212.3	41.7	-46.8	-47.2
Ec Model	Percent Error in Strain -Top VWSG at 160 Days						Percent Error in Strain -Top VWSG at 167 Days					
AASHTO '05 (+)	123.7	69.9	349.7	109.6	-15.4	-16.4	53.9	17.1	213.9	42.1	-41.4	-42.1
ACI 209	123.7	69.9	349.7	109.6	-15.4	-16.4	53.9	17.1	213.9	42.1	-41.4	-42.1
CEB 90-RS	114.1	62.4	336.1	102.4	-21.5	-21.8	47.6	12.1	204.8	37.4	-45.3	-45.6
Constant Ec	114.7	63.0	337.1	102.9	-20.9	-21.7	48.2	12.5	205.7	37.9	-44.8	-45.4
2-Point	114.1	61.7	336.6	102.5	-21.0	-21.7	47.9	11.8	205.5	37.7	-44.8	-45.4

Table E-14: SCC-MS Middle VWSG – Percent Error in Strain

	SCC-MS-1						SCC-MS-2					
	Creep and Shrinkage Model						Creep and Shrinkage Model					
	AASHTO '05 (+)	AASHTO '04 (-)	ACI 209	ACI 209*	CEB 90	Modified CEB 90	AASHTO '05 (+)	AASHTO '04 (-)	ACI 209	ACI 209*	CEB 90	Modified CEB 90
Ec Model	Percent Error in Strain - Middle VWSG After Transfer						Percent Error in Strain - Middle VWSG After Transfer					
AASHTO '05 (+)	20.3	20.3	20.3	20.3	20.3	20.3	17.3	17.3	17.3	17.3	17.3	17.3
ACI 209	20.3	20.3	20.3	20.3	20.3	20.3	17.3	17.3	17.3	17.3	17.3	17.3
CEB 90-RS	0.6	0.6	0.6	0.6	0.6	0.6	-0.6	-0.6	-0.6	-0.6	-0.6	-0.6
Constant Ec	2.4	2.4	2.4	2.4	2.4	2.4	1.7	1.7	1.7	1.7	1.7	1.7
2-Point	2.4	2.4	2.4	2.4	2.4	2.4	1.7	1.7	1.7	1.7	1.7	1.7
Ec Model	Percent Error in Strain -Middle VWSG at 2.88 Days						Percent Error in Strain -Middle VWSG at 3.00 Days					
AASHTO '05 (+)	16.2	7.4	99.3	22.9	-17.9	-17.4	19.4	9.8	109.6	25.4	-17.4	-16.8
ACI 209	16.2	7.4	99.3	22.9	-17.9	-17.4	19.4	9.8	109.6	25.4	-17.4	-16.8
CEB 90-RS	3.7	-9.1	71.7	5.0	-29.6	-28.7	7.6	-6.4	81.3	7.8	-28.2	-27.3
Constant Ec	0.3	-7.9	73.3	6.2	-28.5	-27.9	3.0	-5.6	81.0	8.3	-26.9	-26.2
2-Point	-14.8	-19.4	38.1	-9.8	-28.4	-27.8	-11.6	-16.7	46.8	-6.8	-26.8	-26.1
Ec Model	Percent Error in Strain -Middle VWSG at 7.18 Days						Percent Error in Strain -Middle VWSG at 6.70 Days					
AASHTO '05 (+)	26.8	11.8	125.4	30.0	-19.4	-19.3	23.9	9.5	124.6	26.7	-21.7	-21.5
ACI 209	26.8	11.8	125.4	30.0	-19.4	-19.3	23.9	9.5	124.6	26.7	-21.7	-21.5
CEB 90-RS	13.7	-3.8	98.9	13.3	-30.6	-30.0	12.1	-5.3	98.4	10.8	-31.8	-31.1
Constant Ec	11.4	-2.7	100.5	14.5	-29.6	-29.4	8.8	-4.5	98.7	11.5	-30.5	-30.3
2-Point	0.0	-11.8	74.6	2.5	-29.4	-29.2	-2.2	-13.2	73.3	0.1	-30.4	-30.1
Ec Model	Percent Error in Strain -Middle VWSG at 89.84 Days						Percent Error in Strain -Middle VWSG at 89.84 Days					
AASHTO '05 (+)	75.1	32.1	209.7	54.6	-18.0	-19.3	66.3	25.5	200.6	45.8	-22.8	-24.1
ACI 209	75.1	32.1	209.7	54.6	-18.0	-19.3	66.3	25.5	200.6	45.8	-22.8	-24.1
CEB 90-RS	60.2	20.1	189.4	42.8	-27.9	-28.3	53.2	14.9	182.2	35.3	-31.4	-31.8
Constant Ec	60.9	21.0	190.7	43.6	-27.1	-28.2	54.1	15.9	183.8	36.3	-30.4	-31.5
2-Point	60.9	20.0	190.8	43.4	-26.7	-27.8	54.2	15.0	184.0	36.2	-30.0	-31.2
Ec Model	Percent Error in Strain -Middle VWSG at 160 Days						Percent Error in Strain -Middle VWSG at 167 Days					
AASHTO '05 (+)	74.0	31.3	208.0	51.6	-16.9	-18.5	60.9	21.5	191.0	39.0	-23.6	-25.1
ACI 209	74.0	31.3	208.0	51.6	-16.9	-18.5	60.9	21.5	191.0	39.0	-23.6	-25.1
CEB 90-RS	59.6	20.1	188.9	40.7	-26.5	-27.1	48.6	11.9	174.2	29.7	-31.7	-32.3
Constant Ec	60.5	20.9	190.0	41.4	-25.7	-27.1	49.7	12.8	175.7	30.5	-30.8	-32.1
2-Point	61.3	20.6	191.7	41.9	-25.3	-26.6	50.5	12.6	177.4	31.1	-30.4	-31.7

Table E-15: SCC-MS Bottom VWSG – Percent Error in Strain

	SCC-MS-1						SCC-MS-2					
	Creep and Shrinkage Model						Creep and Shrinkage Model					
	AASHTO '05 (+)	AASHTO '04 (-)	ACI 209	ACI 209*	CEB 90	Modified CEB 90	AASHTO '05 (+)	AASHTO '04 (-)	ACI 209	ACI 209*	CEB 90	Modified CEB 90
Ec Model	Percent Error in Strain - Bottom VWSG After Transfer						Percent Error in Strain - Bottom VWSG After Transfer					
AASHTO '05 (+)	17.2	17.2	17.2	17.2	17.2	17.2	16.2	16.2	16.2	16.2	16.2	16.2
ACI 209	17.2	17.2	17.2	17.2	17.2	17.2	16.2	16.2	16.2	16.2	16.2	16.2
CEB 90-RS	-1.8	-1.8	-1.8	-1.8	-1.8	-1.8	-1.5	-1.5	-1.5	-1.5	-1.5	-1.5
Constant Ec	0.0	0.0	0.0	0.0	0.0	0.0	0.8	0.8	0.8	0.8	0.8	0.8
2-Point	0.0	0.0	0.0	0.0	0.0	0.0	0.8	0.8	0.8	0.8	0.8	0.8
Ec Model	Percent Error in Strain -Bottom VWSG at 2.88 Days						Percent Error in Strain -Bottom VWSG at 3.00 Days					
AASHTO '05 (+)	5.4	0.4	70.1	11.1	-18.9	-18.6	10.4	4.9	82.2	15.9	-16.3	-16.0
ACI 209	5.4	0.4	70.1	11.1	-18.9	-18.6	10.4	4.9	82.2	15.9	-16.3	-16.0
CEB 90-RS	-7.6	-15.2	45.7	-5.5	-30.9	-30.4	-2.1	-10.7	57.1	-0.7	-27.8	-27.2
Constant Ec	-9.3	-14.0	47.3	-4.3	-29.8	-29.5	-4.6	-9.6	57.7	0.2	-26.4	-26.1
2-Point	-19.1	-21.5	24.8	-14.6	-29.7	-29.4	-14.2	-17.0	35.3	-9.7	-26.2	-25.9
Ec Model	Percent Error in Strain -Bottom VWSG at 7.18 Days						Percent Error in Strain -Bottom VWSG at 6.70 Days					
AASHTO '05 (+)	12.0	1.7	88.3	14.2	-21.9	-22.0	6.0	-3.4	81.5	8.0	-26.2	-26.3
ACI 209	12.0	1.7	88.3	14.2	-21.9	-22.0	6.0	-3.4	81.5	8.0	-26.2	-26.3
CEB 90-RS	-1.3	-13.2	64.5	-1.5	-33.3	-33.0	-5.7	-17.0	59.1	-6.3	-36.3	-35.9
Constant Ec	-2.3	-12.0	66.1	-0.3	-32.3	-32.4	-7.2	-16.0	60.0	-5.3	-35.0	-35.1
2-Point	-9.5	-17.9	49.9	-7.8	-32.1	-32.2	-13.8	-21.4	44.7	-12.2	-34.9	-34.9
Ec Model	Percent Error in Strain -Bottom VWSG at 89.84 Days						Percent Error in Strain -Bottom VWSG at 89.84 Days					
AASHTO '05 (+)	47.4	11.3	145.6	26.3	-24.3	-25.7	49.2	12.7	153.9	27.0	-23.9	-25.4
ACI 209	47.4	11.3	145.6	26.3	-24.3	-25.7	49.2	12.7	153.9	27.0	-23.9	-25.4
CEB 90-RS	32.4	-0.6	125.6	14.4	-34.3	-34.8	35.0	1.4	134.6	15.8	-33.3	-33.8
Constant Ec	33.2	0.2	126.8	15.2	-33.5	-34.7	36.1	2.4	136.2	16.9	-32.3	-33.5
2-Point	33.8	-0.3	127.9	15.5	-33.0	-34.2	36.8	2.0	137.5	17.2	-31.8	-33.1
Ec Model	Percent Error in Strain -Bottom VWSG at 160 Days						Percent Error in Strain -Bottom VWSG at 167 Days					
AASHTO '05 (+)	49.8	12.7	150.0	26.4	-22.2	-23.9	-	-	-	-	-	-
ACI 209	49.8	12.7	150.0	26.4	-22.2	-23.9	-	-	-	-	-	-
CEB 90-RS	34.9	1.2	130.5	15.0	-32.2	-32.9	-	-	-	-	-	-
Constant Ec	35.8	2.0	131.6	15.8	-31.4	-32.9	-	-	-	-	-	-
2-Point	37.0	2.0	133.8	16.6	-30.9	-32.3	-	-	-	-	-	-

Table E-16: SCC-HS Top VWSG – Percent Error in Strain

	SCC-HS-1						SCC-HS-2					
	Creep and Shrinkage Model						Creep and Shrinkage Model					
	AASHTO '05 (+)	AASHTO '04 (-)	ACI 209	ACI 209*	CEB 90	Modified CEB 90	AASHTO '05 (+)	AASHTO '04 (-)	ACI 209	ACI 209*	CEB 90	Modified CEB 90
Ec Model	Percent Error in Strain - Top VWSG After Transfer						Percent Error in Strain - Top VWSG After Transfer					
AASHTO '05 (+)	-20.2	-20.2	-20.2	-20.2	-20.2	-20.2	-17.4	-17.4	-17.4	-17.4	-17.4	-17.4
ACI 209	-20.2	-20.2	-20.2	-20.2	-20.2	-20.2	-17.4	-17.4	-17.4	-17.4	-17.4	-17.4
CEB 90-RS	-13.8	-13.8	-13.8	-13.8	-13.8	-13.8	-12.6	-12.6	-12.6	-12.6	-12.6	-12.6
Constant Ec	-27.0	-27.0	-27.0	-27.0	-27.0	-27.0	-24.7	-24.7	-24.7	-24.7	-24.7	-24.7
2-Point	-27.0	-27.0	-27.0	-27.0	-27.0	-27.0	-24.7	-24.7	-24.7	-24.7	-24.7	-24.7
Ec Model	Percent Error in Strain -Top VWSG at 4.88 Days						Percent Error in Strain -Top VWSG at 4.88 Days					
AASHTO '05 (+)	30.3	10.4	208.0	48.9	-57.8	-57.3	16.4	-0.2	177.9	34.1	-64.6	-64.2
ACI 209	30.3	10.4	208.0	48.9	-57.8	-57.3	16.4	-0.2	177.9	34.1	-64.6	-64.2
CEB 90-RS	33.2	4.7	186.2	40.4	-55.1	-54.4	18.3	-7.4	154.6	24.2	-62.9	-62.4
Constant Ec	18.5	-1.9	175.8	33.3	-60.6	-60.1	3.0	-14.6	139.9	15.9	-67.1	-67.2
2-Point	-5.4	-24.4	103.0	1.6	-60.6	-60.1	-15.4	-32.2	83.4	-8.7	-67.2	-66.8
Ec Model	Percent Error in Strain -Top VWSG at 27.62 Days						Percent Error in Strain -Top VWSG at 27.62 Days					
AASHTO '05 (+)	42.7	32.1	290.9	79.1	-61.1	-61.3	45.3	35.3	298.3	82.7	-62.8	-63.1
ACI 209	42.7	32.1	290.9	79.1	-61.1	-61.3	45.3	35.3	298.3	82.7	-62.8	-63.1
CEB 90-RS	45.7	31.1	286.9	77.9	-58.9	-58.8	47.4	32.7	292.9	80.0	-61.2	-61.1
Constant Ec	37.5	25.8	276.8	72.2	-63.4	-63.6	38.9	27.0	281.4	73.7	-65.3	-65.6
2-Point	32.2	17.3	254.4	62.2	-63.5	-63.6	34.1	19.1	260.9	64.6	-65.3	-65.6
Ec Model	Percent Error in Strain -Top VWSG at 93.93 Days						Percent Error in Strain -Top VWSG at 93.93 Days					
AASHTO '05 (+)	57.0	68.2	349.3	120.1	-55.5	-56.1	65.5	77.5	415.2	131.7	-56.7	-57.5
ACI 209	57.0	68.2	349.3	120.1	-55.5	-56.1	65.5	77.5	415.2	131.7	-56.7	-57.5
CEB 90-RS	60.0	69.4	393.2	121.9	-53.3	-53.5	67.8	77.6	419.0	132.5	-55.0	-55.2
Constant Ec	53.5	64.3	382.7	116.3	-57.9	-58.4	61.4	72.4	408.6	127.0	-59.3	-60.0
2-Point	52.7	61.6	378.5	114.3	-57.9	-58.4	60.7	69.8	404.5	125.1	-59.3	-60.0
Ec Model	Percent Error in Strain -Top VWSG at 214 Days						Percent Error in Strain -Top VWSG at 214 Days					
AASHTO '05 (+)	98.7	131.7	560.3	194.7	-36.8	-37.8	122.0	158.6	635.5	228.6	-35.7	-37.1
ACI 209	98.7	131.7	560.3	194.7	-36.8	-37.8	122.0	158.6	635.5	228.6	-35.7	-37.1
CEB 90-RS	102.3	133.9	566.4	197.8	-33.8	-34.4	125.0	159.9	643.6	230.8	-33.3	-34.1
Constant Ec	94.8	127.5	552.9	190.9	-39.7	-40.7	117.3	153.2	630.0	223.8	-39.2	-40.5
2-Point	94.6	126.1	552.4	190.5	-39.8	-40.8	117.2	151.7	629.5	223.4	-39.3	-40.6

Table E-17: SCC-HS Middle VWSG – Percent Error in Strain

	SCC-HS-1						SCC-HS-2					
	Creep and Shrinkage Model						Creep and Shrinkage Model					
	AASHTO '05 (+)	AASHTO '04 (-)	ACI 209	ACI 209*	CEB 90	Modified CEB 90	AASHTO '05 (+)	AASHTO '04 (-)	ACI 209	ACI 209*	CEB 90	Modified CEB 90
Ec Model	Percent Error in Strain - Middle VWSG After Transfer						Percent Error in Strain - Middle VWSG After Transfer					
AASHTO '05 (+)	-1.3	-1.3	-1.3	-1.3	-1.3	-1.3	-0.5	-0.5	-0.5	-0.5	-0.5	-0.5
ACI 209	-1.3	-1.3	-1.3	-1.3	-1.3	-1.3	-0.5	-0.5	-0.5	-0.5	-0.5	-0.5
CEB 90-RS	6.3	6.3	6.3	6.3	6.3	6.3	4.9	4.9	4.9	4.9	4.9	4.9
Constant Ec	-9.4	-9.4	-9.4	-9.4	-9.4	-9.4	-9.0	-9.0	-9.0	-9.0	-9.0	-9.0
2-Point	-9.4	-9.4	-9.4	-9.4	-9.4	-9.4	-9.0	-9.0	-9.0	-9.0	-9.0	-9.0
Ec Model	Percent Error in Strain -Middle VWSG at 4.88 Days						Percent Error in Strain -Middle VWSG at 4.88 Days					
AASHTO '05 (+)	17.6	5.3	134.8	28.8	-36.3	-36.3	23.7	11.2	150.6	36.4	-35.6	-35.7
ACI 209	17.6	5.3	134.8	28.8	-36.3	-36.3	23.7	11.2	150.6	36.4	-35.6	-35.7
CEB 90-RS	22.6	5.4	127.5	27.5	-31.8	-31.4	27.3	8.7	138.5	32.2	-32.4	-32.1
Constant Ec	7.5	-5.0	112.0	16.5	-41.1	-41.0	11.0	-2.1	120.3	20.4	-40.8	-41.0
2-Point	-5.5	-17.5	72.7	-0.8	-41.0	-41.0	-1.1	-13.8	83.4	4.3	-40.7	-40.7
Ec Model	Percent Error in Strain -Middle VWSG at 27.62 Days						Percent Error in Strain -Middle VWSG at 27.62 Days					
AASHTO '05 (+)	38.1	24.5	219.0	57.1	-38.5	-39.2	38.5	25.3	221.7	58.2	-40.6	-41.4
ACI 209	38.1	24.5	219.0	57.1	-38.5	-39.2	38.5	25.3	221.7	58.2	-40.6	-41.4
CEB 90-RS	43.4	26.8	221.7	59.6	-34.3	-34.4	42.2	25.5	222.0	58.7	-37.7	-37.8
Constant Ec	31.0	17.0	204.6	49.2	-42.9	-43.6	30.5	16.5	205.5	48.9	-45.2	-45.9
2-Point	28.0	11.7	191.7	43.4	-42.8	-43.4	27.9	11.6	193.7	43.6	-45.1	-45.8
Ec Model	Percent Error in Strain -Middle VWSG at 93.93 Days						Percent Error in Strain -Middle VWSG at 93.93 Days					
AASHTO '05 (+)	51.0	50.2	282.8	86.9	-33.3	-34.7	38.5	37.9	264.5	71.8	-41.6	-42.9
ACI 209	51.0	50.2	282.8	86.9	-33.3	-34.7	38.5	37.9	264.5	71.8	-41.6	-42.9
CEB 90-RS	56.4	53.9	304.2	91.3	-29.1	-29.7	41.9	39.6	270.3	74.2	-38.9	-39.4
Constant Ec	44.7	44.1	285.7	80.9	-37.9	-39.1	32.4	31.6	255.1	65.7	-45.9	-47.1
2-Point	44.6	42.5	284.4	80.0	-37.7	-38.9	32.3	30.2	253.9	64.9	-45.8	-47.0
Ec Model	Percent Error in Strain -Middle VWSG at 214 Days						Percent Error in Strain -Middle VWSG at 214 Days					
AASHTO '05 (+)	76.6	88.7	395.9	130.2	-16.3	-18.4	50.9	61.1	324.0	96.9	-32.3	-34.2
ACI 209	76.6	88.7	395.9	130.2	-16.3	-18.4	50.9	61.1	324.0	96.9	-32.3	-34.2
CEB 90-RS	82.8	93.4	406.1	135.8	-11.2	-12.4	54.5	63.5	331.9	100.0	-29.2	-30.3
Constant Ec	69.7	82.0	383.8	123.6	-21.8	-23.7	44.7	54.9	315.0	90.9	-37.1	-38.9
2-Point	70.1	81.3	385.3	124.0	-21.5	-23.5	45.0	54.2	316.0	91.1	-37.0	-38.7

Table E-18: SCC-HS Bottom VWSG – Percent Error in Strain

	SCC-HS-1						SCC-HS-2					
	Creep and Shrinkage Model						Creep and Shrinkage Model					
	AASHTO '05 (+)	AASHTO '04 (-)	ACI 209	ACI 209*	CEB 90	Modified CEB 90	AASHTO '05 (+)	AASHTO '04 (-)	ACI 209	ACI 209*	CEB 90	Modified CEB 90
Ec Model	Percent Error in Strain - Bottom VWSG After Transfer						Percent Error in Strain - Bottom VWSG After Transfer					
AASHTO '05 (+)	12.4	12.4	12.4	12.4	12.4	12.4	4.9	4.9	4.9	4.9	4.9	4.9
ACI 209	12.4	12.4	12.4	12.4	12.4	12.4	4.9	4.9	4.9	4.9	4.9	4.9
CEB 90-RS	21.0	21.0	21.0	21.0	21.0	21.0	10.6	10.6	10.6	10.6	10.6	10.6
Constant Ec	3.3	3.3	3.3	3.3	3.3	3.3	-4.0	-4.0	-4.0	-4.0	-4.0	-4.0
2-Point	3.3	3.3	3.3	3.3	3.3	3.3	-4.0	-4.0	-4.0	-4.0	-4.0	-4.0
Ec Model	Percent Error in Strain -Bottom VWSG at 4.88 Days						Percent Error in Strain -Bottom VWSG at 4.88 Days					
AASHTO '05 (+)	21.6	11.2	124.9	30.8	-23.6	-23.7	26.3	15.8	136.9	36.7	-23.0	-23.3
ACI 209	21.6	11.2	124.9	30.8	-23.6	-23.7	26.3	15.8	136.9	36.7	-23.0	-23.3
CEB 90-RS	27.7	13.5	122.4	32.2	-18.0	-17.7	30.6	15.3	130.0	35.1	-19.1	-18.8
Constant Ec	11.3	0.8	103.9	18.9	-29.4	-29.5	13.9	2.9	110.2	21.7	-29.3	-29.5
2-Point	1.5	-8.8	74.3	5.7	-29.3	-29.5	4.8	-6.1	82.3	9.5	-29.2	-29.4
Ec Model	Percent Error in Strain -Bottom VWSG at 27.62 Days						Percent Error in Strain -Bottom VWSG at 27.62 Days					
AASHTO '05 (+)	38.2	23.1	193.6	50.2	-28.1	-29.0	36.1	21.5	190.9	48.6	-31.2	-32.3
ACI 209	38.2	23.1	193.6	50.2	-28.1	-29.0	36.1	21.5	190.9	48.6	-31.2	-32.3
CEB 90-RS	44.5	26.8	199.1	54.3	-23.1	-23.2	40.4	22.9	193.7	50.4	-27.8	-28.0
Constant Ec	30.1	15.1	178.8	41.7	-33.5	-34.3	27.5	12.5	175.1	39.1	-36.7	-37.7
2-Point	28.1	11.0	169.7	37.5	-33.3	-34.2	25.6	8.8	166.8	35.3	-36.6	-37.5
Ec Model	Percent Error in Strain -Bottom VWSG at 93.93 Days						Percent Error in Strain -Bottom VWSG at 93.93 Days					
AASHTO '05 (+)	38.0	32.5	229.5	60.7	-29.1	-30.7	37.0	31.5	230.1	59.8	-32.1	-33.8
ACI 209	38.0	32.5	229.5	60.7	-29.1	-30.7	37.0	31.5	230.1	59.8	-32.1	-33.8
CEB 90-RS	44.0	36.9	240.5	65.7	-24.4	-25.1	41.1	34.0	237.1	63.0	-28.9	-29.5
Constant Ec	31.1	26.0	220.1	54.1	-34.3	-35.7	29.7	24.4	219.1	52.7	-37.4	-38.9
2-Point	31.3	24.9	220.0	53.8	-34.0	-35.5	29.9	23.4	218.9	52.4	-37.2	-38.7
Ec Model	Percent Error in Strain -Bottom VWSG at 214 Days						Percent Error in Strain -Bottom VWSG at 214 Days					
AASHTO '05 (+)	47.5	50.9	279.1	80.1	-19.5	-21.7	48.4	51.6	282.2	81.5	-22.3	-24.6
ACI 209	47.5	50.9	279.1	80.1	-19.5	-21.7	48.4	51.6	282.2	81.5	-22.3	-24.6
CEB 90-RS	53.8	55.9	289.5	85.8	-14.3	-15.6	52.8	54.8	290.9	85.3	-18.7	-19.9
Constant Ec	40.4	44.2	266.9	73.3	-25.2	-27.2	40.9	44.4	270.9	74.3	-28.2	-30.4
2-Point	41.0	43.8	268.8	73.9	-24.9	-26.9	41.4	44.0	272.5	74.8	-28.0	-30.1

APPENDIX F

MEASURED CAMBER

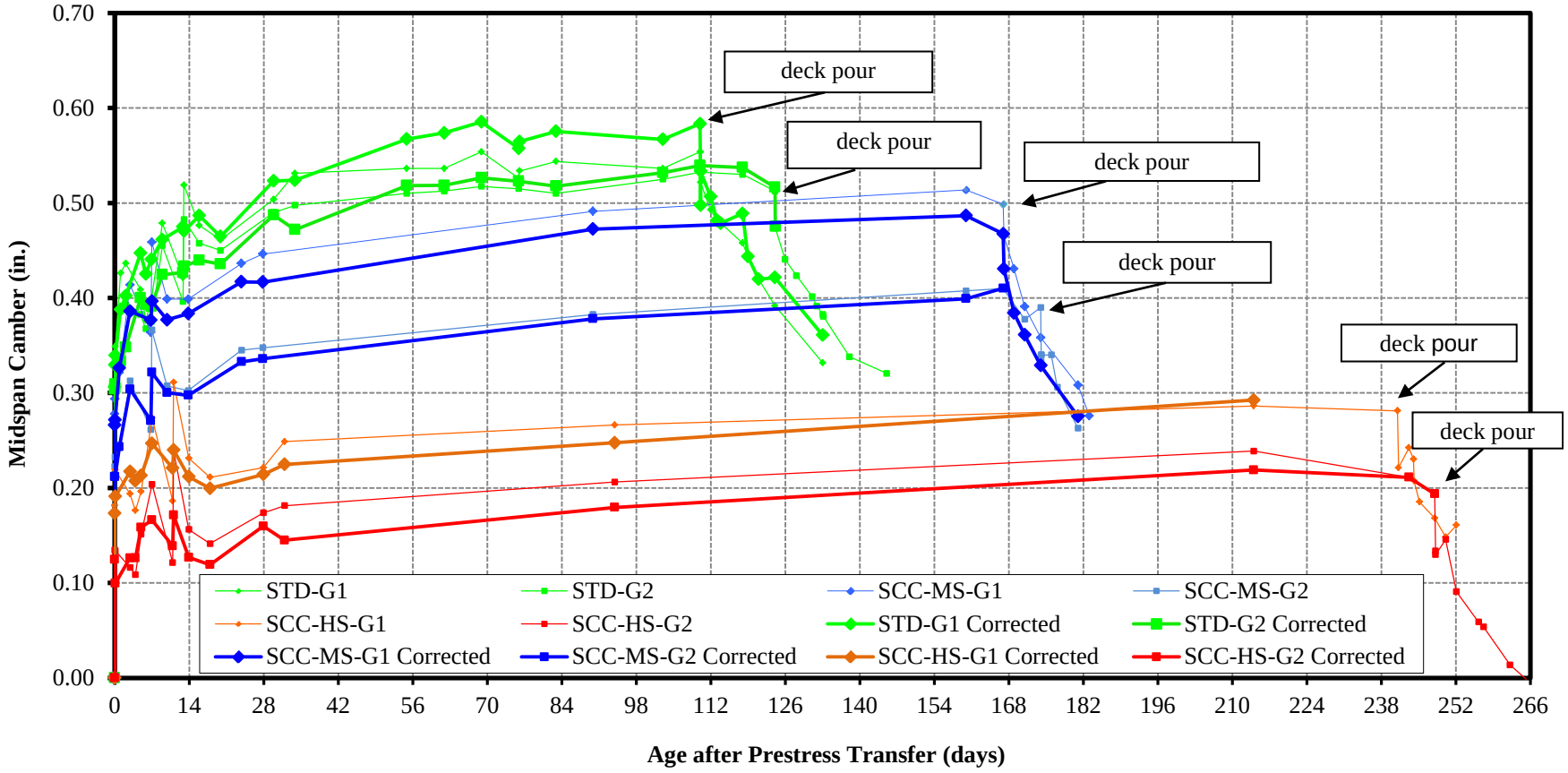

Figure F-1: Measured Midspan Camber versus Time

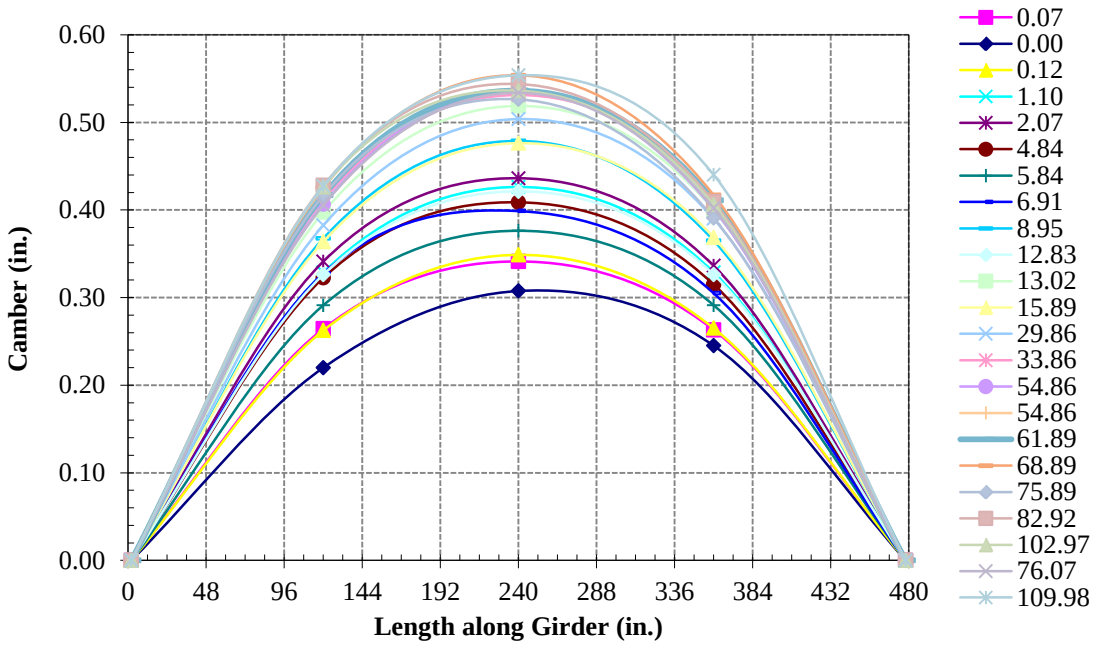

Figure F-2: STD-M-1 Measured Camber

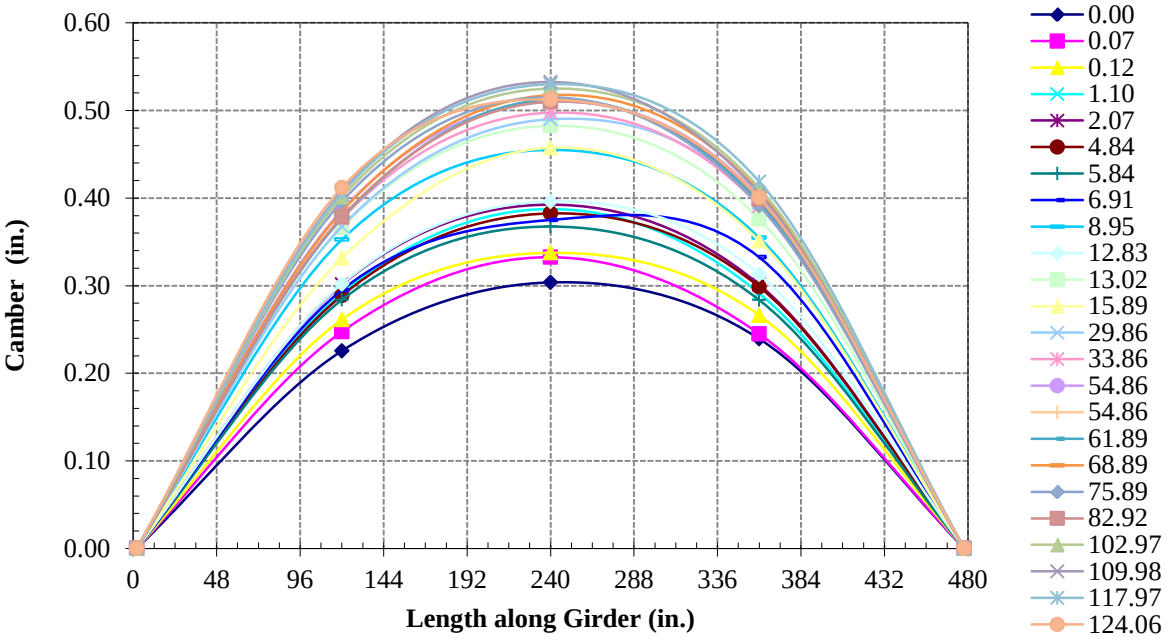

Figure F-3: STD-M-2 Measured Camber

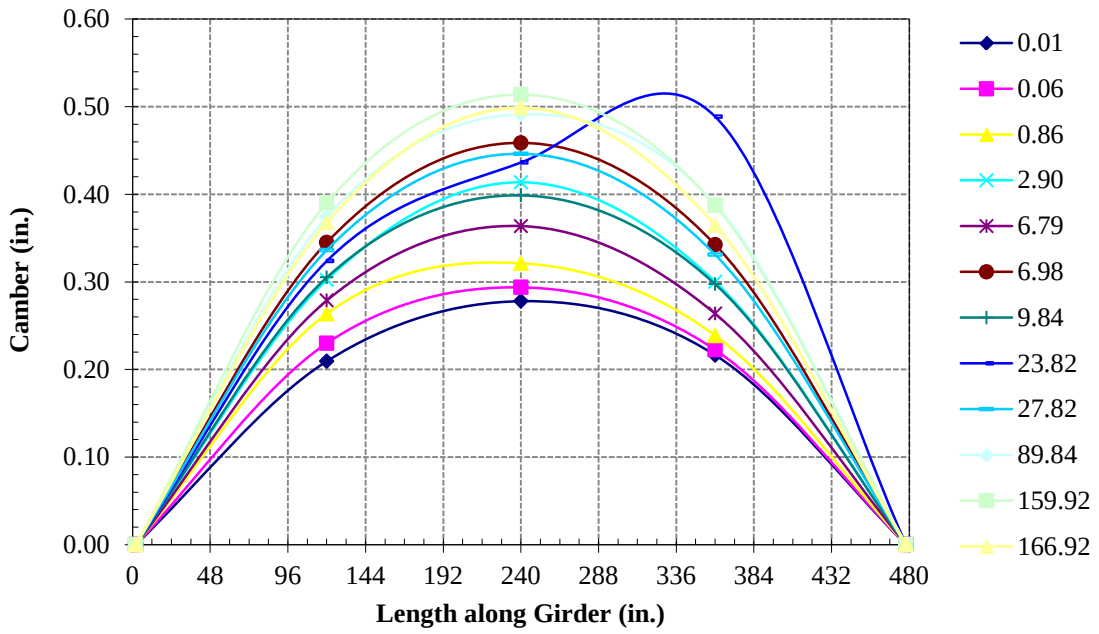

Figure F-4: SCC-MS-1 Measured Camber

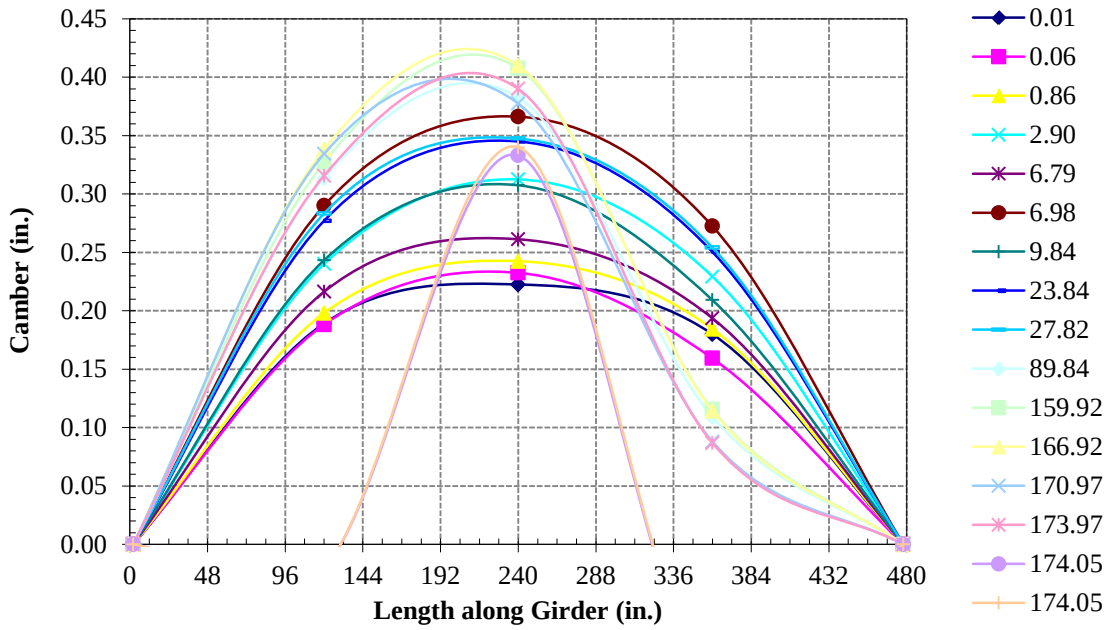

Figure F-5: SCC-MS-2 Measured Camber

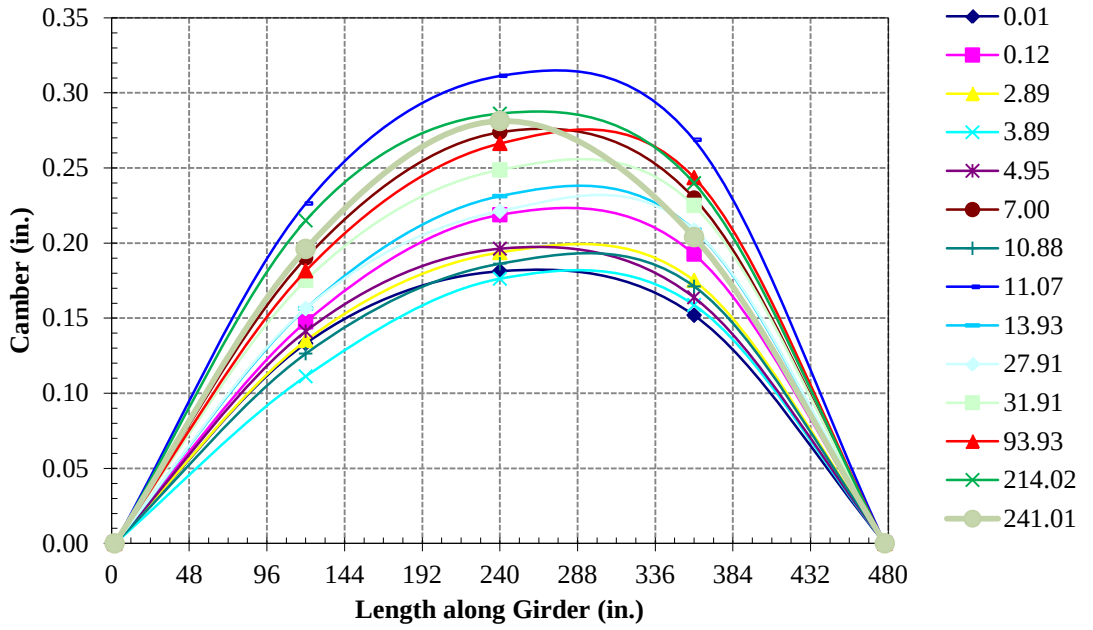

Figure F-6: SCC-HS-1 Measured Camber

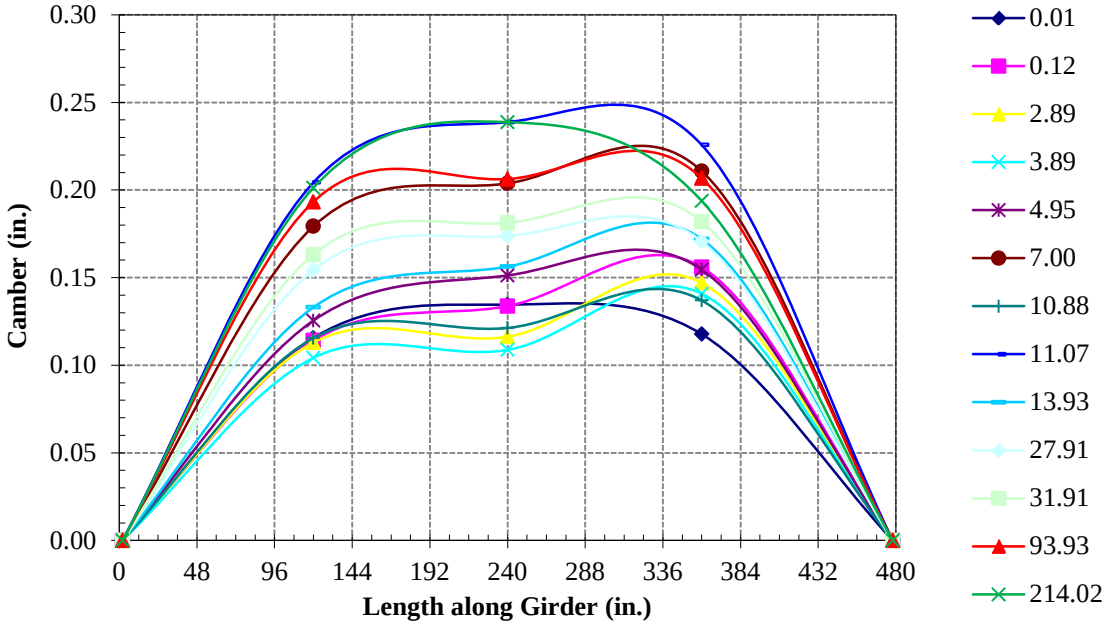

Figure F-7: SCC-HS-2 Measured Camber

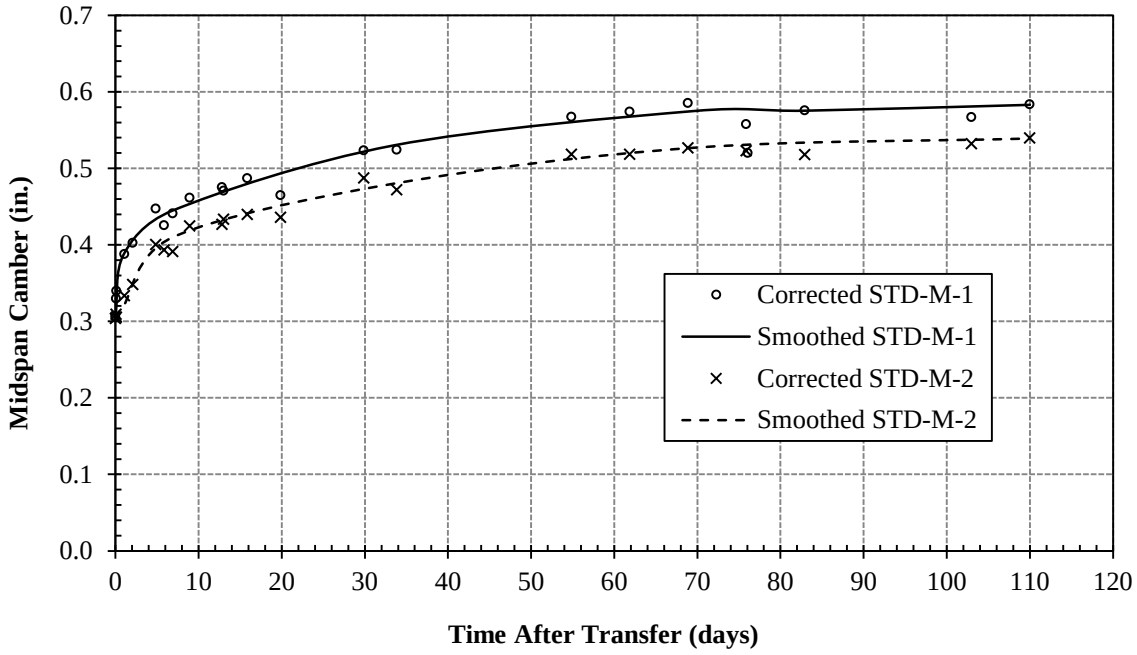

Figure F-8: STD-M Smoothed Camber

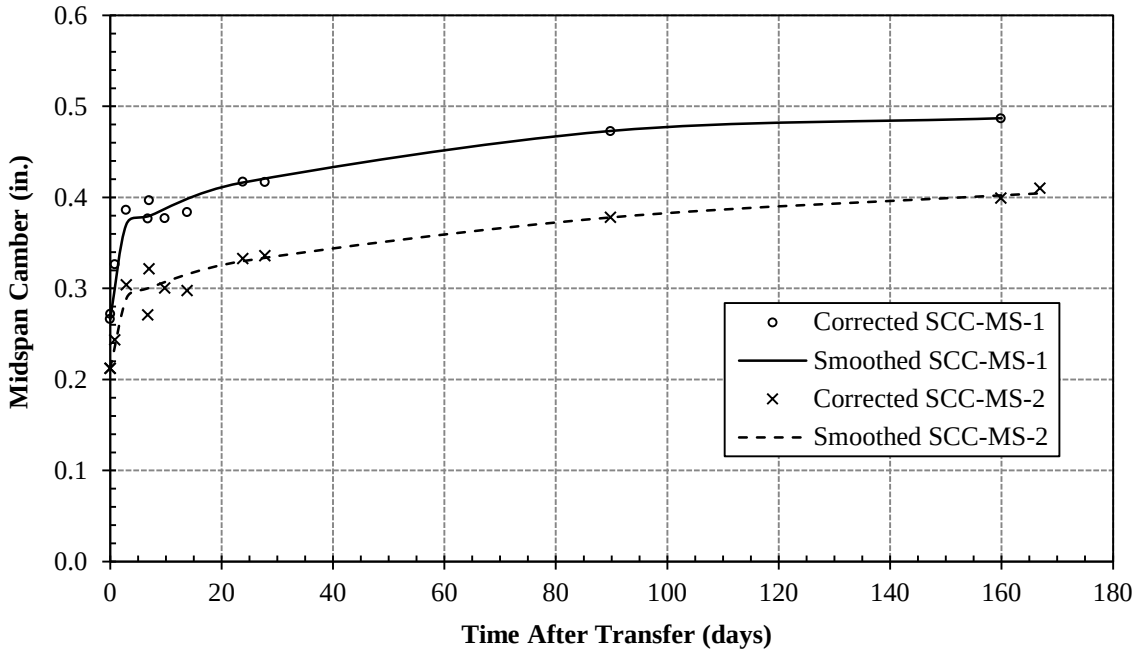

Figure F-9: SCC-MS Smoothed Camber

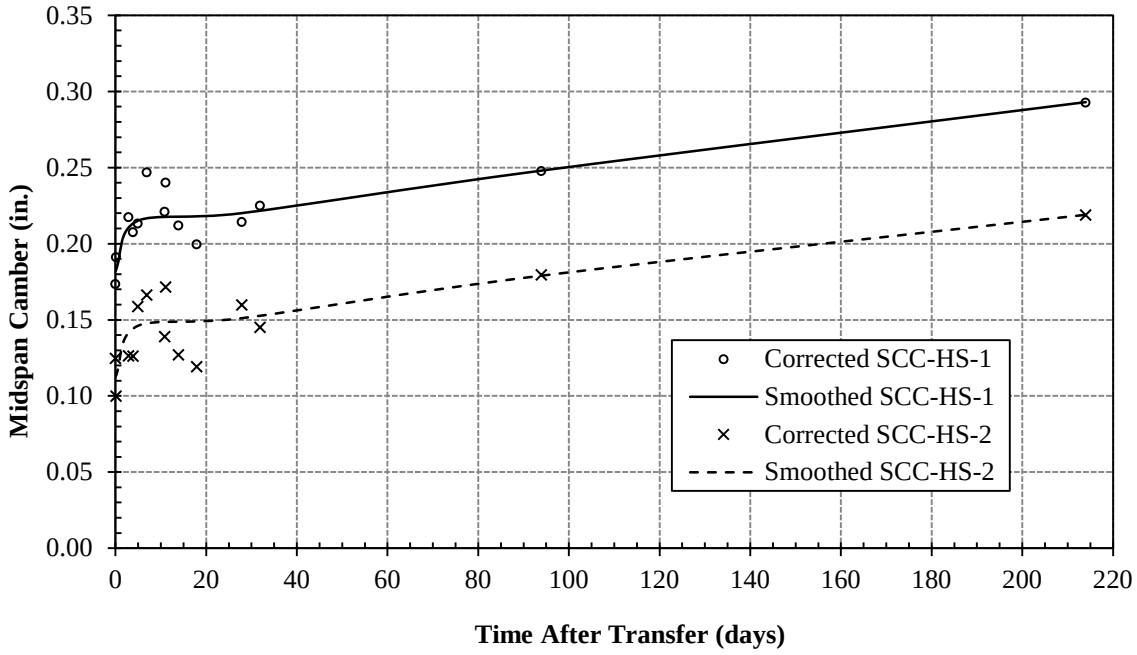

Figure F-10: SCC-HS Smoothed Camber

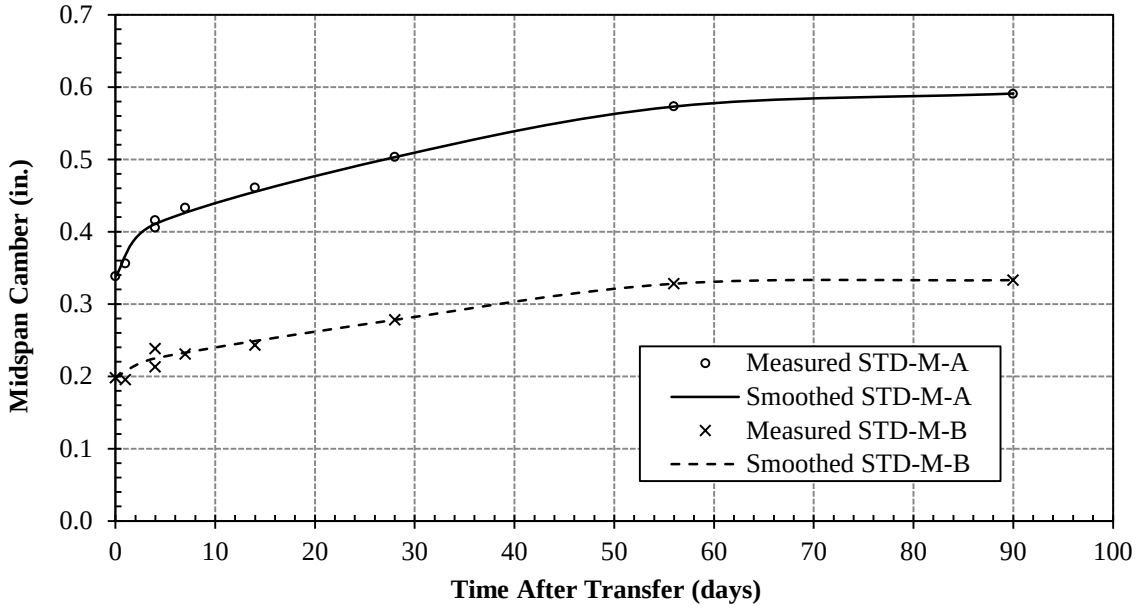

Figure F-11: STD-M-A & -B Smoothed Camber

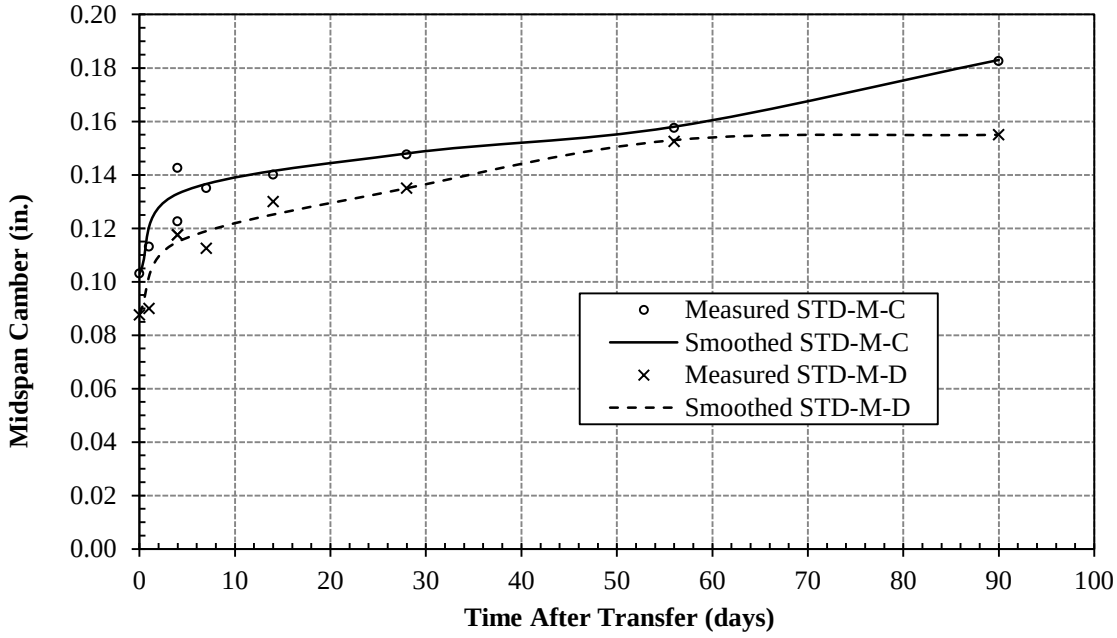

Figure F-12: STD-M-C & -D Smoothed Camber

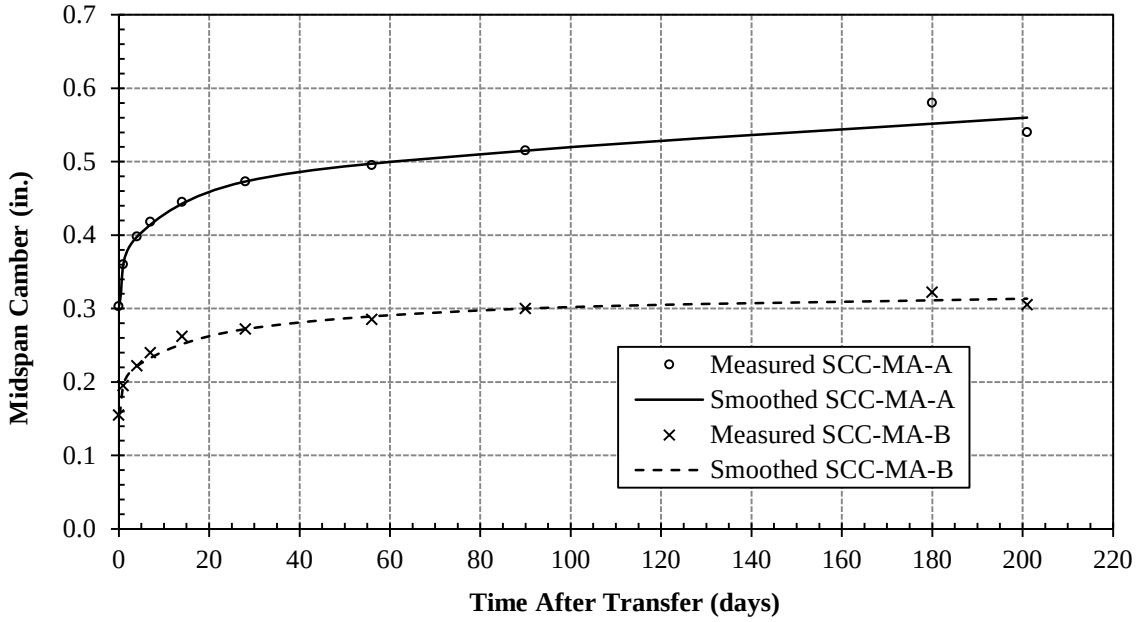

Figure F-13: SCC-MA-A & -B Smoothed Camber

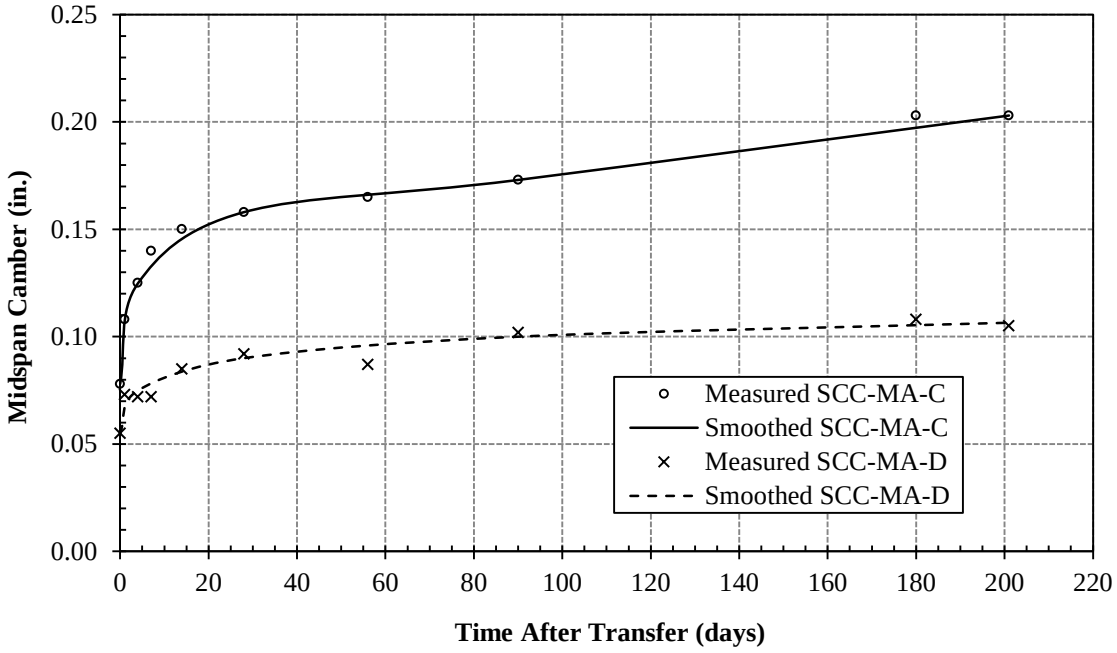

Figure F-14: SCC-MA-C & -D Smoothed Camber

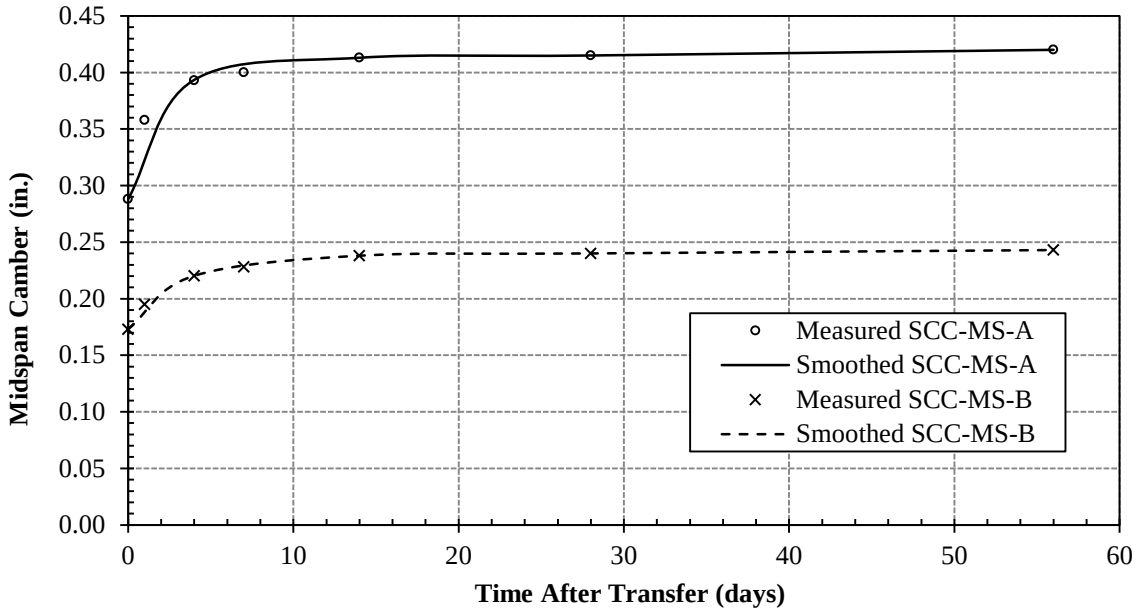

Figure F-15: SCC-MS-A & -B Smoothed Camber

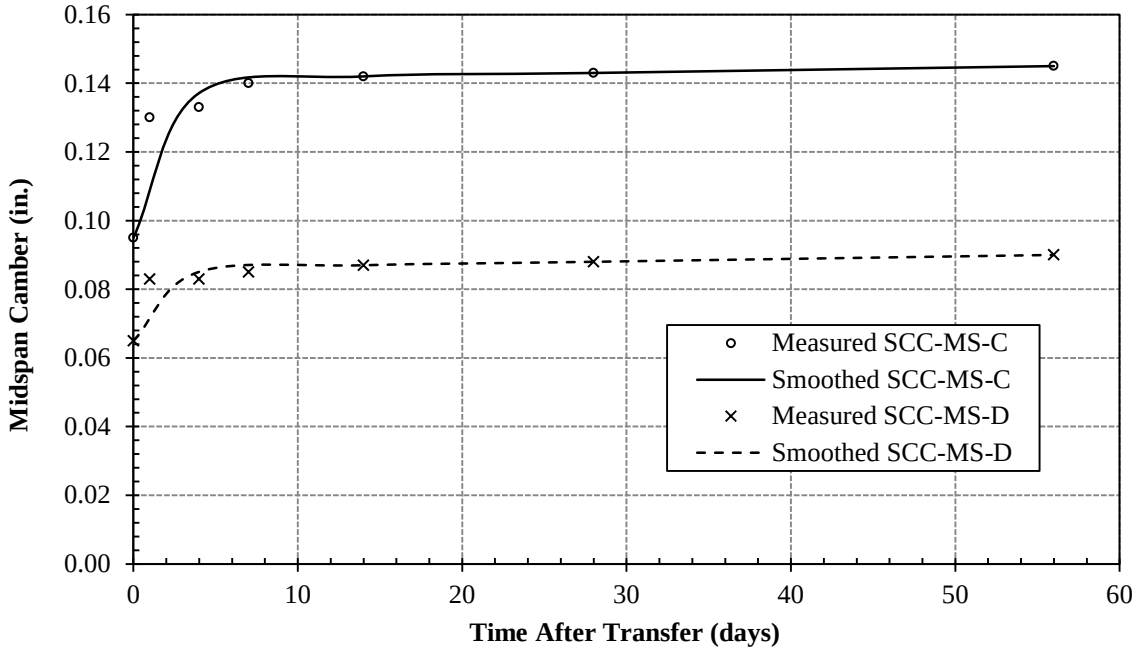

Figure F-16: SCC-MS-A & -B Smoothed Camber

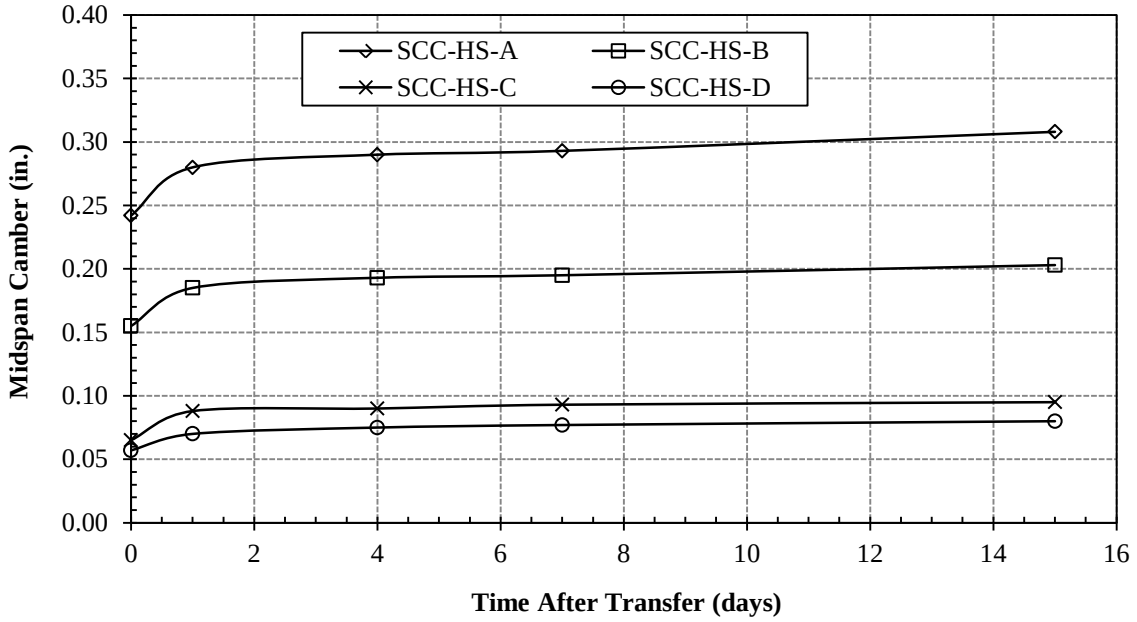

Figure F-17: SCC-HS-A, -B, -C & -D Smoothed Camber

APPENDIX G

PREDICTED CAMBER

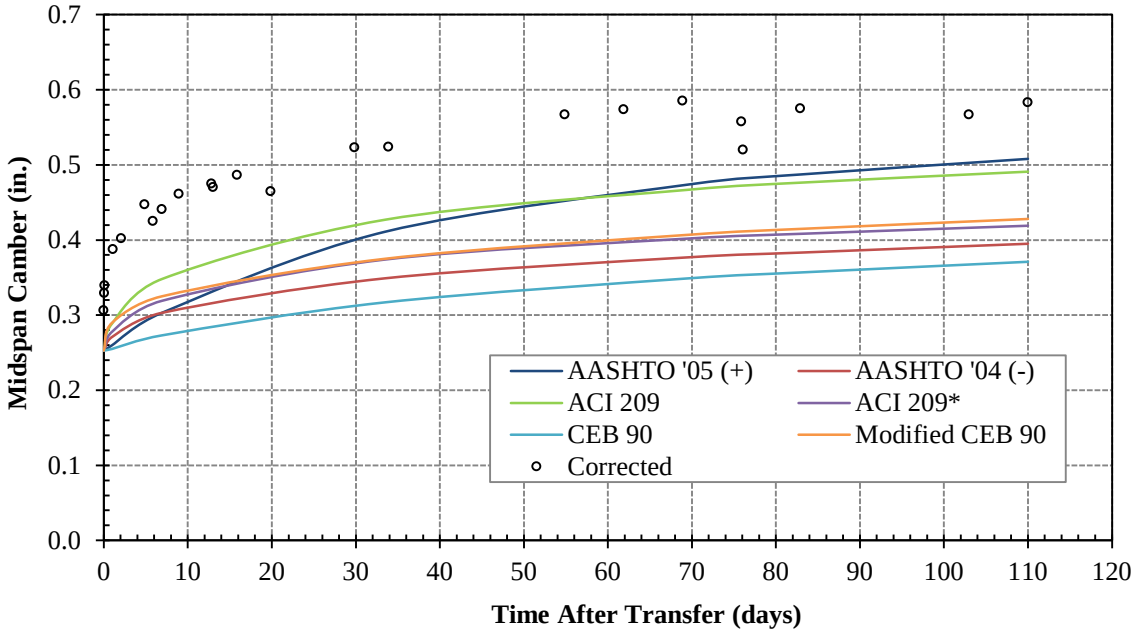

Figure G-1: STD-M-1 Predicted Camber with Two-Point E_c

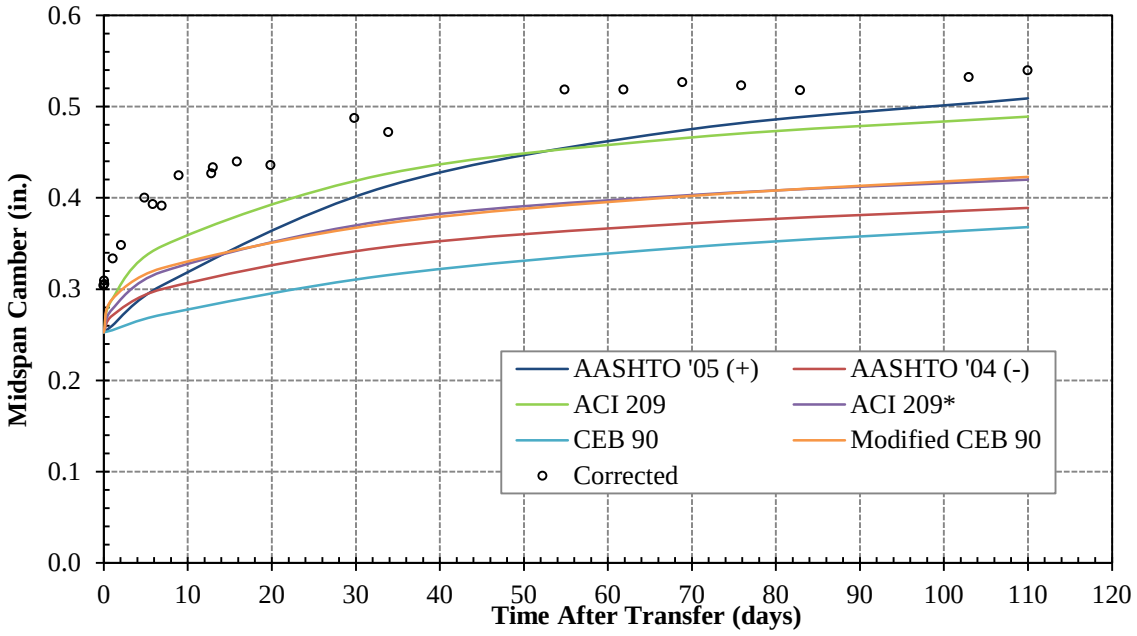

Figure G-2: STD-M-2 Predicted Camber with Two-Point E_c

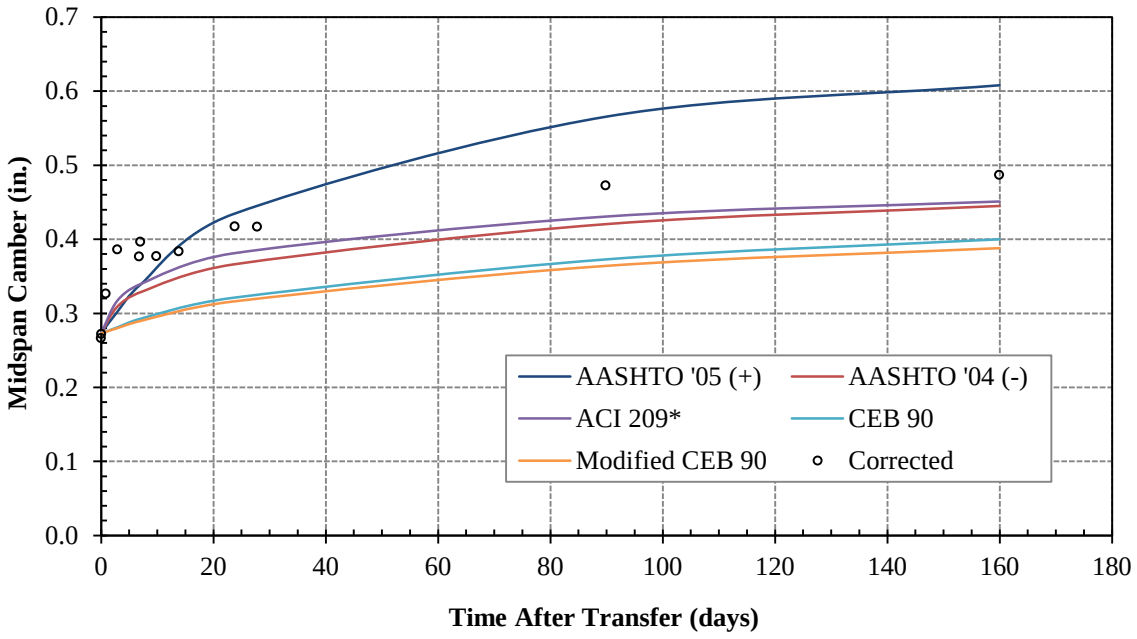

Figure G-3: SCC-MS-1 Predicted Camber with Two-Point E_c

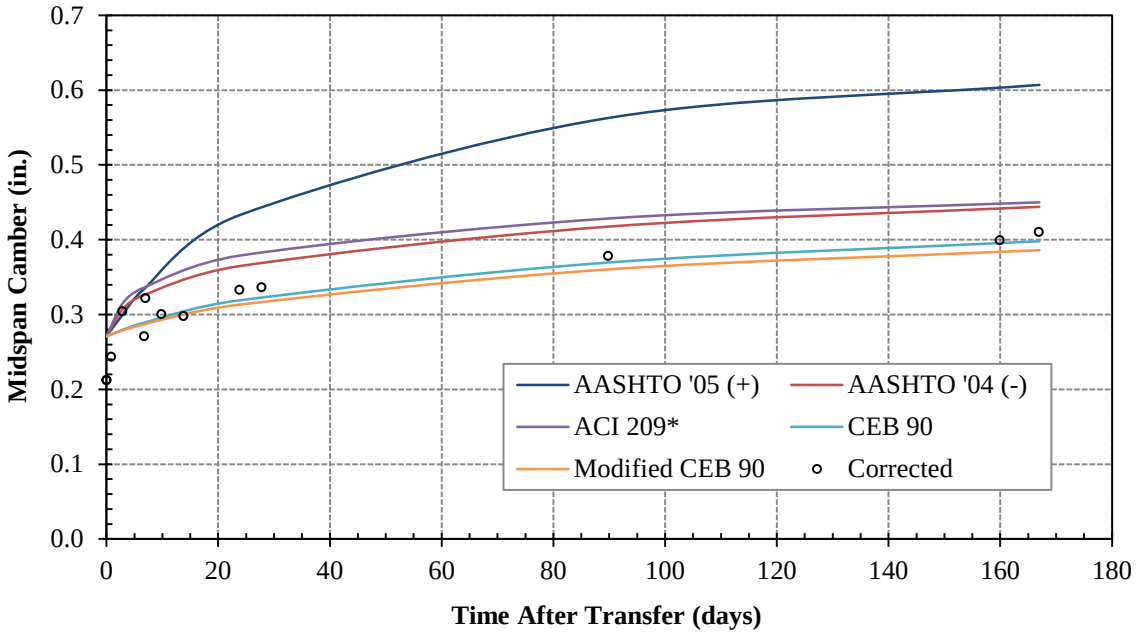

Figure G-4: SCC-MS-2 Predicted Camber with Two-Point E_c

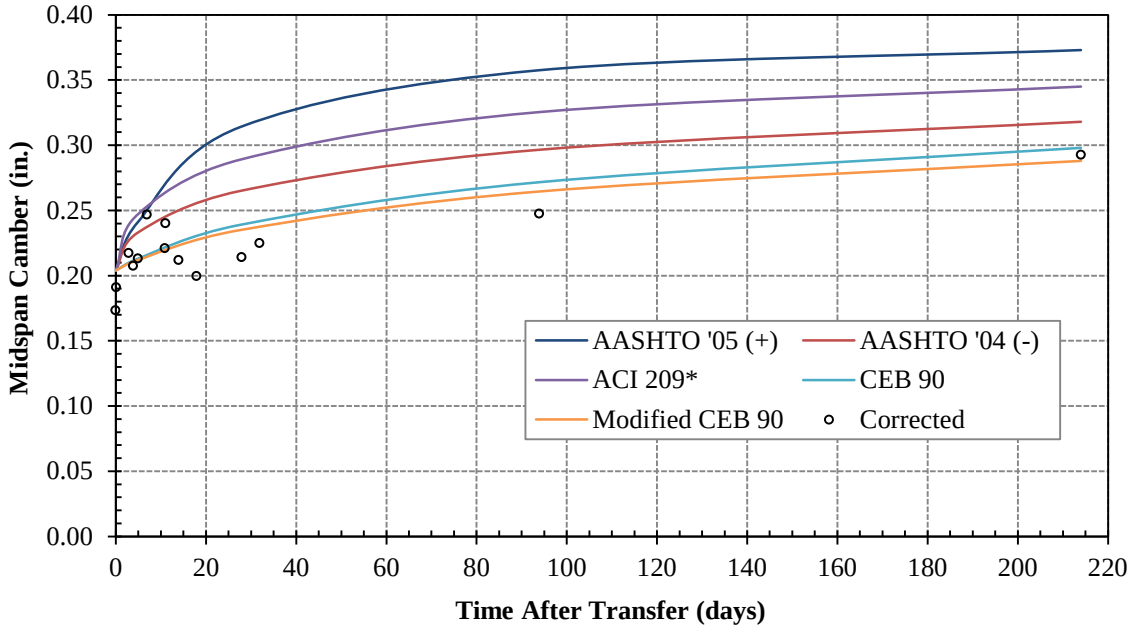

Figure G-5: SCC-HS-1 Predicted Camber with Two-Point E_c

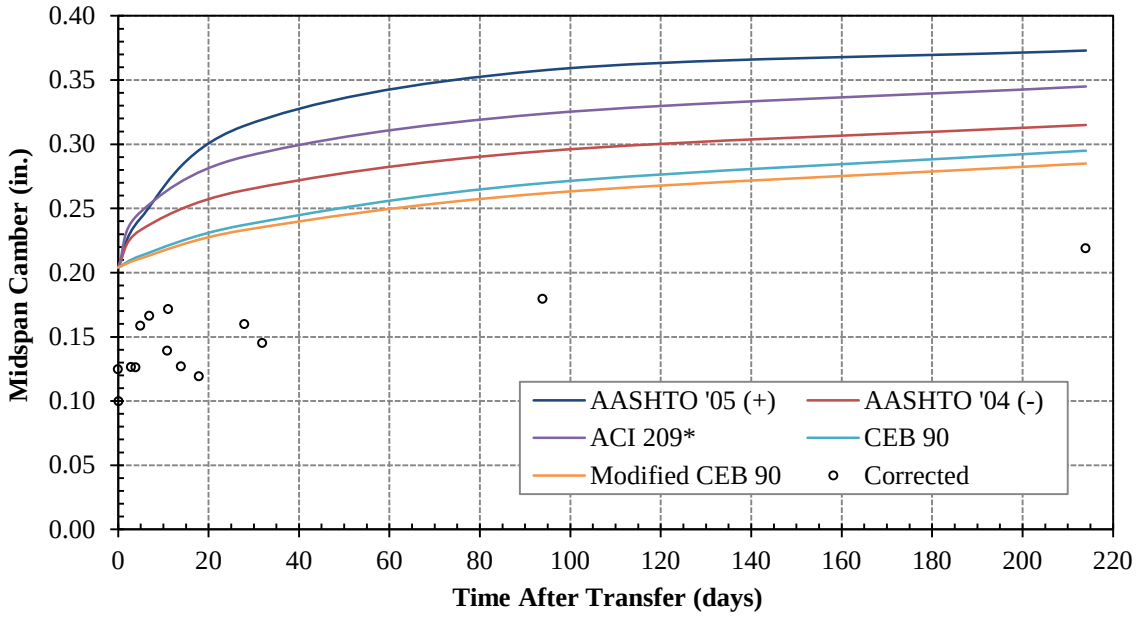

Figure G-6: SCC-HS-2 Predicted Camber with Two-Point E_c

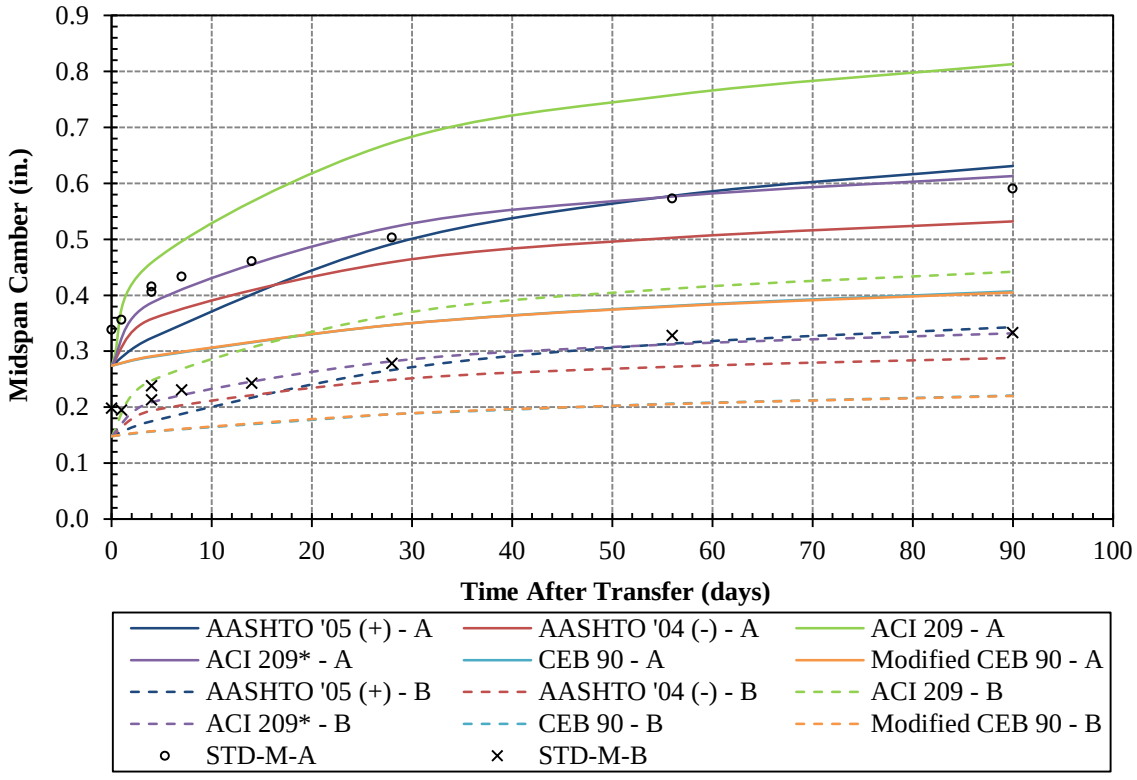

Figure G-7: STD-M-A, B Predicted Camber with Two-Point E_c

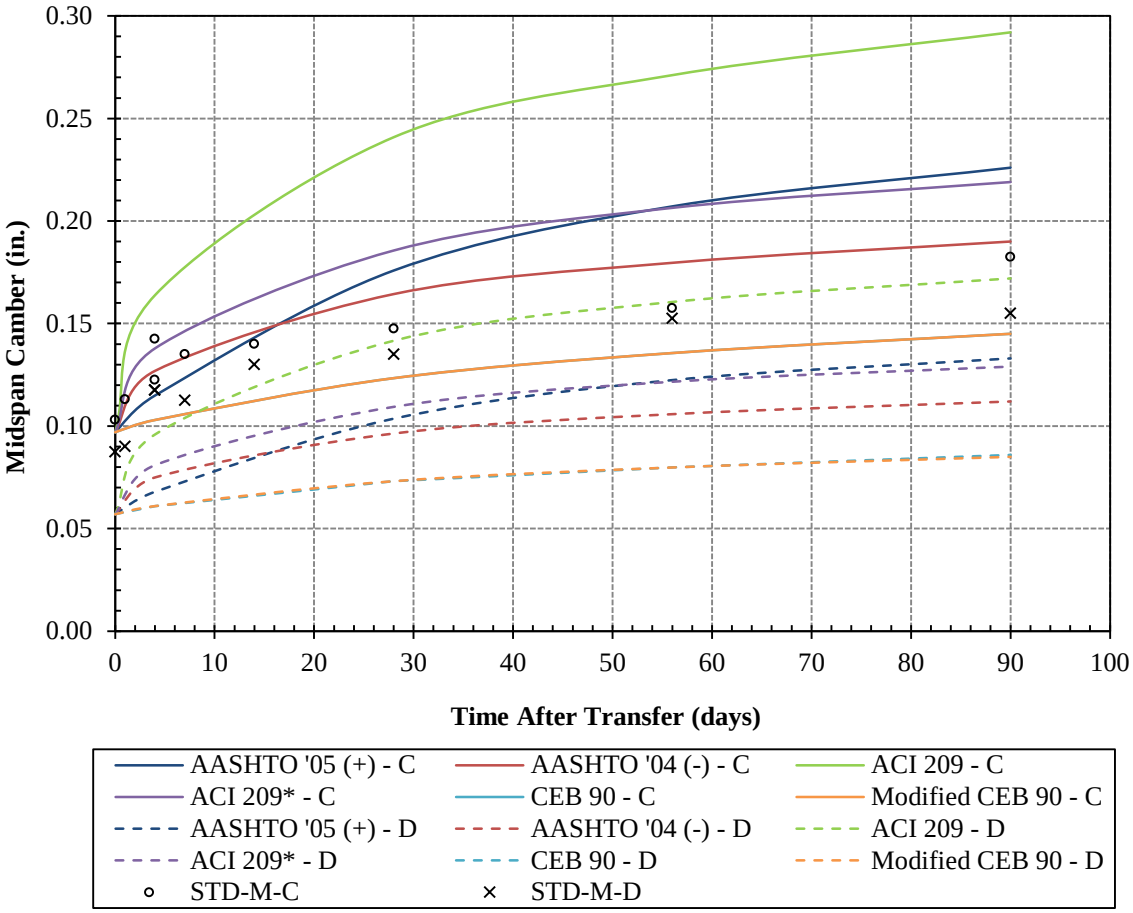

Figure G-8: STD-M-C, D Predicted Camber with Two-Point E_c

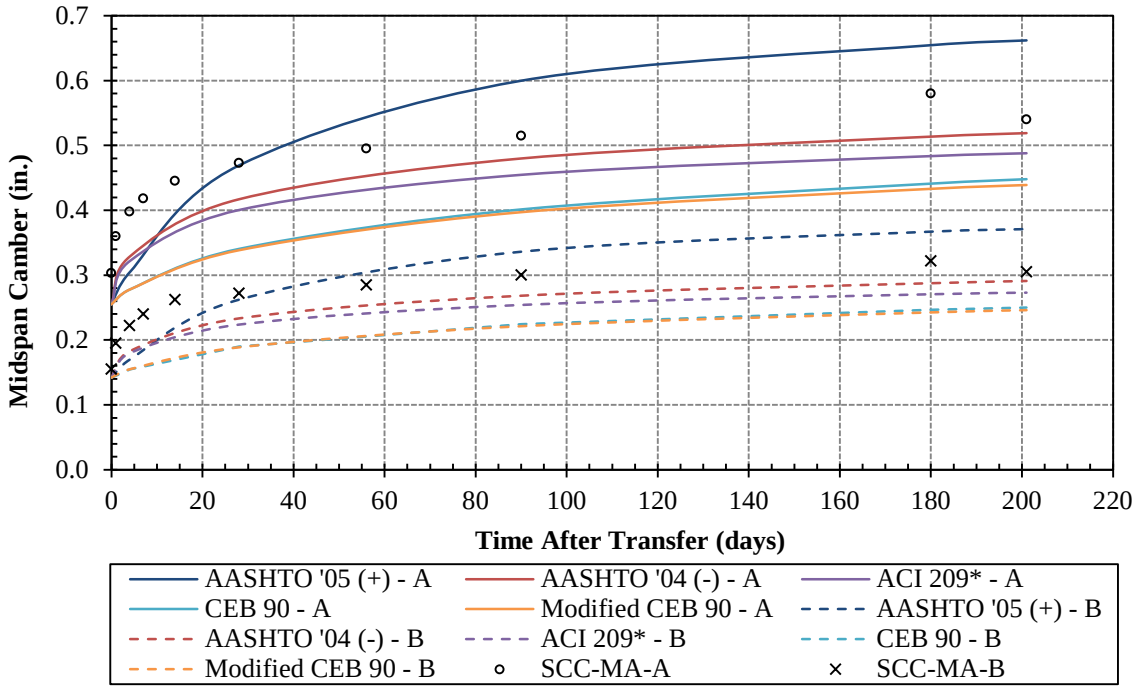

Figure G-9: SCC-MA-A, B Predicted Camber with Two-Point E_c

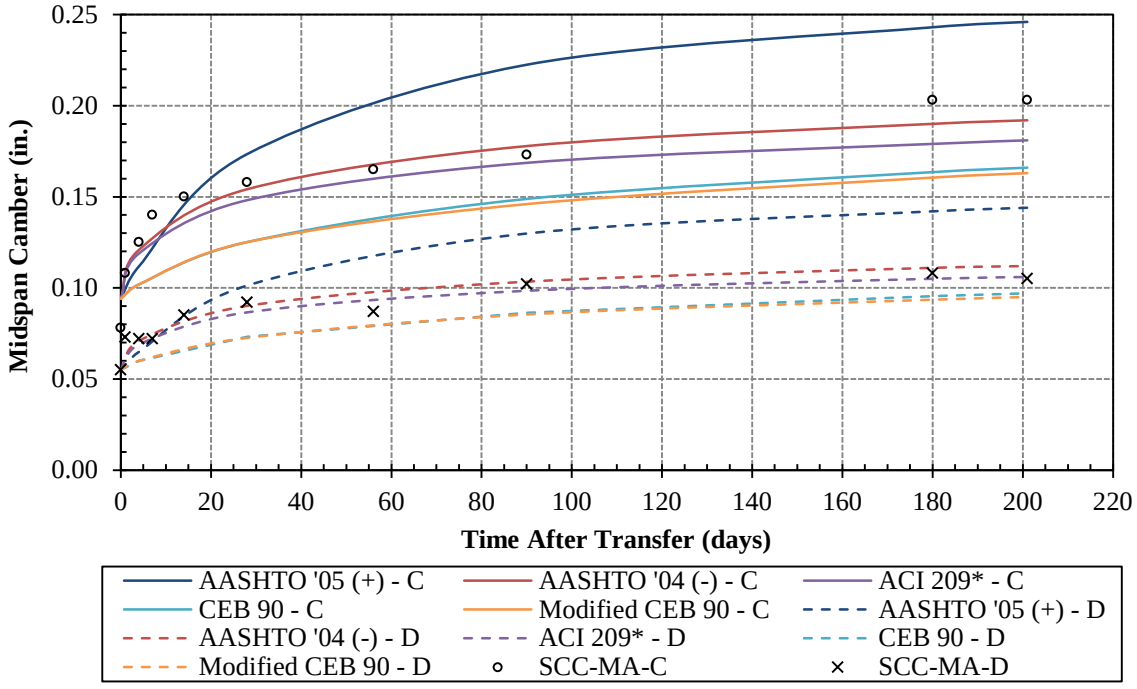

Figure G-10: SCC-MA-C, D Predicted Camber with Two-Point E_c

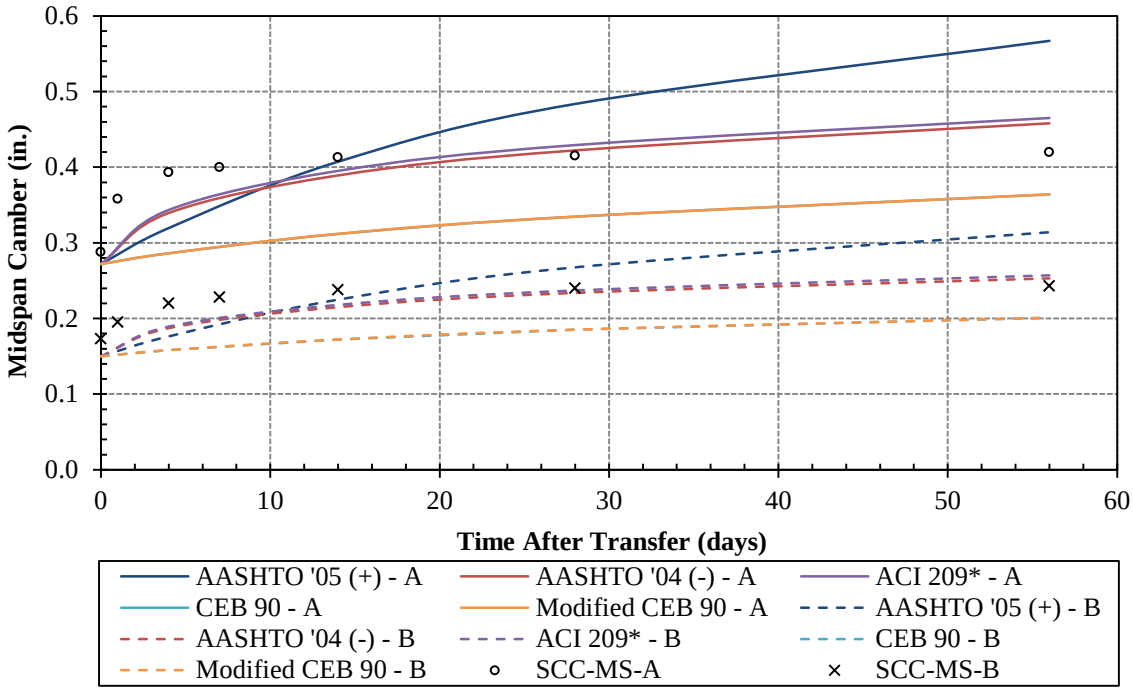

Figure G-11: SCC-MS-A, B Predicted Camber with Two-Point E_c

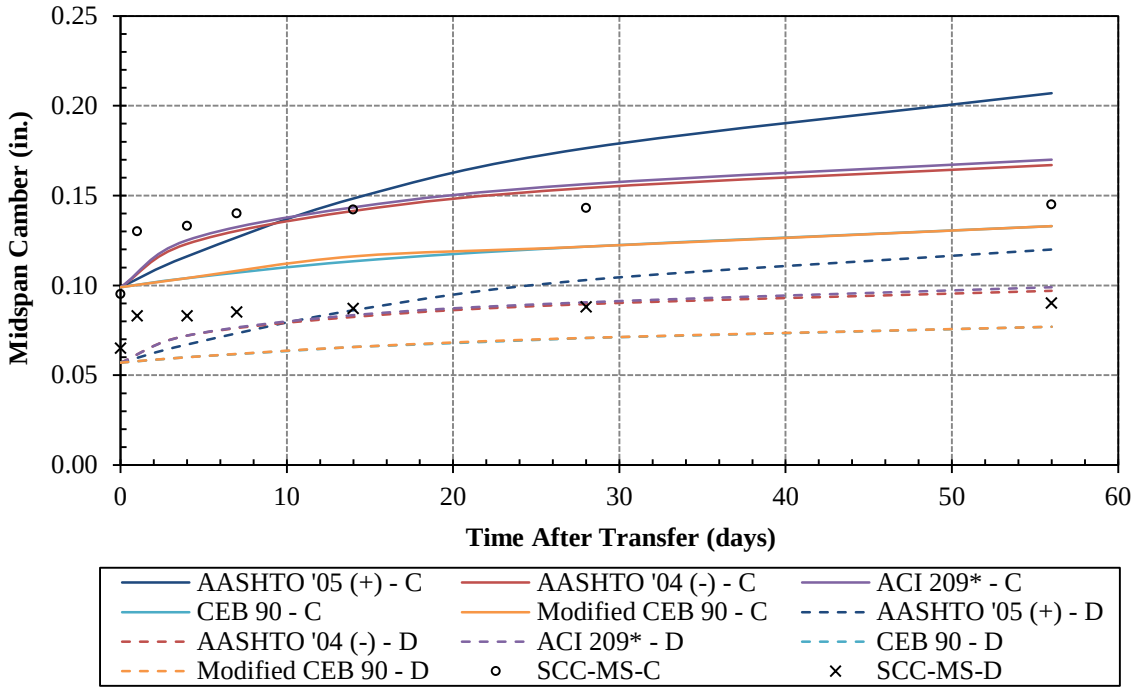

Figure G-12: SCC-MS-C, D Predicted Camber with Two-Point E_c

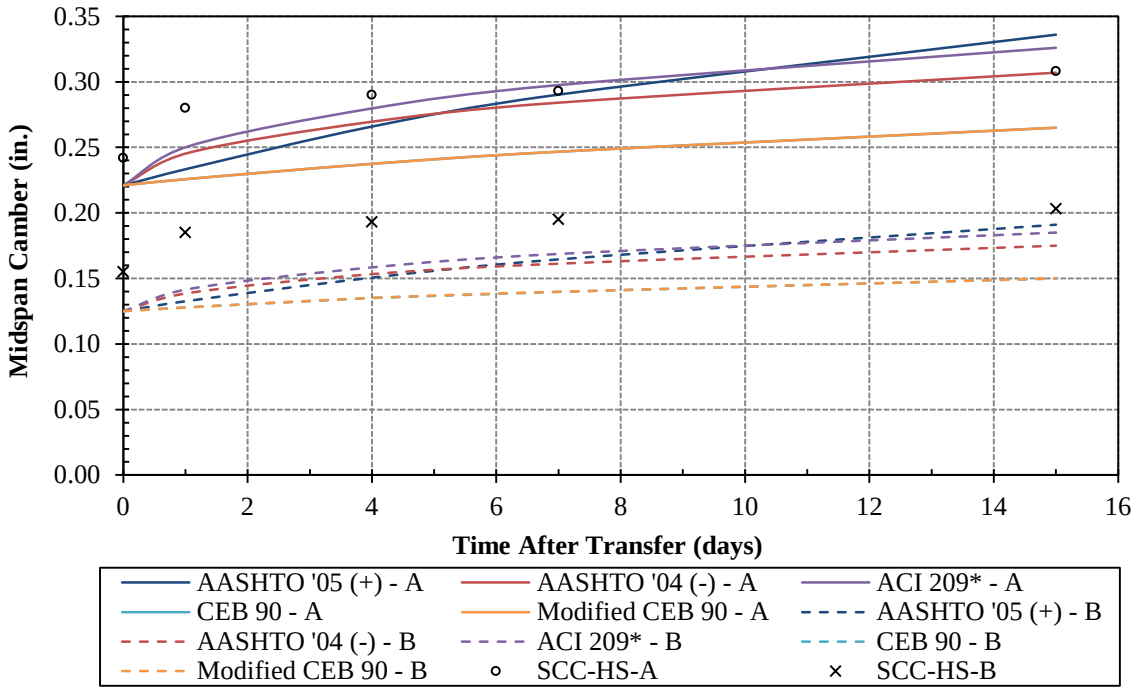

Figure G-13: SCC-HS-A, B Predicted Camber with Two-Point E_c

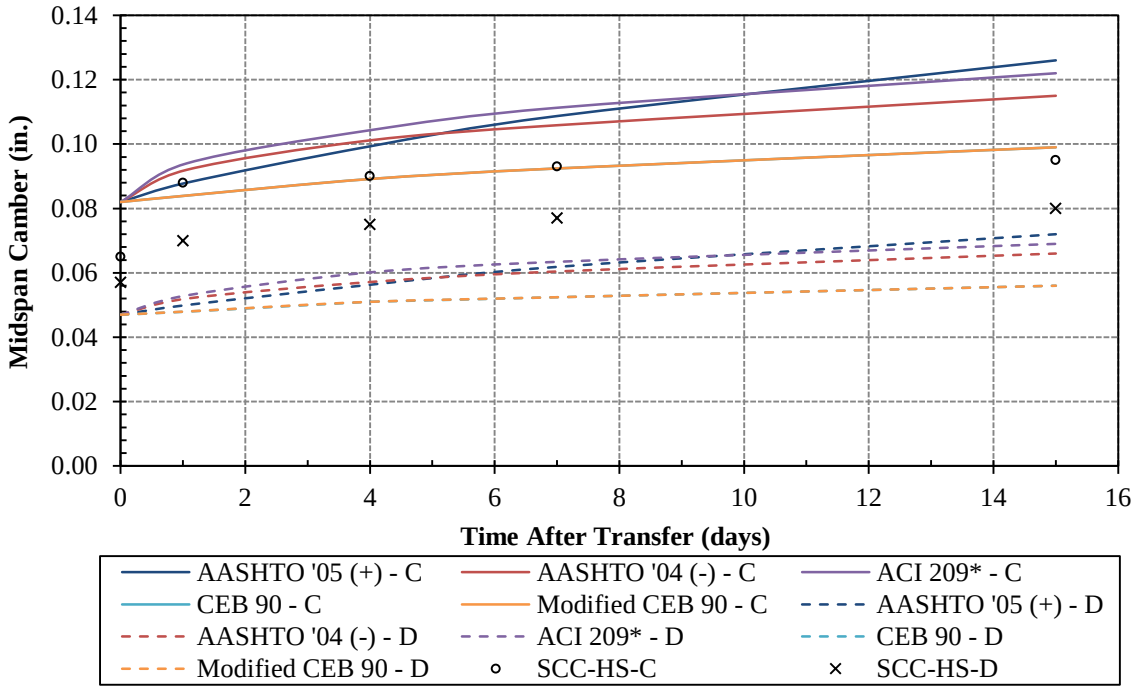

Figure G-14: SCC-HS-C, D Predicted Camber with Two-Point E_c

Table G-1: STD-M (AASHTO Type I) Percent Error in Camber

	STD-M-1						STD-M-2					
	Creep and Shrinkage Model						Creep and Shrinkage Model					
	AASHTO '05 (+)	AASHTO '04 (-)	ACI 209	ACI 209*	CEB 90	Modified CEB 90	AASHTO '05 (+)	AASHTO '04 (-)	ACI 209	ACI 209*	CEB 90	Modified CEB 90
Ec Model	Initial Camber						Initial Camber					
AASHTO '05 (+)	12.3	12.3	12.3	12.3	12.3	12.3	13.3	13.3	13.3	13.3	13.3	13.3
ACI 209	12.3	12.3	12.3	12.3	12.3	12.3	13.3	13.3	13.3	13.3	13.3	13.3
CEB 90-RS	-1.4	-1.4	-1.4	-1.4	-1.4	-1.4	-3.2	-3.2	-3.2	-3.2	-3.2	-3.2
Constant Ec	-17.5	-17.5	-17.5	-17.5	-17.5	-17.5	-16.8	-16.8	-16.8	-16.8	-16.8	-16.8
2-Point	-17.5	-17.5	-17.5	-17.5	-17.5	-17.5	-16.8	-16.8	-16.8	-16.8	-16.8	-16.8
Ec Model	Camber at 1 Day						Camber at 1 Day					
AASHTO '05 (+)	-9.2	-4.8	0.8	-3.0	-10.3	1.3	5.9	10.4	16.9	13.1	4.4	17.5
ACI 209	-9.2	-4.8	0.8	-3.0	-10.3	1.3	5.9	10.4	16.9	13.1	4.4	17.5
CEB 90-RS	-20.6	-16.5	-11.6	-14.9	-21.6	-11.3	-10.0	-5.8	-0.1	-3.7	-11.2	0.2
Constant Ec	-32.7	-30.1	-25.5	-28.3	-34.2	-25.5	-22.3	-19.0	-13.9	-16.9	-23.5	-13.6
2-Point	-33.0	-30.1	-25.5	-28.3	-34.2	-25.2	-22.0	-18.7	-13.3	-16.6	-23.5	-13.3
Ec Model	Camber at 6.91 Days						Camber at 6.91 Days					
AASHTO '05 (+)	-7.2	-6.3	6.2	-2.4	-15.8	-0.4	4.6	4.8	19.4	10.2	-5.4	11.5
ACI 209	-7.2	-6.3	6.2	-2.4	-15.8	-0.4	4.6	4.8	19.4	10.2	-5.4	11.5
CEB 90-RS	-18.8	-18.1	-6.7	-14.2	-26.3	-12.6	-10.8	-10.8	2.0	-5.9	-19.5	-4.9
Constant Ec	-31.2	-31.7	-21.0	-27.6	-38.3	-26.5	-23.0	-23.0	-11.8	-19.0	-30.5	-17.9
2-Point	-31.2	-31.2	-21.0	-27.6	-38.1	-26.3	-22.3	-23.3	-11.3	-18.4	-30.5	-17.4
Ec Model	Camber at 33.48 Days						Camber at 33.48 Days					
AASHTO '05 (+)	5.2	-9.0	9.2	-4.0	-18.1	-3.6	17.0	0.0	20.8	6.8	-9.7	5.9
ACI 209	5.2	-9.0	9.2	-4.0	-18.1	-3.6	17.0	0.0	20.8	6.8	-9.7	5.9
CEB 90-RS	-7.6	-20.4	-4.0	-15.6	-28.2	-15.4	-0.2	-15.0	3.2	-8.9	-23.1	-9.5
Constant Ec	-21.9	-34.1	-18.9	-28.8	-39.7	-28.8	-13.5	-26.7	-10.6	-21.2	-33.7	-21.8
2-Point	-21.6	-33.4	-18.5	-28.6	-39.5	-28.4	-12.7	-26.7	-9.7	-20.5	-33.3	-21.2
Ec Model	Camber at 69.68 Days						Camber at 69.68 Days					
AASHTO '05 (+)	8.0	-12.2	6.6	-7.9	-19.7	-6.7	20.2	-3.7	17.9	2.5	-11.3	2.4
ACI 209	8.0	-12.2	6.6	-7.9	-19.7	-6.7	20.2	-3.7	17.9	2.5	-11.3	2.4
CEB 90-RS	-5.0	-23.3	-6.2	-19.0	-29.4	-18.2	2.9	-18.2	1.0	-12.3	-24.4	-12.5
Constant Ec	-19.5	-36.4	-20.7	-31.7	-40.7	-31.0	-10.9	-29.4	-12.5	-24.2	-34.9	-24.4
2-Point	-19.0	-35.6	-20.2	-31.3	-40.4	-30.5	-9.8	-29.4	-11.5	-23.5	-34.3	-23.7
Ec Model	Camber at 110 Days						Camber at 110 Days					
AASHTO '05 (+)	15.7	-7.9	12.1	-3.8	-14.3	-1.6	25.5	-1.9	20.9	4.2	-8.2	5.1
ACI 209	15.7	-7.9	12.1	-3.8	-14.3	-1.6	25.5	-1.9	20.9	4.2	-8.2	5.1
CEB 90-RS	2.0	-19.4	-1.3	-15.5	-24.7	-13.4	7.5	-16.6	3.4	-10.8	-21.6	-10.1
Constant Ec	-13.7	-33.3	-18.1	-28.7	-36.7	-27.1	-6.8	-27.9	-10.3	-23.1	-32.3	-22.3
2-Point	-12.9	-32.3	-15.8	-28.2	-36.4	-26.6	-5.6	-27.9	-9.3	-22.1	-31.8	-21.6

Table G-2: STD-M (AASHTO Type I) Percent Error in Camber Growth

	STD-M-1						STD-M-2					
	Creep and Shrinkage Model						Creep and Shrinkage Model					
	AASHTO '05 (+)	AASHTO '04 (-)	ACI 209	ACI 209*	CEB 90	Modified CEB 90	AASHTO '05 (+)	AASHTO '04 (-)	ACI 209	ACI 209*	CEB 90	Modified CEB 90
Ec Model	Camber Growth at 1 Day						Camber Growth at 1 Day					
AASHTO '05 (+)	-91.3	-72.7	-48.6	-65.0	-95.6	-46.4	-73.3	-28.7	36.6	-2.0	-88.1	42.6
ACI 209	-91.3	-72.7	-48.6	-65.0	-95.6	-46.4	-73.3	-28.7	36.6	-2.0	-88.1	42.6
CEB 90-RS	-92.5	-72.6	-49.0	-65.1	-97.5	-47.7	-79.1	-30.5	35.5	-6.2	-93.0	39.0
Constant Ec	-87.8	-72.9	-46.2	-62.5	-96.7	-46.2	-74.9	-30.5	38.2	-2.2	-91.1	42.3
2-Point	-89.3	-72.9	-46.2	-62.5	-96.7	-44.7	-70.9	-26.4	46.3	1.9	-91.1	46.3
Ec Model	Camber Growth at 6.91 Days						Camber Growth at 6.91 Days					
AASHTO '05 (+)	-56.9	-54.3	-17.8	-43.0	-82.1	-37.1	-34.3	-33.3	24.3	-12.1	-73.7	-7.0
ACI 209	-56.9	-54.3	-17.8	-43.0	-82.1	-37.1	-34.3	-33.3	24.3	-12.1	-73.7	-7.0
CEB 90-RS	-57.7	-55.5	-17.7	-42.6	-82.6	-37.4	-35.0	-35.0	24.2	-12.5	-75.2	-7.8
Constant Ec	-54.7	-56.5	-14.2	-40.3	-82.7	-35.8	-33.7	-33.7	26.8	-11.7	-73.6	-6.2
2-Point	-54.7	-54.7	-14.2	-40.3	-81.8	-34.9	-29.6	-35.1	29.5	-9.0	-73.6	-3.5
Ec Model	Camber Growth at 33.48 Days						Camber Growth at 33.48 Days					
AASHTO '05 (+)	-15.3	-45.6	-6.7	-34.9	-65.2	-34.1	9.2	-32.8	18.7	-16.0	-56.9	-18.1
ACI 209	-15.3	-45.6	-6.7	-34.9	-65.2	-34.1	9.2	-32.8	18.7	-16.0	-56.9	-18.1
CEB 90-RS	-15.2	-46.4	-6.3	-34.7	-65.5	-34.3	8.7	-34.3	18.6	-16.5	-57.6	-18.3
Constant Ec	-13.0	-48.7	-4.1	-33.1	-64.8	-33.1	10.9	-33.4	20.9	-14.8	-57.0	-17.0
2-Point	-11.9	-46.4	-3.0	-32.5	-64.2	-31.9	13.7	-33.4	23.7	-12.7	-55.6	-14.8
Ec Model	Camber Growth at 69.68 Days						Camber Growth at 69.68 Days					
AASHTO '05 (+)	-8.1	-45.7	-10.6	-37.8	-59.8	-35.5	20.2	-3.7	17.9	2.5	-11.3	2.4
ACI 209	-8.1	-45.7	-10.6	-37.8	-59.8	-35.5	20.2	-3.7	17.9	2.5	-11.3	2.4
CEB 90-RS	-7.6	-46.6	-10.2	-37.5	-59.6	-35.6	2.9	-18.2	1.0	-12.3	-24.4	-12.5
Constant Ec	-5.2	-48.2	-8.3	-36.1	-59.1	-34.3	-10.9	-29.4	-12.5	-24.2	-34.9	-24.4
2-Point	-3.9	-46.1	-7.0	-35.2	-58.2	-33.0	-9.8	-29.4	-11.5	-23.5	-34.3	-23.7
Ec Model	Camber Growth at 110 Days						Camber Growth at 110 Days					
AASHTO '05 (+)	6.4	-38.0	-0.4	-30.3	-49.9	-26.1	25.5	-1.9	20.9	4.2	-8.2	5.1
ACI 209	6.4	-38.0	-0.4	-30.3	-49.9	-26.1	25.5	-1.9	20.9	4.2	-8.2	5.1
CEB 90-RS	7.3	-38.5	0.3	-30.1	-49.8	-25.7	7.5	-16.6	3.4	-10.8	-21.6	-10.1
Constant Ec	9.7	-40.4	-1.5	-28.6	-49.2	-24.7	-6.8	-27.9	-10.3	-23.1	-32.3	-22.3
2-Point	11.6	-37.8	4.2	-27.3	-48.3	-23.4	-5.6	-27.9	-9.3	-22.1	-31.8	-21.6

Table G-3: SCC-MS (AASHTO Type I) Percent Error in Camber

	SCC-MS-1						SCC-MS-2					
	Creep and Shrinkage Model						Creep and Shrinkage Model					
	AASHTO '05 (+)	AASHTO '04 (-)	ACI 209	ACI 209*	CEB 90	Modified CEB 90	AASHTO '05 (+)	AASHTO '04 (-)	ACI 209	ACI 209*	CEB 90	Modified CEB 90
Ec Model	Initial Camber						Initial Camber					
AASHTO '05 (+)	19.8	19.8	19.8	19.8	19.8	19.8	47.2	47.2	47.2	47.2	47.2	47.2
ACI 209	19.8	19.8	19.8	19.8	19.8	19.8	47.2	47.2	47.2	47.2	47.2	47.2
CEB 90-RS	0.7	0.7	0.7	0.7	0.7	0.7	25.0	25.0	25.0	25.0	25.0	25.0
Constant Ec	2.6	2.6	2.6	2.6	2.6	2.6	27.8	27.8	27.8	27.8	27.8	27.8
2-Point	2.6	2.6	2.6	2.6	2.6	2.6	27.8	27.8	27.8	27.8	27.8	27.8
Ec Model	Camber at 2.88 Days						Camber at 3.00 Days					
AASHTO '05 (+)	-9.1	-6.2	22.8	-4.7	-14.8	-15.0	13.2	16.8	55.6	18.5	5.9	5.3
ACI 209	-9.1	-6.2	22.8	-4.7	-14.8	-15.0	13.2	16.8	55.6	18.5	5.9	5.3
CEB 90-RS	-23.8	-21.5	3.4	-20.2	-28.5	-28.5	-3.9	-1.0	32.3	0.7	-10.2	-10.2
Constant Ec	-22.3	-20.2	4.9	-18.6	-27.2	-27.7	-1.6	1.0	35.2	3.0	-8.2	-8.5
2-Point	-21.8	-19.9	6.7	-17.9	-27.2	-27.5	-1.0	1.3	37.5	4.0	-7.9	-8.2
Ec Model	Camber at 7.18 Days						Camber at 6.70 Days					
AASHTO '05 (+)	-0.6	-2.7	40.5	-0.4	-13.8	-14.5	18.5	16.6	70.1	19.4	3.2	2.6
ACI 209	-0.6	-2.7	40.5	-0.4	-13.8	-14.5	18.5	16.6	70.1	19.4	3.2	2.6
CEB 90-RS	-16.8	-18.6	18.3	-16.5	-27.6	-27.9	0.4	-1.1	44.9	1.4	-12.3	-12.3
Constant Ec	-15.3	-17.0	20.3	-15.0	-26.4	-27.1	2.9	1.1	48.0	3.6	-10.4	-11.1
2-Point	-14.3	-17.0	22.6	-14.3	-26.1	-26.9	3.9	1.4	50.8	4.5	-10.1	-10.8
Ec Model	Camber at 23.53 Days						Camber at 23.84 Days					
AASHTO '05 (+)	20.4	3.1	66.9	5.8	-10.3	-11.5	48.1	25.3	109.2	29.8	9.7	7.9
ACI 209	20.4	3.1	66.9	5.8	-10.3	-11.5	48.1	25.3	109.2	29.8	9.7	7.9
CEB 90-RS	1.0	-13.7	40.8	-11.3	-24.7	-25.2	25.7	7.2	78.4	10.2	-6.8	-7.1
Constant Ec	2.7	-12.5	42.7	-9.8	-23.5	-24.7	28.3	9.3	81.7	12.3	-4.9	-6.4
2-Point	4.1	-12.2	45.8	-8.6	-23.0	-24.2	30.1	9.6	85.9	13.8	-4.1	-5.8
Ec Model	Camber at 89.84 Days						Camber at 89.84 Days					
AASHTO '05 (+)	38.0	4.3	82.4	5.6	-8.3	-10.5	68.8	27.4	128.3	29.2	11.8	8.9
ACI 209	38.0	4.3	82.4	5.6	-8.3	-10.5	68.8	27.4	128.3	29.2	11.8	8.9
CEB 90-RS	16.1	-12.8	54.0	-11.6	-23.1	-24.0	43.6	7.8	95.1	9.6	-5.2	-6.3
Constant Ec	17.5	-11.7	55.9	-10.3	-21.9	-23.8	46.0	9.9	98.0	11.4	-3.3	-5.7
2-Point	19.7	-11.0	59.7	-8.9	-21.1	-23.0	48.9	10.5	103.1	13.3	-2.2	-4.7
Ec Model	Camber at 160 Days						Camber at 167 Days					
AASHTO '05 (+)	43.8	7.0	90.3	7.2	-4.7	-7.3	67.8	24.8	127.2	24.8	10.9	7.5
ACI 209	43.8	7.0	90.3	7.2	-4.7	-7.3	67.8	24.8	127.2	24.8	10.9	7.5
CEB 90-RS	21.2	-10.4	60.9	-10.0	-19.9	-21.3	42.9	5.6	94.3	6.1	-5.9	-7.3
Constant Ec	22.7	-9.4	62.5	-9.0	-18.8	-21.1	45.1	7.3	97.3	7.8	-4.2	-7.1
2-Point	24.9	-8.6	66.6	-7.3	-17.8	-20.3	48.0	8.3	102.4	9.7	-3.0	-5.9

Table G-4: SCC-MS (AASHTO Type I) Percent Error in Camber Growth

	SCC-MS-1						SCC-MS-2					
	Creep and Shrinkage Model						Creep and Shrinkage Model					
	AASHTO '05 (+)	AASHTO '04 (-)	ACI 209	ACI 209*	CEB 90	Modified CEB 90	AASHTO '05 (+)	AASHTO '04 (-)	ACI 209	ACI 209*	CEB 90	Modified CEB 90
Ec Model	Camber Growth at 2.88 Days						Camber Growth at 3 Days					
AASHTO '05 (+)	-77.7	-70.0	8.0	-65.9	-93.0	-93.7	-76.4	-68.2	19.0	-64.5	-92.6	-94.1
ACI 209	-77.7	-70.0	8.0	-65.9	-93.0	-93.7	-76.4	-68.2	19.0	-64.5	-92.6	-94.1
CEB 90-RS	-78.4	-71.0	8.6	-66.8	-93.4	-93.4	-76.5	-68.7	19.2	-64.3	-93.0	-93.0
Constant Ec	-78.0	-71.5	7.5	-66.6	-93.5	-95.1	-76.2	-69.4	19.1	-64.3	-93.2	-94.0
2-Point	-76.4	-70.7	13.2	-64.2	-93.5	-94.3	-74.5	-68.5	25.1	-61.7	-92.3	-93.2
Ec Model	Camber Growth at 7.18 Days						Camber Growth at 6.70 Days					
AASHTO '05 (+)	-52.0	-57.1	52.3	-51.4	-85.3	-87.2	-57.2	-60.9	45.7	-55.4	-87.6	-88.8
ACI 209	-52.0	-57.1	52.3	-51.4	-85.3	-87.2	-57.2	-60.9	45.7	-55.4	-87.6	-88.8
CEB 90-RS	-52.8	-58.1	53.1	-52.0	-85.5	-86.3	-57.7	-61.3	46.7	-55.5	-87.6	-87.6
Constant Ec	-52.9	-58.1	52.6	-52.1	-85.8	-88.0	-57.2	-61.5	46.3	-55.8	-87.9	-89.3
2-Point	-49.9	-58.1	59.3	-49.9	-85.0	-87.3	-55.0	-60.7	52.7	-53.6	-87.2	-88.6
Ec Model	Camber Growth at 23.53 Days						Camber Growth at 23.84 Days					
AASHTO '05 (+)	1.3	-38.5	108.7	-32.5	-69.5	-72.3	1.6	-40.9	116.1	-32.6	-70.2	-73.5
ACI 209	1.3	-38.5	108.7	-32.5	-69.5	-72.3	1.6	-40.9	116.1	-32.6	-70.2	-73.5
CEB 90-RS	0.8	-39.4	110.2	-32.8	-69.7	-71.0	1.4	-39.2	117.7	-32.6	-70.2	-70.8
Constant Ec	0.3	-40.5	108.3	-33.4	-70.2	-73.5	1.0	-39.9	116.1	-33.4	-70.7	-73.9
2-Point	4.2	-39.8	116.7	-30.1	-68.9	-72.2	4.9	-39.2	125.0	-30.2	-68.9	-72.6
Ec Model	Camber Growth at 89.84 Days						Camber Growth at 89.84 Days					
AASHTO '05 (+)	34.8	-29.7	119.5	-27.2	-53.8	-58.0	33.4	-30.6	125.4	-27.8	-54.7	-59.2
ACI 209	34.8	-29.7	119.5	-27.2	-53.8	-58.0	33.4	-30.6	125.4	-27.8	-54.7	-59.2
CEB 90-RS	35.0	-30.7	121.3	-28.0	-54.1	-56.2	33.8	-31.3	127.6	-28.1	-54.9	-56.9
Constant Ec	33.5	-31.7	119.1	-28.8	-54.6	-58.9	32.2	-32.0	125.0	-29.3	-55.5	-59.8
2-Point	38.2	-30.3	127.6	-25.5	-52.8	-57.0	37.4	-31.0	134.0	-25.9	-53.6	-57.9
Ec Model	Camber Growth at 160 Days						Camber Growth at 167 Days					
AASHTO '05 (+)	44.2	-23.6	129.7	-23.2	-45.1	-50.0	28.9	-31.4	112.6	-31.4	-51.0	-55.8
ACI 209	44.2	-23.6	129.7	-23.2	-45.1	-50.0	28.9	-31.4	112.6	-31.4	-51.0	-55.8
CEB 90-RS	45.0	-24.3	132.0	-23.4	-45.0	-48.2	29.6	-32.2	114.8	-31.4	-51.2	-53.6
Constant Ec	43.3	-25.7	129.1	-24.8	-46.1	-50.9	27.9	-33.3	112.4	-32.5	-51.8	-56.6
2-Point	48.1	-23.9	137.9	-21.3	-43.8	-49.1	32.6	-31.7	120.7	-29.3	-49.9	-54.6

Table G-5: SCC-HS (AASHTO Type I) Percent Error in Camber

	SCC-HS-1						SCC-HS-2					
	Creep and Shrinkage Model						Creep and Shrinkage Model					
	AASHTO '05 (+)	AASHTO '04 (-)	ACI 209	ACI 209*	CEB 90	Modified CEB 90	AASHTO '05 (+)	AASHTO '04 (-)	ACI 209	ACI 209*	CEB 90	Modified CEB 90
Ec Model	Initial Camber						Initial Camber					
AASHTO '05 (+)	28.1	28.1	28.1	28.1	28.1	28.1	79.0	79.0	79.0	79.0	79.0	79.0
ACI 209	28.1	28.1	28.1	28.1	28.1	28.1	79.0	79.0	79.0	79.0	79.0	79.0
CEB 90-RS	37.9	37.9	37.9	37.9	37.9	37.9	88.7	88.7	88.7	88.7	88.7	88.7
Constant Ec	17.7	17.7	17.7	17.7	17.7	17.7	63.8	63.8	63.8	63.8	63.8	63.8
2-Point	17.7	17.7	17.7	17.7	17.7	17.7	63.8	63.8	63.8	63.8	63.8	63.8
Ec Model	Camber at 4.88 Days						Camber at 4.88 Days					
AASHTO '05 (+)	22.5	18.8	73.2	24.9	8.5	8.0	65.2	60.2	133.9	68.4	46.3	45.0
ACI 209	22.5	18.8	73.2	24.9	8.5	8.0	65.2	60.2	133.9	68.4	46.3	45.0
CEB 90-RS	31.5	27.7	86.4	34.3	16.9	16.9	73.4	68.4	146.6	77.2	53.9	53.9
Constant Ec	12.7	9.4	60.1	15.0	0.0	-0.9	51.3	46.3	115.7	54.5	33.7	33.1
2-Point	13.1	9.4	62.4	16.0	0.0	-0.5	52.6	46.9	118.8	55.8	34.3	33.1
Ec Model	Camber at 27.62 Days						Camber at 27.62 Days					
AASHTO '05 (+)	57.8	35.4	140.9	45.7	20.9	18.6	112.8	81.5	224.9	96.5	62.1	59.0
ACI 209	57.8	35.4	140.9	45.7	20.9	18.6	112.8	81.5	224.9	96.5	62.1	59.0
CEB 90-RS	69.5	44.8	158.2	56.4	29.8	29.3	123.5	90.3	241.8	105.9	70.3	69.6
Constant Ec	45.2	23.7	122.7	34.0	11.1	9.3	95.3	65.2	199.8	79.0	48.3	45.2
2-Point	46.6	23.7	126.0	35.0	11.6	9.7	96.5	65.2	204.2	81.5	48.3	45.8
Ec Model	Camber at 93.93 Days						Camber at 93.93 Days					
AASHTO '05 (+)	55.8	30.7	154.4	41.2	18.6	15.8	116.0	80.3	252.7	95.9	63.2	59.1
ACI 209	55.8	30.7	154.4	41.2	18.6	15.8	116.0	80.3	252.7	95.9	63.2	59.1
CEB 90-RS	66.7	39.7	171.9	51.3	27.5	26.0	126.6	88.7	271.1	105.5	72.0	69.8
Constant Ec	43.2	19.4	134.6	29.5	8.9	6.5	97.6	64.1	225.3	79.2	49.7	45.2
2-Point	44.5	19.8	138.6	31.5	9.8	6.9	99.3	64.2	229.8	80.4	50.3	45.8
Ec Model	Camber at 214 Days						Camber at 214 Days					
AASHTO '05 (+)	37.4	18.3	137.9	27.2	10.1	6.7	84.6	58.1	219.9	70.9	46.7	41.7
ACI 209	37.4	18.3	137.9	27.2	10.1	6.7	84.6	58.1	219.9	70.9	46.7	41.7
CEB 90-RS	47.3	26.5	154.0	36.1	18.3	16.2	93.8	65.4	235.9	79.1	54.0	51.7
Constant Ec	26.5	8.4	119.5	16.6	1.2	-1.9	69.1	43.9	194.7	56.3	34.4	29.8
2-Point	27.5	8.7	122.9	17.9	1.9	-1.5	70.5	43.9	198.9	57.7	34.8	30.2

Table G-6: SCC-HS (AASHTO Type I) Percent Error in Camber Growth

	SCC-HS-1						SCC-HS-2					
	Creep and Shrinkage Model						Creep and Shrinkage Model					
	AASHTO '05 (+)	AASHTO '04 (-)	ACI 209	ACI 209*	CEB 90	Modified CEB 90	AASHTO '05 (+)	AASHTO '04 (-)	ACI 209	ACI 209*	CEB 90	Modified CEB 90
Ec Model	Camber Growth at 4.88 Days						Camber Growth at 4.88 Days					
AASHTO '05 (+)	-23.2	-39.0	189.4	-13.4	-82.3	-84.2	-36.0	-49.1	143.0	-27.7	-85.2	-88.5
ACI 209	-23.2	-39.0	189.4	-13.4	-82.3	-84.2	-36.0	-49.1	143.0	-27.7	-85.2	-88.5
CEB 90-RS	-25.0	-39.6	189.0	-14.0	-81.7	-81.7	-37.7	-50.1	143.1	-28.3	-86.0	-86.0
Constant Ec	-22.9	-37.9	193.6	-12.1	-80.7	-85.0	-35.4	-49.7	147.7	-26.4	-85.6	-87.4
2-Point	-20.7	-37.9	204.3	-7.9	-80.7	-82.9	-31.8	-47.9	156.7	-22.8	-83.8	-87.4
Ec Model	Camber Growth at 27.62 Days						Camber Growth at 27.62 Days					
AASHTO '05 (+)	121.9	30.1	462.5	72.2	-29.2	-38.8	85.7	6.3	369.8	44.4	-42.9	-50.8
ACI 209	121.9	30.1	462.5	72.2	-29.2	-38.8	85.7	6.3	369.8	44.4	-42.9	-50.8
CEB 90-RS	120.4	26.2	458.0	70.6	-30.7	-32.5	83.7	3.9	368.4	41.6	-44.3	-45.8
Constant Ec	122.8	27.0	468.4	72.8	-29.2	-37.5	87.4	4.1	377.1	42.3	-42.7	-51.4
2-Point	129.0	27.0	483.0	77.0	-27.1	-35.5	90.8	4.1	389.2	49.2	-42.7	-49.7
Ec Model	Camber Growth at 93.93 Days						Camber Growth at 93.93 Days					
AASHTO '05 (+)	72.2	6.9	329.2	34.3	-24.6	-31.9	67.5	2.4	317.3	30.9	-28.9	-36.3
ACI 209	72.2	6.9	329.2	34.3	-24.6	-31.9	67.5	2.4	317.3	30.9	-28.9	-36.3
CEB 90-RS	69.7	4.3	324.2	32.5	-25.0	-28.8	65.8	0.1	316.3	29.1	-28.8	-32.7
Constant Ec	72.3	4.9	331.5	33.5	-24.8	-31.8	67.6	0.7	322.6	30.8	-28.1	-37.1
2-Point	75.9	6.0	342.9	39.1	-22.5	-30.6	70.9	0.8	331.6	33.2	-26.9	-35.8
Ec Model	Camber Growth at 214 Days						Camber Growth at 214 Days					
AASHTO '05 (+)	17.9	-18.7	210.6	-1.7	-34.5	-41.0	7.3	-27.1	182.7	-10.5	-41.9	-48.4
ACI 209	17.9	-18.7	210.6	-1.7	-34.5	-41.0	7.3	-27.1	182.7	-10.5	-41.9	-48.4
CEB 90-RS	16.9	-20.3	206.8	-3.2	-34.9	-38.5	6.3	-28.6	181.2	-11.7	-42.6	-45.5
Constant Ec	18.4	-19.4	212.3	-2.3	-34.4	-40.8	7.5	-28.1	185.7	-10.6	-41.7	-48.2
2-Point	20.5	-18.7	219.5	0.5	-33.0	-40.1	9.5	-28.1	191.5	-8.7	-41.1	-47.5

Table G-7: STD-M-A & -B Percent Error in Camber

	STD-M-A						STD-M-B					
	Creep and Shrinkage Model						Creep and Shrinkage Model					
	AASHTO '05 (+)	AASHTO '04 (-)	ACI 209	ACI 209*	CEB 90	Modified CEB 90	AASHTO '05 (+)	AASHTO '04 (-)	ACI 209	ACI 209*	CEB 90	Modified CEB 90
Ec Model	Initial Camber						Initial Camber					
AASHTO '05 (+)	-0.9	-0.9	-0.9	-0.9	-0.9	-0.9	-8.6	-8.6	-8.6	-8.6	-8.6	-8.6
ACI 209	-0.9	-0.9	-0.9	-0.9	-0.9	-0.9	-8.6	-8.6	-8.6	-8.6	-8.6	-8.6
CEB 90-RS	-15.1	-15.1	-15.1	-15.1	-15.1	-15.1	-21.7	-21.7	-21.7	-21.7	-21.7	-21.7
Constant Ec	-18.9	-18.9	-18.9	-18.9	-18.9	-18.9	-25.3	-25.3	-25.3	-25.3	-25.3	-25.3
2-Point	-18.9	-18.9	-18.9	-18.9	-18.9	-18.9	-25.3	-25.3	-25.3	-25.3	-25.3	-25.3
Ec Model	Camber at 4 Days						Camber at 4 Days					
AASHTO '05 (+)	-2.8	7.3	36.9	15.9	-12.7	-12.5	0.0	10.3	40.8	19.2	-10.3	-9.9
ACI 209	-2.8	7.3	36.9	15.9	-12.7	-12.5	0.0	10.3	40.8	19.2	-10.3	-9.9
CEB 90-RS	-16.4	-7.3	18.6	0.1	-24.8	-24.8	-13.6	-4.7	22.1	3.3	-22.5	-22.5
Constant Ec	-20.3	-11.7	13.2	-4.6	-28.5	-28.5	-17.8	-8.9	16.4	-1.9	-26.3	-26.3
2-Point	-20.1	-11.7	13.2	-4.6	-28.5	-28.2	-17.8	-8.9	16.4	-1.9	-26.3	-26.3
Ec Model	Camber at 28 Days						Camber at 28 Days					
AASHTO '05 (+)	18.1	10.4	60.2	24.8	-16.1	-16.1	15.7	8.2	57.4	22.3	-17.8	-17.8
ACI 209	18.1	10.4	60.2	24.8	-16.1	-16.1	15.7	8.2	57.4	22.3	-17.8	-17.8
CEB 90-RS	2.5	-3.9	39.9	8.5	-27.6	-27.6	0.5	-5.9	37.2	6.4	-29.3	-29.3
Constant Ec	-2.3	-8.7	33.5	3.5	-31.2	-31.0	-4.2	-10.5	31.1	1.4	-32.6	-32.6
2-Point	-2.3	-8.7	33.7	3.7	-31.0	-31.0	-4.2	-10.5	31.1	1.4	-32.6	-32.6
Ec Model	Camber at 56 Days						Camber at 56 Days					
AASHTO '05 (+)	21.3	5.9	58.1	21.0	-19.2	-19.4	15.1	0.4	50.1	14.6	-23.7	-23.7
ACI 209	21.3	5.9	58.1	21.0	-19.2	-19.4	15.1	0.4	50.1	14.6	-23.7	-23.7
CEB 90-RS	5.7	-7.7	38.3	5.3	-30.4	-30.4	0.2	-12.7	31.3	-0.3	-34.0	-34.0
Constant Ec	0.6	-12.4	32.0	0.4	-33.7	-33.9	-4.7	-17.0	25.2	-4.8	-37.3	-37.3
2-Point	0.8	-12.3	32.2	0.6	-33.5	-33.7	-4.4	-17.0	25.5	-4.8	-37.1	-37.3
Ec Model	Camber at 90 Days						Camber at 90 Days					
AASHTO '05 (+)	28.4	8.6	64.4	24.6	-16.3	-16.7	23.7	4.5	58.6	20.1	-19.5	-19.8
ACI 209	28.4	8.6	64.4	24.6	-16.3	-16.7	23.7	4.5	58.6	20.1	-19.5	-19.8
CEB 90-RS	11.9	-5.3	44.1	8.7	-27.7	-28.0	7.8	-9.0	38.7	4.5	-30.6	-30.9
Constant Ec	6.5	-10.1	37.5	3.6	-31.2	-31.4	2.7	-13.5	32.4	-0.3	-33.9	-34.2
2-Point	6.9	-9.9	37.7	3.8	-31.1	-31.4	3.0	-13.5	32.7	-0.3	-33.6	-33.9

Table G-8: STD-M-A & -B Percent Error in Camber Growth

	STD-M-A						STD-M-B					
	Creep and Shrinkage Model						Creep and Shrinkage Model					
	AASHTO '05 (+)	AASHTO '04 (-)	ACI 209	ACI 209*	CEB 90	Modified CEB 90	AASHTO '05 (+)	AASHTO '04 (-)	ACI 209	ACI 209*	CEB 90	Modified CEB 90
Ec Model	Camber Growth at 4 Days						Camber Growth at 4 Days					
AASHTO '05 (+)	-11.8	49.5	228.8	101.8	-71.6	-70.1	133.4	293.8	767.8	432.4	-27.1	-19.8
ACI 209	-11.8	49.5	228.8	101.8	-71.6	-70.1	133.4	293.8	767.8	432.4	-27.1	-19.8
CEB 90-RS	-9.3	55.3	238.5	107.6	-68.6	-68.6	147.0	308.8	794.2	453.5	-14.8	-14.8
Constant Ec	-10.5	53.5	238.1	106.5	-70.8	-70.8	140.8	310.3	791.9	444.1	-19.7	-19.7
2-Point	-8.6	53.5	238.1	106.5	-70.8	-68.9	140.8	310.3	791.9	444.1	-19.7	-19.7
Ec Model	Camber Growth at 28 Days						Camber Growth at 28 Days					
AASHTO '05 (+)	58.3	34.8	188.0	79.1	-46.7	-46.7	92.4	63.9	250.9	117.6	-34.9	-34.9
ACI 209	58.3	34.8	188.0	79.1	-46.7	-46.7	92.4	63.9	250.9	117.6	-34.9	-34.9
CEB 90-RS	63.1	40.1	197.3	84.7	-45.1	-45.1	98.8	70.4	261.6	124.9	-33.6	-33.6
Constant Ec	62.6	38.5	197.2	84.4	-46.2	-45.5	97.9	68.5	261.8	123.9	-34.0	-34.0
2-Point	62.7	38.5	198.0	85.1	-45.5	-45.5	97.9	68.5	262.0	124.1	-34.0	-34.0
Ec Model	Camber Growth at 56 Days						Camber Growth at 56 Days					
AASHTO '05 (+)	54.6	16.6	145.2	53.8	-45.2	-45.5	65.3	24.7	162.1	64.1	-41.7	-41.7
ACI 209	54.6	16.6	145.2	53.8	-45.2	-45.5	65.3	24.7	162.1	64.1	-41.7	-41.7
CEB 90-RS	59.6	21.1	153.3	58.5	-43.9	-43.9	70.6	29.0	170.9	69.1	-39.6	-39.6
Constant Ec	58.9	19.6	153.3	58.2	-44.3	-44.9	69.5	27.9	170.4	68.9	-40.8	-40.8
2-Point	59.4	20.1	153.9	58.8	-43.9	-44.3	70.5	27.9	171.3	69.0	-39.9	-40.8
Ec Model	Camber Growth at 90 Days						Camber Growth at 90 Days					
AASHTO '05 (+)	69.0	22.3	154.1	60.2	-36.5	-37.3	87.2	35.3	181.2	77.5	-29.5	-30.3
ACI 209	69.0	22.3	154.1	60.2	-36.5	-37.3	87.2	35.3	181.2	77.5	-29.5	-30.3
CEB 90-RS	74.4	26.9	163.1	65.6	-34.7	-35.6	93.0	40.0	190.5	82.6	-28.1	-29.0
Constant Ec	73.4	25.6	162.8	65.1	-35.5	-36.0	92.3	38.7	190.4	82.3	-28.6	-29.6
2-Point	74.4	26.0	163.3	65.6	-35.0	-36.0	93.2	38.7	191.4	82.3	-27.7	-28.6

Table G-9: STD-M-C & -D Percent Error in Camber

	STD-M-C						STD-M-D					
	Creep and Shrinkage Model						Creep and Shrinkage Model					
	AASHTO '05 (+)	AASHTO '04 (-)	ACI 209	ACI 209*	CEB 90	Modified CEB 90	AASHTO '05 (+)	AASHTO '04 (-)	ACI 209	ACI 209*	CEB 90	Modified CEB 90
Ec Model	Initial Camber						Initial Camber					
AASHTO '05 (+)	15.5	15.5	15.5	15.5	15.5	15.5	-20.0	-20.0	-20.0	-20.0	-20.0	-20.0
ACI 209	15.5	15.5	15.5	15.5	15.5	15.5	-20.0	-20.0	-20.0	-20.0	-20.0	-20.0
CEB 90-RS	-1.0	-1.0	-1.0	-1.0	-1.0	-1.0	-31.4	-31.4	-31.4	-31.4	-31.4	-31.4
Constant Ec	-5.8	-5.8	-5.8	-5.8	-5.8	-5.8	-34.9	-34.9	-34.9	-34.9	-34.9	-34.9
2-Point	-5.8	-5.8	-5.8	-5.8	-5.8	-5.8	-34.9	-34.9	-34.9	-34.9	-34.9	-34.9
Ec Model	Camber at 4 Days						Camber at 4 Days					
AASHTO '05 (+)	-1.8	8.8	38.9	17.2	-11.6	-11.6	-29.4	-22.6	-0.4	-15.7	-37.0	-37.0
ACI 209	-1.8	8.8	38.9	17.2	-11.6	-11.6	-29.4	-22.6	-0.4	-15.7	-37.0	-37.0
CEB 90-RS	-15.1	-6.0	20.0	1.8	-24.2	-23.5	-39.6	-32.8	-14.0	-27.7	-45.5	-45.5
Constant Ec	-19.3	-10.9	15.1	-3.2	-27.7	-27.7	-42.1	-36.2	-18.3	-31.1	-48.1	-48.1
2-Point	-19.3	-10.9	15.1	-3.2	-27.7	-27.7	-42.1	-36.2	-18.3	-31.1	-48.1	-48.1
Ec Model	Camber at 28 Days						Camber at 28 Days					
AASHTO '05 (+)	43.8	34.6	95.3	52.3	1.9	1.9	-7.0	-13.2	26.4	-1.9	-34.6	-34.0
ACI 209	43.8	34.6	95.3	52.3	1.9	1.9	-7.0	-13.2	26.4	-1.9	-34.6	-34.0
CEB 90-RS	24.7	16.9	70.8	31.9	-12.3	-12.3	-19.5	-24.9	10.1	-14.5	-43.5	-43.5
Constant Ec	19.2	10.8	62.7	25.8	-16.4	-16.4	-23.3	-28.6	4.9	-19.0	-45.8	-45.8
2-Point	19.2	11.4	63.3	25.8	-16.4	-16.4	-23.2	-28.6	4.9	-19.0	-45.8	-45.8
Ec Model	Camber at 56 Days						Camber at 56 Days					
AASHTO '05 (+)	58.1	37.5	106.3	57.7	5.1	4.5	-3.4	-16.3	26.1	-3.9	-35.9	-36.5
ACI 209	58.1	37.5	106.3	57.7	5.1	4.5	-3.4	-16.3	26.1	-3.9	-35.9	-36.5
CEB 90-RS	37.2	19.8	80.4	36.8	-9.5	-9.5	-16.4	-26.7	9.8	-16.3	-45.0	-44.9
Constant Ec	30.9	14.0	72.1	30.5	-13.9	-13.9	-20.3	-30.7	5.2	-20.3	-47.7	-47.7
2-Point	31.5	14.0	72.1	31.1	-13.9	-13.9	-19.7	-30.6	5.3	-20.3	-47.7	-47.7
Ec Model	Camber at 90 Days						Camber at 90 Days					
AASHTO '05 (+)	49.0	26.0	91.2	44.7	-3.6	-3.6	3.9	-12.3	32.9	0.6	-32.9	-32.9
ACI 209	49.0	26.0	91.2	44.7	-3.6	-3.6	3.9	-12.3	32.9	0.6	-32.9	-32.9
CEB 90-RS	29.9	9.6	67.1	26.0	-16.2	-16.7	-9.7	-23.9	16.1	-12.3	-41.9	-41.9
Constant Ec	23.8	4.1	59.5	20.0	-20.5	-20.5	-14.2	-27.7	11.0	-16.8	-44.5	-45.2
2-Point	23.8	4.1	60.0	20.0	-20.5	-20.5	-14.2	-27.7	11.0	-16.8	-44.5	-45.2

Table G-10: STD-M-C & -D Percent Error in Camber Growth

	STD-M-C						STD-M-D					
	Creep and Shrinkage Model						Creep and Shrinkage Model					
	AASHTO '05 (+)	AASHTO '04 (-)	ACI 209	ACI 209*	CEB 90	Modified CEB 90	AASHTO '05 (+)	AASHTO '04 (-)	ACI 209	ACI 209*	CEB 90	Modified CEB 90
Ec Model	Camber Growth at 4 Days						Camber Growth at 4 Days					
AASHTO '05 (+)	-54.0	-21.1	73.1	5.2	-84.7	-84.7	-45.8	-12.5	95.8	20.8	-83.3	-83.3
ACI 209	-54.0	-21.1	73.1	5.2	-84.7	-84.7	-45.8	-12.5	95.8	20.8	-83.3	-83.3
CEB 90-RS	-51.4	-18.2	76.4	9.9	-84.7	-82.1	-46.5	-7.6	99.3	21.5	-80.6	-80.6
Constant Ec	-51.6	-19.4	80.1	10.2	-83.9	-83.9	-43.7	-7.9	99.6	22.8	-79.5	-79.5
2-Point	-51.6	-19.4	80.1	10.2	-83.9	-83.9	-43.7	-7.9	99.6	22.8	-79.5	-79.5
Ec Model	Camber Growth at 28 Days						Camber Growth at 28 Days					
AASHTO '05 (+)	81.1	54.6	228.9	105.4	-39.0	-39.0	46.4	24.3	164.8	64.1	-52.0	-49.7
ACI 209	81.1	54.6	228.9	105.4	-39.0	-39.0	46.4	24.3	164.8	64.1	-52.0	-49.7
CEB 90-RS	86.0	60.0	240.3	110.2	-37.9	-37.9	49.3	27.0	172.1	70.0	-50.1	-50.1
Constant Ec	88.2	58.7	241.2	111.4	-37.1	-37.1	50.2	27.2	173.5	69.2	-47.9	-47.9
2-Point	88.2	60.8	243.3	111.4	-37.1	-37.1	50.6	27.2	173.5	69.2	-47.9	-47.9
Ec Model	Camber Growth at 56 Days						Camber Growth at 56 Days					
AASHTO '05 (+)	106.5	54.9	227.1	105.4	-26.1	-27.6	48.7	11.0	135.2	47.3	-46.7	-48.4
ACI 209	106.5	54.9	227.1	105.4	-26.1	-27.6	48.7	11.0	135.2	47.3	-46.7	-48.4
CEB 90-RS	111.5	60.5	237.5	110.1	-24.8	-24.8	51.5	16.0	141.2	51.7	-46.6	-46.2
Constant Ec	112.6	60.8	239.3	111.4	-24.8	-24.8	52.4	15.0	144.2	52.6	-46.1	-46.1
2-Point	114.6	61.0	239.3	113.2	-24.8	-24.8	54.5	15.3	144.5	52.6	-46.1	-46.1
Ec Model	Camber Growth at 90 Days						Camber Growth at 90 Days					
AASHTO '05 (+)	66.6	20.8	150.4	57.9	-37.9	-37.9	68.5	22.2	151.9	59.3	-37.0	-37.0
ACI 209	66.6	20.8	150.4	57.9	-37.9	-37.9	68.5	22.2	151.9	59.3	-37.0	-37.0
CEB 90-RS	71.5	24.5	157.8	62.6	-35.2	-36.5	72.8	25.3	159.3	64.2	-35.2	-35.2
Constant Ec	72.3	24.2	159.1	63.0	-35.9	-35.9	72.8	25.1	161.5	63.7	-34.0	-36.3
2-Point	72.3	24.2	160.5	63.0	-35.9	-35.9	72.8	25.1	161.5	63.7	-34.0	-36.3

Table G-11: SCC-MA-A & -B Percent Error in Camber

	SCC-MA-A						SCC-MA-B					
	Creep and Shrinkage Model						Creep and Shrinkage Model					
	AASHTO '05 (+)	AASHTO '04 (-)	ACI 209	ACI 209*	CEB 90	Modified CEB 90	AASHTO '05 (+)	AASHTO '04 (-)	ACI 209	ACI 209*	CEB 90	Modified CEB 90
Ec Model	Initial Camber						Initial Camber					
AASHTO '05 (+)	-10.2	-10.2	-10.2	-10.2	-10.2	-10.2	-2.6	-2.6	-2.6	-2.6	-2.6	-2.6
ACI 209	-10.2	-10.2	-10.2	-10.2	-10.2	-10.2	-2.6	-2.6	-2.6	-2.6	-2.6	-2.6
CEB 90-RS	-15.2	-15.2	-15.2	-15.2	-15.2	-15.2	-7.7	-7.7	-7.7	-7.7	-7.7	-7.7
Constant Ec	-15.8	-15.8	-15.8	-15.8	-15.8	-15.8	-8.4	-8.4	-8.4	-8.4	-8.4	-8.4
2-Point	-15.8	-15.8	-15.8	-15.8	-15.8	-15.8	-8.4	-8.4	-8.4	-8.4	-8.4	-8.4
Ec Model	Camber at 4 Days						Camber at 4 Days					
AASHTO '05 (+)	-18.3	-12.1	27.9	-13.8	-25.6	-25.6	-18.5	-12.2	27.9	-14.0	-25.7	-25.7
ACI 209	-18.3	-12.1	27.9	-13.8	-25.6	-25.6	-18.5	-12.2	27.9	-14.0	-25.7	-25.7
CEB 90-RS	-22.9	-16.6	21.4	-18.6	-29.9	-29.9	-23.0	-16.7	21.2	-18.5	-30.2	-30.2
Constant Ec	-23.4	-17.3	20.4	-19.1	-30.4	-30.4	-23.4	-17.6	20.3	-19.4	-30.6	-30.6
2-Point	-23.4	-17.3	20.6	-19.1	-30.2	-30.2	-23.4	-17.6	20.7	-18.9	-30.2	-30.2
Ec Model	Camber at 28 Days						Camber at 28 Days					
AASHTO '05 (+)	5.5	-6.1	61.9	-9.7	-23.4	-23.7	2.5	-8.9	57.8	-12.4	-25.6	-26.0
ACI 209	5.5	-6.1	61.9	-9.7	-23.4	-23.7	2.5	-8.9	57.8	-12.4	-25.6	-26.0
CEB 90-RS	-0.2	-11.0	53.5	-14.7	-27.6	-28.0	-3.1	-13.5	49.7	-17.2	-29.9	-30.3
Constant Ec	-1.2	-12.1	52.2	-15.3	-28.2	-28.6	-4.0	-14.6	48.4	-17.9	-30.4	-30.6
2-Point	-0.8	-11.8	52.7	-15.3	-28.0	-28.5	-3.6	-14.2	48.8	-17.8	-30.3	-30.6
Ec Model	Camber at 90 Days						Camber at 90 Days					
AASHTO '05 (+)	24.0	-0.8	79.4	-5.9	-16.8	-17.8	19.1	-4.9	73.3	-9.6	-20.2	-21.2
ACI 209	24.0	-0.8	79.4	-5.9	-16.8	-17.8	19.1	-4.9	73.3	-9.6	-20.2	-21.2
CEB 90-RS	17.4	-6.0	70.2	-11.1	-21.5	-22.5	12.7	-9.6	64.6	-14.6	-24.8	-25.6
Constant Ec	16.0	-7.2	68.4	-11.9	-22.3	-23.3	11.7	-10.9	62.8	-15.4	-25.6	-26.3
2-Point	16.5	-6.8	69.1	-11.7	-22.1	-22.9	12.0	-10.6	63.5	-15.3	-25.2	-26.2
Ec Model	Camber at 201 Days						Camber at 201 Days					
AASHTO '05 (+)	30.6	2.4	87.2	-3.7	-11.5	-13.1	29.5	1.3	87.5	-4.6	-12.5	-14.1
ACI 209	30.6	2.4	87.2	-3.7	-11.5	-13.1	29.5	1.3	87.5	-4.6	-12.5	-14.1
CEB 90-RS	23.5	-3.0	78.0	-9.1	-16.5	-18.1	22.6	-3.9	78.0	-9.8	-17.4	-19.0
Constant Ec	22.0	-4.3	75.9	-10.0	-19.8	-21.3	21.3	-5.2	76.1	-10.8	-18.4	-19.7
2-Point	22.6	-3.9	76.7	-9.6	-17.0	-18.7	21.6	-4.6	76.7	-10.5	-18.0	-19.3

Table G-12: SCC-MA-A & -B Percent Error in Camber Growth

	SCC-MA-A						SCC-MA-B					
	Creep and Shrinkage Model						Creep and Shrinkage Model					
	AASHTO '05 (+)	AASHTO '04 (-)	ACI 209	ACI 209*	CEB 90	Modified CEB 90	AASHTO '05 (+)	AASHTO '04 (-)	ACI 209	ACI 209*	CEB 90	Modified CEB 90
Ec Model	Camber Growth at 4 Days						Camber Growth at 4 Days					
AASHTO '05 (+)	-37.9	-8.5	177.9	-16.7	-71.9	-71.9	-54.0	-32.6	103.8	-38.7	-78.6	-78.6
ACI 209	-37.9	-8.5	177.9	-16.7	-71.9	-71.9	-54.0	-32.6	103.8	-38.7	-78.6	-78.6
CEB 90-RS	-37.9	-6.9	180.5	-16.9	-72.7	-72.7	-54.7	-32.1	103.8	-38.5	-80.6	-80.6
Constant Ec	-37.5	-7.4	180.2	-16.2	-72.5	-72.5	-54.4	-33.2	103.6	-39.7	-80.4	-80.4
2-Point	-37.5	-7.4	181.4	-16.2	-71.2	-71.2	-54.4	-33.2	105.3	-38.1	-78.8	-78.8
Ec Model	Camber Growth at 28 Days						Camber Growth at 28 Days					
AASHTO '05 (+)	48.8	12.7	223.6	1.6	-40.7	-41.7	12.0	-15.0	144.1	-23.4	-55.0	-55.9
ACI 209	48.8	12.7	223.6	1.6	-40.7	-41.7	12.0	-15.0	144.1	-23.4	-55.0	-55.9
CEB 90-RS	49.2	13.7	225.5	1.5	-40.8	-42.1	11.7	-14.5	144.8	-23.8	-55.8	-56.7
Constant Ec	48.6	12.5	224.8	1.6	-41.0	-42.1	11.1	-15.8	144.2	-24.2	-55.9	-56.4
2-Point	49.7	13.2	226.6	1.6	-40.3	-41.7	12.1	-14.8	145.1	-23.8	-55.5	-56.4
Ec Model	Camber Growth at 90 Days						Camber Growth at 90 Days					
AASHTO '05 (+)	92.7	25.6	242.4	11.8	-17.7	-20.5	46.1	-4.9	161.2	-15.0	-37.5	-39.6
ACI 209	92.7	25.6	242.4	11.8	-17.7	-20.5	46.1	-4.9	161.2	-15.0	-37.5	-39.6
CEB 90-RS	93.3	26.3	244.6	11.7	-18.1	-21.0	45.9	-4.3	162.2	-15.5	-38.3	-40.2
Constant Ec	92.0	24.9	243.3	11.4	-18.5	-21.5	45.4	-5.7	160.9	-15.8	-38.8	-40.5
2-Point	93.3	26.1	245.1	11.9	-18.0	-20.3	46.1	-4.9	162.4	-15.6	-38.1	-40.3
Ec Model	Camber Growth at 201 Days						Camber Growth at 201 Days					
AASHTO '05 (+)	103.5	32.1	247.4	16.6	-3.2	-7.4	67.0	8.1	188.1	-4.2	-20.6	-24.0
ACI 209	103.5	32.1	247.4	16.6	-3.2	-7.4	67.0	8.1	188.1	-4.2	-20.6	-24.0
CEB 90-RS	104.0	32.8	250.2	16.4	-3.5	-8.0	66.9	8.4	189.0	-4.6	-21.2	-24.8
Constant Ec	102.6	31.4	248.4	15.8	-10.8	-14.8	65.9	7.0	187.4	-5.4	-22.1	-25.0
2-Point	104.1	32.4	250.5	16.8	-3.2	-7.7	66.6	8.4	188.9	-4.7	-21.4	-24.3

Table G-13: SCC-MA-C & -D Percent Error in Camber

	SCC-MA-C						SCC-MA-D					
	Creep and Shrinkage Model						Creep and Shrinkage Model					
	AASHTO '05 (+)	AASHTO '04 (-)	ACI 209	ACI 209*	CEB 90	Modified CEB 90	AASHTO '05 (+)	AASHTO '04 (-)	ACI 209	ACI 209*	CEB 90	Modified CEB 90
Ec Model	Initial Camber						Initial Camber					
AASHTO '05 (+)	28.2	28.2	28.2	28.2	28.2	28.2	5.5	5.5	5.5	5.5	5.5	5.5
ACI 209	28.2	28.2	28.2	28.2	28.2	28.2	5.5	5.5	5.5	5.5	5.5	5.5
CEB 90-RS	20.5	20.5	20.5	20.5	20.5	20.5	0.0	0.0	0.0	0.0	0.0	0.0
Constant Ec	20.5	20.5	20.5	20.5	20.5	20.5	0.0	0.0	0.0	0.0	0.0	0.0
2-Point	20.5	20.5	20.5	20.5	20.5	20.5	0.0	0.0	0.0	0.0	0.0	0.0
Ec Model	Camber at 4 Days						Camber at 4 Days					
AASHTO '05 (+)	-4.0	3.2	50.4	0.8	-12.8	-12.8	-2.8	4.2	52.8	2.8	-12.5	-12.5
ACI 209	-4.0	3.2	50.4	0.8	-12.8	-12.8	-2.8	4.2	52.8	2.8	-12.5	-12.5
CEB 90-RS	-9.6	-2.4	42.4	-4.8	-17.6	-17.6	-8.3	-1.4	44.4	-2.8	-16.7	-16.7
Constant Ec	-10.4	-3.2	41.6	-4.8	-18.4	-18.4	-9.7	-1.4	43.1	-4.2	-16.7	-16.7
2-Point	-10.4	-3.2	41.6	-4.8	-18.4	-18.4	-9.7	-1.4	43.1	-4.2	-16.7	-16.7
Ec Model	Camber at 28 Days						Camber at 28 Days					
AASHTO '05 (+)	16.7	3.6	80.4	-0.2	-15.4	-15.7	17.1	3.9	80.7	0.2	-15.1	-15.7
ACI 209	16.7	3.6	80.4	-0.2	-15.4	-15.7	17.1	3.9	80.7	0.2	-15.1	-15.7
CEB 90-RS	10.4	-1.4	70.9	-5.6	-20.2	-20.8	10.6	-1.6	71.0	-5.9	-20.0	-20.5
Constant Ec	9.4	-2.7	69.3	-6.5	-20.8	-21.1	9.5	-2.6	69.9	-6.4	-20.5	-21.1
2-Point	9.8	-2.4	69.6	-6.2	-20.8	-20.8	10.1	-2.0	69.9	-5.9	-20.5	-21.1
Ec Model	Camber at 90 Days						Camber at 90 Days					
AASHTO '05 (+)	36.7	9.2	99.8	3.8	-8.6	-9.9	36.1	8.3	98.1	2.4	-9.4	-10.4
ACI 209	36.7	9.2	99.8	3.8	-8.6	-9.9	36.1	8.3	98.1	2.4	-9.4	-10.4
CEB 90-RS	29.6	3.4	89.4	-1.9	-13.4	-14.5	28.3	2.4	88.3	-2.7	-14.3	-15.3
Constant Ec	28.0	2.2	87.7	-3.1	-14.5	-15.7	27.3	1.4	86.3	-3.7	-15.3	-16.3
2-Point	28.6	2.8	88.3	-2.5	-14.0	-15.6	27.3	1.4	87.3	-3.5	-15.3	-16.3
Ec Model	Camber at 201 Days						Camber at 201 Days					
AASHTO '05 (+)	29.1	1.0	87.2	-4.9	-12.8	-14.8	45.7	14.3	112.4	7.6	-1.9	-3.8
ACI 209	29.1	1.0	87.2	-4.9	-12.8	-14.8	45.7	14.3	112.4	7.6	-1.9	-3.8
CEB 90-RS	22.2	-4.4	77.8	-10.3	-17.7	-19.2	38.1	7.6	101.9	1.0	-7.6	-8.6
Constant Ec	20.7	-5.4	75.9	-11.3	-18.7	-20.2	36.2	6.7	99.0	0.0	-8.6	-9.5
2-Point	21.2	-5.4	76.4	-10.8	-18.2	-19.7	37.1	6.7	100.0	1.0	-7.6	-9.5

Table G-14: SCC-MA-C & -D Percent Error in Camber Growth

	SCC-MA-C						SCC-MA-D					
	Creep and Shrinkage Model						Creep and Shrinkage Model					
	AASHTO '05 (+)	AASHTO '04 (-)	ACI 209	ACI 209*	CEB 90	Modified CEB 90	AASHTO '05 (+)	AASHTO '04 (-)	ACI 209	ACI 209*	CEB 90	Modified CEB 90
Ec Model	Camber Growth at 4 Days						Camber Growth at 4 Days					
AASHTO '05 (+)	-66.8	-51.9	46.0	-56.9	-85.1	-85.1	-33.1	-5.2	190.1	-10.8	-72.1	-72.1
ACI 209	-66.8	-51.9	46.0	-56.9	-85.1	-85.1	-33.1	-5.2	190.1	-10.8	-72.1	-72.1
CEB 90-RS	-66.5	-50.6	48.3	-55.9	-84.1	-84.1	-35.3	-5.9	188.2	-11.8	-70.6	-70.6
Constant Ec	-68.2	-52.3	46.5	-55.9	-85.9	-85.9	-41.2	-5.9	182.4	-17.6	-70.6	-70.6
2-Point	-68.2	-52.3	46.5	-55.9	-85.9	-85.9	-41.2	-5.9	182.4	-17.6	-70.6	-70.6
Ec Model	Camber Growth at 28 Days						Camber Growth at 28 Days					
AASHTO '05 (+)	-17.7	-37.9	80.4	-43.7	-67.1	-67.7	27.4	-3.7	177.5	-12.5	-48.4	-49.8
ACI 209	-17.7	-37.9	80.4	-43.7	-67.1	-67.7	27.4	-3.7	177.5	-12.5	-48.4	-49.8
CEB 90-RS	-16.6	-36.0	82.5	-42.8	-66.7	-67.7	26.2	-3.9	176.4	-14.7	-49.8	-51.0
Constant Ec	-18.2	-38.1	79.9	-44.3	-67.7	-68.1	23.5	-6.6	173.7	-15.8	-51.0	-52.5
2-Point	-17.6	-37.6	80.5	-43.8	-67.7	-67.7	25.1	-5.0	173.7	-14.7	-51.0	-52.5
Ec Model	Camber Growth at 90 Days						Camber Growth at 90 Days					
AASHTO '05 (+)	12.1	-27.1	101.7	-34.6	-52.3	-54.1	63.1	5.8	190.7	-6.3	-30.5	-32.6
ACI 209	12.1	-27.1	101.7	-34.6	-52.3	-54.1	63.1	5.8	190.7	-6.3	-30.5	-32.6
CEB 90-RS	13.8	-25.9	104.1	-33.9	-51.2	-53.0	61.4	5.2	191.6	-5.9	-31.0	-33.1
Constant Ec	11.4	-27.6	101.5	-35.7	-53.0	-54.7	59.3	3.0	187.4	-8.1	-33.1	-35.3
2-Point	12.2	-26.8	102.4	-34.8	-52.1	-54.6	59.3	3.0	189.5	-7.6	-33.1	-35.3
Ec Model	Camber Growth at 201 Days						Camber Growth at 201 Days					
AASHTO '05 (+)	1.1	-34.5	74.7	-42.0	-52.0	-54.4	80.2	17.6	212.9	4.3	-14.7	-18.4
ACI 209	1.1	-34.5	74.7	-42.0	-52.0	-54.4	80.2	17.6	212.9	4.3	-14.7	-18.4
CEB 90-RS	2.2	-33.6	77.2	-41.6	-51.5	-53.5	80.0	16.0	214.0	2.0	-16.0	-18.0
Constant Ec	0.2	-34.9	74.6	-42.9	-52.9	-54.9	76.0	14.0	208.0	0.0	-18.0	-20.0
2-Point	0.9	-34.9	75.3	-42.2	-52.2	-54.2	78.0	14.0	210.0	2.0	-16.0	-20.0

Table G-15: SCC-MS-A & -B Percent Error in Camber

	SCC-MS-A						SCC-MS-B					
	Creep and Shrinkage Model						Creep and Shrinkage Model					
	AASHTO '05 (+)	AASHTO '04 (-)	ACI 209	ACI 209*	CEB 90	Modified CEB 90	AASHTO '05 (+)	AASHTO '04 (-)	ACI 209	ACI 209*	CEB 90	Modified CEB 90
Ec Model	Initial Camber						Initial Camber					
AASHTO '05 (+)	6.6	6.6	6.6	6.6	6.6	6.6	-2.3	-2.3	-2.3	-2.3	-2.3	-2.3
ACI 209	6.6	6.6	6.6	6.6	6.6	6.6	-2.3	-2.3	-2.3	-2.3	-2.3	-2.3
CEB 90-RS	-11.1	-11.1	-11.1	-11.1	-11.1	-11.1	-18.5	-18.5	-18.5	-18.5	-18.5	-18.5
Constant Ec	-5.6	-5.6	-5.6	-5.6	-5.6	-5.6	-13.3	-13.3	-13.3	-13.3	-13.3	-13.3
2-Point	-5.6	-5.6	-5.6	-5.6	-5.6	-5.6	-13.3	-13.3	-13.3	-13.3	-13.3	-13.3
Ec Model	Camber at 4 Days						Camber at 4 Days					
AASHTO '05 (+)	-8.1	-2.8	44.5	-1.5	-17.8	-17.6	-9.5	-4.1	42.7	-3.2	-19.1	-19.1
ACI 209	-8.1	-2.8	44.5	-1.5	-17.8	-17.6	-9.5	-4.1	42.7	-3.2	-19.1	-19.1
CEB 90-RS	-23.4	-18.3	21.6	-17.6	-31.6	-31.3	-24.5	-19.5	20.0	-18.6	-32.3	-32.3
Constant Ec	-18.8	-13.7	28.5	-12.7	-27.5	-27.2	-20.0	-15.0	26.8	-14.1	-28.6	-28.2
2-Point	-18.8	-13.7	28.5	-12.7	-27.2	-27.2	-20.0	-15.0	26.8	-14.1	-28.2	-28.2
Ec Model	Camber at 14 Days						Camber at 14 Days					
AASHTO '05 (+)	11.1	6.1	81.2	7.7	-14.8	-14.6	6.5	1.6	74.2	3.3	-18.4	-18.3
ACI 209	11.1	6.1	81.2	7.7	-14.8	-14.6	6.5	1.6	74.2	3.3	-18.4	-18.3
CEB 90-RS	-7.0	-11.0	53.1	-9.8	-28.8	-28.8	-10.9	-14.6	47.1	-13.5	-31.9	-31.7
Constant Ec	-1.7	-6.0	61.3	-4.6	-24.7	-24.7	-5.5	-10.1	54.9	-8.4	-28.0	-28.0
2-Point	-1.4	-5.8	61.8	-4.3	-24.5	-24.5	-5.5	-9.7	55.7	-8.4	-27.7	-27.7
Ec Model	Camber at 28 Days						Camber at 28 Days					
AASHTO '05 (+)	31.1	14.7	107.7	16.6	-8.8	-8.8	25.5	9.5	99.4	11.6	-12.9	-12.9
ACI 209	31.1	14.7	107.7	16.6	-8.8	-8.8	25.5	9.5	99.4	11.6	-12.9	-12.9
CEB 90-RS	9.8	-3.8	75.8	-2.4	-24.0	-24.0	5.3	-7.9	68.8	-6.7	-27.4	-27.4
Constant Ec	16.1	1.3	84.7	2.9	-19.6	-19.6	11.1	-3.0	77.4	-1.3	-23.2	-23.2
2-Point	16.5	1.7	85.9	3.4	-19.4	-19.4	11.5	-2.6	78.3	-1.2	-22.8	-22.8
Ec Model	Camber at 56 Days						Camber at 56 Days					
AASHTO '05 (+)	51.4	22.6	131.9	24.8	-2.1	-2.1	45.3	17.3	123.0	19.3	-6.6	-6.6
ACI 209	51.4	22.6	131.9	24.8	-2.1	-2.1	45.3	17.3	123.0	19.3	-6.6	-6.6
CEB 90-RS	27.4	3.1	96.7	4.5	-18.3	-18.3	21.8	-1.2	88.9	0.0	-21.8	-22.2
Constant Ec	34.0	8.3	106.4	10.2	-13.6	-13.8	28.4	3.7	98.4	5.3	-17.7	-17.7
2-Point	35.0	9.0	107.9	10.7	-13.3	-13.3	29.2	4.1	100.0	5.8	-17.3	-17.3

Table G-16: SCC-MS-A & -B Percent Error in Camber Growth

	SCC-MS-A						SCC-MS-B					
	Creep and Shrinkage Model						Creep and Shrinkage Model					
	AASHTO '05 (+)	AASHTO '04 (-)	ACI 209	ACI 209*	CEB 90	Modified CEB 90	AASHTO '05 (+)	AASHTO '04 (-)	ACI 209	ACI 209*	CEB 90	Modified CEB 90
Ec Model	Camber Growth at 4 Days						Camber Growth at 4 Days					
AASHTO '05 (+)	-51.8	-33.0	133.2	-28.5	-85.7	-84.8	-34.7	-8.5	215.8	-4.2	-80.4	-80.4
ACI 209	-51.8	-33.0	133.2	-28.5	-85.7	-84.8	-34.7	-8.5	215.8	-4.2	-80.4	-80.4
CEB 90-RS	-51.8	-30.4	137.9	-27.1	-86.1	-85.0	-34.7	-6.0	221.1	-0.8	-79.1	-79.1
Constant Ec	-52.6	-32.4	135.0	-28.4	-86.9	-85.9	-36.2	-9.2	216.6	-4.3	-82.8	-80.4
2-Point	-52.6	-32.4	135.0	-28.4	-85.9	-85.9	-36.2	-9.2	216.6	-4.3	-80.4	-80.4
Ec Model	Camber Growth at 14 Days						Camber Growth at 14 Days					
AASHTO '05 (+)	13.8	-1.6	231.4	3.4	-66.3	-65.7	33.2	14.8	286.6	21.1	-60.3	-59.9
ACI 209	13.8	-1.6	231.4	3.4	-66.3	-65.7	33.2	14.8	286.6	21.1	-60.3	-59.9
CEB 90-RS	15.4	0.2	238.7	4.7	-65.9	-65.9	34.2	17.4	294.6	22.5	-60.0	-59.5
Constant Ec	13.5	-1.6	233.8	3.4	-67.0	-67.0	32.8	13.4	288.2	20.5	-61.9	-61.9
2-Point	14.5	-0.8	235.7	4.3	-66.4	-66.2	32.8	15.2	291.2	20.5	-60.6	-60.6
Ec Model	Camber Growth at 28 Days						Camber Growth at 28 Days					
AASHTO '05 (+)	75.1	24.7	309.8	30.6	-47.3	-47.3	102.0	43.3	373.0	51.0	-38.9	-38.9
ACI 209	75.1	24.7	309.8	30.6	-47.3	-47.3	102.0	43.3	373.0	51.0	-38.9	-38.9
CEB 90-RS	77.0	26.9	319.5	32.2	-47.2	-47.2	104.4	46.5	383.5	52.0	-39.2	-39.2
Constant Ec	74.8	23.6	312.4	29.4	-48.6	-48.6	100.7	42.5	374.8	49.4	-41.1	-41.1
2-Point	76.4	25.2	316.4	31.1	-47.8	-47.8	102.5	44.3	378.2	49.8	-39.4	-39.4
Ec Model	Camber Growth at 56 Days						Camber Growth at 56 Days					
AASHTO '05 (+)	133.8	47.8	374.0	54.2	-26.1	-26.1	169.1	69.6	445.5	76.9	-15.2	-15.2
ACI 209	133.8	47.8	374.0	54.2	-26.1	-26.1	169.1	69.6	445.5	76.9	-15.2	-15.2
CEB 90-RS	137.8	50.9	385.8	56.0	-25.9	-25.9	171.7	73.5	457.4	78.8	-14.1	-15.9
Constant Ec	133.4	46.8	377.3	53.2	-27.0	-27.8	166.9	68.1	447.0	74.6	-17.6	-17.6
2-Point	136.6	49.2	382.1	54.8	-26.2	-26.2	170.2	69.7	453.6	76.3	-16.0	-16.0

Table G-17: SCC-MS-C & -D Percent Error in Camber

	SCC-MS-C						SCC-MS-D					
	Creep and Shrinkage Model						Creep and Shrinkage Model					
	AASHTO '05 (+)	AASHTO '04 (-)	ACI 209	ACI 209*	CEB 90	Modified CEB 90	AASHTO '05 (+)	AASHTO '04 (-)	ACI 209	ACI 209*	CEB 90	Modified CEB 90
Ec Model	Initial Camber						Initial Camber					
AASHTO '05 (+)	17.9	17.9	17.9	17.9	17.9	17.9	0.0	0.0	0.0	0.0	0.0	0.0
ACI 209	17.9	17.9	17.9	17.9	17.9	17.9	0.0	0.0	0.0	0.0	0.0	0.0
CEB 90-RS	-2.1	-2.1	-2.1	-2.1	-2.1	-2.1	-16.9	-16.9	-16.9	-16.9	-16.9	-16.9
Constant Ec	4.2	4.2	4.2	4.2	4.2	4.2	-12.3	-12.3	-12.3	-12.3	-12.3	-12.3
2-Point	4.2	4.2	4.2	4.2	4.2	4.2	-12.3	-12.3	-12.3	-12.3	-12.3	-12.3
Ec Model	Camber at 4 Days						Camber at 4 Days					
AASHTO '05 (+)	-1.5	4.5	55.6	6.0	-12.0	-11.3	-8.4	-2.4	44.6	-1.2	-18.1	-18.1
ACI 209	-1.5	4.5	55.6	6.0	-12.0	-11.3	-8.4	-2.4	44.6	-1.2	-18.1	-18.1
CEB 90-RS	-18.0	-12.0	30.8	-11.3	-26.3	-26.3	-22.9	-18.1	21.7	-18.1	-31.3	-31.3
Constant Ec	-12.8	-7.5	38.3	-6.0	-21.8	-21.8	-19.3	-13.3	28.9	-13.3	-27.7	-27.7
2-Point	-12.8	-7.5	38.3	-6.0	-21.8	-21.8	-19.3	-13.3	28.9	-13.3	-27.7	-27.7
Ec Model	Camber at 14 Days						Camber at 14 Days					
AASHTO '05 (+)	17.9	12.3	92.7	14.2	-9.5	-9.5	11.7	6.3	83.2	8.6	-14.1	-14.1
ACI 209	17.9	12.3	92.7	14.2	-9.5	-9.5	11.7	6.3	83.2	8.6	-14.1	-14.1
CEB 90-RS	-1.7	-5.5	62.6	-4.6	-24.8	-24.8	-6.7	-10.7	53.9	-9.5	-29.0	-29.0
Constant Ec	4.0	-0.6	71.2	1.0	-20.6	-20.1	-0.9	-6.1	62.8	-4.1	-24.4	-24.4
2-Point	4.5	-0.4	71.7	1.0	-20.1	-18.2	-0.9	-5.2	63.1	-4.1	-24.4	-24.4
Ec Model	Camber at 28 Days						Camber at 28 Days					
AASHTO '05 (+)	38.6	21.1	120.8	23.2	-3.9	-3.9	30.7	14.3	108.6	16.6	-9.3	-9.3
ACI 209	38.6	21.1	120.8	23.2	-3.9	-3.9	30.7	14.3	108.6	16.6	-9.3	-9.3
CEB 90-RS	16.4	1.7	86.7	3.1	-19.9	-19.9	10.2	-3.9	77.1	-2.7	-24.1	-24.1
Constant Ec	22.7	7.3	96.5	9.2	-15.1	-15.0	15.9	1.8	86.1	2.0	-19.8	-19.8
2-Point	23.4	7.8	97.8	9.4	-15.0	-15.0	17.1	1.8	87.1	3.0	-19.5	-19.5
Ec Model	Camber at 56 Days						Camber at 56 Days					
AASHTO '05 (+)	60.7	29.7	146.9	31.7	3.4	3.4	50.0	21.1	132.2	23.3	-3.3	-3.3
ACI 209	60.7	29.7	146.9	31.7	3.4	3.4	50.0	21.1	132.2	23.3	-3.3	-3.3
CEB 90-RS	34.5	9.0	109.0	10.3	-13.8	-13.8	26.7	2.2	96.7	3.3	-18.9	-18.9
Constant Ec	42.1	14.5	120.0	16.6	-9.0	-9.0	33.3	7.8	106.7	8.9	-14.4	-14.4
2-Point	42.8	15.2	121.4	17.2	-8.3	-8.3	33.3	7.8	107.8	10.0	-14.4	-14.4

Table G-18: SCC-MS-C & -D Percent Error in Camber Growth

	SCC-MS-C						SCC-MS-D					
	Creep and Shrinkage Model						Creep and Shrinkage Model					
	AASHTO '05 (+)	AASHTO '04 (-)	ACI 209	ACI 209*	CEB 90	Modified CEB 90	AASHTO '05 (+)	AASHTO '04 (-)	ACI 209	ACI 209*	CEB 90	Modified CEB 90
Ec Model	Camber Growth at 4 Days						Camber Growth at 4 Days					
AASHTO '05 (+)	-57.6	-39.7	112.1	-35.3	-88.8	-86.6	-38.9	-11.1	205.6	-5.6	-83.3	-83.3
ACI 209	-57.6	-39.7	112.1	-35.3	-88.8	-86.6	-38.9	-11.1	205.6	-5.6	-83.3	-83.3
CEB 90-RS	-57.0	-35.5	117.7	-32.8	-86.6	-86.6	-33.1	-6.4	214.3	-6.4	-79.9	-79.9
Constant Ec	-57.1	-39.4	114.6	-34.3	-87.4	-87.4	-36.6	-5.0	216.8	-5.0	-81.0	-81.0
2-Point	-57.1	-39.4	114.6	-34.3	-87.4	-87.4	-36.6	-5.0	216.8	-5.0	-81.0	-81.0
Ec Model	Camber Growth at 14 Days						Camber Growth at 14 Days					
AASHTO '05 (+)	-0.1	-14.3	191.6	-9.4	-70.3	-70.3	46.3	24.8	329.0	33.9	-55.8	-55.8
ACI 209	-0.1	-14.3	191.6	-9.4	-70.3	-70.3	46.3	24.8	329.0	33.9	-55.8	-55.8
CEB 90-RS	1.4	-10.5	199.6	-7.7	-70.2	-70.2	48.8	29.8	337.3	35.3	-57.7	-57.7
Constant Ec	-0.7	-13.9	194.2	-9.2	-72.0	-70.5	51.3	28.2	338.8	37.2	-54.7	-54.7
2-Point	0.8	-13.3	195.7	-9.2	-70.5	-65.0	51.3	32.0	340.2	37.2	-54.7	-54.7
Ec Model	Camber Growth at 28 Days						Camber Growth at 28 Days					
AASHTO '05 (+)	52.3	8.2	260.2	13.5	-55.1	-55.1	117.4	54.8	415.7	63.5	-35.6	-35.6
ACI 209	52.3	8.2	260.2	13.5	-55.1	-55.1	117.4	54.8	415.7	63.5	-35.6	-35.6
CEB 90-RS	56.2	11.5	270.3	15.8	-54.0	-54.0	125.1	60.2	432.8	65.4	-33.0	-33.0
Constant Ec	52.7	8.8	263.9	14.4	-55.2	-54.8	123.1	61.6	429.5	62.6	-32.6	-32.6
2-Point	54.7	10.4	267.5	14.8	-54.8	-54.8	128.1	61.6	433.5	66.6	-31.6	-31.6
Ec Model	Camber Growth at 56 Days						Camber Growth at 56 Days					
AASHTO '05 (+)	105.3	28.9	317.3	34.0	-35.5	-35.5	180.0	76.0	476.0	84.0	-12.0	-12.0
ACI 209	105.3	28.9	317.3	34.0	-35.5	-35.5	180.0	76.0	476.0	84.0	-12.0	-12.0
CEB 90-RS	108.4	32.8	329.0	36.9	-34.6	-34.6	188.9	83.0	492.2	87.8	-8.5	-8.5
Constant Ec	105.4	28.6	322.2	34.3	-36.7	-36.7	187.4	82.5	488.4	87.0	-8.8	-8.8
2-Point	107.3	30.5	326.1	36.3	-34.7	-34.7	187.4	82.5	493.0	91.6	-8.8	-8.8

Table G-19: SCC-HS-A & -B Percent Error in Camber

	SCC-HS-A						SCC-HS-B					
	Creep and Shrinkage Model						Creep and Shrinkage Model					
	AASHTO '05 (+)	AASHTO '04 (-)	ACI 209	ACI 209*	CEB 90	Modified CEB 90	AASHTO '05 (+)	AASHTO '04 (-)	ACI 209	ACI 209*	CEB 90	Modified CEB 90
Ec Model	Initial Camber						Initial Camber					
AASHTO '05 (+)	-12.8	-12.8	-12.8	-12.8	-12.8	-12.8	-23.2	-23.2	-23.2	-23.2	-23.2	-23.2
ACI 209	-12.8	-12.8	-12.8	-12.8	-12.8	-12.8	-23.2	-23.2	-23.2	-23.2	-23.2	-23.2
CEB 90-RS	-2.5	-2.5	-2.5	-2.5	-2.5	-2.5	-14.2	-14.2	-14.2	-14.2	-14.2	-14.2
Constant Ec	-8.7	-8.7	-8.7	-8.7	-8.7	-8.7	-19.4	-19.4	-19.4	-19.4	-19.4	-19.4
2-Point	-8.7	-8.7	-8.7	-8.7	-8.7	-8.7	-19.4	-19.4	-19.4	-19.4	-19.4	-19.4
Ec Model	Camber at 1 Day						Camber at 1 Day					
AASHTO '05 (+)	-24.6	-24.6	-24.6	-24.6	-24.6	-24.6	-35.7	-35.7	-35.7	-35.7	-35.7	-35.7
ACI 209	-24.6	-24.6	-24.6	-24.6	-24.6	-24.6	-35.7	-35.7	-35.7	-35.7	-35.7	-35.7
CEB 90-RS	-15.7	-15.7	-15.7	-15.7	-15.7	-15.7	-28.1	-28.1	-28.1	-28.1	-28.1	-28.1
Constant Ec	-21.1	-21.1	-21.1	-21.1	-21.1	-21.1	-32.4	-32.4	-32.4	-32.4	-32.4	-32.4
2-Point	-21.1	-21.1	-21.1	-21.1	-21.1	-21.1	-32.4	-32.4	-32.4	-32.4	-32.4	-32.4
Ec Model	Camber at 4 Days						Camber at 4 Days					
AASHTO '05 (+)	-12.8	-11.2	33.1	-7.7	-21.6	-21.6	-25.7	-24.7	13.6	-21.5	-33.6	-32.8
ACI 209	-12.8	-11.2	33.1	-7.7	-21.6	-21.6	-25.7	-24.7	13.6	-21.5	-33.6	-32.8
CEB 90-RS	-2.7	-0.8	48.0	3.0	-12.7	-12.7	-16.9	-15.4	26.5	-12.3	-25.8	-25.8
Constant Ec	-8.7	-7.0	39.3	-3.5	-18.2	-18.1	-22.0	-21.0	45.2	-17.9	-30.4	-30.4
2-Point	-8.3	-7.0	39.3	-3.5	-18.1	-18.1	-22.0	-20.6	18.8	-17.9	-30.0	-30.0
Ec Model	Camber at 7 Days						Camber at 7 Days					
AASHTO '05 (+)	-5.5	-7.5	48.7	-3.1	-19.6	-19.6	-19.7	-21.4	27.0	-17.3	-31.9	-31.9
ACI 209	-5.5	-7.5	48.7	-3.1	-19.6	-19.6	-19.7	-21.4	27.0	-17.3	-31.9	-31.9
CEB 90-RS	5.4	3.3	65.4	8.0	-10.3	-10.3	-10.0	-11.9	41.1	-7.8	-23.7	-23.7
Constant Ec	-1.1	-3.2	55.3	1.4	-15.8	-15.8	-15.6	-17.3	32.7	-13.5	-28.3	-28.3
2-Point	-0.9	-3.0	55.7	1.6	-15.8	-15.8	-15.6	-17.3	33.2	-13.5	-28.3	-28.3
Ec Model	Camber at 15 Days						Camber at 15 Days					
AASHTO '05 (+)	4.2	-4.5	67.2	1.0	-17.9	-17.9	-10.8	-18.2	44.3	-12.8	-29.6	-29.6
ACI 209	4.2	-4.5	67.2	1.0	-17.9	-17.9	-10.8	-18.2	44.3	-12.8	-29.6	-29.6
CEB 90-RS	15.9	6.5	85.4	12.3	-8.4	-8.4	0.0	-8.4	60.1	-3.0	-21.2	-21.2
Constant Ec	8.8	-0.3	74.4	5.5	-14.0	-14.3	-6.4	-14.3	50.7	-9.4	-26.1	-26.1
2-Point	9.1	-0.3	75.0	5.8	-14.0	-14.0	-5.9	-13.8	51.2	-8.9	-26.1	-26.1

Table G-20: SCC-HS-A & -B Percent Error in Camber Growth

	SCC-HS-A						SCC-HS-B					
	Creep and Shrinkage Model						Creep and Shrinkage Model					
	AASHTO '05 (+)	AASHTO '04 (-)	ACI 209	ACI 209*	CEB 90	Modified CEB 90	AASHTO '05 (+)	AASHTO '04 (-)	ACI 209	ACI 209*	CEB 90	Modified CEB 90
Ec Model	Camber Growth at 1 Day						Camber Growth at 1 Day					
AASHTO '05 (+)	-60.8	-27.6	171.6	-12.5	-84.9	-84.9	-69.6	-43.6	125.8	-26.2	-87.0	-87.0
ACI 209	-60.8	-27.6	171.6	-12.5	-84.9	-84.9	-69.6	-43.6	125.8	-26.2	-87.0	-87.0
CEB 90-RS	-62.2	-29.8	167.1	-16.3	-86.5	-86.5	-68.9	-41.7	121.4	-26.2	-88.3	-84.5
Constant Ec	-62.5	-28.0	170.9	-13.6	-85.6	-85.6	-66.9	-42.1	119.1	-29.7	-87.6	-87.6
2-Point	-62.5	-28.0	170.9	-13.6	-85.6	-85.6	-66.9	-42.1	119.1	-29.7	-87.6	-87.6
Ec Model	Camber Growth at 4 Days						Camber Growth at 4 Days					
AASHTO '05 (+)	-35.0	-51.5	42.5	-42.0	-73.6	-73.6	-43.5	-58.9	15.0	-53.7	-79.4	-74.5
ACI 209	-35.0	-51.5	42.5	-42.0	-73.6	-73.6	-43.5	-58.9	15.0	-53.7	-79.4	-74.5
CEB 90-RS	-35.4	-50.7	41.8	-40.3	-74.3	-74.3	-43.7	-57.8	16.3	-53.6	-78.1	-81.2
Constant Ec	-33.4	-51.6	42.4	-42.3	-74.8	-74.5	-46.5	-60.5	134.3	-52.8	-79.9	-79.9
2-Point	-31.3	-51.6	42.6	-42.3	-74.5	-74.5	-46.0	-58.0	17.3	-52.8	-77.2	-77.2
Ec Model	Camber Growth at 7 Days						Camber Growth at 7 Days					
AASHTO '05 (+)	48.0	35.2	405.2	64.1	-44.4	-44.4	22.3	11.6	319.0	37.7	-54.9	-54.9
ACI 209	48.0	35.2	405.2	64.1	-44.4	-44.4	22.3	11.6	319.0	37.7	-54.9	-54.9
CEB 90-RS	46.1	33.8	399.7	62.0	-46.3	-46.3	24.0	12.8	314.0	36.1	-53.8	-53.8
Constant Ec	47.8	34.3	402.6	63.1	-44.8	-44.8	22.6	12.5	314.4	35.5	-54.0	-54.0
2-Point	48.7	35.5	404.7	64.4	-44.8	-44.8	22.6	12.5	317.5	35.5	-54.0	-54.0
Ec Model	Camber Growth at 15 Days						Camber Growth at 15 Days					
AASHTO '05 (+)	91.2	44.2	428.3	73.8	-27.0	-27.0	68.2	27.5	372.2	57.4	-34.9	-34.9
ACI 209	91.2	44.2	428.3	73.8	-27.0	-27.0	68.2	27.5	372.2	57.4	-34.9	-34.9
CEB 90-RS	88.0	42.9	420.5	70.9	-28.5	-28.5	70.0	28.7	366.2	55.4	-34.4	-34.4
Constant Ec	89.1	42.7	424.3	72.5	-27.0	-28.7	67.9	26.6	367.6	52.4	-35.4	-35.4
2-Point	90.8	42.7	427.6	74.2	-27.0	-27.0	70.5	29.2	370.2	55.0	-35.4	-35.4

Table G-21: SCC-HS-C & -D Percent Error in Camber

	SCC-HS-C						SCC-HS-D					
	Creep and Shrinkage Model						Creep and Shrinkage Model					
	AASHTO '05 (+)	AASHTO '04 (-)	ACI 209	ACI 209*	CEB 90	Modified CEB 90	AASHTO '05 (+)	AASHTO '04 (-)	ACI 209	ACI 209*	CEB 90	Modified CEB 90
Ec Model	Initial Camber						Initial Camber					
AASHTO '05 (+)	21.5	21.5	21.5	21.5	21.5	21.5	-21.1	-21.1	-21.1	-21.1	-21.1	-21.1
ACI 209	21.5	21.5	21.5	21.5	21.5	21.5	-21.1	-21.1	-21.1	-21.1	-21.1	-21.1
CEB 90-RS	27.7	27.7	27.7	27.7	27.7	27.7	-12.3	-12.3	-12.3	-12.3	-12.3	-12.3
Constant Ec	26.2	26.2	26.2	26.2	26.2	26.2	-17.5	-17.5	-17.5	-17.5	-17.5	-17.5
2-Point	26.2	26.2	26.2	26.2	26.2	26.2	-17.5	-17.5	-17.5	-17.5	-17.5	-17.5
Ec Model	Camber at 1 Day						Camber at 1 Day					
AASHTO '05 (+)	-10.2	-10.2	-10.2	-10.2	-10.2	-10.2	-35.7	-35.7	-35.7	-35.7	-35.7	-35.7
ACI 209	-10.2	-10.2	-10.2	-10.2	-10.2	-10.2	-35.7	-35.7	-35.7	-35.7	-35.7	-35.7
CEB 90-RS	-5.7	-5.7	-5.7	-5.7	-5.7	-5.7	-28.6	-28.6	-28.6	-28.6	-28.6	-28.6
Constant Ec	-6.8	-6.8	-6.8	-6.8	-6.8	-6.8	-32.9	-32.9	-32.9	-32.9	-32.9	-32.9
2-Point	-6.8	-6.8	-6.8	-6.8	-6.8	-6.8	-32.9	-32.9	-32.9	-32.9	-32.9	-32.9
Ec Model	Camber at 4 Days						Camber at 4 Days					
AASHTO '05 (+)	4.8	6.8	31.5	11.3	-6.5	-6.5	-27.8	-26.7	9.9	-23.8	-35.8	-35.8
ACI 209	4.8	6.8	31.5	11.3	-6.5	-6.5	-27.8	-26.7	9.9	-23.8	-35.8	-35.8
CEB 90-RS	17.2	19.2	78.8	23.7	5.6	5.6	-19.8	-18.5	21.9	-15.8	-28.0	-28.0
Constant Ec	10.3	12.4	67.7	15.9	-0.9	-0.9	-24.9	-23.8	15.3	-19.8	-32.0	-32.0
2-Point	10.3	12.4	68.6	16.8	-0.9	-0.9	-24.9	-23.8	15.3	-19.8	-32.0	-32.0
Ec Model	Camber at 7 Days						Camber at 7 Days					
AASHTO '05 (+)	11.0	8.4	76.3	14.3	-5.5	-5.5	-23.6	-25.4	21.7	-21.5	-35.1	-35.1
ACI 209	11.0	8.4	76.3	14.3	-5.5	-5.5	-23.6	-25.4	21.7	-21.5	-35.1	-35.1
CEB 90-RS	24.4	21.3	95.1	27.2	5.8	5.8	-14.5	-16.3	34.7	-12.4	-28.2	-28.8
Constant Ec	16.9	13.8	83.8	19.7	-0.6	-0.6	-19.7	-21.5	26.9	-17.6	-31.9	-31.9
2-Point	16.9	13.8	83.8	19.7	-0.6	-0.6	-19.7	-21.5	26.9	-17.6	-31.9	-31.9
Ec Model	Camber at 15 Days						Camber at 15 Days					
AASHTO '05 (+)	26.3	15.8	104.2	23.2	-1.1	-1.1	-15.0	-22.5	38.8	-17.5	-32.5	-32.5
ACI 209	26.3	15.8	104.2	23.2	-1.1	-1.1	-15.0	-22.5	38.8	-17.5	-32.5	-32.5
CEB 90-RS	41.1	29.5	126.3	36.8	10.5	10.5	-5.0	-12.5	53.8	-7.5	-25.0	-25.0
Constant Ec	32.6	21.1	112.6	28.4	4.2	4.2	-10.0	-17.5	43.8	-13.8	-30.0	-30.0
2-Point	32.6	21.1	113.7	28.4	4.2	4.2	-10.0	-17.5	45.0	-12.5	-30.0	-30.0

Table G-22: SCC-HS-C & -D Percent Error in Camber Growth

	SCC-HS-C						SCC-HS-D					
	Creep and Shrinkage Model						Creep and Shrinkage Model					
	AASHTO '05 (+)	AASHTO '04 (-)	ACI 209	ACI 209*	CEB 90	Modified CEB 90	AASHTO '05 (+)	AASHTO '04 (-)	ACI 209	ACI 209*	CEB 90	Modified CEB 90
Ec Model	Camber Growth at 1 Day						Camber Growth at 1 Day					
AASHTO '05 (+)	-85.7	-71.4	21.6	-60.6	-96.4	-96.4	-80.5	-51.3	85.1	-41.5	-90.3	-90.3
ACI 209	-85.7	-71.4	21.6	-60.6	-96.4	-96.4	-80.5	-51.3	85.1	-41.5	-90.3	-90.3
CEB 90-RS	-66.0	-48.9	43.0	-42.1	-76.2	-76.2	-73.7	-47.4	84.2	-38.6	-91.2	-91.2
Constant Ec	-79.3	-65.5	24.1	-58.6	-93.1	-93.1	-72.0	-53.4	86.6	-44.0	-90.7	-90.7
2-Point	-79.3	-65.5	24.1	-58.6	-93.1	-93.1	-72.0	-53.4	86.6	-44.0	-90.7	-90.7
Ec Model	Camber Growth at 4 Days						Camber Growth at 4 Days					
AASHTO '05 (+)	-64.6	-72.7	-87.6	-70.7	-86.5	-86.5	-51.8	-68.3	-8.7	-61.8	-85.2	-85.2
ACI 209	-64.6	-72.7	-87.6	-70.7	-86.5	-86.5	-51.8	-68.3	-8.7	-61.8	-85.2	-85.2
CEB 90-RS	-65.2	-75.3	-25.3	-70.6	-85.6	-85.6	-57.3	-70.9	-8.8	-65.8	-81.4	-81.4
Constant Ec	-66.6	-74.1	-27.5	-71.5	-84.1	-84.1	-60.1	-68.6	-8.1	-57.3	-80.2	-80.2
2-Point	-66.6	-74.1	-25.6	-69.2	-84.1	-84.1	-60.1	-68.6	-8.1	-57.3	-80.2	-80.2
Ec Model	Camber Growth at 7 Days						Camber Growth at 7 Days					
AASHTO '05 (+)	-28.7	-35.8	149.7	-19.8	-74.0	-74.0	-12.3	-21.3	208.4	-2.3	-68.3	-68.3
ACI 209	-28.7	-35.8	149.7	-19.8	-74.0	-74.0	-12.3	-21.3	208.4	-2.3	-68.3	-68.3
CEB 90-RS	-8.5	-16.5	175.2	-1.3	-56.9	-56.9	-9.7	-17.8	206.1	-0.7	-69.9	-72.4
Constant Ec	-24.4	-32.5	151.9	-17.1	-70.5	-70.5	-9.9	-18.6	207.4	-0.4	-67.1	-67.1
2-Point	-24.4	-32.5	151.9	-17.1	-70.5	-70.5	-9.9	-18.6	207.4	-0.4	-67.1	-67.1
Ec Model	Camber Growth at 15 Days						Camber Growth at 15 Days					
AASHTO '05 (+)	12.4	-15.0	215.4	4.2	-58.9	-58.9	26.7	-6.4	263.5	15.7	-50.4	-50.4
ACI 209	12.4	-15.0	215.4	4.2	-58.9	-58.9	26.7	-6.4	263.5	15.7	-50.4	-50.4
CEB 90-RS	33.1	4.4	244.6	22.7	-42.6	-42.6	28.9	-0.9	261.8	19.0	-50.4	-50.4
Constant Ec	16.3	-12.8	217.1	5.7	-55.1	-55.1	31.8	0.2	258.6	16.0	-52.5	-52.5
2-Point	16.3	-12.8	219.7	5.7	-55.1	-55.1	31.8	0.2	263.8	21.3	-52.5	-52.5

APPENDIX H

VISUAL BASIC PROGRAM

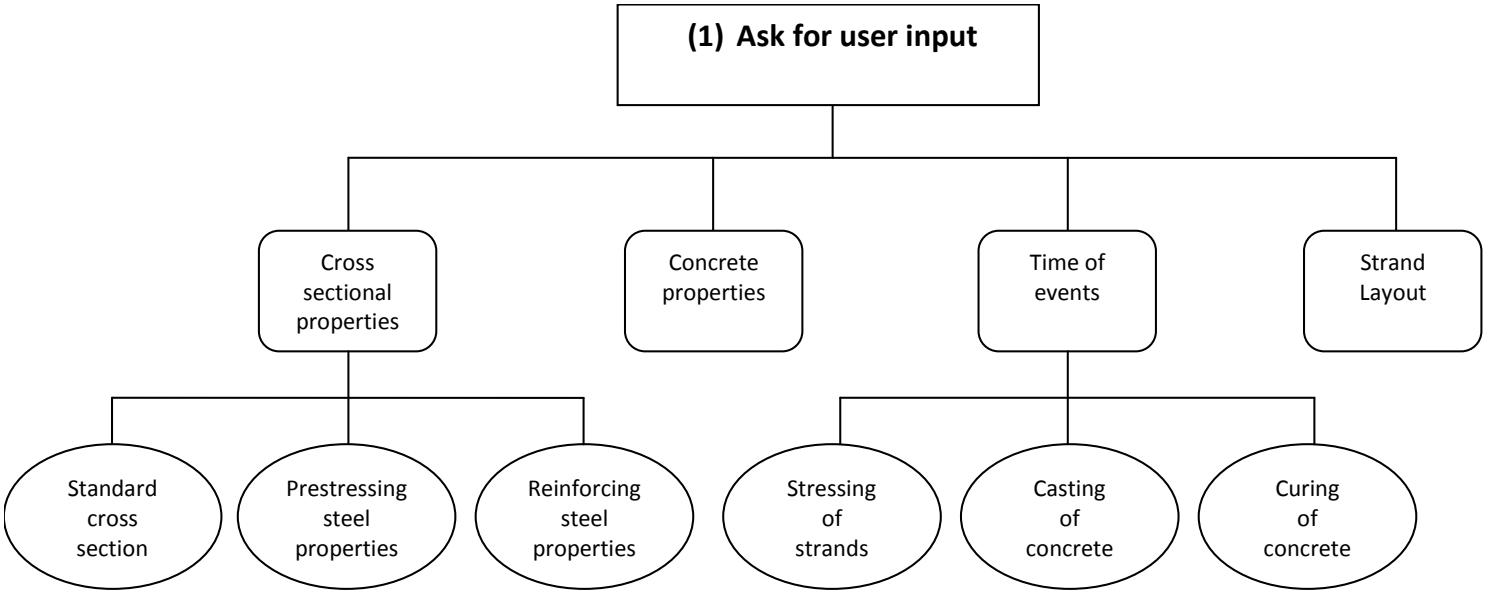

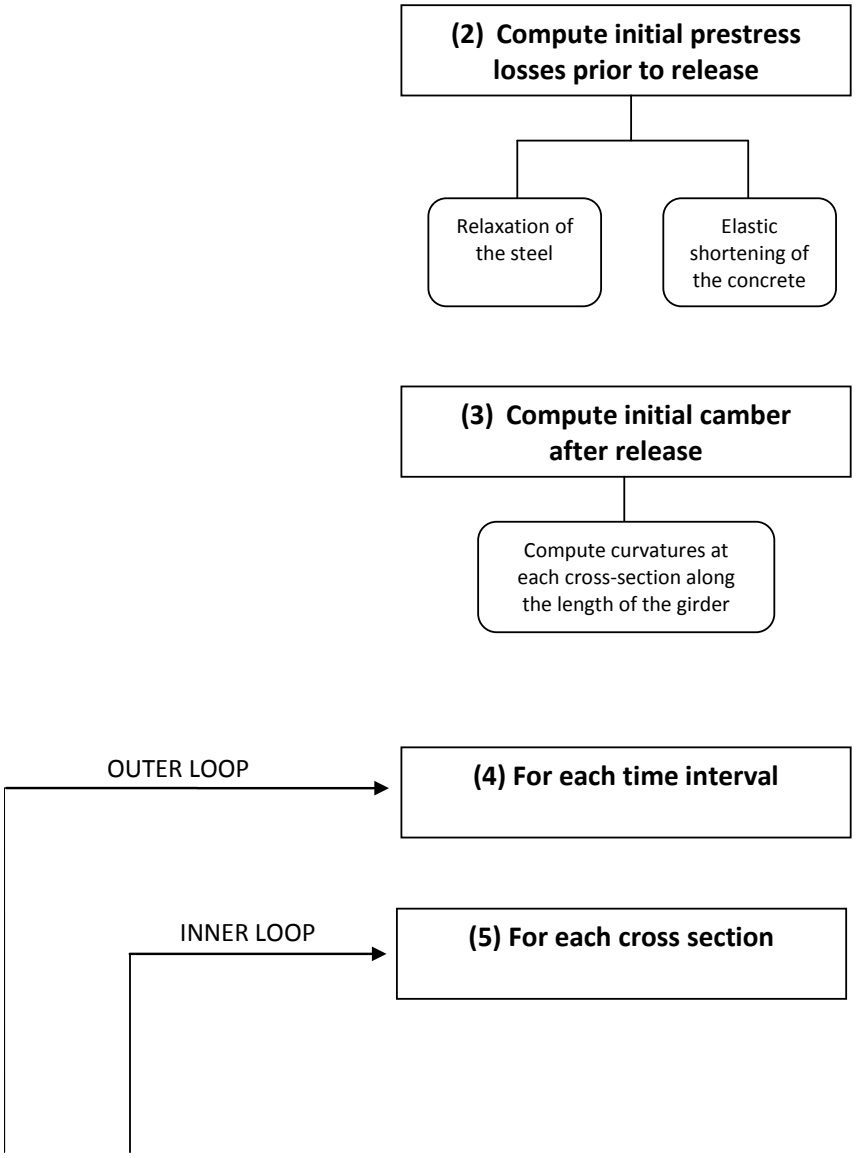
(2) Compute initial prestress losses prior to release
Relaxation of the steel
Elastic shortening of the concrete
(3) Compute initial camber after release
Compute curvatures at each cross-section along the length of the girder
OUTER LOOP
(4) For each time interval
INNER LOOP
(5) For each cross section

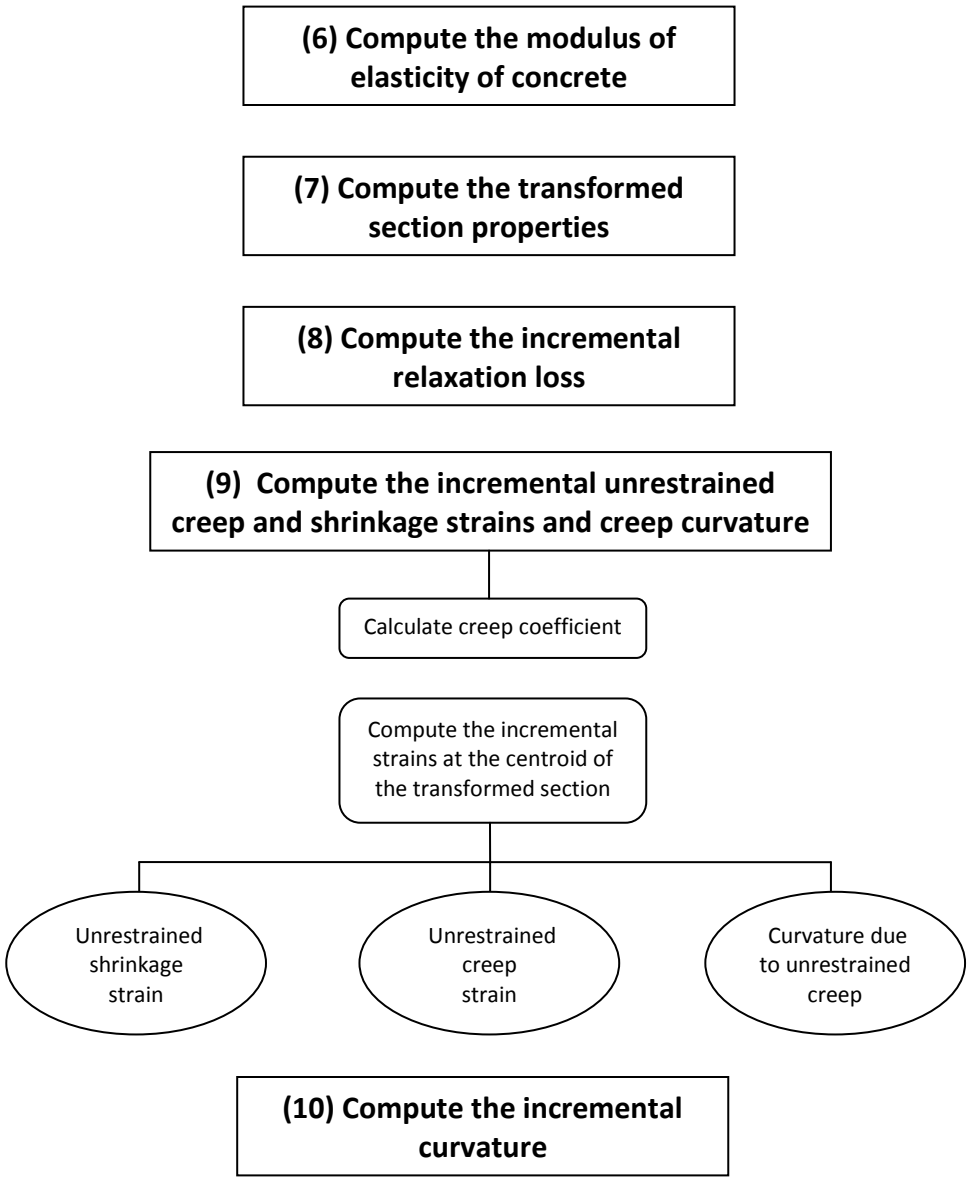
(6) Compute the modulus of elasticity of concrete
(7) Compute the transformed section properties
(8) Compute the incremental relaxation loss
(9) Compute the incremental unrestrained creep and shrinkage strains and creep curvature
Calculate creep coefficient
Compute the incremental strains at the centroid of the transformed section
Unrestrained shrinkage strain
Unrestrained creep strain
Curvature due to unrestrained creep
(10) Compute the incremental curvature

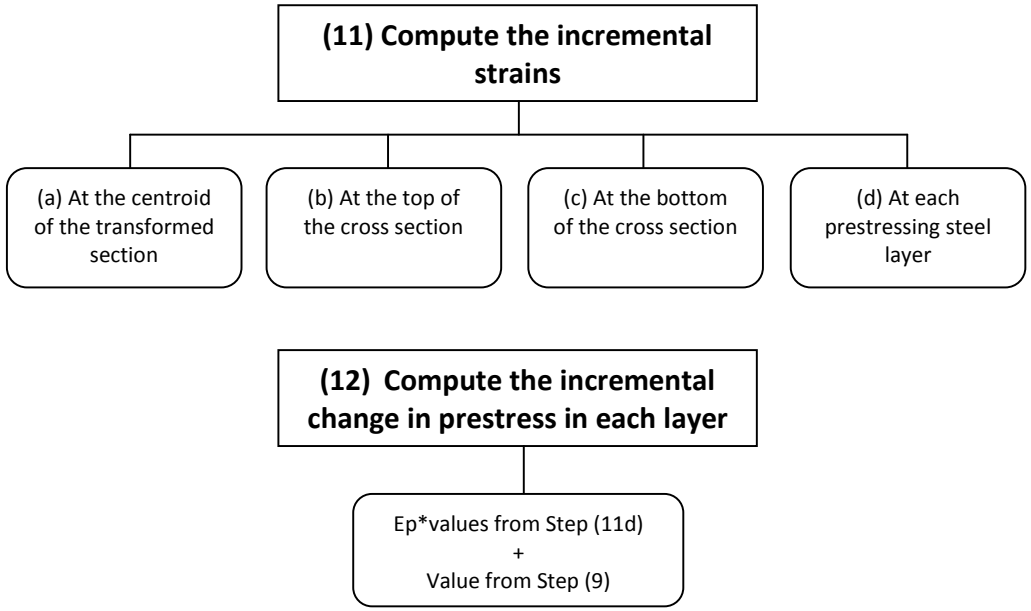
(11) Compute the incremental strains
(a) At the centroid of the transformed section
(b) At the top of the cross section
(c) At the bottom of the cross section
(d) At each prestressing steel layer
(12) Compute the incremental change in prestress in each layer
Ep*values from Step (11d)
+
Value from Step (9)

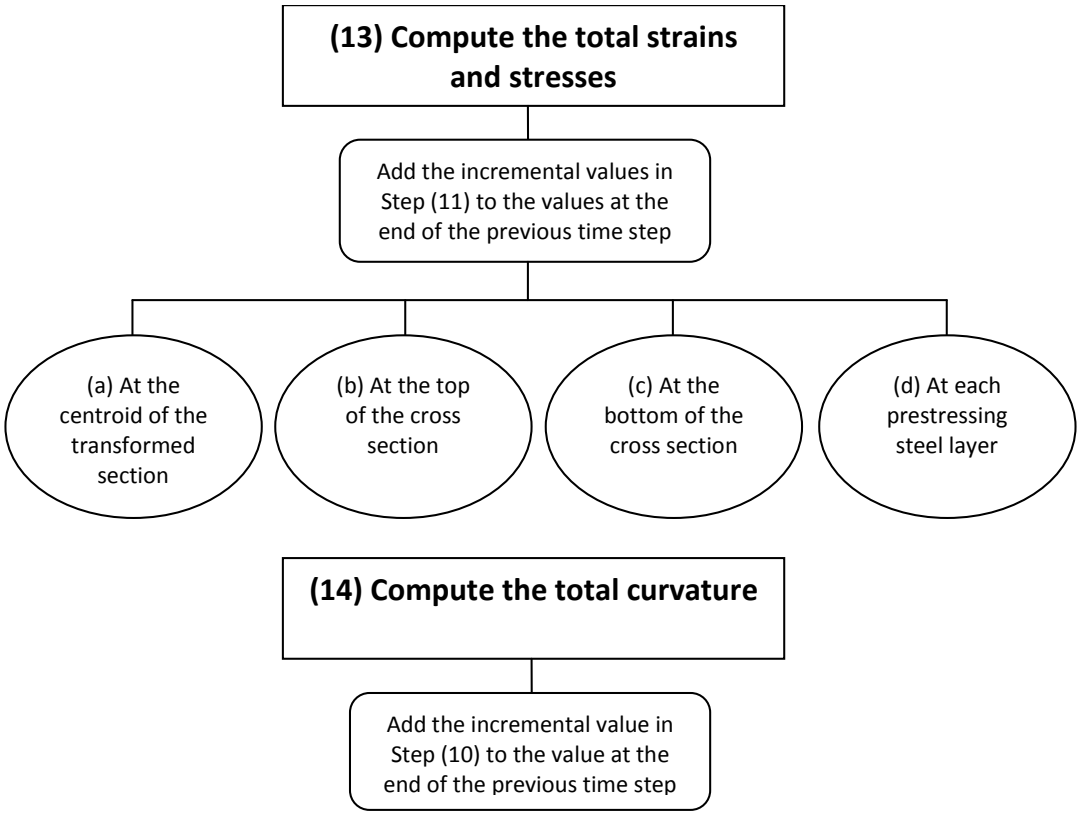
(13) Compute the total strains and stresses
Add the incremental values in Step (11) to the values at the end of the previous time step
(a) At the centroid of the transformed section
(b) At the top of the cross section
(c) At the bottom of the cross section
(d) At each prestressing steel layer
(14) Compute the total curvature
Add the incremental value in Step (10) to the value at the end of the previous time step

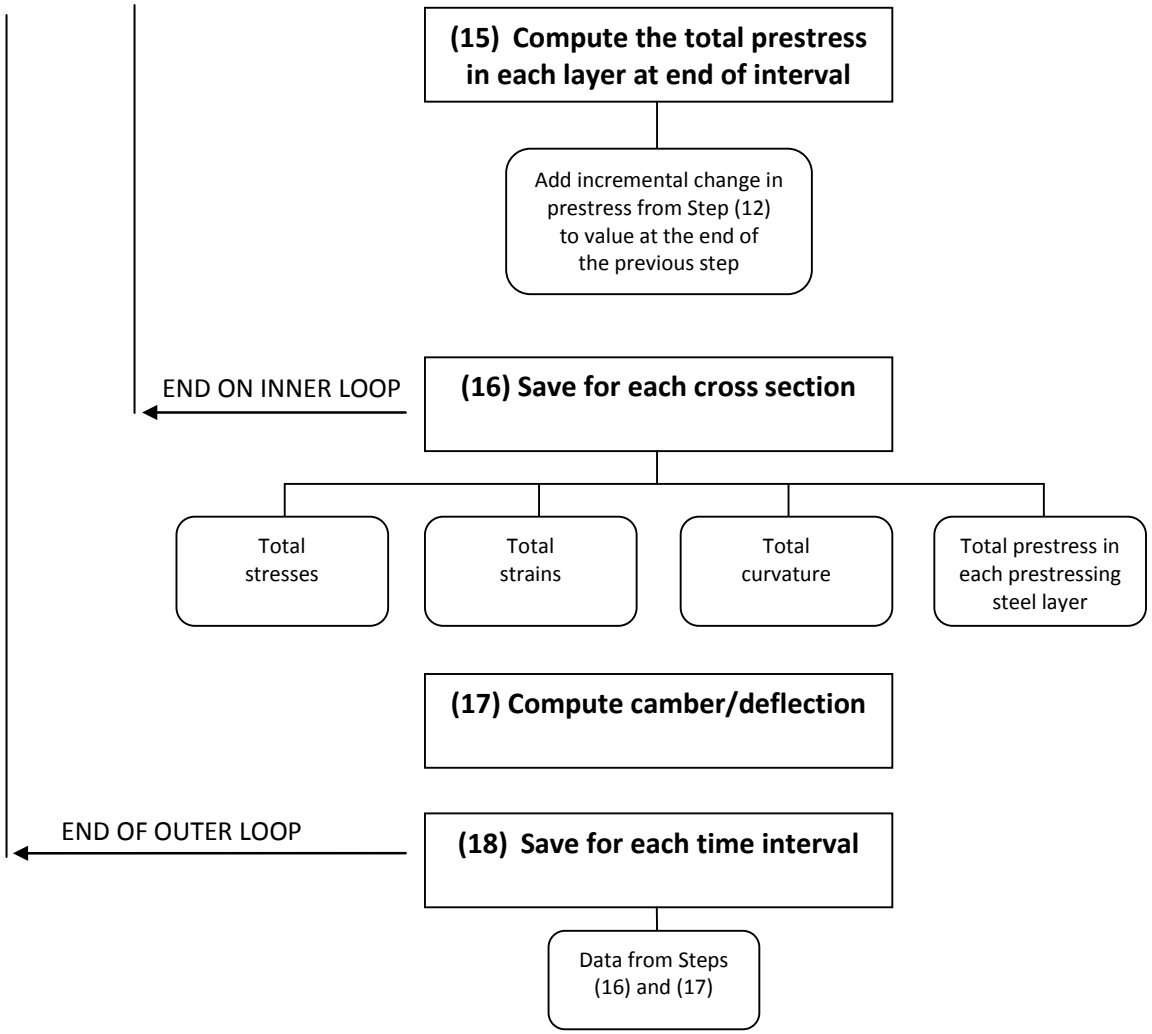

Figure H-1: Visual Basic Program Flow Chart

Table H-1: Property and Event Summary

			Gross Cross Sectional Properties						Hardened Concrete Properties				Fresh Properties				Mix	Cement	
	Beam ID	Standard CS	A_g ($in.^2$)	I_g ($in.^4$)	y_b (in.)	h (in.)	V/S (in.)	L (in.)	f'_{ci} (psi)	E_{ci} (ksi)	$f'_{c,28}$ (psi)	$E_{c,28}$ (ksi)	Air (%)	Slump* (in.)	Slump (in.)	w_c (pcf)	FA (%)	Type (I or III)	Content (pcy)
AASHTO TYPE 1	STD-M-1	Type I	276	22750	12.59	28	3.07	480	4780	5700	6600	6750	3.4	1	6.75	148	35.3	III	640
	STD-M-2	Type I	276	22750	12.59	28	3.07	480	4780	5700	7200	7300	3	1	6.5	148	35.3	III	640
	SCC-MS-1	Type I	276	22750	12.59	28	3.07	480	5540	5250	9780	7400	3.8	0	26.25	148.5	45	III	790
	SCC-MS-2	Type I	276	22750	12.59	28	3.07	480	5540	5250	9790	7500	1.8	0	27.75	150.3	45	III	790
	SCC-HS-1	Type I	276	22750	12.59	28	3.07	480	10430	7000	13160	8600	1.5	0	28	153.6	44.2	III	929
	SCC-HS-2	Type I	276	22750	12.59	28	3.07	480	10430	7000	13580	8300	1.5	0	28.25	153.2	44.2	III	929
T-BEAMS	STD-M-A	-	144	2943	9.75	15	1.85	276	5000	4900	6320	5150	11	1	9.5	142.2	46	III	640
	STD-M-B	-	144	2943	9.75	15	1.85	196	5000	4900	6320	5150	11	1	9.5	142.2	46	III	640
	STD-M-C	-	144	2943	9.75	15	1.85	156	5000	4900	6320	5150	11	1	9.5	142.2	46	III	640
	STD-M-D	-	144	2943	9.75	15	1.85	116	5000	4900	6320	5150	11	1	9.5	142.2	46	III	640
	SCC-MA-A	-	144	2943	9.75	15	1.85	276	5500	4900	8540	5400	2	0	29	151.8	46	III	750
	SCC-MA-B	-	144	2943	9.75	15	1.85	196	5500	4900	8540	5400	2	0	29	151.8	46	III	750
	SCC-MA-C	-	144	2943	9.75	15	1.85	156	5500	4900	8540	5400	2	0	29	151.8	46	III	750
	SCC-MA-D	-	144	2943	9.75	15	1.85	116	5500	4900	8540	5400	2	0	29	151.8	46	III	750
	SCC-MS-A	-	144	2943	9.75	15	1.85	276	5300	4950	9170	6150	5	0	28.5	148.4	46	III	750
	SCC-MS-B	-	144	2943	9.75	15	1.85	196	5300	4950	9170	6150	5	0	28.5	148.4	46	III	750
	SCC-MS-C	-	144	2943	9.75	15	1.85	156	5300	4950	9170	6150	5	0	28.5	148.4	46	III	750
	SCC-MS-D	-	144	2943	9.75	15	1.85	116	5300	4950	9170	6150	5	0	28.5	148.4	46	III	750
	SCC-HS-A	-	144	2943	9.75	15	1.85	276	9990	6050	13380	7050	3	0	26	155.2	46	III	929
	SCC-HS-B	-	144	2943	9.75	15	1.85	196	9990	6050	13380	7050	3	0	26	155.2	46	III	929
	SCC-HS-C	-	144	2943	9.75	15	1.85	156	9990	6050	13380	7050	3	0	26	155.2	46	III	929
	SCC-HS-D	-	144	2943	9.75	15	1.85	116	9990	6050	13380	7050	3	0	26	155.2	46	III	929
BT-54	BT-1 thru 5	BT-54	659	268,077	27.63	54	3.01	1362	8540	5740	9920	5740	4.2	0.5	8	149.7	37	III	904

Table H-1 Cont'd: Property and Event Summary

			Ambient	Prestressing Steel			Reinforcing Steel		Time of Events		Curing Details			Analysis Intervals		
	Beam ID	Standard CS	RH (%)	E_p (ksi)	f_{pu} (ksi)	f_{py} (ksi)	E_s (ksi)	f_y (ksi)	Jacking (hrs)	Transfer (hrs)	Type (M or S)	Ave Temp (˚C)	Length (hrs)	Number of CS	Max Time	Number of TI
AASHTO TYPE 1	STD-M-1	Type I	75	28900	270	243	-	-	6	21	S	50	18	35	110	40
	STD-M-2	Type I	75	28900	270	243	-	-	6	21	S	50	18	35	110	40
	SCC-MS-1	Type I	75	28900	270	243	-	-	6	23	M	44	18	35	160	40
	SCC-MS-2	Type I	75	28900	270	243	-	-	6	23	M	46	18	35	167	40
	SCC-HS-1	Type I	75	28900	270	243	-	-	6	22	M	48	18	35	214	40
	SCC-HS-2	Type I	75	28900	270	243	-	-	6	22	M	52	18	35	214	40
T-BEAMS	STD-M-A	-	55	28900	270	243	29000	60	96	72	M		66	35	90	40
	STD-M-B	-	55	28900	270	243	29000	60	96	72	M		66	35	90	40
	STD-M-C	-	55	28900	270	243	29000	60	96	72	M		66	35	90	40
	STD-M-D	-	55	28900	270	243	29000	60	96	72	M		66	35	90	40
	SCC-MA-A	-	55	28900	270	243	29000	60	24	30	M		24	35	201	40
	SCC-MA-B	-	55	28900	270	243	29000	60	24	30	M		24	35	201	40
	SCC-MA-C	-	55	28900	270	243	29000	60	24	30	M		24	35	201	40
	SCC-MA-D	-	55	28900	270	243	29000	60	24	30	M		24	35	201	40
	SCC-MS-A	-	55	28900	270	243	29000	60	96	72	M		66	35	56	40
	SCC-MS-B	-	55	28900	270	243	29000	60	96	72	M		66	35	56	40
	SCC-MS-C	-	55	28900	270	243	29000	60	96	72	M		66	35	56	40
	SCC-MS-D	-	55	28900	270	243	29000	60	96	72	M		66	35	56	40
	SCC-HS-A	-	55	28900	270	243	29000	60	192	30	M		24	35	15	40
	SCC-HS-B	-	55	28900	270	243	29000	60	192	30	M		24	35	15	40
	SCC-HS-C	-	55	28900	270	243	29000	60	192	30	M		24	35	15	40
	SCC-HS-D	-	55	28900	270	243	29000	60	192	30	M		24	35	15	40
BT-54	BT-1 thru 5	BT-54	70	27500	270	243	-	-	6	20	S		20	35	311	40

Table H-2: Prestressing Strand and Reinforcing Steel Summary

	Beam ID	Layer Group	Group Type	Number of Strands	Strand Type	Nominal Diameter	Jacking Stress	Distance from Bottom	Detail Length	Steel Layer	Number of Bars	Bar Size	Distance from Bottom
AASHTO TYPE I	STD-M-1	1	Fully Bonded, Straight	6	Low-relax	1/2" Oversized (0.164)	202.5	3	0	-	-	-	-
		2	Fully Bonded, Straight	2	Low-relax	1/2" Oversized (0.164)	30.5	25	0	-	-	-	-
	STD-M-2	1	Fully Bonded, Straight	6	Low-relax	1/2" Oversized (0.164)	202.5	3	0	-	-	-	-
		2	Fully Bonded, Straight	2	Low-relax	1/2" Oversized (0.164)	30.5	25	0	-	-	-	-
	SCC-MS-1	1	Fully Bonded, Straight	6	Low-relax	1/2" Oversized (0.164)	202.5	3	0	-	-	-	-
		2	Fully Bonded, Straight	2	Low-relax	1/2" Oversized (0.164)	30.5	25	0	-	-	-	-
	SCC-MS-2	1	Fully Bonded, Straight	6	Low-relax	1/2" Oversized (0.164)	202.5	3	0	-	-	-	-
		2	Fully Bonded, Straight	2	Low-relax	1/2" Oversized (0.164)	30.5	25	0	-	-	-	-
	SCC-HS-1	1	Fully Bonded, Straight	6	Low-relax	1/2" Oversized (0.164)	202.5	3	0	-	-	-	-
		2	Fully Bonded, Straight	2	Low-relax	1/2" Oversized (0.164)	30.5	25	0	-	-	-	-
	SCC-HS-2	1	Fully Bonded, Straight	6	Low-relax	1/2" Oversized (0.164)	202.5	3	0	-	-	-	-
		2	Fully Bonded, Straight	2	Low-relax	1/2" Oversized (0.164)	30.5	25	0	-	-	-	-
T-BEAMS	STD-M-A	1	Fully Bonded, Straight	2	Low-relax	1/2" Oversized (0.164)	212.4	2	0	1	4	#3	13.25
	STD-M-B	1	Fully Bonded, Straight	2	Low-relax	1/2" Oversized (0.164)	205	2	0	1	4	#3	13.25
	STD-M-C	1	Fully Bonded, Straight	2	Low-relax	1/2" Oversized (0.164)	205	2	0	1	4	#3	13.25
	STD-M-D	1	Fully Bonded, Straight	2	Low-relax	1/2" Oversized (0.164)	212.4	2	0	1	4	#3	13.25
	SCC-MA-A	1	Fully Bonded, Straight	2	Low-relax	1/2" Oversized (0.164)	202.2	2	0	1	4	#3	13.25
	SCC-MA-B	1	Fully Bonded, Straight	2	Low-relax	1/2" Oversized (0.164)	198	2	0	1	4	#3	13.25
	SCC-MA-C	1	Fully Bonded, Straight	2	Low-relax	1/2" Oversized (0.164)	198	2	0	1	4	#3	13.25
	SCC-MA-D	1	Fully Bonded, Straight	2	Low-relax	1/2" Oversized (0.164)	202.2	2	0	1	4	#3	13.25
	SCC-MS-A	1	Fully Bonded, Straight	2	Low-relax	1/2" Oversized (0.164)	214.5	2	0	1	4	#3	13.25
	SCC-MS-B	1	Fully Bonded, Straight	2	Low-relax	1/2" Oversized (0.164)	210.3	2	0	1	4	#3	13.25
	SCC-MS-C	1	Fully Bonded, Straight	2	Low-relax	1/2" Oversized (0.164)	210.3	2	0	1	4	#3	13.25
	SCC-MS-D	1	Fully Bonded, Straight	2	Low-relax	1/2" Oversized (0.164)	214.5	2	0	1	4	#3	13.25
	SCC-HS-A	1	Fully Bonded, Straight	2	Low-relax	1/2" Oversized (0.164)	213.7	2	0	1	4	#3	13.25
	SCC-HS-B	1	Fully Bonded, Straight	2	Low-relax	1/2" Oversized (0.164)	213.7	2	0	1	4	#3	13.25
	SCC-HS-C	1	Fully Bonded, Straight	2	Low-relax	1/2" Oversized (0.164)	213.7	2	0	1	4	#3	13.25
	SCC-HS-D	1	Fully Bonded, Straight	2	Low-relax	1/2" Oversized (0.164)	213.7	2	0	1	4	#3	13.25

Table H-2 Cont'd: Prestressing Strand and Reinforcing Steel Summary

	Beam ID	Layer Group	Group Type	Number of Strands	Strand Type	Nominal Diameter	Jacking Stress	Distance from Bottom	Detail Length	Steel Layer	Number of Bars	Bar Size	Distance from Bottom
AASHTO BT-54	All BT-54 Girders	1	Fully Bonded, Straight	6	Low-relax	0.6"	202.5	2.5	0	-	-	-	-
		2	Debonded	4	Low-relax	0.6"	202.5	2.5	48	-	-	-	-
		3	Fully Bonded, Straight	6	Low-relax	0.6"	202.5	4.5	0	-	-	-	-
		4	Debonded	4	Low-relax	0.6"	202.5	4.5	48	-	-	-	-
		5	Fully Bonded, Straight	4	Low-relax	0.6"	202.5	6.5	0	-	-	-	-
		6	Debonded	2	Low-relax	0.6"	202.5	6.5	48	-	-	-	-
		7	Fully Bonded, Straight	2	Low-relax	0.6"	202.5	8.5	0	-	-	-	-
		8	Draped	2	Low-relax	0.6"	202.5	4.5	120	-	-	-	38.5
		9	Draped	2	Low-relax	0.6"	202.5	6.5	120	-	-	-	40.5
		10	Draped	2	Low-relax	0.6"	202.5	8.5	120	-	-	-	42.5
		11	Draped	2	Low-relax	0.6"	202.5	10.5	120	-	-	-	44.5
		12	Draped	2	Low-relax	0.6"	202.5	12.5	120	-	-	-	46.5
		13	Draped	2	Low-relax	0.6"	202.5	14.5	120	-	-	-	48.5
		14	Draped	2	Low-relax	0.6"	202.5	16.5	120	-	-	-	50.5
		15	Fully Bonded, Straight	4	Low-relax	1/2"	50	52	0	-	-	-	-

Table H-3: Reinforcing Steel Properties

Bar Size Designation		Nominal Dimensions		
		Diameter	Area	Weight
U.S. Customary	SI	(in.)	($in.^2$)	(lb/ft)
#3	#10	0.375	0.11	0.376
#4	#13	0.500	0.20	0.668
#5	#16	0.625	0.31	1.043
#6	#19	0.750	0.44	1.502
#7	#22	0.875	0.60	2.044
#8	#25	1.000	0.79	2.670
#9	#29	1.128	1.00	3.400
#10	#32	1.270	1.27	4.303
#11	#36	1.410	1.56	5.313
#14	#43	1.693	2.25	11.380
#18	#57	2.257	4.00	20.240

Table H-4: Prestressing Steel Properties

Seven-Wire Strand					
Nominal Diameter	(in.)	1/2	1/2 Special	1/2 Special	3/5
Area	(sq. in.)	0.153	0.164	0.167	0.217
Weight	(plf)	0.52	0.53	0.53	0.74

Table H-5: AASHTO Girder Section Properties

Type	Area ($in.^2$)	Moment of Inertia ($in.^4$)	y_{bottom} (in.)	Weight (lb/ft)
I	276	22,750	12.59	287
II	369	50,980	15.83	384
III	560	125,390	20.27	583
IV	789	260,730	24.73	822
V	1,013	521,180	31.96	1,055
VI	1,085	733,320	36.38	1,130

Table H-6: AASHTO Girder Dimensions

Type	D1 (in.)	D2 (in.)	D3 (in.)	D4 (in.)	D5 (in.)	D6 (in.)
I	28.0	4.0	0.0	3.0	5.0	5.0
II	36.0	6.0	0.0	3.0	6.0	6.0
III	45.0	7.0	0.0	4.5	7.5	7.0
IV	54.0	8.0	0.0	6.0	9.0	8.0
V	63.0	5.0	3.0	4.0	10.0	8.0
VI	72.0	5.0	3.0	4.0	10.0	8.0

Type	B1 (in.)	B2 (in.)	B3 (in.)	B4 (in.)	B5 (in.)	B6 (in.)
I	12.0	16.0	6.0	3.0	0.0	5.0
II	12.0	18.0	6.0	3.0	0.0	6.0
III	16.0	22.0	7.0	4.5	0.0	7.5
IV	20.0	26.0	8.0	6.0	0.0	9.0
V	42.0	28.0	8.0	4.0	13.0	10.0
VI	42.0	28.0	8.0	4.0	13.0	10.0

Table H-7: Maximum Number of Strands in AASHTO Girders

Type	Layer of Reinforcement (from bottom of section)							
	1	**2**	**3**	**4**	**5**	**6**	**7**	**8**
I	6	6	4	2	2	2	2	2
II	8	8	6	4	2	2	2	2
III	10	10	10	8	6	4	2	2
IV	12	12	12	10	8	6	4	2
V	12	12	12	12	10	8	6	4
VI	12	12	12	12	10	8	6	4

Type	Layer of Reinforcement (from bottom of section)					
	9-13	**14-17**	**18-21**	**22-26**	**27-30**	**31-35**
I	2	-	-	-	-	-
II	2	2	-	-	-	-
III	2	2	2	-	-	-
IV	2	2	2	2	-	-
V	2	2	2	2	2	-
VI	2	2	2	2	2	2

APPENDIX I

SENSITIVITY ANALYSIS – INTERVAL SELECTION

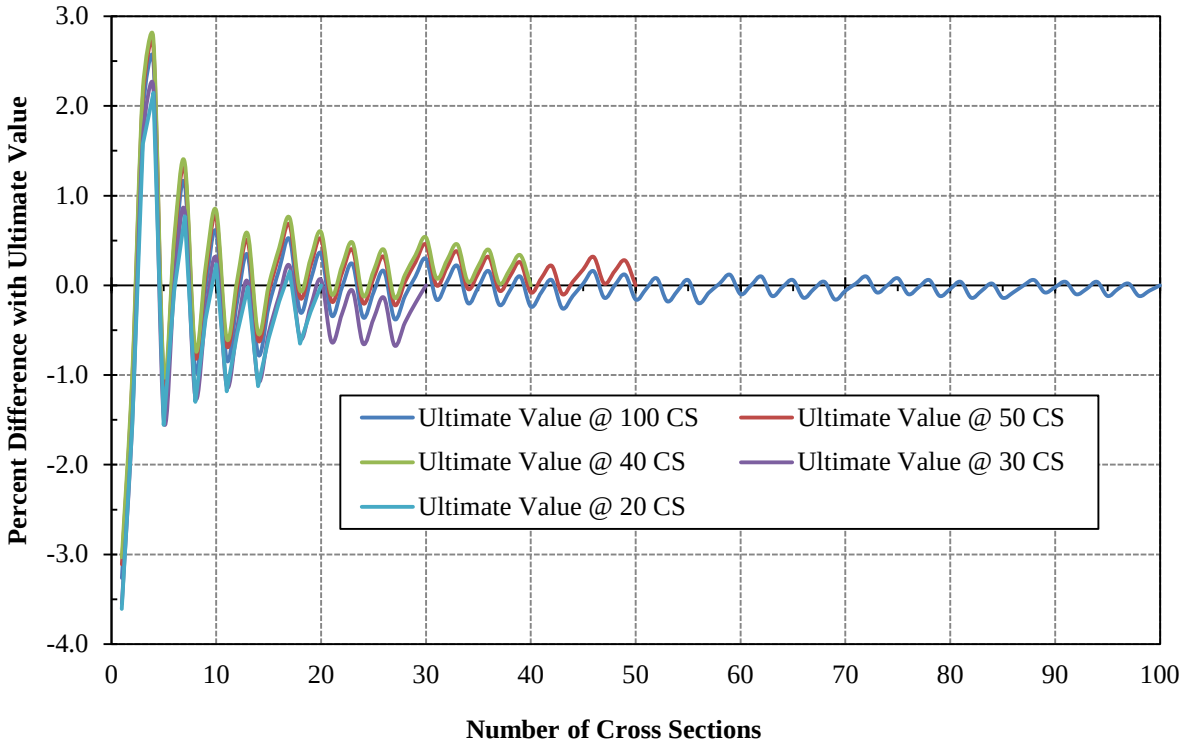

Figure I-1: Comparison of Percent Differences in Initial Midspan Camber

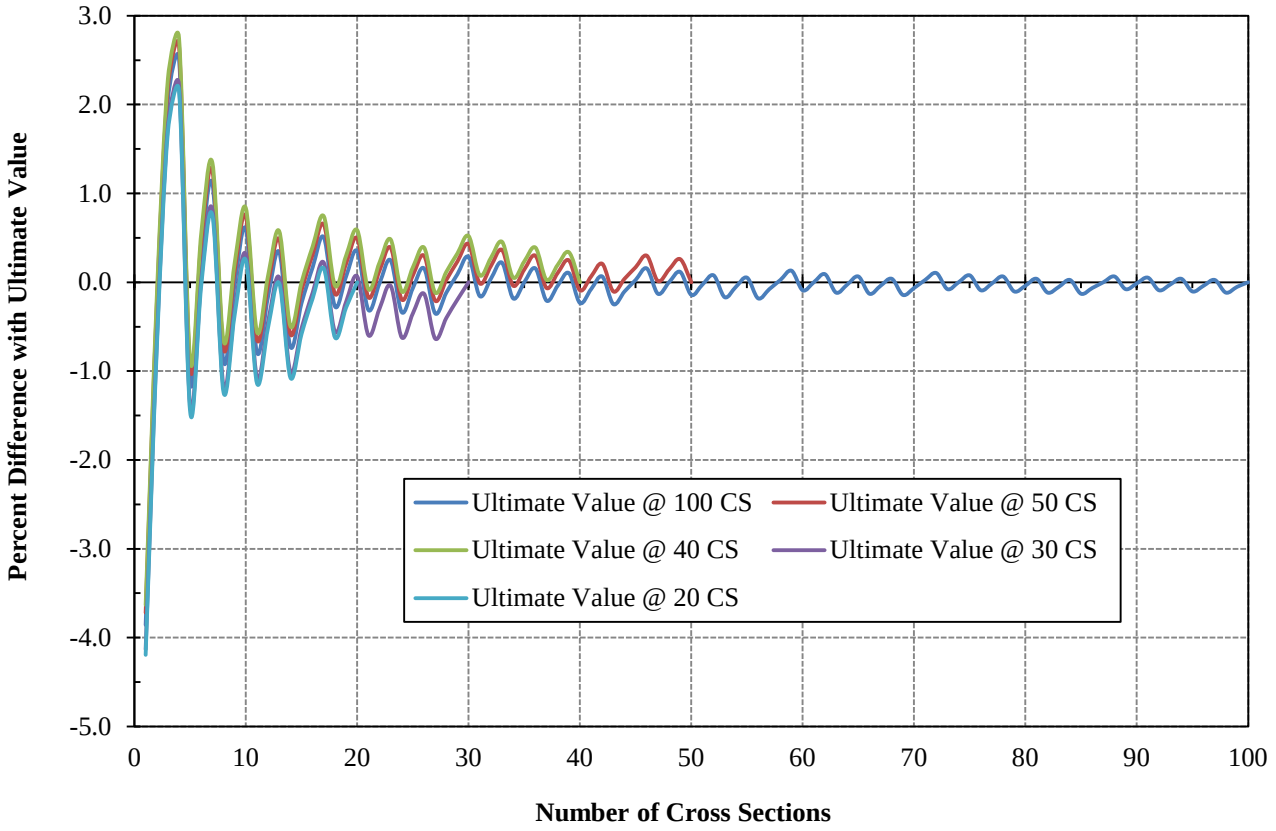

Figure I-2: Comparison of Percent Differences in 28-Day Midspan Camber

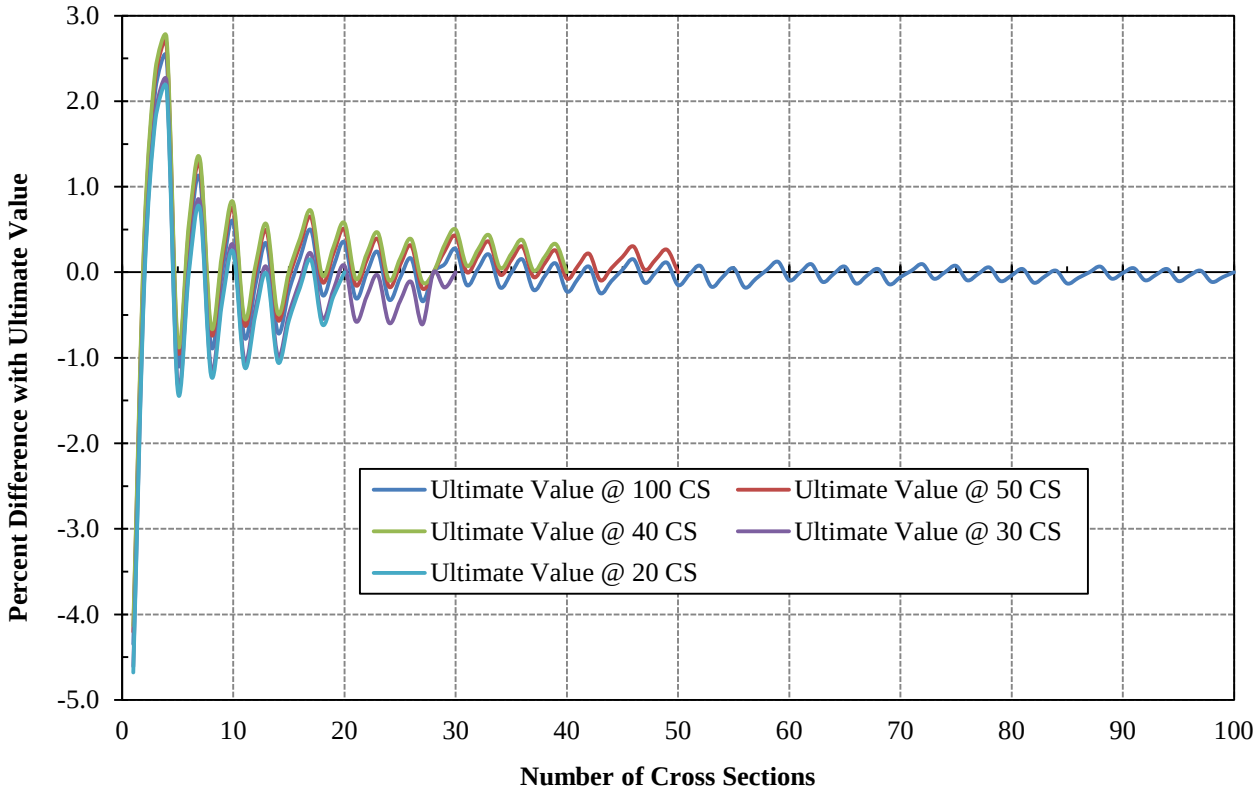

Figure I-3: Comparison of Percent Differences in 365-Day Midspan Camber

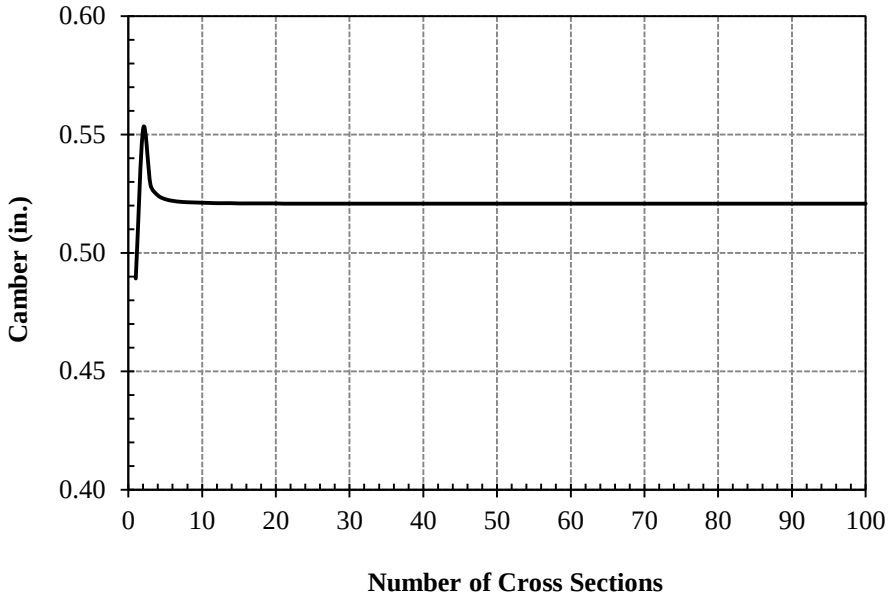

Figure I-4: Initial Midspan Camber vs. Number of Cross Sections (Straight)

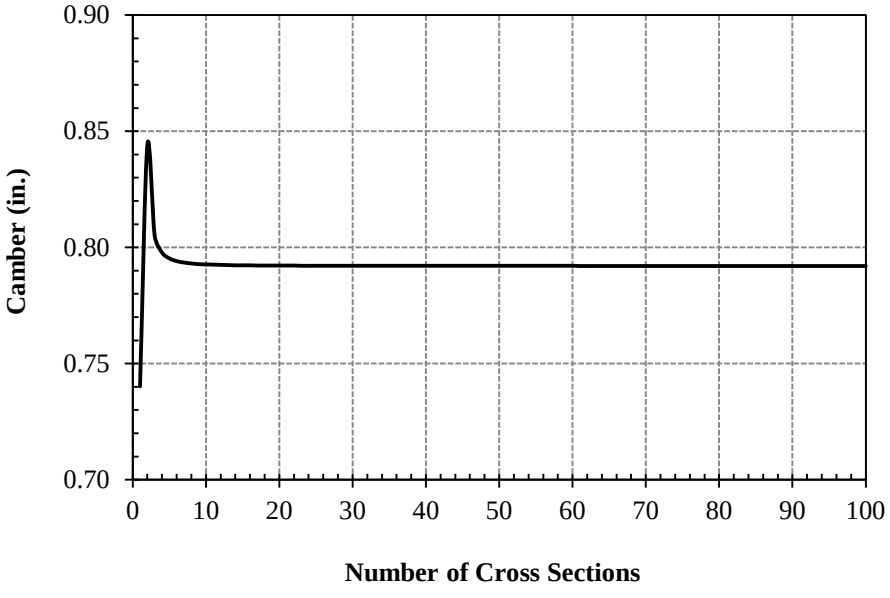

Figure I-5: Midspan Camber at 28 Days vs. Number of Cross Sections (Straight)

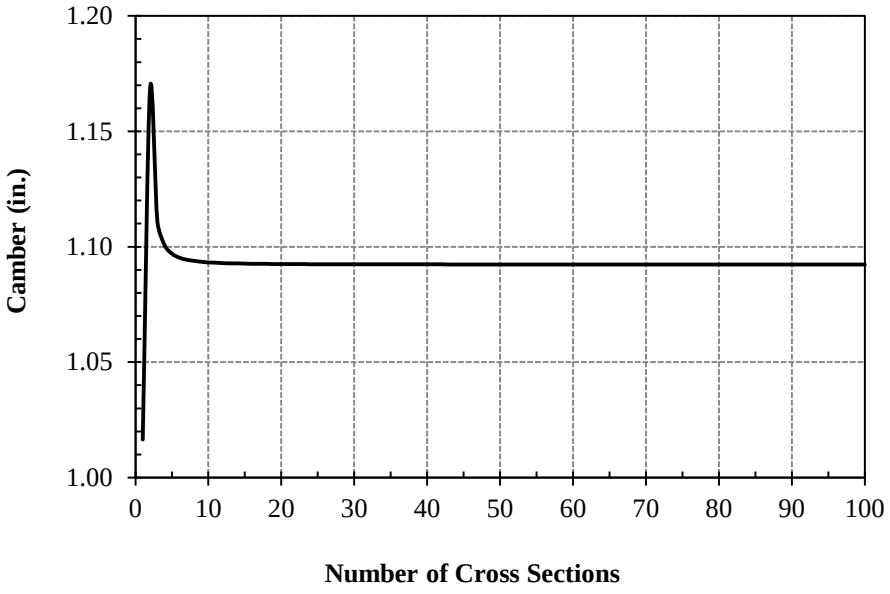

Figure I-6: Midspan Camber at 365 Days vs. Number of Cross Sections (Straight)

APPENDIX J

SENSITIVITY ANALYSIS – VISUAL BASIC PROGRAM

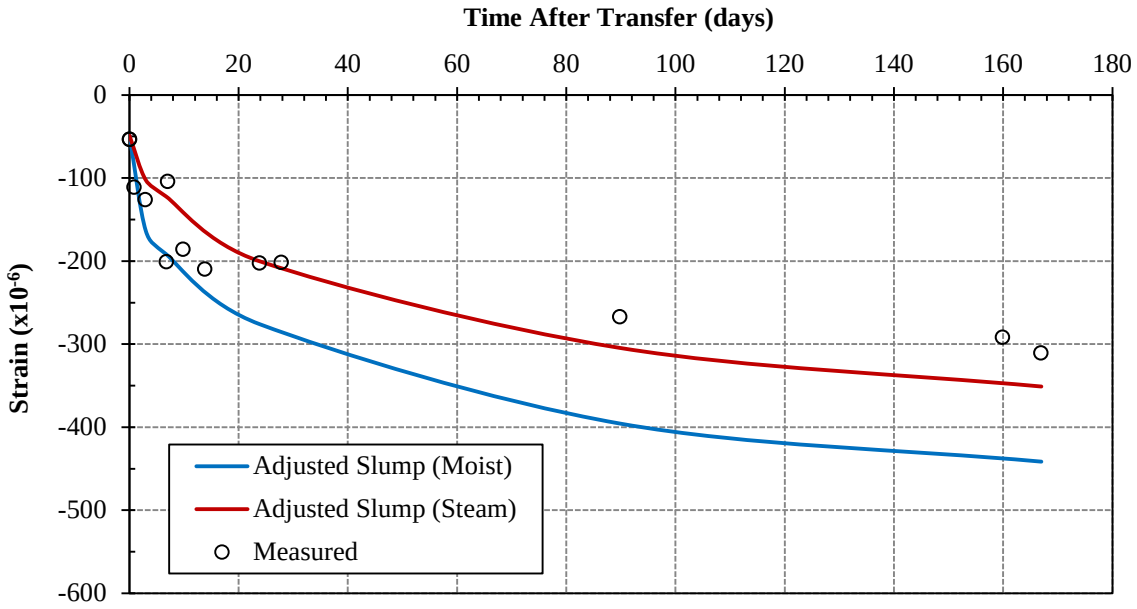

Figure J-1: SCC-MS-2 Predicted Strains at Top VWSG – Varying Cure Type

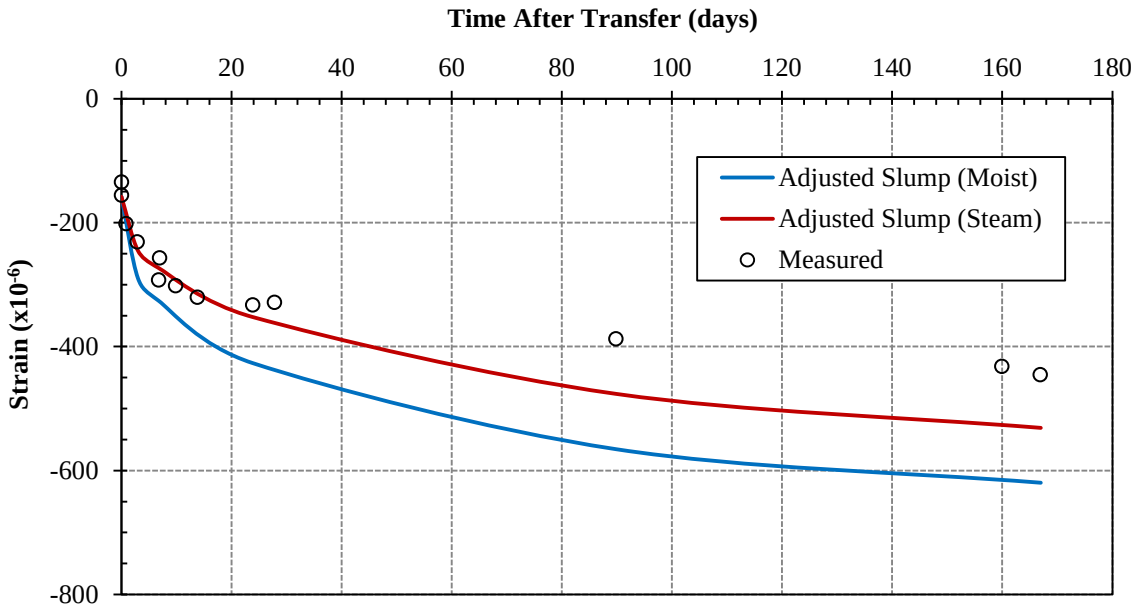

Figure J-2: SCC-MS-2 Predicted Strains at Middle VWSG – Varying Cure Type

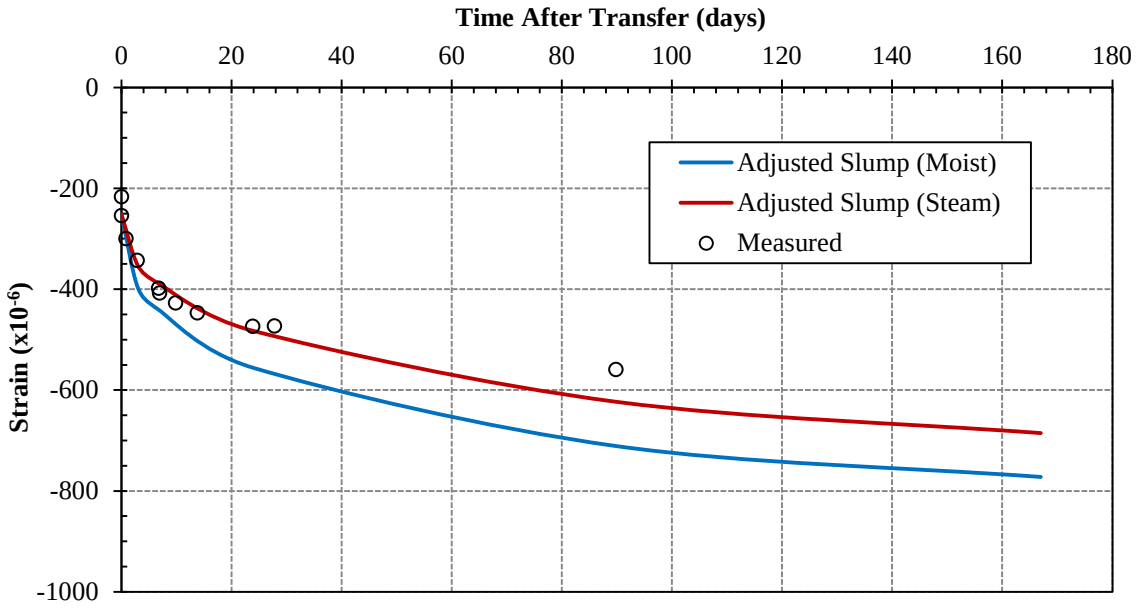

Figure J-3: SCC-MS-2 Predicted Strains at Bottom VWSG – Varying Cure Type

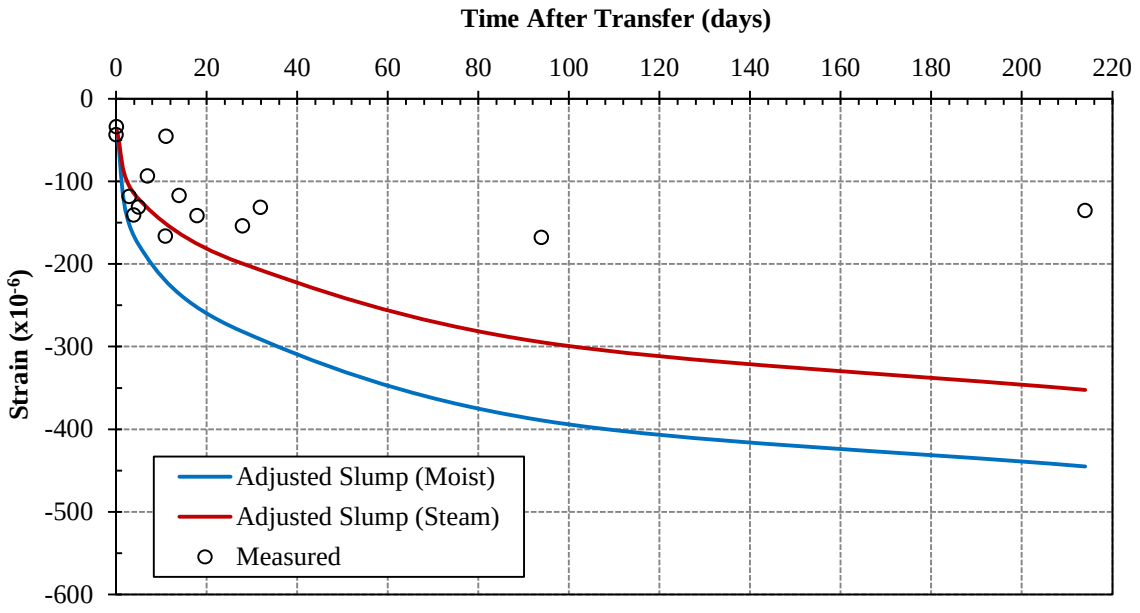

Figure J-4: SCC-HS-2 Predicted Strains at Top VWSG – Varying Cure Type

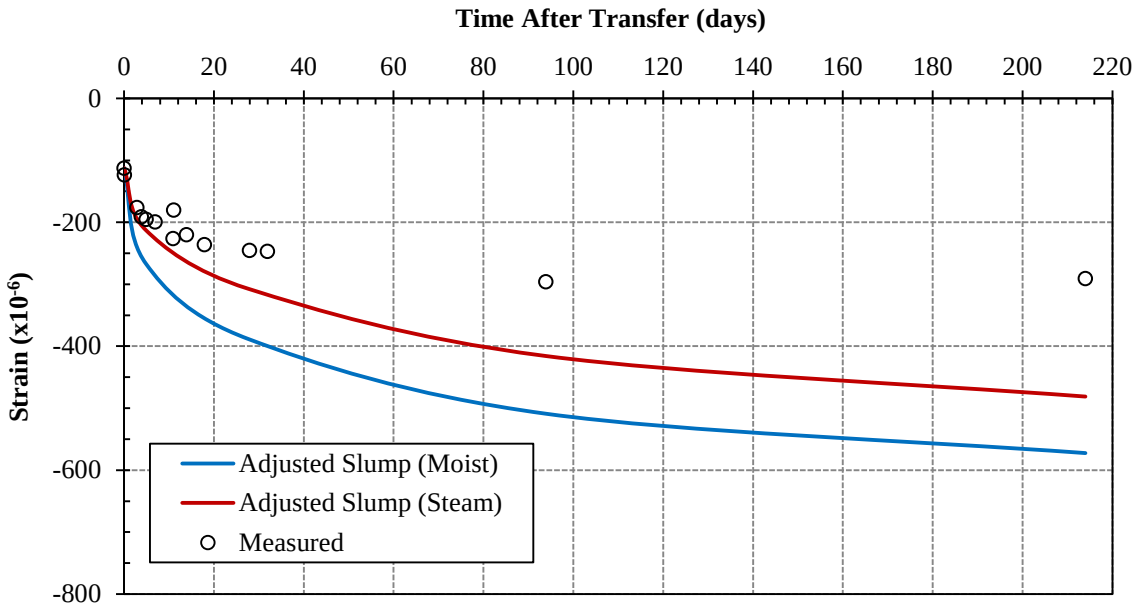

Figure J-5: SCC-HS-2 Predicted Strains at Middle VWSG – Varying Cure Type

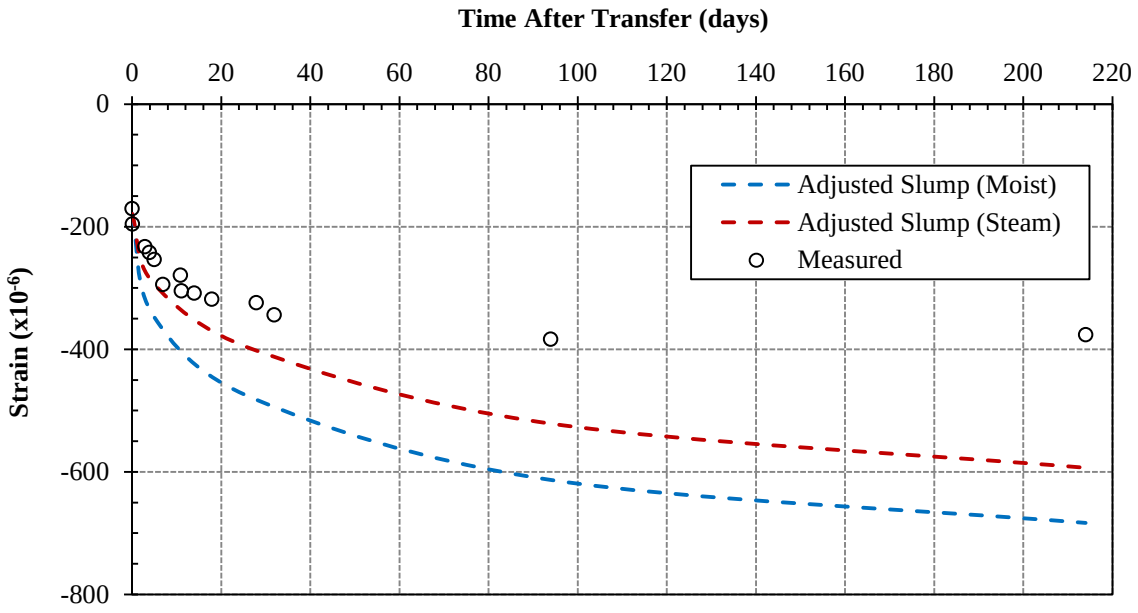

Figure J-6: SCC-HS-2 Predicted Strains at Bottom VWSG – Varying Cure Type

APPENDIX K

VISUAL BASIC PROGRAM USER INTERFACE

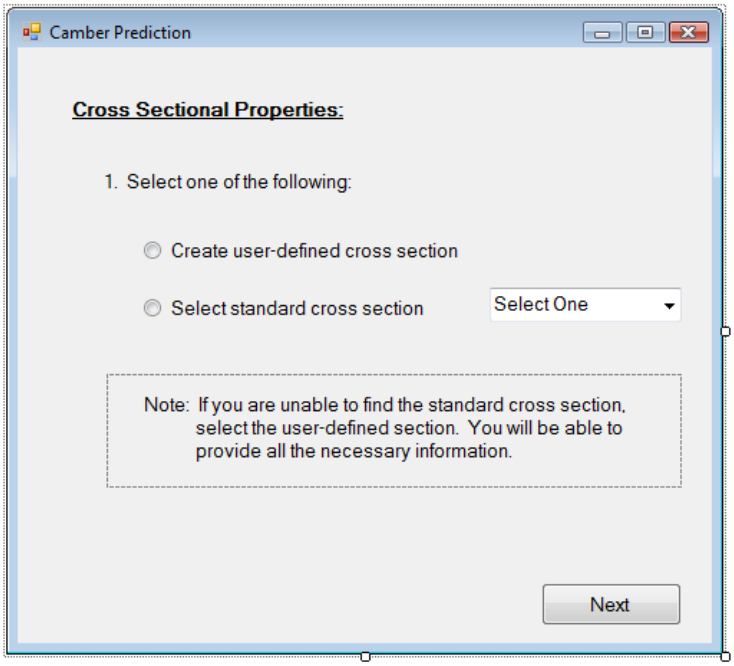

Figure K-1: Selection of Standard or User-Defined Cross Section

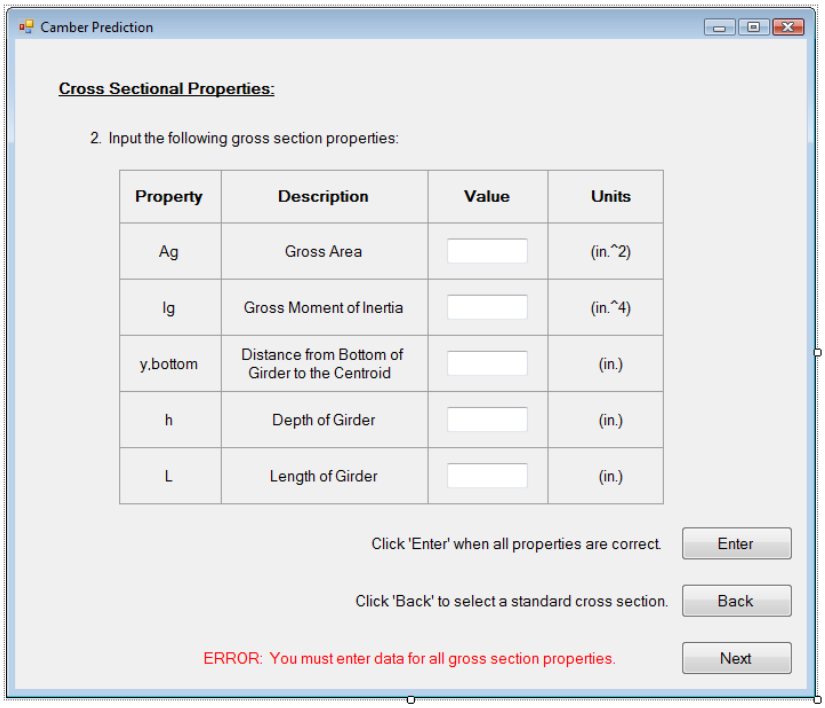

Figure K-2: Input of Cross-Sectional Properties

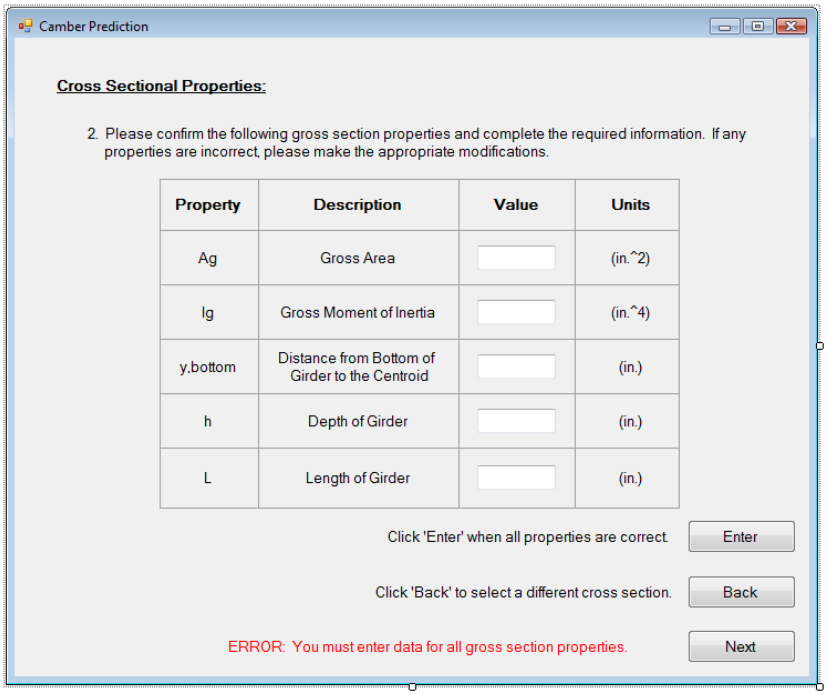

Figure K-3: Confirmation of Standard Cross-Sectional Properties

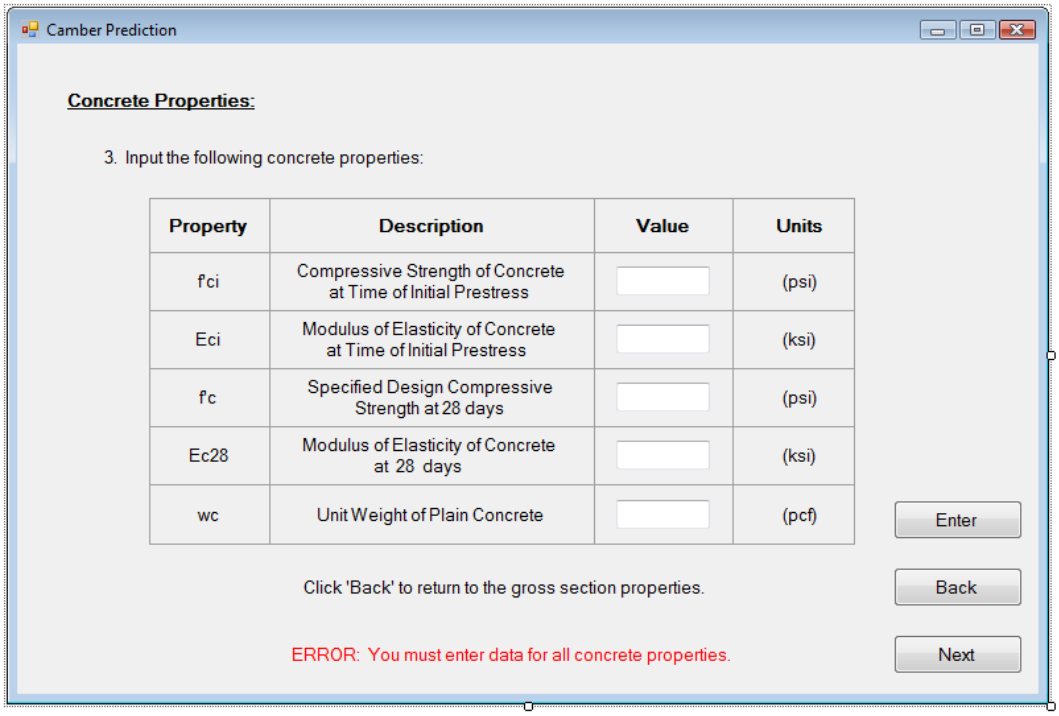

Figure K-4: Input of Concrete Properties

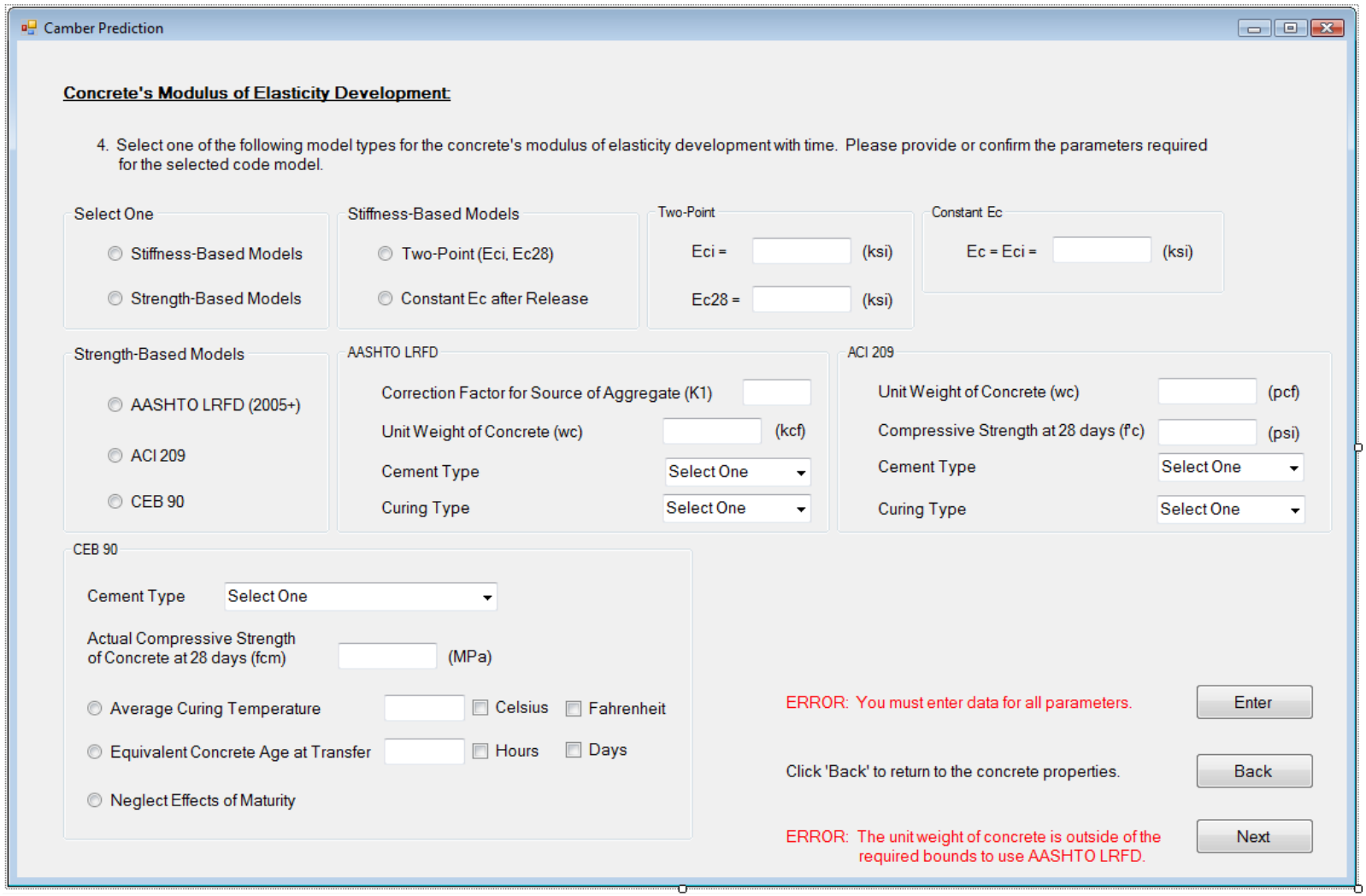

Figure K-5: Concrete Modulus of Elasticity Development

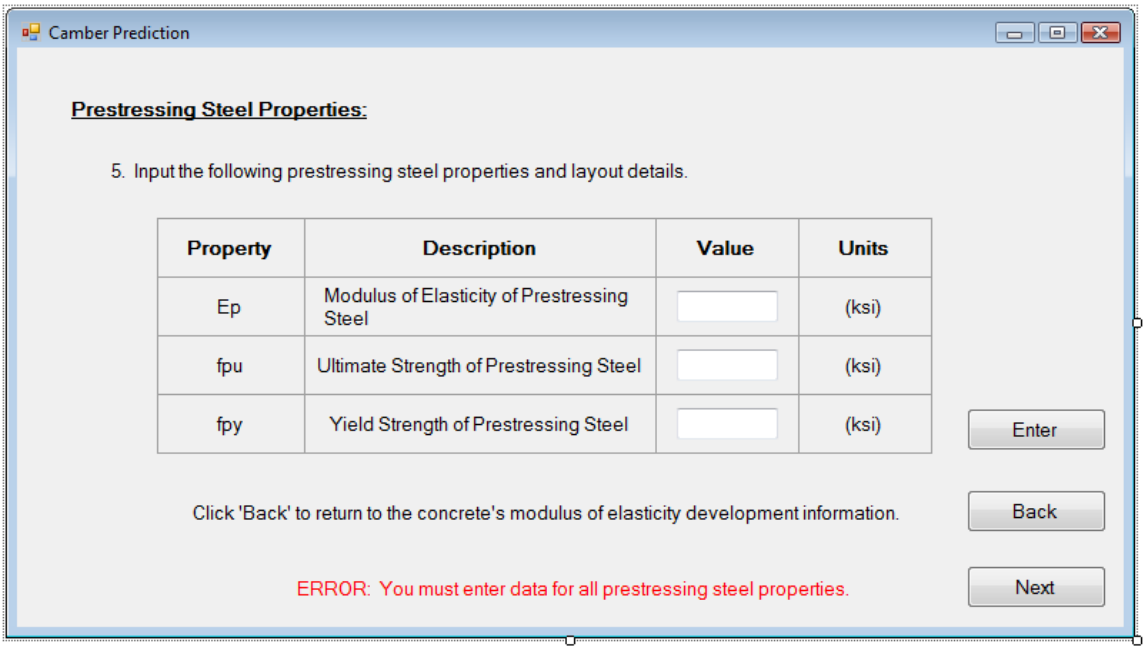

Figure K-6: Input of Prestressing Steel Properties

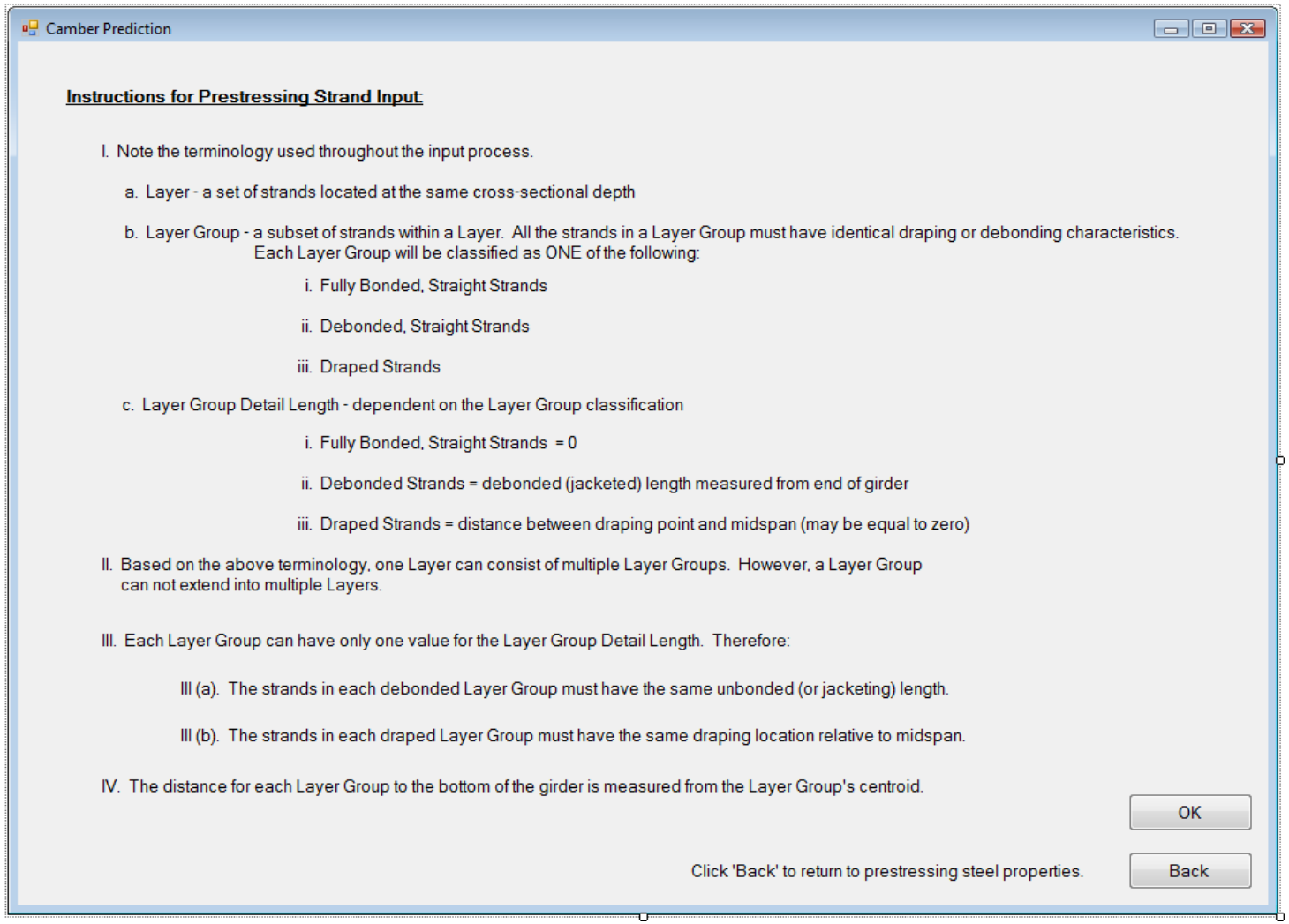

Figure K-7: Instructions for Prestressing Strand Input

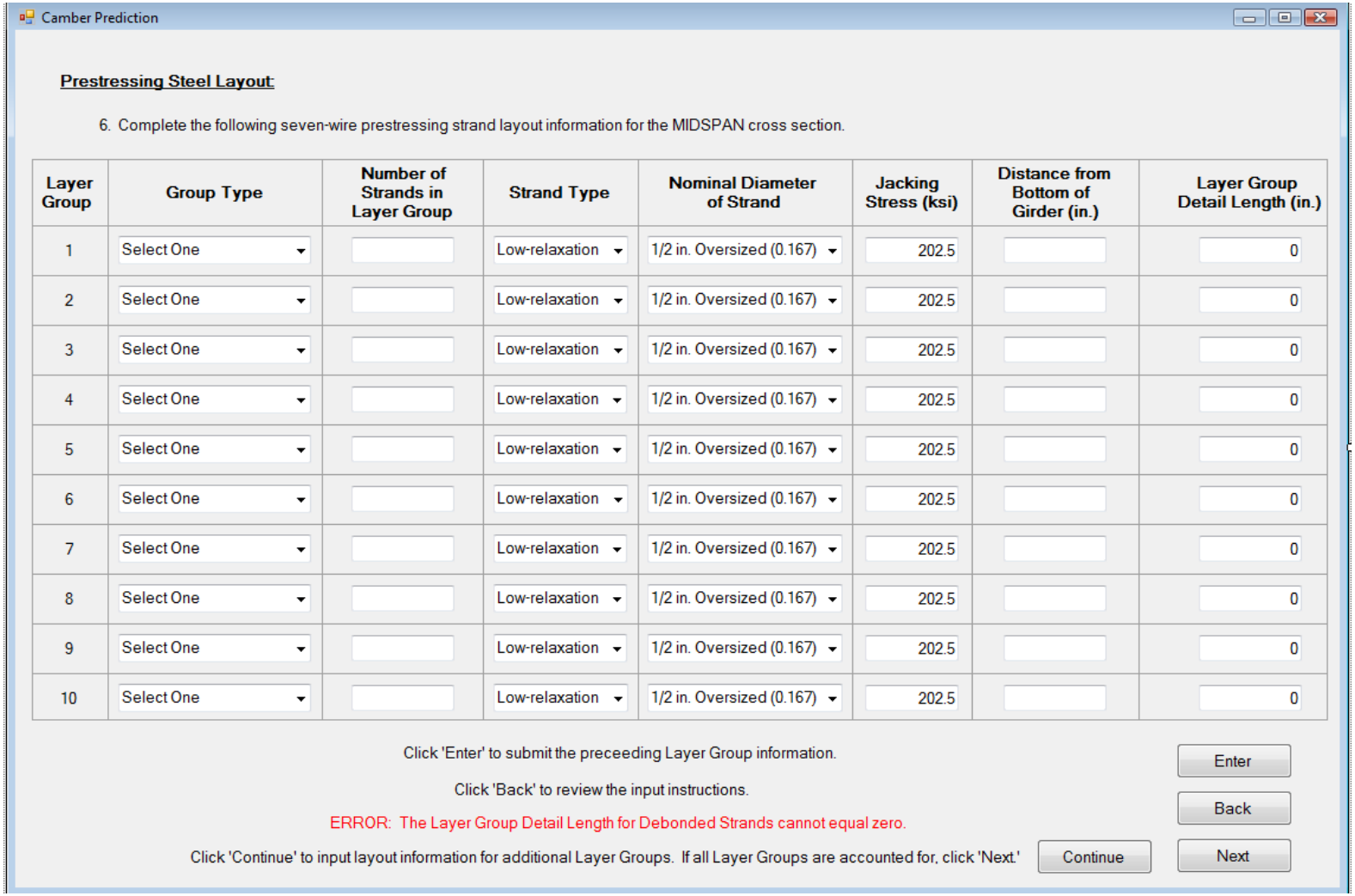

Figure K-8: Input of Prestressing Steel Layout

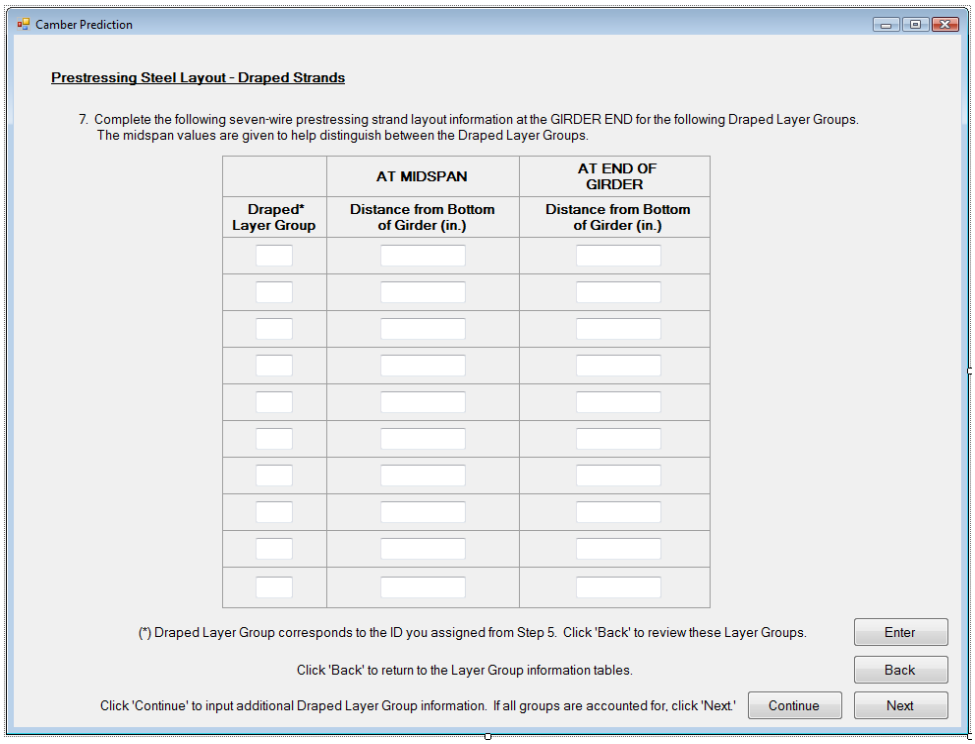

Figure K-9: Input of Prestressing Steel Layout – Draped Strands

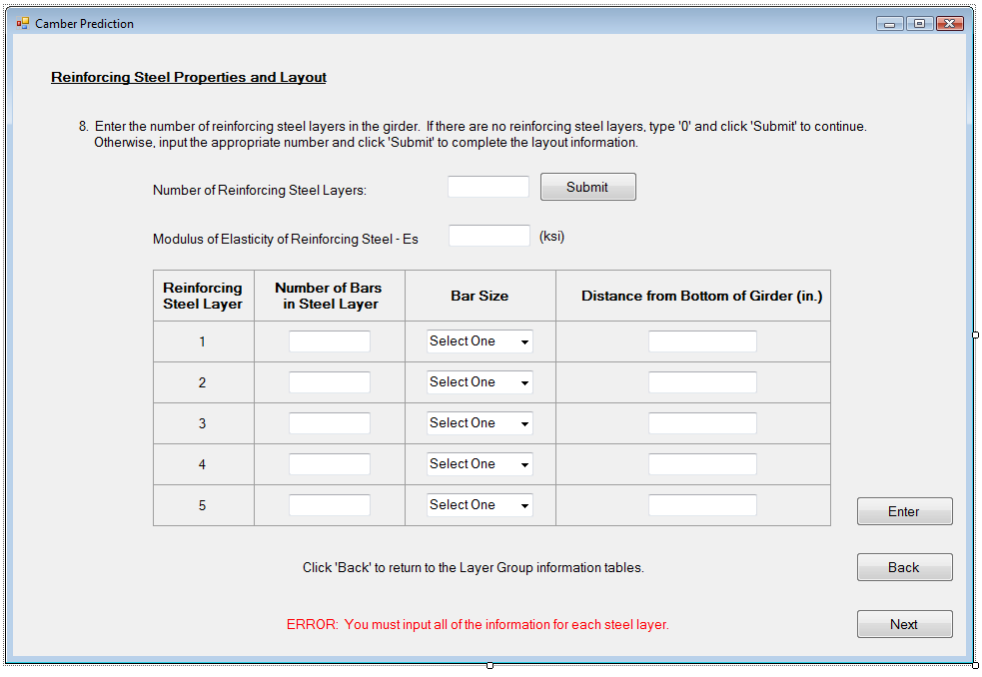

Figure K-10: Input of Reinforcing Steel Properties and Layout

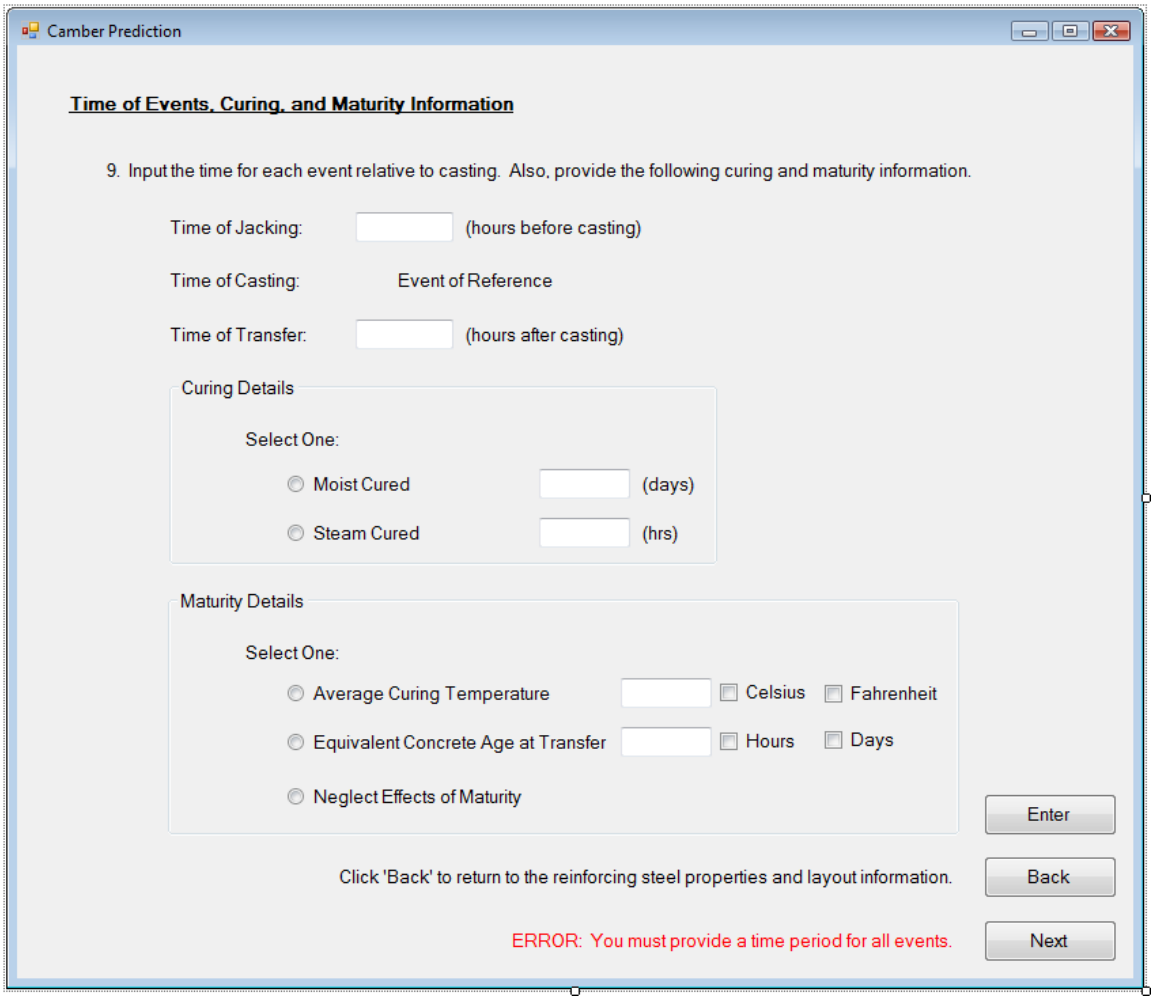

Figure K-11: Input of Event Times, Curing, and Maturity Information

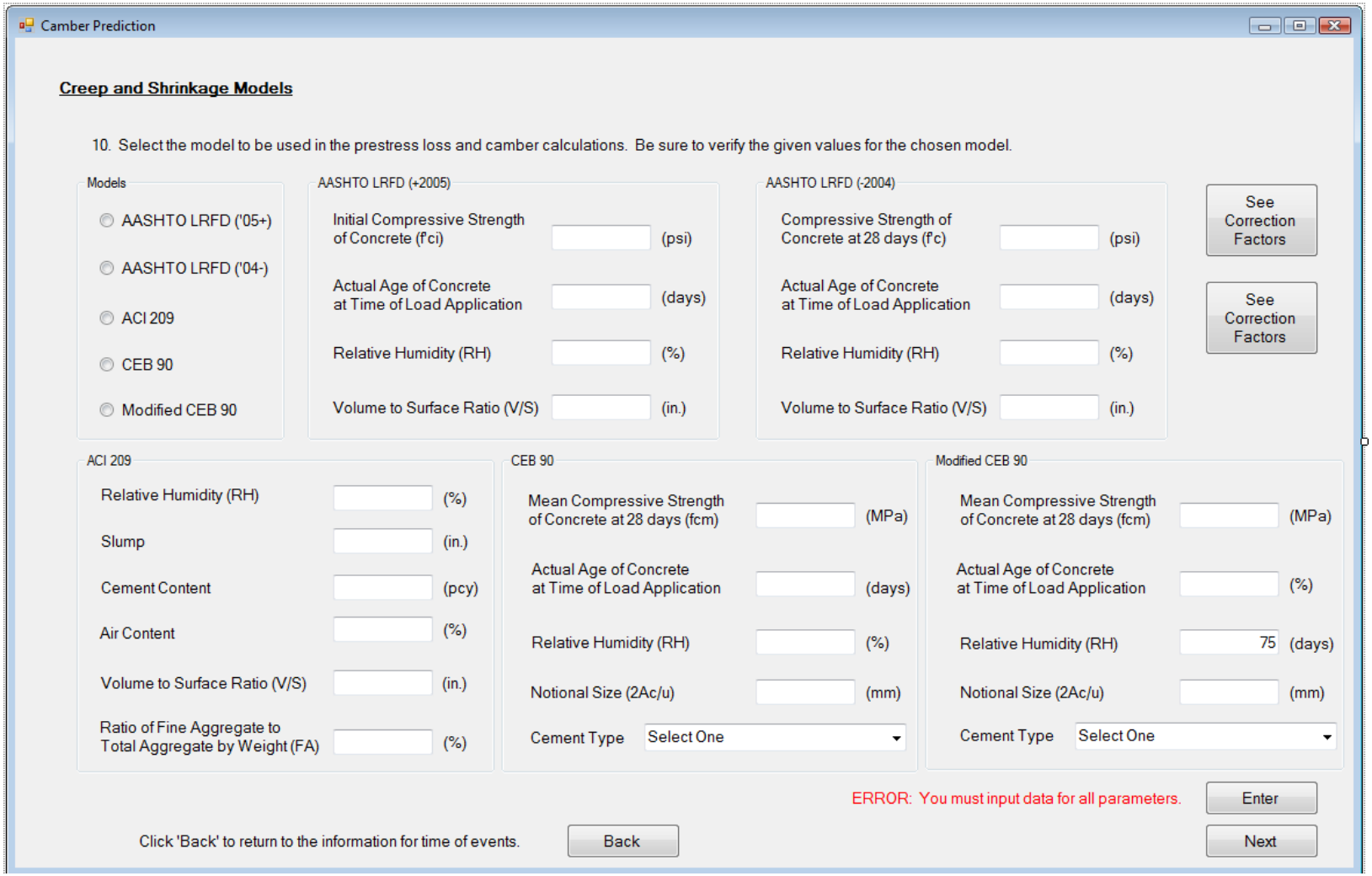

Figure K-12: Selection and Input of Creep and Shrinkage Model Information

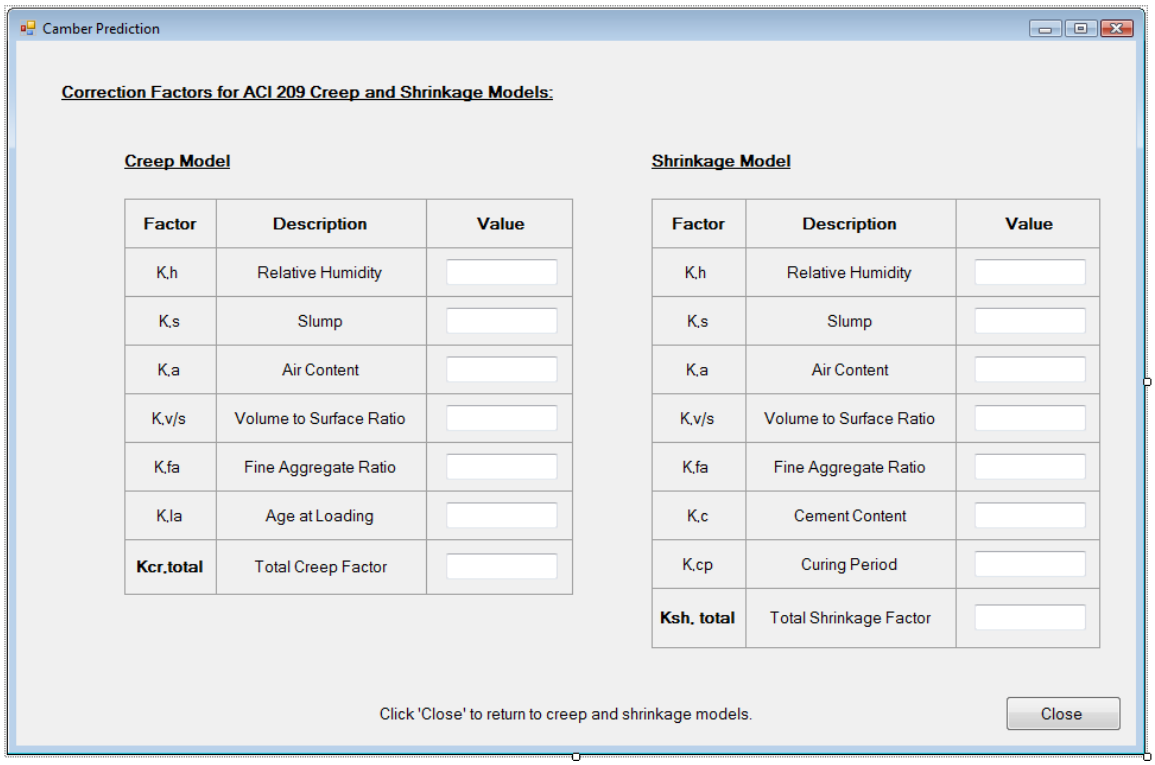

Figure K-13: Display of ACI 209 Creep and Shrinkage Correction Factors

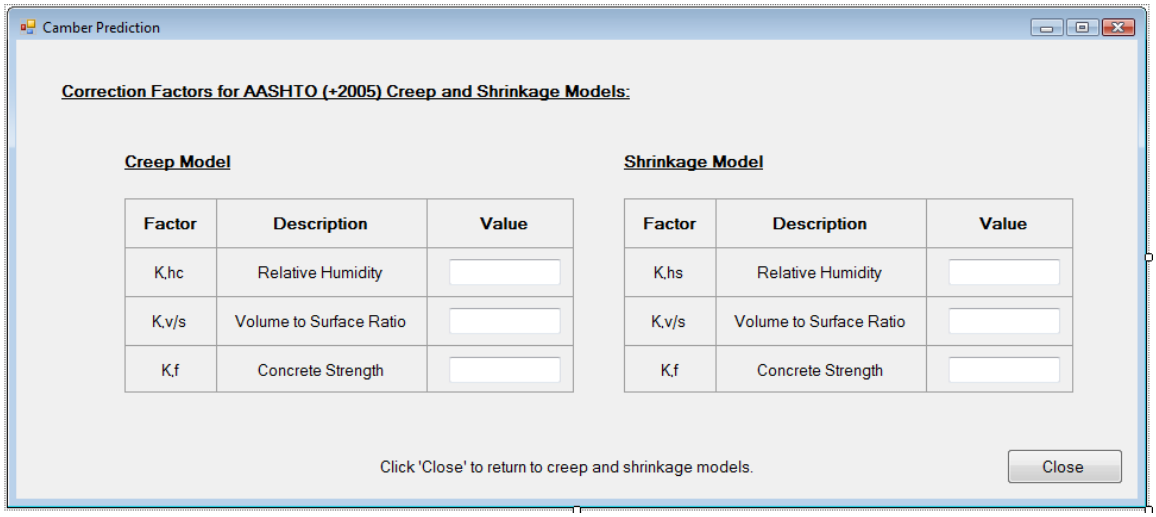

Figure K-14: Display of AASHTO (+'05) Creep and Shrinkage Correction Factors

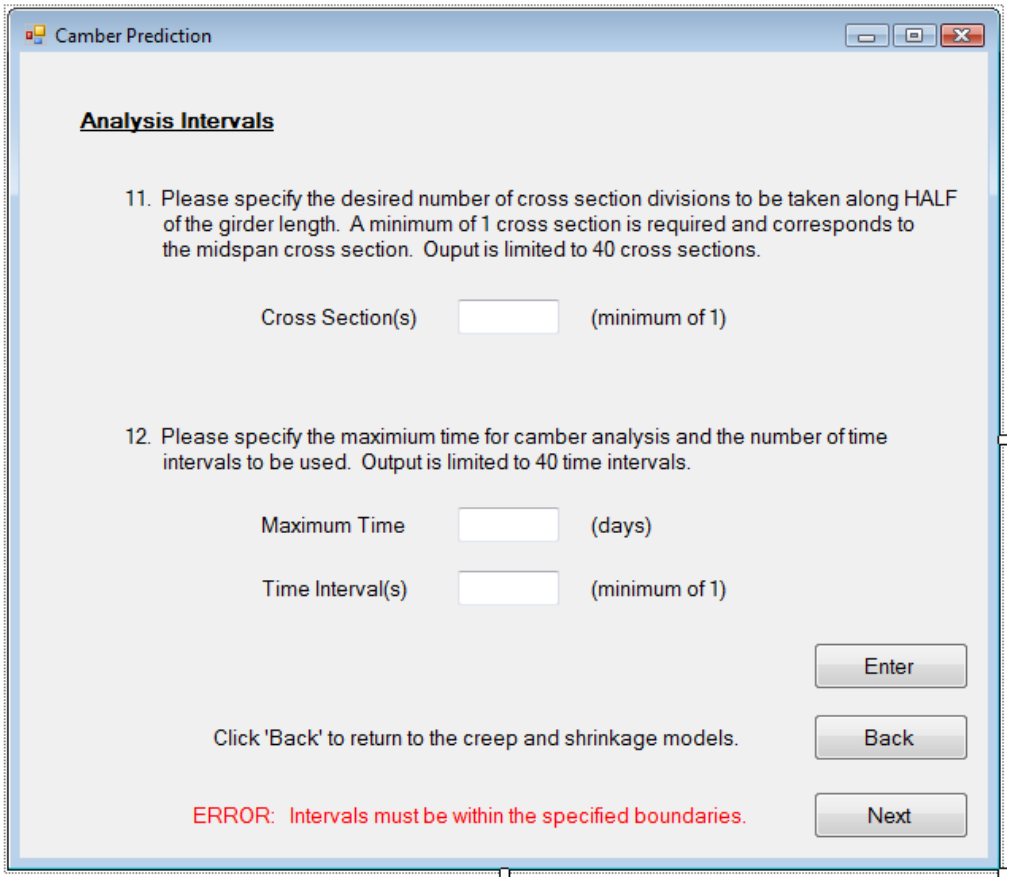

Figure K-15: Input of Analysis Intervals

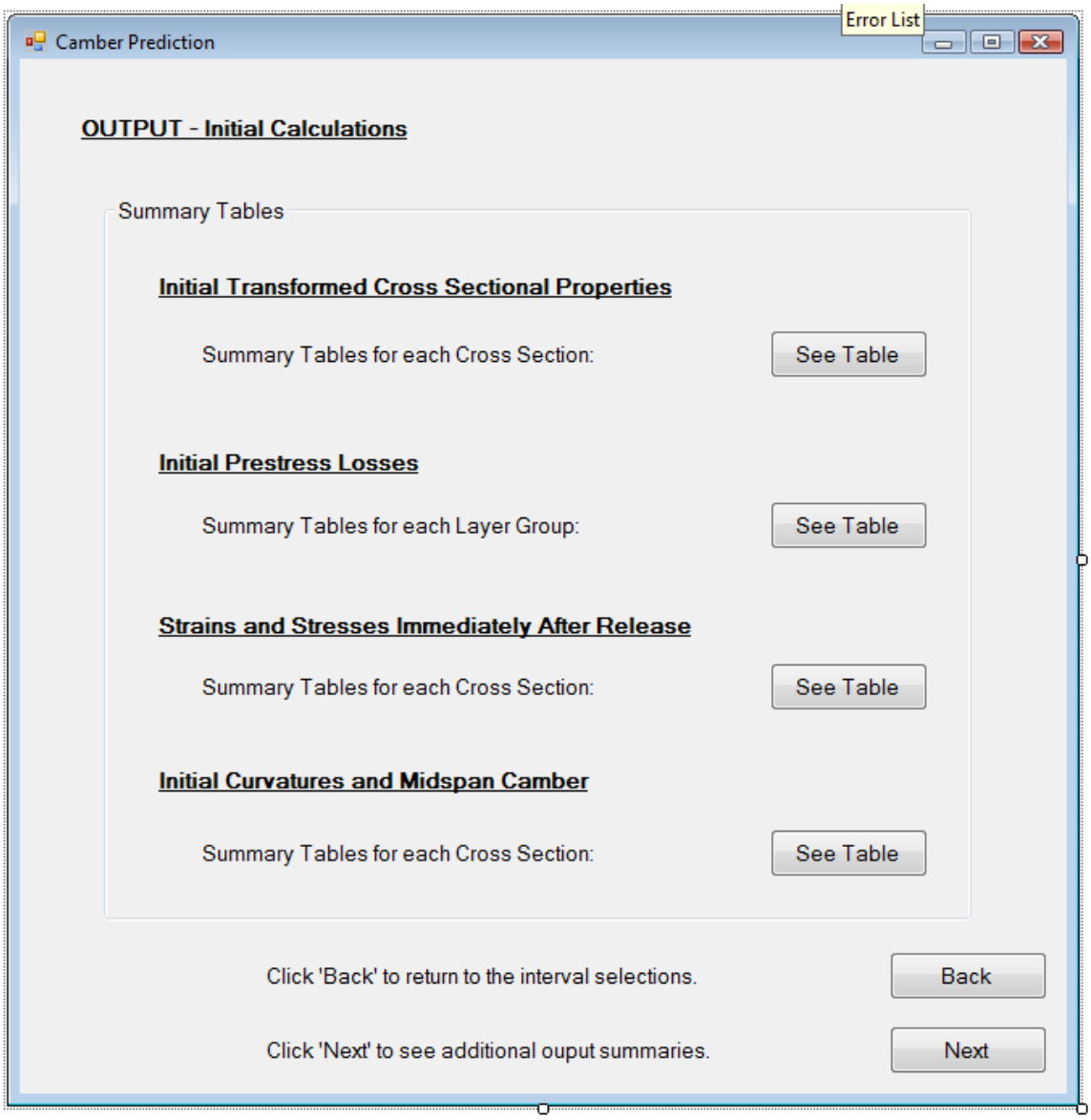

Figure K-16: Output Summary Form – Initial Calculations

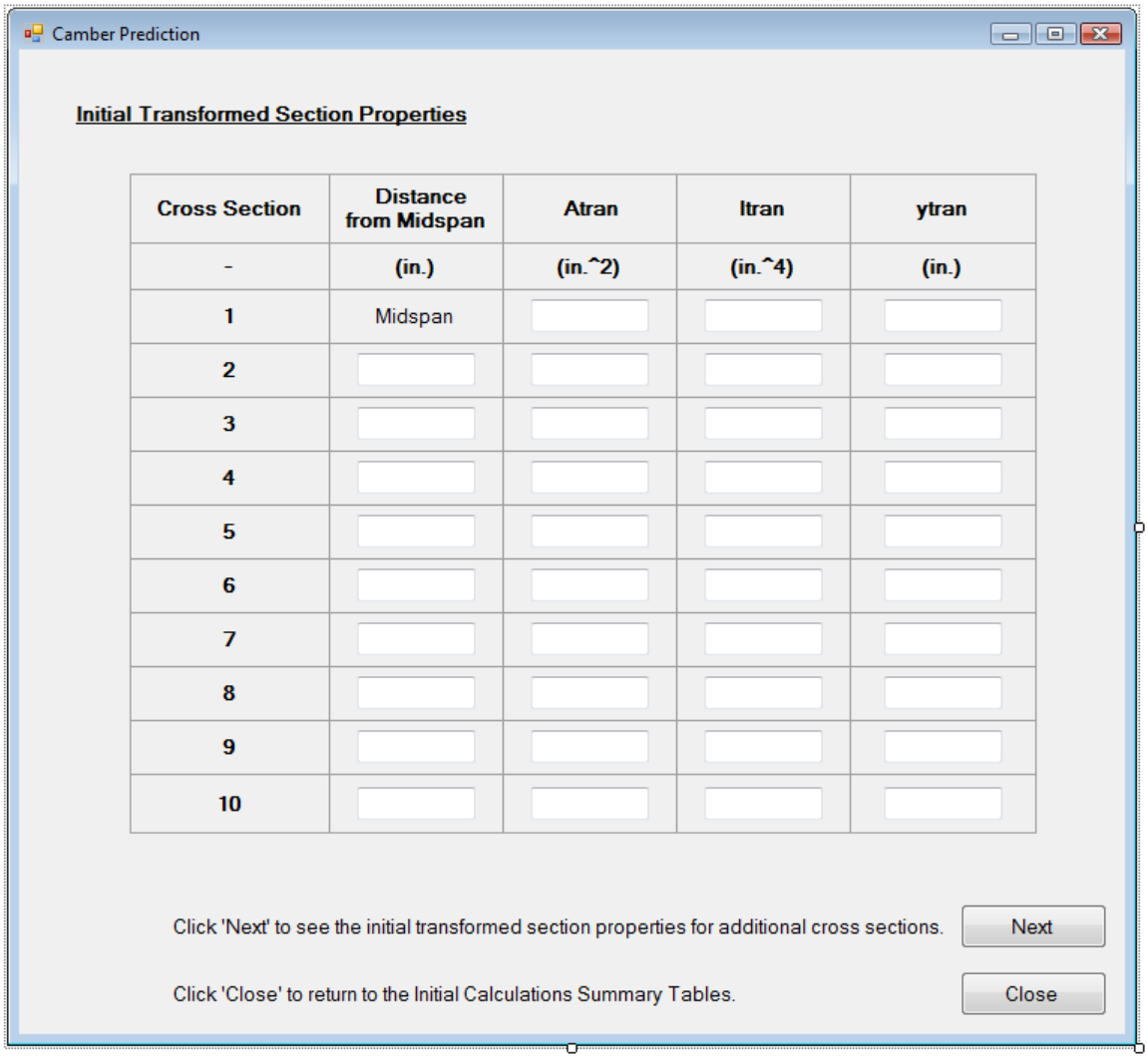

Figure K-17: Initial Transformed Section Properties

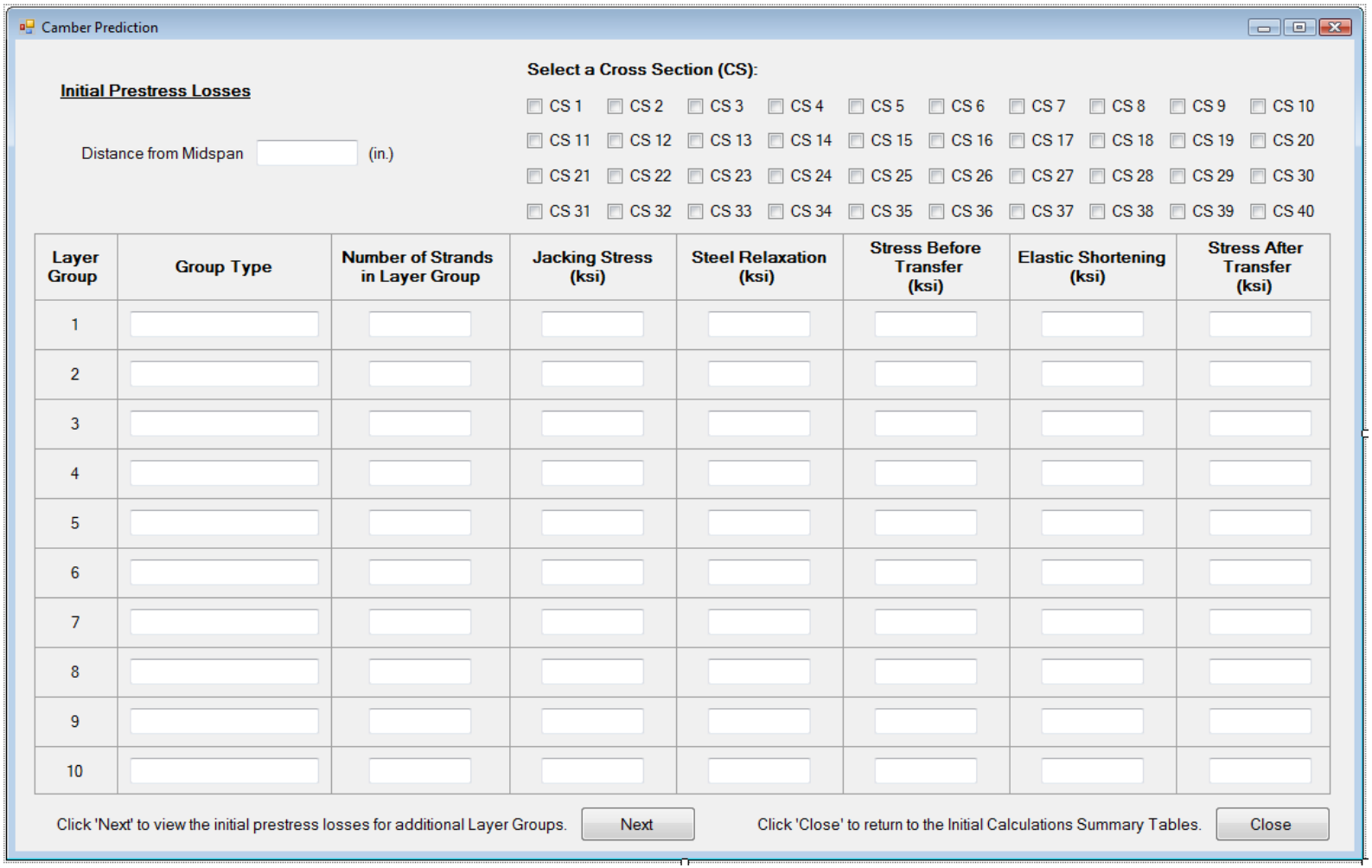

Figure K-18: Initial Prestress Losses and Stress Immediately after Transfer

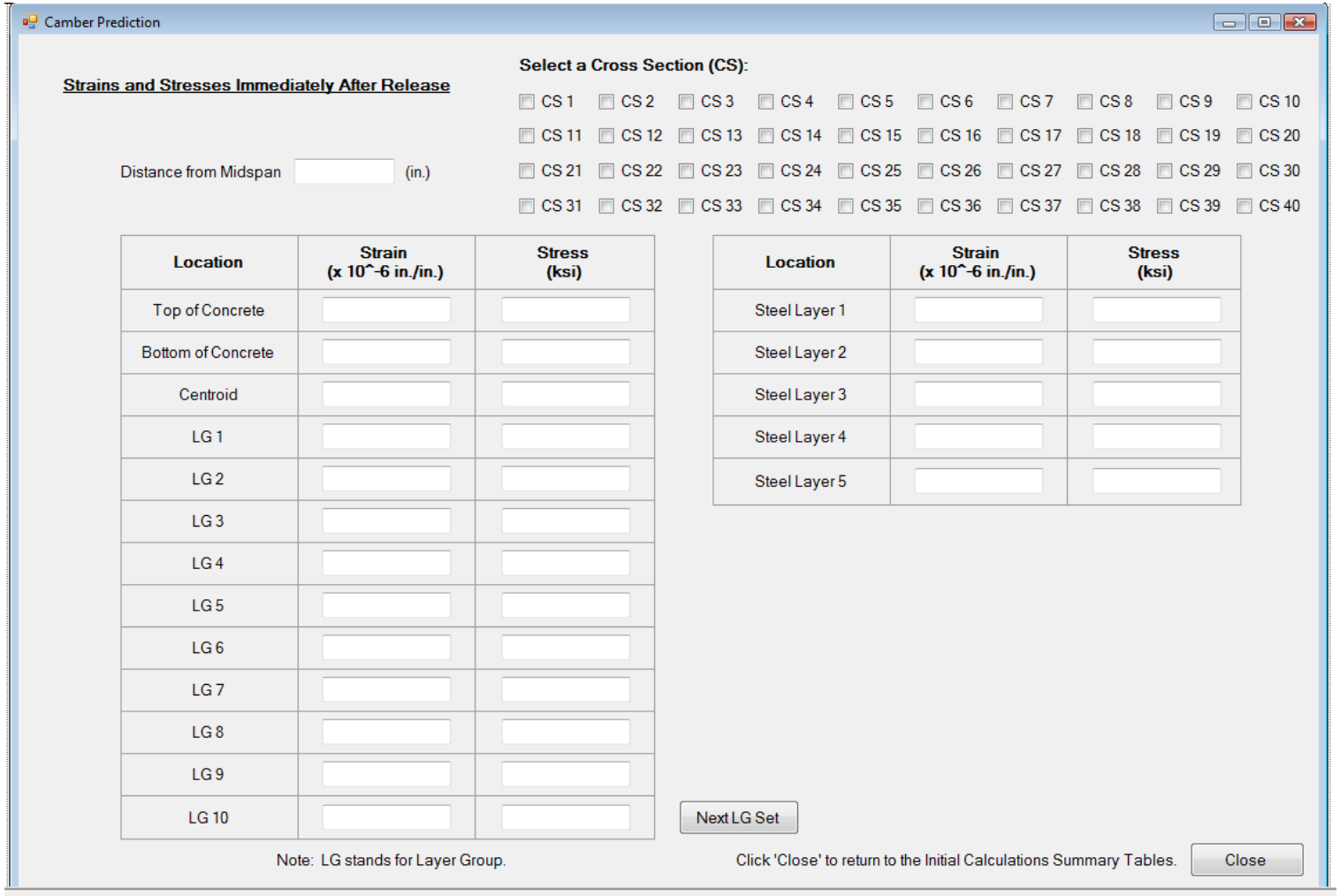

Figure K-19: Strains and Stresses Immediately after Release

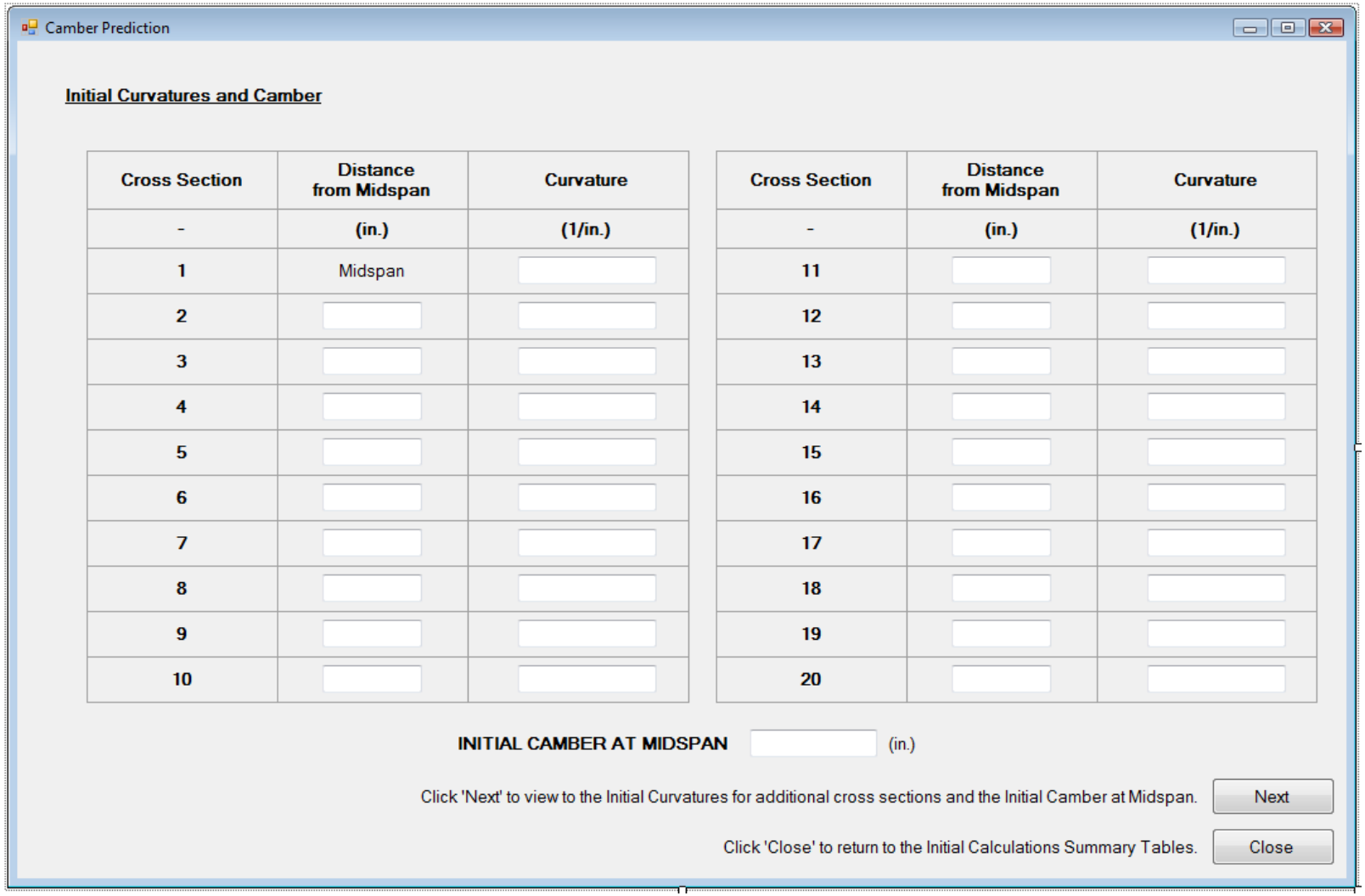

Figure K-20: Initial Curvatures and Midspan Camber

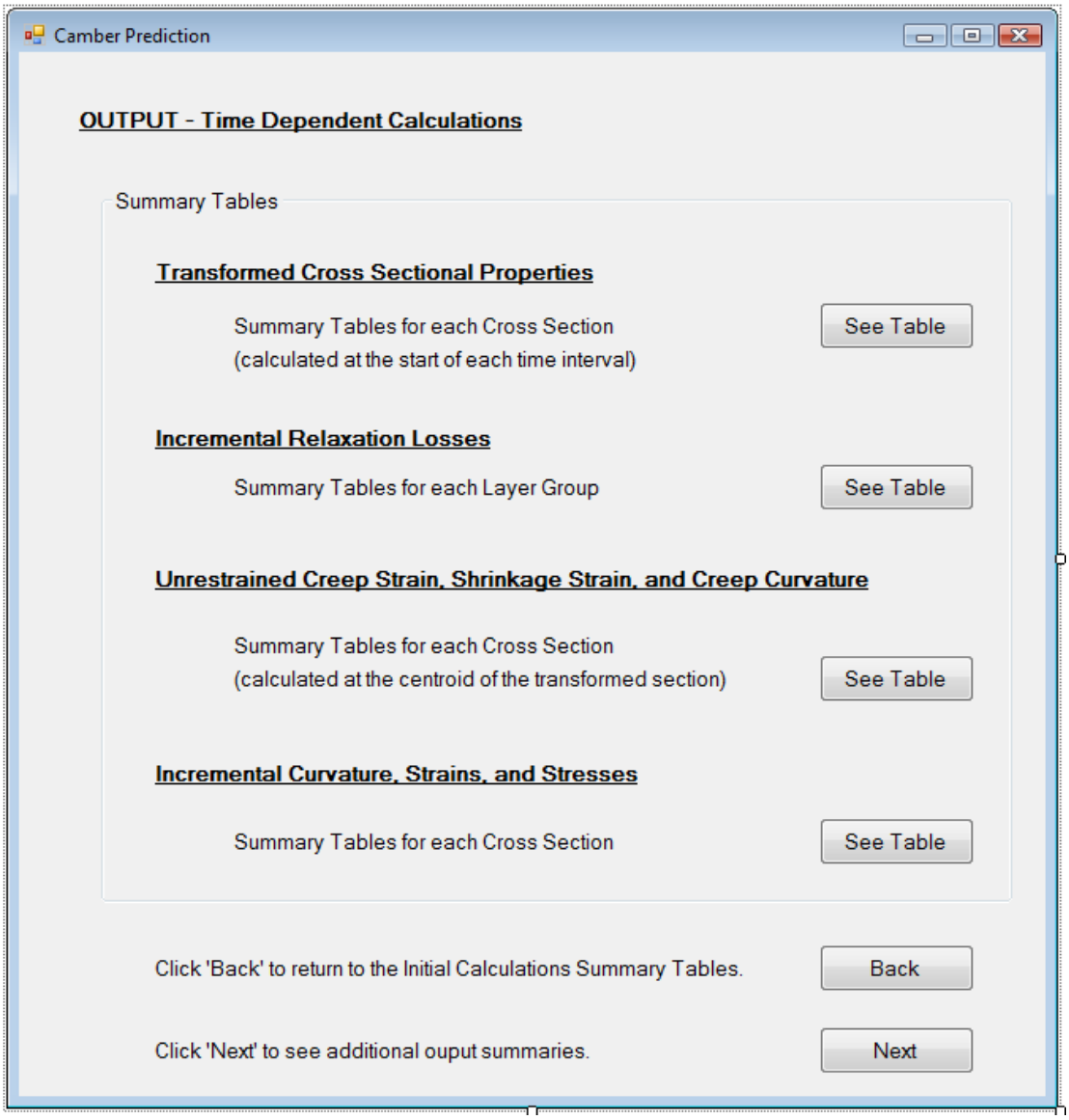

Figure K-21: Output Summary Form – Time-Dependent Calculations

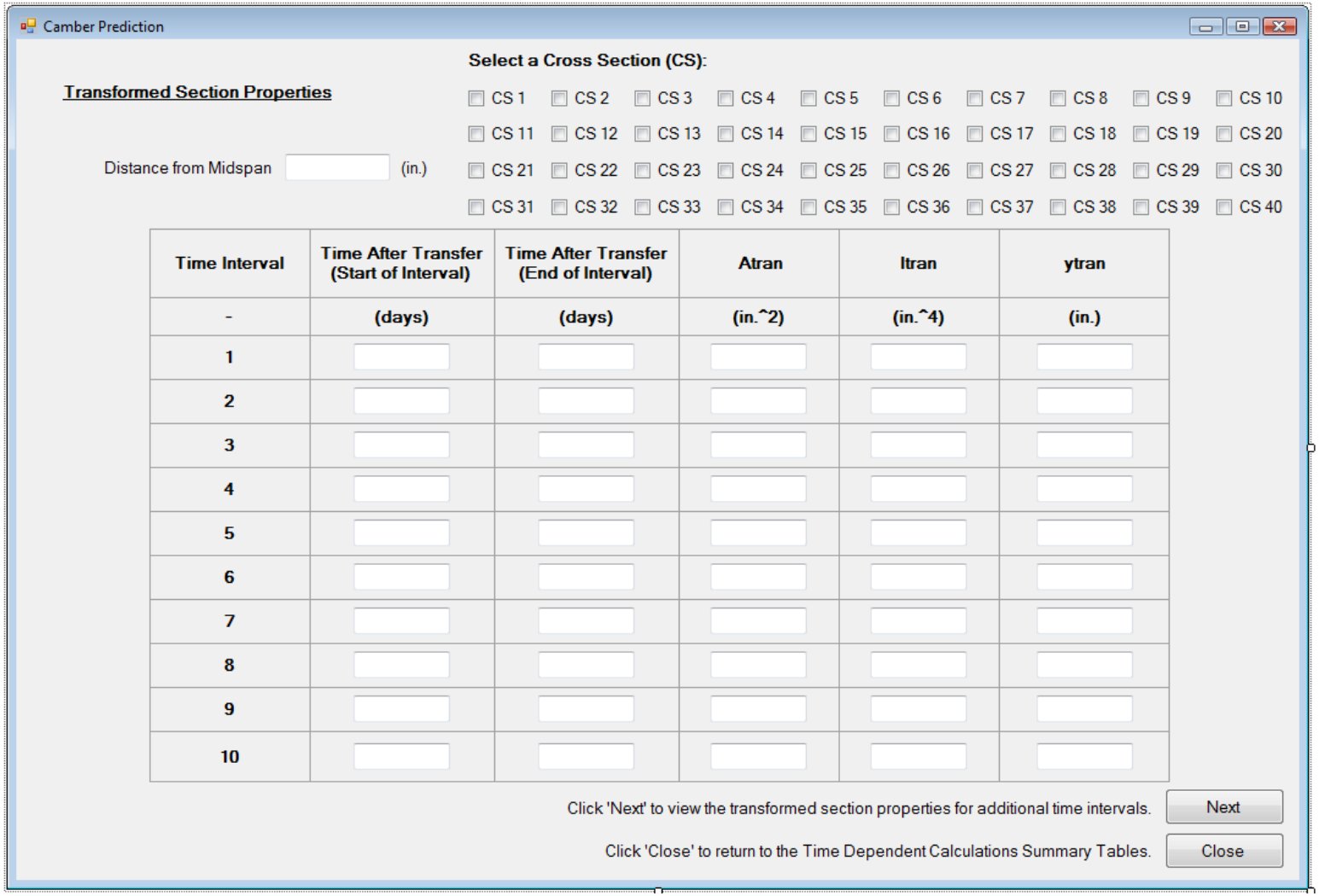

Figure K-22: Transformed Section Properties

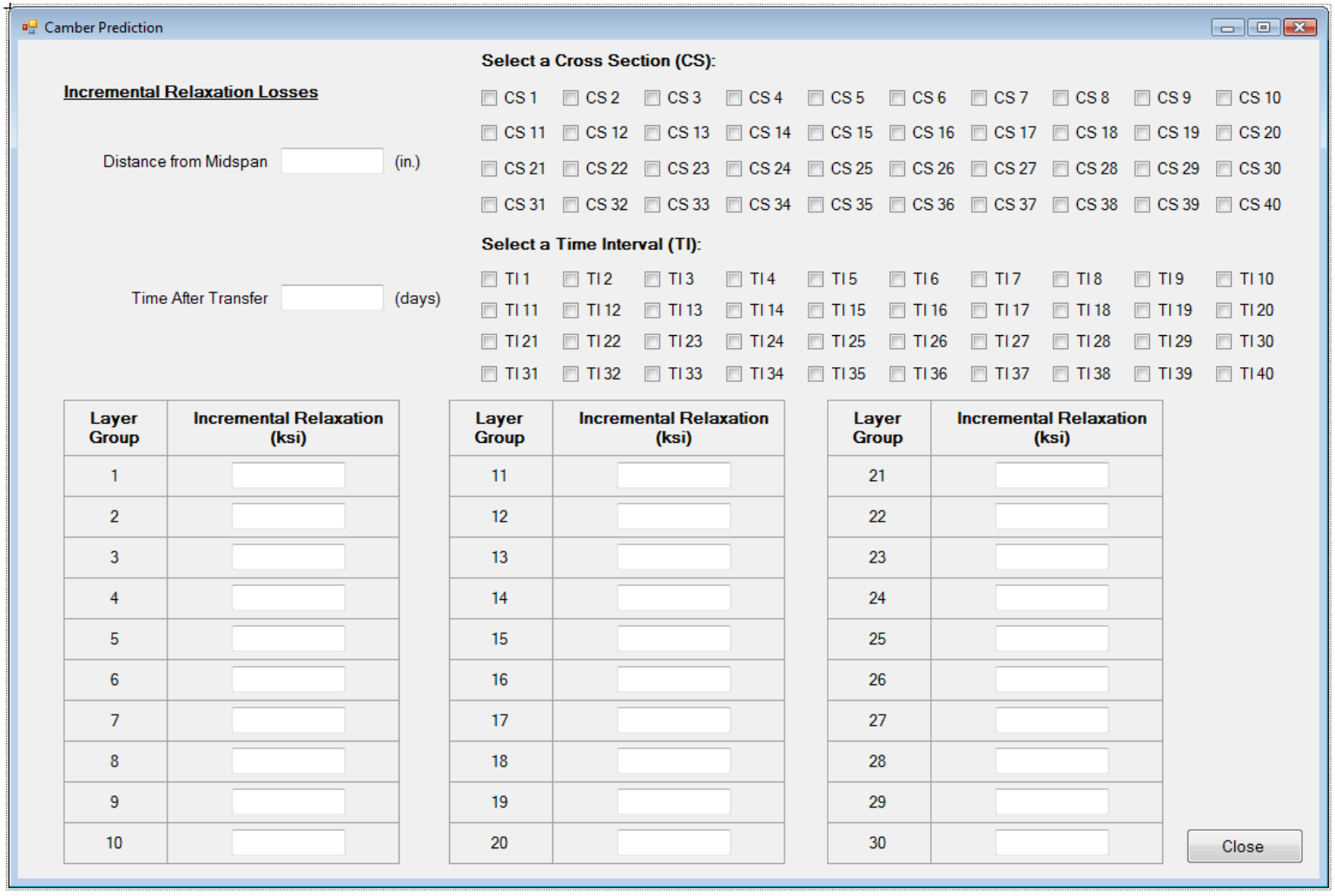

Figure K-23: Incremental Relaxation Losses

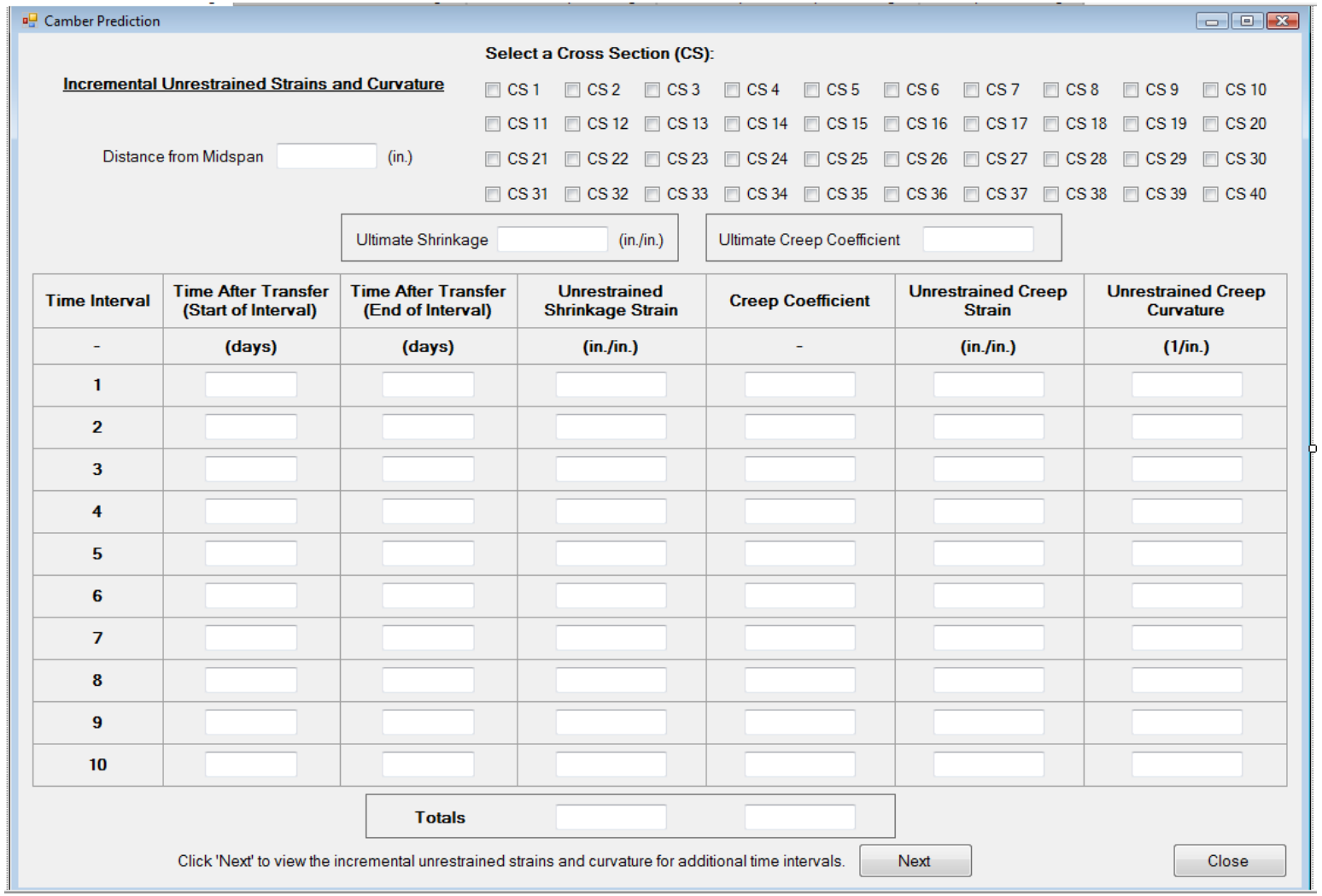

Figure K-24: Incremental Unrestrained Strains and Curvature

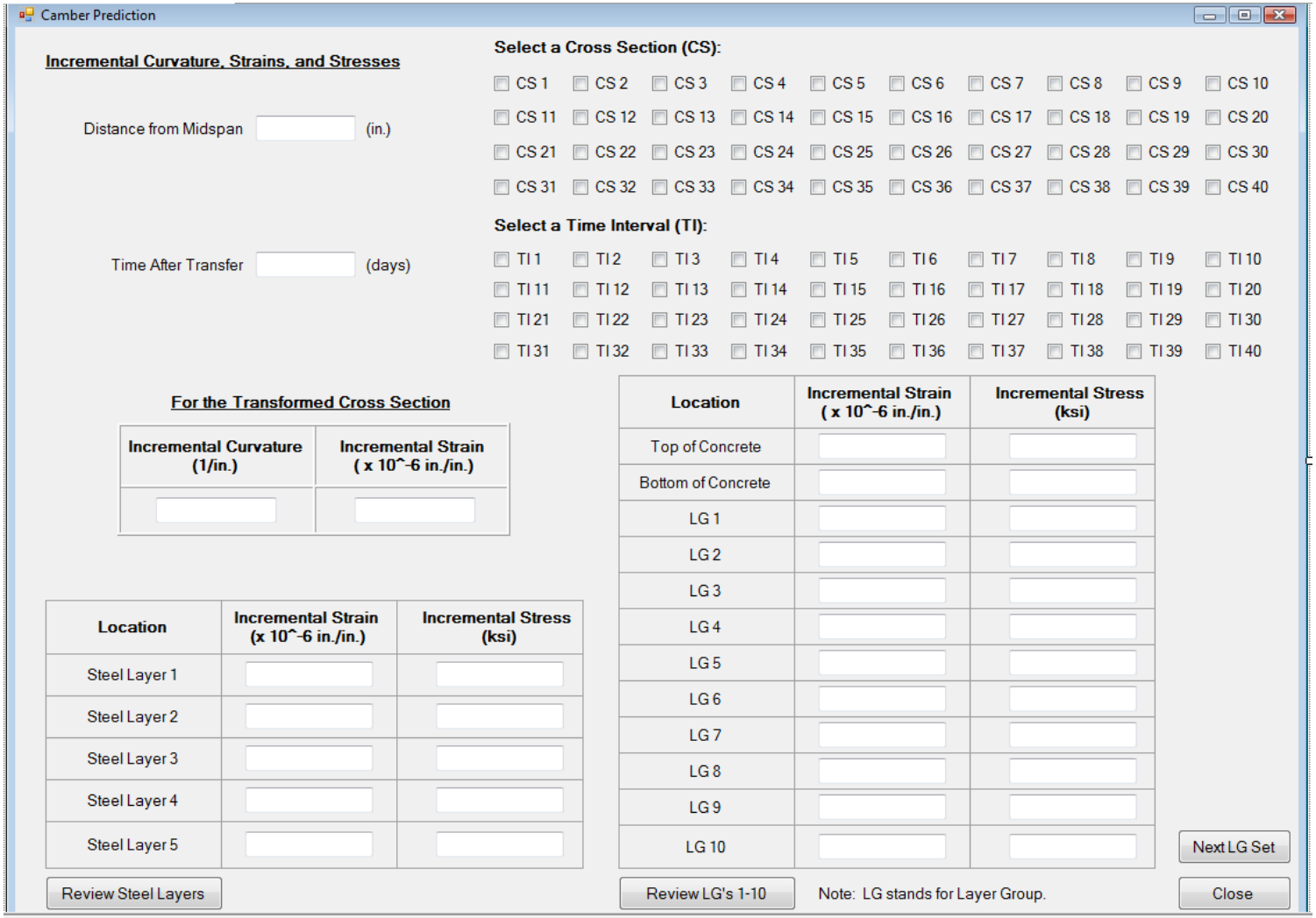

Figure K-25: Incremental Curvature, Strains, and Stresses

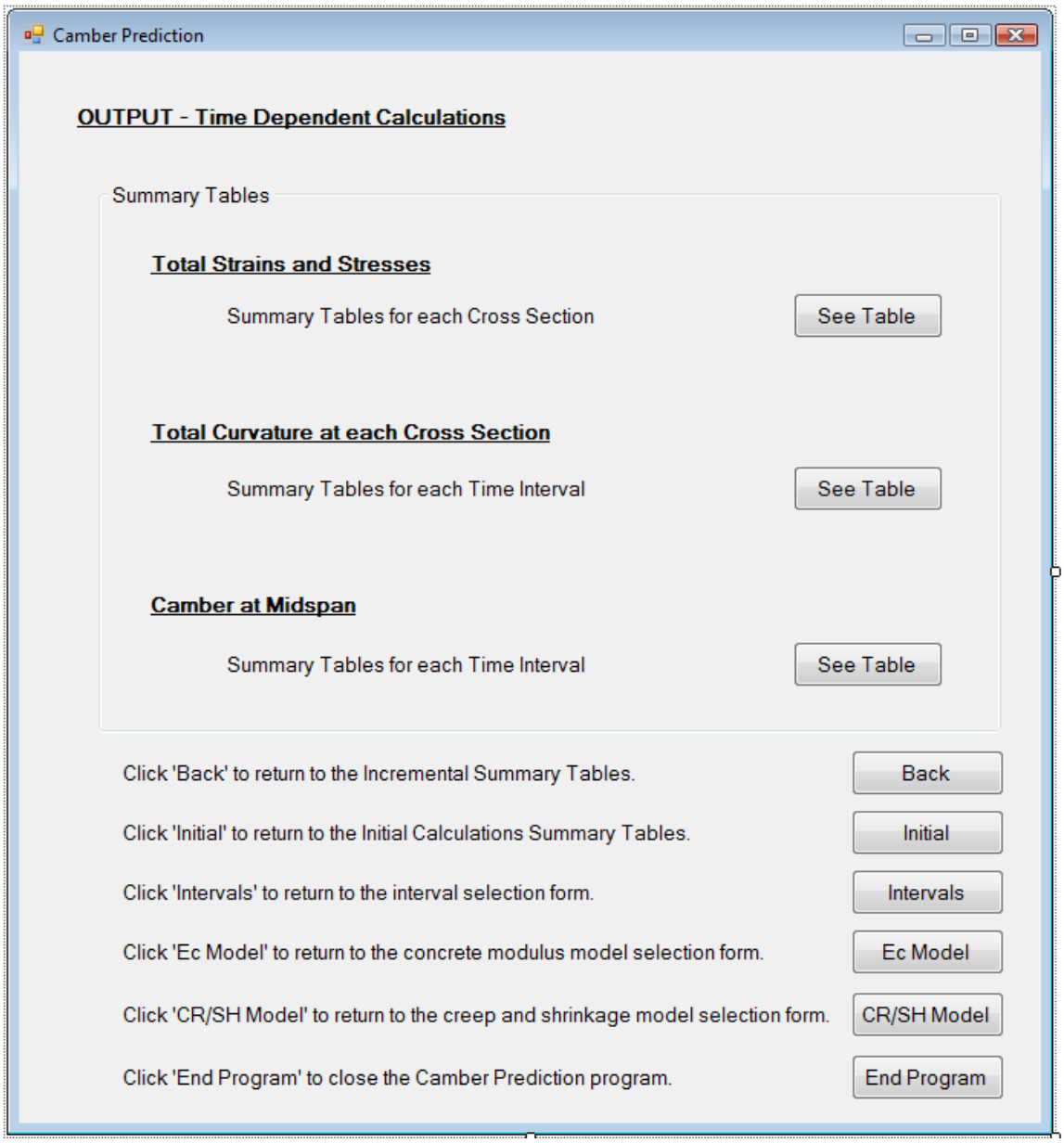

Figure K-26: Output Summary Form – Final Results

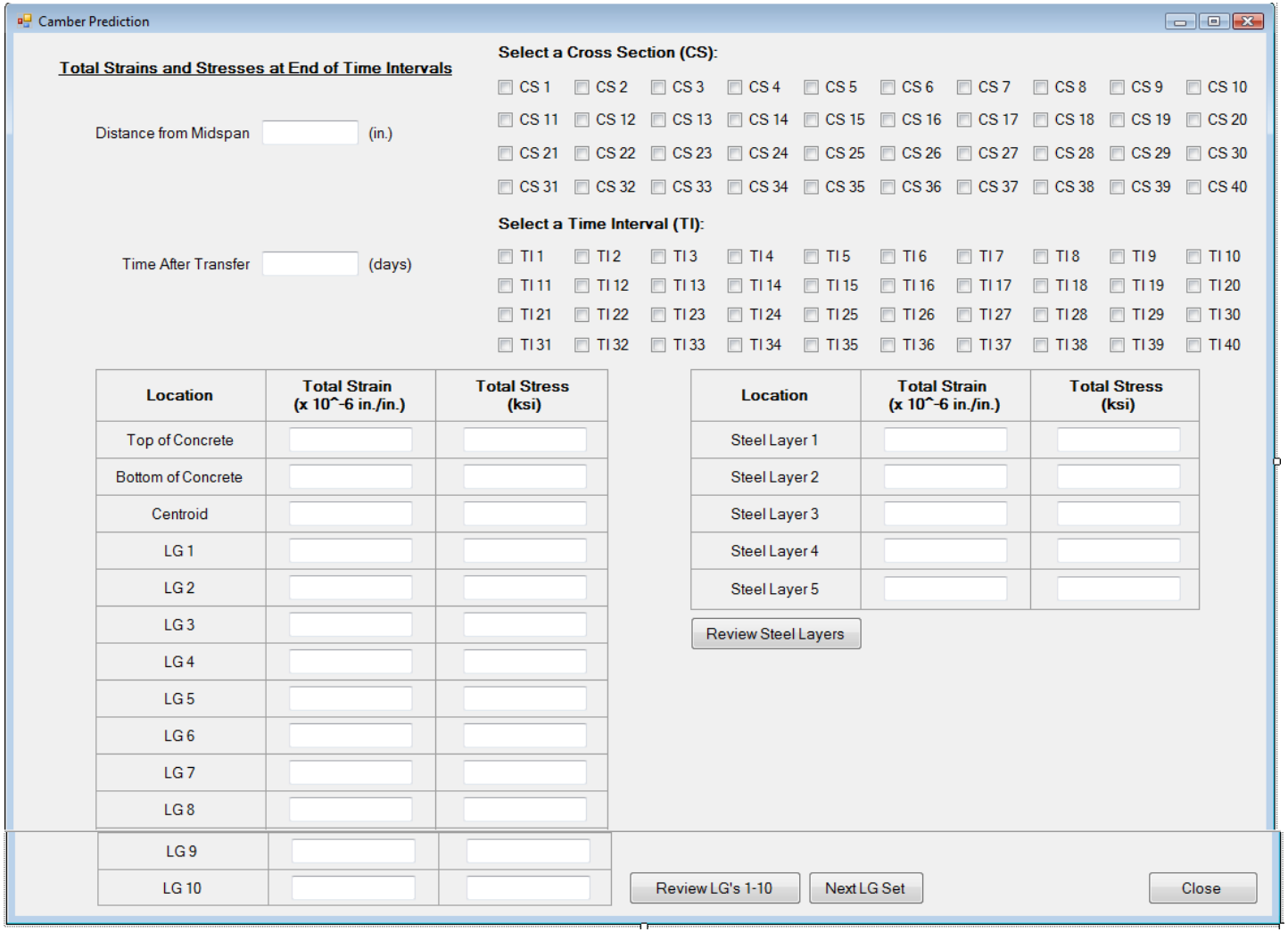

Figure K-27: Total Strains and Stresses

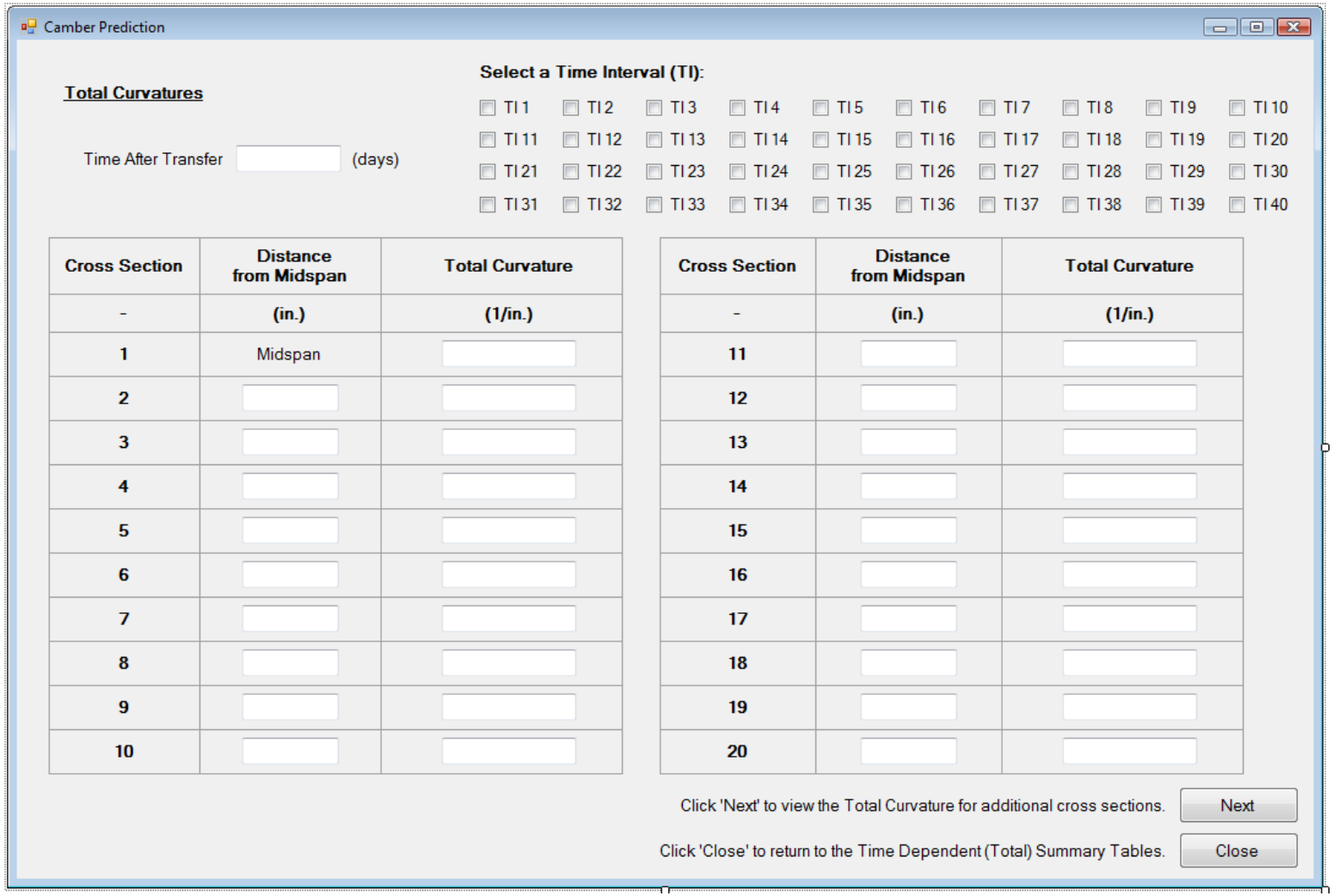

Figure K-28: Total Curvatures

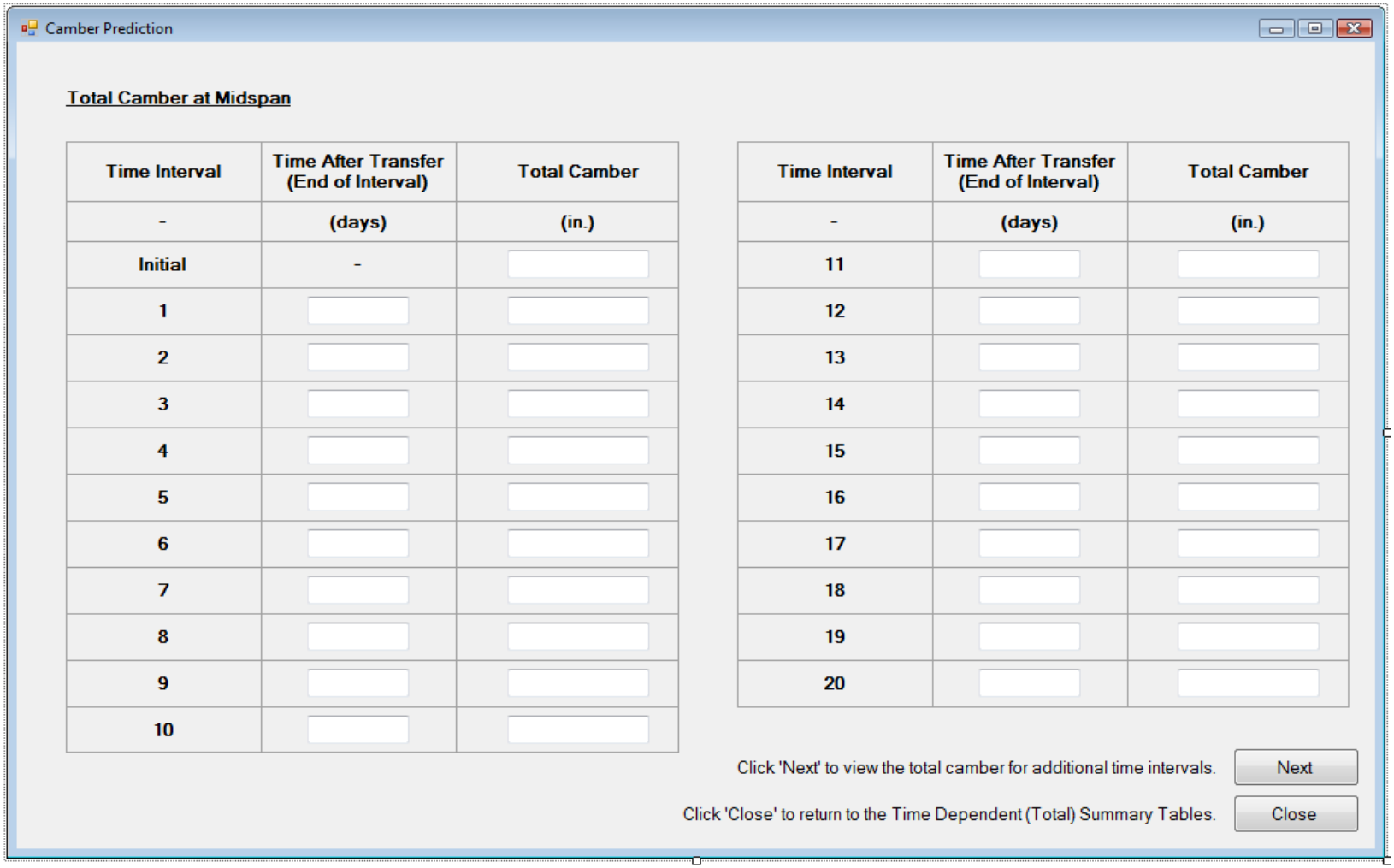

Figure K-29: Total Camber at Midspan

APPENDIX L

VISUAL BASIC PROGRAM CODE

Module 1: Global Variables (Partial Code)

```
Module GlobalVariables

    Public Ag, Ig, yb, wg, L, h, fci, Ec_initial, fc28, Ec28, wc, Mg, Ep,
    fpu, fpy, Es, Ec As Single…Public TimeIntervals As Integer

Sub GVariables(ByRef Ag As Single…ByRef h_CEB As Single)

        'Intervals

        NumberCS = Val(Intervals.txbNumberCS.Text)
        MaxTime = Val(Intervals.txbMaxTime.Text)
        TimeIntervals = Val(Intervals.txbTimeIntervals.Text)

        'GROSS CROSS SECTION PROPERTIES

        Ag = Math.Max(Val(InputSectProp.TextBox1.Text),
            Val(VerifySectProp.TextBox1.Text))
        Ig = Math.Max(Val(InputSectProp.TextBox2.Text),
            Val(VerifySectProp.TextBox2.Text))
        yb = Math.Max(Val(InputSectProp.TextBox3.Text),
            Val(VerifySectProp.TextBox3.Text))
        ' No longer using wg as input.  Only displaying as output later
          on when it is calculated
        h = Math.Max(Val(InputSectProp.TextBox5.Text),
            Val(VerifySectProp.TextBox5.Text))
        L = Math.Max(Val(InputSectProp.TextBox6.Text),
            Val(VerifySectProp.TextBox6.Text))

        'CONCRETE PROPERTIES

        fci = Val(ConcProp.TextBox1.Text)
        Ec_initial = Val(ConcProp.TextBox2.Text)
        fc28 = Val(ConcProp.TextBox3.Text)
        Ec28 = Val(ConcProp.TextBox4.Text)
        wc = Val(ConcProp.TextBox5.Text)

        'PRESTRESSING STEEL INPUT
```

```
Ep = Val(PrestressProp.TextBox1.Text)
fpu = Val(PrestressProp.TextBox2.Text)
fpy = Val(PrestressProp.TextBox3.Text)

'PRESTRESSING STRAND TYPES

ST1 = LayerGroupInfo1.cb1LG1.SelectedItem : ST2 =
LayerGroupInfo1.cb1LG2.SelectedItem : ST3 =
LayerGroupInfo1.cb1LG3.SelectedItem
: ST4 = LayerGroupInfo1.cb1LG4.SelectedItem : ST5 =
LayerGroupInfo1.cb1LG5.SelectedItem : ST6 =
LayerGroupInfo1.cb1LG6.SelectedItem
: ST7 = LayerGroupInfo1.cb1LG7.SelectedItem : ST8 =
LayerGroupInfo1.cb1LG8.SelectedItem : ST9 =
LayerGroupInfo1.cb1LG9.SelectedItem
: ST10 = LayerGroupInfo1.cb1LG10.SelectedItem : ST11 =
LayerGroupInfo2.cb1LG11.SelectedItem : ST12 =
LayerGroupInfo2.cb1LG12.SelectedItem
: ST13 = LayerGroupInfo2.cb1LG13.SelectedItem : ST14 =
LayerGroupInfo2.cb1LG14.SelectedItem : ST15 =
LayerGroupInfo2.cb1LG15.SelectedItem
: ST16 = LayerGroupInfo2.cb1LG16.SelectedItem : ST17 =
LayerGroupInfo2.cb1LG17.SelectedItem : ST18 =
LayerGroupInfo2.cb1LG18.SelectedItem
: ST19 = LayerGroupInfo2.cb1LG19.SelectedItem : ST20 =
LayerGroupInfo2.cb1LG20.SelectedItem : ST21 =
LayerGroupInfo3.cb1LG21.SelectedItem
: ST22 = LayerGroupInfo3.cb1LG22.SelectedItem : ST23 =
LayerGroupInfo3.cb1LG23.SelectedItem : ST24 =
LayerGroupInfo3.cb1LG24.SelectedItem
: ST25 = LayerGroupInfo3.cb1LG25.SelectedItem : ST26 =
LayerGroupInfo3.cb1LG26.SelectedItem : ST27 =
LayerGroupInfo3.cb1LG27.SelectedItem
: ST28 = LayerGroupInfo3.cb1LG28.SelectedItem : ST29 =
LayerGroupInfo3.cb1LG29.SelectedItem : ST30 =
LayerGroupInfo3.cb1LG30.SelectedItem

'DRAPED LAYER GROUPS

GT1 = LayerGroupInfo1.cbGT1.SelectedItem : GT2 =
LayerGroupInfo1.cbGT2.SelectedItem : GT3 =
LayerGroupInfo1.cbGT3.SelectedItem
: GT4 = LayerGroupInfo1.cbGT4.SelectedItem : GT5 =
LayerGroupInfo1.cbGT5.SelectedItem : GT6 =
LayerGroupInfo1.cbGT6.SelectedItem
: GT7 = LayerGroupInfo1.cbGT7.SelectedItem : GT8 =
LayerGroupInfo1.cbGT8.SelectedItem : GT9 =
LayerGroupInfo1.cbGT9.SelectedItem
: GT10 = LayerGroupInfo1.cbGT10.SelectedItem : GT11 =
LayerGroupInfo2.cbGT11.SelectedItem : GT12 =
LayerGroupInfo2.cbGT12.SelectedItem
: GT13 = LayerGroupInfo2.cbGT13.SelectedItem : GT14 =
LayerGroupInfo2.cbGT14.SelectedItem : GT15 =
LayerGroupInfo2.cbGT15.SelectedItem
```

```
: GT16 = LayerGroupInfo2.cbGT16.SelectedItem : GT17 =
LayerGroupInfo2.cbGT17.SelectedItem : GT18 =
LayerGroupInfo2.cbGT18.SelectedItem
: GT19 = LayerGroupInfo2.cbGT19.SelectedItem : GT20 =
LayerGroupInfo2.cbGT20.SelectedItem : GT21 =
LayerGroupInfo3.cbGT21.SelectedItem
: GT22 = LayerGroupInfo3.cbGT22.SelectedItem : GT23 =
LayerGroupInfo3.cbGT23.SelectedItem : GT24 =
LayerGroupInfo3.cbGT24.SelectedItem
: GT25 = LayerGroupInfo3.cbGT25.SelectedItem : GT26 =
LayerGroupInfo3.cbGT26.SelectedItem : GT27 =
LayerGroupInfo3.cbGT27.SelectedItem
: GT28 = LayerGroupInfo3.cbGT28.SelectedItem : GT29 =
LayerGroupInfo3.cbGT29.SelectedItem : GT30 =
LayerGroupInfo3.cbGT30.SelectedItem

'LAYER GROUP DETAIL LENGTH

DL1 = Val(LayerGroupInfo1.txb3LG1.Text) : DL2 =
Val(LayerGroupInfo1.txb3LG2.Text) : DL3 =
Val(LayerGroupInfo1.txb3LG3.Text)
: DL4 = Val(LayerGroupInfo1.txb3LG4.Text) : DL5 =
Val(LayerGroupInfo1.txb3LG5.Text) : DL6 =
Val(LayerGroupInfo1.txb3LG6.Text)
: DL7 = Val(LayerGroupInfo1.txb3LG7.Text) : DL8 =
Val(LayerGroupInfo1.txb3LG8.Text) : DL9 =
Val(LayerGroupInfo1.txb3LG9.Text)
: DL10 = Val(LayerGroupInfo1.txb3LG10.Text) : DL11 =
Val(LayerGroupInfo2.txb3LG11.Text) : DL12 =
Val(LayerGroupInfo2.txb3LG12.Text)
: DL13 = Val(LayerGroupInfo2.txb3LG13.Text) : DL14 =
Val(LayerGroupInfo2.txb3LG14.Text) : DL15 =
Val(LayerGroupInfo2.txb3LG15.Text)
: DL16 = Val(LayerGroupInfo2.txb3LG16.Text) : DL17 =
Val(LayerGroupInfo2.txb3LG17.Text) : DL18 =
Val(LayerGroupInfo2.txb3LG18.Text)
: DL19 = Val(LayerGroupInfo2.txb3LG19.Text) : DL20 =
Val(LayerGroupInfo2.txb3LG20.Text) : DL21 =
Val(LayerGroupInfo3.txb3LG21.Text)
: DL22 = Val(LayerGroupInfo3.txb3LG22.Text) : DL23 =
Val(LayerGroupInfo3.txb3LG23.Text) : DL24 =
Val(LayerGroupInfo3.txb3LG24.Text)
: DL25 = Val(LayerGroupInfo3.txb3LG25.Text) : DL26 =
Val(LayerGroupInfo3.txb3LG26.Text) : DL27 =
Val(LayerGroupInfo3.txb3LG27.Text)
: DL28 = Val(LayerGroupInfo3.txb3LG28.Text) : DL29 =
Val(LayerGroupInfo3.txb3LG29.Text) : DL30 =
Val(LayerGroupInfo3.txb3LG30.Text)



'REINFORCING STEEL INPUT

NumberSteelLayers = Val(ReinforcingSteel.TextBox1.Text)
```

```
        Es = Val(ReinforcingSteel.txbEs.Text)

        yr1 = Val(ReinforcingSteel.tb2SL1.Text) : yr2 =
        Val(ReinforcingSteel.tb2SL2.Text) : yr3 =
        Val(ReinforcingSteel.tb2SL3.Text)
        : yr4 = Val(ReinforcingSteel.tb2SL4.Text) : yr5 =
        Val(ReinforcingSteel.tb2SL5.Text)

        nr1 = Val(ReinforcingSteel.tb1SL1.Text) : nr2 =
        Val(ReinforcingSteel.tb1SL2.Text) : nr3 =
        Val(ReinforcingSteel.tb1SL3.Text)
        : nr4 = Val(ReinforcingSteel.tb1SL4.Text) : nr5 =
        Val(ReinforcingSteel.tb1SL5.Text)

        'TIME OF EVENTS

        MoistPeriod = Val(TimeOfEvents.txbMoistDays.Text)
        SteamPeriod = Val(TimeOfEvents.txbSteamDays.Text) / 24

        JackingTime = Val(TimeOfEvents.txbJackingTime.Text)
        TransferTime = Val(TimeOfEvents.txbTransferTime.Text)

        'CREEP AND SHRINKAGE MODELS

        'CEB 90 and Modified CEB Models:
        RH_CEB = Math.Max(Val(SelectModel.txbRH_CEB.Text),
            Val(SelectModel.txbRH_CEB_Mod.Text))
        fcm_CEB = Math.Max(Val(SelectModel.txbfcm_CEB.Text),
            Val(SelectModel.txbfcm_CEB_Mod.Text))
        h_CEB = Math.Max(Val(SelectModel.txbh_CEB.Text),
            Val(SelectModel.txbh_CEB_Mod.Text))

    End Sub

End Module
```

Module 2: Global Arrays (Partial Code)

```
Module GlobalArrays

    Public Ag, Ig, yb, wg, L, h, fci, Ec_initial, fc28, Ec28, wc, Ep, fpu,
    fpy, Es As Single…Public Acon_array(1, NumberCS, TimeIntervals) As Single

    Sub GArrays(ByRef Ag As Single…ByRef AdjustedAge As Single)

        'Creates the yps_array based on the number of cross sections and
        layer group details.

        Dim yps_array(NumberLayerGroups, NumberCS) As Single

        If NumberCS = "1" Then

            For j = 1 To NumberCS
```

```
            For k = 1 To NumberLayerGroups
                If j = 1 Then
                    yps_array(k, j) = yp_mid_array(k)
                ElseIf j = 2 Then
                    yps_array(k, j) = yp_end_array(k)
                End If
            Next k
        Next j

        yp_array = yps_array

        Dim CS_Division_array(1, NumberCS) As Single

        If NumberCS = "1" Then
            CS_Division_array(1, 1) = 0
        ElseIf NumberCS = "2" Then
            CS_Division_array(1, 1) = 0
            CS_Division_array(1, 2) = L / 2
        End If

        CS_Segments_array = CS_Division_array

        'Creates an array of Mg based on the number of cross sections.

        Dim M_self_wt_array(1, NumberCS) As Single

        'In case we use lightweight beams, use wc + 5 instead of wg in
        the self-weight moment calculations.

        For j = 1 To NumberCS
            If j = 1 Then
              M_self_wt_array(1, j) = (((wc + 5) * (Ag / 144)) * L ^ 2) /
              (8 * 12000)
            ElseIf j = 2 Then
                M_self_wt_array(1, j) = 0
            End If
        Next j

        Mg_array = M_self_wt_array

    End If

    If NumberCS >= "2" Then

        AdditionalCS = NumberCS - 1

        CS_Segments = (L / 2) / AdditionalCS

        'Creates an array of the distances for all cross sections from
        the midspan.

        Dim CS_division_array(1, NumberCS) As Single

        For j = 1 To NumberCS
            CS_division_array(1, j) = CS_Segments * (j - 1)
```

```
            Next j

            CS_Segments_array = CS_division_array

            'Creates the yp_array for all cross sections based on their
            distances from midspan and group type.

Dim yp_CrossSections_array(NumberLayerGroups, NumberCS) As Single

            For j = 1 To NumberCS
                For k = 1 To NumberLayerGroups
                    If j = 1 Then
                        yp_CrossSections_array(k, j) = yp_mid_array(k)
                    ElseIf j >= 2 Then
                        If GT_array(k) = "Fully Bonded, Straight" Or
                        GT_array(k) = "Debonded" Then
                            yp_CrossSections_array(k, j) = yp_mid_array(k)
                        ElseIf GT_array(k) = "Draped" And DL_array(k) >=
                        CS_Segments_array(1, j) Then
                            yp_CrossSections_array(k, j) = yp_mid_array(k)
                        ElseIf GT_array(k) = "Draped" And DL_array(k) <
                        CS_Segments_array(1, j) Then
                            yp_CrossSections_array(k, j) = yp_end_array(k) -
                            ((L / 2) - CS_division_array(1, j)) *
                            (yp_end_array(k) - yp_mid_array(k)) / ((L / 2) -
                            DL_array(k))
                        End If
                    End If
                Next k
            Next j

            yp_array = yp_CrossSections_array

            'Creates an array of Mg based on the number of cross sections.

            Dim M_self_wt_array(1, NumberCS) As Single

            For j = 1 To NumberCS
            M_self_wt_array(1, j) = ((L / 2) - CS_Segments_array(1, j)) *
            ((((wc + 5) * (Ag / 144)) * L / 2) - (((wc + 5) * (Ag / 144)) *
            ((L / 2) - CS_Segments_array(1, j)) / 2)) * (1 / 12000)
            Next

            Mg_array = M_self_wt_array

        End If

        'Calculates the area of prestressing steel in each prestressing layer
        group and total area of prestressing steel.

        Dim Apst_array(NumberLayerGroups, NumberCS) As Single
        Dim yApst_array(NumberLayerGroups, NumberCS) As Single

        For j = 1 To NumberCS
            For k = 1 To NumberLayerGroups
```

```
        If j = 1 Then
            Apst_array(k, 1) = Ap_array(k) * nps_array(k)
        ElseIf j >= 2 Then
            If GT_array(k) = "Fully Bonded, Straight" Or
            GT_array(k) = "Draped" Then
                Apst_array(k, j) = Ap_array(k) * nps_array(k)
            ElseIf GT_array(k) = "Debonded" And DL_array(k) >
            ((L / 2) - CS_Segments_array(1, j)) Then
                Apst_array(k, j) = 0
            ElseIf GT_array(k) = "Debonded" And DL_array(k) <=
            ((L / 2) - CS_Segments_array(1, j)) Then
                Apst_array(k, j) = Ap_array(k) * nps_array(k)
            End If
        End If
    Next k
Next j

Aps_array = Apst_array

Dim Aps_total_array(1, NumberCS) As Single

For j = 1 To NumberCS
    For k = 1 To NumberLayerGroups
        Aps_total_array(1, j) = Aps_total_array(1, j) +
        Aps_array(k, j)
    Next k
Next j

Aps_sum_array = Aps_total_array

'Calculates the distance from bottom fiber to centroid of
prestressing steel.

For j = 1 To NumberCS
    For k = 1 To NumberLayerGroups
        yApst_array(k, j) = yp_array(k, j) * Aps_array(k, j)
    Next k
Next j

yAps_array = yApst_array

Dim yAps_total_array(1, NumberCS) As Single

For j = 1 To NumberCS
    For k = 1 To NumberLayerGroups
        yAps_total_array(1, j) = yAps_total_array(1, j) +
        yAps_array(k, j)
    Next k
Next j

yAps_sum_array = yAps_total_array

Dim yps_total_array(1, NumberCS) As Single

For j = 1 To NumberCS
```

```
    yps_total_array(1, j) = yAps_sum_array(1, j) /
    Aps_sum_array(1, j)
Next j

yps_sum_array = yps_total_array

'Creates the yrs_array based on the number of cross sections
and layer group details.

Dim yr_constant_array(NumberSteelLayers, NumberCS) As Single

For j = 1 To NumberCS
    For k = 1 To NumberSteelLayers
        yr_constant_array(k, j) = yr_array(k)
    Next k
Next j

yrs_array = yr_constant_array

Dim Arst_array(NumberSteelLayers, NumberCS) As Single
Dim yArst_array(NumberSteelLayers, NumberCS) As Single

'Calculates the area of reinforcing steel in each reinforcing steel
layer and total area of reinforcing steel.

For j = 1 To NumberCS
    For k = 1 To NumberSteelLayers
        Arst_array(k, j) = Ar_array(k) * nrs_array(k)
    Next k
Next j

Ars_array = Arst_array

Dim Ars_total_array(1, NumberCS) As Single

For j = 1 To NumberCS
    For k = 1 To NumberSteelLayers
        Ars_total_array(1, j) = Ars_total_array(1, j) +
        Ars_array(k, j)
    Next k
Next j

Ars_sum_array = Ars_total_array

'Calculates the distance from bottom fiber to centroid of reinforcing
steel.

For j = 1 To NumberCS
    For k = 1 To NumberSteelLayers
        yArst_array(k, j) = yrs_array(k, j) * Ars_array(k, j)
    Next k
Next j

yArs_array = yArst_array
```

```
Dim yArs_total_array(1, NumberCS) As Single

For j = 1 To NumberCS
    For k = 1 To NumberSteelLayers
        yArs_total_array(1, j) = yArs_total_array(1, j) +
        yArs_array(k, j)
    Next k
Next j

yArs_sum_array = yArs_total_array

Dim yrs_total_array(1, NumberCS) As Single

For j = 1 To NumberCS
    yrs_total_array(1, j) = yArs_sum_array(1, j) /
    Ars_sum_array(1, j)
Next j

yrs_sum_array = yrs_total_array

'TIME INTERVALS

Dim t_array(TimeIntervals) As Single

For i = 1 To TimeIntervals
    t_array(i) = MaxTime * (1 / ((1 - (1 / 0.2) * (Log(i /
    TimeIntervals))) ^ 2))
Next i

time_array = t_array

'CONCRETE AGE ARRAY AND ADJUSTED AGE

Dim concrete_age_array(TimeIntervals) As Single
Dim AdjustedAge1 As Single

'TEMPERATURE ADJUSTED CONCRETE AGE (MATURITY)

If TimeOfEvents.cbC.Checked = True Then
    CureTemp = Val(TimeOfEvents.txbCureTemp.Text)
ElseIf TimeOfEvents.cbF.Checked = True Then
 CureTemp = ((Val(TimeOfEvents.txbCureTemp.Text) - 32) * 5 / 9)
End If

If SelectModel.rbCEB.Checked = True Then

    If TimeOfEvents.rbAveCureTemp.Checked = True Then
        AdjustedAge1 = (TransferTime / 24) * Exp(13.65 - (4000
        / (273 + (CureTemp / 1))))
    ElseIf TimeOfEvents.cbHours.Checked = True Then
        AdjustedAge1 = Val(TimeOfEvents.txbEqAge.Text) / 24
    ElseIf TimeOfEvents.cbDays.Checked = True Then
        AdjustedAge1 = Val(TimeOfEvents.txbEqAge.Text)
    ElseIf TimeOfEvents.rbNeglect.Checked = True Then
        AdjustedAge1 = (TransferTime / 24)
```

```
        End If

        If SelectModel.ComboBoxCementType2.Text = "Rapid hardening,
        high-strength RS" Then
            AdjustedAge = AdjustedAge1 * ((9 / (2 + AdjustedAge1 ^
            1.2)) + 1)
        ElseIf SelectModel.ComboBoxCementType2.Text = "Normal/Rapid
        hardening N and R" Then
            AdjustedAge = AdjustedAge1
        ElseIf SelectModel.ComboBoxCementType2.Text = "Slowly
        hardening SL" Then
            AdjustedAge = AdjustedAge1 * (((9 / (2 + AdjustedAge1 ^
            1.2)) + 1) ^ (-1))
        End If

    ElseIf SelectModel.rbCEB_Mod.Checked = True Then
        If TimeOfEvents.rbAveCureTemp.Checked = True Then
            AdjustedAge1 = (TransferTime / 24) * Exp(18.47 - (5410
            / (273 + (CureTemp / 1))))
        ElseIf TimeOfEvents.cbHours.Checked = True Then
            AdjustedAge1 = Val(TimeOfEvents.txbEqAge.Text) / 24
        ElseIf TimeOfEvents.cbDays.Checked = True Then
            AdjustedAge1 = Val(TimeOfEvents.txbEqAge.Text)
        ElseIf TimeOfEvents.rbNeglect.Checked = True Then
            AdjustedAge1 = (TransferTime / 24)
        End If

        If SelectModel.ComboBoxCementType2Mod.Text = "Rapid
        hardening, high-strength RS" Then
            AdjustedAge = AdjustedAge1 * ((9 / (2 + AdjustedAge1 ^
            1.2)) + 1)
        ElseIf SelectModel.ComboBoxCementType2Mod.Text =
        "Normal/Rapid hardening N and R" Then
            AdjustedAge = AdjustedAge1
        ElseIf SelectModel.ComboBoxCementType2Mod.Text = "Slowly
        hardening SL" Then
            AdjustedAge = AdjustedAge1 * (((9 / (2 + AdjustedAge1 ^
            1.2)) + 1) ^ (-1))
        End If

    Else
        If TimeOfEvents.rbAveCureTemp.Checked = True Then
            AdjustedAge = (TransferTime / 24) * Exp(13.65 - (4000 /
            (273 + (CureTemp / 1))))
        ElseIf TimeOfEvents.cbHours.Checked = True Then
            AdjustedAge = Val(TimeOfEvents.txbEqAge.Text) / 24
        ElseIf TimeOfEvents.cbDays.Checked = True Then
            AdjustedAge = Val(TimeOfEvents.txbEqAge.Text)
        ElseIf TimeOfEvents.rbNeglect.Checked = True Then
            AdjustedAge = (TransferTime / 24)
        End If

    End If

        concrete_age_array(0) = AdjustedAge
```

```
  For i = 1 To TimeIntervals
      concrete_age_array(i) = time_array(i) + AdjustedAge
  Next i

  age_array = concrete_age_array

  'SHRINKAGE TIME ARRAY

Dim time_after_initial_curing_array(TimeIntervals) As Single

  For i = 1 To TimeIntervals
      If TimeOfEvents.rbMoistCure.Checked = True Then
          time_after_initial_curing_array(i) = age_array(i) -
          MoistPeriod
      ElseIf TimeOfEvents.rbSteamCure.Checked = True Then
          time_after_initial_curing_array(i) = age_array(i) –
          SteamPeriod
      End If
  Next i

  shrink_time_array = time_after_initial_curing_array

  'JACKING AGE ARRAY

  Dim time_after_jacking_array(TimeIntervals) As Single

  time_after_jacking_array(0) = (JackingTime / 24) +
  (TransferTime / 24)

  For i = 1 To TimeIntervals
      time_after_jacking_array(i) = time_array(i) +
      (JackingTime / 24) + (TransferTime / 24)
  Next i

  jack_time_array = time_after_jacking_array

  'MODULUS OF ELASTICITY MODELS

  Dim Econcrete_array(TimeIntervals) As Single

  If ModulusOfElasticity.rbConstantEc.Checked = True Then

      For i = 1 To TimeIntervals
          Econcrete_array(i) = Ec_initial
      Next i

  End If

  If ModulusOfElasticity.rbTwoPoint.Checked = True Then

      Dim s_stiffness As Single
      Dim beta_cc(TimeIntervals) As Single

      s_stiffness = (Log(Ec_initial / Ec28)) / (1 - ((28 /
```

```
    (TransferTime / 24)) ^ 0.5))

For i = 1 To TimeIntervals
    beta_cc(i) = Exp(s_stiffness * (1 - ((28 / age_array(i
    - 1)) ^ 0.5)))
Next

For i = 1 To TimeIntervals
    Econcrete_array(i) = Ec28 * beta_cc(i)
Next i

End If

If ModulusOfElasticity.rbACI.Checked = True Then

    Ec_initial = (33 * (((wc ^ 3) * fci) ^ 0.5)) / 1000

    If ModulusOfElasticity.ComboBoxCuringType.Text = "Moist
    Cured" And ModulusOfElasticity.ComboBoxCementType.Text
    = "Type I" Then
        alpha = 4
        beta = 0.85
    ElseIf ModulusOfElasticity.ComboBoxCuringType.Text =
    "Moist Cured" And
    ModulusOfElasticity.ComboBoxCementType.Text = "Type
    III" Then
        alpha = 2.3
        beta = 0.92
    ElseIf ModulusOfElasticity.ComboBoxCuringType.Text =
    "Steam Cured" And
    ModulusOfElasticity.ComboBoxCementType.Text = "Type I"
    Then
        alpha = 1.0
        beta = 0.95
    ElseIf ModulusOfElasticity.ComboBoxCuringType.Text =
    "Steam Cured" And
    ModulusOfElasticity.ComboBoxCementType.Text = "Type
    III" Then
        alpha = 0.7
        beta = 0.98
    End If

    Dim fconcrete_array(TimeIntervals) As Single

    For i = 1 To TimeIntervals
        fconcrete_array(i) = Max((age_array(i - 1) / (alpha
        + (beta * age_array(i - 1)))) * fc28, fci)
    Next i

    fcon_array = fconcrete_array

    For i = 1 To TimeIntervals
        Econcrete_array(i) = (33 * (((wc ^ 3) *
        fcon_array(i)) ^ 0.5)) / 1000
    Next i
```

```
End If

If ModulusOfElasticity.rbAASHTO.Checked = True Then

    Dim K1 As Single

    K1 = Val(ModulusOfElasticity.TextBox3.Text)

    Ec_initial = 33000 * K1 * ((wc / 1000) ^ 1.5) * ((fci /
    1000) ^ 0.5)

    'Uses ACI 209 strength development equation to compute
    AASHTO's stiffness development.

    If ModulusOfElasticity.cbCuringType.Text = "Moist
    Cured" And ModulusOfElasticity.cbCementType.Text =
    "Type I" Then
        alpha = 4
        beta = 0.85
    ElseIf ModulusOfElasticity.cbCuringType.Text = "Moist
    Cured" And ModulusOfElasticity.cbCementType.Text =
    "Type III" Then
        alpha = 2.3
        beta = 0.92
    ElseIf ModulusOfElasticity.cbCuringType.Text = "Steam
    Cured" And ModulusOfElasticity.cbCementType.Text =
    "Type I" Then
        alpha = 1.0
        beta = 0.95
    ElseIf ModulusOfElasticity.cbCuringType.Text = "Steam
    Cured" And ModulusOfElasticity.cbCementType.Text =
    "Type III" Then
        alpha = 0.7
        beta = 0.98
    End If

    Dim fconcrete_array(TimeIntervals) As Single

    For i = 1 To TimeIntervals
        fconcrete_array(i) = Max((age_array(i - 1) / (alpha
        + (beta * age_array(i - 1)))) * fc28, fci)
    Next i

    fcon_array = fconcrete_array

    For i = 1 To TimeIntervals
        Econcrete_array(i) = 33000 * K1 * ((wc / 1000) ^
        1.5) * (((fcon_array(i) / 1000) ^ 0.5))
    Next i

End If

If ModulusOfElasticity.rbCEB.Checked = True Then
```

```
If ModulusOfElasticity.rbAveCureTemp.Checked = True Then
    AdjustedAge1 = (TransferTime / 24) * Exp(13.65 –
    (4000 / (273 + (CureTemp / 1))))
ElseIf ModulusOfElasticity.cbHours.Checked = True Then
    AdjustedAge1 = Val(TimeOfEvents.txbEqAge.Text) / 24
ElseIf ModulusOfElasticity.cbDays.Checked = True Then
    AdjustedAge1 = Val(TimeOfEvents.txbEqAge.Text)
ElseIf ModulusOfElasticity.rbNeglect.Checked = True
Then
    AdjustedAge1 = (TransferTime / 24)
End If

If ModulusOfElasticity.ComboBoxCementType2.Text =
"Rapid hardening, high-strength RS" Then
    AdjustedAge = AdjustedAge1 * ((9 / (2 +
    AdjustedAge1 ^ 1.2)) + 1)
ElseIf ModulusOfElasticity.ComboBoxCementType2.Text =
"Normal/Rapid hardening N and R" Then
    AdjustedAge = AdjustedAge1
ElseIf ModulusOfElasticity.ComboBoxCementType2.Text =
"Slowly hardening SL" Then
    AdjustedAge = AdjustedAge1 * (((9 / (2 +
    AdjustedAge1 ^ 1.2)) + 1) ^ (-1))
End If

concrete_age_array(0) = AdjustedAge

For i = 1 To TimeIntervals
    concrete_age_array(i) = time_array(i) + AdjustedAge
Next i

age_array = concrete_age_array

If ModulusOfElasticity.ComboBoxCementType2.Text =
"Rapid hardening, high-strength RS" Then
    s = 0.2
ElseIf ModulusOfElasticity.ComboBoxCementType2.Text =
"Normal/Rapid hardening N and R" Then
    s = 0.25
ElseIf ModulusOfElasticity.ComboBoxCementType2.Text =
"Slowly hardening SL" Then
    s = 0.38
End If

Dim beta_2c_array(TimeIntervals) As Single

For i = 1 To TimeIntervals
    beta_2c_array(i) = Exp(s * (1 - ((28 / age_array(i
    - 1)) ^ 0.5)))
Next i

beta_cc_array = beta_2c_array

Dim fconcrete_array(TimeIntervals) As Single
```

```
                For i = 1 To TimeIntervals
                    fconcrete_array(i) = Max(beta_cc_array(i) * fc28,
                    fci)
                Next i

                fcon_array = fconcrete_array

                Dim beta_e_array(TimeIntervals) As Single

                For i = 1 To TimeIntervals
                    beta_e_array(i) = (beta_cc_array(i)) ^ 0.5
                Next i

                Dim fc28_CEB As Single

                fc28_CEB = fc28 * 0.00689475729

                Dim Ec28_CEB As Single

                Ec28_CEB = (2.15 * (10 ^ 4)) * ((fc28_CEB / 10) ^ (1 /
                3)) / 6.89475729

                For i = 1 To TimeIntervals
                    Econcrete_array(i) = beta_e_array(i) * Ec28_CEB
                Next i

                Ec_initial = Econcrete_array(1)

            End If

            Econ_array = Econcrete_array

            Dim Aconcrete_initial_array(1, NumberCS) As Single

            For j = 1 To NumberCS
                Aconcrete_initial_array(1, j) = Ag - Aps_sum_array(1,
                j) - Ars_sum_array(1, j)
            Next j

            Acon_initial_array = Aconcrete_initial_array

            Dim Aconcrete_array(1, NumberCS, TimeIntervals) As Single

            For i = 1 To TimeIntervals
                For j = 1 To NumberCS
                    Aconcrete_array(1, j, i) = Ag - Aps_sum_array(1, j)
                    - Ars_sum_array(1, j)
                Next j
            Next i

            Acon_array = Aconcrete_array

    End Sub

End Module
```

Module 3: Initial Transformed Section Properties

```
Module TransformedSectionCalcs

    'Variables previously calculated within other modules.
      Public Ag, Ig, yb, Ep, Econ_array(TimeIntervals), Ec_initial, Es, Aps,
      yp_mid_array(30), yp_end_array(30), Ar_array(5), nrs_array(5),
      yr_array(5) As Single
      Public yp_array(NumberLayerGroups, NumberCS),
      Aps_array(NumberLayerGroups, NumberCS), Aps_sum_array(1, NumberCS),
      yAps_array(NumberLayerGroups, NumberCS), yAps_sum_array(1, NumberCS),
      yps_sum_array(1, NumberCS), yrs_array(NumberSteelLayers, NumberCS),
      Ars_array(NumberSteelLayers, NumberCS), Ars_sum_array(1,NumberCS),
      yArs_array(NumberSteelLayers, NumberCS), yArs_sum_array(1, NumberCS),
      yrs_sum_array(1, NumberCS) As Single
      Public NumberLayerGroups, NumberSteelLayers, TimeIntervals, NumberCS,
      i, j, k As Integer

    'Variables calculated within this module.
      Public np_initial, ns_initial, np_array(TimeIntervals),
      ns_array(TimeIntervals), Aps_y2_initial(1, NumberCS), Ars_y2_initial(1,
      NumberCS), Aps_y2(1, NumberCS, TimeIntervals), Ars_y2(1, NumberCS,
      TimeIntervals), ytr_initial_array(1, NumberCS), ytr_array(1, NumberCS,
      TimeIntervals), yp_cen_initial_array(NumberLayerGroups, NumberCS),
      yr_cen_initial_array(NumberSteelLayers, NumberCS),
      yp_cen_array(NumberLayerGroups, NumberCS, TimeIntervals), _
      yr_cen_array(NumberSteelLayers, NumberCS, TimeIntervals),
      Atr_initial_array(1, NumberCS), Atr_array(1, NumberCS, TimeIntervals),
      Itr_initial_array(1, NumberCS), Itr_array(1, NumberCS, TimeIntervals)
      As Single

    Function Atran_initial_array(ByVal Ep As Single, ByVal Es As
             Single, ByVal Ec_initial As Single, ByVal Ag As Single, _
             ByVal Aps_sum_array(,) As Single, ByVal Ars_sum_array(,)
             As Single, ByVal NumberCS As Integer, ByRef np_initial As
             Single, ByRef ns_initial As Single)

        'Defines variables to be used during transformed section
        calculations.

        np_initial = Ep / Ec_initial
        ns_initial = Es / Ec_initial

        Dim Atrans_initial_array(1, NumberCS) As Single

        For j = 1 To NumberCS
            Atrans_initial_array(1, j) = Ag + ((np_initial - 1) *
            Aps_sum_array(1, j)) + ((ns_initial - 1) * Ars_sum_array(1,
            j))
        Next

        Atran_initial_array = Atrans_initial_array

    End Function
```

```
Function ytran_initial_array(ByVal Ag As Single, ByVal yb As
         Single, ByVal np_initial As Single, ByVal ns_initial As
         Single, ByVal yAps_sum_array(,) As Single, ByVal
         yArs_sum_array(,) As Single, ByVal Aps_sum_array(,) As
         Single, ByVal Ars_sum_array(,) As Single, ByVal NumberCS
         As Integer)

    Dim ytrans_initial_array(1, NumberCS) As Single

    For j = 1 To NumberCS
        ytrans_initial_array(1, j) = ((Ag * yb) + ((np_initial - 1)
        * yAps_sum_array(1, j)) + ((ns_initial - 1) *
        yArs_sum_array(1, j))) / _
       (Ag + ((np_initial - 1) * Aps_sum_array(1, j)) +
       ((ns_initial - 1) * Ars_sum_array(1, j)))
    Next

    ytran_initial_array = ytrans_initial_array

End Function

Function yp_centroid_initial_array(ByVal NumberLayerGroups As
         Integer, ByVal NumberCS As Integer, ByVal
         ytr_initial_array(,) As Single, ByVal yp_array(,) As
         Single)

    Dim yp_cen_initial_array(NumberLayerGroups, NumberCS) As Single

    For j = 1 To NumberCS
        For k = 1 To NumberLayerGroups
            yp_cen_initial_array(k, j) = ytr_initial_array(1, j) –
            yp_array(k, j)
        Next k
    Next j

    yp_centroid_initial_array = yp_cen_initial_array

End Function

Function yr_centroid_initial_array(ByVal NumberSteelLayers As
         Integer, ByVal NumberCS As Integer, ByVal
         ytr_initial_array(,) As Single, ByVal yrs_array(,) As
         Single)

    Dim yr_cen_initial_array(NumberSteelLayers, NumberCS) As Single

    For j = 1 To NumberCS
        For k = 1 To NumberSteelLayers
            yr_cen_initial_array(k, j) = ytr_initial_array(1, j) –
            yrs_array(k, j)
        Next k
    Next j

    yr_centroid_initial_array = yr_cen_initial_array
```

```
End Function

Function Itran_initial_array(ByVal Ag As Single, ByVal Ig As
         Single, ByVal yb As Single, ByVal yp_cen_initial_array(,)
         As Single, ByVal yr_cen_initial_array(,) As Single, ByVal
         ytr_initial_array(,) As Single, ByVal Aps_array(,) As
         Single, ByVal Ars_array(,) As Single, ByVal np_initial As
         Single, ByVal ns_initial As Single, ByVal
         NumberLayerGroups As Integer, ByVal NumberSteelLayers As
         Integer, ByVal NumberCS As Integer, ByRef
         Aps_y2_initial(,) As Single, ByRef Ars_y2_initial(,) As
         Single)

    'Calculates the contribution of the prestressing steel layers to the
    moment of inertia.

    Dim Aps_y2_array(NumberLayerGroups, NumberCS)

    For j = 1 To NumberCS
        For k = 1 To NumberLayerGroups
            Aps_y2_array(k, j) = Aps_array(k, j) *
            ((yp_cen_initial_array(k, j)) ^ 2)
        Next k
    Next j

    Dim Aps_y2_sum(1, NumberCS) As Single

    For j = 1 To NumberCS
        For k = 1 To NumberLayerGroups
            Aps_y2_sum(1, j) = Aps_y2_sum(1, j) + Aps_y2_array(k,
            j)
        Next k
    Next j

    Aps_y2_initial = Aps_y2_sum


    'Calculates the contribution of the reinforcing steel layers to the
    moment of inertia.

    Dim Ars_y2_array(NumberSteelLayers, NumberCS)

    For j = 1 To NumberCS
        For k = 1 To NumberSteelLayers
            Ars_y2_array(k, j) = Ars_array(k, j) *
           ((yr_cen_initial_array(k, j)) ^ 2)
        Next k
    Next j

    Dim Ars_y2_sum(1, NumberCS) As Single

    For j = 1 To NumberCS
        For k = 1 To NumberSteelLayers
            Ars_y2_sum(1, j) = Ars_y2_sum(1, j) + Ars_y2_array(k,
```

```
                j)
            Next k
        Next j

        Ars_y2_initial = Ars_y2_sum


        ' Calculates the moment of interia immediately before release.

        Dim Itrans_initial_array(1, NumberCS) As Single

        For j = 1 To NumberCS
            Itrans_initial_array(1, j) = Ig + (Ag * ((yb –
            ytr_initial_array(1, j)) ^ 2)) + ((np_initial - 1) *
            Aps_y2_initial(1, j)) + ((ns_initial - 1) *
            Ars_y2_initial(1, j))
        Next

        Itran_initial_array = Itrans_initial_array

    End Function
```

Module 4: Initial Prestress Losses Prior to Release

```
Module InitialPrestressLosses

'Variables previously calculated in other modules.
      Public NumberSteelLayers, NumberLayerGroups, NumberCS, i, j, k As
            Integer
      Public ST_array(30) As String
      Public Mg, Ep, Ec_initial, fpy, fpj_array(30), Atr_initial,
            Itr_initial, ytr_initial, yp_mid_array(30), Ap_array(30),
            nps_array(30), TransferTime, JackingTime As Single

'Variables calculated in this module.
      Public t_initial, KL_array(NumberLayerGroups) As Single
      Public yp_cen_initial_array(NumberLayerGroups, NumberCS),
            ep_initial_array(NumberLayerGroups), No_initial_array(1,
            NumberCS), Mo_initial_array(1, NumberCS),
            delta_phi_initial_array(1, NumberCS), delta_ecen_initial_array(1,
            NumberCS), _
            delta_ep_es_initial_array(NumberLayerGroups),
            delta_fp_es_initial_array(NumberLayerGroups), _
            fpbt_array(NumberLayerGroups, NumberCS) As Single


    Function InitialSteelRelax_array(ByVal TransferTime As Single,
      ByVal NumberLayerGroups As Integer, ByVal ST_array() As String, ByVal
      fpj_array() As Single, ByVal fpy As Single, ByVal JackingTime As
      Single, ByVal NumberCS As Integer, ByRef t_initial As Single, ByRef
      KL_array() As Integer)

        t_initial = (TransferTime + JackingTime) / 24
```

```
'Creates an array of the KL factor to be used in relaxation of the steel
calculation.

      Dim K_L_array(NumberLayerGroups) As Integer

      For k = 1 To NumberLayerGroups
            If ST_array(k) = "Low-relaxation" Then
                K_L_array(k) = 45
            ElseIf ST_array(k) = "Stress-Relieved" Then
                K_L_array(k) = 10
            End If
        Next k

        KL_array = K_L_array

'Calculates the steel relaxation for each prestressing steel layer.

      Dim delta_fp_r_initial_array(NumberLayerGroups, NumberCS) As
            Single

      For j = 1 To NumberCS
            For k = 1 To NumberLayerGroups
                delta_fp_r_initial_array(k, j) = Math.Min(((-
                  fpj_array(k) / KL_array(k)) * (Log10(24 * t_initial)) *
                  (((fpj_array(k) / fpy)) - 0.55)), 0)
            Next k
      Next j

        InitialSteelRelax_array = delta_fp_r_initial_array

    End Function

'Calculates the elastic shortening for each prestressing steel layer.

    Function PrestressBeforeTransfer_array(ByVal fpj_array() As Single,
      ByVal InitialSteelRelaxation_array(,) As Single,
      ByVal NumberLayerGroups As Single, ByVal NumberCS As Single)

      Dim fpbt_array(NumberLayerGroups, NumberCS) As Single

      For j = 1 To NumberCS
            For k = 1 To NumberLayerGroups
                fpbt_array(k, j) = fpj_array(k) +
                  InitialSteelRelaxation_array(k, j)
            Next k
        Next j

        PrestressBeforeTransfer_array = fpbt_array

    End Function

    Function ep_i_array(ByVal NumberLayerGroups As Integer, ByVal
      NumberCS As Integer, ByVal fpbt_array(,) As Single, ByVal Ep As Single)
```

```
    Dim ep_initial_array(NumberLayerGroups, NumberCS) As Single

    For j = 1 To NumberCS
        For k = 1 To NumberLayerGroups
            ep_initial_array(k, j) = (fpbt_array(k, j)) / Ep
        Next k
    Next j

    ep_i_array = ep_initial_array

End Function

Function delta_ep_es_i_array(ByVal NumberLayerGroups As Single,
  ByVal NumberCS As Integer, ByVal Ep As Single, ByVal
  ep_initial_array(,) As Single, ByVal Ec_initial As Single, ByVal
  Atr_initial_array(,) As Single, ByVal yp_cen_initial_array(,) As
  Single, ByVal Itr_initial_array(,) As Single, ByVal Mg_array(,) As
  Single, ByVal Aps_array(,) As Single, ByVal fpbt_array(,) As Single,
  ByRef No_initial_array(,) As Single, ByRef Mo_initial_array(,) As
  Single, ByRef delta_ecen_initial_array(,) As Single, ByRef
  delta_phi_initial_array(,) As Single)

    Dim No_i_array(NumberLayerGroups, NumberCS) As Single

    For j = 1 To NumberCS
        For k = 1 To NumberLayerGroups
            No_i_array(k, j) = fpbt_array(k, j) * Aps_array(k, j)
        Next k
    Next j

    Dim No_i_sum_array(1, NumberCS) As Single

    For j = 1 To NumberCS
        For k = 1 To NumberLayerGroups
            No_i_sum_array(1, j) = No_i_sum_array(1, j) +
              No_i_array(k, j)
        Next k
    Next j

    No_initial_array = No_i_sum_array

    Dim delta_ecen_i_array(1, NumberCS) As Single

    For j = 1 To NumberCS
        delta_ecen_i_array(1, j) = -No_initial_array(1, j) /
              (Ec_initial * Atr_initial_array(1, j))
    Next j

    delta_ecen_initial_array = delta_ecen_i_array

    Dim Mo_i_array(NumberLayerGroups, NumberCS) As Single

    For j = 1 To NumberCS
        For k = 1 To NumberLayerGroups
            Mo_i_array(k, j) = No_i_array(k, j) *
```

```
            yp_cen_initial_array(k, j)
        Next k
    Next j

    Dim Mo_i_sum_array(1, NumberCS) As Single

    For j = 1 To NumberCS
        For k = 1 To NumberLayerGroups
            Mo_i_sum_array(1, j) = Mo_i_sum_array(1, j) +
              Mo_i_array(k, j)
        Next k
    Next j

    Mo_initial_array = Mo_i_sum_array

    Dim delta_phi_i_array(1, NumberCS) As Single

    For j = 1 To NumberCS
        delta_phi_i_array(1, j) = (Mg_array(1, j) –
              Mo_initial_array(1, j)) / (Ec_initial *
              Itr_initial_array(1, j))
    Next j

    delta_phi_initial_array = delta_phi_i_array

    Dim delta_ep_es_initial_array(NumberLayerGroups, NumberCS) As
        Single

    For j = 1 To NumberCS
        For k = 1 To NumberLayerGroups
          delta_ep_es_initial_array(k, j) =
              delta_ecen_initial_array(1, j) +
              (delta_phi_initial_array(1, j) * yp_cen_initial_array(k,
              j))
        Next k
    Next j

    delta_ep_es_i_array = delta_ep_es_initial_array

End Function

Function InitialElasticShort_array(ByVal Ep As Single, ByVal
  delta_ep_es_initial_array(,) As Single,                    ByVal
  NumberLayerGroups As Integer, ByVal NumberCS As Integer)

    Dim delta_fp_es_initial_array(NumberLayerGroups, NumberCS) As
        Single

    For j = 1 To NumberCS
        For k = 1 To NumberLayerGroups
            delta_fp_es_initial_array(k, j) = Ep *
              delta_ep_es_initial_array(k, j)
        Next k
    Next j
```

```
        InitialElasticShort_array = delta_fp_es_initial_array

    End Function


    Function PrestressAfterTransfer_array(ByVal fpbt_array(,) As
      Single, ByVal InitialElasticShortening_array(,) As Single, _
      ByVal NumberLayerGroups As Single, ByVal NumberCS As Integer)

        Dim fpt_array(NumberLayerGroups, NumberCS) As Single

        For j = 1 To NumberCS
            For k = 1 To NumberLayerGroups
                fpt_array(k, j) = fpbt_array(k, j) +
                  InitialElasticShortening_array(k, j)
            Next k
        Next j

        PrestressAfterTransfer_array = fpt_array

    End Function

End Module
```

Module 5: Initial Strains and Stresses

```
Module InitialStrainStress

'Variables previously calculated in other modules.
    Public NumberLayerGroups, NumberSteelLayers, NumberCS, j, k As
      Integer
    Public h, Ec_initial, Ep, ytr_initial_array(1, NumberCS),
      yr_cen_initial_array2(NumberSteelLayers, NumberCS), ytop_array(1,
      NumberCS), ep_initial_array(NumberLayerGroups, NumberCS),
      delta_ep_es_initial_array(NumberLayerGroups, NumberCS), _
      delta_ecen_initial_array(1, NumberCS), delta_phi_initial_array(1,
      NumberCS), fpj_array(NumberLayerGroups) As Single

'Variables calculated in this module.
    Public ec_array(2, NumberCS), fc_array(2, NumberCS),
      er_array(NumberSteelLayers, NumberCS), fr_array(NumberSteelLayers,
      NumberCS), _
      ep_array(NumberLayerGroups, NumberCS) As Single

    Function PrestressStrain_array(ByVal NumberLayerGroups As Integer,
      ByVal NumberCS As Integer, ByVal fpj_array() As Single, _
      ByVal delta_ep_es_initial_array(,) As Single, ByVal Ep As Single)

        Dim eps_array(NumberLayerGroups, NumberCS) As Single

        For j = 1 To NumberCS
            For k = 1 To NumberLayerGroups
                eps_array(k, j) = delta_ep_es_initial_array(k, j) +
```

```
            (fpj_array(k) / Ep)
        Next k
    Next j

    PrestressStrain_array = eps_array

End Function

Function SteelStrain_array(ByVal NumberSteelLayers As Integer,
  ByVal NumberCS As Integer, ByVal delta_ecen_initial_array(,) As Single,
  ByVal delta_phi_initial_array(,) As Single, _
  ByVal yr_cen_initial_array(,) As Single)

    Dim ers_array(NumberSteelLayers, NumberCS) As Single

    For j = 1 To NumberCS
        For k = 1 To NumberSteelLayers
            ers_array(k, j) = delta_ecen_initial_array(1, j) +
              (delta_phi_initial_array(1, j) * yr_cen_initial_array(k,
              j))
        Next k
    Next j

    SteelStrain_array = ers_array

End Function

Function SteelStress_array(ByVal NumberSteelLayers As Integer,
  ByVal NumberCS As Integer, ByVal Es As Single, _
  ByVal initial_er_array(,) As Single)

    Dim frs_array(NumberSteelLayers, NumberCS) As Single

    For j = 1 To NumberCS
        For k = 1 To NumberSteelLayers
            frs_array(k, j) = Es * initial_er_array(k, j)
        Next k
    Next j

    SteelStress_array = frs_array

End Function

Function ConcreteStrain_array(ByVal delta_ecen_initial_array(,) As
  Single, ByVal delta_phi_initial_array(,) As Single, _
  ByVal ytr_initial_array(,) As Single, ByVal h As Single, ByVal NumberCS
  As Integer, ByRef ytop_array(,) As Single)

    Dim yt_array(1, NumberCS) As Single

    For j = 1 To NumberCS
        yt_array(1, j) = ytr_initial_array(1, j) - h
    Next j

    ytop_array = yt_array
```

```
    Dim econ_array(2, NumberCS) As Single

    For j = 1 To NumberCS
        econ_array(1, j) = delta_ecen_initial_array(1, j) +
          (delta_phi_initial_array(1, j) * ytr_initial_array(1, j))
          econ_array(2, j) = delta_ecen_initial_array(1, j) +
          (delta_phi_initial_array(1, j) * ytop_array(1, j))
    Next

    ConcreteStrain_array = econ_array

End Function

Function ConcreteStress_array(ByVal NumberCS As Integer, ByVal
  initial_ec_array(,) As Single, ByVal Ec_initial As Single)

    Dim fcon_array(2, NumberCS) As Single

    For j = 1 To NumberCS
        fcon_array(1, j) = Ec_initial * initial_ec_array(1, j)
        fcon_array(2, j) = Ec_initial * initial_ec_array(2, j)
    Next

    ConcreteStress_array = fcon_array

End Function

Function Initial_Strain_array(ByVal delta_ecen_initial_array(,) As
  Single, ByVal NumberCS As Integer)

    Dim initial_ecen_array(1, NumberCS) As Single

    For j = 1 To NumberCS
        initial_ecen_array(1, j) = delta_ecen_initial_array(1, j)
    Next j

    Initial_Strain_array = initial_ecen_array

End Function

Function Initial_Stress_array(ByVal initial_ecen_array(,) As
  Single, ByVal Ec_initial As Single, ByVal NumberCS As Integer)

    Dim initial_fcen_array(1, NumberCS) As Single

    For j = 1 To NumberCS
        initial_fcen_array(1, j) = initial_ecen_array(1, j) *
              Ec_initial
    Next j

    Initial_Stress_array = initial_fcen_array

End Function
```

```
End Module
```

Module 6: Transformed Section Properties

```
    Function Atran_array(ByVal Ep As Single, ByVal Es As Single, ByVal
             Econ_array() As Single, ByVal Ag As Single, ByVal
             Aps_sum_array(,) As Single, ByVal Ars_sum_array(,) As
             Single, ByVal NumberCS As Integer, ByVal TimeIntervals As
             Integer, ByRef np_array() As Single, ByRef ns_array() As
             Single)

        'Defines variables to be used during transformed section
        calculations.

        Dim np(TimeIntervals) As Single

        For i = 1 To TimeIntervals
            np(i) = Ep / Econ_array(i)
        Next i

        np_array = np

        Dim ns(TimeIntervals) As Single

        For i = 1 To TimeIntervals
            ns(i) = Es / Econ_array(i)
        Next i

        ns_array = ns

        Dim Atrans_array(1, NumberCS, TimeIntervals) As Single

        For i = 1 To TimeIntervals
            For j = 1 To NumberCS
                Atrans_array(1, j, i) = Ag + ((np_array(i) - 1) *
                Aps_sum_array(1, j)) + ((ns_array(i) - 1) *
                Ars_sum_array(1, j))
            Next j
        Next i

        Atran_array = Atrans_array

    End Function

    Function ytran_array(ByVal Ag As Single, ByVal yb As Single, ByVal
             np_array() As Single, ByVal ns_array() As Single, _
             ByVal NumberCS As Integer, ByVal TimeIntervals As Integer,
             ByVal yAps_sum_array(,) As Single, ByVal yArs_sum_array(,)
             As Single, ByVal Aps_sum_array(,) As Single, ByVal
             Ars_sum_array(,) As Single)

        Dim ytrans_array(1, NumberCS, TimeIntervals) As Single
```

```
        For i = 1 To TimeIntervals
            For j = 1 To NumberCS
                ytrans_array(1, j, i) = ((Ag * yb) + ((np_array(i) - 1)
                * yAps_sum_array(1, j)) + ((ns_array(i) - 1) *
                yArs_sum_array(1, j))) / _
                (Ag + ((np_array(i) - 1) * Aps_sum_array(1, j)) +
                ((ns_array(i) - 1) * Ars_sum_array(1, j)))
            Next j
        Next i

        ytran_array = ytrans_array

    End Function

    Function yp_centroid_array(ByVal NumberLayerGroups As Integer,
             ByVal NumberCS As Integer, ByVal TimeIntervals As Integer,
             ByVal ytr_array(,,) As Single, ByVal yp_array(,) As
             Single)

Dim yp_cen_array(NumberLayerGroups, NumberCS, TimeIntervals) As Single

        For i = 1 To TimeIntervals
            For j = 1 To NumberCS
                For k = 1 To NumberLayerGroups
                    yp_cen_array(k, j, i) = ytr_array(1, j, i) –
                    yp_array(k, j)
                Next k
            Next j
        Next i

        yp_centroid_array = yp_cen_array

    End Function

    Function yr_centroid_array(ByVal NumberSteelLayers As Integer,
           ByVal NumberCS As Integer, ByVal TimeIntervals As Integer,
           ByVal ytr_array(,,) As Single, ByVal yrs_array(,) As  Single

Dim yr_cen_array(NumberSteelLayers, NumberCS, TimeIntervals) As Single

        For i = 1 To TimeIntervals
            For j = 1 To NumberCS
                For k = 1 To NumberSteelLayers
                    yr_cen_array(k, j, i) = ytr_array(1, j, i) –
                    yrs_array(k, j)
                Next k
            Next j
        Next i

        yr_centroid_array = yr_cen_array

    End Function

    Function Itran_array(ByVal Ag As Single, ByVal Ig As Single, ByVal
             yb As Single, ByVal yp_cen_array(,,) As Single, _
```

```
     ByVal yr_cen_array(,,) As Single, ByVal ytr_array(,,) As
     Single, ByVal Aps_array(,) As Single, ByVal Ars_array(,)
     As Single, ByVal np_array() As Single, ByVal ns_array() As
     Single, ByVal NumberLayerGroups As Integer, ByVal
     NumberSteelLayers As Integer, ByVal NumberCS As Integer, _
     ByVal TimeIntervals As Integer, ByRef Aps_y2(,,) As
     Single, ByRef Ars_y2(,,) As Single)


'Calculates the contribution of the prestressing steel layers to the
moment of inertia.

Dim Aps_y2_array(NumberLayerGroups, NumberCS, TimeIntervals)

For i = 1 To TimeIntervals
    For j = 1 To NumberCS
        For k = 1 To NumberLayerGroups
            Aps_y2_array(k, j, i) = Aps_array(k, j) *
           ((yp_cen_array(k, j, i)) ^ 2)
        Next k
    Next j
Next i

Dim Aps_y2_sum(1, NumberCS, TimeIntervals) As Single

For i = 1 To TimeIntervals
    For j = 1 To NumberCS
        For k = 1 To NumberLayerGroups
            Aps_y2_sum(1, j, i) = Aps_y2_sum(1, j, i) +
            Aps_y2_array(k, j, i)
        Next k
    Next j
Next i

Aps_y2 = Aps_y2_sum


'Calculates the contribution of the reinforcing steel layers to the
moment of inertia.

Dim Ars_y2_array(NumberSteelLayers, NumberCS, TimeIntervals)

For i = 1 To TimeIntervals
    For j = 1 To NumberCS
        For k = 1 To NumberSteelLayers
            Ars_y2_array(k, j, i) = Ars_array(k, j) *
           ((yr_cen_array(k, j, i)) ^ 2)
        Next k
    Next j
Next i

Dim Ars_y2_sum(1, NumberCS, TimeIntervals) As Single

For i = 1 To TimeIntervals
    For j = 1 To NumberCS
```

```
                For k = 1 To NumberSteelLayers
                    Ars_y2_sum(1, j, i) = Ars_y2_sum(1, j, i) +
                    Ars_y2_array(k, j, i)
                Next k
            Next j
        Next i

        Ars_y2 = Ars_y2_sum


        ' Calculates the moment of interia at the beginning of each
        time interval.

        Dim Itrans_array(1, NumberCS, TimeIntervals) As Single

        For i = 1 To TimeIntervals
            For j = 1 To NumberCS
                Itrans_array(1, j, i) = Ig + (Ag * ((yb - ytr_array(1,
                j, i)) ^ 2)) + ((np_array(i) - 1) * Aps_y2(1, j, i)) +
                ((ns_array(i) - 1) * Ars_y2(1, j, i))
            Next j
        Next i

        Itran_array = Itrans_array

    End Function

End Module
```

Module 7: Net Concrete Properties

```
Module NetProp

    Public NumberLayerGroups, NumberSteelLayers, NumberCS,
    TimeIntervals, i, j, k As Integer
    Public Ep, Es, Ec_initial, Econ_array(TimeIntervals) As Single
    Public Atr_initial_array(1, NumberCS), ytr_initial_array(1,
    NumberCS), Atr_array(1, NumberCS, TimeIntervals), _
    ytr_array(1, NumberCS, TimeIntervals), Acon_initial_array(1,
    NumberCS), Acon_array(1, NumberCS, TimeIntervals), _
    yAps_sum_array(1, NumberCS), yArs_sum_array(1, NumberCS),
    yp_array(NumberLayerGroups, NumberCS), yrs_array(,) As Single
    Public np_initial, ns_initial, np_array(TimeIntervals),
    ns_array(TimeIntervals), yc_net_initial_array(1, NumberCS), _
    yc_net_array(1, NumberCS, TimeIntervals), yp_net_initial_array(1,
    NumberCS), yp_net_array(NumberLayerGroups, NumberCS,
    TimeIntervals), yr_net_initial_array(1, NumberCS),
    yr_net_array(NumberSteelLayers, NumberCS, TimeIntervals) As Single

    Sub NetConcreteProp(ByVal NumberLayerGroups As Integer, ByVal
                        NumberCS As Integer, ByVal TimeIntervals As  Integer,
                        ByVal i As Integer, ByVal j As Integer, ByVal k As
                        Integer, ByVal Ep As Single, ByVal Es As Single, _
```

```
                    ByVal Ec_initial As Single, ByVal Econ_array() As
                    Single, ByVal Atr_initial_array(,) As Single, ByVal
                    ytr_initial_array(,) As Single, ByVal Atr_array(,,)
                    As Single, ByVal ytr_array(,,) As Single, _
                    ByVal Acon_initial_array(,) As Single, ByVal
                    Acon_array(,,) As Single, ByVal yAps_sum_array(,) As
                    Single, _
                    ByVal yArs_sum_array(,) As Single, ByRef np_initial
                    As Single, ByRef ns_initial As Single, ByRef
                    np_array() As Single, _
                    ByRef ns_array() As Single, ByRef
                    yc_net_initial_array(,) As Single, ByRef
                    yc_net_array(,,) As Single, _
                    ByRef yp_net_initial_array(,) As Single, ByRef
                    yp_net_array(,,) As Single, ByRef
                    yr_net_initial_array(,) As Single, _
                    ByRef yr_net_array(,,) As Single, ByVal yp_array(,)
                    As Single, ByVal yrs_array(,) As Single, ByVal
                    NumberSteelLayers As Integer)

np_initial = Ep / Ec_initial
ns_initial = Es / Ec_initial

Dim np(TimeIntervals) As Single
Dim ns(TimeIntervals) As Single

For i = 1 To TimeIntervals
    np(i) = Ep / Econ_array(i)
    ns(i) = Es / Econ_array(i)
Next i

np_array = np
ns_array = ns

Dim yc_initial_array(1, NumberCS) As Single

For j = 1 To NumberCS
    yc_initial_array(1, j) = ((Atr_initial_array(1, j) *
    ytr_initial_array(1, j)) - (np_initial * yAps_sum_array(1,
    j)) - (ns_initial * yArs_sum_array(1, j))) /
    Acon_initial_array(1, j)
Next j

yc_net_initial_array = yc_initial_array

Dim yc_array(1, NumberCS, TimeIntervals) As Single

For i = 1 To TimeIntervals
    For j = 1 To NumberCS
        yc_array(1, j, i) = ((Atr_array(1, j, i) * ytr_array(1,
        j, i)) - (np_array(i) * yAps_sum_array(1, j)) _
        - (ns_array(i) * yArs_sum_array(1, j))) / Acon_array(1,
        j, i)
    Next j
Next i
```

```
        yc_net_array = yc_array

        Dim yp_net_concrete_initial_array(NumberLayerGroups, NumberCS)
            As Single
        Dim yr_net_concrete_initial_array(NumberSteelLayers, NumberCS)
            As Single

        For j = 1 To NumberCS
            For k = 1 To NumberLayerGroups
                yp_net_concrete_initial_array(k, j) =
                yc_net_initial_array(1, j) - yp_array(k, j)
            Next k
        Next j

        For j = 1 To NumberCS
            For k = 1 To NumberSteelLayers
                yr_net_concrete_initial_array(k, j) =
                yc_net_initial_array(1, j) - yrs_array(k, j)
            Next k
        Next j

        yp_net_initial_array = yp_net_concrete_initial_array
        yr_net_initial_array = yr_net_concrete_initial_array

        Dim yp_net_concrete_array(NumberLayerGroups, NumberCS,
            TimeIntervals) As Single
        Dim yr_net_concrete_array(NumberSteelLayers, NumberCS,
            TimeIntervals) As Single

        For i = 1 To TimeIntervals
            For j = 1 To NumberCS
                For k = 1 To NumberLayerGroups
                    yp_net_concrete_array(k, j, i) = yc_net_array(1, j,
                    i) - yp_array(k, j)
                Next k
            Next j
        Next i

        For i = 1 To TimeIntervals
            For j = 1 To NumberCS
                For k = 1 To NumberSteelLayers
                    yr_net_concrete_array(k, j, i) = yc_net_array(1, j,
                    i) - yrs_array(k, j)
                Next k
            Next j
        Next i

        yp_net_array = yp_net_concrete_array
        yr_net_array = yr_net_concrete_array

    End Sub

End Module
```

Module 8: Creep and Shrinkage Correction Factors

```
Module K_Calculations

    Public RH, Slump, CementContent, AirContent, VS, FA, CureAge, LoadingAge,
    Kh_creep, Ks_creep, Ka_creep, Kvs_creep, _
    Kfa_creep, Kla_creep, K_CreepTotal, Kh_shrink, Ks_shrink, Ka_shrink,
    Kvs_shrink, Kfa_shrink, Kc_shrink, Kcp_shrink, _
    K_ShrinkTotal, TransferTime, MoistPeriod, fci, ti, fc28, SteamPeriod,
    Kcure_shrink As Single

    Sub K_Calcs(ByRef RH As Single, ByRef Slump As Single, ByRef
                CementContent As Single, ByRef AirContent As Single, _
                ByRef VS As Single, ByRef FA As Single, ByRef CureAge
                As Single, ByRef LoadingAge As Single, _
                ByVal MoistPeriod As Single, ByRef Kh_creep As Single,
                ByRef Ks_creep As Single, ByRef Ka_creep As Single, _
                ByRef Kvs_creep As Single, ByRef Kfa_creep As Single,
                ByRef Kla_creep As Single, ByRef K_CreepTotal As
                Single, ByRef Kh_shrink As Single, ByRef Ks_shrink As
                Single, ByRef Ka_shrink As Single, ByRef Kvs_shrink As
                Single, ByRef Kfa_shrink As Single, ByRef Kc_shrink As
                Single, ByRef Kcp_shrink As Single, ByRef K_ShrinkTotal
                As Single, ByRef fci As Single, ByRef ti As Single,
                ByRef Khc As Single, ByRef Ks As Single, ByRef Kf As
                Single, ByRef Khs As Single, ByRef fc28 As Single,
                ByVal SteamPeriod As Single, ByRef Kcure_shrink As
                Single)

        'Imports the variables from the user input to be used in the
        calculations.

        If SelectModel.rbACI.Checked = True Then
            RH = Val(SelectModel.txbRH_ACI.Text)
            Slump = Val(SelectModel.txbSlump_ACI.Text)
            CementContent = Val(SelectModel.txbCementContent_ACI.Text)
            AirContent = Val(SelectModel.txbAirContent_ACI.Text)
            VS = Val(SelectModel.txbVS_ACI.Text)
            FA = Val(SelectModel.txbFA_ACI.Text)
            LoadingAge = (Val(TimeOfEvents.txbTransferTime.Text) / 24)
            CureAge = Val(TimeOfEvents.txbMoistDays.Text)
        ElseIf SelectModel.rbAASHTO_05.Checked = True Then
            RH = Val(SelectModel.txbRH_AASHTO_05.Text)
            VS = Val(SelectModel.txbVS_AASHTO_05.Text)
            fci = Val(SelectModel.txbfci_AASHTO_05.Text)
            If TimeOfEvents.rbSteamCure.Checked = True Then
                ti = Val(SelectModel.txbti_AASHTO_05.Text)
            ElseIf TimeOfEvents.rbMoistCure.Checked = True Then
                ti = Val(SelectModel.txbti_AASHTO_05.Text) / 7
            End If
        ElseIf SelectModel.rbAASHTO_04.Checked = True Then
            RH = Val(SelectModel.txbRH_AASHTO_04.Text)
            VS = Val(SelectModel.txbVS_AASHTO_04.Text)
            fc28 = Val(SelectModel.txbfc28_AASHTO_04.Text)
```

```
    If TimeOfEvents.rbSteamCure.Checked = True Then
        ti = Val(SelectModel.txbti_AASHTO_04.Text) * 7
    ElseIf TimeOfEvents.rbMoistCure.Checked = True Then
        ti = Val(SelectModel.txbti_AASHTO_04.Text)
    End If
End If

'ACI Correction Factors

If SelectModel.rbACI.Checked = True Then

    'ACI Creep Correction Factors

    If RH > "40" Then
        Kh_creep = 1.27 - (0.0067 * RH)
    Else
        K_Values_ACI.txb1.Text = "RH < 40%"
    End If

    Ks_creep = 0.82 + (0.067 * Slump)
    Ka_creep = Math.Max((0.46 + (0.09 * AirContent)), 1)
    Kvs_creep = (2 / 3) * (1 + (1.13 * Exp((-0.54 * VS))))
    Kfa_creep = 0.88 + (0.0024 * FA)

    If TimeOfEvents.rbMoistCure.Checked = True And LoadingAge >
    7 Then
        Kla_creep = 1.25 * ((LoadingAge) ^ (-0.118))
    ElseIf TimeOfEvents.rbSteamCure.Checked = True And
    LoadingAge > 3 Then
        Kla_creep = 1.13 * ((LoadingAge) ^ (-0.094))
    Else
        Kla_creep = 1
    End If

    Dim K_Creep_Total As Single

    K_Creep_Total = Kh_creep * Ks_creep * Ka_creep * Kvs_creep
                    * Kfa_creep * Kla_creep

    K_CreepTotal = K_Creep_Total

    'ACI Shrinkage Correction Factors

    If RH >= "40" And RH <= "80" Then
        Kh_shrink = 1.4 - (0.01 * RH)
    ElseIf RH > "80" And RH <= "100" Then
        Kh_shrink = 3.0 - (0.03 * RH)
    End If

    Ks_shrink = 0.89 + (0.041 * Slump)
    Ka_shrink = 0.95 + (0.008 * AirContent)
    Kvs_shrink = 1.2 * Exp((-0.12 * VS))
    Kc_shrink = 0.75 + (0.00036 * CementContent)

    If FA <= "50" Then
```

```
            Kfa_shrink = 0.3 + (0.014 * FA)
        ElseIf FA > "50" Then
            Kfa_shrink = 0.9 + (0.002 * FA)
        End If

        If MoistPeriod = "7" Or TimeOfEvents.rbSteamCure.Checked =
        True Then
            Kcp_shrink = 1
        Else
            Kcp_shrink = (-0.1015 * Log(CureAge)) + 1.202
        End If

        Dim K_Shrink_Total As Single

        K_Shrink_Total = Kh_shrink * Ks_shrink * Ka_shrink *
                         Kvs_shrink * Kfa_shrink * Kc_shrink *
                         Kcp_shrink

        K_ShrinkTotal = K_Shrink_Total

        'AASHTO Creep and Shrinkage Correction Factors

    ElseIf SelectModel.rbAASHTO_05.Checked = True Then

        Khc = 1.56 - 0.008 * RH
        Khs = 2.0 - 0.014 * RH
        Ks = Max(1.45 - 0.13 * VS, 1.0)
        Kf = 5 / (1 + (fci / 1000))

        If TimeOfEvents.rbMoistCure.Checked = True And MoistPeriod
        < 5 Then
            Kcure_shrink = 1.2
        ElseIf TimeOfEvents.rbSteamCure.Checked = True And
        SteamPeriod < 0.7142857 Then
            Kcure_shrink = 1.2
        Else
            Kcure_shrink = 1.0
        End If

    ElseIf SelectModel.rbAASHTO_04.Checked = True Then

        Kf = 1 / (0.67 + ((fc28 / 1000) / 9))

        If TimeOfEvents.rbMoistCure.Checked = True And MoistPeriod
        < 5 Then
            Kcure_shrink = 1.2
        ElseIf TimeOfEvents.rbSteamCure.Checked = True And
        SteamPeriod < 0.7142857 Then
            Kcure_shrink = 1.2
        Else
            Kcure_shrink = 1.0
        End If

        If RH < 80 Then
            Khs = (140 - RH) / 70
```

```
            ElseIf RH >= 80 Then
                Khs = 3 * (100 - RH) / 70
            End If

        End If

    End Sub

End Module
```

Module 9: Time Loop (Partial Code)

```
Module TIME_LOOP

    Public i, j, k, NumberLayerGroups, NumberSteelLayers, NumberCS,
    TimeIntervals As Integer
    Public h…Total_fnet_array(1, NumberCS, TimeIntervals) As Single

    Sub time_interval_loop(ByVal NumberLayerGroups As Integer…ByVal
                           Kcure_shrink As Single)

'START OF THE TIME LOOP.

        For i = 1 To TimeIntervals

'COMPUTES THE INCREMENTAL RELAXATION LOSS.

            For j = 1 To NumberCS
                For k = 1 To NumberLayerGroups
                    If i = 1 Then
delta_fpr_array(k, j, i) = Math.Min(((-fpt_array(k, j) / KL_array(k)) *
                           (Log10(24 * jack_time_array(i)) - Log10(24 *
                           jack_time_array(i - 1))) * (((fpt_array(k, j)
                           / fpy) - 0.55))), 0)
                    ElseIf i >= 2 Then
delta_fpr_array(k, j, i) = Math.Min((((-fps_array(k, j, i - 1) /
                           KL_array(k)) * (Log10(24 *
                           jack_time_array(i)) - Log10(24 *
                           jack_time_array(i - 1))) * (((fps_array(k,
                           j, i - 1)) / fpy) - 0.55))), 0)
                    End If
                Next k
            Next j

'COMPUTES THE CREEP COEFFICIENT.

            If SelectModel.rbACI.Checked = True Then

                ultimate_creep_co = K_CreepTotal * 2.35

'Calculate at the beginning and end of the time interval...need the change in
vt.
```

```
                vt_array_begin(i) = (time_array(i - 1) ^ 0.6) / (10 +
                                    (time_array(i - 1) ^ 0.6))
                vt_array_end(i) = (time_array(i) ^ 0.6) / (10 +
                                  (time_array(i) ^ 0.6))
                delta_vt_array(i) = vt_array_end(i) - vt_array_begin(i)

                Creep_Co_array(i) = ultimate_creep_co *
                                    delta_vt_array(i)

                Total_Creep_Co = Total_Creep_Co + Creep_Co_array(i)

            ElseIf SelectModel.rbAASHTO_05.Checked = True Then

                ultimate_creep_co = 1.9 * Ks * Khc * Kf * (ti ^ (-
                                    0.118))

'Calculate at beginning and end of time interval...need the change in Ktd.

                Ktd_array_begin(i) = time_array(i - 1) / (61 - (4 *
                                     (fci / 1000)) + time_array(i - 1))
                Ktd_array_end(i) = time_array(i) / (61 - (4 * (fci /
                                   1000)) + time_array(i))
                delta_Ktd_array(i) = Ktd_array_end(i) -
                                     Ktd_array_begin(i)

                Creep_Co_array(i) = ultimate_creep_co *
                                    delta_Ktd_array(i)

                Total_Creep_Co = Total_Creep_Co + Creep_Co_array(i)

            ElseIf SelectModel.rbAASHTO_04.Checked = True Then



Ktd_array_begin(i) = (time_array(i - 1)) ^ 0.6 / (10 + ((time_array(i –
                     1)) ^ 0.6))
Ktd_array_end(i) = (time_array(i)) ^ 0.6 / (10 + ((time_array(i)) ^
                    0.6))
delta_Ktd_array(i) = Ktd_array_end(i) - Ktd_array_begin(i)

Kc_array(i) = (((age_array(i) - ti) / ((26 * Exp(0.36 * VS)) +
              (age_array(i) - ti))) / ((age_array(i) - ti) / (45 +
              (age_array(i) - ti)))) * ((1.8 + (1.77 * Exp(-0.54 *
              VS))) / 2.587)

ultimate_creep_co = 3.5 * Kf * (ti ^ -0.118) * ((10000 / ((26 *
                    Exp(0.36 * VS)) + 10000)) / (10000 / (45 + 10000)))
                    *((1.8 + (1.77 * Exp(-0.54 * VS))) / 2.587)

Creep_Co_array(i) = 3.5 * Kc_array(i) * Kf * (ti ^ -0.118) *
                    delta_Ktd_array(i)

 Total_Creep_Co = Total_Creep_Co + Creep_Co_array(i)

            ElseIf SelectModel.rbCEB.Checked = True Then
```

```
notional_creep_co = (1 + ((1 - (RH_CEB / 100)) / (0.46 * ((h_CEB / 100)
                    ^ (1 / 3))))) * (5.3 / ((fcm_CEB / 10) ^ 0.5)) _
                    * (1 / (0.1 + ((TransferTime) ^ 0.2)))

ultimate_creep_co = notional_creep_co

beta_h = Math.Min(((150 * (1 + ((1.2 * RH_CEB / 100) ^ 18)) * (h_CEB /
         100)) + 250), 1500)

beta_c_begin(i) = (age_array(i - 1) / (beta_h + age_array(i - 1))) ^
                  0.3

beta_c_end(i) = (age_array(i) / (beta_h + age_array(i))) ^ 0.3
                delta_beta_c(i) = beta_c_end(i) - beta_c_begin(i)

Creep_Co_array(i) = notional_creep_co * delta_beta_c(i)

Total_Creep_Co = Total_Creep_Co + Creep_Co_array(i)


            ElseIf SelectModel.rbCEB_Mod.Checked = True Then

beta_h = Math.Min(((150 * (1 + ((1.2 * RH_CEB / 100) ^ 18)) * (h_CEB /
         100)) + 250), 1500)

                If TimeOfEvents.rbMoistCure.Checked = True Then

notional_creep_co = (1 + ((1 - (RH_CEB / 100)) / (0.46 * ((h_CEB / 100)
                    ^ (1 / 3))))) * (5.3 / ((fcm_CEB / 10) ^ 0.5)) _
                    * (1 / (0.26 + ((TransferTime) ^ 0.18)))

beta_c_begin(i) = (age_array(i - 1) / (beta_h + age_array(i - 1))) ^
                  0.27
beta_c_end(i) = (age_array(i) / (beta_h + age_array(i))) ^ 0.27
                delta_beta_c(i) = beta_c_end(i) - beta_c_begin(i)

                ElseIf TimeOfEvents.rbSteamCure.Checked = True Then

notional_creep_co = (1 + ((1 - (RH_CEB / 100)) / (0.46 * ((h_CEB / 100)
                    ^ (1 / 3))))) * (4.65 / ((fcm_CEB / 10) ^ 0.5)) _
                    * (1 / (0.26 + ((TransferTime) ^ 0.18)))

beta_c_begin(i) = (time_array(i - 1) / (beta_h + time_array(i - 1))) ^
                  0.35

beta_c_end(i) = (time_array(i) / (beta_h + time_array(i))) ^ 0.35

delta_beta_c(i) = beta_c_end(i) - beta_c_begin(i)

                End If

ultimate_creep_co = notional_creep_co

Creep_Co_array(i) = notional_creep_co * delta_beta_c(i)
```

```
Total_Creep_Co = Total_Creep_Co + Creep_Co_array(i)

            End If

'COMPUTES THE INCREMENTAL UNRESTRAINED CREEP STRAIN AT THE CENTROID OF THE
TRANSFORMED SECTION BY UPDATING No.

            For j = 1 To NumberCS
                For k = 1 To NumberLayerGroups
                    If i = 1 Then
                        ep_array(k, j, i) = (fpt_array(k, j)) / Ep
                    ElseIf i >= 2 Then
                        ep_array(k, j, i) = (fps_array(k, j, i - 1)) /
                        Ep
                    End If
                Next k
            Next j

            For j = 1 To NumberCS
                For k = 1 To NumberLayerGroups
                    If i = 1 Then
                        No_array(k, j, i) = fpt_array(k, j) *
                        Aps_array(k, j)
                    ElseIf i >= 2 Then
                        No_array(k, j, i) = Ep * ep_array(k, j, i) *
                        Aps_array(k, j)
                    End If
                Next k
            Next j




            For j = 1 To NumberCS
                For k = 1 To NumberLayerGroups
                    No_sum_array(1, j, i) = No_sum_array(1, j, i) +
                    No_array(k, j, i)
                Next k
            Next j

            For j = 1 To NumberCS
                delta_e_cen_array(1, j, i) = -No_sum_array(1, j, i) /
               (Ec_initial * Atr_initial_array(1, j))
            Next j

            For j = 1 To NumberCS
                delta_creep_e_cen_array(1, j, i) = Creep_Co_array(i) *
                delta_e_cen_array(1, j, i)
            Next j

'COMPUTES THE INCREMENTAL UNRESTRAINED CREEP CURVATURE BY UPDATING Mo.

            For j = 1 To NumberCS
                For k = 1 To NumberLayerGroups
```

```
                Mo_array(k, j, i) = No_array(k, j, i) *
                yp_cen_array(k, j, i)
            Next k
        Next j

        For j = 1 To NumberCS
            For k = 1 To NumberLayerGroups
                Mo_sum_array(1, j, i) = Mo_sum_array(1, j, i) +
                Mo_array(k, j, i)
            Next k
        Next j

        For j = 1 To NumberCS
            delta_phi_array(1, j, i) = (Mg_array(1, j) –
            Mo_sum_array(1, j, i)) / (Ec_initial *
            Itr_initial_array(1, j))
        Next j

        For j = 1 To NumberCS
            delta_creep_phi_array(1, j, i) = Creep_Co_array(i) *
            delta_phi_array(1, j, i)
        Next j

'COMPUTES THE INCREMENTAL UNRESTRAINED CREEP STRAIN AT THE CENTROID OF THE
NET CONCRETE SECTION.

        For j = 1 To NumberCS
            delta_creep_e_net_array(1, j, i) =
            delta_creep_e_cen_array(1, j, i) +
            (delta_creep_phi_array(1, j, i) * (ytr_array(1, j, i) _
             - yc_net_array(1, j, i)))
        Next j

'COMPUTES THE INCREMENTAL UNRESTRAINED SHRINKAGE STRAIN FOR EACH CROSS
SECTION.

        If SelectModel.rbACI.Checked = True Then

          ultimate_shrink_strain = K_ShrinkTotal * -780 * (10 ^ -6)

'Calculate at beginning and end of time interval...need the change in
gamma_array.

            If TimeOfEvents.rbMoistCure.Checked = True Then
gamma_array_begin(i) = shrink_time_array(i - 1) / (35 +
                       shrink_time_array(i - 1))
gamma_array_end(i) = shrink_time_array(i) / (35 + shrink_time_array(i))
            ElseIf TimeOfEvents.rbSteamCure.Checked = True Then
gamma_array_begin(i) = shrink_time_array(i - 1) / (55 +
                       shrink_time_array(i - 1))
gamma_array_end(i) = shrink_time_array(i) / (55 + shrink_time_array(i))
            End If

delta_gamma_array(i) = gamma_array_end(i) - gamma_array_begin(i)
```

```
                For j = 1 To NumberCS
                    delta_shrink_e_cen_array(1, j, i) =
                    ultimate_shrink_strain * delta_gamma_array(i)
                Next j

                For j = 1 To NumberCS
                    Total_Shrink_Strain_array(1, j) =
                    Total_Shrink_Strain_array(1, j) +
                    delta_shrink_e_cen_array(1, j, i)
                Next j


            ElseIf SelectModel.rbAASHTO_05.Checked = True Then

                ultimate_shrink_strain = Ks * Khs * Kf * Kcure_shrink * -0.48
                * (10 ^ -3)

'Calculate at beginning and end of time interval...need the change in Ktd.

Ktd_array_begin(i) = shrink_time_array(i - 1) / (61 - (4 * (fci /
                     1000)) + shrink_time_array(i - 1))
Ktd_array_end(i) = shrink_time_array(i) / (61 - (4 * (fci / 1000)) +
                   shrink_time_array(i))
delta_Ktd_array(i) = Ktd_array_end(i) - Ktd_array_begin(i)

                For j = 1 To NumberCS
                    delta_shrink_e_cen_array(1, j, i) =
                    ultimate_shrink_strain * delta_Ktd_array(i)
                Next j



                For j = 1 To NumberCS
                    Total_Shrink_Strain_array(1, j) =
                    Total_Shrink_Strain_array(1, j) +
                    delta_shrink_e_cen_array(1, j, i)
                Next j

            ElseIf SelectModel.rbAASHTO_04.Checked = True Then

Ks_array(i) = (((age_array(i) - ti) / ((26 * Exp(0.36 * VS)) +
              (age_array(i) - ti))) / ((age_array(i) - ti) / (45 +
              (age_array(i) - ti)))) * ((1064 - (94 * VS)) / 923)

                If TimeOfEvents.rbMoistCure.Checked = True Then

ultimate_shrink_strain = -Khs * ((10000 / ((26 * Exp(0.36 * VS)) +
                         10000)) / ((10000 / (45 + 10000))) _
                         * ((1064 - (94 * VS)) / 923)) * Kcure_shrink *
                         0.51 * 10 ^ -3

Ktd_array_begin(i) = shrink_time_array(i - 1) / (35 +
                     shrink_time_array(i - 1))
Ktd_array_end(i) = shrink_time_array(i) / (35 + shrink_time_array(i))
                   delta_Ktd_array(i) = Ktd_array_end(i) –
```

```
                    Ktd_array_begin(i)

                     For j = 1 To NumberCS
                         delta_shrink_e_cen_array(1, j, i) = -
                         Ks_array(i) * Kcure_shrink * Khs *
                         delta_Ktd_array(i) * 0.51 * 10 ^ -3
                     Next j

                ElseIf TimeOfEvents.rbSteamCure.Checked = True Then

ultimate_shrink_strain = -Khs * Kcure_shrink * ((10000 / ((26 *
                          Exp(0.36 * VS)) + 10000)) / ((10000 / (45 +
                          10000))) * ((1064 - (94 * VS)) / 923)) * 0.56
                          * 10 ^ -3

Ktd_array_begin(i) = shrink_time_array(i - 1) / (55 +
                      shrink_time_array(i - 1))
Ktd_array_end(i) = shrink_time_array(i) / (55 + shrink_time_array(i))
                    delta_Ktd_array(i) = Ktd_array_end(i) –
                    Ktd_array_begin(i)

                     For j = 1 To NumberCS
                         delta_shrink_e_cen_array(1, j, i) = -
                         Ks_array(i) * Kcure_shrink * Khs *
                         delta_Ktd_array(i) * 0.56 * 10 ^ -3
                     Next j

                End If



                For j = 1 To NumberCS
                    Total_Shrink_Strain_array(1, j) =
                    Total_Shrink_Strain_array(1, j) +

                    delta_shrink_e_cen_array(1, j, i)
                Next j

            ElseIf SelectModel.rbCEB.Checked = True Or
            SelectModel.rbCEB_Mod.Checked = True Then

                beta_SRH = 1 - (RH_CEB / 100) ^ 3

                If RH_CEB >= 40 And RH_CEB < 99 Then
                    beta_RH = -1.55 * beta_SRH
                ElseIf RH_CEB >= 99 Then
                    beta_RH = 0.25
                End If

                If SelectModel.ComboBoxCementType2.Text = "Slowly
                hardening SL" Or
                SelectModel.ComboBoxCementType2Mod.Text = "Slowly
                hardening SL" Then
                    beta_SC = 4
```

```
                ElseIf SelectModel.ComboBoxCementType2.Text =
                "Normal/Rapid hardening N and R" Or
                SelectModel.ComboBoxCementType2Mod.Text = "Normal/Rapid
                hardening N and R" Then
                    beta_SC = 5
                ElseIf SelectModel.ComboBoxCementType2.Text = "Rapid
                hardening, high-strength RS" Or
                SelectModel.ComboBoxCementType2Mod.Text = "Rapid
                hardening, high-strength RS" Then
                    beta_SC = 8
                End If

notional_shrink_co = ((160 + (10 * beta_SC * (9 - (fcm_CEB / 10)))) *
                      10 ^ -6) * beta_RH

ultimate_shrink_strain = notional_shrink_co

beta_s_begin(i) = (shrink_time_array(i - 1) / (350 * ((h_CEB / 100) ^
                   2) + shrink_time_array(i - 1))) ^ 0.5

beta_s_end(i) = (shrink_time_array(i) / (350 * ((h_CEB / 100) ^ 2) +
                 shrink_time_array(i))) ^ 0.5

delta_beta_s(i) = beta_s_end(i) - beta_s_begin(i)

                For j = 1 To NumberCS
                    delta_shrink_e_cen_array(1, j, i) =
                    notional_shrink_co * delta_beta_s(i)
                Next j



                For j = 1 To NumberCS
                    Total_Shrink_Strain_array(1, j) =
                    Total_Shrink_Strain_array(1, j) +
                    delta_shrink_e_cen_array(1, j, i)
                Next j

            End If

'COMPUTES THE INCREMENTAL CURVATURE.

            delta_relax_array = delta_fpr_array
            delta_ecr_array = delta_creep_e_cen_array
            delta_esh_array = delta_shrink_e_cen_array
            delta_phi_cr_array = delta_creep_phi_array

            For j = 1 To NumberCS
                For k = 1 To NumberLayerGroups
                    Aps_yp_cen_array(k, j, i) = Aps_array(k, j) *
                    yp_cen_array(k, j, i)
                Next k
            Next j

            For j = 1 To NumberCS
```

```
    For k = 1 To NumberLayerGroups
        Aps_yp_cen(1, j, i) = Aps_yp_cen(1, j, i) +
        Aps_yp_cen_array(k, j, i)
    Next k
Next j

For j = 1 To NumberCS
    For k = 1 To NumberLayerGroups
        Aps_delta_fr_array(k, j, i) = Aps_array(k, j) *
        delta_fpr_array(k, j, i)
    Next k
Next j

For j = 1 To NumberCS
    For k = 1 To NumberLayerGroups
        Aps_delta_fr(1, j, i) = Aps_delta_fr(1, j, i) +
        Aps_delta_fr_array(k, j, i)
    Next k
Next j

For j = 1 To NumberCS
    For k = 1 To NumberLayerGroups
        Aps_yp_delta_fr_array(k, j, i) =
        Aps_yp_cen_array(k, j, i) * delta_fpr_array(k,j,i)
    Next k
Next j




For j = 1 To NumberCS
    For k = 1 To NumberLayerGroups
        Aps_yp_delta_fr(1, j, i) = Aps_yp_delta_fr(1, j, i)
        + Aps_yp_delta_fr_array(k, j, i)
    Next k
Next j

For j = 1 To NumberCS
    For k = 1 To NumberSteelLayers
        Ars_yr_cen_array(k, j, i) = Ars_array(k, j) *
        yr_cen_array(k, j, i)
    Next k
Next j

For j = 1 To NumberCS
    For k = 1 To NumberSteelLayers
        Ars_yr_cen(1, j, i) = Ars_yr_cen(1, j, i) +
        Ars_yr_cen_array(k, j, i)
    Next k
Next j

For j = 1 To NumberCS
    delta_curvature_array(1, j, i) =
```

```
                (delta_creep_phi_array(1, j, i) * (1 - (((np_array(i) *
                Aps_y2(1, j, i)) + (ns_array(i) * Ars_y2(1, j, i))) /
                Itr_array(1, j, i)))) - ((((delta_ecr_array(1, j, i) +
                delta_esh_array(1, j, i)) * ((np_array(i) *
                Aps_yp_cen(1, j, i)) + (ns_array(i) * Ars_yr_cen(1, j,
                i)))) + ((1 / Ep) * (np_array(i) *
                Aps_yp_delta_fr(1, j, i)))) / Itr_array(1, j, i))
            Next j

'COMPUTES THE INCREMENTAL STRAIN AT THE CENTROID OF THE TRANSFORMED SECTION.

            For j = 1 To NumberCS
                delta_ecen_array(1, j, i) = ((Acon_array(1, j, i) /
                Atr_array(1, j, i)) * (delta_ecr_array(1, j, i) +
                delta_esh_array(1, j, i))) -(((delta_creep_phi_array(1,
                j, i) * ((np_array(i) * Aps_yp_cen(1, j, i)) +
                (ns_array(i) * Ars_yr_cen(1, j, i)))) + ((1 /
                Econ_array(i)) * (Aps_delta_fr(1, j, i)))) /
                Atr_array(1, j, i))
            Next j

'COMPUTES THE INCREMENTAL STRAIN AT THE CENTROID OF THE NET CONCRETE SECTION.

            For j = 1 To NumberCS
                delta_enet_array(1, j, i) = delta_ecen_array(1, j, i) +
                (delta_curvature_array(1, j, i) * (ytr_array(1, j, i) _
                - yc_net_array(1, j, i)))
            Next j

'COMPUTES THE INCREMENTAL STRAIN AT THE TOP AND BOTTOM OF THE CROSS SECTION.

            For j = 1 To NumberCS
                y_net_top_array(1, j, i) = yc_net_array(1, j, i) - h
                y_net_bottom_array(1, j, i) = yc_net_array(1, j, i)
            Next j

            For j = 1 To NumberCS
                delta_e_top_array(1, j, i) = delta_enet_array(1, j, i)
                + (y_net_top_array(1, j, i) * delta_curvature_array(1,
                j, i))

                delta_e_bottom_array(1, j, i) = delta_enet_array(1, j,
                i) + (y_net_bottom_array(1, j, i) *
                delta_curvature_array(1, j, i))
            Next j

'COMPUTES THE INCREMENTAL STRAIN IN EACH REINFORCING STEEL LAYER.

            For j = 1 To NumberCS
                For k = 1 To NumberSteelLayers
                    delta_er_array(k, j, i) = delta_enet_array(1, j, i)
                    + (yr_net_array(k, j, i) * delta_curvature_array(1,
                    j, i))
                Next k
            Next j
```

```
'COMPUTES THE INCREMENTAL STRAIN IN EACH LAYER GROUP.

            For j = 1 To NumberCS
                For k = 1 To NumberLayerGroups
                    delta_ep_array(k, j, i) = delta_enet_array(1, j, i)
                    + (yp_net_array(k, j, i) * delta_curvature_array(1,
                    j, i))
                Next k
            Next j

'COMPUTES THE INCREMENTAL STRESS AT THE TOP AND BOTTOM OF THE CROSS SECTION.

'Translates the unrestrained incremental creep strain from the centroid to
the top and bottom of the cross section using the incremental curvature due
to the unrestrained creep.  The unrestrained incremental shrinkage strain is
constant across the entire cross section.

            For j = 1 To NumberCS

delta_creep_etop_array(1, j, i) = delta_creep_e_net_array(1, j, i) +
                                  (y_net_top_array(1, j, i) *
                                  delta_creep_phi_array(1, j, i))

delta_creep_ebottom_array(1, j, i) = delta_creep_e_net_array(1, j, i) +
                                     (y_net_bottom_array(1, j, i) *
                                     delta_creep_phi_array(1, j, i))

delta_shrink_etop_array(1, j, i) = delta_shrink_e_cen_array(1, j, i)

delta_shrink_ebottom_array(1, j, i) = delta_shrink_e_cen_array(1, j, i)
            Next j


            For j = 1 To NumberCS
delta_stress_cen_array(1, j, i) = (delta_ecen_array(1, j, i) –
                                  delta_creep_e_cen_array(1, j, i) –
                                  delta_shrink_e_cen_array(1, j, i)) *
                                  Econ_array(i)

delta_stress_net_array(1, j, i) = (delta_enet_array(1, j, i) –
                                  delta_creep_e_net_array(1, j, i) -
                                  delta_shrink_e_cen_array(1, j, i)) *
                                  Econ_array(i)

delta_stress_top_array(1, j, i) = (delta_e_top_array(1, j, i) –
                                  delta_creep_etop_array(1, j, i) -
                                  delta_shrink_etop_array(1, j, i)) *
                                  Econ_array(i)

delta_stress_bottom_array(1, j, i) = (delta_e_bottom_array(1, j, i) –
                                     delta_creep_ebottom_array(1, j, i)
                                     - delta_shrink_ebottom_array(1, j,
                                     i)) * Econ_array(i)
            Next j
```

```
'COMPUTES THE INCREMENTAL STRESS IN EACH REINFORCING STEEL LAYER.

            Es = Val(ReinforcingSteel.txbEs.Text)

            For j = 1 To NumberCS
                For k = 1 To NumberSteelLayers
                    delta_stress_r_array(k, j, i) = Es *
                    delta_er_array(k, j, i)
                Next k
            Next j

'COMPUTES THE INCREMENTAL STRESS IN EACH LAYER GROUP.

            For j = 1 To NumberCS
                For k = 1 To NumberLayerGroups
                    delta_stress_p_array(k, j, i) = (Ep *

                    delta_ep_array(k, j, i)) + delta_fpr_array(k, j, i)
                Next k
            Next j




'UPDATES THE PRESTRESS FORCE IN EACH LAYER GROUP BASED ON THE LOSSES DUE TO
RELAXATION, CREEP, AND SHRINKAGE.

            For j = 1 To NumberCS
                For k = 1 To NumberLayerGroups
                    If i = 1 Then
                        fps_array(k, j, 1) = fpt_array(k, j) +
                        delta_stress_p_array(k, j, i)
                    ElseIf i >= 2 Then
                        fps_array(k, j, 1) = fpt_array(k, j) +
                        delta_stress_p_array(k, j, 1)

                        fps_array(k, j, i) = fps_array(k, j, i - 1) +
                        delta_stress_p_array(k, j, i)
                    End If
                Next k
            Next j

'COMPUTES THE TOTAL STRAIN AT VARIOUS LOCATIONS WITHIN THE CROSS SECTION.

            For j = 1 To NumberCS
total_strain_cen_array(1, j, 0) = delta_ecen_initial_array(1, j)
total_strain_net_array(1, j, 0) = delta_ecen_initial_array(1, j) +
                                  (delta_phi_initial_array(1, j) * _
                                  (ytr_initial_array(1, j) -
                                  yc_net_initial_array(1, j)))
total_strain_top_array(1, j, 0) = initial_ec_array(2, j)
total_strain_bottom_array(1, j, 0) = initial_ec_array(1, j)
```

```
total_strain_cen_array(1, j, i) = total_strain_cen_array(1, j, i - 1) +
                                  delta_ecen_array(1, j, i)
total_strain_net_array(1, j, i) = total_strain_net_array(1, j, i - 1) +
                                  delta_enet_array(1, j, i)
total_strain_top_array(1, j, i) = total_strain_top_array(1, j, i - 1) +
                                  delta_e_top_array(1, j, i)
total_strain_bottom_array(1, j, i) = total_strain_bottom_array(1, j, i
                                     - 1) + delta_e_bottom_array(1, j, i)
            Next j

            For j = 1 To NumberCS
                For k = 1 To NumberLayerGroups
total_strain_p_array(k, j, 0) = initial_ep_array(k, j)
total_strain_p_array(k, j, i) = total_strain_p_array(k, j, i - 1) +
                                delta_ep_array(k, j, i)
                Next k
            Next j

            For j = 1 To NumberCS
                For k = 1 To NumberSteelLayers
total_strain_r_array(k, j, 0) = initial_er_array(k, j)
total_strain_r_array(k, j, i) = total_strain_r_array(k, j, i - 1) +
                                delta_er_array(k, j, i)
                Next k
            Next j
'COMPUTES THE TOTAL STRESS AT VARIOUS LOCATIONS WITHIN THE CROSS SECTION.

            For j = 1 To NumberCS
total_stress_cen_array(1, j, 0) = delta_ecen_initial_array(1, j) *
                                  Ec_initial
total_stress_net_array(1, j, 0) = (delta_ecen_initial_array(1, j) +
                                  (delta_phi_initial_array(1, j) * _
                                  (ytr_initial_array(1, j) –
                                  yc_net_initial_array(1, j)))) *
                                  Ec_initial
total_stress_top_array(1, j, 0) = initial_fc_array(2, j)
total_stress_bottom_array(1, j, 0) = initial_fc_array(1, j)

total_stress_cen_array(1, j, i) = total_stress_cen_array(1, j, i - 1) +
                                  delta_stress_cen_array(1, j, i)
total_stress_net_array(1, j, i) = total_stress_net_array(1, j, i - 1) +
                                  delta_stress_net_array(1, j, i)
total_stress_top_array(1, j, i) = total_stress_top_array(1, j, i - 1) +
                                  delta_stress_top_array(1, j, i)
total_stress_bottom_array(1, j, i) = total_stress_bottom_array(1, j, i
                                     - 1) +
                                     delta_stress_bottom_array(1, j, i)
            Next j

'COMPUTES THE TOTAL STRESS IN EACH REINFORCING STEEL LAYER.

            For j = 1 To NumberCS
                For k = 1 To NumberSteelLayers
total_stress_r_array(k, j, 0) = initial_fr_array(k, j)
total_stress_r_array(k, j, i) = total_stress_r_array(k, j, i - 1) +
```

```
                                delta_stress_r_array(k, j, i)
                    Next k
                Next j

'COMPUTES THE TOTAL PRESTRESS IN EACH LAYER GROUP.

                For j = 1 To NumberCS
                    For k = 1 To NumberLayerGroups
                        If i = 1 Then
total_stress_p_array(k, j, i) = fpt_array(k, j) +
                                delta_stress_p_array(k, j, i)
                        ElseIf i >= 2 Then
total_stress_p_array(k, j, 1) = fpt_array(k, j) +
                                delta_stress_p_array(k, j, 1)
total_stress_p_array(k, j, i) = total_stress_p_array(k, j, i - 1) +
                                delta_stress_p_array(k, j, i)
                        End If
                    Next k
                Next j




'COMPUTES THE TOTAL CURVATURE.

                For j = 1 To NumberCS
                   total_phi_array(1, j, 0) = delta_phi_initial_array(1, j)
                   total_phi_array(1, j, i) = total_phi_array(1, j, i - 1)
                                            + delta_curvature_array(1, j, i)
                Next j


            Next i

'END OF THE TIME LOOP.

    End Sub

End Module
```

Module 10: Camber Calculations (Initial and Time Dependent)

```
Module CamberCalc

    Public NumberCS, j, i, TimeIntervals As Integer
    Public L, delta_phi_initial_array(1, NumberCS),
      CS_Segments_array(1, NumberCS), Total_Curvature_array(1, NumberCS,
      TimeIntervals), Total_Camber(1, NumberCS - 1, TimeIntervals),
      Total_Camber_Calculation(TimeIntervals), Initial_Camber As Single

    Function Initial_Camber_Calc(ByVal NumberCS As Integer, ByVal L As
```

```
  Single, ByVal delta_phi_initial_array(,) As Single,
  ByVal CS_Segments_array(,) As Single, ByRef Initial_Camber_array(,) As
  Single, ByRef Initial_Camber_Calculation As Single)


    Dim Initial_Camber(1, NumberCS - 1) As Single
    Dim Initial_Camber_1CS As Single

    If NumberCS = "1" Then

        Initial_Camber_1CS = -(delta_phi_initial_array(1, 1) *
              (L ^ 2) / 8)

    ElseIf NumberCS >= "2" Then

        For j = 1 To NumberCS - 1
            Initial_Camber(1, j) = -(((CS_Segments_array(1, j + 1)
              - CS_Segments_array(1, j)) / 2) *
              ((delta_phi_initial_array(1, j) * (((L / 2) - (2 / 3) *
              CS_Segments_array(1, j)) - ((1 / 3) * CS_Segments_array(1,
              j + 1)))) + (delta_phi_initial_array(1, j + 1) * (((L / 2)
              - (1 / 3) * CS_Segments_array(1, j)) - ((2 / 3) *
              CS_Segments_array(1, j + 1))))))
        Next j

        Initial_Camber_array = Initial_Camber

    End If

    If NumberCS = "1" Then

        Initial_Camber_Calculation = Initial_Camber_1CS

    ElseIf NumberCS >= "2" Then

        Dim Initial_Camber_sum As Single

        For j = 1 To NumberCS - 1
            Initial_Camber_sum = Initial_Camber_sum +
              Initial_Camber_array(1, j)
        Next j

        Initial_Camber_Calculation = Initial_Camber_sum

    End If

    Initial_Camber_Calc = Initial_Camber_Calculation

End Function

Function Total_Camber_array(ByVal NumberCS As Integer, ByVal
  TimeIntervals As Integer, ByVal L As Single, ByVal
  Total_Curvature_array(,,) As Single, ByVal CS_Segments_array(,) As
  Single, ByRef Total_Camber(,,) As Single, ByRef Total_Camber_Calc() As
  Single)
```

```
        Dim Camber(1, NumberCS - 1, TimeIntervals) As Single
        Dim Camber_1CS(TimeIntervals) As Single

        If NumberCS = "1" Then

            For i = 1 To TimeIntervals

                Camber_1CS(i) = -(Total_Curvature_array(1, 1, i) *
                  (L ^ 2) / 8)

            Next i

            Total_Camber_Calc = Camber_1CS


        ElseIf NumberCS >= "2" Then

            For i = 1 To TimeIntervals

                For j = 1 To NumberCS - 1

                    Camber(1, j, i) = -(((CS_Segments_array(1, j + 1) –
                        CS_Segments_array(1, j)) / 2) *
                        ((Total_Curvature_array(1, j, i) *
                        (((L / 2) - (2 / 3) * CS_Segments_array(1, j)) - ((1
                        / 3) * CS_Segments_array(1, j + 1))))
                        + (Total_Curvature_array(1, j + 1, i) * (((L / 2) -
                        (1 / 3) * CS_Segments_array(1, j)) -
                        ((2 / 3) * CS_Segments_array(1, j + 1))))))
                Next j

            Next i

            Total_Camber = Camber

            Dim Camber_sum(TimeIntervals) As Single

            For i = 1 To TimeIntervals
                For j = 1 To NumberCS - 1
                    Camber_sum(i) = Camber_sum(i) + Total_Camber(1,j,i)
                Next j
            Next i

            Total_Camber_Calc = Camber_sum

        End If

        Total_Camber_array = Total_Camber_Calc

    End Function

End Module
```